FRIB PROJECT: MOVING TO PRODUCTION PHASE *

K. Saito#, H. Ao, B. Barker, B. Bird, N. Bultman, E. Burkhardt, F. Casagrande, S. Chandrasekaran, S. Chouhan, C. Compton, J. Crisp, K. Davidson, K. Elliott, A. Feyzi, A. Fox, P. Gibson, K. Holland, L. Hodges, G. Kiupel, S. Lidia, D. Morris, I. Malloch, E. Metzgar, D. Miller, S. Miller, D. Norton, J. Popielarski, L. Popielarski, A. Rauch, R. Rose, T. Russo, S. Shanab, M. Shuptar, S. Stark, M. Thrush, N. Usher, G. Velianoff, D. Victory, J. Wei, T. Xu, Y. Xu, M. Xu, Y. Yamazaki, Q. Zhao, W. Zheng
Facility for Rare Isotope Beams, Michigan State University, East Lansing, MI 48824, USA
A. Facco, INFN - Laboratori Nazionali di Legnaro, Legnaro (Padova), Italy
K. Hosoyama, M. Masuzawa, High Energy Accelerator Research Organisation, Tsukuba, Japan
R.E. Laxdal TRIUMF, Vancouver, Canada

Abstract

The Facility of Rare Isotope Beams (FRIB) project was presented in SRF2013 [1]. This paper reports the progressed situation of this project since SRF2013. FRIB project is now moving to production phase. FRIB superconducting RF (SRF) linac project and challenges are presented. This paper address the status of the SRF hardware production, SRF infrastructure status and plans for ramping to full production, and also focus on information that can be relevant for future large proton/ion SRF linac projects.

FRIB PROJECT

FRIB is a Department of Energy (DOE) joint project operated at MSU and obtained CD3-B approval in August 2014. Conventional facilities construction began in March 2014. Accelerator system construction also started in October 2014, and will be completed in 2022 (CD4). Early commissioning is schedule in 2017 - 2020 starting with the Front end [2]. SRF is the core technology in this project [3].

Figure 1: FRIB conventional facility contraction status on August 2015.

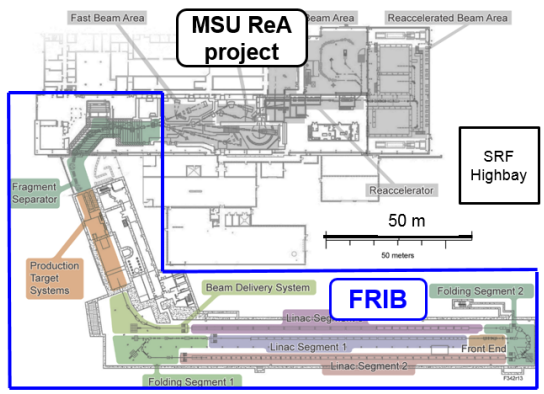

Figure 2: FRIB configuration in MSU campus.

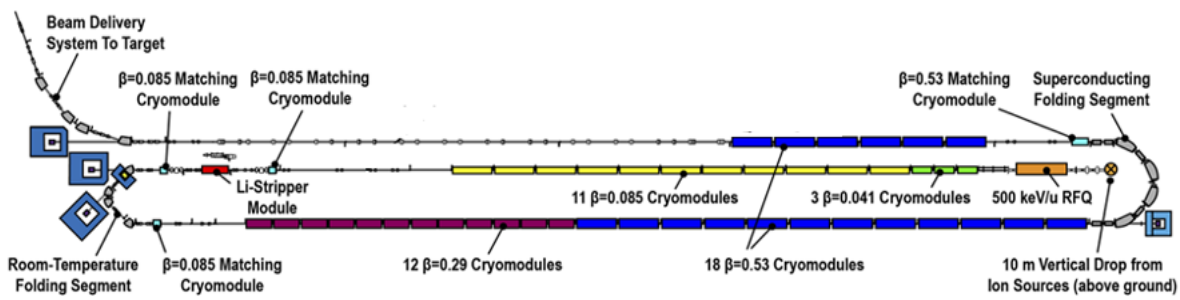

Figure 3: FRIB linac configuration.

* This material is based upon work supported by the U.S. Department of Energy Office of Science under Cooperative Agreement DE-SC0000661, the State of Michigan and Michigan State University
# Saito@frib.msu.edu

ISBN 978-3-95450-178-6

RECENT PROGRESS WITH EU-XFEL*

D. Reschke#, DESY, Hamburg, Germany
for the European XFEL Accelerator Consortium

Abstract

The superconducting accelerator of the European XFEL consists of the injector part and the main linac. The injector includes one 1.3 GHz accelerator module and one 3.9 GHz third-harmonic module, while the main linac will consist of 100 accelerator modules, operating at an average design gradient of 23.6 MV/m. The fabrication and surface treatment by industry as well as RF acceptance tests of the required 808 superconducting 1.3 GHz cavities are close to an end by the time of SRF 2015. The accelerator module assembly, testing and installation in the tunnel is in full swing. First steps of commissioning have been made. The status and results of cavity and module RF tests at 1.3 GHz and 3.9 GHz are presented.

INTRODUCTION

The 17.5 GeV SRF linac for the European XFEL is currently under construction by a consortium consisting of several European institutes [1]. An enhanced cryomodule production rate of 1.25 eight-cavity-module per week since beginning of 2015 requires an average vertical acceptance testing rate and delivery of at least ten cavities per week. The average cryomodule testing rate has to match this production rate. Testing of both, individual cavities and cryomodules, is performed in a dedicated test facility at DESY (AMTF) [2,3,4,5]. As of July 31, 2015 approximately 740 of the 800 series EU-XFEL TESLA-type 1.3 GHz SRF cavities have been produced, and have each undergone at least one vertical acceptance test at AMTF. As of September 10, 2015 ~57 of the 102 EU-XFEL cryomodules (see below) have been tested at AMTF. Vertical and module testing is performed by a team from IFJ-PAN Krakow as an in-kind contribution. The installation of cryomodules and first steps of commission for the injector as well as for the main linac are in full swing.

XFEL CAVITIES AND VERTICAL ACCEPTANCE TEST AT AMTF

Production Overview

Series production of the 1.3 GHz TESLA cavities is equally divided between E. Zanon Spa. (EZ), Italy, and Research Instruments GmbH (RI), Germany. Production includes both mechanical fabrication and surface preparation [6] with the required extensive documentation [7]. Details about the RF measurements for quality assurance during the cavity production and the devices used for frequency measurement and tuning can be found in [8,9,10]. The 800 series cavities required for XFEL (400 per vendor) are delivered complete with a helium tank, ready for vertical testing in AMTF (Fig.1) at DESY. Each vendor also produces an additional 12 cavities without helium tank for the ILC-HiGrade programme [11], which are used as a quality control tool as well as for further R&D. For 8 of these 24 cavities a subsequent assembly of the He-tank will be made. Both vendors must exactly follow well-defined specifications for the mechanical fabrication and surface treatments, but no RF performance guarantee is given. The surface preparation at both vendors starts with a bulk EP followed by 800° annealing, but for the final surface treatment two alternative recipes are in use: EZ applies a final chemical surface removal ("Flash-BCP"); RI applies a final electrochemical surface removal (EP). All cavities are fully equipped with their HOM antennas, pick-up probe and a High-Q input coupler antenna with fixed coupling. The procedures before and after the vertical acceptance test at 2K are described in [12].

At the time of SRF 2015 the mechanical cavity production is nearly finished. The tested ~740 cavities clearly demonstrate that the chosen scheme for mechanical production and surface preparation is successful at both vendors.

Due to pores out of DESY specification found in the longitudinal welds of the Helium service pipe made of Titanium about 750 He-tanks had to be modified, partially on He tanks already welded onto cavities. This major effort including the necessary qualification steps has been performed successfully over the last two years and is described in detail in [13].

Vertical Testing Rates

In order to achieve the desired testing rate of at least eight to ten cavities per week, the vertical acceptance tests are made using two independent test systems, each consisting of an independent bath cryostat and RF test stand. Each test cryostat accepts an "insert" which supports up to four cavities, greatly increasing the efficiency of cool-down / warm-up cycles. The test infrastructure at DESY (Fig.1) has been in full operation since October 2013 and has achieved a stable average of about 42 vertical tests per month (Fig. 2). All vertical acceptance tests of the 824 cavities will be finished within the current project schedule (end of 2015). Each vertical test is categorized according to well-defined "test reasons". Depending on the result a categorized "decision" is taken and documented in the cavity and cryomodule managing system [14] of the AMTF as well as in the XFEL cavity data base [15]. Cavities without non-conformities and with acceptable performance usual have only one vertical acceptance test ("as received") after which they receive the decision "send to string

#detlef.reschke@desy.de

ISBN 978-3-95450-178-6

OVERVIEW OF RECENT SRF DEVELOPMENTS FOR ERLS*

S. Belomestnykh#,1,2

1) Brookhaven National Laboratory, Upton, NY 11973-5000, U.S.A.
2) Stony Brook University, Stony Brook, NY 11794, U.S.A.

Abstract

This presentation reviews SRF technology for Energy Recovery Linacs (ERLs). In particular, recent developments and results reported at the ERL2015 Workshop are highlighted. The paper covers facilities under construction, commissioning or operation, such as cERL at KEK, b*ERL*inPro at HZB and R&D ERL at BNL, as well as facilities in the development phase. Future perspectives will be discussed.

INTRODUCTION

Energy recovery linacs still generate a lot of interest in the accelerator and user communities as the recent Workshop on Energy Recovery Linacs [1] has demonstrated, attracting more than one hundred participants. Along with "traditional" applications of ERLs for X-ray light sources and FELs [2, 3], electron-ion colliders [4], and electron coolers [5, 6], several new proposals and ideas were presented at the workshop as reported in [7]. Among those are: a compact ultra-high flux X-ray and THz source at John Adams Institute [8], ERLs for nuclear physics research MESA at Mainz University [9] and particle physics experiments at the jointly proposed BNL/Cornell demonstration multi-pass FFAG machine [10], γ-ray sources [11, 12], an ERL facility at CERN for applications [13] and even a concept of lepton ERL scalable to TeV energies [14]. However, only a few big proposals are actually funded. The field is very active, but is still in the development/demonstration stage. Tigner in his talk [15] outlined challenges to realization of ERLs. Some R&D needs related to SRF are:

- CW operation of large-scale SRF installations: high Q_0 at relevant accelerating gradients.
- Unprecedented beam currents and number of spatially superimposed high charge bunches in the SRF linacs: beam break up, halo, other beam dynamics issues.
- Photoinjectors producing high-brightness beams.
- Precise phase and amplitude control of narrow-bandwidth SRF cavities required over large spatial extent with varying ground vibration conditions.

As SRF linacs are essential to realize full benefits of the ERL approach, a significant portion of the ERL'2015 was devoted to the SRF technology, which was discussed in several working groups [16-18]. ERLs operate in CW mode and as a result, an optimal accelerating gradient for their SRF structures lie in a range between 15 and 20 MV/m (see [19] for example). Cryogenic power in such installations is dominated by the dynamic heat loads and hence achieving high quality factors in CW SRF cavities is very important. There was a lot of progress in this area recently, started with pioneering work on nitrogen doping at Fermilab [20], which was adopted for LCLS-II [21]. Other laboratories around the world joined the efforts trying to shed a light on the physics behind this effect, which is not fully understood yet. This is a very "hot topic" that will be widely discussed at this conference and warrants a separate review paper as many new and exciting results will be presented. As this topic will be outside the scope of present paper, I concentrate on such aspects as SRF injectors, HOM-damped SRF structures and cryomodules for ERLs. I review recent developments of the SRF technology for ERL projects around the world reported at the ERL'2015 workshop as well as some results obtained after the workshop.

RECENT RESULTS FROM SRF INJECTORS FOR ERLS

Significant progress was made since the last SRF conference in developing superconducting RF electron guns. As this will be covered in two other reviews talks [22, 23], here I highlight only some results relevant for ERLs. While we see more SRF guns generating first beams, there are still issues to be resolved. The photocathode materials survive well in the SRF guns when installed properly. However, contamination of the gun cavities photoemission materials often causes multipacting and field emission. Particulate-free installation of the cathodes is not always successful either and sometimes results in performance degradation.

SRF Gun II at ELBE

A new SRF gun for ELBE (SRF Gun II), shown in Figure 1, was developed, installed and commissioned at HZDR [24, 25]. This gun has an improved 3.5-cell niobium cavity with a better accelerating filed distribution: peak field ratio of 0.8:1 between the half-cell and TESLA cells. A superconducting solenoid is integrated into the gun cryomodule. There were also several smaller modifications.

An accelerating gradient of 10 MV/m was achieved in the first RF test of the gun without a cathode [24], which is a significant improvement as compared with SRF Gun I as one can see from Figure 2. Beam dynamics simulations showed that higher gradient should result in reduced emittance and bunch length. The first beam test has been carried out with a copper photocathode with gradients up to 9 MV/m. Installation of a Cs_2Te photocathode was not successful as it resulted in very low quantum efficiency

* Work is supported by Brookhaven Science Associates, LLC under contract No. DE-AC02-98CH10886 with the US DOE
#sbelomestnykh@bnl.gov

STATUS OF THE RISP SUPERCONDUCTING HEAVY ION ACCELERATOR*

Dong-O Jeon# representing the RISP
Institute for Basic Science, Daejeon, Republic of Korea

Abstract

Construction of the RISP heavy ion accelerator facility is in-progress in Korea with the In-flight Fragment (IF) and Isotope Separation On-Line (ISOL) facilities. The driver linac for the IF facility is a superconducting linac. Prototyping of major components and their tests are proceeding including superconducting cavities, superconducting magnets and cryomodules, the 28-GHz ECR ion source and the RFQ. Prototype superconducting cavities were fabricated through domestic vendors and tested at the TRIUMF showing promising vertical tests results. Progress report of the RISP accelerator systems is presented.

INTRODUCTION

The RISP heavy ion accelerator facility is a unique facility that has the 400-kW In-flight Fragmentation (IF) facility and the Isotope Separator On-Line (ISOL) facility [1,2]. The driver accelerator for the IF facility is a superconducting linac (SCL) that can accelerate up to 200 MeV/u for the uranium beam delivering more than 400 kW of beam power to the IF target and various other targets.

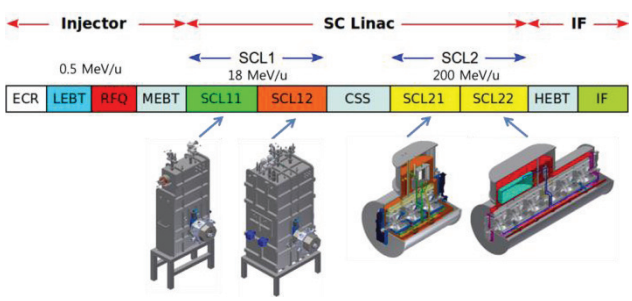

Figure 1: Plot of the RISP superconducting linac lattice.

Figure 1 shows the schematic drawing of the driver linac. The superconducting linac adopts the normal conducting quadrupole doublets as focusing elements. This design is free from the quench of superconducting solenoids induced by the beam loss.

Adoption of short cryomodules also provides flexibility in operation and maintenance. For example, cryomodules can be removed for repair while operating the facility. Also it is easy to reshuffle better performing cavities or cryomodules to enhance the performance. For long cryomodules, removal of one cryomodule stops the beam operation.

Studies show that cryogenic load of the RISP linac is similar to that of the FRIB adopting long cryomodule design. The heat-load of warm-cold transition is offset by that of the current leads of superconducting solenoids. Cost comparisons shows that the construction cost is very similar and only differs by a few percent.

Detailed design of the accelerator systems has been completed, and prototyping and testing of critical components and systems have been performed. In this paper, the status of the RISP accelerator systems is presented along with prototyping progress.

DRIVER LINAC

The driver linac consists of an injector (28-GHz ECR ion source, 500-keV/u RFQ) and SCL1 (QWR, HWR type), CSS (Charge Stripper Section) and SCL2 (SSR1, SSR2 type) that can accelerate a uranium beam to 200 MeV/u, delivering 400-kW beam power to the target. The driver linac can accelerate beams from proton to uranium.

Injector

28-GHz ECR ion source (ECRIS) for the driver linac was fabricated with a saddle-type sextupole and four solenoids made of NbTi wires [3]. Figure 2 shows the plot of the superconducting magnet assembly, the plot of ECRIS cryostat and actual ECRIS. Superconducting magnet tests have been carried out, achieving 95% (80%) of the design goal for the hexapole (solenoid) in a combined operation mode. Further magnet training is in progress. Preliminary beam extraction test was conducted for of the 28-GHz ECRIS with a part of the LEBT installed along with it. Preliminary beam extraction test is shown in Fig. 3.

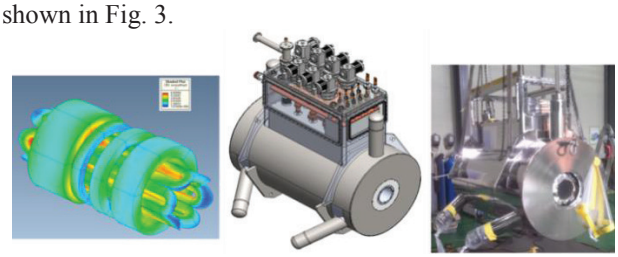

Figure 2: Plot of 28 GHz ECR ion source and its superconducting magnet assembly.

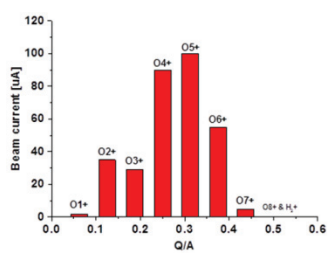

Figure 3: Initial ECR IS beam extraction test while maintain the magnets at the 50% of the design.

*Work supported by Ministry of Science, ICT and Future Planning
#jeond@ibs.re.kr

ISBN 978-3-95450-178-6

SENSITIVITY OF NIOBIUM SUPERCONDUCTING RF CAVITIES TO MAGNETIC FIELD*

D. Gonnella†, M. Liepe, and J. Kaufman

CLASSE, Cornell University, Ithaca, NY 14853, USA

Abstract

One important characteristic of nitrogen-doped cavities is their very high sensitivity to increased residual surface resistance from trapped ambient magnetic flux. We have performed a systematic study on the losses by trapped flux, and their dependence on the mean-free-path (MFP) of the niobium RF penetration layer. Cavities with a wide range of MFP values were tested in uniform ambient magnetic fields to measure trapped magnetic flux and resulting increase in RF surface resistance. MFP values were determined from surface impedance measurements. It was found that larger mean free paths lead to lower sensitivity to trapped magnetic flux.

INTRODUCTION

With SRF cavities reaching ever high intrinsic quality factors and reaching new, unprecedented levels of efficiency, the impact of the magnetic field present in the vicinity of the cavities becomes ever more important. During cool down, part of the ambient magnetic field will get trapped in the superconductor. This trapped flux in the RF penetration layer then causes losses in RF fields, resulting in an increase in the residual resistance of the cavity. However, the exact material parameter dependence of the impact of trapped magnetic field on the cavity's residual resistance had yet to be studied systematically Here we present the results of an experiment at Cornell to study how the cavity preparation method impacts a cavity's sensitivity to the magnetic field trapped in its walls.

EXPERIMENTAL SETUP

A total of eight cavities were prepared with a variety of methods: 6 nitrogen-doped cavities with varying levels of doping and two cavities prepared in a more standard fashion, one electropolished and one electropolished followed by a 48 hour 120°C bake. Each cavity was then assembled on a vertical test stand and surrounded by a Helmholtz coil. This coil applied a uniform external magnetic field parallel to the cavity's axis. A fluxgate magnetometer was placed on the cavity's iris to measure both applied magnetic field and trapped magnetic flux. Three temperature sensors were also placed on the cavity, one on each flange, and one on the equator in order to measure cool down rates and spatial temperature gradients. A picture of the experimental setup is shown in Fig. 1.

Figure 1: The experimental setup. A 1.3 GHz ILC shaped single-cell cavity was surrounded in a Helmholtz coil to induce a uniform external magnetic field parallel to the cavity axis.

Each cavity was cooled down in a variety of magnetic fields in order to trap different amounts of magnetic field in the cavity walls. Figure 2 shows a typical cool down. For each cool down, Q_0 versus temperature was measured, allowing us to extract residual resistance by BCS fitting using SRIMP [1] using the method described in [2]. Additionally, resonance frequency versus temperature was measured for each cavity to extract mean free path by converting to change in penetration depth versus temperature in order to extract mean free path.

EXPERIMENTAL RESULTS

The results of these measurements are shown in Fig. 3. The mangetic flux sensitivity is defined as

$$\text{Sensitivity} = \frac{dR_{\text{res}}}{dB_{\text{trapped}}}, \tag{1}$$

the slope shown in Fig. 3. We can see that there is a large spread in cavity sensitivity to trapped flux. The stronger doped cavities showed higher sensitivity and all nitrogen-doped cavities showed higher sensitivity than the EP and EP+120°C baked cavities. The EP cavity shows a sensitivity slightly larger than the EP+120°C baked cavity but still

* Work Supported by the US DOE and the LCLS-II High Q Program and NSF Grant PHY-1416318

† dg433@cornell.edu

HIGH-Q OPERATION OF SRF CAVITIES: THE IMPACT OF THERMOCURRENTS ON THE RF SURFACE RESISTANCE

J.-M. Köszegi, O. Kugeler, J. Knobloch, Helmholtz-Zentrum Berlin, Germany

Abstract

We present a study concerning the operation of a superconducting RF cavity (non-doped niobium) in horizontal testing with the focus on understanding the thermoelectrically induced contribution to the surface resistance. Starting in 2009, we suggested a means of reducing the residual resistance by warming up a cavity after initial cooldown to about 20 K and cooling it down again [1]. In subsequent studies we used this technique to manipulate the residual resistance by more than a factor of 2 [2]. We postulated that thermocurrents during cooldown generate additional trapped magnetic flux that impacts the cavity quality factor. Since several questions remained open, we present here a more extensive study including measurement of two additional passband modes of the 9-cell cavity that confirms the effect. We also discuss simulations that substantiate the claim. While the layout of the cavity LHe tank system is cylindrically symmetric, we show that the temperature dependence of the material parameters result in a non-symmetric current distribution. Hence a significant amount of magnetic flux can be generated at the RF surface resulting in an increased surface resistance [3].

SETUP

A fully equipped TESLA-type cavity welded into a titanium tank and with a TTF-3 input coupler installed was mounted horizontally inside the HoBiCaT [4] cryostat. The TESLA-type cavity reported on here received a heavy BCP (about 150 µm) prior to a 2 h bakeout at 800 °C (no N_2 anneal). A light BCP etch followed the heat treatment. Before the helium tank was welded onto the cavity a quality factor of about $2 \cdot 10^{10}$ in the π mode at 2 K was measured in a vertical test which corresponds to a residual resistance R_{res} of 1.2 nΩ if one assumes that the BCS resistance R_{BCS} did not change between vertical and horizontal test (fitting parameters for R_{BCS} in horizontal test are listed below).

The cavity was equipped with Cernox sensors on the helium vessel head and beam pipes near the Nb-Ti joints. Furthermore two heaters were attached, one on each beam pipe. The setup including the helium supply is sketched in Figure 1.

HoBiCaT can cool the cavity with different schemes. The cryoplant fills the helium via the filling line at the bottom left and/or the 2-phase-pipe from the top right. As discussed below, we used three different cooling schemes: The initial cooldown, the thermal cycle and the parked cooldown.

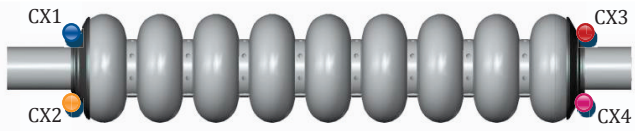

Figure 1: TESLA cavity in the LHe tank and equipped with four Cernox sensors and two heaters. The tank can be filled via the filling line and via the two phase pipe.

The heaters were used to create a temperature difference between the cavity ends if desired. The targeted difference could be adjusted by varying the heater power. Values chosen were typical of those encountered during normal cooldowns. The "parked cooldown" (Figure 2c) from room temperature combines properties of both the initial cooldown and the thermal cycle. The cooling procedure of the initial cooldown was adapted to stop well before the sc phase transition. The cryoplant was balanced to maintain a constant temperature for 48 h. The set point was first set to 30 K and then continuously lowered to 14 K during this period. After all temperature sensors were clearly in equilibrium the set point was further lowered towards 1.8 K and the cavity tank system transitioned with a small $\Delta T <$ 10 K into the sc state.

THERMOELECTRIC EFFECT IN THE CAVITY HELIUM TANK SYSTEM

With the described setup, we investigated the hypothesis that thermoelectrically induced currents and their associated magnetic flux is responsible for the change of R_s upon thermal cycling. In the horizontal setup, the system is fabricated of two materials: Niobium (cavity) and titanium (helium tank) which create bimetal junctions. If a temperature difference is applied along the system (from left to right), a current is driven along the cavity and back through the tank. The additional temperature difference from bottom to top breaks the cylindrical symmetry of the system because the dc resistance of Nb and Ti is temperature dependent. Thus, even though mechanically the system is symmetric, the current is not and a magnetic field can be generated at the RF surface and get trapped during sc phase transition.

RF MEASUREMENTS

For the evaluation of the residual resistance in the nine cells of the cavity we measured the quality factor Q_0 in three different passband modes: The π mode (1299 MHz), the 8/9π mode (1298 MHz) and the 1/9π mode (1274 MHz).

ISBN 978-3-95450-178-6

NATURE OF QUALITY FACTOR DEGRADATION IN SRF CAVITIES DUE TO QUENCH*

M. Checchin†, M. Martinello, FNAL, Batavia, IL 60510, USA and IIT, Chicago, IL 60616, USA
A. Romanenko, A. Grassellino, D.A. Sergatskov, O. Melnychuk, S. Posen,
FNAL, Batavia, IL 60510, USA
J.F. Zasadzinski, IIT, Chicago, IL 60616, USA

Abstract

Superconductive quench is a well-known phenomenon that causes magnetic flux trapping in superconducting accelerating cavities increasing the radio-frequency surface resistance. This paper is addressed to the understanding of the quench-induced losses nature. We present the proof that the real origin of quench-related quality factor degradation is consequence only of ambient magnetic field trapped at the quench spot. Also, we show how the quality factor can be fully recovered after it was highly deteriorated quenching several times in presence of external magnetic field. Such phenomenon was found to be completely reliable up to certain values of applied magnetic field, above that the cavity quality factor cannot be fully recovered anymore.

INTRODUCTION

Superconducting radio frequency (SRF) accelerating cavities are resonating structures that allow to accelerate charged particles up to energies of TeV. The limiting factors of such accelerating structures are represented by the finite value of intrinsic quality factor (Q_0), related to the cryogenic cost needed to their operation, and by the radio frequency (RF) field breakdown due to quench, that limits the maximum accelerating gradient (E_{acc}) achievable.

During the quench event a large area of the cavity becomes normal-conducting. This leads to a sudden increase of the surface resistance, that causes the suppression of the RF field in the cavity. Many well-known mechanisms [1–5] may lead to such phenomenon, and it was hypothesized that when the normal conducting region is created some magnetic flux can be trapped causing extra dissipation [7].

The origin of such trapped magnetic flux was ascribed to different mechanisms, such as: thermocurrents driven by the local thermal gradient in the quench zone [7], RF field trapped within the penetration depth region, or ambient magnetic field [8]. Anyhow, the real origin of Q_0 degradation after a quench is still not well understood and source of discussion in the SRF community.

Some studies [8] were performed at Fermi National Accelerator Laboratory (FNAL) on the degradation of the quality factor of superconducting resonators (high and medium β), with the purpose of finding a criterion to define the amount of ambient magnetic field trapped during the quench. In such work was also discussed the possibility of the complete recovery of the quality factor quenching in absence of external magnetic field.

In the present study we report the experimental prove that the Q_0 degradation due to quench is direct consequence of trapped ambient magnetic field, ruling out any other possible mechanism. We also demonstrate that fully recovery of the Q_0 after a quench can be achieved when the cavity is quenched in absence of external magnetic field, without warming the cavity above the critical temperature.

We discuss the configuration of the magnetic field trapped at the quench spot, and how this is the key to understand the recovery phenomenon.

It was also observed that not always the recovery of the quality factor is possible. If the trapped field is large enough, it migrates far from the quench spot, and the quality factor cannot be completely recovered anymore.

EXPERIMENTAL SET-UP

Some quench experiments were performed using several niobium nitrogen doped [6] 1.3 GHz TESLA-type cavities (TABLE 1), which were tested at the FNAL vertical test facility (VT). A scheme of the single cell cavities instrumentation is sketched in Fig. 1.

Single cell cavities were equipped with a T-map system [9] in order to map the temperature variation of the cavity

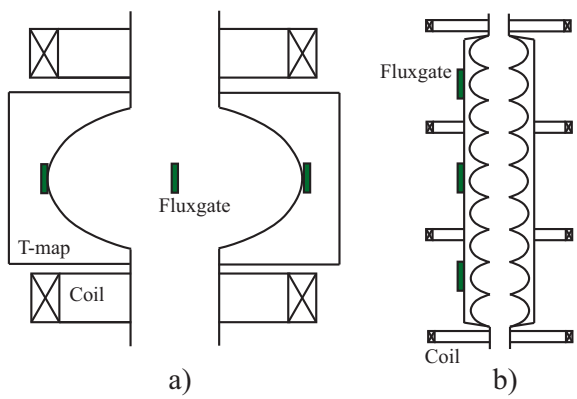

Figure 1: Experimental set-up for: a) single cell cavities, b) 9-cells fully dressed LCLS-II cavity.

* Work supported by the US Department of Energy, Office of High Energy Physics.
† checchin@fnal.gov

ISBN 978-3-95450-178-6

N DOPING: PROGRESS IN DEVELOPMENT AND UNDERSTANDING*

A. Grassellino, A. Romanenko, S Posen, Y. Trenikhina, O. Melnychuk, D.A. Sergatskov, M. Merio,
Fermilab, Batavia, IL 60510, USA
M. Checchin, M. Martinello, Fermilab and Illinois Institute of Technology,
Chicago, IL 60616, USA

Abstract

Following the 2012 discovery at Fermilab of a systematic increase of the quality factor of SRF bulk niobium cavities via nitrogen doping of the RF surface, Fermilab has moved forward with the development of this new technology, expanding from single cell to multicell cavities and to cavities of different frequencies. Extensive effort has been dedicated to the understanding of the underlying phenomena leading to the improved performance. This contribution will summarize the recent state of the art development and understanding of the N doping technology at FNAL.

INTRODUCTION

N doping was discovered in 2012 at FNAL and proven to systematically raise Q factors in the mid accelerating field region Bpk > 60 mT. In particular, N doping is found to lower the BCS surface resistance compared to 120C baked and unbaked niobium by a factor of ~ 2 at fields > 60 mT, and to lower non trapped flux related residual resistance < 2 nΩ [1]. Following the discovery on single cells, FNAL worked on: a) understanding the parameters in play leading to the improved performance; b) searching for the optimal doping recipe leading to best performance, in particular for Q, quench fields and trapped flux induced losses; c) develop quickly the technology on 1.3 GHz nine cells for LCLS-2 [2,3]; d) study cavity cutout and flat samples with various surface techniques looking for correlation with performance [4]; and e) apply the findings to 650 MHz cavities. A timeline summarizing the N doping R&D at FNAL is shown in Fig. 1.

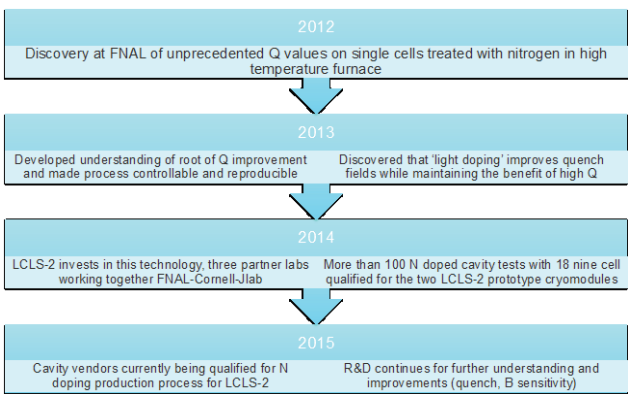

Figure 1: Timeline summarizing the development of the N doping technology from the 2012 discovery to today.

*Work supported.
#cee@aps.anl.gov

PROGRESS IN N DOPING DEVELOPMENT: LCLS-2 AND PIP-2

A variety of doping bake regimes have been explored at FNAL for single and multicell cavities of different frequencies 1.3 GHz and 650 MHz, in the context of development of a baseline surface treatment protocol for the LCLS-2 [5] and PIP-2 projects [6]. In both cases Q maximization at medium accelerating gradients ~ 17 MV/m and operating temperatures of ~ 2K is desired for minimization of cryogenic costs. Figure 2 shows the so far optimal recipe found and currently adopted as LCLS-2 baseline cavity surface processing protocol, the recipe known as "2/6" which stands for 2 minutes nitrogen injection, 6 minutes anneal, all at 800C, followed by 5 microns electro polishing average surface removal [7]. As it can be seen from Fig. 2 the processing sequence is a small variation from the standard protocol for example adopted by XFEL, involving small changes during the furnace treatment, the post furnace EP, and the removal of the final 120C bake. The 120C bake does not bring performance benefit to N doped surfaces, actually a decrease in Q and quench fields has been observed to N doped cavities that have been also 120C baked.

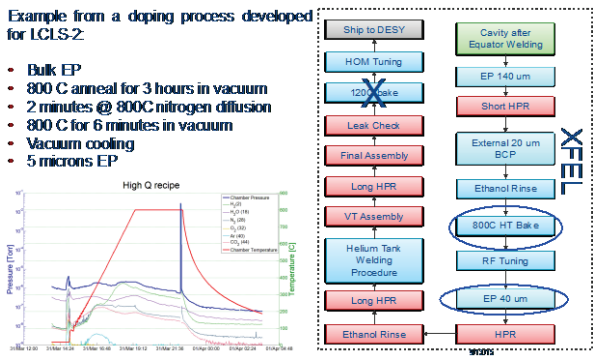

Figure 2: Example of doping protocol, small variation from the standard surface processing sequence.

The development of N doping for LCLS-2 is extensively described in [2,3]. Figure 3 shows one of the milestone plots which is the vertical test qualification of the nine cell cavities, treated with the 2/6 recipe, for the two LCLS-2 prototype cryomodules. All cavities meet the specification of 2.7e10 at 2K, 16 MV/m, and a record average quality factor is achieved of ~ 3.5e10 at 2 K, 16 MV/m. The bottom plot shows the same recipe applied to 650 MHz cavities, compared to standard 120C bake processing. Also in this case a gain up to a factor of 2 in quality factor at mid-field is found, and a record Q of ~ 7e10 at 16 MV/m, 2 K is reached.

NIOBIUM IMPURITY-DOPING STUDIES AT CORNELL AND CM COOL-DOWN DYNAMIC EFFECT ON Q_0 *

M. Liepe,† B. Clasby, R. Eichhorn, F. Furuta, G.M. Ge, D. Gonnella, T. Gruber, D.L. Hall, G. Hoffstaetter, J. Kaufman, P. Koufalis, J.T. Maniscalco, T. O'Connel, P. Quigley, D. Sabol, J. Sears, E.N. Smith, V. Veshcherevich,
CLASSE, Cornell University, Ithaca, NY 14853, USA

Abstract

As part of a multi-laboratory research initiative on high Q_0 niobium cavities for LCLS-II and other future CW SRF accelerators, Cornell has conducted an extensive research program during the last two years on impurity-doping of niobium cavities and related material characterization. Here we give an overview of these activities, and present results from single-cell studies, from vertical performance testing of nitrogen-doped nine-cell cavities, and from cryomodule testing of nitrogen-doped nine-cell cavities. We show that 2K quality factors at 16 MV/m well above the nominal LCLS-II specification of 2.7×10^{10} can be reached reliably by nitrogen doping of the RF penetration layer. We demonstrate that the nitrogen furnace pressure is not a critical parameter in the doping process. We show that higher nitrogen doping levels generally result in reduced quench fields, with substantial variations in the quench field between cavities treated similarly. We propose that this can be explained by the reduced lower critical field H_{c1} in N-doped cavities and the typical variation in the occurrence of defects on a cavity surface. We report on the results from five cryomodule tests of nitrogen-doped 9-cell cavities, and show that fast cool-down with helium mass flow rates above 2 g/s is reliable in expelling ambient magnetic fields, and that no significant change in performance occurs when a nitrogen-doped cavity is installed in a cryomodule with auxiliary components.

INTRODUCTION

Future CW operated large scale SRF linacs rely on the availability of very high efficiency SRF cavities, i.e. cavities with high intrinsic quality factors Q_0 at operating temperature (typically 1.8K to 2K) and operating accelerating fields (typically 15 to 20 MV/m). A prime example is LCLS-II, a CW SRF driven FEL to be constructed at SLAC, calling for nominal SRF nine-cell operating parameters of E_{acc} =16 MV/m and Q_0 of 2.7×10^{10} at 2K. [1] For many years now Cornell has been working on high efficiency niobium SRF cavities, initially as part of developing the technology for the Cornell Energy-Recovery-Linac (ERL), resulting in a proof-of-principle operation of a seven-cell 1.3 GHz cavity in a test cryomodule with unprecedented high 2K Q_0 of 3.5×10^{10}. [2] Motivated partly by such promising results, and partly by the recent demonstration that high temperature diffusion of small amounts of foreign atoms into the niobium rf surface can yield a dramatically reduced BCS surface resistance [3, 4], the LCLS-II project was adopted to employ high Q_0 SRF cavities. A collaborative effort between FNAL, JLab, and Cornell University was established in order to support the rapid development of procedures to minimize the LCLS-II cryogenic heat load by maximizing the Q_0 of nine-cell 1.3 GHz cavities for use in the LCLS-II linac. [5–7] The collaboration decided early on to focus on high temperature diffusion of nitrogen impurities into the niobium cavity wall as the technical route to increasing Q_0 in the LCLS-II cavities, a process discovered at FNAL to lower cryogenic loads by ≈50%. [3] The nitrogen doping process has the advantage of requiring only small changes to the standard cavity treatment process, but still needed to be fully developed and demonstrated on multi-cell cavities, including on cavities in cryomodule environments at the time the LCLS-II high Q_0 collaboration was formed. In this paper we give an updated overview of Cornell's contributions to this development process.

SINGLE-CELL N-DOPING STUDIES

As part of developing the nitrogen-doping protocol for the LCSL-II cavities, Cornell performed two dedicated studies on single-cell 1.3 GHz cavities. The goal was to explore optimal parameters, demonstrate robustness of the process in meeting specifications, study the impact of environmental factors and the cool-down process on cavity performance, and to improve understanding of the underlaying processes resulting in reduced BCS resistance, but also reduced maximum fields. The cavity treatment parameters used in these two studies were as follows:

A 20 min N-doping at 800°C, follow by 30 min anneal in vacuum at 800°C ("20N30" process), followed by different final vertical electropolishing (VEP) amounts. This process was applied to 5 single-cell cavities. The 2K performance results of the cavities in vertical test are shown in Fig. 1. [8] The average quench field of these 5 cavities is 27 MV/m, and the average Q_0 is 3.6×10^{10} at 2K and 16 MV/m.

B 20 min N-doping at 900°C, follow by 30 min anneal in vacuum at 900°C, followed by alternating vertical electropolishing (VEP) and vertical performance testing. This heavy doping ("over-doing") process was applied to one single-cell cavity to study the impact of heavy N-doping, especially reducing the quench field. The

* Work supported, in part, by the US DOE and the LCLS-II Project and by NSF grant PHYS-1416318.
† MUL2@cornell.edu

ISBN 978-3-95450-178-6

RF PERFORMANCE OF INGOT NIOBIUM CAVITIES OF MEDIUM-LOW PURITY*

G. Ciovati#, P. Dhakal, P. Kneisel, J. Spradlin, G. Myneni, JLab, Newport News, VA 23606, USA

Abstract

Superconducting radio-frequency cavities made of ingot niobium with residual resistivity ratio (RRR) greater than 250 have proven to have similar or better performance than fine-grain Nb cavities of the same purity, after standard processing. The high purity requirement contributes to the high cost of the material. As superconducting accelerators operating in continuous-wave typically require cavities to operate at moderate accelerating gradients, using lower purity material could be advantageous not only to reduce cost but also to achieve higher Q_0-values, because of the well-known dependence of the BCS-surface resistance on mean free path. In this contribution we present the results from cryogenic RF tests of 1.3-1.5 GHz single-cell cavities made of ingot Nb of medium (RRR=100-150) and low (RRR=60) purity from different suppliers. Cavities made of medium-purity ingots routinely achieved peak surface magnetic field values greater than 70 mT with Q_0-values above 1.5×10^{10} at 2 K. The performances of cavities made of low-purity ingots were affected by significant pitting of the surface after chemical etching.

INTRODUCTION

The performance of superconducting radio-frequency (RF) cavities is described by a plot of the quality factor, Q_0, as a function of the accelerating gradient, E_{acc}, or as a function of the peak surface magnetic or electric fields, B_p and E_p, respectively, measured at or below 4 K. R&D efforts throughout the world over the last decade demonstrated that the performance of SRF cavities built from large-grain, ingot material is comparable to that achieved using standard fine-grain, bulk Nb [1]. A relatively small production series of 1.3 GHz, 9-cell cavities made of high-purity (RRR~300) ingot Nb material showed that high gradients, greater than ~40 MV/m, could be achieved reproducibly and that higher Q_0-values than those of cavities of the same shape made of fine-grain, high-purity Nb, were achieved at 2 K [2]. The push for higher purity material stemmed from the need to increase the thermal conductivity of the Nb in order to "thermally stabilize" defects in the material which can cause quenches at reduced gradients [3]. The production of high-purity, fine-grain Nb sheets requires many elaborate steps during which foreign metallic impurities can be embedded in the material and therefore requiring time-consuming quality control of the sheets [4]. The cost of high-purity, fine-grain Nb sheets is significant and exceeds ~600 $/kg. The production of ingot Nb discs is comparatively much simpler and therefore lower cost is to be expected. Whereas SRF cavities for high-energy particle colliders need to operate at gradients corresponding to B_p-values greater than ~100 mT, SRF cavities for continuous wave (CW) accelerators require operation at 70-80 mT but with high (> $\sim1\times10^{10}$ at 2 K) quality factor. The purity of the Nb material is a parameter which affects cost, quench field and surface resistance. In this contribution, we present the results of RF tests of 1.3-1.5 GHz single-cell cavities made of ingot Nb material with RRR in the range 60-150 to evaluate whether an "optimum" RRR from the cost-performance point of view can be found for CW accelerator cavities. The treatment processes included buffered chemical polishing (BCP), electropolishing (EP), centrifugal barrel polishing (CBP), annealing in vacuum (HT), low-temperature baking (LTB) and HF rinse (HF). The mechanical properties of medium-purity ingot Nb cavities have been recently evaluated and the yield pressure was found to be higher than that of high-purity, fine-grain Nb cavities [5].

CAVITY MATERIAL

Table 1 summarizes the cavities, material supplier and RRR used for this study. 1.3 GHz cavities are of the TESLA center-cell shape [6], whereas the 1.5 GHz cavities are of the original CEBAF shape [7]. The RRR was calculated from the resistance of $1 \times 1 \times 30$ mm^3 samples, measured with the standard four-probe method with an estimated error of 10%. The RRR calculated from the thermal conductivity at 4 K measured on another set of samples from ingots F, G, H was 126, 144 and 93, respectively.

Table 1: Cavity label, frequency, material supplier and average RRR values from 4-probe method and thermal conductivity at 4 K.

Cavity Label	Freq. (MHz)	Nb supplier /Ingot label	RRR
LG-RG	1.5	Tokyo Denkai	140 ± 10
F1F2	1.3	CBMM/F	118 ± 11
F5F6	1.5	CBMM/F	118 ± 11
G1G2	1.5	CBMM/G	125 ± 20
H1H2	1.5	CBMM/H	100 ± 10
H3H4	1.5	CBMM/H	100 ± 10
TC1N1	1.3	OTIC	60 ± 6
OCC1N2	1.5	OTIC	60 ± 6

* This manuscript has been authored by Jefferson Science Associates, LLC under U.S. DOE Contract No. DE-AC05-06OR23177. The U.S. Government retains a non-exclusive, paid-up, irrevocable, world-wide license to publish or reproduce this manuscript for U.S. Government purposes.
#gciovati@jlab.org

ISBN 978-3-95450-178-6

OBSERVATION OF HIGH FIELD Q-SLOPE IN 3 GHz Nb CAVITIES*

G. Eremeev†, F. Hannon
Thomas Jefferson National Accelerator Facility, Newport News, VA 23606, U.S.A.

Abstract

A degradation of the unloaded quality factor is commonly observed above about 100 mT in elliptical niobium cavities. The cause of this degradation has not been fully understood yet, but the empirically found solution of heating to about 100-120 °C for 24-48 hrs. eliminates the degradation in electropolished fine grain or large grain niobium cavities. While numerous experiments related to this phenomenon have been done at 1.3 GHz and 1.5 GHz, little data exists at other frequencies, and the frequency dependence of this degradation is not clear. We have measured the unloaded quality factor of 3 GHz fine grain niobium cavities, which were chemically polished as the final treatment before RF tests in a vertical Dewar and observed the characteristic degradation in two cavities. The measurement of the quality factor degradation at different bath temperatures points to a field-dependent rather than a temperature-related effect.

INTRODUCTION

As a part of new material development, several 3 GHz single cell cavities were built out of niobium to serve as a substrate for future new material coatings. The cavities received the standard modern cavity processing and were measured at T_{bath} = 2.0 K to confirm their suitability as a substrate. Two of the cavities reached fields significantly higher than we anticipated and were limited by a Q-slope reminiscent of the high field Q-slope.

The high field Q-slope was identified in the 1990s [1], when advances with high pressure rinsing allowed for a field emission free cavities reaching to above B_{peak} = 100 mT. At this field a strong degradation in the quality factor was consistently observed in many cavities. Further experiments with temperature mapping indicated broad heating in the high magnetic field regions. Significant effort has been spent in the 2000s to understand the phenomenon and several dissertation were written on the topic [2, 3, 4, 5, 6]. Also, in the late 1990s - early 2000s an empirical solution was found to avoid the degradation: electropolishing followed by 120 °C baking for 48 hours [7, 8]. The solution allowed for high gradient niobium cavities and is used today as a standard treatment.

The 2000s were dominated by oxygen pollution hypothesis as the explanation for the high field Q-slope [9, 10]. Oxygen pollution layer in the RF penetration layer was postulated, and interstitial oxygen was known to degrade superconducting properties of niobium [11]. While the presence and the role of oxygen at the interface is still not completely elucidated, ample evidence eliminate the oxygen pollution layer as a sole culprit behind the Q-drop. With oxygen out of the picture, hydrogen filled the void.

High concentration hydrogen has been known to degrade the quality factor of superconducting cavities due to formation of Nb-H at low temperature [12]. Due to high mobility of hydrogen, it was assumed that hydrogen cannot be involved with mild baking effect, but present models involving hydrogen-crystal defects speculate that Nb-H systems are the cause of the high field Q-slope [13, 14]. Recently, material surface studies have provided some support for the hypothesis [15], but most questions regarding the phenomenon remain standing: why the difference between electropolishing and buffered chemical polishing, why anodizing removes benefit, why the grain size matters, etc.

One of the questions is the frequency dependance of the degradation. Since most of the data related to the degradation were collected at 1.3 or 1.5 GHz, models are required to predict what happens when one goes up or down in frequency. A couple of papers addressed the topic using the data sets available at the time [16, 17]. Our measurements reported here contribute to the data set on the frequency dependence of the high field Q-slope.

RF RESULTS

The half cells were stamped from 3mm RRR niobium sheet, mechanically polished, and electron beam welded together to form 3 GHz cavity. The cavity received 80 μm of bench chemical polishing BCP(1:1:1). After bulk chemistry the cavities were annealed in a vacuum furnace at 600 °C for 10 hours. After annealing, the cavities were chemically polished with BCP (1:1:1) solution for 10 μm, high pressure rinsed, assembled for cold RF test, and tested in the dewar. All three cavities were tested at 2.0 K to check their suitability for subsequent new material development. FH3C was also tested at 1.8 and 1.6 K while still in the dewar. FH3D was removed from the dewar after 2.0 K, baked "in-situ" at 120 °C for 48 hours, and tested again at 2.0 K.

FH3A had a low field $Q_0 = 6{\cdot}10^9$ and was limited by quench at about 13 MV/m. The cavity Q_0 curve also exhibits a strong slope starting from very low gradient, Fig. 1.

*Authored by Jefferson Science Associates, LLC under U.S. DOE Contract No. DE-AC05-06OR23177. The U.S. Government retains a non-exclusive, paid-up, irrevocable, world-wide license to publish or reproduce this manuscript for U.S. Government purposes.

† grigory@jlab.org

SUPERCONDUCTING CAVITY FOR THE MEASUREMENTS OF FREQUENCY, TEMPERATURE, RF FIELD DEPENDENCE OF THE SURFACE RESISTANCE*

HyeKyoung Park[1,2#], S.U. De Silva[1], J.R. Delayen[1]
[1] Center for Accelerator Science, ODU, Norfolk, VA 23529, USA
[2] Thomas Jefferson National Accelerator Facility, Newport News VA 23606, USA

Abstract

In order to better understand the contributions of the various physical processes to the surface resistance of superconductors, the Old Dominion University (ODU) Center for Accelerator Science (CAS) is developing a half-wave resonator capable of operating between 325 MHz and 1.3 GHz. This will allow the measurement of the temperature and RF field dependence of the surface resistance on the same surface over the range of frequency of interest for particle accelerators and identify the various sources of power dissipation.

MOTIVATION AND RESEARCH OBJECTIVES

The surface resistance is the fundamental source of power dissipation. Yet, we do not have a complete understanding of the loss mechanisms. For a low field region the Bardeen-Cooper-Schrieffer (BCS) theory provides the determining factors such as critical temperature (T), frequency (ω), and material properties of penetration depth (λ), energy gap (Δ), coherence length which expressed as following [1]:

$$R_{BCS} \cong \frac{\mu_0^2 \omega^2 \lambda^3 \sigma_n \Delta}{k_B T} \ln\left[\frac{c_1 k_B T}{\hbar \omega}\right] \exp\left[-\frac{\Delta}{k_B T}\right].$$

Here μ_0, k_B, $\hbar$ are permeability in free space, the Boltzmann constant, and the Planck constant respectively.

The test results of actual cavities show that there is a temperature independent residual resistance (R_{res}), which remains unexplained. Several contributions (e.g.; trapped vortices, metallic suboxides or hydrides, grain boundaries, etc [1]) to the residual resistance have been studied. They all seem to contribute to the loss but largely on a case by case basis. So far the residual resistance tends to be treated as a material defect rather than a fundamental intrinsic phenomenon.

One of the basic limitations of all the experimental work to-date is that the tests have been performed on each cavity or surface at a single frequency. To vary the frequency, different cavities were built and tested. Even with careful control, fabrication techniques do not guarantee identical, repeatable surfaces. This variation adds difficulty when attempting to extract accurate frequency dependence. Even when the same cavity was measured at different frequencies in different modes, typically elliptical cavities where the frequencies were relatively close, the surface magnetic and electric field distributions were quite different in the various modes. To be able to systematically study the frequency dependence, the cavity should provide the identical surface and the same field distribution. This requires a multi-mode cavity. A simple geometry that would fulfill those requirements is a cylindrical coaxial resonator [2] shown in Fig. 1.

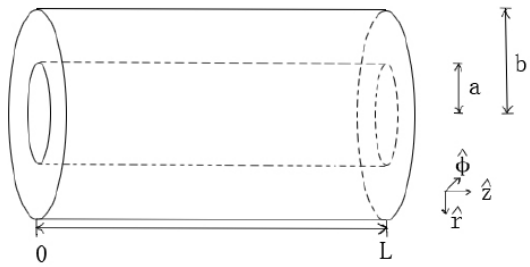

Figure 1: Coaxial half wave resonator.

ODU CAS optimized and fabricated such a cavity and are ready to carry out the experiments to see the frequency, field, temperature dependence of the surface resistance.

ELECTROMAGNETIC DESIGN

Cavity Parameters

Besides the usual TE and TM modes in cylindrical resonators, a coaxial resonator has a series of TEM modes where the high surface magnetic field is concentrated on the inner cylinder with the same sinusoidal profile (although of different wavelength).

Its simple geometry allows analytical solutions of Maxwell's equations [3] as follows.

$$\boldsymbol{E}_T = \hat{r}\frac{V_0}{\ln\left(\frac{b}{a}\right)}\frac{1}{r}\sin\left(\frac{n\pi z}{L}\right)e^{-i\left(\omega t-\frac{\pi}{2}\right)}$$

$$\boldsymbol{H}_T = \hat{\varphi}\,\frac{V_0}{\ln\left(\frac{b}{a}\right)}\frac{1}{r}\sqrt{\frac{\varepsilon_0}{\mu_0}}\cos\left(\frac{n\pi z}{L}\right)e^{-i\omega t}$$

where V_0 is the peak voltage at the inner conductor and ω is the RF frequency.

*Research supported by NSF Award PHY-1416051.
#hkpark@jlab.org

UNDERSTANDING THE FIELD DEPENDENCE OF SURFACE RESISTANCE IN NITROGEN-DOPED CAVITIES *

P. N. Koufalis†, D. Gonnella, M. Liepe, J. T. Maniscalco, I. Packtor
CLASSE, Cornell University, Ithaca, NY 14853

Abstract

An important limiting factor in the performance of superconducting radio frequency (SRF) cavities in medium and high field gradients is the intrinsic quality factor and, thus, the surface resistance of the cavity [1]. The exact dependence of the surface resistance on the magnitude of the RF field is not well understood. We present an analysis of experimental data of LT1-3 and LT1-4, 1.3 GHz single-cell nitrogen-doped cavities prepared and tested at Cornell [2]. Most interestingly, the cavities display anti-Q slopes in the medium field region (i.e. R_s decreases with increasing accelerating field). We extract the temperature dependent surface resistances of the cavities, analyze field dependencies, and compare with theoretical predictions. These comparisons and analyses provide new insights into the field dependence of the surface resistance and improve our understanding of the mechanisms behind this effect.

CAVITY PREPARATION

Two single-cell, 1.3 GHz, TESLA-shaped cavities (LT1-3 and LT1-4) were nitrogen-doped using the following preparation methods inspired by [3].

1. 150 μm vertical electropolish (VEP)
2. 800 °C bake
   (a) 3 hours in vacuum
   (b) 20 minutes in 60 mTorr of N_2 gas
   (c) 30 minutes in vacuum
3. LT1-3 received a 12 μm VEP
4. LT1-4 received a 24 μm VEP

After preparation, the cavities were RF tested vertically in cw mode. The quality factor, Q_0, was measured at various temperatures and accelerating fields. The surface resistance, R_s, was then calculated from the Q_0 data. The temperature dependent part of the surface resistance, R_{BCS}, was then extracted from the R_s values. Figure 1 summarizes the R_{BCS} data obtained from measurements.

DATA ANALYSIS AND MODELING

We begin our analysis of the data using an approximate model describing the relation between the the Bardeen-Cooper-Schrieffer resistance, R_{BCS}, temperature, T, and two model parameters.

$$R_{BCS} = \frac{A}{T} e^{-\epsilon/k_B T} \tag{1}$$

The pre-exponential factor, A, and the effective energy gap, ϵ, are the model parameters which in general are assumed to be functions of E_{acc}. Letting both parameters vary simultaneously with the accelerating field resulted in a sloppy fit of the data. Because of this, we let only one parameter vary while holding the other fixed. In this way, we were able to independently extract the field dependence of each model parameter. Naturally, this leads to two possibilities, summarized in Eqs. 2 and 3:

$$R_{BCS}(E_{acc}) = \frac{A(E_{acc})}{T} e^{-\epsilon/k_B T} \tag{2}$$

$$R_{BCS}(E_{acc}) = \frac{A}{T} e^{-\epsilon(E_{acc})/k_B T} \tag{3}$$

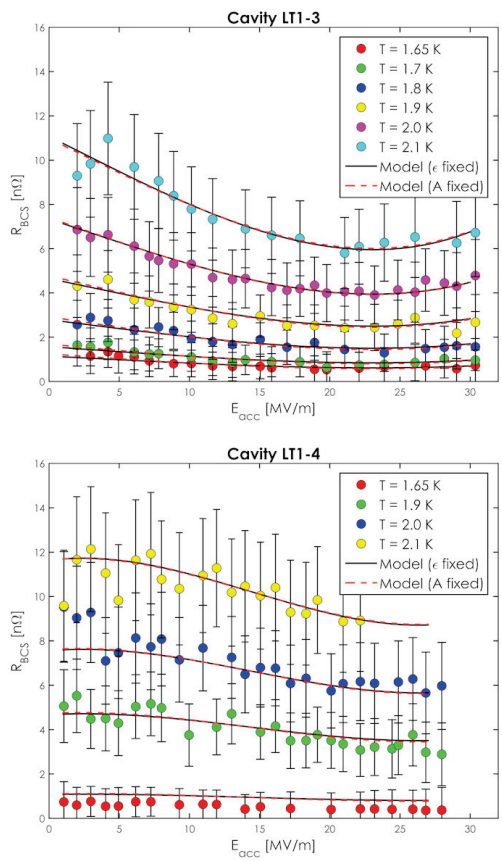

Figure 1: R_{BCS} vs. E_{acc} at various temperatures with both models from Eq. 2 and 3 plotted against the measurement data.

* Work supported by NSF grant PHYS-1416318
† pnk9@cornell.edu

DEVELOPING A SETUP TO MEASURE FIELD DEPENDENCE OF BCS SURFACE RESISTANCE*

J. T. Maniscalco† and M. Liepe
CLASSE, Cornell University, Ithaca, NY, 14853, USA

Abstract

The temperature-dependent part of the microwave surface resistance of superconducting radio-frequency (SRF) cavities has been shown experimentally to depend on the strength of the applied magnetic surface field. Several theories have recently been proposed to describe this phenomenon. In this paper we present work on the development of a microwave cavity setup for measuring the field-dependence with an applied DC magnetic field.

INTRODUCTION

The Bardeen-Cooper-Schreiffer (BCS) theory of superconductivity shows that the surface resistance R_S of superconductors in radio-frequency (RF) fields exhibits a strong dependence on temperature [1]. Experimental results have shown that this temperature-dependent component also depends on the strength of the magnetic field on the surface [2, 3]. In particular, this has been observed especially for niobium surfaces with small mean free path ℓ on the order of the coherence length ξ of clean niobium.

Several theories have been proposed to explain this field dependence with adjustments to the density of states of Cooper pair electrons in the RF-exposed superconducting surface [4, 5]. Cornell is developing a new cavity to study this field dependence and test these theories.

The motivation of the design of this new cavity was the desired ability to measure the BCS surface resistance as a function of the strength of an applied DC magnetic field on the RF surface. To probe this phenomenon effectively, it is necessary to have a fairly uniform DC field in the area dominating RF losses, so that the effects of the desired DC field can be isolated from losses on the surface where DC field strength may be higher or lower. In addition, we sought the ability to measure R_{BCS} as a function of the RF field, at least up to medium-field values. Finally, we wanted to use a high-frequency design in order to facilitate construction and testing.

The initial design phase of this cavity has now been completed. Details on this design process, outcomes of simulations, and future plans and expectations are outlined below.

CAVITY DESIGN

As previously mentioned, the main design goal of this new cavity was to establish a large area of homogenous DC magnetic field along the inner surface of the cavity in the peak RF magnetic field region. This was achieved by using a pillbox-like cylindrical design for the central "body" section of the cavity, connected to the beam tubes by a conical "loft" section, with the DC field generated by an external electromagnet. Because of the Meissner effect, any magnetic flux that enters the cavity through one beam tube must exit through the other beam tube. This flux expands uniformly to fill the body of the cavity, projecting the desired uniform field along the central cylinder. Due to this expansion/compression, the field is stronger on the inner surface of the beam tube than on the body surface; we sought to design the cavity in such a way that the strength of the RF field in this region was highly attenuated to limit the impact of the beam tubes on the measurements of surface resistance, which will be performed with RF-off Q_0 measurements.

After preliminary pen-and-paper sketching, we performed initial modeling and refinement of the cavity design in CST's Microwave Studio (MWS) simulation software, seeking to define a 6 GHz fundamental TM mode with high quality factor and high attenuation of the RF field in the beam tubes.

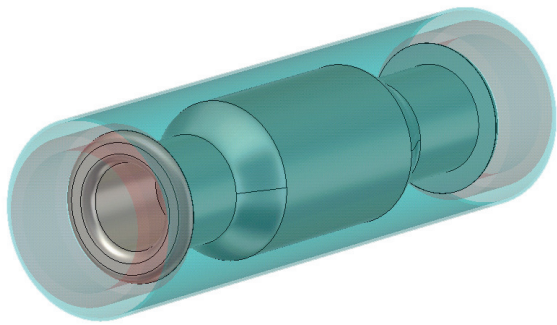

Figure 1: A CAD depiction of the field dependence cavity, shown with dressing. The magnetic shielding is shown in transparent blue, and the twin solenoids are shown in transparent red.

Table 1: Field-Dependence Cavity Parameters

Parameter	Value
Frequency	6.06 GHz
Geometry factor G	396 Ω
Quality factor Q_0	1.29×10^{10}
$B_{\mathrm{solenoid}}/B_{\mathrm{surface\ DC}}$	6.5
RF mode	TM_{010}
Total cavity length	141 mm
Cavity body radius	39 mm

* This work was supported by the NSF grant PHYS-1416318.
† jtm288@cornell.edu

ISBN 978-3-95450-178-6

H_{C2} MEASUREMENTS OF SUPERCONDUCTORS*

J. T. Maniscalco†, D. Gonnella, D. L. Hall, M. Liepe, and E. Smith
CLASSE, Cornell University, Ithaca, NY, 14853, USA

Abstract

Recently, Cornell has improved a method for extracting the upper critical field H_{c2} of a thin-film superconductor using four-point resistivity measurements. In the field of superconducting radio-frequency accelerators (SRF), novel materials and processes such as nitrogen-doped niobium and Nb_3Sn may allow for improved SRF performance and cost efficiency over traditional niobium. In this paper we present updated results on H_{c2} measurements for Nb_3Sn, as well as results for niobium prepared with an 800° C bake. We also extract important material properties from these measurements, such as the Ginzburg Landau parameter, the mean free path, and coherence length, which are critical for determining SRF performance.

INTRODUCTION

When considering the utility of alternative materials for use in constructing SRF cavities, several figures of merit exist including the mean free path ℓ, the coherence length ξ, and the Ginzburg-Landau parameter κ which can help gauge the performance of candidate materials against each other. These are related to and can be derived from the upper critical field H_{c2} of the material. Since H_{c2} can only be observed directly at a temperature of 0 K, it must be found through extrapolation. Cornell has developed a method to find H_{c2} of SRF materials, from which the aforementioned parameters can be derived [1]. The method uses a Physical Property Measurement System (PPMS), a device which allows for resistivity measurements at precisely controlled temperatures, magnetic fields, and excitation currents.

APPARATUS AND METHOD

For measurement of SRF materials, a sample up to 1 cm × 1 cm and several millimeters thick is placed on a sample puck (Fig. 1). Four spring-loaded press contacts are applied to the surface, and the assembly is inserted into and sealed inside the cryostat of the PPMS. The four contacts are used in a four-point resistivity configuration.

For a given measurement, the strength of the magnetic field applied by the solenoid and the excitation current for the resistivity measurements are both fixed, and the temperature is swept across the superconducting transition region for the given field and current. We perform resistivity measurements at 0.1 K intervals along the sweep. The result of each

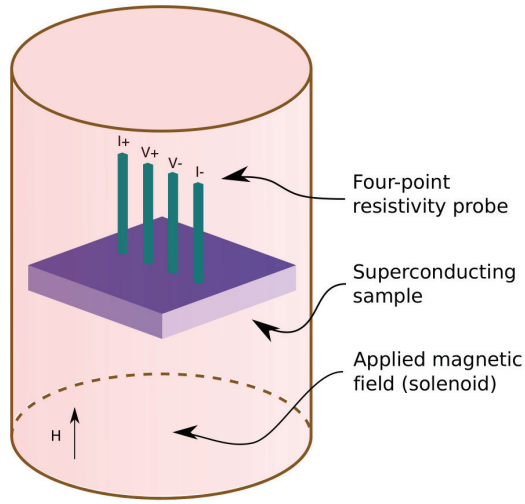

Figure 1: A schematic of a material sample loaded inside the PPMS with four-point resistivity probes attached.

sweep is a characteristic "cliff" graph (Fig. 2). From this, we perform a piecewise linear fit to extract the transition temperature with a 50% resistivity criteria. Uncertainty on $T_c(H,I)$ is taken as the width of the transition region (the steeply ascending central part of the "cliff" shape).

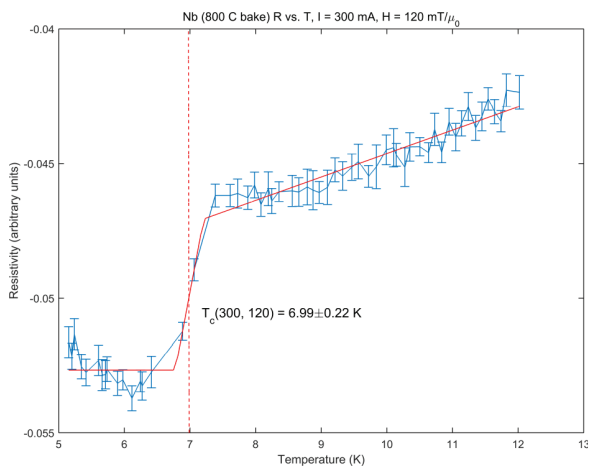

Figure 2: Resistivity measurements at varied temperatures with fixed magnetic field and excitation current. The superconducting transition temperature, $T_c(H,I)$ is chosen with a 50% resistivity criteria.

This temperature sweep is performed at a range of field strengths and excitation currents. Typically, we use the excitation currents 100 mA, 300 mA, and 500 mA. We perform

* This work was supported in part by the NSF grant PHYS-1416318 and by the DOE grant DE-SC0008431. This work made use of the Cornell Center for Materials Research Shared Facilities which are supported through the NSF MRSEC program (DMR-1120296).
† jtm288@cornell.edu

ISBN 978-3-95450-178-6

TEMPERATURE EXCURSIONS IN Nb SHEETS WITH IMBEDDED DELAMINATION CRACKS

Peng Xu, Neil T. Wright, MSU, East Lansing, MI, 48824, USA
Chris Compton, FRIB, East Lansing, MI, 48824, USA
Thomas R. Bieler, Michigan State University, East Lansing, MI, 48824, USA

Abstract

Delamination cracks can form in rolled Nb sheets, and between layers with different micro-structures. Such cracks cause resistance to heat conduction from the RF surface to the liquid He bath. A delamination crack can negate the advances in manufacturing processes that have enhanced the thermal conductivity of Nb. Here, temperature excesses are calculated as functions of crack size and location, and the power dissipated at an imperfection in the RF surface. A disk shape of Nb sheet is modeled as having adiabatic sides. A hemispherical defect is located on the RF surface at the center of this section. A crack is modeled as a void within the Nb disk. The Kapitza resistance between the Nb surface and liquid He is varied. The results indicate that an incipient crack leads to a decrease in the magnetic flux required to cause thermal breakdown. The decrease in the field is gradual with increasing crack radius, until the crack radius nearly equals the section radius, after which the field required for breakdown decreases sharply. To a lesser extent, the field strength for thermal breakdown also decreases with increased crack depth.

INTRODUCTION

Maintaining super-conducting state is crucial for SRF applications. Thermal breakdown of a superconducting radio frequency (SRF) cavity occurs when the rf surface temperature reaches its critical temperature [1]. Recent progresses in Nb cavities for particle accelerators has resulted in significant increase in thermal breakdown field up to 180~200 mT, which is close to the thermodynamic critical field (200 mT) [2, 3]. However, imperfections such as defects or dislocations can cause to a sharp decrease of thermal breakdown field [4]. Delamination cracks might also be a factor to decrease the field because of its resistance to heat conduction between the rf surface and liquid He bath. Recent studies at FRIB of MSU [5] shows that after EB spot welding, a crack in the 2 mm Nb sheet of the outer conductor was discovered. The crack is approximately in the middle of the sheet, splitting the sheet in two parts and propagating around 25 mm along the circumference, the depth of crack cannot be determined. Fig.1 and Fig. 2 are the picture and microscopic image of the delaminating crack, respectively. It is essential to study the influence of crack on thermal breakdown field and surface temperature of Nb.

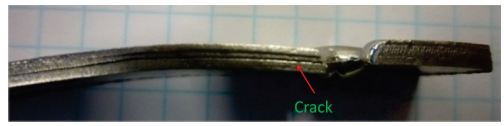

Figure 1: Picture of the delamination crack.

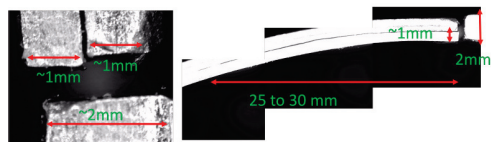

Figure 2: Microscopic image of the delamination crack.

MODELING

While a one dimensional thermal resistance network model might be used, a two dimensional transient heat transfer problem considering edge effects, crack effects, and temperature dependent thermal conductivity coupled with surface-surface radiation is modeled using multi-physics COMSOL. Fig.3 shows the geometry of the model, where r_c and r_{Nb} are the radius of the crack and Nb, respectively. h is the crack thickness and r_d is the radius of the defect. A finite cylindrical Nb disk with thickness d and radius r bounded by liquid helium on the lower surface and by a uniform rf magnetic field H on the top surface is modeled.

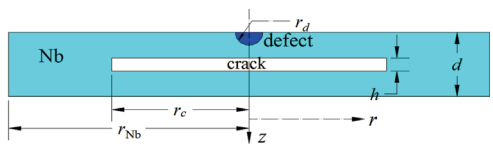

Figure 3: Geometry of the heat transfer model.

The governing equation of this model can be written as:

$$\frac{\partial^2 T}{\partial r^2} + \frac{1}{r}\frac{\partial T}{\partial r} + \frac{\partial^2 T}{\partial z^2} = \frac{1}{\alpha(T)}\frac{\partial T}{\partial t} \qquad (1)$$

where $\alpha(T)$ is the thermal diffusivity of Nb and is defined as $\alpha(T) = k(T)/(\rho C)$, $k(T)$ is the temperature dependent thermal conductivity, shown in Fig. 4. C is the heat capacity and ρ is the mass density.

Initial and Boundary Conditions

Initial temperature of Nb can be set to any temperature below 9.25 K (critical temperature of Nb), here T_0 is chosen to be the liquid He temperature (1.6 K). T_0 is the temperature when time is 0.

ISBN 978-3-95450-178-6

THEORETICAL FIELD LIMIT AND CAVITY SURFACE CONDITIONS: NANO-SCALE TOPOGRAPHY AND SUB-MILLIMETER PIT*

Takayuki Kubo†
KEK, High Energy Accelerator Research Organization, Tsukuba, Ibaraki, Japan

Abstract

The recent two theoretical papers [1] and [2] are briefly introduced. The former [1] addresses the superheating field (B_s) suppression due to nano-defects distributing almost continuously on the cavity surface. We introduce a model of the nano-defect. An analytical formula for B_s suppression factor is derived in the framework of the London theory. By using the formula, suppression factors of bulk or multilayer superconductors and those after various surface processing technologies can be evaluated. The latter [2] addresses the magnetic field enhancement (MFE) at the sub-millimeter pit on the surface of cavity, which is thought to cause quench. There exists the famous well-type pit model, but many of pits are not well-type but have gentle slopes. Impacts of the slope angle on MFE have not been well understood. We introduce a model that can describe a pit with an arbitrary slope angle. A formula to evaluate the MFE factor is derived. A pit with a gentle slope angle yields a much smaller MFE factor than the well-type pit. The formula can be applied to the calculation of MFE factors of real pits with arbitrary slope angles.

INTRODUCTION

The fundamental limit of the peak magnetic-field $B_{\rm pk}$ of the superconducting (SC) radio-frequency (RF) cavity is thought to be imposed by the superheating field, B_s, at which the Bean-Livingston barrier for penetration of vortices disappears. According to studies on surface topographies of SCRF materials, nano-scale defects almost continuously exists and distribute with a much higher density than micrometer or sub-millimeter scale defects. B_s is reduced at each nano-defect, and thus the limit of $B_{\rm pk}$ of a real cavity would be imposed not by B_s but by an effective superheating field $\widetilde{B}_s = \eta B_s$, where η is a suppression factor that contains effects of nano-defects. Ref. [1] studies the field limit of SCRF cavity made of a type II SC with a large GL parameter, taking effects of nano-defects into account. An analytical formula for η is derived in the framework of the London theory. Its results can be applied not only to a bulk SC but also to a multilayer SC [4]. The half of the present contribution is devoted to introducing results of Ref. [1].

Actually, rather macroscopic defects, such as pits associated with cavity fabrication processes, which cause the thermal magnetic breakdown, is (will be) the major obstacle to achieving a high $B_{\rm pk}$ by the present Nb cavity (future cavities made from alternative materials). The magnetic-field enhancement (MFE) effect is the key to understand the thermal magnetic breakdown at a pit. The surface magnetic-field in the vicinity of a pit is generally written as $H(\mathbf{r}) = \beta(\mathbf{r})H_0$ with $0 \le \beta(\mathbf{r}) \le \beta_{\rm M}$, where $\mathbf{r}$ is a position, H_0 is the surface magnetic-field far from the pit, and $\beta(\mathbf{r})$ is a coefficient introduced to reflect an effect of a pit geometry. $\beta(\mathbf{r})$ reaches its maximum value, $\beta_{\rm M}$, at an edge of a pit. If the enhanced field, $\beta_{\rm M}H_0$, is large enough, the edge becomes normal conducting due to thermal and magnetic effects, which triggers a thermal runaway. A difference of edge shape affects the $\beta_{\rm M}$-factor and thus the breakdown field. To reveal the relation between the $\beta_{\rm M}$-factor and the geometry of pit is the first step to understand the quench due to a pit. While many of pits found on cavity surfaces are not well-type but have gentle slopes, pits with general slope angles had not been studied. Impacts of the slope angle on the $\beta_{\rm M}$-factor had not been well understood. Ref. [2] studies the model of pit that can describe a pit with arbitrary slope angle, edge radius, and pit width. A formula to evaluate the MFE factor is derived. A pit with a gentle slope angle yields a much smaller MFE factor than the well-type pit model. Application of the formula to evaluations of MFE factors of real pits is also shown. In the last half of this contribution, the results of Ref. [2] are introduced.

NANO-DEFECTS AND SUPERHEATING FIELD SUPPRESSIONS

In this section, results of Reference [1] are briefly introduced.

A nano-defect is modeled by a groove with a depth smaller than the penetration depth (see Fig. 1). The surface of SC is parallel to the xz plane. The groove and the applied magnetic-field are parallel to the z-axis. The geometry of the groove is specified by the depth, δ, and the angle, $\pi\alpha$ ($1 < \alpha < 2$). The slope angle is then given by $\theta = \pi(\alpha - 1)/2$. The material is a type II SC with a large GL parameter, and its coherence length and penetration depth are given by ξ and λ ($\gg \xi$), respectively. Furthermore, the assumption $\xi \ll \delta$ is necessary for treating the model in the framework of the London theory.

The detailed derivation process of the superheating field suppression factor due to the nano defect is found in

* The work is supported by JSPS Grant-in-Aid for Young Scientists (B) Grant Number 26800157, JSPS Grant-in-Aid for Challenging Exploratory Research Grant Number 26600142, and Photon and Quantum Basic Research Coordinated Development Program from the Ministry of Education, Culture, Sports, Science and Technology, Japan
† kubotaka@post.kek.jp

MODEL OF FLUX TRAPPING IN COOLING DOWN PROCESS*

Takayuki Kubo†
KEK, High Energy Accelerator Research Organization, Tsukuba, Ibaraki, Japan

Abstract

The flux trapping that occurs in the process of cooling down of the superconducting cavity is studied. The critical fields B_{c2} and B_{c1} depend on a position when a material temperature is not uniform. In a region with $T \simeq T_c$, B_{c2} and B_{c1} are strongly suppressed and can be smaller than the ambient magnetic field, B_a. A region with $B_{c2} \leq B_a$ is normal conducting, that with $B_{c1} \leq B_a < B_{c2}$ is in the vortex state, and that with $B_{c1} > B_a$ is in the Meissner state. As a material is cooled down, these three domains including the vortex state domain sweep and pass through the material. In this process, vortices contained in the vortex state domain are trapped by pinning centers distributing in the material. A number of trapped fluxes can be evaluated by using the analogy with the beam-target collision event, where beams and a target correspond to pinning centers and the vortex state domain, respectively. We find a number of trapped fluxes and thus the residual resistance are proportional to the ambient magnetic field and the inverse of the temperature gradient. The obtained formula for the residual resistance is consistent with experimental results. The present model focuses on what happens at the phase transition fronts during a cooling down, reveals why and how the residual resistance depends on the temperature gradient, and naturally explains how the fast cooling works.

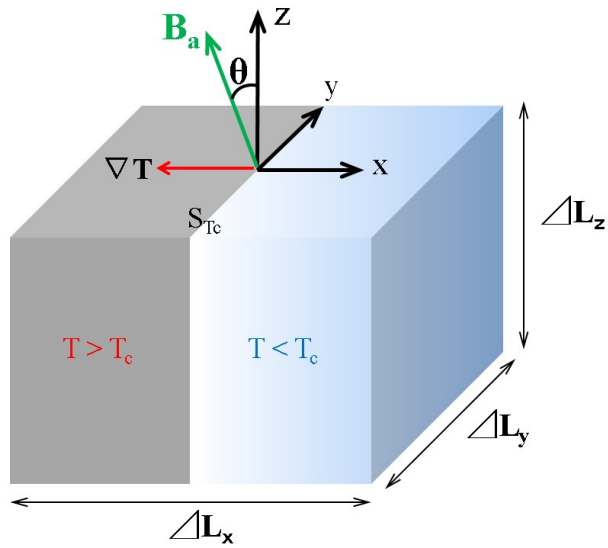

Figure 1: SC material of a cavity wall under cooling down. The gray and blue region represent the domains with $T > T_c$ and $T < T_c$, respectively. The origin of the x-axis is located at the interface of these two regions, which we call S_{T_c}. The SC material is cooled down from the right to the left. The ambient magnetic field $\mathbf{B}_a$ is parallel to the z-x plane, and θ is the angle between $\mathbf{B}_a$ and the z-axis.

INTRODUCTION

The surface resistance of the superconducting (SC) radio frequency (RF) cavity consists of the temperature dependent part and the temperature independent part. The latter is called the residual resistance, $R_{\rm res}$, and limits the quality factor of SCRF cavity at $T \ll T_c$.

Magnetic fluxes trapped in a process of cooling down of a cavity degrade $R_{\rm res}$. Thus decreasing a number of trapped fluxes is necessary for a reduction of $R_{\rm res}$. Recent studies show that cooling down conditions affect a number of trapped fluxes [1, 2, 3, 4]. In particular, researchers in Fermilab found a fast cooling with a larger temperature gradient leads to a better expulsion of fluxes and thus yields a lower residual resistance $R_{\rm res}$ [3, 4]. They achieved an ultra high Q_0 ($\simeq 2 \times 10^{11}$) by the fast cooling method [4].

While many experimental studies on the flux trapping have been conducted, not much theoretical progress followed on it. In the present paper, we theoretically study the flux trapping that occurs in the process of cooling down by focusing on the dynamics in the vicinity of the phase transition fronts. We do not consider effects of the thermal current. We show a number of trapped fluxes and thus $R_{\rm res}$ are proportional to the ambient magnetic field and the inverse of the temperature gradient. The present model reveals why and how the residual resistance depends on the temperature gradient, and naturally explains how the fast cooling works.

MODEL

Let us consider the SC material shown in Figure 1, which represents a part of a cavity wall. The gray and blue regions represent the domains with $T > T_c$ and $T < T_c$, respectively. The origin of the x-axis is located at the interface of these two regions, which we call S_{T_c} in the following. The SC material is cooled down from the right to the left: ∇T is parallel to the negative direction of the x-axis; $dT/dx < 0$ and $dT/dy = dT/dz = 0$. The ambient magnetic field $\mathbf{B}_a$ is parallel to the z-x plane, and θ is the angle between $\mathbf{B}_a$ and the z-axis. Its magnitude $|\mathbf{B}_a|$ is given by B_a.

Let us look at the vicinity of S_{T_c}. Since $T \simeq T_c$ in the vicinity of S_{T_c}, the lower critical field $B_{c1}(T(x))$ and the upper critical field $B_{c2}(T(x))$ are strongly suppressed and can be smaller than the ambient magnetic field B_a (typically

* The work is supported by JSPS Grant-in-Aid for Young Scientists (B) Grant Number 26800157, JSPS Grant-in-Aid for Challenging Exploratory Research Grant Number 26600142, and Photon and Quantum Basic Research Coordinated Development Program from the Ministry of Education, Culture, Sports, Science and Technology, Japan.
† kubotaka@post.kek.jp

FIELD-DEPENDENT SURFACE RESISTANCE FOR SUPERCONDUCTING NIOBIUM ACCELERATING CAVITIES: THE CASE OF N-DOPING

W. Weingarten, visiting fellow at Cornell University*
R. Eichhorn, Cornell Laboratory for Accelerator-Based Sciences and Education, Ithaca, NY, USA

Abstract

The dependence of the Q-value on the RF field (Q-slope) for superconducting RF cavities is actively studied in various accelerator laboratories. Although remedies against this dependence have been found, the physical cause still remains obscure. A rather straightforward two-fluid model description of the Q-slope in the low and high field domains is extended to the case of the experimentally identified increase of the Q-value with the RF field obtained by so-called "N-doping".

INTRODUCTION

So-called "N-doped" niobium superconducting (sc) cavities obtained increased interest, because they hold the promise of large Q-values at technically still useful accelerating gradients. They exhibit an increase of the Q-value below 2.1-2.5 K with the RF magnetic surface field B (negative Q-slope) up to about 60-80 mT, equivalent to 15-20 MV/m accelerating gradient. This observation was repeatedly observed in different laboratories [1, 2, 3]. A typical data set is shown in Fig. 1.

It shows the Q-value vs the magnetic surface field B of a 1.3 GHz single cell cavity, made of bulk niobium and fired in a N_2 atmosphere [p=50 mTorr (66 hPa), 800°C, 20 minutes], electro-polished, prepared at FNAL and tested at Cornell at different temperatures (from top to bottom, 1.6, 1.7, 1.8, 1.9, 2.0, 2.1, 2.5, 3.0 and 4.2 K) [4]. For an accelerating gradient of 10 MV/m the surface magnetic field B amounts to 42 mT. The continuous lines result from the fit to the data with Q=270.7 Ω/R_s, with R_s described by eq. 4. The maximum gradient was limited by a quench.

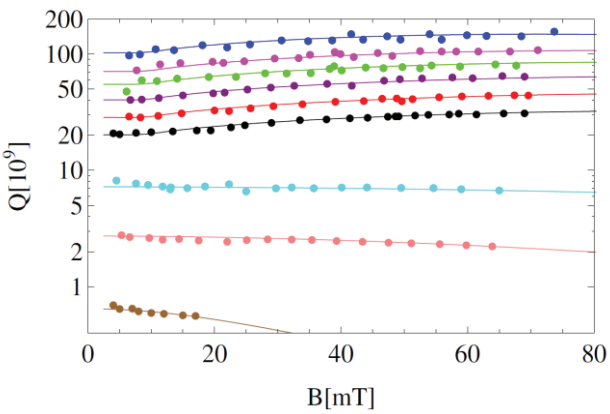

Figure 1: Q vs. B curve of 1.3 GHz N-doped cavity.

Accelerating cavities treated by N-doping are not free from the previously observed decrease of the Q-value with the RF magnetic field (Q-slope and Q-drop). These observations were described in several models [5, 6, 7, 8], but a unanimously accepted explanation is missing. Recipes to improve cavity performance were nevertheless found [5]. The present paper presents a data analysis of the experimental results as of Fig. 1 and presents a common description of the observed Q-increase and Q-decrease.

Our paper is organized as such. In a first step we present the model as of ref. 6 for weak sc defects at the surface caused by oxygen. Then we extend the model for similar defects in the bulk made up of nitrogen. Secondly, by a zero level analysis, we identify the important variables describing the data (Table 1). "Zero level" alludes to using Microsoft EXCEL® as fitting tool. We then use the MATHEMATICA® software for fitting the data related to the N-doped cavity of Fig. 1, discuss the results, and draw a conclusion.

DESCRIPTION OF MODEL

RF Magnetic Field Dependence of Weak SC Defects

Our analysis is based on the two-fluid model of RF superconductivity with emphasis on the electrical conductivity of the nc component of the superconductor.

For a **weak sc defect located at the surface**, we apply the model as outlined in ref. 6, however no longer for the specific case of an Nb/NbO composite but instead for an Nb/NbN composite. This model states that the surface layer is non-uniform in terms of having defects being only weak superconductors. The defect has mesoscopic size, embedded in the sc "host" metal of high purity and in close contact with this. The weak sc defect would be nc if not in the vicinity of a sc host metal. The defect is supposed to have sc properties induced from, and weaker than, the sc "host" metal Nb (Cooper pairs, characteristic coherence length ξ_N, lower critical field B_c* and lower critical temperature than the sc host metal). The defect also induces normal-conducting (nc) charge carriers into the otherwise sc host metal. All these features are typical of the sc proximity-effect.

The model states the entry of magnetic flux above relatively small magnetic fields and an increase of the Q-slope above the "surface percolation temperature" T*, which is typically in the order of 2.1 K (for an Nb/NbO composite). Energy balance considerations lead to the following results. The magnetic field B_c* for the first entry of magnetic flux at the weak sc defect as nucleation centre,

* wolfgang.weingarten@cern.ch

ISBN 978-3-95450-178-6

HOW UNIFORM ARE COOL-DOWNS?

J. Robbins and R. Eichhorn#
CLASSE Cornell University, Ithaca, NY 14853, USA

Abstract

Since the last SRF conference it has become clear that achieving extremely high quality factors of SRF cavities depends on the cool-down scenario. While some findings favor a fast cool-down, others suggest a slow cycle to be advantageous, and many variations to that have been investigated: the role of thermo-currents, the amount of ambient magnetic field and flux trapping. This paper will investigate how uniform different cool-down procedures are and if they can explain the more efficient magnetic flux expulsion.

INTRODUCTION

In the effort to produce superconducting cavities with higher Q-factors, recent experiments have been conducted to determine how different cavity cool-down processes result in different amounts of trapped magnetic flux [1-3]. Faster cool-downs have been speculated to sweep the magnetic flux out of the cavity more efficiently than slow cool-downs [1]. Furthermore, it seems unclear if this applies only to nitrogen doped cavities and large grain cavities. However, the mechanism for this effect is poorly understood and is the subject of ongoing study.

In an earlier paper, we [3] measured the movement of the transition line of a superconducting cavity using our T-Map system. Results there indicated that a slow cool-down leads to less temperature variations on the surface but gave no answer to the question if this is more likely to generate normal conducting islands that are susceptible to flux trapping.

In practice, the superconducting-normal conducting (SC-NC) interface is never completely uniform during cool-down. Defects in the niobium and thermal fluctuations perturb the SC-NC interface and increase the probability of producing normal-conducting islands, resulting in trapped magnetic flux.

As a factor that determine the uniformity of the cool-down we want to studie the size and number of perturbations to the SC-NC interface and the rate at which those perturbations shrink.

We have run simulations using ANSYS® to determine the relative size and decay time of perturbations applied to the SC-NC interface during cavity cool-down. Understanding the behavior of deviations in the superconducting phase boundary from an ideally moving cold front should help answering the question of how the cool-down rate affects the amount of trapped magnetic flux.

#r.eichhorn@cornell.edu

METHODS

Niobium Parameters

The thermal conductivity values that we used in our simulations were taken from a combination of theoretical models and experimental data. The theoretical model that we used was the thermal conductivity equation given by [4].

$$Ks(T) = \frac{Kes}{Ken}\left(\frac{\rho_{295K}}{L \cdot RRR \cdot T} + aT^2\right)^{-1} + \left(\frac{1}{De^{\frac{\alpha T_c}{T}}T^2} + \frac{1}{B \cdot l \cdot T^3}\right)^{-1}$$

$K_{es}/K_{en}\,(T)$ is the ratio of superconducting to normal-conducting electron contributions to thermal conductivity. Constant parameters are given in Table 1. This model is valid for $T < 5.8\,K$. For temperatures above $5.8\,K$, an experimental data set was used [5].

The specific heat of the niobium cylinder was assumed to follow the Debye model $C_v = \gamma\,T + A\,T^3$. Using experimental data from [6], values for the parameters were calculated as $\gamma = 0.0946\ \frac{J}{kg \cdot K^2}$ and $A = 1.28 \times 10^{-3}\ \frac{J}{kg \cdot K^4}$ (for $T > T_c$) and $\gamma = 0$ and $A = 5.01 \times 10^{-3}\ \frac{J}{kg \cdot K^4}$ for $T < T_c$.

Table 1: Parameters for Theoretical Thermal Conductivity Model, Taken from [4]

Param.	Value	Definition
RRR	400	resid. res. ratio
ρ_{295K}	$14.5 \times 10^{-8}\Omega m$	res. at 295 K
l	$50\ \mu m$	Nb phonon mfp
T_c	$9.2\ K$	Nb critical temp
L	$2.45 \times 10^{-8}\ V^2K^{-2}$	param of Eq. 1
a	$2.30 \times 10^{-5}\ mW^{-1}K^{-1}$	param of Eq. 1
B	$7.0 \times 10^{-3}\ Wm^{-2}K^{-4}$	param of Eq. 1
$1/D$	$300\ m\,K^3W^{-1}$	param of Eq. 1
α	1.76	param of Eq. 1

SIMULATION OF GEOMETRY DEPENDENT FLUX TRAPPING

J. May-Mann, and R. Eichhorn#
Cornell Laboratory for Accelerator-Based Sciences and Education, Ithaca, NY 14853-5001, USA

Abstract

Trapping or expulsion of ambient magnetic field has become an important factor in the performance of superconducting cavities with very high Q. As experimental data is limited, we set up a numerical field calculation model to study this effect in more details.

We will present the results of simulations describing a cavity transitioning from a normal conducting to a superconducting state in a constant magnetic field in either a longitudinal or transverse direction. This will show that the orientation of the field during cool down can affect the amount of magnetic field being vulnerable for trapping.

Our simulations will also explain, how flux trapping, partial trapping or Meissner expulsion will change the field configuration, the field remaining at the RF surface of the cavity and the field strength measureable on the outside of the cavity where usually the fluxgate magnetometers are placed.

INTRODUCTION

Residual magnetic fields, and in particular flux pinning can be a major contribution to surface resistivity of a superconducting cavity [1]. In an a-priory approach there is an easy explanation to this: Since during the transition, magnetic field cannot pass through an already superconducting region, it is possible for magnetic flux to not be expelled and eventually become trapped inside a shrinking normal conducting area in the superconductor.

As this is a purely geometric effect, the orientation of a magnetic field is suspected to be of relevance [2]. In this paper, we investigated this behavior for an ideal as well as an non-ideal superconductor under certain field configurations.

CAVITY TRANSITION SIMULATION

In order to study the configuration of the field during the cavity transition, CST® EM-Studio® was used to gain qualitative features of the transition. For this simulation, the transition of a superconducting cavity is taken to be a sharp normal-conducting/super-conducting boundary moving up cavity corresponding to a moving thermal gradient. This transition was simulated by separating a single cavity into two parts along a plane perpendicular to longitudinal axis of the cavity at varying heights (see Fig. 1). The bottom half was assumed to be a perfect electric conductor (to simulate the superconducting part) and the top half was made into a normal conducting material with no magnetic properties

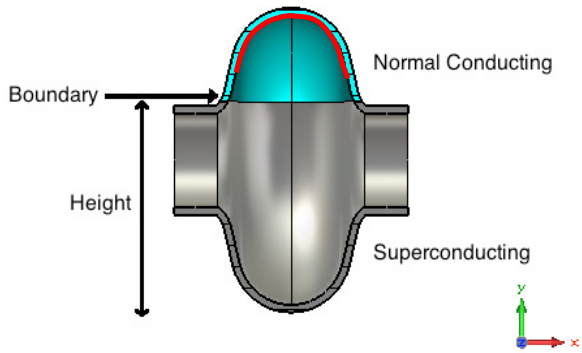

Figure 1: (a) Model of the cavity used for the cavity transition simulations. The red curve depicts the curve on which the magnitude of field will be given in the figures below.

(ensured by applying a μ-value of 1). This assumption would represent an ideal superconductor with perfect Meissner flux expulsion. A constant magnetic field with a magnitude of 1.26 μT was applied in either the longitudinal (here after referred to as +X) direction or the transverse (here after referred to as +Y) direction (see Fig. 1a).

The cavity itself had an equator diameter of 206.6 mm and wall thickness of 5 mm. Simulations were done with the normal conducting superconducting boundary at heights 28.3 mm, 103.3 mm, 143.3 mm, 178.3 mm, 188.3 mm, and 198.3 mm, measured from the bottom of the cell. At each of these heights, the field magnitude was then calculated along the inner surface at the top of cavity in order to get an understanding about the field level that are subject to trapping (see Fig. 1b).

All simulations were afterwards repeated with the bottom half portion having a μ-value of .05. This was found to correspond to a non-ideal superconductor that traps around half the magnetic field and expelled the other half.

TRANSITION SIMULATION RESULTS

Perfectly Superconducting Bottom Portion

The field configuration (see Fig. 2 and Fig. 3), and the value of the magnetic field along the inner surface of the top of the cavity (see Fig 4. and Fig. 5) are shown for both initial fields in the +X and +Y directions where the bottom portion was assumed to be a perfect superconductor with complete flux expulsion. In examining the results, the focus was primarily on two features:

#reichhorn@cornell.edu

ISBN 978-3-95450-178-6

MAGNETIC FLUX EXPULSION IN HORIZONTALLY COOLED CAVITIES *

M. Martinello†, M. Checchin, FNAL, Batavia, IL 60510, USA and IIT, Chicago, IL 60616, USA
A. Grassellino, A. Romanenko, D.A. Sergatskov, O. Melnychuk, FNAL, Batavia, IL 60510, USA
J. Zasadzinski, IIT, Chicago, IL 60616, USA

Abstract

The cool down details of superconducting accelerating cavities are crucial parameters that have to be optimize in order to obtain very high quality factors. The temperature all around the cavity is monitored during its cool down across the critical temperature, in order to visualize the different dynamics of fast and slow cool-down, which determine considerable difference in terms of magnetic field expulsion and cavity performance. The study is performed placing a single cell 1.3 GHz elliptical cavity perpendicularly to the helium cooling flow, which is representative of how SRF cavities are cooled in an accelerator. Hence, the study involves geometrical considerations regarding the cavity horizontal configuration, underling the different impact of the various magnetic field components on the surface resistance. Experimental data also proves that under established conditions, flux lines are concentrated at the cavity top, in the equatorial region, leading to temperature rise.

INTRODUCTION

During the cool down of a superconducting radio-frequency (SRF) cavity some magnetic flux may be trapped in the cavity walls. This trapped magnetic field causes additional losses, therefore it is important to minimize this contribution for radio-frequency (RF) applications [1].

This is particular significant in case of particle accelerators in continuous wave (CW) that need low dissipated power (high Q-factors) in order to minimize the cryogenic cost during the operation [2].

The trapped flux contribution can be minimized by maintaining large thermal gradient along the cavity surface [3, 4] during its cool down through the critical temperature (T_c). Fast cool downs guarantee large thermal gradients, especially when the starting temperature is much higher than the critical temperature. Slow cool downs with starting temperature close to T_c promotes instead the magnetic flux to be trapped.

In this paper we studied the cool down details of a cavity placed perpendicularly to the helium cooling flow (horizontal cool down) and for the first time a T-map system was used to map the temperature around the cavity during the cooling.

This study reveals that after a slow cool down the heating is more uniformly distributed around the cavity than after a fast cool down. Also, cooling the cavity with magnetic field component orthogonal to the cavity axis leads to a localized heating on top of the cavity equator.

EXPERIMENTAL SET-UP

The cavity used for the study presented in this paper is a single cell 1.3 GHz TESLA type nitrogen doped niobium cavity, the same studied in previous works [4, 5].

For this experiment the cavity was instrumented with: two pairs of Helmontz coils orhtogonally placed to each other, four single-axis Bartington Mag-01H cryogenic fluxgate magnetometers and four Cernox thermometers. The thermometers (orange squares in Fig. 1a) were placed on the cavity equator, in the following positions: bottom, mid, mid-top and top. Two fluxgates magnetometers (green rectangles in Fig. 1a) were installed one perpendicular and one parallel to the cavity axis at the top position, while the others were placed with the same directions of the previous ones but at the mid position.

The cavity was also instrumented with a T-map (Fig. 1b), an advanced diagnostic technique which allows to measure and map the temperature all around the cavity [1]. The FNAL T-map system consist on 570 thermometers installed on 36 boards that are assembled around the cavity every 10 degrees each. Every board counts 16 thermometers. In the experiments discuss in this paper the T-map system is used for two different reason: 1) to detect the temperature all around the cavity during the cavity cooling below its critical temperature and 2) to measure the temperature around the cavity during the RF measurement.

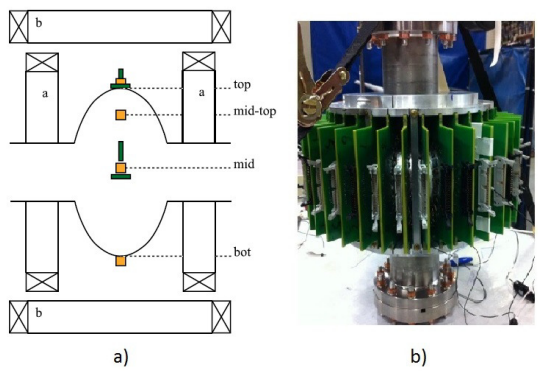

Figure 1: a)Sketch of the cavity instrumentation: four thermometers (orange squares), four fluxgates magnetometers (green rectangles), two pairs of Helmontz coils. b) Picture of the T-map system assembled on the cavity.

* Work supported by the US Department of Energy, Office of High Energy Physics.
† mmartine@fnal.gov

TRAPPED FLUX SURFACE RESISTANCE ANALYSIS FOR DIFFERENT SURFACE TREATMENTS*

M. Martinello†, M. Checchin, FNAL, Batavia, IL 60510, USA and IIT, Chicago, IL 60616, USA
A. Grassellino, O. Melnychuk, S. Posen, A. Romanenko, D. Sergatskov, FNAL, Batavia, IL 60510, USA
J.F. Zasadzinski, IIT, Chicago, IL 60616, USA

Abstract

The trapped flux surface resistance is one of the main contributions on cavity losses which appears when cavities are cooled in presence of external magnetic field. The study is focused on the understanding of the different parameters which determine the trapped flux surface resistance, and how this change as a function of different surface treatments. The study is performed on 1.3 GHz niobium cavities processed with different surface treatments after the 800 °C bake: electro-polishing (EP), 120 °C baking, and N-doping varying the time of the Nitrogen exposure. The trapped flux surface resistance normalized for the trapped magnetic flux is then analyzed as a function of the mean free path in order to find the surface treatment which minimized the trapped flux sensitivity.

INTRODUCTION

When type II superconductors are cooled below their critical temperature the material pass through the mixed stated before stabilizing in the Meissner state. While in the mixed state the magnetic field is free to penetrate the superconductor, in the Meissner state the superconductor behaves as a perfect diamagnet.

During the transition between these two states the Meissner effect guarantees the magnetic flux expulsion from the superconductor. However, whenever defects are present inside the superconductor, magnetic flux may be energetically favorable to stay pinned inside the material, and the Meissner effect would be incomplete [1].

Some studies [2, 3] highlighted the fact that when the cavity is cooled below its critical temperature, the amount of trapped magnetic field depends on the thermal gradients at the transition phase front. Large thermal gradients are usually achieved with fast cooldowns with starting temperature as higher as possible than the critical temperature. On the other hand, the amount of trapped flux increases when the cavity is cooled with slow cooldowns with starting temperature close to the critical one. In particular when the cooldown is done really slow all the external magnetic field is trapped into the cavity walls.

The magnetic field trapped into the superconductor causes additional losses which substantially lower the Q-factor of the accelerating cavity.

This effect becomes particularly important in the case of N-doped cavities since they are more sensitive at the trapped flux compared to non doped cavities [4].

In this paper the trapped flux sensitivity is studied for cavities processed with different surface treatments after the baking at 800 °C: electro-polishing (EP), 120 °C baking, and various N-doping recipes.

The trapped flux sensitivity was found to be dependent on the mean free path l, and experimentally was observed the presence of a maximum of magnetic trapped flux sensibility around $l \simeq 50$ nm.

EXPERIMENTAL SET-UP

All the cavities analyzed are single cell 1.3 GHz Tesla-type niobium cavities. A scheme of the instrumentation of those cavities is shown in Fig. 1. They were instrumented with a pair of Helmholtz coils in order to adjust the magnetic field around the cavity as desired. Four Barlington single axis flux gate magnetometers (green rectangular in the figure) were placed equidistantly around the cavity equator in order to monitor the external magnetic field during the cavity cooldown. In order to supervise the cooldown details the cavity was also equipped with three thermometers (orange squares in the figure), one at the lower iris, one at the equator and one at the upper iris.

Every cavity was measured after both fast ans slow cooldowns:

1. Fast cooldown:
   - Compensating the magnetic field outside the cavity in order to minimize its value during the SC cavity transition
   - With Helmholtz coils switched off making sure that the magnetic expulsion was total
2. Slow cooldown with 10 mG of applied magnetic field

The detailed explanation of such procedures will be explained in the following sections.

All the RF tests performed were conducted at the vertical test facility (VTS) of Fermi National Accelerator Laboratory (FNAL).

ORIGIN OF TRAPPED MAGNETIC FLUX

As mentioned in the introduction, the magnetic flux can be trapped during the normal conducting (NC) - superconducting (SC) transition of the cavity.

* Work supported by the US Department of Energy, Office of High Energy Physics.
† mmartine@fnal.gov

ISBN 978-3-95450-178-6

INTRODUCTION OF PRECISELY CONTROLLED MICROSTRUCTURAL DEFECTS INTO SRF CAVITY NIOBIUM SHEETS AND THEIR IMPACT ON LOCAL SUPERCONDUCTING PROPERTIES*

M. Wang, T.R. Bieler, D. Kang, Michigan State University, East Lansing, MI 48824, USA
C.C. Compton, Facility for Rare Isotope Beams, East Lansing, MI 48824, USA
D. C. Larbalestier, P. J. Lee, A. A. Polyanskii, Z. H. Sung, Applied Superconductivity Center, National High Magnetic Field Laboratory, Tallahassee, FL 32310, USA

Abstract

When SRF (superconducting radio frequency) cavity half cells are formed from niobium sheets, the metallurgical processing introduces microstructural defects such as dislocations and low-angle grain boundaries that may degrade cavity performance. And the density and distribution of these defects may vary with the prior processing of the sheet. To build and understand the relationship between magnetic flux behavior and microstructural defects in SRF niobium we have strategically strained tensile samples cut from an SRF niobium sheet to produce specific types of microstructural defects that could then be examined for their impact on local weakness to magnetic flux penetration using magneto-optical (MO) imaging. Laue X-ray and electron backscatter diffraction (also known as orientation imaging microscopy™, EBSD or OIM) crystallographic analyses of large grain ingot slices were used to characterize microstructural defects in order to enable eventual prediction of which grain and sample orientations will produce defects due to tensile deformation. Grain orientations were chosen to favor specific slip systems, which generate dislocations with particular angles with respect to the sample surface. The generated defect structures were characterized using OIM and transmission electron microscopy (TEM). MO imaging showed, for the first time, preferential flux penetration associated with local regions with high dislocation density.

INTRODUCTION

High purity niobium, with the highest critical temperature of the elemental superconductors, is widely used for superconducting radio frequency (SRF) cavities [1]. As particle accelerators have important applications in several fields, increasing the accelerating electric field and quality factor of cavities have always been pursued. The limit value of maximum accelerating field has been reached, but not in a reproducible way [2, 3]. This variability of cavity performance needs to be minimized to reduce the cost of future instruments.

From the view point of materials science, microstructural evolution during processes, such as rolling, drawing, welding and heat treatment, can generate many possible defects that could account for the some of the inconsistencies in cavity performance. Hence, it is desirable to understand and ultimately control the amount and kinds of microstructural defects in niobium that can interact with the magnetic field in the cavity and degrade cavity performance. The maximum magnetic field occurs in the equator area of elliptical niobium cavities, where "hot spots" (local overheated areas) are often observed during operation of the cavities. The magnetic field is caused by the high superconducting currents going around the equator region along the innermost layer of material (10's of nanometers). Evidence has been found that these "hot spots" originate from trapped magnetic flux within niobium [4]. Local thermal gradients can displace the trapped flux and weaken the "hot spots" [4]. Pinning centers that tend to trap magnetic flux include dislocations and low angle grain boundaries (LAGB) that are introduced during the fabrication of niobium cavities. These defects with magnetic flux pinned around them could lead to the loss of superconductivity in local areas, where the density of superconducting electrons is close to zero [5]. This perturbation for the superconducting currents due to grain boundaries has been observed using cryogenic magneto-optical (MO) imaging [6].

Not only does flux trapping limit the accelerating field, it also generates extra heat that has to be transferred out through liquid helium coolant which needs extra energy to keep it at a low temperature (<9.3K). Although magnetic flux behavior due to microstructural defects is believed to cause problems, few researchers have investigated the mechanism. Flux penetration has been observed when grain boundaries are perpendicular to the surface of the MO sample and parallel to the magnetic field [6]. To discover the mechanisms, it is necessary to investigate correlations between microstructural defects and magnetic flux behavior within niobium.

In this work, high purity SRF niobium tensile samples were strategically deformed in a way similar to that of typical cavity forming processes to introduce dislocations that have specific angles with respect to the sample surface. This is based on the assumption that screw dislocations dominate the microstructure, as commonly observed in BCC metals [7]. The cryogenic MO imaging

*Research supported by DOE/OHEP (contract number DE-FG02-09ER41638 at MSU and DE-SC0009960 at FSU) and the State of Florida.

HORIZONTAL TESTING AND THERMAL CYCLING OF AN N-DOPED TESLA TYPE CAVITY

O. Kugeler, J. Köszegi, J. Knobloch, Helmholtz Zentrum Berlin, Germany
A. Grassellino, O. Melnychuk, A. Romanenko, D. Sergatskov, Fermilab, USA

Abstract

An N-doped TESLA type cavity treated at FERMILAB has been tested in the HoBiCaT horizontal test stand. Temperatures and magnetic fields occurring during the superconducting transition were recorded at various positions and directions on the outer cavity surface. Several thermal cycling runs were performed yielding different Q_0 factors just like in undoped cavities. The resulting residual and BCS resistance values were correlated to the thermal and magnetic conditions during cooldown and compared to values obtained in a vertical test at Fermilab.

INTRODUCTION

In the strife for maximizing Q_0 of superconducting Nb cavities, two technical developments have led to major advances in the past few years: The controlled contamination of the material by N-doping [1] and the optimization of magnetic flux expulsion by thermal cycling [2]. The amount of trapped flux is given by the total amount of ambient flux in the instance of the superconducting transition [3] and the efficiency of the expulsion driven by the Meissner effect [4-6].

The total ambient flux is given by the fraction of the Earth magnetic field that is not removed by the magnetic shielding (typically <1% or <0.5 μT) plus a contribution due to thermal currents [7]. Thermal currents occur when conducting loops of different materials with different Seebeck coefficients (Nb, Ti, NbTi, …) exist in the cavity-tank system and these loops are subject to a superimposed temperature profile.

The efficiency of the Meissner expulsion is correlated to the temperature gradients in the instance of the transition. While in conduction cooled model systems a small gradient leads to better expulsion and reduced trapped flux [8] the opposite is observed in vertical cavity tests, where faster cooling through Tc results in larger quality factors [5]. The dependence of the obtained Q_0 factor on the cooling gradient can even be different for horizontal and vertical tests. In order to extract which observations might be due to systematic influence of the testing environment and which measurements from the cavity by itself, a joint effort has been established to test one particular cavity in different cryostats at different labs. The measurements presented here have been done at the horizontal test facility at HZB, HoBiCaT [9]. Previous measurements were done horizontally at Cornell [10] and vertically with and without tank at Fermilab.

EXPERIMENTAL SETUP

All measurements have been performed on the TB9AES11 cavity, a TESLA type cavity that was N-doped with the standard Fermilab recipe [1]. The cavity was encased in a magnetic shielding, a second magnetic shield was present the inside wall of the HoBiCaT cryostat. Fluxgate magnetic field sensors were attached at the cavity walls at different positions and with different orientations: Fluxgate FG1, FG3 and FG4 were placed radially on the outer and middle cells parallel to the cavity surface near the equator, to monitor the Meissner transition. FG2 was placed azimuthally on one of the outer cells in order to observe thermal currents due to the toroidal current loop formed by cavity (Nb) and tank (Ti). Cernox temperature sensors CX7, CX8, and CX5 were placed on top of the outer cells and the middle cell in order to measure temperature differences in axial direction of the cavity, CX6 was placed at the bottom of an outer cell which in combination with CX5 allowed for the measurement of a vertical temperature difference

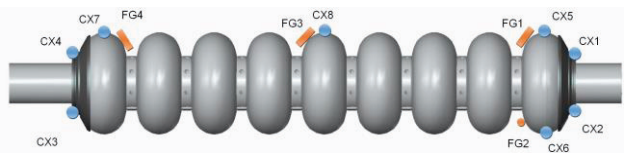

Figure 1: Positions and orientations of CERNOX temperature sensors and Fluxgate magnetometers on the TB9AES11 cavity.

across one cell. The beam pipe and the outer helium vessel were equipped with further CERNOX temperature sensors CX1 and CX2 on the input coupler side and CX3 and CX4 on the other side. All measured values were recorded with a Labview and EPICS system on a one second basis. Heaters were attached at both beam pipes in order impose temperature gradients during cool down. The cavity was equipped with a near critically coupled fixed, low-power input antenna. The resulting high loaded $Q_L > 1 \cdot 10^{10}$ allowed for precise measurement of the high expected Q_0 values. The pickup probe had an external Q of ca. $1 \cdot 10^{12}$. RF operation of the cavity was performed with a PLL. Due to the HoBiCaT infrastructure the RF drive signal was amplified with a 15 kW Bruker solid state amp, passed through a 17 m of HCA300-50J flexible coaxial cable, then through a WR-650 waveguide with circulator and three-stub-tuner. From there it was adapted to N type connector and LMR-400 cable and connected to a feedthrough at the cryostat. Inside the vacuum it was further adapted to SMA connectors and Huber+Suhner K_03252_D-06 cable.

ISBN 978-3-95450-178-6

MEAN FREE PATH DEPENDENCE OF THE TRAPPED FLUX SURFACE RESISTANCE*

M. Checchin†, M. Martinello, Fermilab, Batavia, IL 60510, USA and IIT, Chicago, IL 60616, USA
A. Grassellino, A. Romanenko, Fermilab, Batavia, IL 60510, USA
J.F. Zasadzinski, IIT, Chicago, IL 60616, USA

Abstract

In this article a calculation of the trapped flux surface resistance is presented. The two main mechanisms considered in such approach are the oscillation of the magnetic flux trapped in the superconductor due to the Lorentz force, and the static resistance associated to the normal conducting vortex core. The model derived shows a good description of the available experimental data, highlighting that the radio frequency vortex dissipation is mostly due to the static part of the surface resistance. We show that the surface resistance for 100% trapped flux normalized to the trapped field (expressed in nΩ/mG) can be approximated to $R_{flux}/B \approx 18.3(\text{n}\Omega\sqrt{\text{s nm}}/\text{mG}) \cdot \left(\sqrt{l\,f}/\,(50.1(\text{nm}) + l)\right)$ with l the mean free path in nm and f the frequency in GHz.

INTRODUCTION

When the superconductive transition is performed in presence of external magnetic field, magnetic flux can be trapped in superconducting materials as energetically stable fluxoids in the mixed state of II type superconductors, or as vortexes pinned at defects in the Meissner state of I and II type superconductors. In some circumstances, magnetic flux lines can penetrate in the Meissner state without needing of pinning sites to exist in the so called intermediate state, as consequence of the demagnetization effect.

All such magnetic flux structures can introduce dissipation in both dc and radio frequency (RF) domains.

Controlling the pinning force of the superconducting material, it is possible to minimize the vortex dc dissipation, enabling superconductors to transport very high currents, without any dissipation, up to the depinning current.

On the other hand, in RF applications the vortexes dissipation is less controllable, and superconducting radio frequency (SRF) devices often operates in presence of such extra dissipation. The trapped flux problem is indeed critical for superconducting accelerating cavities, especially when high quality factors are needed for applications in continuous wave (CW) accelerators.

With the discovery of the nitrogen doping treatment [1] of SRF niobium cavities, it becames extremely important to deeply understand the origin of such extra dissipation. The nitrogen doping process modifies the niobium mean free path and energy gap [2, 3], introducing a beneficial effect on the quality factor Q_0, but at the same time it affects negatively the magnetic flux dissipation [4–6].

* Work supported by the US Department of Energy, Office of High Energy Physics.
† checchin@fnal.gov

In this work a model to describe the dissipation introduced by such flux structures in superconductors operating in RF field as a function of the mean free path is presented. The calculation will consider the following assumptions:

1. The vortex description is local
2. No interaction between vortexes are considered
3. $T << T_c$, no temperature dependencies are introduced
4. The single vortex resistance is defined as constituted by two contributions:
   (a) Static, due to the RF dissipation of the normal-conducting core
   (b) Dynamic, due to the Lorentz force acting on the flux
      - The pinning potential is approximated as parabolic
      - Only a single pinning point per vortex is considered
      - Every vortex experiences the same pinning potential
5. The applied magnetic field is 100% trapped during the superconductive transition.

In the non-local description, a vortex is described as a modulation of the order parameter of the superconductor tending to zero at the center of the vortex, and approaching to its finite value far from it [7].

Differently, in the local description introduced by C. Caroli *et al.* [8], the vortex is described as a normal conducting core with dimension of the order of the coherence length ξ_0. The superconducting currents that spin around it screening the magnetic flux confined inside.

In the model here presented, the dimension of the single vortex is described as in the work of J. Bardeen and M.J. Stephen [9]. The radius $a = \hbar/(2P_c)$ of the normal conducting core is defined as the distance from the center of the vortex at which the superelectrons' momentum assumes critical value P_c, and the superconducting energy gap Δ, otherwise constant at infinite, goes to zero.

In the clean limit where the electrons mean free path l is higher than the coherence length ξ_0 ($l > \xi_0$), the superelectrons' momentum critical value and the correspondent vortex radius are [9]

$$P_c = \frac{2.178\hbar}{2\pi\xi_0} \quad \rightarrow \quad a_{cln} = 1.16\xi_0 \qquad (1)$$

ISBN 978-3-95450-178-6

DETECTORS SENSING SECOND SOUND EVENTS INDUCED BY THERMAL QUENCHES OF SRF CAVITIES IN HE II

M. Fouaidy, D. Longuevergne, F. Dubois, O. Pochon, J-F Yaniche, Institut de Physique Nucléaire d'Orsay Unité mixte de recherche CNRS-IN2P3 Université Paris-Sud 91406 ORSAY cedex

Abstract

SRF bulk Nb cavities are often limited by quench due to anomalous losses (Joule heating due normal defects or Field Emission). We continued R&D on Quench Detectors (QD) activity for locating quench in SRF cavities via 2nd sound in superfluid helium. We investigated 2 kinds of QD: Capacitive OST (COST) and Low Response time resistive Thermometers (LRT). A test stand operating in LHe (Temperature: T_0) was used for full characterization of the QD by means of precise experimental simulation of SRF cavity quench: various heaters subjected to a pulsed heat flux q_P were used. For improving spatial resolution of QD, smaller COSTs were developed and tested. We investigated the dynamic response of QD as function of different parameters (heater size/geometry, T_0, q_P) and data are reported. Further, a 2nd Sound Resonator (SSR) equipped with a pair of COSTs at its 2 extremities as 2nd Sound Generator (SSG) and Detector (SSD) respectively, a low heat capacity heater (SSG) and a LRT (SSD) was developed. The experimental data obtained, with SSR operated in resonating mode or in a pulsed mode are presented. The results concerning location of quenches in QWR and Double-spoke cavities are discussed.

INTRODUCTION

Thanks to an important R&D effort made by different laboratories around the world during ~35 years , to the use of high purity material (e.g. Nb with RRR>300) and the improvement of fabrication process as well as preparation procedures, SRF bulk Nb cavities are nowadays operated reliably at high accelerating gradient E_{acc}. For example, in the frame ILC R&D program, the achieved E_{acc} in the TTF/FLASH superconducting linac at DESY increased from 18 MV/m for the 1st cryomodules housing 8 nine cells 1.3 GHz cavities to 30 MV/m for the 7th cryomodules. These 2 values of E_{acc} correspond to surface magnetic fields B_S =76 mT and 126 mT respectively [1]. However, the maximum RF surface magnetic field (B_{Smax}) achieved with SRF bulk Nb cavities is often limited by anomalous RF losses due to Joule heating of normal-resistive defects embedded onto the RF surface or heating induced by impacting field emitted electrons on the RF surface. The typical effective diameter and surface resistance of normal defects are respectively in the range 1-100 µm and 1-10 mΩ. Considering a ILC cavity operating at E_{acc}=33 MV/m, the heat flux density q_{Defect} due to Joule heating of a defect area is 31 MW/m^2 (Fig.1), in contrast to RF losses in the superconducting RF surface region (q_{BCS}~82 W/m^2). Due to such very high heat flux in the defect zone, and to the

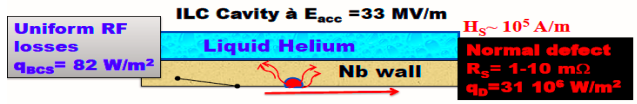

Figure 1: Sketch of the thermal model used (2D axisymmetric problem).

quadratic dependence of Joule RF losses with B_S (e.g. q α $R_S.B_S^2$), the temperature of the RF surface T_{RF} increases strongly with B_S especially in the defect area. As illustration of such strong heating $\Delta T = T_{RF}-T_0$, the computed temperature profile is presented in Fig.2 for a field jute above the quench field.

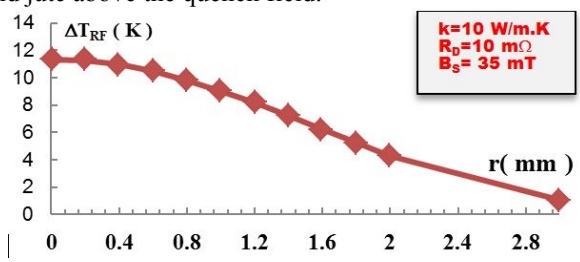

Figure 2: Computed heating profile (ΔT versus distance r to defect center) on the RF surface (Bath Temperature: T_0=2K, defect radius: 200 µm, E_{acc}=9 MV/m).

As E_{acc} is increased, The Joule heating increases the RF surface temperature (Fig. 3) in the vicinity of the defect up to the critical temperature T_C (B_S) of niobium. When the quench field is reached, a dramatic increase (e.g. by 5 to 6 orders of magnitude) of the local RF losses is observed.

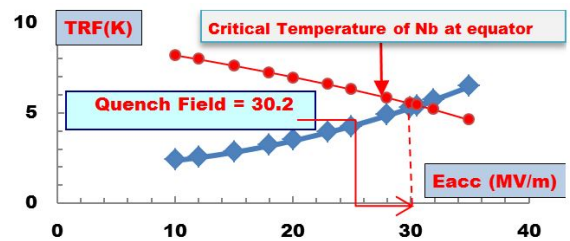

Figure 3: Computation of quench field for ILC cavity.

This catastrophic process leads to the quench of the SRF cavity as soon as the hot spot area effective diameter exceeds a critical value D_C~1-10 cm, for which the unloaded quality factor Q_0 decreases strongly. Obviously, the thermal quench of a SRF cavity is easily detectable with RF probes (i.e. transmitted or reflected RF power). However, as it is an overall measurement, RF signals are insufficient to characterize completely the thermal runaway and are unable to locate quench source. Dedicated diagnostic tools are then needed in order to study and investigate in details quench phenomena.

ISBN 978-3-95450-178-6

SRF CAVITY BREAKDOWN CALCULATION PROCEDURE USING FEA-SOFTWARE

Roman Kostin#, Alexei Kanareykin, Euclid Techlabs, LLC, Solon, Ohio, USA
Ivan Gonin, Fermilab, Batavia, IL 60510, USA
Evgeniy Zaplatin, Forschungszentrum Juelich, Juelich, Germany

Abstract

SRF cavity thermal breakdown can be analyzed analytically using thermodynamics equation. This technique is suitable for simple geometries when surface magnetic field variation can be omitted. Thermal radiation effect which is crucial for SRF gun calculations is also hard to implement properly because of complicated geometry. All of these can be overcome by using multiphysics FEA-software. This paper shows the procedure of cavity thermal breakdown calculation in coupled multiphysics analysis with dependable parameters.

INTRODUCTION

The goal of this work was implementation of thermal multiphysics analysis of SRF cavities in FEA software with temperature dependant parameters such as surface resistance and thermal conductivity. Kapitza resistance was assumed to be constant with constant bath temperature. ANSYS APDL scripts were developed to perform the analysis.

3.9 GHz elliptical cavity QvsB curves which were obtained at Fermilab for DESY FLASH module were used to check ANSYS results. Thermal conduction coefficient, Kapitza conductance and surface resistance was obtained for better matching with measured QvsB curves. The first attempts to fit the curves were done in the reference [1]. Simple model with constant thermal conduction coefficient was implemented in Mathcad. The results did not show an agreement for each case. In this paper 9 cell 3.9 GHz elliptical cavity data was used to fit ANSYS results and show a good agreement for almost the same quench fields. This proves the accuracy of developed ANSYS macros and opens the way to use it for different geometries as a "plug and play" solution.

The developed algorithm also was tested on 1.4 cell HZB SRF gun [2]. It represents L-band 1.4-cell SRF gun with warm cathode which has a very tiny gap between the cathode and niobium walls in superconducting state. Although, global thermal breakdown is not possible in L-band cavities, superheating field is greater than critical magnetic field of niobium, accurate thermal analysis is required to determine cathode temperature and its longitudinal thermal expansion. The thermal radiation was not included in our simulations yet but will be implemented in later works.

r.kostin@euclidtechlabs.com

3.9 GHz CAVITY MULTIPHYSICS ANALYSIS

Global thermal breakdown of SRF cavities is determined by temperature dependence of surface resistance which in terms depends on RF magnetic field heating. Heat flux from RF heating depends on the temperature:

$$q = \frac{R_s}{2} \cdot H_\tau{}^2 \qquad (1),$$

$$R_s = R_{BCS}(T) + R_{Res} \qquad (2),$$

where q - thermal heat flux, R_{BCS} - temperature dependant BCS surface resistance, R_{Res} - residual constant surface resistance and H_τ – surface magnetic field.

Heat flux from RF heating changes temperature distribution which in its term should change the applied heat flux at constant fields. Special APDL macro was developed to take into account this heat flux dependence on temperature by iterative thermal calculations. Surface resistance, thermal conductivity and Kapitza resistance has been set as functions of temperature, i.e. their values are calculated by ANSYS according to temperature distribution. Kapitza resistance depends on bath temperature which is constant but could be evaluated for different regimes which eliminate the need of correction for different bath temperatures. There are only two input parameters - magnetic field and bath temperature, the others were set through functions.

Fermilab 3.9 GHz 9 cell cavity experimental data (QvsB curves) were used to compare with simulation results. The corresponding thermal conductivity, Kapitza and surface resistance were required to match experimental curves with simulation results. A 1D simplified model was developed to find proper material properties and save time on simulation. The length of the model equals to the cavity wall thickness. Heat flux was applied to one side and convection coefficient that equals to Kapitza conductance for the other side. Temperature dependent thermal conductivity was also applied. Several Kapitza resistance models (Amrit1, Amrit3, Mittag), residual resistance and thermal conductivity coefficients (see Fig. 1) were used to obtain global thermal breakdown at fields as close as possible to quench fields from the experimental data. The calculated results can be found in Table 1.

MODIFICATIONS OF SUPERCONDUCTING PROPERTIES OF NIOBIUM CAUSED BY NITROGEN DOPING OF ULTRA-HIGH QUALITY FACTOR CAVITIES*

A. Vostrikov#, Y.-K. Kim, L. Horyn, University of Chicago, Chicago, IL 60637, USA
A. Romanenko, A. Grassellino, FNAL, Batavia, IL 60510, USA
T. Murat, University of Wisconsin – Madison, Madison, WI 53706, USA

Abstract

A study is presented on the superconducting properties of niobium used for the fabrication of the SRF cavities after treating by recently discovered nitrogen doping methods [12]. Cylindrical niobium samples have been subjected to the standard surface treatments applied to the cavities (electro-polishing, low temperature bake-out) and compared with samples treated by additional nitrogen doping recipes routinely used to reach ultra-high quality factor values (over $3 \cdot 10^{10}$ at 2 K, 16 MV/m). The DC magnetization curves and the complex magnetic AC susceptibility have been measured. Crosscheck resistivity measurements of the critical surface magnetic field (B_{c3}) are also presented.

Evidence for the lowered field of first flux penetration after nitrogen doping is found confirming the correlation with the lowered quench fields. Superconducting critical temperatures T_c = 9.25 K are found to be in agreement with previous measurements. Wider transition gap for nitrogen treated samples is observed. No strong effect on the critical surface field from nitrogen doping is found. The results of B_{c3} measurements via AC susceptibility are confirmed by resistivity measurements.

In addition, the results of low energy muon spin rotation (LE-μSR) spectroscopy measurements of magnetic field penetration into superconducting niobium are presented. A strong correlation between London penetration depth behavior and niobium treatment is demonstrated. Such behavior is in agreement with anti-Q-slope effect measured previously.

INTRODUCTION

Superconducting radio frequency (SRF) cavities are the key technology for future particle accelerators for high-energy physics, nuclear physics, light sources, and accelerator-driven subcritical reactors. Several decades of SRF research and development at laboratories and universities worldwide have led to the successful realization of niobium cavities that reliably achieve very high gradients and quality factors.

Recent breakthrough discovery at Fermilab demonstrated positive impact on cavity's quality factor from the doping of certain amount of nitrogen into niobium cavity walls. However, this treatment reduces somewhat the maximum gradient achievable in the cavity, i.e. reduction of quench field takes place. It was demonstrated that SRF cavities, which surfaces prepared with electrolytic polishing (EP) method and low temperature (120ºC) bake-out for 48 hours, can have quench fields over 40 MV/m, while cavities which undergone nitrogen doping are limited by a quench field of 25-30 MV/m. [1, 12]

Magnetic measurements on niobium samples are a useful tool to investigate the effect of nitrogen doping on niobium critical fields. The experimental studies on the magnetization and susceptibility of niobium samples presented in the paper have been carried out with the aim to gain an understanding of superconducting properties change by nitrogen doping.

MAGNETOMETER EXPERIMENTAL PROCEDURE

The samples for the magnetization and susceptibility measurements are cylinders with diameter of 2.85 mm and a height of 7.0 mm, which are cut from RRR~300 fine grain niobium sheets used for SRF cavity production. Bulk EP of about 120 μm removal was done on all samples. After that, one of the samples was baked for 48 hours at 120ºC in the vacuum. Such surface preparation in SRF cavities typically leads to maximum accelerating fields of 40 MV/m and above. Two other samples are prepared using different nitrogen doping recipes, which found to deliver SRF cavities with optimal quality factor (over $2.7 \cdot 10^{10}$ and above at 2 K, 16 MV/m). The procedure of surface treatment (after initial bulk EP) is the following:

- high temperature bake at 800ºC for 3 hours in vacuum;
- bake at 800ºC for time t_1 with nitrogen gas in the chamber (diffusion of nitrogen into niobium happens);
- after diffusion bake at 800ºC for time t_2 in vacuum (diffused nitrogen redistributes inside the niobium walls to produce desired nitrogen concentration profile);
- 5 μm surface layer removal by EP (nitrides formed at the surface removed, desired surface concentration of nitrogen is achieved).

Time parameters t_1 and t_2 are subject to optimization. Optimal in terms of quality factor recipes have the following parameters: t_1 = 2 min, t_2 = 6 min and t_1 = 20 min, t_2 = 30 min. Cavities prepared with the first recipe have quench fields of up to about 30 MV/m. Cavities prepared with the second recipe have quench fields of up

*Work supported by DOE HEP.
#vostrikov@uchicago.edu

PRESERVATION OF VERY HIGH QUALITY FACTORS OF 1.3 GHZ NINE CELL CAVITIES FROM BARE VERTICAL TEST TO DRESSED HORIZONTAL TEST

A. Grassellino[1], A. Romanenko[1], O. Melnychuk[1], D. A. Sergatskov[1], G. Wu[1], M. Martinello[1,2], M. Checchin[1,2], A. C. Crawford[1], S. Posen[1], C. Grimm[1], A. Hocker[1], J. Ozelis[1], S. Aderholt[1], A.Rowe[1], N. Solyak[1], R. Stanek[1], D. Gonnella[3], M. Liepe[3], J. Vogt[4]

[1]Fermilab, Batavia, IL 60510, USA, [2]Illinois Institute of Technology, Chicago, IL 60616, USA, [3]CLASSE, Cornell, Ithaca, NY 14853, USA, [4]HZB, Berlin, Germany

Abstract

At FNAL, a series of 1.3 GHz nine cell cavities have been treated with nitrogen doping, and vertically tested first as bare cavities, then dressed in different styles of Helium vessels (ILC and LCLS-2), tested vertically again post dressing and then horizontally tested in a one cavity cryomodule configuration, with magnetic shielding, RF ancillaries etc. In this contribution we summarize the quality factor evolution from vertical bare test to final cryomodule configuration horizontal test and highlight the important parameters we found for Q preservation.

INTRODUCTION

Record high operational quality factors have been routinely and systematically demonstrated in nitrogen doped niobium cavities in more than hundred vertical tests at different laboratories [1, 2, 3]. In the past years lots of attention has been dedicated to the potential effect of Q changes because of change in trapped flux induced residual resistance, depending on the details of cooling in dressed cavities. This is now understood to be potentially coming from different sources: a) the strong effect of cooldown through critical temperature on the efficiency of magnetic flux expulsion [4, 5, 6]; b) the change in magnetic fields surrounding the cavity surface during cooldown [7] that may arise depending on temperature differences between cavity, vessel, and other potential circuit loops of dissimilar metals. In this work, we study for the first time the full step-to-step evolution of the quality factor of very high Q N doped nine cell cavities from bare vertical test, to vertical test post dressing, to horizontal test with unity coupling and finally in full cryomodule environment with high power coupler all RF ancillaries. This way we can track if changes in Q occur at any of these steps and trace clearly to their origin. We find that even in very low magnetic fields < 4 mGauss - achieved via double cryoperm shields plus active compensation [8]- slow and homogeneous cooling through transition in horizontal tests always leads to worse quality factors then for fast cooling in agreement with the findings from vertical tests of single and nine cells [4]. A procedure yielding repeatedly optimal Q in horizontal dressed cavity configuration is described, together with the key parameters/knobs that may lead to better or worse final Q results. Non-trapped flux related conditions encountered that can deteriorate Q will also be described.

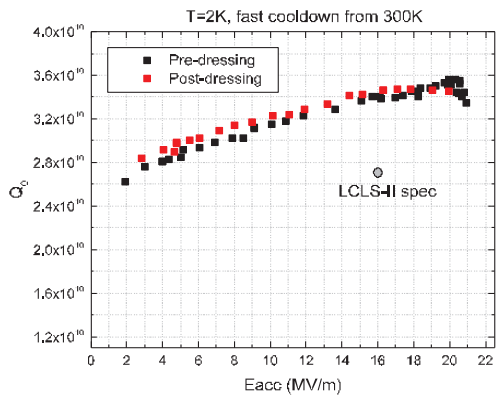

Figure 1: High N doped nine cell pre and post dressing performance comparison in vertical test. No degradation is encountered with He vessel welding.

VERTICAL TEST RESULTS FOR DOPED NINE CELL BARE VERSUS DRESSED CAVITIES

More than 10 nine cell 1.3 GHz cavities have been doped at FNAL as part of this study, mostly treated with the LCLS-2 baseline doping recipe known as "2/6" + 5 microns EP, meaning that nitrogen gas is injected at 800°C for 2 minutes at partial pressure of ~25 mTorr, then cavity is annealed at 800°C in HV for 6 minutes, then 5 microns EP. This is one of the optimal doping recipes found so far, leading to optimal R_{BCS} (16MV/m, 2K, 1.3GHz) = 4.5 nΩ, optimal non flux related residual < 2nΩ, and to a sensitivity to trapped magnetic flux of ~1.2 nΩ/mGauss [9]. One of the nine cell studied TB9AES011 was doped with a different recipe yielding to a much larger sensitivity to trapped flux of ~2 nΩ/mGauss. The plots below (Fig. 1) show this particular cavity before and after helium vessel welding in vertical test, both curves for fast cooldowns from 300K in 5 mGauss dewar ambient field. The results show that no degradation occurs during the dressing process, even for these very

ISBN 978-3-95450-178-6

MEASUREMENTS OF THERMAL IMPEDANCE ON SUPERCONDUCTING RADIOFREQUENCY CAVITIES*

Pashupati Dhakal†, Gianluigi Ciovati and Ganapati Rao Myneni
Jefferson Lab, Newport News, VA 23606, USA

Abstract

The thermal impedance of niobium plays an important role in the thermal stability of the superconducting radio frequency (SRF) cavities used in particle accelerators. During the operation of SRF cavities, the RF power dissipates on the inner surface of the cavities and the heat transport to the helium bath depends on the thermal conductivity of niobium and Kapitza conductance at the interface between the niobium and superfluid helium. Thermal impedance was measured on three 1.3 GHz single cell cavities made from ingot niobium with different purity. The results show the influence of surface preparation on thermal impedance and the results are qualitatively in agreement to the power law dependence with temperature as reported in the literature.

INTRODUCTION

Superconducting radio frequency cavities are the building blocks of particle accelerators for basic physics research. It is based on niobium superconducting hollow structures ("cavities") to accelerate the beam of charged particles to the velocity of light. The superiority of superconducting material is its ability to efficiently store large amount of energy with no or very little dissipation. The performance of SRF cavities is measured in terms of the quality factor expressed as Q_0=$\omega U/P$, where U is stored energy and (P/ω) is the power dissipation on inner cavity wall per rf cycle. Ideally, the quality factor of SRF cavities is independent of the accelerating field (or peak magnetic field) as the breakdown occurs at superheating field. However, due to the finite resistance of the superconductor in rf field, power dissipates on the cavity walls due to the interaction of the rf field with normal conducting electrons. At high peak magnetic field the dissipation is believed to be of magnetic origin, where the surface resistance increases due to pair-breaking by the increasing rf field gives rise to the non-linear BCS surface resistance [1]. The cavity then goes to the magneto-thermal instability and finally "quench". The dissipated power is given by $P_{diss} = (1/2\mu_0)R_s(T)B_p^2$, where μ_0 is magnetic permeability, $R_s(T)$ is surface resistance, and B_p is peak rf magnetic field on the inner surface of the cavity.

The power dissipated (heat) on the inner surface of SRF cavities during the operation is conducted through the cavity wall into the helium bath. The efficient transport of heat from the inner cavity wall to the helium bath depends on the thermal conductivity of niobium and the Kapitza conductance between the outer cavity surface and the superfluid helium. The thermal conductivity of niobium is material dependent, for example the impurities contents (related to the residual resistivity ratio-RRR), crystal grain sizes, mechanical deformation, defects and dislocations in niobium. The Kapitza resistance is an intrinsic thermal resistance due to the phonon mismatch at the boundary between Nb and the superfluid He and depends on the nature of solid surface. In this contribution, we present some preliminary results in an attempt to understand the effect of surface preparations on the thermal resistance on SRF cavities.

EXPERIMENTAL SETUP

Previously, thermal impedance measurements on SRF niobium samples were carried out in an experimental cell which allows us to measure the thermal conductivity and Kapitza resistance [2–4] by measuring the temperature jump across the niobium samples. Palmieri *etal.*, [5] measured the thermal boundary resistance via the rf surface resistance measurement in SRF cavities and showed the change in thermal boundary resistance as the outer surface of cavity was modified. In our present study, we have estimated the thermal impedance of SRF cavity using the method used in refs. [2,3]. The schematic representation of the experimental set up is shown in Fig. 1.

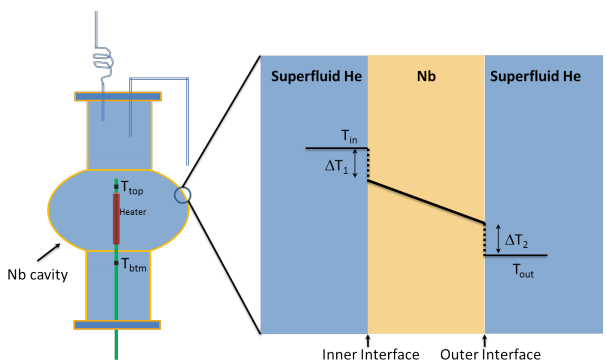

Figure 1: Schematic of experimental set up.

Niobium SRF cavity of thickness ~ 2.9 mm is immersed in superfluid helium bath and filled with superfluid He via a capillary tube of diameter ~1.5mm. Two capillary tubes are used, one for filling and other for exhaust to He gas during filling , welded to a ~ 9.5mm thick stainless steel flange sealed to one cavity flange with indium wire. A cryogenic heater of resistance ~8.5 Ω is inserted along the axis of the cavity using a G10 rod. Two calibrated thermometers are attached at the both ends of the G10 rod, measuring the

† dhakal@jlab.org

ISBN 978-3-95450-178-6

LCLS-II SRF CAVITY PROCESSING PROTOCOL DEVELOPMENT AND BASELINE CAVITY PERFORMANCE DEMONSTRATION*

P. Bishop,[1] M. Checchin,[2] H. Conklin,[1] A. Crawford,[2] E. Daly,[4] K. Davis,[4] M. Drury,[4] R. Eichhorn,[1] J. Fischer,[4] F. Furuta,[1] G.M. Ge,[1] D. Gonnella,[1] A. Grassellino,[2] C. Grimm,[2] T. Gruber,[1] D. Hall,[1] A. Hocker,[2] G. Hoffstaetter,[1] J. Kaufman,[1] G. Kulina,[1] M. Liepe,[1†] J. Maniscalco,[1] M. Martinello,[2] O. Melnychuk,[2] T. O'Connel,[1] J. Ozelis,[2] A.D. Palczewski,[4] P. Quigley,[1] C. Reece,[4] A. Romanenko,[2] M. Ross,[3] A. Rowe,[2] D. Sabol,[1] J. Sears,[1] D.A. Sergatskov[2] W. Soyars,[2] R. Stanek,[2] V. Veshcherevich,[1] R. Wang,[2] G. Wu[2]
[1] CLASSE, Cornell University, Ithaca, NY 14853, USA
[2] FNAL, Batavia, IL 60510, USA
[3] SLAC, Menlo Park, CA 94025, USA
[4] TJNAF, Newport News, VA 23606, USA

Abstract

The Linac Coherent Light Source-II Project will construct a 4 GeV CW superconducting RF linac in the first kilometer of the existing SLAC linac tunnel. The baseline design calls for 280 1.3 GHz nine-cell cavities with an average intrinsic quality factor Q_0 of 2.7×10^{10} at 2K and 16 MV/m accelerating gradient. The LCLS-II high Q_0 cavity treatment protocol utilizes the reduction in BCS surface resistance by nitrogen doping of the RF surface layer, which was discovered originally at FNAL. Cornell University, FNAL, and TJNAF conducted a joint high Q_0 R&D program with the goal of (a) exploring the robustness of the N-doping technique and establishing the LCLS-II cavity high Q_0 processing protocol suitable for production use, and (b) demonstrating that this process can reliably achieve LCLS-II cavity specification in a production acceptance testing setting. In this paper we describe the LCLS-II cavity protocol and analyze combined cavity performance data from both vertical and horizontal testing at the three partner labs, which clearly shows that LCLS-II specifications were met, and thus demonstrates readiness for LCLS-II cavity production.

INTRODUCTION

The very significant successes of the LCLS research program have produced a keen interest in the high research value of high repitition rate coherent photon sources. In order to expedite realization of such a facility in the US, the US DOE asked SLAC to rework their proposed LCLS-II concept into one providing MHz pulse structure via the use of CW SRF technology in the old SLAC tunnel. [1] Rather than take the time to develop an optimized purpose-built SRF accelerator, the decision was taken to seek to adopt the electron accelerator system developed for the European XFEL project, making only necessary changes to enable CW operation.

* Work supported, in part, by the US DOE and the LCLS-II Project under U.S. DOE Contract No. DE-AC05-06OR23177 and DE-AC02-76SF00515.
† MUL2@cornell.edu

The principal characteristic that required adaptation relates to the significance of the increased dynamic cryogenic load. Re-engineering of the cryogenic plumbing internal to the cryomodules and also the distribution system was required. The scale of the required cryoplant was also quite significant. Extrapolation from the heatload performance of the EXFEL cryomodules implied either two or three plants of the scale of the CEBAF 2 K Central Helium Liquefier would be required.

Contemporaneous with the reworking of the LCLS-II construction project, a technical route to lowering of CW SRF cryogenic loads by factors of more than 50% via diffusion of nitrogen impurities in the cavity was discovered at FNAL. [2] This lowering of the rf surface resistance, frequently known as "high Q_0," stimulated great interest because of the prospect of dramatic cost savings in both capital and operations. High temperature diffusion of small amounts of foreign atoms into the niobium rf surface was found empirically to yield the dramatically improved performance. [2,3] Using nitrogen for this purpose was found to be accomplished quite conveniently, with only small alteration of the rather standard cavity treatment processes used for EXFEL, 12GeV CEBAF, ILC R&D, and other projects.

This set of circumstances set the stage for a focused R&D effort to probe the reliability of such new treatment methods, and to flush out specifications of the cryomodule environmental conditions required to realize the new performance standards in operational conditions.

JOINT HIGH Q_0 R&D PROGRAM

In order to support the rapid development of procedures to minimize the LCLS-II cryogenic heat load FNAL, JLab, and Cornell University were asked to join the LCLS-II collaboration in R&D on methods to confidently maximize the Q_0 of nine-cell cavities for use in LCLS-II linac. [4,5]

The initial work centered on development of systematic methods for controlled high-temperature diffusion doping of Nb cavities with nitrogen, controlled thickness removal of the interior surface of the doped Nb cavity by electropolishing, and the development of well-specified and controlled cool-

ISBN 978-3-95450-178-6

NATURE AND IMPLICATION OF FOUND ACTUAL PARTICULATES ON THE INNER SURFACE OF CAVITIES IN A FULL-SCALE CRYOMODULE PREVIOUSLY OPERATED WITH BEAM*

J. Fischer, R.L. Geng#, A. McEwen, O. Trofimova

Jefferson Lab, Newport News, VA 23606, U.S.A.

Abstract

We report on the preliminary results of the first study of found actual particulates on the inner surface of 5-cell CEBAF cavities in a full-scale cryomodule previously operated with beam. The procedure of particle collection is illustrated. The nature of studied particulates is presented. The implication of the findings will be discussed in view of reliable and efficient operation of CEBAF and future large-scale SRF accelerators.

INTRODUCTION

Field emission in an SRF cavity often has its root in small foreign particulates, lodging on the cavity inner surface. Although it is known that not all the surface particulates are active field emitters, the general practice nowadays is to avoid particulate contamination by careful cleaning and handling of individual cavities, as well as clean room assembly of cavity strings. Despite these elaborate processes, adequately clean cavity surface is still difficult to obtain for a beam-ready cavity placed in the accelerator tunnel. Consequentially, degradation in field emission onset is sometimes observed from vertical qualification test of an individual cavity to its test in a cryomodule. Moreover, as will be shown in this contribution, new particulates, shed from beam line components, may travel and arrive at the cavity surface, after a cryomodule has been placed in the accelerator tunnel. The nature of these "traveling beam-line particulates" landed on the inner surface of a beam-accelerating cavity is largely unknown for two reasons: (1) lack of access to such surfaces; (2) lack of a workable procedure for investigation without destroying the cavity.

In the decades-long history of large scale SRF machine operation in CEBAF, it has been known that the field emission in cavities placed in the tunnel might deteriorate over some time of beam operation. Among the consequences of this deterioration is an increased machine trip rate via its charging effect on cryogenic ceramic RF windows. In order to keep the trip rate to stay within the tolerable limit, the operation gradient of some cavities must be lowered. This results in an apparent "gradient loss", or more precisely a loss in "usable gradient", which in turn reduces the attainable beam energy for stable machine operation. Historically, two practical counter-measures are used in CEBAF to restore the "lost" gradient: (1) Helium processing; (2) cryomodule refurbishment [1-3]. Each of these two countermeasures has its own advantages and dis-advantages. Helium processing is less expensive and can be done *in-situ* in accelerator tunnel; but sometimes it produces a rather small effect. It is also possible that a cavity may be degraded from helium processing, as observed in some helium processed 7-cell cavities, newly installed for the 12 GeV energy upgrade of CEBAF [4]. Cryomodule refurbishment is more effective in raising the gradient capability of the original CEBAF cavities, for a superior cavity surface is obtained from reprocessing these cavities wit modern cleaning techniques and assembly procedures; but the cost for refurbishment is relatively high.

The root cause of the field emission deterioration problem in CEBAF is not known and has not been studied before. Recently, there has been an increased interest in gaining a clear understanding of the problem. A driving force is the need to run the 418 SRF cavities together stably for the upcoming physics run. Among these cavities, 80 of them are new 7-cells installed for the 12 GeV upgrade. They are operated at a nominal gradient of 17.5 MV/m. The corresponding peak surface electric field is ~40 MV/m, which is significantly higher than the typical values of 25-30 MV/m in the original 5-cell cavities. Due to the exponential nature of field emission, *the new 7-cell cavities are therefore at a higher risk as compared to the original 5-cell cavities, if the root cause is the same*. It should be noted that trips rooted from emission in the new 7-cell cavity cryomodules have its unique symptoms such as beam line vacuum spikes etc. In this contribution, we report on the preliminary results of our effort in identifying actual particulates on the inner surface of 5-cell CEBAF cavities in a full-scale cryomodule, which was previously operated with beam. The nature of the found and studied particulates is presented. The implication of the findings will be discussed in view of reliable and efficient operation of CEBAF and future large-scale SRF accelerators.

CAVITIES

The cavities were originally embedded in cryomodule FEL2, which was previously operated with beam. This module is slated to be refurbished in a similar fashion as the past 11 refurbishment modules, all of which successfully raised the acceleration voltage per module from 20 MV to 50 MV. It should be mentioned that the module FEL2 (now known as C50-12) suffered a vacuum accident at one point, in which the cavity inner surface was exposed to a shockwave and atmospheric pressure. This resulted in a large degradation in field emission onset

*Authored by Jefferson Science Associates, LLC under U.S. DOE Contract No. DE-AC05-06OR23177.
Work partially supported by the US-Japan Collaboration Fund.
#geng@jlab.org

TOF-SIMS STUDY OF NITROGEN DOPING NIOBIUM SAMPLES*

Z. Q. Yang, X. Y. Lu#, L. Lin, J. F. Zhao, D. Y. Yang, W. W. Tan
State Key Laboratory of Nuclear Physics and Technology, Peking University, Beijing, China

Abstract

Nitrogen doping treatment with the subsequent electropolishing (EP) of the niobium superconducting cavity can significantly increase the cavity's quality factor up to a factor of 3. The nitrogen doping experiment has been successfully repeated and demonstrated on both single cell and 9-cell cavities and the best nitrogen doping recipe has been searched. But the mechanism of the nitrogen doping effect remains unclear. Nitrogen doping study on niobium samples was carried out in Peking University. The niobium samples were manual processed to avoid heat generation. The experiment condition is close to that of the Fermilab. After the nitrogen doping treatment, the samples were mildly electropolished with the thickness of 1.3μm, 1.9μm, 3.3μm, 4.2μm, 5.1μm, 5.9μm and 7.0μm. The time of flight secondary ion mass spectrometry (TOF-SIMS) measurements show that the samples directly after nitrogen doping have a much higher nitrogen concentration in the depth of about 90nm. When the EP removal is larger than 1.3 μm , the samples' impurity elements is remarkably reduced and their distribution is similar to each other. Also the measured results to some extent prove that EP removal can introduce H to the niobium surface.

INTRODUCTION

Quality factor Q is one of the most important factors of radio-frequency niobium superconducting cavities. High quality factor can efficiently decrease the cryogenic load of superconducting cavities, and the post treatment has an important influence on the cavities' radio-frequency performance. The average unloaded Q_0 of linac coherent light source (LCLS-II) 9-cell 1.3GHz cavities and cryomodules were set to be exceeding 2.7×10^{10} at a gradient of 16MV/m at 2K [1]. It means that the surface resistance of the cavity is less than 10nΩ, and the standard surface treatment procedures including a combination of chemical treatments like electropolishing (EP), buffered chemical polishing (BCP) and heat treatments [2] cannot meet this requirement. Grassellino [3, 4, 5] from FNAL has reported a new surface treatment, nitrogen doping, that can systematically improve the quality factor of radio-frequency niobium superconducting cavities up to a factor of about 3 compared to the standard surface treatment procedures. Nitrogen doping consists of three steps, namely heat treatment at 800^0C for several minutes in a nitrogen atmosphere of about 25 mTorr, heat treatment at 800^0C for several minutes in high vacuum and EP removal of cavity material to several microns. After that Cornell University [6] and JLAB [7] have successfully repeated and demonstrated the nitrogen doping experiment on both single cell and 9-cell cavities. On one hand, Cornell University and JLAB together with FNAL have been searching for the best nitrogen doping recipe [8, 9]. A widely accepted one is the so called " Fermilab 2/6", that is 800^0C degasing for 3 hours in high vacuum, then heat treatment at 800^0C for two minutes in a nitrogen atmosphere of about 25 mTorr, with the subsequent heat preservation of six minutes in high vacuum. After that the cavity was EP removed 5μm to obtain the best performance. On the other hand, fundamental understanding of the nitrogen doping mechanism is being carried out extensively, but yet remains unclear. But more and more studies [10, 11, 12, 13] show that hydrogen content may play an important role in the remarkable increase of the quality factor of superconducting niobium cavity after nitrogen doping treatment. The nitrogen impurities can reduce the diffusion coefficient of hydrogen in nitrogen doped niobium [14], but exorbitant nitrogen content may degrade the quality factor of the superconducting niobium cavity. The cavity directly after nitrogen treatment shows the quality factor of the order of 10^7[3], for the possible poorly superconducting nitrides on the cavity inner surface [15]. Nitrogen doping study on niobium samples was carried out in Peking University to seek the physical explanation of it. In the first stage, the niobium samples, with different EP removal, have been analysed using TOF-SIMS to measure their depth profiles of impurity elements, which can be helpful to understand the nitrogen doping effect.

SAMPLE PREPARATION AND NITROGEN DOPING EXPERIMENT

Sample Preparation

To avoid heat generation, instead of wire electrodischarge machining (EDM), the niobium samples were manual processed. Firstly, niobium strips with the dimensions of about 40mm×4mm×2.8mm, were cut out from the same niobium plate using the same saw. Secondly, the niobium strips were polished smoothly on 180-grit sandpaper, 300-grit sandpaper and 1200-grit sandpaper. The samples' treatments were attempted to replicate that of the cavities' to the extent possible. So the niobium strips were etched by EP 1:9, with the depth of about 150μm, to remove a mechanical damage layer and surface contaminations introduced during handling. Taking into account the higher oxygen content in the mixed acid surface layer which may result in a bad etched surface and the convenience of cutting down the polished samples without damaging the surfaces to be measured,

*Work supported by Major Research Plan of National Natural Science Foundation of China (91026001)
#E-mail: xylu@pku.edu.cn

ISBN 978-3-95450-178-6

ANALYSIS OF BCS RF LOSS DEPENDENCE ON N-DOPING PROTOCOLS*

A. D. Palczewski#, P. Dhakal, and C. E. Reece
Thomas Jefferson National Accelerator Facility, Newport News, VA 23606, USA

Abstract

We present a study on two parallel-path SRF cavities (one large grain and one fine grain, 1.3 GHz) which seeks to explain the correlation between the amount of nitrogen on the inner surface of a "nitrogen doped" SRF cavity and the change in the temperature dependant (packaged into term BCS) RF losses. For each doping/EP, the cavities were tested at multiple temperatures (2.0 K to 1.5 K in 0.1 K steps) to create a Q_0 vs. E_{acc} vs. T matrix which then could be used to extract temperature dependant and independent components. After each test, the cavities were thermally cycled to 120 K and then re-cooled and retested to assess if evidence of hydrogen migration might appear even at a small level. In addition, TD-5 was also tested at fixed low field (Q_0 vs. T) to fit standard BCS theory. In parallel, SIMS data was taken on like-treated samples to correlate the amount of nitrogen within the RF surface to the change in the temperature dependant fitting parameter "A".

INTRODUCTION

During the last one and a half years, while developing guidance for the nitrogen doping protocols for the LCLS-II cryomodules, JLab has systematically doped over 20 single and multi-cell cavities, with most cavities being doped more than once. The wide range of cavity dopings was done to better understand the feasibility of nitrogen doping for project. For all test RF measurements each cavity was tested at multiple temperatures (Q_0 vs. E_{acc} vs. T) in order to enable decomposition of the RF losses into temperature dependant and temperature independent portions. Initial analysis of RF losses on multiple cavities was presented at IPAC 2015 [1]. These results suggest that there is a correlation between the doping/electropolish parameters and the temperature dependent RF losses, but it is unclear what mechanism would explain this correlation.

Another mystery that arose during the initial phase of development was the occurrence of lower than expected temperature independent losses after a surface reset of 35 to 50 μm.[2] These so-called "re-baselined" cavities had performance similar to standard preparation EP cavities but with the Q_0 vs. E_{acc} @ 2.0 K curve shifted up. This suggested that there was still a substantial amount of nitrogen left in the niobium and that the nitrogen may play more than one role in the niobium.

In this paper we present a new study on two cavities which seeks to explain the correlation between the temperature dependant portion of the surface resistance with doping/EP as well as the higher than expected Q_0 at 2.0 K after surface reset.

CAVITY HISTORY

The two cavities chosen for this study were RDT-13 and TD-5; both cavities are 1.3 GHz TESLA shaped single cell cavities. RDT-13 uses the symmetric long end cell design (geometry factor of 279) made out of fine grain niobium RRR>250 from Tokyo-Denki. The cavity had been doped multiple times before this study, with a 40-45 μm chemistry reset between doping and an 80 μm reset before this study. After its last doping (800°C 3hrs N1A10 EP5), the cavity had a rather strange temperature independent component to its Q_0 vs. E_{acc} performance, similar to a medium field Q_0 slope. At the time this was presumed to be caused by a "bad" EP, and therefore 80 μm was taken off the inner surface to ensure what was thought to be a full surface reset, i.e. no doping left.

TD-5 is symmetric center cell design (geometry factor of 270) cavity made out of large grain niobium RRR>300 from Tokyo-Denki. After manufacturing and before the baseline test, the cavity was post purified at 1250°C with titanium. The full cavity histories after half-cell machining are presented in Table 1.

TEST PLAN

This study was designed to follow two different cavities through a single nitrogen doping followed by multiple EP removals with RF tests. After the first RF test for each EP, each cavity was warmed up to 120 K for a minimum of 5 hours and then re-cooled and tested. Such incremental steps with removal by EP continued until there was a positive slope in the temperature dependant portion of the surface resistance. In addition, after the first EP removal of 5 μm EP, the outsides of the cavities were BCP'ed removing 10 μm and retested. The full test outline is shown in Table 2.

RESULTS

This study was designed to follow two different cavities through a single nitrogen doping followed by multiple EP removals with an RF test after each removal. The RF data is presented in multiple ways; Q_0 vs. E_{acc} at 2.0 K, temperature independent and dependant surface resistance vs field, as well as low field Q_0 vs. T on TD-5.

* Authored by Jefferson Science Associates, LLC under U.S. DOE Contract No. DE-AC05-06OR23177 with supplemental funding from the LCLS-II Project U.S. DOE Contract No. DE-AC02-76SF00515
#ari@jlab.org

PERFORMANCE OF DRESSED CAVITIES FOR THE JEFFERSON LABORATORY LCLS-II PROTOTYPE CRYOMODULE - WITH COMPARISON TO THE PRE-DRESSED PERFORMANCE*

A. D. Palczewski# and K. Davis, JLAB, Newport News, VA, USA
F. Furuta, M. Ge, D. Gonnella and M. Liepe Cornell University, Ithaca, NY, USA

Abstract

Initial vertical RF test results and quench studies for six of the eight undressed 9 cell cavities slated for use in the Jefferson laboratory LCLS-II prototype cryomodule were presented at IPAC2015[1]. For the final string 2 more cavities AES029 and AES030 (work done at Cornell) are being processed and tested for qualification before helium vessel welding. In addition, AES034 (initial R&D treatment) is being reworked with the current production protocol after a surface reset to improve the overall performance. After final qualification all 8 cavities will be welded into helium vessels and equipped with HOM couplers. In this paper we will present the final undressed and dressed vertical RF data comparing the changes in the surface resistance before their installation in the cryomodule string.

INTRODUCTION

The current doping protocol for the baseline design as well as for production is N2/6 + EP5 (nitrogen injection @ 800C for 2 minutes at an average pressure of 25mtorr, followed by 6 minutes under vacuum and then a 5µm electro-polish)[1-4]. The cavities used in the prototype module were already used in doping studies during the R&D phase. Because of this, all but one cavity was doped more than once. Two of the cavities used in the prototype string will not have the baseline doping. One is AES031 which was the only cavity to receive only one doping, and AES030 which was accidentally doped for 6 minutes rather than 2 and received a larger EP (14µm rather than 5 µm) which at the time was intended to compensate for the extra nitrogen. The final doping parameters and number of dopings for each cavity is shown in Table 1.

Table 1: Doping Parameters for 9 Cell Cavities and Total Doping Cycles

Cavity ID	Final doping	Times doped
AES029	N2/6 EP5	2
AES030	N6/6 EP14	2
AES031	N20/30 EP26	1
AES032	N2/6 EP5	2
AES033	N2/6 EP5	2
AES034	N2/6 EP5	3
AES035	N2/6 EP5	2
AES036	N2/6 EP5	2

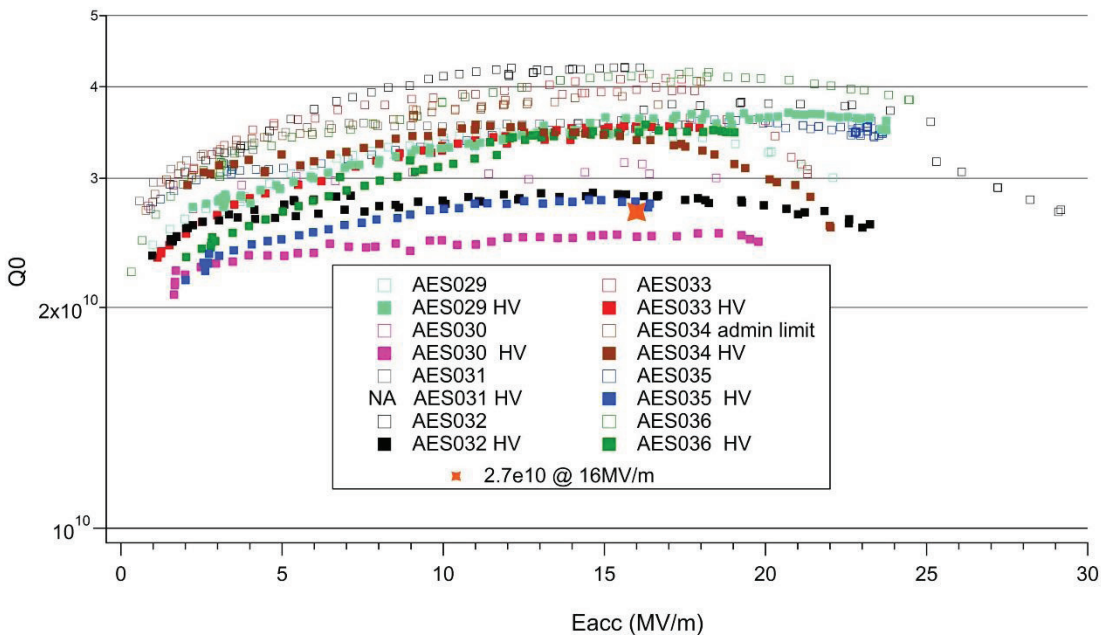

Figure 1: Q vs Eacc @ 2.0K before (solid squares) or after (open squares) HV welding and HOM installation. All data corrected to superconducting flanges if SS flanges were used.

* Authored by Jefferson Science Associates, LLC under U.S. DOE Contract No. DE-AC05-06OR23177 with supplemental funding from the LCLS-II Project U.S. DOE Contract No. DE-AC02-76SF00515
#ari@jlab.org

CRYOMODULE TESTING OF NITROGEN-DOPED CAVITIES*

D. Gonnella†[1], B. Clasby[1], R. Eichhorn[1], B. Elmore[1], F. Furuta[1], M. Ge[1], A. Grassellino[2], C. Grimm[2], D. Hall[1], Y. He[1], G. Hoffstaetter[1], J. Holzbauer[2], J. Kaufman[1], P. Koufalis[1], M. Liepe[1], J.T. Maniscalco[1], O. Melnychuk[2], T. O'Connell[1], A. Palczewski[3], Y. Pischalnikov[2], C. Reece[3], P. Quigley[1], A. Romanenko[2], D. Sabol[1], W. Schappert[2], J. Sears[1], D. Sergatskov[2], E. Smith[1], and V. Veshcherevich[1]

[1]CLASSE, Cornell University, Ithaca, NY 14853, USA
[2]FNAL, Batavia, IL 60510, USA
[3]TJNAF, Newport News, VA 23606, USA

Abstract

The Linac Coherent Light Source-II (LCLS-II) is a new FEL x-ray source that is planned to be constructed in the existing SLAC tunnel. In order to meet the required high Q_0 specification of 2.7×10^{10} at 2 K and 16 MV/m, nitrogen-doping has been proposed as a preparation method for the SRF cavities in the linac. In order to test the feasibility of these goals, four nitrogen-doped cavities have been tested at Cornell in the Horizontal Test Cryomodule (HTC) in five separate tests. The first three tests consisted of cavities assembled in the HTC with high Q input coupler. The fourth test used the same cavity as the third but with the prototype high power LCLS-II coupler installed. Finally, the fifth test used a high power LCLS-II coupler, cavity tuner, and HOM antennas. Here we report on the results from these tests along with a systematic analysis of change in performance due to the various steps in preparing and assembling LCLS-II cavities for cryomodule operation. These results represent one of the final steps to demonstrate readiness for full prototype cryomodule assembly for LCLS-II.

INTRODUCTION

The Linac Coherent Light Source II (LCLS-II) is a new CW FEL that will be built in the existing SLAC tunnel. Due to requirements for high cryogenic efficiency, the SRF cavities in the machine will be prepared using nitrogen-doping [1]. A large collaborative effort has been undertaken between Fermilab, Jefferson Lab, and Cornell to research and develop the SRF technology for LCLS-II's main linac. The final step before building prototype cryomodules was a serious of single-cavity cryomodule tests at the three labs. This paper will discuss the results of five cryomodule tests in the Cornell Horizontal Test Cryomodule (HTC). The HTC is a full cryomodule capable of holding a single 9-cell cavity. Its design is very similar to the design for the full LCLS-II main linac cryomodule. For details on the HTC and it's adaption to use LCLS-II cavities, see [2].

* Work supported by the US DOE and the LCLS-II High Q Program.
† dg433@cornell.edu

ORGANIZATION OF CRYOMODULE TESTS

A total of five cryomodule tests were completed at Cornell. These represent a systematic study of the SRF technology to be used in the LCLS-II main linac cryomodules. Of the five tests, four different cavities were used. Details on the cavities and the tests are shown in Table 1. These tests were organized in such a way to first test the feasibility of the high Q_0 specification (by installing with High Q input couplers), then to test the LCLS-II high power coupler (by measuring potential degradation as a result of the coupler installation on a previously tested cavity), and finally to test a fully dressed cavity with LCLS-II coupler and tuner. The results here are broken up by main topic rather than by each tests: changes from vertical to horizontal test, coupler studies, tuner studies, and cool down and flux trapping studies.

CHANGES FROM VERTICAL TO HORIZONTAL TEST

There is much concern in differences in how a cavity performs when tested vertically versus horizontally. Since assembly in cyomodule is much more difficult and involved that assembly on a vertical test stand, it has been widely accepted that some loss in cavity Q_0 will occur. Here we present a systematic look at how cryomodule assembly affects Q_0.

HTC9-1

The first HTC test consisted of a cavity dressed in an ILC helium vessel and assembled with high Q input coupler. The purpose of this test was to check the feasibility of meeting the LCLS-II Q_0 specifications after an assembly in cryomodule. The Q_0 vs E performance of the cavity at 2.0 K before dressing in vertical test and after assembly in the HTC is shown in Fig. 1. Before dressing, the cavity quenched at 15 MV/m at a Q of $(3.5 \pm 0.4)\times10^{10}$. After dressing and assembly in the HTC, the cavity quenched at 14 MV/m with a Q_0 of $(3.2 \pm 0.3)\times10^{10}$. This drop in Q_0 was attributed to a 1 ± 0.1 nΩ increase in residual resistance.

FUNDAMENTAL STUDIES ON DOPED SRF CAVITIES*

D. Gonnella†, T. Gruber, J. Kaufman, P. Koufalis, M. Liepe, and J.T. Maniscalco
CLASSE, Cornell University, Ithaca, NY 14853, USA

Abstract

Recently, doping with nitrogen has been demonstrated to help SRF cavities reach significantly higher intrinsic quality factors than with standard procedures. However, the quench fields of these cavities have also been shown to be frequently reduced. Here we report on fundamental studies of doped cavities, investigating the source of reduced quench field and exploring alternative dopants. We have focused on studying the quench of nitrogen-doped cavities with temperature mapping and measurements of the flux penetration field using pulsed power to investigate maximum fields in nitrogen doped cavities. We also report on studies of cavities doped with other gases such as helium. These studies have enabled us to shed light on the mechanisms behind the higher Q and lower quench fields that have been observed in cavities doped with impurities.

INTRODUCTION

Nitrogen-doping of SRF cavities has recently been developed as a new cavity preparation technique in order to reach higher intrinsic quality factors Q_0 than have been previously achievable with standard niobium cavities [1]. Nitrogen-doping consists of treating niobium cavities in a UHV furnace at high temperatures with a small amount of nitrogen gas. This treatment has been shown to cause an anti-Q slope in the medium field region (between 5 and 20 MV/m) opposite the usual medium field Q slope observed. However, this improvement is not without its trade offs: more often than not nitrogen-doped cavities quench at lower fields than undoped cavities. The cause of this lower field quench is not yet well understood.

In order to better understand the underlying mechanisms of the success and potential pitfalls of nitrogen-doped cavities (and cavities doped with other gases) a research program is ongoing at Cornell. Here we discuss our latest results specifically focusing on the development of a new nitrogen diffusion simulation, quench studies in both CW and pulsed mode, and doping a cavity with helium gas.

DOPING PROCESS STUDIES

The diffusion of nitrogen into niobium is well described in [2]. We have developed a code based on this model to accurately predict nitrogen concentration in niobium for a given set of treatment parameters (temperature, time, etc.). In addition to implementing the model in [2], we have added a calculation for how the nitrogen diffuses further into the niobium when the source is removed; i.e. when the niobium continues to "bake" in vacuum after the doping. By having a good understanding of how the treatment parameters affect material properties we can better predict a good "recipe" for doped cavities. Figure 1 shows an example run of our model. Shown is the nitrogen concentration in niobium as a function of depth for a treatment at 800°C for 20 minutes with nitrogen followed by 30 minutes in vacuum (anneal time). Also shown are results of secondary ion mass spectroscopy (SIMS) on a sample treated in this way. We can clearly see that in the bulk the simulation agrees with the SIMS data. This result is very promising: it shows that the model can accurately predict nitrogen concentration.

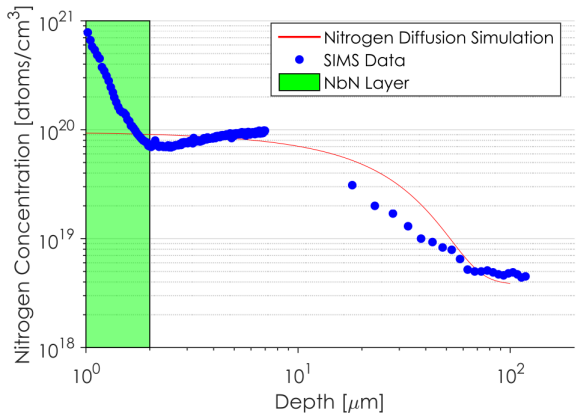

Figure 1: A plot of the N_2 concentration as predicted by the diffusion model compared with measurements on a nitrogen-doped niobium sample. Sample was treated with three cavities at 800°C for 3 hours in vacuum followed by 800°C in 60 mTorr of N_2 for 20 minutes followed by an additional 30 minutes in vacuum.

The model also can predict the drop in nitrogen pressure during the doping that we observe as cavities take nitrogen. The results of this simulation along with pressure drop data from a nitrogen-doping is shown in Fig. 2. We can see that the model accurately predicts the correct pressure drop for a given treatment. More importantly however, this confirms that the pressure of nitrogen during the doping does not affect the amount of nitrogen taken in by the niobium. The model described in [2] leads to a change in pressure that depends only on $\sqrt{t}$. This is a very important result that demonstrates that it is indeed feasible to reproduce similarly prepared cavities in different furnaces and at slightly different pressures. This is also consistent with measurements observed in which cavities that were prepared with almost the same parameters - except for differences in the nitrogen

* Work supported by NSF grant PHY-1416318 and the US DOE and the LCLS-II High Q Program
† dg433@cornell.edu

ISBN 978-3-95450-178-6

STUDY OF SLIP AND DEFORMATION IN HIGH PURITY SINGLE CRYSTAL NB FOR ACCELERATOR CAVITIES*

D. Kang, D.C. Baars, A. Mapar, T.R. Bieler#, F. Pourboghrat, MSU, East Lansing, MI 48824, USA
C. Compton, FRIB, East Lansing, MI 48824, USA

Abstract

High purity Nb has been used to fabricate accelerator cavities over the past couple decades, and there is a growing interest in using large grain ingot Nb as an alternative to the fine grain sheets. Plastic deformation governed by slip is complicated in body-centered cubic metals like Nb. Besides the crystal orientation with respect to the applied stress (Schmid effect), slip is also affected by other factors including temperature, strain rate, strain history, and non-Schmid effects such as non-glide shear stresses and twinning/anti-twinning asymmetry. A clear understanding of slip is an essential step towards modeling the deep drawing of ingot slices, and hence predicting the final microstructure/performance of cavities. Two groups of single crystals, with and without a prior heat treatment, were deformed to about 40% engineering strain in uniaxial tension. Differences in flow stresses and active slip systems between the two groups were observed, likely due to the removal of pre-existing dislocations. Crystal plasticity modeling of the stress-strain behavior suggests that the non-Schmid effect is small in Nb, and that the deep drawing process might be approximated with a Schmid model.

INTRODUCTION

Large grain Nb is being investigated for fabricating superconducting radiofrequency (SRF) cavities for particle accelerators, as a promising alternative to the traditional approach using fine grain Nb sheets [1-4]. In the cavity forming process, grain orientations, active slip systems, dislocation substructure, and recrystallization during heat treatments are interrelated from the metallurgical point of view [4] – slip behavior depends on how grains are oriented with respect to the applied stress; slip and interactions of slip systems result in a certain dislocation substructure; the dislocation substructure determines whether recovery or recrystallization occurs, and resulting dislocation substructure may be defective regions that trap magnetic flux [5]. Establishing the correct model for slip systems is particularly important for predicting the microstructural evolution during deep drawing.

For body-centered cubic (bcc) metals, the close packed (hence slip) directions are one of the four <111> directions, and there are no close packed planes like there are in face-centered cubic metals [6]. Planes containing the close packed direction in a decreasing order of inter-planar spacing are {110}, {112}, and {123}. As no stable stacking faults have been found in bcc metals, no slip planes are defined by dislocation dissociations. These features complicate slip in bcc metals.

In bcc metals, edge dislocations have lower lattice friction and are more mobile than screw dislocations at room temperature, and the movement of screw dislocations is the rate controlling factor during plastic deformation [4]. Since screw dislocation motion is thermally activated, it will likely occur by nucleation of kink pairs on well-defined atomic planes. The kink pair nucleation mechanism gives rise to the temperature and strain rate dependence of the flow stress in bcc metals [6].

The low mobility of bcc screw dislocations can be partly explained by the core relaxation theory [7, 8]. The core of a <111> bcc screw dislocation tends to spread onto three symmetric {110} or {112} planes, which results in a non-planar core and lowers the mobility of screw dislocations. Consequently, screw dislocations are affected by non-glide (out of slip plane) shear stresses, which violates the Schmid law. This relaxation also adds to the waviness of slip traces, since cross slip can occur on two of the three {110} or {112} planes to follow a slip plane with a high resolved shear stress. As a result, long, drawn-out screw dislocations are left behind during plastic deformation and are observable.

There has been no consensus thus far regarding the core structure of screw dislocations in Nb [6]. Seeger has argued that the core relaxation depends on both temperature and purity [9, 10]. The fundamental slip planes change from {110} at low temperatures (<100 K) to {112} at higher temperatures due to a change in the core structure. Experimental results from many bcc metals support this theory, though there are exceptions [11-15]. On the other hand, interstitial impurities such as hydrogen stabilize the {110} relaxation [8, 16]. SRF cavities are fabricated from high purity Nb at room temperature, so {112} relaxation should be favored over {110}. However, the forming process could easily lead to hydrogen contamination, so both relaxations may coexist [7].

Another phenomenon unique to bcc metals is the twinning/anti-twinning asymmetry, in which a smaller resolved shear stress is required to move a screw dislocation in the twinning sense of slip than in the anti-twinning sense [7, 17]. The non-planar screw dislocation cores and the twinning/anti-twinning asymmetry give rise to the non-Schmid effects in bcc metals, and affect the critical resolved shear stress for a given slip system to varying extents [7].

The relationship between slip systems changes with deformation due to rotation of the crystal with respect to

*Work supported by the U.S. Department of Energy, Office of High Energy Physics, through Grant No. DE-FG02-09ER41638.
#bieler@egr.msu.edu

ISBN 978-3-95450-178-6

SECONDARY ELECTRON YIELD OF ELECTRON BEAM WELDED AREAS OF SRF CAVITIES

M. Basovic, S. Popovic, M. Tomovic, L. Vuskovic, Center for Accelerator Science, Old Dominion University, Norfolk, VA 23529, USA
A. Samolov, F. Cuckov, Department of Engineering, University of Massachusetts, Boston, MA 02125, USA

Abstract

Secondary Electron Emission (SEE) is a phenomenon that contributes to the total electron activity inside the Superconducting Radiofrequency (SRF) cavities during the accelerator operation. SEE is highly dependent on the state of the surface. During electron beam welding process, significant amount of heat is introduced into the material causing the microstructure change of Niobium (Nb). Currently, all simulation codes for field emission and multipacting are treating the inside of the cavity as a uniform, homogeneous surface. Due to its complex shape and fabricating procedure, and the sensitivity of the SEE on the surface state, it would be interesting to see if the Secondary Electron Yield (SEY) parameters vary in the surface area on and near the equator weld. For that purpose, we have developed experimental setup that can measure accurately the energy distribution of the SEY of coupon-like like samples. To test the influence of the weld area on the SEY of Nb, dedicated samples are made from a welded plate using electron beam welding parameters common for cavity fabrication. SEY data matrix of those samples will be presented.

INTRODUCTION

Intrinsic quality factor (Q factor) is a measure of quality of Superconducting Radiofrequency (SRF) cavities. Q factor is highly dependent of the state of the cavity surface and therefore all fabrication and preparation processes are having an effect on the final shape of the Q factor curve. Impurities and defects are introduced to Niobium (Nb) surface during fabrication and preparation process and are added to the previously existing impurities of Nb sheet metal. Most of the imperfections of the surface are introduced during forming and welding of the half cells. Performance of the cavities is reduced due to the presence of these surface imperfections and is limiting the overall performance of linear accelerators. In order to mitigate the influence of surface irregularities and improve the operation, cavities are subjected to an extensive etching and cleaning procedure [1]. This procedure has had a great success in increasing the maximum achievable accelerating gradient [2]. Regardless of the all surface processing so far, theoretical accelerating gradient maximum for Nb is yet to be achieved [3]. In ideal case, accelerating cavities are under perfect vacuum allowing only presence of accelerated particles. In real case, combination of imperfect vacuum, cavity surface irregularities, and presence of high electric and magnetic fields provide the initial number of free particles and the means for their multiplication. Phenomenon which describes the multiplications of free charged particles inside the cavity is called Secondary Electron Emission (SEE). At high accelerating gradients main power losses in the cavities are due to field emission [4] and multipacting [5]. Magnetic and electric field confined inside the cavity can accelerate free particles toward the surface. Due to the impact more free electrons can be released into vacuum causing a net increase in the number of free charged particles. The magnitude that describes the SEE is called Secondary Electron Yield (SEY). SEY is defined as the number of emitted electrons per impacting electron. If the value of SEY is larger than one, buildup of free particles will cause the increasing power losses, leading to the "quenching" of cavity.

Manipulating the SEY curve of a material has been a research topic ever since the discovery of SEE. Depending on the application goal can be to increase or decrease the SEY values of the material. Magnitude of the SEY is a function of the impacting electrons [6] and the angle at which they are impacting the surface [7]. For cavities and beam tubes research has been conducted towards the reducing the SEY magnitude of the used material. Several methods have been developed and used for decreasing the value of SEY. Some of those methods include surface coatings [8], baking [9], exposure to glow discharge [10], and electron beam irradiation [6].

Multipacting and field emission simulation codes are currently modeling the cavity as uniform homogeneous structure with uniform properties of SEY across its surface. Based on the research showing the effect of baking on SEY and the fact that during welding amount of heat induced in material is changing its microstructure in an area of the weld, we believe that it is important to determine if and to what extent the SEY has changed in the area of weld.

Accelerating cavity is a very complex structure to fabricate. During the fabrication process of cavities is when the majority of the surface impurities are introduced. Joining of cavity half cells is performed by electron beam welding. Significant amount of heat is induced in material during the process causing the microstructure changes in the area of and close to welding. Three separate microstructures can be observed in the weld area of equator and iris [11, 12]. At the equator, weld zone is formed from melted Nb during welding process. This zone has a distinct microstructure. Heat affected zone is found on both sides of the weld zone and formed during welding but without melting of

ISBN 978-3-95450-178-6

HIGH FLUX THREE DIMENSIONAL HEAT TRANSPORT IN SUPERFLUID HELIUM AND ITS APPLICATION TO A TRILATERATION ALGORITHM FOR QUENCH LOCALIZATION WITH OSTS

T. Junginger - TRIUMF Canada's National Laboratory for Particle and Nuclear Physics and Helmholtz-Zentrum Berlin fuer Materialien und Energie (HZB), Germany *
P. Horn, Dresden Institute of Technology (TU Dresden), Germany
T. Koettig, K. Liao, A. MacPherson CERN, Geneva, Switzerland
B.J. Peters Karlsruhe Institute of Technology (KIT), Germany

Abstract

Oscillating superleak transducers of second sound can be used to localize quench spots on superconducting cavities by trilateration. However propagation speeds faster than the velocity of second sound are usually observed impeding the localization. Dedicated experiments show that the fast propagation cannot be correlated to the dependence of the velocity on the heat flux density, but rather to boiling effects in the vicinity of the hot spot. 17 OSTs were used to detect quenches on a 704 MHz one-cell elliptical cavity. Two different algorithms for quench localization have been tested and implemented in a computer program enabling direct cross-checks. The new algorithm gives more consistent results for different OST signals analyzed for the same quench spot.

INTRODUCTION

Small defects on the inner surface of superconducting cavities can result in a quench, the transition to the normal state. Heat fluxes in the kW/cm^2 range can occur at the cavity surface during a quench. For quality assurance and improvement of the production process defects have to be localized and investigated. So-called Oscillating Superleak Transducers (OST) have been used since 2008 for this localization [1]. Several OST sensors and the time of flight information make it possible to localize the defect by trilateration. In such tests however it is usually observed that the speed of heat propagation exceeds the speed of second sound literature values. There are several reasons for this effect. The second sound velocity depends on the heat flux density as will be discussed below. There could be a delay between the generation of second sound and the detection of dissipation by the RF signal [2]. In [3] we have shown that the heat transport in superconducting niobium can be significantly faster than the speed of second sound. Based on this result Eichhorn and Markhan have performed calculations taking into account the geometry between the OST detectors and the quench spot [4]. As a practical solution to cope with this effect at DESY an algorithm has been developed that uses a minimization method with the geometrical constraint that the quench spot needs to be on the cavity surface [5]. The algorithm will give accurate results if the quench spot is on or close to the equator. The applicability to different cavity geometries is not obvious. In order to develop a more suitable algorithm for non-elliptical cavities the physics of high flux heat transport in superfluid helium needs to be understood in detail. Here we present dedicated experiments with heaters as simulated quench hot spots. We have extended the Matlab code from [5] to allow to be used for arbitrary cavity shapes and added a new algorithm for quench localization. The two algorithms were finally tested for consitency with data obtained from a quench on a single-cell cavity equipped with 17 OSTs.

Dependence of the Second Sound Velocity on the Heat Flux Density in the Two-Dimensional Case

A possible explanation for propagation speeds exceeding literature values of the second sound velocity could be the dependence of the second sound speed on the heat flux density. Two publications from 1951 have addressed this theoretically in [6] and experimentally in [7]. In particular the measurements presented in [7] have qualitatively proven that the second sound velocity v_2 depends on the heat flux density q. This dependence of v_2 on q is based on two assumptions. First, the temperature of the second sound for greater heating pulses is significantly higher than the bath temperature due to localized heating, so that the propagation velocity is different. Second, the normal fluid component carries the entire entropy and a temperature rise means creation of more normal fluid component. In order to describe the change in velocity of the second sound Dessler and Fairbank introduced a correction factor Γ that reflects the sensitivity to heat flux density [8]. The measurable velocity of second sound v_2 is thus composed of the velocity for very small heating pulses $v_{2,0}$ and a term which is linearly dependent on the heat flux density q [8].

$$v_2 = v_{2,0} + \Gamma \cdot q \quad (1)$$

This relation was obtained in a two dimensional setup, from measurement in channels having constant cross section, so that the heating power density remains also constant. For a statement about the three-dimensional spread, the change of the heating power density must also be considered.

EXPERIMENTAL SETUP AND RESULTS

We have carried out experiments to determine the second sound velocity at different heat flux densities in three-

* tobi@triumf.ca

ISBN 978-3-95450-178-6

CHARACTERIZATION OF SRF MATERIALS AT THE TRIUMF μSR FACILITY

R.E. Laxdal, T. Buck, T. Junginger, P. Kolb, Y. Ma, L. Yang, Z. Yao,
TRIUMF, Vancouver, Canada
R. Kiefl, UBC, Vancouver, Canada
S.H. Abidi, U. of Toronto, Toronto, Canada

Abstract

μSR is a powerful tool to probe local magnetism and hence it can be used to diagnose flux penetration in Type-II superconductors. Samples produced at TRIUMF and with collaborators in both coin shaped and ellipsoidal geometries have been characterized by applying either transverse or parallel fields between 0 and 300mT and measuring flux entry as a function of applied field. Samples include Nb treated in standard ways including forming, chemistry, and heat treatments. Further, Nb samples have been doped with Nitrogen and coated with a 2 micron layer of Nb3Sn by collaborators from FNAL and Cornell respectively and measured in three field/geometry configurations. Analysis of the method in particular the effects of geometry and the role of pinning will be presented. Results of the measurements will be presented.

INTRODUCTION

μSR (muon spin rotation) is a powerful condensed matter technique to understand superconductors in terms of their magnetic-phase diagram and penetration depth, as well as characterize impurities based on muon diffusion. In the early 1970's new high-intensity, intermediate-energy accelerators were built at PSI, TRIUMF and LAMPF. These new "meson factories" produced pions (and therefore muons) several orders of magnitude more than previous sources - and in doing so, ushered in a new era in the techniques and applications of μSR. Since 2010 the SRF group at TRIUMF has been using the μSR technique to characterize materials and processing techniques typical for the SRF community using the TRIUMF surface muon beam [1]. Typical samples have been prepared from RRR Nb either as coins (flat and formed) and in a machined ellipsoid geometry. The samples are then treated with a number of surface and bulk techniques and subsequently tested with μSR to determine characteristics of the superconducting state. This paper gives details on the samples and preparation, geometrical effects and measurement results.

μSR TECHNIQUE

Surface muons are emitted from a production target 100% spin polarized with momentum and energy of 29.8MeV/c and 4.1MeV respectively and are implanted one at a time into the sample. When the muon decays (half life=2.2μsec) it emits a fast decay positron preferentially along the direction of its spin at the time of the decay. By detecting the rate of emitted positrons as a function of time with two detectors placed symmetrically around the sample the time evolution of the spin precession of the muon and therefore the magnetic field properties experienced by the muon can be inferred from the time dependent asymmetry in the positron decay.

The samples are placed in a cryostat surrounded by field inducing coils. Field penetration measurements are primarily done by cooling the sample to below T_c (2K is common) in zero field and then applying a static magnetic field perpendicular to the initial spin polarization to see if field is in the sample. Specifically the asymmetry signal gives information on the volume fraction of the host material sampled by the muon that does not contain magnetic field.

This signal can be used to characterize the superconducting state, particularly the transition from Meissner state to mixed state. When completely in the Meissner state there is no field in the sample and the asymmetry is maximized. As the field increases flux will eventually enter the superconductor as it enters the mixed state and the asymmetry signal will be reduced. Further the rate of de-coherence of the asymmetry signal gives a measure of the non-uniformity of the sampled field.

The muon beam has a Gaussian transverse distribution with a physical half-width of approximately 8mm. The spin-polarized muons are implanted into the sample, and quickly stop at interstitial sites in the bulk. The energy of the surface muons means that they are deposited about 150 μm into the sample so the measurement represents a bulk as opposed to a surface probe.

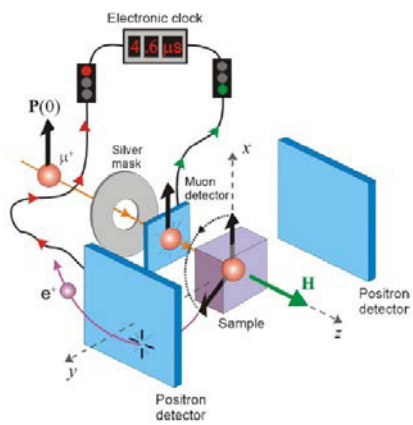

Figure 1: TF-μSR setup with the initial muon spin polarization perpendicular to the magnetic field. The silver mask in front of the sample restricts the muon implantation to the central region of the sample.

ISBN 978-3-95450-178-6

MUON SPIN ROTATION ON TREATED NB SAMPLES IN PARALLEL FIELD GEOMETRY

S. Gheidi, T. Buck, UBC, Vancouver, Canada
M. Dehn, Technische Universität München, München, Germany
R. Kiefl, R. E. Laxdal, G. Morris, T. Junginger, TRIUMF, Vancouver, Canada

Abstract

Muon Spin Rotation (μSR) is a powerful tool to probe local magnetism in matter and hence can be used to diagnose the entry of magnetic flux in superconductors. First measurements on SRF samples were done with an external DC field applied perpendicular to the sample [1] (transverse geometry) with the muons applied to the sample face. Here, the results are strongly impacted by demagnetization, pinning strength and edge effects. A new spectrometer has been developed to allow sample testing with a field varying from 0 to 300 mT applied along the sample face (parallel geometry) analogous to RF fields in SRF resonators. The geometry is characterized by a small demagnetization factor reducing the impact of pinning and edge effects on field of first flux entry. The beamline installation and first results comparing transverse and parallel results will be presented.

MOTIVATION

Superconducting radio frequency (SRF) cavities face a limiting issue in which as the RF power input increases to achieve higher acceleration gradients, the surface resistance in the cavity walls increases causing the quality factor (Q) of the cavity to drop significantly (Figure 1).

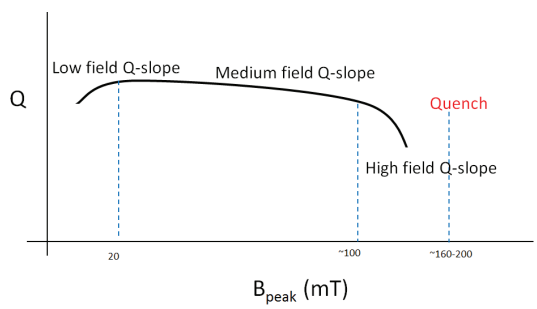

Figure 1: The quality factor of SRF cavities drops significantly peak magnetic fields are increased.

The reason for this shortcoming is not yet fully understood, however, it has been found that the performance of the cavity is heavily influenced by its surface preparations [2]. Common preparations include surface etching, bake-outs, and introducing impurities to the niobium. It is difficult and costly to test treatments on cavities so a technique such as μSR, which allows for the testing of small samples mirroring potential cavity treatments with high sensitivity is important for making significant progress in the improvement of SRF cavities.

EXPERIMENTAL SETUP

Muon Spin Rotation

Muon Spin Rotation (μSR) is a magnetic probe that can be used to detect the local magnetic properties of materials with extremely high sensitivity. μSR takes advantage of the preferential emission of a positron along the polarization of the muon before its decay. By detecting the location of emitted positrons as a function of time with two detectors, in the case of parallel geometry “up" and “down", the spin precession of the muons and therefore magnetic field properties can be inferred through an Asymmetry signal:

$$Asy(t) = \frac{N_U(t) - \alpha N_D(t)}{N_U(t) + \alpha N_D(t)} \quad (1)$$

Here, $N_U(t)$ is the number of counts in the “Up" detector and $N_D(t)$ is the number of counts in the “Down" detector. The parameter α is added to account for detector efficiencies and to remove any bias between telescopes caused by uneven solid angles; in the case where the detectors are identical in efficiency, α assumes a value of 1.

Previous μSR experiments on superconducting Nb samples had used a geometry where the applied magnetic field is perpendicular to the sample face. It was concluded that the treatments affect the strength of pinning in the nb [1]. The experiment presented in this paper involves an applied magnetic field parallel to the sample face in order to achieve a more accurate model of field interactions inside the cavity, namely the boundary condition that, $B_\perp = 0$.

A spectrometer capable of providing fields up to 300 mT parallel to sample faces was built using TRIUMF’s M20 C-leg beamline. The spectrometer consists of a dipole magnet which provides the applied field, an internal and external muon counter used to specify muon location, and “up" and “down" detectors for detecting emitted positrons (Figure 2(a)). Due to the presence of the Lorentz Force in parallel geometry, a steering magnet is also employed to pre-steer the μ^+ beam such that by the time the beam enters the dipole’s field domain, the beam is steered back to the center of the sample (Figure 2(b)).

The beamline delivers muons with energy of 3.87 MeV +/- 6% and momentum of 28.9 MeV/c. The muons have an average stopping distance of 100μm in the nb, as simulated by TRIM [3] (Figure 3).

ISBN 978-3-95450-178-6

DETERMINATION OF BULK AND SURFACE SUPERCONDUCTING PROPERTIES OF N_2-DOPED COLD WORKED, HEAT TREATED AND ELECTRO-POLISHED SRF GRADE NIOBIUM

S. Chetri, D.C. Larbalestier, P.J. Lee, Applied Superconductivity Center,
National High Magnetic Field Laboratory, FSU, FL 32310, USA
P. Dhakal, Thomas Jefferson National Accelerator Facility, VA 23606, USA
Z-H Sung, United States Steel Research and Technology Center, PA 15120, USA

Abstract

Nitrogen-doped cavities show significant performance improvement (Q_0) beyond the expected limits due to lowered RF surface resistance [1,2]. However, such cavities quench in the medium accelerating field regime (B_{peak} = 80 - 120 mT) for reasons that remain to be clearly explained. In this study we explore the influence of N_2-doping on the surface and bulk superconducting properties of cold worked SRF Nb, and then compare these results with those previously obtained on similarly cold worked samples given conventional cavity processing without N_2 treatments. We present DC magnetization and AC susceptibility characteristics of a polycrystalline Nb rod drawn to a true strain of 4.2, after standard cavity chemical, thermal, and N_2-doping treatments. DC magnetic hysteresis showed that the N_2-doping significantly decreases the field of first flux penetration, H_{cp}. Temperature-variation-mode AC susceptibility showed that N_2-doping after an 800 °C anneal enhances the surface critical temperature, $T_{c,onset}$ ~9.4 K to values similar to that observed for 120 °C baking, suggestive of strong surface charging by nitrogen. Use of DC as well as AC techniques allows us to see that the bulk $T_{c,peak}$ shifts back to the typical T_c of annealed Nb, ~ 9.2 K after 800 °C, even as $T_{c,onset}$ is enhanced by N_2. It is also observed that r_{32} (H_{c3}/H_{c2}) ratio reverts to the Ginzburg-Landau (GL) value of ~1.7. The implication is clearly that N_2-doping affects the surface superconductivity of SRF-Nb without deteriorating the bulk properties.

INTRODUCTION

Recently, a nitrogen doping step has been introduced into the processing of SRF cavities which has resulted in an enhanced quality factor (Q_0) beyond the previously assumed theoretical limits [1]- [2]. However, this enhanced performance is offset by quenching in the mid RF field regime ($\boldsymbol{B_{peak}}$ ≈ 80 - 120 mT) [2]. The mid field quench phenomenon of the N_2-doped cavity appears near the lower critical field of niobium, thus implicating vortex penetration as its cause. Measurement of H_{cp}, the field of first flux penetration and its relationship to the often enhanced surface superconductivity critical field, H_{c3}, thus seems important. Our previous study of SRF-grade polycrystalline Nb [3] by surface-sensitive AC susceptibility showed that cold work can enhance the surface superconducting properties ($T_{c,onset}$ and the r_{32} (H_{c3}/H_{c2}) ratio), an observation that is in agreement with Casalbuoni's earlier study which showed that standard chemical and thermal cavity treatments enhance the surface superconductivity well beyond the GL ratio of ~ 1.7 [4]. Following our previous study, here we have investigated the surface and bulk superconductivity of Nb samples given the same processing history as the earlier samples, but with an additional recrystallization at 800 °C and N_2-doping step as recently employed in cavity fabrication. To characterize variations of surface and bulk superconductivity, we combined AC susceptibility with DC magnetic hysteresis. We are also implementing X-ray Photoelectron Spectroscopy (XPS), surface chemistry analysis in order to provide additional interpretation of the current findings.

EXPERIMENTAL

A SRF-grade poly-crystalline Nb rod was drawn to a true strain of 4.2, and then processed using the standard SRF Nb cavity fabrication steps established for the ILC (international linear collider): EP (electro-polishing), BCP (buffered chemical polishing), 120 °C/48h bake, and 800 °C/2h anneal. Our previous study [3] employing these processing steps showed a strong relationship between surface superconductivity and mechanical deformation. In order to clarify the new effects of N_2-doping, several sets of these drawn Nb samples were sent to Thomas Jefferson National Accelerator Facility (TJNAF) for recrystallization and nitrogen doping. These samples were in the as-drawn, 3h EP'ed and 95min BCP'ed condition, with diameter (0.75-1 mm).

These Nb rods were first annealed at 800 °C for 3 h in a chamber used for cavity heat treatments and at the end of the anneal nitrogen gas was injected into the furnace at a partial pressure of ~25 mTorr for 2 minutes after which the N_2 was removed and a final anneal at 800 °C for 10 minutes was given in order to diffuse N into the bulk. After return to room temperature, the N2-doped samples were further treated with an extra 10 min EP that removed ~5 μm of surface to follow the previous practice established for N_2-doped cavity processing.

After the doping process, the Nb wires were cut into ~7 mm lengths with a diamond saw in order to fit into the cryostat of the surface and bulk superconducting property measurement system. AC susceptibility was characterized in DC field-swept and temperature-variation mode with a 9 T Quantum Design PPMS (Physical Property Measurement System). Since the relevant layer for SRF performance is that within a penetration depth of the

AN INVESTIGATION OF CORRELATIONS BETWEEN MECHANICAL AND MICROSTRUCTURAL PROPERTIES OF HIGH PURITY POLYCRYSTALLINE NIOBIUM*

M. Zhao, D. Kang, T.R. Bieler#, Michigan State University, East Lansing, MI 48824, USA
C.C. Compton, Facility for Rare Isotope Beams, East Lansing, MI 48824, USA

Abstract

Superconducting radiofrequency (SRF) cavities made from high purity niobium are commonly used in particle accelerators. An understanding of the relationship between mechanical and functional properties and the processing history is essential in order to manufacture cavities with uniform performance. The crystallographic texture and microstructure in polycrystalline sheet varies considerably, and identifying its influence on properties is needed to achieve a better understanding of how to control properties of high purity niobium. Texture (preferred crystal orientations) strongly affects mechanical properties and formability of metals and alloys. Samples received from many lots of material from two suppliers, A and B, for building cavities for the Facility for Rare Isotopes were examined to identify relationships between these two properties. Texture of the undeformed niobium samples through the thickness was measured using Orientation Imaging Microscopy™ (OIM). Texture is identified with pole figures (PF), orientation distribution functions (ODF) and grain misorientation relationships. Stress-strain testing was done to identify ultimate tensile stress (UTS), elongation, 0.2% yield strength, and the hardening rate. From tests on many lots, there is no clear trend between the mechanical and material properties in high purity niobium. Correlations between various microstructural and mechanical properties show significant scatter and few apparent correlations.

INTRODUCTION

In order to manufacture cavities with uniform performance, understanding of the relationship between mechanical and microstructural properties is necessary. Niobium sheets can be ordered from many suppliers that meet established cavity specifications. However, the properties of the niobium sheets often show a large range of variability and exhibit random variations in properties.

It is well established that crystallographic texture is an inherent characteristic of metals produced by deformation processing and heat treatment, and has a significant influence on mechanical, physical as well as chemical properties of materials [1]. In general, there are relationships between the mechanical and material properties, which can provide useful information for improving a manufacturing process. For high purity niobium, these correlations are still not understood. As mechanical properties change throughout the fabrication process, the correlation between mechanical properties and texture is useful to predict the mechanical properties of the final product. Understanding of these relationships should enable manufacturing cavities with similar mechanical properties. Moreover, the large data set obtained can support additional research, so that when problems arise in manufactured cavities, there is a database to consult.

During the rolling process, different strain conditions take place in the surface and center, because the shear on the surface activates slip systems that rotate crystals differently from the plane-strain compression in the center [2]. Due to these differences, the plane-strain compression typically causes {111} to be approximately parallel to the sheet normal direction (ND) in the middle, which is blue orientation in the default color scale of OIM maps [2]. Shear on the surface normally causes {001} || ND, which is a red orientation [2].

MATERIALS AND METHODS

To study the mechanical and microstructural properties of high purity niobium, samples were cut from unused material area, as shown as Figures. 1 and 2 [3]. An Instron 4302 universal testing machine was used to measure tensile behavior systematically in experiments. SEM-EBSD measurements were made on a Camscan

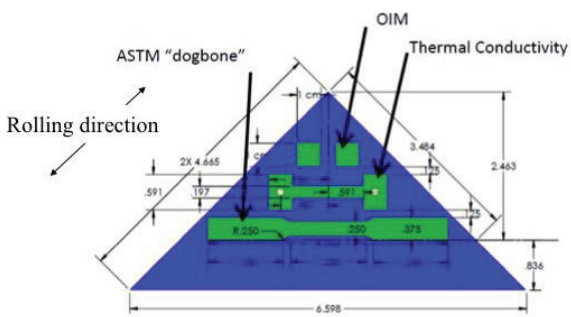

Figure 1: Layout of supplier A test samples [3].

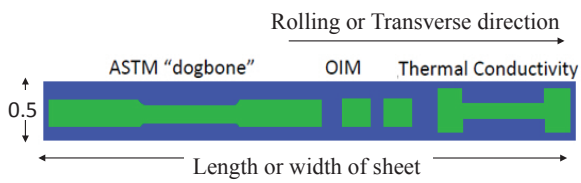

Figure 2: Layout of supplier B test samples.

*Work supported by the U.S. Department of Energy, Office of High Energy Physics, through Grant No. DE-FG02-09ER41638, and the Facility for Rare Isotope Beams
#bieler@egr.msu.edu

ISBN 978-3-95450-178-6

CHARACTERIZATION OF NITROGEN DOPING RECIPES FOR THE Nb SRF CAVITIES

Y. Trenikhina, A. Grassellino, O. Melnychuk, A. Romanenko, FNAL, Fermilab, USA

Abstract

Nitrogen doping enabled a new state-of-the-art performance standard for Nb SRF cavities. For the future development of this technology, it's vital to understand the mechanisms behind the performance benefits of N-doped cavities as well as the performance limitations, such as quench field. Following various doping recipes, cavity cutouts and flat niobium samples have been evaluated with XRD, SEM, SIMS and TEM in order to relate structural and compositional changes in the niobium near-surface to the quality of SRF performance. Annealing with nitrogen for various durations and at various temperatures, the Nb cavities demonstrated non-superconducting Nb nitride phases, followed by unreacted Nb with elevated N-interstitials concentration. We found that EP of the annealed cavities removes the unwanted niobium nitride phases, confirming that performance benefits are originating from the elevated concentration of N interstitials. The role of low temperature Nb hydride precipitants in the performance limitation of N-doped cavities was evaluated by TEM temperature dependent studies. Finally, characterization of the original cavity cutouts from the N-doped RF tested cavity sheds some light on quenching mechanisms.

INTRODUCTION

Fermilab's search for an optimal solution to the medium field performance degradation, led to the discovery of "nitrogen doping" of Nb cavities. Nitrogen doping of Nb cavities enabled new higher standards for Nb SRF cavity performance. This recipe yields reproducible improvement of the quality factor in addition to the reversal of the Medium Field Q-Slope [1] . Reported values of Q_0 are up to 3 times higher than for electropolished (EP) standardly prepared cavities, and up to 2 times higher than for EP cavities which had mild bake at 120°C. Cavities with non-typical, reversed MFQS show low values of microwave surface resistance.

N-doping of single- and nine-cells Nb 1.3 GHz cavities has a great potential to be adopted for a number of future particle accelerators. However, problems like limited quench field, remain unexplained as well as the origin of the performance benefits. Our characterization work was initiated to reveal the mechanisms leading to the unique SRF performance after N-doping. Our investigations consist of tracking material features of the Nb near-surface induced by the nitrogen doping and relating them to the results of RF cavity testing.

N-doping of Nb cavities includes two major processing steps: annealing of the cavity in the presence of nitrogen gas, and material removal through EP. Annealing of Nb cavities at 800°C in a UHV furnace with nitrogen partial pressure of $\approx 2*10^2$ Torr for different time durations is followed by EP and high pressure water rinsing (HPR). The amount of material that has to be removed depends on the duration of the 800°C annealing with nitrogen. Figure [need recent Q vs. E curve(s)] shows the results of RF characterization of the N-doped Nb cavities, which were subject to the described sequence with various experimental parameters.

X-Ray Diffraction (XRD), Scanning Electron Microscopy (SEM) and Transmission Electron Microscopy (TEM) at room and cryogenic temperatures were performed on Nb samples as well as on the cutouts taken directly from N-doped Nb cavities. A combination of those characterization techniques provides complete insight into the chemical and structural details of the near-surface on different length scales.

EXPERIMENTAL METHODS

Description of Nb Samples and Cavity Cutouts

Square samples were cut from the niobium sheets used for cavity fabrication. All Nb samples were electropolished (EP) prior to treatment with nitrogen. In order to reproduce the effect of the first step of nitrogen doping, Nb samples had been annealed in a UHV furnace at 800°C for time durations of 2 min and 20 min. After characterization of the effects of the first step of nitrogen doping, some Nb samples had been EP and characterized again.

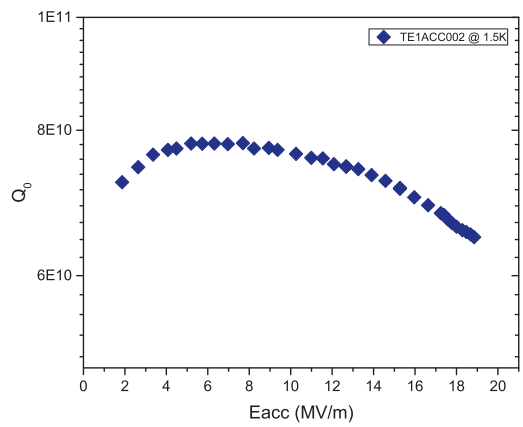

Figure 1: Performance of the Cavity 2 which was baked at 800°C for 20 min in nitrogen atmosphere and 5 μm were removed via EP.

Cavity cutouts for material characterization were taken from two TESLA shape 1.3 GHz fine grain cavities which underwent nitrogen doping with different parameters. The first cavity (labeled "Cavity 1" for the following) was baked in a UHV furnace at 1000°C with nitrogen gas for 10 min.

ISBN 978-3-95450-178-6

CRYSTAL PLASTICITY MODELING OF SINGLE CRYSTAL Nb*

A. Mapar, D. Kang, T. R. Bieler#, F. Pourboghrat, Michigan State University, East Lansing, MI 48824, USA
C. C. Compton, Facility for Rare Isotope Beams, East Lansing, MI 48824, USA

Abstract

Deformation behavior of niobium (Nb) is not thoroughly studied, although it is heavily used for superconducting applications. This deficiency of knowledge makes use of fine grain sheets desirable because they are easier to deform uniformly than anisotropic large grain sheets. Simulation models for deformation of Nb are limited. Therefore, design of a new manufacturing procedure is costly because models predicting the deformation of Nb are inaccurate.

Tensile tests were performed on single crystals with different orientations, to study the deformation behavior of Nb. Several crystal plasticity models were developed, calibrated and used to predict the deformation of single crystal tensile samples. This study compares the predictions of these models. As polycrystals are aggregates of single crystals, the model will also be useful for polycrystals.

INTRODUCTION

High-gradient SRF cavities are key enabling devices for high energy and high intensity science. Over the last decade the best cavities have achieved performance close to the theoretical limit (50 MV/m), but it has been challenging to fabricate cavities with reproducible properties and reproducible high performance. An increasing number of cavities are made from large-grain (≥ ~5-10 mm, low GB density), high purity (RRR ≥ 200) niobium (Nb) slices, which have often shown superior properties to similarly processed cavities made from polycrystalline sheet metal with ~50 μm grain size, notably higher quality factors (Q). There is still variability in cavity performance that limits the ability to build accelerator cavities that consistently achieve accelerating gradients above 35 MV/m, which is not understood. Until the origins of this variability are understood and brought under control, (or at least detectable at an early stage of fabrication), the ability to build next generation accelerators capable of detecting phenomena comparable to the convincing evidence for the Higgs Boson in 2012 [1], may not be achieved at an acceptable cost.

Mechanical cavity shape fabrication by traditional deep drawing, hydroforming, or other deformation history affects cavity performance. Defect structures that develop during deformation include dislocations, sub-structures with low and high angle boundaries, and altering the character of initial grain boundaries (GBs). These all influence the performance of surface chemical and thermal treatments on the cavity during the fabrication process.

This study is a continuation of [2] that was presented at SRF 2013, which along with [3], provides more details on development of the crystal plasticity model and experimental procedures.

CRYSTAL PLASTICITY CONSTITUTIVE MODEL DEVELOPMENT

Unlike continuum based finite element constitutive models that are in common use in finite element codes, crystal plasticity models simulate the physical slip processes that take place in a particular grain orientation in response to an imposed stress (or strain). Constitutive model development that is capable of simulating the stress-strain behavior of Nb single crystals is challenging, requiring novel approaches motivated by physical understanding to develop suitable hardening rules.

The inverse pole figure in Fig. 1a shows the orientation of the tensile axis nine single crystal tensile samples. Fig. 1b shows the stress-strain behavior of these samples. The long nearly flat flow stress evolution in many of the orientation near the center of the inverse pole figure triangle implies that very little dislocation accumulation took place, i.e. dislocations enter and

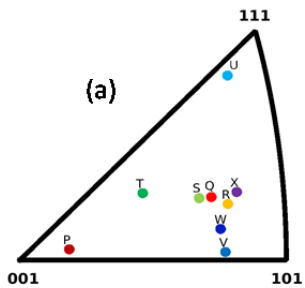

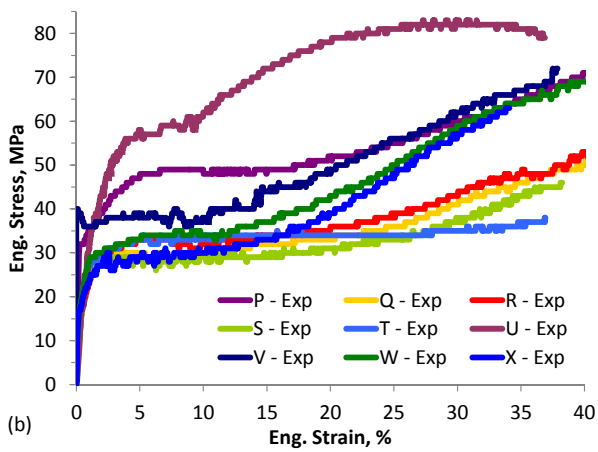

Figure 1: (a) The tensile axis of samples used in this study. (b) Stress-strain response of annealed single crystal samples.

*Work supported by the U.S. Department of Energy, Office of High Energy Physics, through Grant No. DE-FG02-09ER41638.
#bieler@egr.msu.edu

FIELD EMISSION FROM A THERMALLY OXIDIZED Nb SAMPLE

S. Lagotzky*, G. Müller, University of Wuppertal, D-42097 Wuppertal, Germany

Abstract

The activation of enhanced field emission (EFE) on Nb is strongly influenced by the thickness d_{ox} of the surface oxide. EFE measurements on a single crystal Nb sample with an increased d_{ox} of about 100 nm after thermal oxidation (TO) revealed first EFE at 100 (150) MV/m and emitter number densities N up to 30 (40) cm^{-2} at 225 MV/m after cleaning with ionized N_2 (dry ice cleaning, DIC). These results mean an improvement compared to wet anodized Nb. Moreover, TO is able to reduce N at the intended electric peak field of future accelerating structures for the International Linear Collider (ILC) by a factor 20 compared to the actually used Nb after DIC. The remaining EFE was mainly caused by surface defects and partially molten features with onset fields above 90 MV/m. Removal of the oxide by a heat treatment under ultra-high vacuum activated additional emitters and confirmed the suppression of EFE by the Nb oxide.

INTRODUCTION

Enhanced field emission (EFE) from particulates and surface defects is one of the main field limitations of superconducting Nb cavities required for the International Linear Collider (ILC) [1]. The activation field E_{act} of such emitters and the emitter number density N is strongly influenced by the thickness d_{ox} of the Nb oxide layer. Removal of the native oxide layer (d_{ox} = 5 nm [2]), e.g. by heat treatments (HT) under UHV up to 800°C, increases N significantly for E_{act} up to 160 MV/m with onset fields E_{on} down to 40 MV/m [3, 4]. Former EFE measurements on electrochemically oxidized Nb samples yielded for increasing d_{ox} between 53 and 463 nm a reduction of N from 18 to 2 cm^{-2} at an E_{act} of 95 MV/m [5]. Similarly oxidized cavities proved that their quality factor is not affected by oxide layers up to 100 nm [6–8].

In order to improve the EFE performance of Nb surfaces with respect to ILC requirements (electric peak fields of 70 MV/m), we report here on a combination of Nb oxidation with advanced surface cleaning techniques. Single crystal Nb was used to avoid any grain boundary effects. Thermal oxidation (TO) in air was applied to receive a homogeneous layer with d_{ox} of about 100 nm. Such a TO should also be applicable for cavities. Systematic EFE measurements by means of a field emission scanning microscope (FESM) and a scanning electron microscope (SEM) on the same sample were performed both after TO with N_2-cleaning or dry ice cleaning (DIC) [9]. Supplementary measurements after removal of the oxide in both cases by a heat treatment (HT) under ultra-high vacuum (UHV) were carried out to prove the EFE suppression by the Nb oxide.

*s.lagotzky@uni-wuppertal.de

EXPERIMENTAL DETAILS

Samples

We have used single crystal Nb discs (Ø=28 mm) with an RRR of 250 welded to a Nb support rod. Such samples were polished in two steps: 1. buffered chemical polishing (BCP, HF (48%): HNO_3 (65%): H_3PO_4 (85%), 1:1:2) of 40 µm and 2. electropolishing (EP, HF (40%): H_2SO_4 (98%) 1:9) of 140 µm. The resulting linear (square) roughness was about 80 nm (100 nm) as measured by means of optical profilometry [4]. Each sample has two marks on the edge for repositioning in different measurement systems with an accuracy of about 500 µm.

At first, wet anodizing in H_2SO_4 (10%) with a voltage of 25 V and a Nb sheet (~50 cm^2) as counter electrode in a distance of about 8 cm was tried on N_2-cleaned sample at room temperature. The resulting colour of the anodized surfaces was dark blue, but rather inhomogeneous. SEM analysis of the surfaces revealed many round features of about 10 µm in size on the initially flat surface. Therefore, the wet oxidation was replaced by a TO within a muffle furnace. Heating at 360 °C for 40 min in air and subsequent natural cool-down resulted in a rather homogenous yellow colour (Fig. 1a) that correspond to an oxide thickness of about 100 nm.

Before and after TO the sample was cleaned with ionized and filtered N_2 (*Simco-Ion Top Gun*, filter size 10 nm) at a pressure of 5 bar and immediately installed into the FESM. After the initial EFE measurements the oxide was removed in a resistive furnace inside the load-lock of the FESM (see Fig. 2) under UHV conditions (<10^{-4} Pa). The HT cycle consisted of a warm-up ramp (6.3 °C/min) from room temperature, the annealing at 400°C for 2 h and a natural cool-down phase (3 h). The temperature was controlled with a thermocouple (Pt10Rh-Pt type S) and regulated by a commercial PID-controller (JUMO cTRON 04) within ± 1°C. After this HT, the sample showed its initial metallic appearance.

For comparison, DIC (*CryoSnow* SJ-10) in a clean room (ISO 2) instead of the N_2-cleaning was applied before and after the TO. In order to avoid particulate contamination the sample was protected by an Al cap, as shown in Fig. 1b. This cap was also cleaned by DIC and not removed until the sample faced UHV conditions.

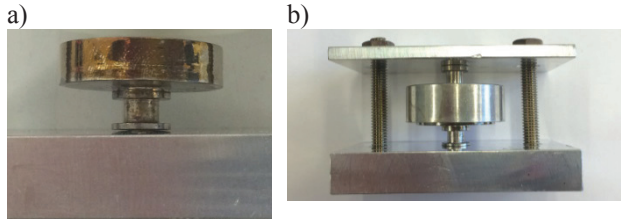

Figure 1: Colour of Nb sample after TO (a) and fixation of Al protection cap for the second TO step after DIC (b).

ISBN 978-3-95450-178-6

FIELD EMISSION INVESTIGATION OF CENTRIFUGAL-BARREL-POLISHED Nb SAMPLES

S. Lagotzky*, G. Müller, University of Wuppertal, D-42097 Wuppertal, Germany
A. Navitski, DESY, D-22603 Hamburg, Germany
A. Prudnikava, Y. Tamashevich, University of Hamburg, D-20148 Hamburg, Germany

Abstract

Centrifugal barrel polishing (CBP) of superconducting Nb cavities is recently reconsidered as alternative or complementary to buffered chemical polishing (BCP) and electropolishing (EP). First investigations of the enhanced field emission (EFE) on a Nb sample, which received CBP in a special coupon cavity, were performed. Despite of the rather smooth surface and dry ice cleaning (DIC), EFE already occurred at activation fields E_{act} of 60 MV/m resulting in low onset fields E_{on} of 40 MV/m. This is caused by Al_2O_3 inclusions from the polishing media, which can be removed by 20 µm BCP. Thereby, EFE is shifted to much higher E_{act} of more than 175 MV/m and E_{on} more than 80 MV/m, where EFE is caused by hole-like features with still somewhat sharp edges.

INTRODUCTION

Actual and future linear electron accelerators require high accelerating gradients E_{acc} and quality factors Q_0, which are often limited by enhanced field emission (EFE) in the superconducting Nb cavities [1]. Systematic measurements on Nb samples have revealed particulate contaminations and surface defects as the main origin of EFE [2]. Various elaborate surface preparation (buffered chemical polishing (BCP) and electropolishing (EP)) and cleaning (high-pressure ultra-pure water rinsing (HPR)) techniques are actually used to remove such emitters and obtain a sufficient surface quality. Recently, centrifugal barrel polishing (CBP) has been reconsidered to achieve a smooth surface as after EP but with less effort [3]. Moreover, CBP has been recognized to remove the surface defects like deep scratches, welding splatters, and foreign inclusions, some of which remain unaffected by the EP/BCP. A combination of CBP and EP/BCP was already applied and tested on single-cell Nb cavities with resulting Q_0 of more than 10^{10} and E_{acc} of 25 to 40 MV/m [4-5]. Accordingly, a similar polishing is also considered for the accelerating structures of the future International Linear Collider (ILC) as alternative for the established EP procedure [6-7]. A systematic investigation of the EFE from such CBP surfaces, however, is still pending. Therefore, we have started to investigate the surface quality, EFE statistics and local properties of a Nb sample, which was prepared as a coupon in a modified single-cell 1.3 GHz cavity close to the electric peak field region by an optimized four step CBP process. Instead of HPR, dry ice cleaning (DIC) [8] was used before and after BCP of 20 µm to avoid any particulate emitters.

EXPERIMENTAL DETAILS

Sample Preparation

We have used a polycrystalline Nb disc (Ø of 8.6 mm, thickness of 3 mm, and RRR of 300) with a central thread and small off-axis hole (Ø of 1 mm), which serves for the fixation on a suitable holder during CBP in the cavity. The thread is compatible with the sample holder for the different measurement techniques, while the hole enables a sample repositioning with an accuracy of ~500 µm. The coupon position close to the iris of the modified cavity can be seen in Fig. 1. The CBP was performed in 4 steps with different mixtures of polishing media [9]:

1. Ceramic angle-cut triangles (KM, 9 x 9 mm^2), surfactant (TS compound), and de-ionized (DI) water (8 h, removal rate 3 to 9 µm/h);
2. Plastic cones (RG-22, 12.5 mm), TS compound, and DI water (15 h, removal rate 1 to 2.5 µm/h);
3. 600 mesh Al_2O_3, cubic hardwood blocks (5 mm), and DI water (30 h, removal rate 0.1 to 0.7 µm/h);
4. Colloidal SiO_2 (40 nm) and cubic hardwood blocks (5 mm) (40 h, removal rate less than 0.1 µm/h).

After the CBP, the coupon cavity was rinsed by DI water and cleaned in an ultrasonic bath first with a solvent (TICKOPUR R-33) and then in pure DI water. The CBP sample has received additional DI water rinsing, drying, and protection by a Teflon cap in a clean room.

Finally, CBP sample and Teflon cap were cleaned by DIC with a commercial system (CryoSnow SJ-10) in a cleanroom class ISO 2 for 5 and 3 min, respectively. The

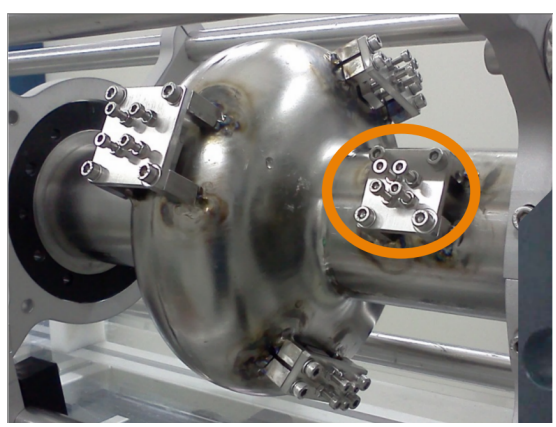

Figure 1: Coupon cavity for the CBP of Nb samples. The circle marks the location of the investigated sample.

*s.lagotzky@uni-wuppertal.de

ISBN 978-3-95450-178-6

A GPU BASED 3D PARTICLE TRACKING CODE FOR MULTIPACTING SIMULATION*

T. Xin#,1,2, I. Ben-Zvi1,2, S. Belomestnykh1,2, J. C. Brutus1, V. N. Litvinenko1,2,
I. Pinayev1, J. Skaritka1, Q. Wu1, B. Xiao1
1Brookhaven National Laboratory, Upton NY 11973, USA
2Stony Brook University, Stony Brook NY, 11794, USA

Abstract

A new GPU based 3D electron tracking code is developed at BNL and benchmarked with both popular existing parallel tracking code and experimental results. The code takes advantage of massive concurrency of GPU cards to track electrons under RF field in 3D Tetrahedron meshed structures. Approximately ten times more FLOPS can be achieved by utilizing GPUs compare to CPUs with same level of power consumption. Different boundary materials can be specified and the 3D EM field can be imported from the result of Omega3P calculation. CUDA_OpenGL interop was implemented so that the emerging of multipactors can be monitored in real time while the simulation is undergoing. Code also has GPU farm version that can run on multiple GPUs to further increase the turnover of multipacting simulation.

INTRODUCTION

Electron multipacting (MP) study in an SRF cavity and power coupler is of great importance in both designing and operating phase of the device. There are several 2D codes that can handle structures with cylindrical symmetry such as Multipac and Fishpact. To deal with 3D structures we have Track3P solver in the ACE3P package and Particle Studio in the CST suite. For 2D codes the limitation is obvious, especially when we are facing a power coupler problem where the structures are usually lack azimuthal symmetry. The Track3P code is extremely powerful in terms of the range of problems it can handle but it also requires a cluster such as NERSC to fully harness this power. Therefore we developed this GPU based 3D tracking code to increase the turnover of the multipacting simulation in SRF structures with only several GPU cards. This code can run on either PC or workstation as long as a GPU that support Nvidia CUDA computing capability 1.3 and above is available.

STRUCTURE OF THE CODE

The idea of this code is to take the advantage of high concurrency of the GPU to run a large scale Monte Carlo process to simulate the multipacting phenomenon. There are three primary parts in the code.

Main (Master) Function

The main function is a host function that runs on CPU and controls the work flow of the program. All the kernels running on GPU are launched from the main host code. First, the input parameters are read into the main function from an input file. Then the geometry model of an RF structure and the field distribution from Omega3P eignesolver are read in. The mesh model will be pre-processed before it is sent to the GPU so that the particles can be more easily located when it is going through the tracking process. Then the main function calls the sequence of the core kernels in the display call back function of the OpenGL so that the tracking process is synchronized with the rendering process. The core tracking kernels will be discussed below.

Momentum Update

Initial locations, momentums and relative RF phases of the particles are generated by a kernel called init_par on GPU. Then the field strength at the location of the particle is calculated by using first order shape function of the Tetrahedral element and the field info on the vertex of the element in which the particle is located. After the field information is ready, the momentum updating kernel takes the pointer to the chunk of global memory that stores the information and starts calculating the new momentum of the particles. The momentum update task was done by a fourth order Runge-Kutta method. After the momentum is updated, the new location of the particle is also updated as if there is no collision. We call this a virtual movement of the particle. The further steps will be conducted by the particle locating kernel, which will be discussed in the following section.

Since momentum updating does not involve the memory copying between GPU and CPU, it can save us considerable amount of time. Each momentum updating kernel requires 90 registers, which still needs some optimization. But even with this amount of register requirement a low tier GeForce GTX 860M GPU can run about 50 thousands of the kernels simultaneously and do one iteration in about 30 ms for 2 million particles.

Particle Locating

The code spends major portion of time on locating the particle after each virtual movement of the particle. The data structure of the mesh model is organized so that each mesh element also stores the ID of the four neighbor elements as well as the internal ID of the surfaces they shared. Every time after the particle is virtually moved by

* This work was carried out at Brookhaven Science Associates, LLC under Contracts No. DE-AC02-98CH10886 and at Stony Brook University under grant DE-SC0005713 with the U.S. DOE.

#txin@bnl.gov

SUPRESSION OF UPSTREAM FIELD EMISSION IN RF ACCELERATORS*

F. Marhauser#, S.V. Benson, D.R. Douglas,
Thomas Jefferson National Accelerator Facility, Newport News, VA 23606, U.S.A.
L.J.P. Ament, ASML US Inc., Wilton, CT 06897, U.S.A.

Abstract

This paper illustrates the idea of suppressing prevalent field emission in RF accelerators in the upstream direction with a rather minor change to the typical configuration, i.e. not requiring a modification to the accelerating structures, but the interconnecting beam tube lengths. An example is presented for a pair of superconducting RF cavities for simplification.

INTRODUCTION

So-called electron loading in radio-frequency (RF) accelerating cavities is the primary cause for cavity performance limitations today. Electron loading can limit the desired energy gain, add cryogenic heat load, damage accelerator components and increase accelerator downtime depending on the induced trip rates. Trip rates are of particular concern for next generation facilities such as Accelerator Driven Subcritical Reactors or Energy Recovery Linacs for Free Electron Lasers.

Electron loading can be attributed to mainly three phenomena, i.e. field emission (FE), multiple impact electron amplification (short: multipacting) and RF electrical breakdown. In all cases, electrons are involved either being released from the enclosing RF surfaces or generated directly within the RF volume by ionization processes with the rest gas (even in ultra high vacuum), e.g. due to cosmic radiation. The free electrons can absorb a considerable amount of the RF energy provided by external power sources thereby constraining the achievable field level and/or causing operational failures.

Field emission has been a prevalent issue, particularly in superconducting RF (SRF) cavities [1], whereas RF electrical breakdown and multipacting can be controllable within limits by adequate design choices. Though SRF cavities may readily exceed accelerating fields (E_{acc}) of 20 MV/m, the onset of parasitic electron activities may start at field levels as low as a few MV/m. Field emission becomes a major concern when the electrons emitted are captured by the accelerating RF field and directed close to the beam axis through a series of cavities or cryomodules.

The electrons can then accumulate a comparable amount of energy as the main beam would over the same distance. This can present a considerable 'dark current' with damaging risks (e.g. when hitting undulator magnets). The electrons can be directed either down- or upstream the accelerator depending on the site and time of origin.

Figure 1 exemplarily shows the energy range of field-emitted electrons numerically computed for an upgrade cryomodule of JLab's electron recirculator CEBAF depending on the initial field emitter location along the cryomodule [2].

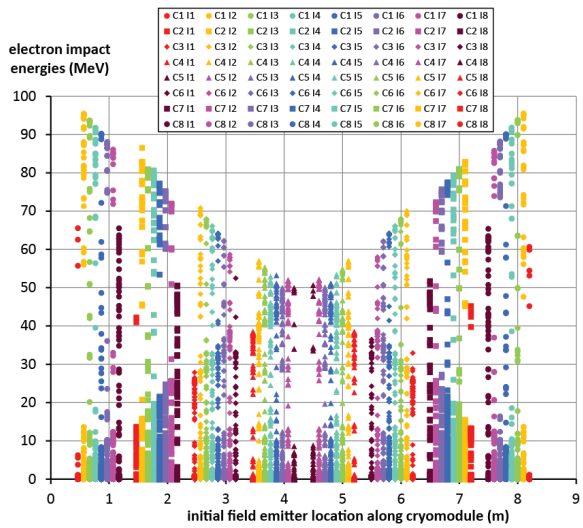

Figure 1: Possible impact energy range of electrons in an upgrade CEBAF cryomodule with all cavities operating at the nominal field level of E_{acc} = 19.2 MV/m totaling 108 MeV energy gain. The results are not fully mirror-symmetric due to numerical differences start conditions.

Housing eight seven-cell cavities, this covers all probable emitter sites seeded around irises, where the electrical surface field peaks (E_{peak}). The energies are plotted over the initial 8 × 8 iris regions covering all possible field emitting surfaces. Same colors represent same iris regions (1 through 8 for each cavity). A color code is given in the legend with C = cavity and I = iris with the corresponding number denoting the site of origin.

* Authored by Jefferson Science Associates, LLC under U.S. DOE Contract No. DE-AC05-06OR23177. The U.S. Government retains a non-exclusive, paid-up, irrevocable, world-wide license to publish or reproduce this manuscript for U.S. Government purposes.
# marhause@jlab.org

DESIGN OF THE SUPERCONDUCTING LINAC FOR SARAF

C. Madec, N. Bazin, L. Boudjaoui, R. Cubizolles, G. Ferrand, B. Gastineau, Ph. Hardy, C. Pes, N. Pichoff, N. Sellami, Ph. Bredy, CEA, Saclay, France
P. Bertrand, GANIL, Caen, France

Abstract

CEA is committed to delivering a Medium Energy Beam Transfer line and a superconducting linac (SCL) [1] for SARAF accelerator in order to accelerate 5mA beam of either protons from 1.3 MeV to 35 MeV or deuterons from 2.6 MeV to 40.1 MeV. The SCL consists 4 cryomodules equipped with warm diagnostics. The first two identical cryomodules host 6 half-wave resonator (HWR) low beta cavities (β = 0.091), 176 MHz. As the last two identical welcome 7 HWR high-beta cavities (β = 0.181), 176 MHz. The beam is focused through the superconducting solenoids located between cavities and housing steering coils. A Beam Position Monitor is placed upstream each solenoid. A diagnostic box containing a beam profiler, a bunch length monitor and a vacuum pump will be inserted between 2 consecutive cryomodules. The HWR cavities, the solenoid package, the cryomodules and the warm sections are being designed. These studies will be presented in this contribution.

CAVITIES DESIGN

RF Design of the Half Wave Resonators

Two different half wave cavity resonators are being studied for the SARAF Linac project, for two different β_opt parameters: 0.091 and 0.181 respectively referred as low and high beta cavities. The frequency of the cavity corresponds to the frequency of the bunches : 176 MHz. These cavities are designed for a 5 mA continuous beam current.

To reach the high accelerating voltage per cavity, the electromagnetic design was carefully optimized:

- The peak surface electric field has to be minimized to reduce field emission; 35 MV/m is considered as a reasonable peak electric field;
- The peak magnetic field was set to 70 mT in order to be lower than the 180 mT transition magnetic field from superconducting state to normal;
- The dissipated power on the walls of the cavity must be minimized to reduce the cryogenic cost.

Specific cavity geometrical parameters have been used for the optimization. They are shown on Figure 1 and defined as:

- R_{in}: radius of the central drift tube element;
- R_{ext}: outer radius of the cavity;
- R_b: small radius of the torus;
- Z_c: thickness of the drift tube;

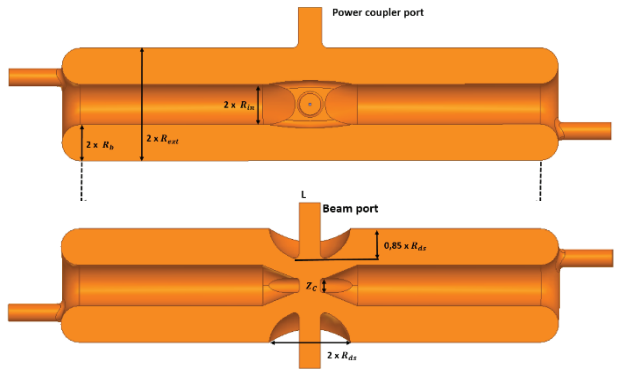

Figure 1: Main parameters of the cavities. Top diagram: cut perpendicular to the beam axis. Bottom diagram: cut perpendicular to the coupler antenna axis.

- R_{ds}: radius of the beam nozzle;
- L: length of the cavity.

The optimization has to take into account constraints imposed by the beam dynamic studies. The cavity flange-to-flange distance is defined as 280 mm and 410 mm for the low and high beta cavities respectively. When considering the flange dimensions and the helium tank design, this defines a maximum value for R_{ext} as 95 mm and 160 mm for the low and high beta cavities respectively.

The cavities will be placed vertically, thus, the liquid helium will flow through the drift tube in order to avoid helium bubbles and local heat. A channel of 10mm diameter was considered as a minimum for ensuring a comfortable helium flow at 4 K. We chose to manufacture the drift tube by digital machining to reduce the welding risk in this part of the cavity that shows very high electric field. These defines the minimum value of R_{in} to 34 mm. Simulations were carried out with the Ansys HFSS software. The results of the optimization are detailed in Table 1. The table shows that magnetic and electric field peak limits, 70 mT and 35 MV/m are respected by this design, at the nominal acceleration field.

Mechanical Design of the Low Beta HWR and its Helium Tank

The nominal value of Q_{ext} ($1.21.10^6$) sets the cavity 3 dB bandwidth at nominal beam current to 289 Hz for the low beta HWR. The amplitude of the He pressure fluctuations in the 4.45 K cryostat is expected to be +/-5 mBar. This implies that He pressure sensitivity df /dP in the order of 10 to 5 Hz/mbar has to be reached in order to limit the extra RF power consumption.

RECENT MEASUREMENTS ON THE SC 325 MHz CH-CAVITY*

M. Busch†, M. Basten, F. Dziuba, H. Podlech, U. Ratzinger, IAP, Frankfurt am Main, Germany
M. Amberg, Helmholtz-Institut Mainz (HIM), Mainz, Germany

Abstract

At the Institute for Applied Physics (IAP), Frankfurt University, a superconducting 325 MHz CH-Cavity has been designed and built and extensive tests have successfully been performed. The cavity is determined for a 11.4 AMeV, 10 mA ion beam at the GSI UNILAC. This cavity consists of 7 gaps and is envisaged to deliver a gradient of 5 MV/m. Novel features of this structure are a compact design, low peak fields, improved surface processing and power coupling. Furthermore a tuner system based on bellow tuners attached inside the resonator and driven by a stepping motor and a piezo actuator will control the frequency. In this contribution measurements performed at 4.2 K and 2.1 K at the cryo lab in Frankfurt will be presented.

INTRODUCTION

Currently planned projects like the sc cw Heavy Ion Linac at GSI/HIM [1] require compact and efficient cavities to deliver beams of high intensity, quality and availabilty. For those applications the superconducting CH-cavity has

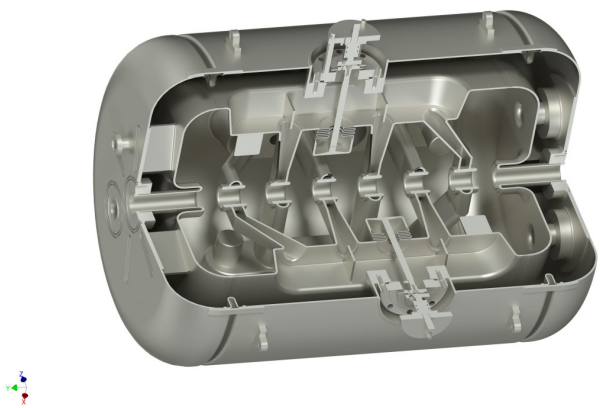

Figure 1: Rendering of the cavity with welded helium vessel.

already proved to be an appropiate candidate being characterized by a small number of drift spaces between neighboring cavities compared to conventional low-β ion linacs [2]. Additionally the KONUS beam dynamics, which decreases the transverse rf defocusing and allows the development of long lens free sections, yields high real estate gradients with moderate electric and magnetic peak fields. At the Institute for Applied Physics, Frankfurt University, a new cavity operating at 325.224 MHz, consisting of 7 cells, $\beta = 0.16$ and an effective length of 505 mm (see Table 1) has been designed [3] and extensively measured after all fabrication and processing steps at Research Instruments [4]. In the final stage the cavity is being welded to a helium vessel to provide a closed helium circulation (see Fig. 1).

Table 1: Specifications of the 325 MHz CH-Cavity.

β	0.16
frequency [MHz]	325.224
no. of cells	7
length ($\beta\lambda$-def.) [mm]	505
diameter [mm]	352
E_a (design) [MV/m]	5
E_p/E_a	5
B_p/E_a [mT/(MV/m)]	13
G [Ω]	66
R_a/Q_0	1260
R_aR_s [$k\Omega^2$]	80

MEASUREMENT SETUP

At the cryo lab of the IAP a measurement setup comprising a vertical cryostat has been installed for various test purposes (see Fig. 2) allowing power measurements at 4.2 K and 2.1 K, respectively. In this system the spent Helium can be extracted to a recovery system or the cryostat can be evacuated by a roots pump to reach 2 K. The CH-cavity

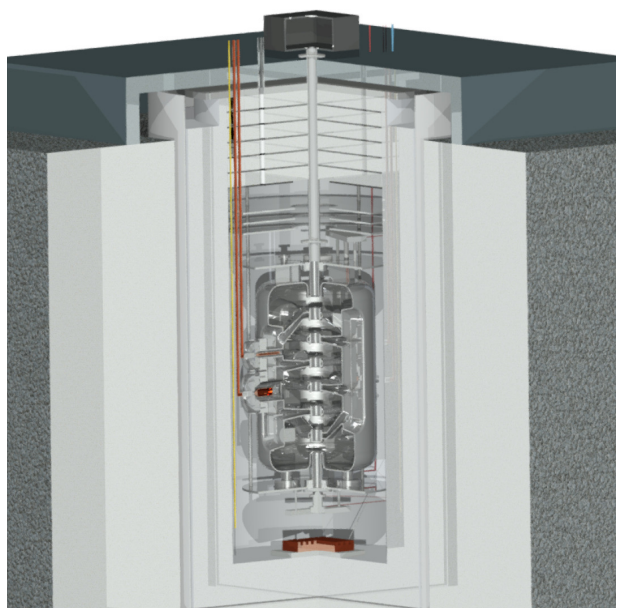

Figure 2: Schematic layout of the vertical test environment.

has been provided with four low-temperature probes, 40 **T**hermo-**L**uminescence-**D**osimeter (see Fig. 3) to record

* Work supported by GSI, BMBF Contr. No. 06FY7102
† busch@iap.uni-frankfurt.de

ISBN 978-3-95450-178-6

R&D STATUS OF THE NEW SUPERCONDUCTING CW HEAVY ION LINAC@GSI

M. Basten[1,*], M. Amberg[1,3], K. Aulenbacher[3,4], W. Barth[2,3], M. Busch[1], F. Dziuba[1], V. Gettmann[3], M. Heilmann[2], D. Mäder[1], S. Mickat[2,3], M. Miski-Oglu[3], H. Podlech[1], M. Schwarz[1]

[1]IAP University of Frankfurt, 60438 Frankfurt am Main, Germany
[2]GSI Helmholtzzentrum, 64291 Darmstadt, Germany
[3]Helmholtz-Institut Mainz (HIM), 55099 Mainz, Germany
[4]KPH Mainz University, 55128 Mainz, Germany

Abstract

To keep the ambitious Super Heavy Element (SHE) physics program at GSI competitive a superconducting (sc) continuous wave (cw) high intensity heavy ion LINAC is currently under progress as a multi-stage R&D program of GSI, HIM and IAP [2]. The baseline linac design consists of a high performance ion source, a new low energy beam transport line, an (cw) upgraded High Charge State Injector (HLI), and a matching line (1.4 MeV/u) which is followed by the new sc-DTL LINAC for post acceleration up to 7.3 MeV/u. In the present design the new cw-heavy ion LINAC comprises constant-beta sc Crossbar-H-mode (CH) cavities operated at 217 MHz. The advantages of the proposed beam dynamics concept applying a constant beta profile are easy manufacturing with minimized costs as well as a straightforward energy variation [6]. An important milestone will be the full performance test of the first CH cavity (Demonstrator), in a horizontal cryo module with beam. An advanced Demonstrator setup comprising a string of cavities and focussing elements is proposed to build from 10 short CH-cavities with 8 gaps. The corresponding simulations and technical layout of the new cw heavy ion LINAC will be presented.

INTRODUCTION

At the moment the Demonstrator for the sc cw-LINAC at GSI is under construction and its successful beam operation will be the first milestone realizing the new sc cw-LINAC at GSI [1]. The advanced Demonstrator which is presented here will be the second milestone for the sc LINAC at GSI. The Demonstrator will be the first cavity for the sc LINAC followed by 5 additional cryomodules with 2 CH-cavities per cryomodule [2,3]. The design of the advanced Demonstrator will be used for all cavities in the sc cw-LINAC after the Demonstrator. The 8 cell cavity is designed and optimized for high power applications and has a design gradient of 5 MV/m. Its frequency is the second harmonic of the High Charge Injector (HLI) at GSI, Darmstadt. Table 1 shows the main parameters and figure 1 shows the Layout of the sc 217 MHz CH-cavity.

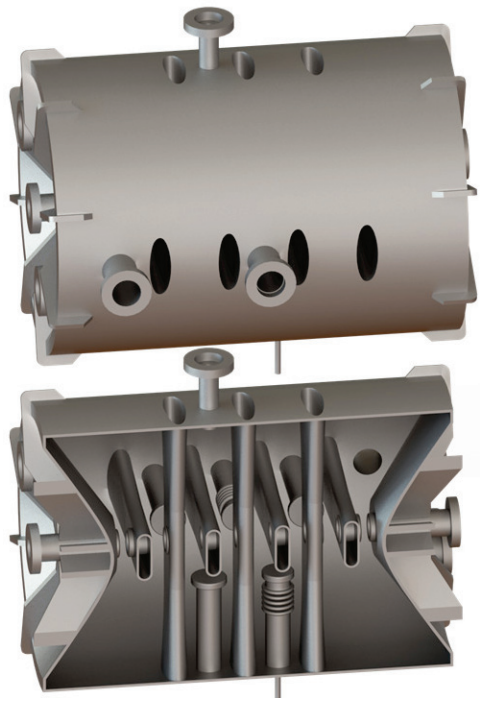

Figure 1: Layout of the sc 217 MHz CH-cavity.

Table 1: Main Parameters of the 217 MHz CH-cavity

Parameter	Unit	
β		0.069
Frequency	MHz	215
Accelerating cells		8
Length ($\beta\lambda$-definition)	mm	381.6
Cavity diameter (inner)	mm	392.3
Cell length	mm	47.7
Aperture diameter	mm	30
Static tuner		3
Dynamic bellow tuner		2
Wall thickness	mm	3-4
Accelerating gradient	MV/m	5
E_p/E_a		5.2
B_p/E_a	mT/(MV/m)	<10
G	Ω	50
R_a/Q_0	Ω	1070

* Basten@iap.uni-frankfurt.de

STEPS TOWARDS SUPERCONDUCTING CW-LINAC FOR HEAVY IONS AT GSI

M. Miski-Oglu*, M. Amberg, V. Gettmann HIM, Mainz, Germany
W. Barth, GSI, Darmstadt; HIM, Mainz, Germany
K. Aulenbacher HIM Mainz, IKP Mainz, Germany
M. Heilmann, S. Mickat, S. Yaramyshev, GSI, Darmstadt, Germany
M. Basten, D. Bänsch, F. Dziuba, H. Podlech, U. Ratzinger,
IAP Frankfurt University, Frankfurt, Germany

Abstract

Providing heavy ion beams for the ambitious experiment program at GSI, the Universal Linear Accelerator (UNILAC) serves as a powerful high duty factor (25%) accelerator. Beam time availability for SHE-research will be decreased due to the limitation of the UNILAC providing a proper beam for FAIR simultaneously. To keep the GSI-SHE program competitive on a high level, a standalone sc cw-LINAC in combination with the upgraded GSI High Charge State injector is planned to build. In preparation for this the first linac section (financed by HIM and partly by HGF-ARD-initiative) will be tested in 2015 as a demonstrator. After successful testing the construction of an extended cryomodule comprising two further, but shorter CH cavities is foreseen to test until end of 2017. In this contribution the measurement of the beam parameters at the entrance of cw-demonstrator, the preliminary simulation of beam dynamics for the first stage of advanced demonstrator will be presented. As a final R&D step towards an entire linac an advanced cryo modules comprising up to five CH cavities is envisaged for 2019 serving for first user experiments at the coulomb barrier.

DEMONSTRATOR ENVIRONMENT AT GSI

The commissioning of the cw-demonstrator [1] consisting of 2 superconducting (**sc**) solenoids and the superconducting CH-cavity is scheduled for the first quarter of 2016. Figure 1 shows the demonstrator environment at GSI.

The beam with an energy of $1.4\,\mathrm{MeV/u}$ from existing high charge state injector (HLI) operating at $108\,\mathrm{MHz}$ is transported through the line comprising of quadrupole lenses for transversal matching and two rebuncher cavities for longitudinal matching to the demonstrator sc CH-cavity [2, 3]. The liquid He cryostat maintains the cooling of the cavity and two sc solenoids [4, 5] is placed within the radiation protection shelter.

EMITTANCE MEASUREMENT OF HLI BEAM

Within the preparations to commissioning of cw-demonstrator, during a beam time in 2015 the transverse emittance of the Ar^{7+} and Ar^{10+} beams from HLI injector was measured. The measurements was done by a slit-grid device [6]. Two stepping motor driven slits of $0.2\,\mathrm{mm}$ width, one in vertical and another in horizontal plane are installed in the vacuum chamber at the position of the cw-

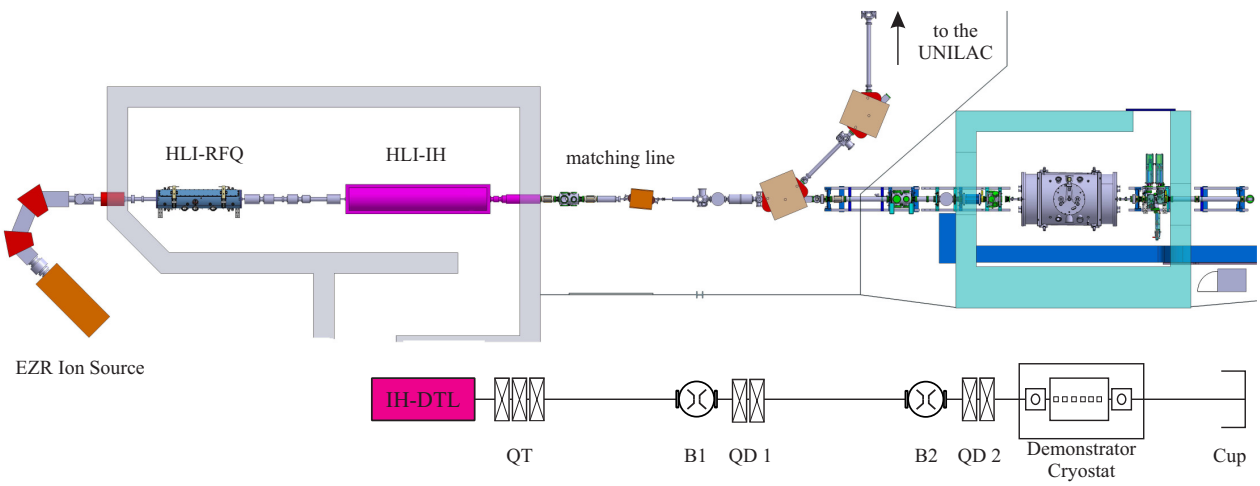

Figure 1: Top: footprint of the demonstrator test environment at GSI. Bottom: scheme of the beam line. The main elements of the beam line: quadrupole triplet QT, quadrupole doublets QD1 and QD2 and two buncher cavities B1, B2.

* m.miskioglu@gsi.de

PULSED SC ION LINAC AS AN INJECTOR TO BOOSTER OF ELECTRON ION COLLIDER*

P.N. Ostroumov#, Z.A. Conway, and B. Mustapha, ANL, Argonne, IL 60439, U.S.A
B. Erdelyi, Department of Physics, NIU, DeKalb, IL 60115, U.S.A.

Abstract

The medium energy electron-ion collider (MEIC) being developed at JLAB requires a new ion accelerator complex (IAC). The IAC includes a new linac and a new booster accelerator. The new facility is required for the acceleration of ions from protons to lead for colliding beam experiments with electrons in the EIC storage ring. Originally, we proposed a pulsed linac with a NC front-end up to 5 MeV/u and a SC section for higher energies. The linac is capable of providing 285 MeV protons and ~100 MeV/u lead ions for injection into the IAC booster. A recent cost optimization study of the IAC suggested that lower injection energy into the booster may reduce the overall cost of the project with ~130 MeV protons and ~42 MeV/u lead ions. Stronger space charge effects in the booster caused by lower injection energy will be mitigated by the appropriate booster design. In this paper we discuss both linac options.

INTRODUCTION

Several years ago we developed a multi-ion injector linac design for the medium energy EIC (MEIC) capable of providing ~285 MeV protons and ~100 MeV/u lead ions [1,2]. This linac consisted of 122 superconducting (SC) cavities housed in 16 cryomodules. Recently, significant progress has been made at ANL with the developments of high-performance quarter-wave resonators (QWRs) and half-wave resonators (HWRs). Particularly, both QWRs and HWRs can provide very high accelerating gradients by operating at peak electric and magnetic fields up to 60 MV/m and 90 mT respectively. If we apply this technology to the design of a pulsed multi-ion linac, the cavity and cryomodule count can be notably reduced. In addition, by lowering the injection energy of lead ions to ~42 MeV/u and implementing newly developed technologies, the cost of the multi-ion superconducting linac may be reduced by nearly a factor of 3 relative to the current proposed 100 MeV/u linac option. The cost reduction is driven by the reduced number of SC cavities and cryomodules.

HEAVY-ION LINAC PARAMETERS

A block-diagram of the new linac is shown in Figure 1 and the basic design parameters are listed in Table 1. The economic acceleration of lead ions to 42 MeV/u requires a stripper in the linac with an optimum stripping energy of ~8.2 MeV/u, obtained from the plot of total accelerating voltage as a function of the stripping energy shown in Figure 2. The stripping efficiency of lead ions to the most abundant charge state 61+ is 17.5%.

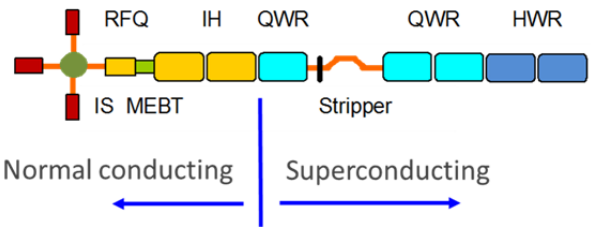

Figure 1: A schematic drawing of the MEIC ion linac.

Table 1: Main Parameters of the Linac

Parameter	Units	Value
Ion species		H^+ to Pb
Fundamental frequency	MHz	100
Kinetic energy of protons & lead ions	MeV/u	130&42
Maximum pulse current		
Light ions (A/q≤3)	mA	2
Heavy ions (A/q>3)	mA	0.5
Pulse repetition rate	Hz	up to 10
Pulse length		
Light ions (A/q≤3)	ms	0.5
Heavy ions (A/q>3)	ms	0.25
Maximum pulsed beam power	kW	260
# of QWR cryomodules		3
# of HWR cryomodules		2
Total length	m	~55

The MEIC ion linac will use several ion sources (IS)

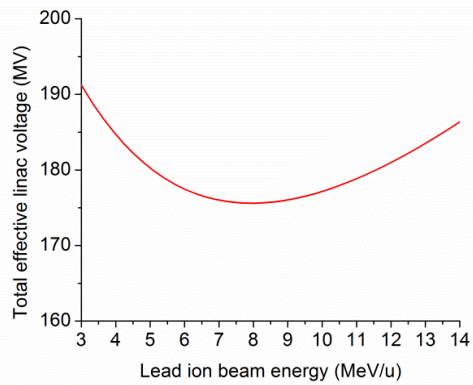

Figure 2: Total effective linac voltage as a function of the stripping energy of lead ions.

*This work was supported by the U.S. Department of Energy, Office of Nuclear Physics, under Contract DE-AC02-06CH11357. This research used resources of ANL's ATLAS facility, which is a DOE Office of Science User Facility.
#ostroumov@anl.gov

ISBN 978-3-95450-178-6

SUPERCONDUCTING LINAC UPGRADE PLAN FOR THE SECOND TARGET STATION PROJECT AT SNS*

S-H. Kim#, M. Doleans, J. Galambos, M. Howell, J. Mammosser,
ORNL, Oak Ridge, TN 37831, USA

Abstract

The beam power of the Linac for the Second Target Station (STS) at the Spallation Neutron Source (SNS) will be doubled to 2.8 MW. For the energy upgrade, seven additional cryomodules will be installed in the reserved space at the end of the linac tunnel to produce linac output energy of 1.3 GeV. The cryomodules for STS will have the same physical length but will incorporate some design changes based on the lessons learned from operational experience over the last 10 years and from the high beta spare cryomodule developed in house. The average macro-pulse beam current for the STS will be 38 mA which is about a 40 % increase from the present beam current for 1.4 MW operation. Plans for the new cryomodules and for the existing cryomodules to support higher beam current for the STS are presented in this paper.

INTRODUCTION

The proposed Second Target Station (STS) concept is based on a short pulse configuration by 10-Hz, 470 kW proton beam, which is optimized for cold neutrons with high peak brightness [1]. In order to provide required beam to the First Target Station (FTS) and STS, the plan for the SNS accelerator upgrade is to increase the linac output energy from 940 MeV to 1 GeV and to increase average macro pulse beam current from 26 mA to 38 mA. The total beam repetition rate will be the same at 60 Hz; 50 Hz for the FTS and 10 Hz for the STS. As a result the accelerator capacity will be doubled in terms of beam power from 1.4 MW to 2.8 MW.

The original SNS Power Upgrade Project (PUP) plan [2] was to upgrade the SNS linac to 3-MW capability by increasing the linac beam energy to 1.3 GeV with nine additional high beta cryomodules and by increasing the average macro pulse beam current to 42 mA. There are empty slots at the end of the linac tunnel for nine additional high beta cryomodules, and space for the high power RF and control racks in the klystron gallery that were prepared during the original construction. The design accelerating gradient of the new SRF cavities for the PUP was 14 MV/m mainly due to two concerns; 1) the average accelerating gradient of existing high beta SRF cavities are lower than the original design gradient that is 15.8 MV/m, 2) The klystron power at saturation for the upgrade will provide 700 kW that limits the accelerating gradient at 15 MV/m for the 42-mA beam loading.

* This work was supported by SNS through UT-Battelle, LLC, under contract DE-AC05-00OR22725 for the U.S. DOE.
# kimsh@anl.gov

The spare high beta cryomodule was developed and commissioned in 2012 and has been in service in the tunnel for the neutron production since then [3, 4]. All cavities in this cryomodule are running at 16 MV/m stably limited by the available RF power. The existing high power RF system provides 550 kW. The average macro pulse beam current is 38 mA that is about 10 % less than the beam current for the PUP. For the STS, these two factors are basis for the design accelerating gradient of the new SRF cavities at 16 MV/m. Thus, seven additional high beta cryomodules are required for the STS. Installing seven cryomodules in the nine available slots helps the practical issues. Currently some of the chases for the upgrade section between the klystron gallery and the tunnel have been already filled with cables. Removing these cables will affect the machine operation and will generate additional cost.

The optimum geometric beta of the cavities for STS is higher than that of the original high-beta cavities but the module length and accordingly cavity geometric beta will be kept same due to economic reasons. All helium transfer lines are already installed during the SNS project with bayonets for the high beta cryomodules. Waveguides penetrations from the klystron gallery to the linac tunnel were also installed for the length of the high beta cryomodules. Some changes, that do not require changes of overall layout, will be made based on the lessons learned from operational experiences over the last 10 years and the pressure-vessel compliance issue. Table 1 summarizes the design changes between the original SNS high beta cryomodule and the high beta cryomodule for the STS.

Table 1: Cryomodule Design Changes for the STS

Parameters	Original	STS
E_{acc} at β=0.81 (MV/m)	15.8	16.0
Fundamental power coupler rating, peak/average (kW)	550/48	700/65
End group Nb	Reactor grade	High RRR
Fast tuner	Piezo	none
HOM coupler per cavity	2	none
Pressure vessel	Good Engineering Practice	Code Stamp required

PRELIMINARY CONCEPTUAL DESIGN OF THE CEPC SRF SYSTEM

J.Y. Zhai#, J. Gao, T.M. Huang, Z.C. Liu, Z.H. Mi, P. Sha, Y. Sun, H.J. Zheng, IHEP, China
Carlo Pagani, University of Milano and INFN-LASA, Italy
Sergey Belomestnykh, BNL and Stony Brook University, USA

Abstract

CEPC is a circular electron positron collider operating at 240 GeV center-of-mass energy as a Higgs factory, recently proposed by the Chinese high energy physics community. The CEPC study group, together with the FCC and ILC community, will contribute to the development of future high energy colliders and experiments which will ensure that the elementary particle physics remain a vibrant and exciting field of fundamental investigation for decades to come. Superconducting RF (SRF) system is one of the most important technical systems of CEPC and is a key to achieving its design energy and luminosity. It will dominate, with the associated RF power source and cryogenic system, the overall machine cost, efficiency and performance. The CEPC SRF system will be one of the largest and most powerful SRF accelerator installations in the world. The preliminary conceptual design of the CEPC SRF system is summarized in this paper, including the machine layout, key parameter choices and some critical issues such as HOM damping, emphasizing the new technology requirement and R&D focuses.

INTRODUCTION

CEPC-SPPC is the most ambitious accelerator project ever proposed in China and even in the world. It will be housed in a 54 km circular tunnel (current baseline; 100 km as alternative). The first phase is an electron-positron Higgs factory at a centre-of-mass energy of 240 GeV (CEPC) for precise measurements of the newly discovered Higgs boson. The experiment is planned to start in 2028 and run though the 2030's. Experiments at the Z pole and the WW production threshold will be also possible. Then the tunnel will be filled by a proton-proton collider with a 70 TeV centre-of-mass energy (SPPC) with next-generation superconducting magnets, to explore the energy frontier [1].

Figure 1 is a layout of the CEPC. The circumference is about 54.4 km. There are 8 arcs and 8 straight sections. Four straight sections, 944 m each, are for the interaction regions and RF; another four, also 944 m each, are for the RF, injection, beam dump, etc. Among the four IPs, IP1 and IP3 will be used for e+e– collisions, whereas IP2 and IP4 are reserved for pp collisions. Both the electron and positron beams will circulate in the same beam pipe with an energy of 120 GeV each. The peak luminosity goal of CEPC is 2×10^{34} $cm^{-2}s^{-1}$ at each interaction point. The total synchrotron radiation loss is limited to ~100 MW.

The CEPC tunnel will accommodate two ring accelerators: the collider and a full energy Booster. While the two colliders will be mounted on the floor, the Booster will hang from the ceiling.

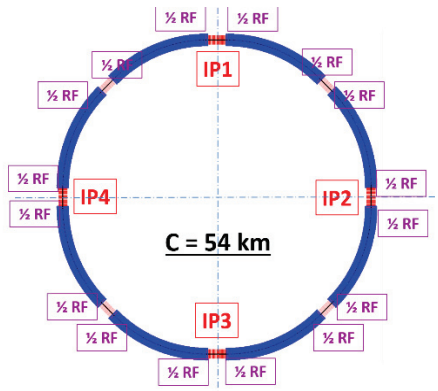

Figure 1: CEPC layout.

Superconducting RF (SRF) system is the most demanding technical system of CEPC. Because the Booster beam current is relatively low (0.8 mA), it is decided to use a 1.3 GHz SRF system, a mature technology that has been used in the ILC, XFEL and LCLS-II. The collider beam current is very high (33 mA) and both beams use the same RF cavity; the average RF power is bigger than in any exiting SRF system, and a large power coupler is required. Even more difficult is the HOM damper, which must extract most of the HOM power from the cavity. Therefore, it is decided to use a 650 MHz SRF system, which is used in the China ADS project and PIP-II at Fermilab.

CEPC SRF SYSTEM LAYOUT

Eight RF stations are placed in eight straight sections of the tunnel, and each of them split into two half stations. The total RF station length is approximately 1.4 km with 12 GeV of RF voltage. Table 1 shows the main parameters of the CEPC SRF system.

CEPC will use 384 five-cell 650 MHz cavities for the collider (main ring) and 256 nine-cell 1.3 GHz cavities for the Booster. The collider cavities operate in CW. The Booster cavities operate in quasi-CW mode. The collider module will be mounted on the tunnel floor and the Booster module hangs from the ceiling in series with the collider module string at a different beamline height.

During the conceptual design phase, significant effort is needed to identify high-risk challenges that require R&D. The highest priority items are efficient and economical damping of the huge HOM power with minimum dynamic cryogenic heat load, achieving the cavity gradient with high quality factor in the vertical test and real accelerator environment, robust 300 kW high power

#zhaijy@ihep.ac.cn

TECHNOLOGY READINESS LEVELS APPLIED TO CURRENT SRF ACCELERATOR TECHNOLOGY FOR ADS

R. Edinger, PAVAC, Richmond, Canada
R. E. Laxdal, TRIUMF, Vancouver, Canada
L. Yang, TRIUMF/PAVAC, Vancouver, Canada

Abstract

Accelerator Driven Systems (ADS) are comprised of high power accelerators supplying a proton beam to a reactor vessel. The reactor vessel could contain nuclear fuels such as used Uranium or Thorium [1]. The proton beam will be used to produce Neutrons by spallation in the reactor vessel. Technology readiness levels (TRL's) can be used to chart technology status with respect to end goal and as such can be used to outline a road map to complete an ADS system. TRL1 defines basic principles observed and reported, whereas TRL9 is defined as system ready for full scale deployment. SRF technology when applied to ADS reflects a mix of TRL levels since worldwide many SRF Accelerators are in operation [2]. The paper will identify the building blocks of an ADS accelerator and analyze each for technical readiness for industrial scale deployment. The integrated ADS structure is far more complex than the individual systems, but the use of proven sub-systems allows the construction of SRF accelerators that can deliver the beam required. An analysis of the technical readiness of SRF technology for ADS will be presented.

INTRODUCTION

PAVAC and TRIUMF [2] developed an initial plan for a ADS facility named TP-ADS Demonstrator staged in 2 phases with a final goal of a <10mA proton beam with an energy of ~100MeV resulting in up to 1 MW of beam power on a Thorium / target facility. The facility includes a proton source with a normal temperature RFQ. This front end (linac injector) is composed of an ion source and a radiofrequency quadrupole (RFQ) accelerator. The ion source has to deliver high brightness beams (intensity, emittance, stability).

Direct current proton sources using 2.45GHz ECR plasma heating, delivering stable beams with high availability and small emittances are now available as injectors for accelerators. The RFQ, which includes RF electric transverse focusing, bunches and accelerates the beam from about 100 keV to a few (3) MeV. These structures are well suited to keep the beam quality (longitudinal and transverse) at high intensity. Four vane RFQs at 162/325MHz are now in production and testing for high intensity application and therefore for the purpose of this review are not included.

Downstream of the RFQ are six super conducting (SRF) cryomodules, which accelerate the proton beam efficiently to higher energies. Downstream of the last cryomodule is a target facility used as a test bed for future ADS target/reactor systems.

Our focus is on the super conducting accelerator, Proton source and target technology required for a Thorium and related processes will be described later. We will be using technology readiness levels to describe the maturity of the technology similar as being used by NEA [3] for nuclear fuels.

SRF ACCELERATOR CONFIGURATION

The SRF section consists of 6 cryomodules similar in design as shown in Figure 1, named CM0 to CM5. CM0 is considered the injector module capturing the protons coming from the RFQ section and is the only SRF module in Phase 1 of the plan. After CM0 the proton beam can be tested up to <10mA and with an energy of 10MeV. CM1 to CM 5 are accelerating stages with a mix of SRF cavity types, design specs and frequencies for all cryomodules are as shown in Table 1 and a concept shown in Figure 2.

Table 1: TP-ADS Demonstrator Technical Draft Specification

	PHASE 1			GOAL	PHASE 2					GOAL
	PROTON SOURCE	RFQ	CM0		CM1	CM2	CM3	CM4	CM5	
CURRENT	10mA	9.5mA	9.5mA	DEMO OF HIGH BEAM CURRENT ON TARGET	9.5mA	9.5mA	9.5mA	9.5mA	9.5mA	DEMO OF HIGH BEAM CURRENT
NUMBER OF CAVITIES			6		7	7	7	8	8	43
CAVITY TECHNOLOGY		NORMAL CONDUCTING	SRF		SRF	SRF	SRF	SRF	SRF	
TYPE OF CAVITY			HWR		HWR	HWR	HWR	HWR OR SPOKE	HWR OR SPOKE	
ENERGY PER CAVITY (MeV)			1.4		1.4	3.3	3.3	3.7	3.7	
BETA			0.11		0.11	0.24	0.24	0.4	0.4	
RF Power Coupler/kW			14		14	33	33	37	37	
RF (MHz)			162.5		162.5	162.5	162.5	325	325	
Period length/mm			570		570	950	950	1700	1700	
CM length/m			3.42		3.99	6.65	6.65	6.8	6.8	
TOTAL ENERGY (MeV)	0.03	3	9.5		17	35.2	54	76.6	100.7	1 MEGAWATT ON Th TRAGET

ISBN 978-3-95450-178-6

CHARACTERIZATION OF SURFACE DEFECTS ON EXFEL SERIES AND ILC-HIGRADE CAVITIES*

A. Navitski#, E. Elsen, V. Myronenko, J. Schaffran, and O. Turkot DESY, Hamburg, Germany
Y. Tamashevich, University of Hamburg, Hamburg, Germany

Abstract

A detailed analysis of surface quality of around 100 EXFEL series and ILC-HiGrade SRF cavities has been performed applying high-resolution optical system OBACHT and replica. Typical surface features and defects as well as their influence on the cavity performance and possible repair methods are presented and discussed.

INTRODUCTION

Superconducting radio-frequency (SRF) niobium cavities are a key component of current and future efficient particle accelerators producing high-energy and high-intensity beams. The technology is a key to next-generation light sources, accelerator-driven sub-critical nuclear reactors and nuclear-fuel treatment, and new accelerators for material science and medical applications. The SRF cavities are made from high-purity niobium and undergo a complex multi-step production process to achieve high accelerating gradient, E_{acc}, and unloaded quality factor, Q_0 [1]. These quantities, together with the manufacturing yield, drive cost and performance factors such as cryogenics, beam energy, and machine length. The European X-ray Free Electron Laser (EXFEL) [2], currently under construction in Hamburg, requires for example 800 Tesla-shape nine-cell 1.3 GHz SRF niobium cavities operating at nominal average E_{acc} of 23.6 MV/m with Q_0 of at least 10^{10}. The future International Linear Collider (ILC) [3] would require the production of 16,000 such cavities operating at nominal average gradient of 31.5 MV/m with almost the same Q_0 factor. With such a quantity of cavities to be fabricated, an appropriate quality control (QC), failure reason clarification, possibilities for retreatment and repair of the SRF cavities, and the resulting manufacturing yield become very important issues.

The ability to detect performance-limiting defects, especially in early production steps, would significantly reduce repetition of expensive cold RF tests and retreatments of the cavities.

Inspection of the inner cavity surface by an optical system is an inexpensive and useful means for surface control and identification of critical or suspicious features.

*Work supported by EU FP7/2007-2013 under grant agreement number 283745 (CRISP) and "Construction of New Infrastructures - Preparatory Phase", ILC-HiGrade, contract number 206711, BMBF project 05H12GU9, and Alexander von Humboldt Stiftung/Foundation.

#aliaksandr.navitski@desy.de

MEASUREMENT TECHNIQUE

OBACHT

Optical inspections of the cavities have been performed applying the high-resolution OBACHT system. OBACHT is a semi-automated inspection tool of the inner cavity surface and is based on the Kyoto camera system. It allows inspection of a large number of cavities with and without a He-tank as well as of the components that make up a complete cavity such as "dumbbells" and end groups. A "standard" cavity inspection concentrates on the welding seams at the equator and irises plus the area to the left and right of the equator welding seams and yields approximately 3000 images in 8 hours. One OBACHT image covers a cavity area of 12x9 mm^2 at the equator with at least 10 µm resolution. The positioning accuracy of a cavity mounted on a movable sled is about 10 µm, whereas the angular accuracy of the camera positioning is about 0.01°.

Replica

To gain information about the 3D topography of surface features or defects, a replica technique has been applied additionally on some defects, especially if an unambiguous interpretation of defects could not be performed based on the OBACHT images. Replica is a non-destructive surface-study method reaching resolution down to 1 µm by imprinting the details of the surface onto a hardened rubber. The footprint is subsequently investigated with a microscope or profilometer. 3D laser scanning microscope (Keyence VK-X100K) has been applied for topographic investigations of the replica-samples and provides up to 0.2 μm lateral and 10 nm height resolution.

SURFACE DEFECTS

Based on the optical inspections of the EXFEL series and ILC-HiGrade cavities, the following seven types of surface "defects" could be identified. These are scratches, foreign inclusions, welding errors, rough polishing, defects called "cat eyes", etching pits, and dust.

Scratches

The scratches (Fig. 1) are usually localized in the iris region of the cavities and are indications of some mishandling or errors during the production steps leading to contacts or collisions between production tools and cavities thus resulting in mechanical damages of the niobium surface. The main impact of such defects on the cavity performance is an excessive x-ray radiation in the

ISBN 978-3-95450-178-6

SURFACE ANALYSES AND OPTIMIZATION OF CENTRIFUGAL BARREL POLISHING OF Nb CAVITIES

A. Navitski#, E. Elsen DESY, Hamburg, Germany
B. Foster[1], A. Prudnikava, Y. Tamashevich, University of Hamburg, Germany

Abstract

Detailed microscopy investigations of the niobium surface quality after centrifugal barrel polishing (CBP) have been performed applying metallographic techniques. The results imply the need for further optimisation of the polishing procedure, mainly to reduce the thickness of the layer that is damaged at the surface as well as pollution by the polishing media. The most realistic application of CBP is a combination using CBP initially to remove surface defects followed by chemical polishing to obtain a chemically clean niobium surface.

INTRODUCTION

Centrifugal barrel polishing (CBP) is an acid-free surface-polishing technique based on abrasive media. It considerably reduces the usage of chemicals in the preparation of Nb cavities, typically requiring only a final light electropolishing (EP) or buffered chemical polishing (BCP) step and achieving considerably smaller roughness than in chemical treatments alone [1, 2]. CBP addresses in particular the removal of pits, welding spatters, deep scratches, and inclusions of foreign material that occasionally occur in the production process and often remain unaffected by the EP/BCP treatment. A mirror-smooth surface without chemical contamination is also an important enabling step for thin-film technologies of SRF cavities.

A combination of CBP and EP/BCP was already applied and tested on single- and nine-cell Nb cavities with resulting quality factor Q_0 of cavities of more than 10^{10} and accelerating gradients E_{acc} of 25 to 40 MV/m [3, 4]. Accordingly, similar polishing is also considered for the accelerating structures of the future International Linear Collider (ILC) [5] as an alternative or partial replacement of the established EP procedure.

Dedicated studies of the CBP process using a "coupon" cavity and applying microscopy and metallographic techniques have been performed and reported here.

EXPERIMENTAL DETAILS

CBP Machine

The CBP machine (Fig. 1) has been purchased by the University of Hamburg and is used in the ILC-HiGrade Lab at DESY within a common R&D program [6]. The machine is custom built for this purpose by Mass Finishing Inc. and can be used to polish up to two single- or nine-cell 1.3 GHz SRF cavities at once. During the polishing process the cavity, approximately 50% filled with a polishing media, rotates around the central shaft of the machine at up to 110 rpm, while at the same time counter-rotating around its own axis with the same speed. The rotation speed of the main shaft determines the centrifugal force acting between the polishing media and the cavity walls, while the counter-rotation of the cavity lets the polishing media move across the surface and polish it.

Different polishing media and variation of the rotation speed is used to achieve an optimum polishing result.

Figure 1: CBP machine in the ILC-HiGrade Lab.

Coupon Cavity

Since quality of the inner surface plays a key role for the RF performance of the cavities, it is necessary to characterise the surface after the applied polishing procedure. The inner surface is, however, hidden in the cavity and difficult to access by conventional microscopy techniques. To overcome this, a special "coupon" cavity has been fabricated in cooperation with our colleagues from KEK, Japan. This is a niobium single-cell cavity with six openings into which removable samples (coupons) can be placed at the most interesting regions of the cavity (Fig. 2). The usage of the coupons allows polishing characterisation and optimisation by direct measurements of the surface roughness, removal rate, and removal profile as well as further detailing the amount of contamination left behind after the polishing process. This allows detailed surface studies after a series of CBP tests

*Work supported by EU FP7/2007-2013 under grant agreement number 283745 (CRISP), BMBF project 05H12GU9, and Alexander von Humboldt Stiftung/Foundation.
[1]Also at DESY and University of Oxford, UK
#aliaksandr.navitski@desy.de

CERN'S BULK NIOBIUM HIGH GRADIENT SRF PROGRAMME: DEVELOPMENTS AND RECENT COLD TEST RESULTS

A. Macpherson*, K. Hernandez Chahin, C. Jarrige, P. Maesen,
F. Pillon, K.-M. Schirm, R. Torres-Sanchez, N. Valverde Alonso.
CERN, Geneva, Switzerland

Abstract

Recent results from the bulk niobium high-gradient cavity development program at CERN are presented, with particular focus on test results for the 704 MHz bulk niobium 5-cell elliptical cavity prototypes produced for the Superconducting Proton Linac (SPL) project. Successive cold tests of bare cavities have been used to refine the cavity preparation and testing process, with all steps done in-house at CERN. Current performance results are discussed with reference to observables such as ambient magnetic field, field emission levels, and quenches.

INTRODUCTION

As part of CERN's ongoing programme of accelerator development, an R&D programme on bulk Niobium cavities has been established, with the focus on achievement of high gradients for elliptical cavities. For this programme, the work is a follow-on from the SPL project [1], and is designed to update the in-house competencies in superconducting RF, but also put in place the necessary infrastructure. Over the last 2 years, significant investment has occurred, with an ISO4 cleanroom and high pressure water rinsing facility, refurbished vertical and horizontal test-stand cryostats, and new measurement and diagnostic capabilities coming online.

Using the SPL 5-cell bulk niobium $\beta = 1$ elliptical cavities designed with a fundamental TM mode frequency at 2K of 704.4MHz as the primary test structures (see Fig. 1), a series of cold tests have been conducted to validate the SPL cavity RF performance. As part of this process, cavity surface preparation, measurement and analysis have also been improved. The SPL cavities specifications require an operating acceleration gradient of 25 MV/m with a $Q_0 = 1.0 \times 10^{10}$ at 2K, and the challenge has been to achieve this level of performance. Four prototype cavities have been produced in industry and two have been tested to date.

EXPERIMENTAL SETUP

Surface preparation and vertical testing of the cavity prototypes has been done entirely at CERN, including high pressure rinse, bakeout and assembly, with all but the chemistry being done in CERN's recently commissioned SRF cleanroom facility [2]. Vertical cold tests were performed in CERN's SM18 4 m deep vertical cryostat, and a summary of the RF surface preparation steps are:

- Degreasing by submersion in a NetInox solution
- Bulk electro-polishing: average removal of 160 µm
- 650 °C bake for 12 hrs then 12 hrs cool down
- Final electro-polishing: average removal of 20 µm
- High Pressure Rinsing, in a 100 bar rinsing cabinet.
- Drying in ISO4 clean room in laminar air flow.
- Assembly in an ISO4 cleanroom environment
- Mounting on the cryostat insert and leak testing
- [OPTIONAL] Bakeout at 120 °C for 40 hrs
- Cool down to 2 K: ambient magnetic field below 30 nT.

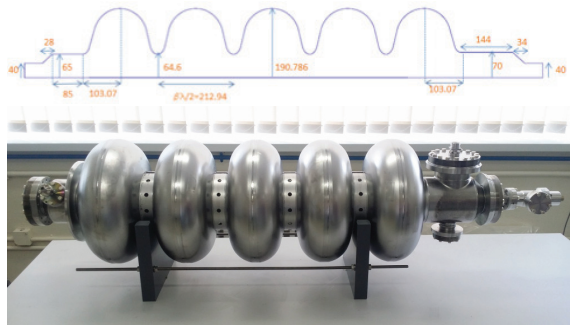

Figure 1: Mechanical dimensions of the $\beta = 1$ SPL cavity and a photo of the assembled cavity ready for testing.

Electropolishing of the first prototype (SPL1) was done with a simple solid body copper cathode, resulting in a surface containing numerous pinhole defects and shallow grooves. Both defects are understood in terms of excessive surface contact of hydrogen gas bubbles during the electropolishing process, with the former seen as a potential source of field emmission sites. For this reason the electropolishing cathode was redesigned with a mesh structure to allow improved flow through the cavity [3]. The second prototype (SPL2) was electropolished with the redesigned cathode. As can be seen from Fig. 2 the redefined cathode produced a much improved surface that was visibly free of pinholes and grooves.

High pressure rinsing of the cavities is done with a vertical 100 bar High Pressure Rinsing (HPR) cabinet with di-jet nozzle. A standard HPR rinse is composed of 6 cycles, each taking 50 min and is with a vertical nozzle speed of 0.5 mm/s, and a cavity rotation of 3 RPM.

Standard monitoring and diagnostic systems are deployed on the cavity; these include a 30 sensor OST array, 18 channels of temperature monitoring using contact temperature resistors (CERNOX, RuO_2, and Allen Bradley), cavity and Helium bath pressure gauges, and 3 single axis magnetic flux probes for ambient magnetic field measurement. The fully instrumented insert can be seen in Fig. 3.

* alick.macpherson@cern.ch

ISBN 978-3-95450-178-6

EXPERIENCES ON RETREATMENT OF EU-XFEL SERIES CAVITIES AT DESY

A. Matheisen, B.v.d. Horst, N. Steinhau-Kühl, N. Krupka, P. Schilling, S. Saegebarth
DESY Hamburg, Germany

Abstract

For the European XFEL, two industrial companies are responsible for the manufacture and surface preparation of the eight hundred superconducting cavities. The companies had to follow strictly the XFEL specification and to document all production and preparation steps. No performance guaranties were required. Each cavity delivered by industry to DESY is tested in a vertical test at 2K. Resonators not reaching the performances defined for application at the XFEL linear accelerator modules or showing leakage during cold RF tests have undergone a subsequent retreatment at DESY. Nearly 20% of the cavity production required retreatment, most of them by an additional High Pressure Rinsing. Some cavities received additional BCP flash chemical treatment when the initial HPR did not cure the problem. The analysis of retreatments and quality control data available from the retreatment sequences and the workflow of retreatment will be presented.

INTRODUCTION

The two companies, E. Zanon SpA (Italy) and Research Instruments (Germany), were contracted to build accelerator structures for the EU-XFEL accelerator. Each company had to manufacture 412 super conducting (s.c.) cavities by following strictly the procedures for cavity manufacturing and surface treatment as given in the document “Series surface and acceptance test preparation of superconducting cavities for the European EU-XFL (XFEL/A - D), revision B / JUNE 30, 2009 [1]. Handover of these cavities to DESY for acceptance test had to be in status “integrated to Helium tank (HT) and ready for acceptance test”.

No performance guaranty was requested when companies could show that they strictly followed the specification. In case specified procedures are followed and cavities did not fulfill the criteria for module assembly, the retreatment for performance improvement had to be done at DESY.

Until May 2014 permission for installation to modules was given, when usable gradient [2] above 26 MV/m was reached. After analysis of data on retreatments the acceptance level was reduced to usable gradients [3] above 20 MV/m.

Until August 2015 more than 90% of the EU-XFEL resonator were manufactured and handed out for acceptance test. About 20 % failed the acceptance criteria for module assembly or showed leaks during test at 2K were retreated at DESY [2].

RESPONSIBILITIES AND WARRANTIES

The fact that EU-XFEL production is the first time that the complete surface treatment is done at industry, no performance guaranty is asked for. The specification and the criteria for quality control (QC) defined in there [1] had to be followed strictly by industry. In case no deviations from specification are found, but cavities do not match performance, the retreatment is done by DESY.

It was agreed that the specification and the parameters specified there may not cover all conditions and unpredictable situations of a serial production. When problems showed up and were not covered by the specification a solution was found in close collaboration between companies and DESY.

In case of non-conformances at a late phase of production or for deviation of process data like TOC value of the ultra-pure water (UPW) or sulfur accumulation in vacuum systems [4] or only limited data from preparation phase of the EU-XFEL were on hand, a so called “limited acceptance” for handout of cavities to DESY was given. In this case companies did not stop processing of the cavities and took the responsibility for that. Cavities holding limited acceptance were recalled for retreatment by the companies, when the cavities failed the vertical acceptance test.

Leak tightness of the cavities is controlled at room temperature at the companies and at DESY during incoming inspection. Accessories like antennas or valves [1] are provided by DESY and responsibility for leak tightness or functionality of these components is at DESY.

In case leaks or suspect of leaks during cold test were detected at 2K but not detectable at room temperature, repair and retreatment was done at DESY. Leaks reproducible detected after cold test at a gasket or flange area were on the responsibly of the companies and cavities were send back for retreatment and control of gaskets and sealing surfaces.

RETREATMENT PASSES AT DESY

The general retreatment sequence (RP) for cavities to be retreated at DESY consist of four processing levels (table 1 to 4), which based on the experiences gained during preparation phase for the XFEL project [3].

The standard retreatment in first pass (RP1) was done by six times high pressure rinsing (HPR) at 100 bar of the inner surface. In case cavities not recovered in performance in first reprocessing the second retreatment pass (RP2) with removal of the Niobium surface by buffered chemical polishing (BCP) is executed. Cavities

ISBN 978-3-95450-178-6

HORIZONTAL RF TEST OF A FULLY EQUIPPED 3.9 GHz CAVITY FOR THE EUROPEAN XFEL IN THE DESY AMTF

C. Maiano, C. Albrecht, R. Böspflug, J. Branlard, L. Butkowski, T. Delfs, J. Eschke, A. Goessel, F. Hoffmann, M. Hüning, K. Jensch, R. Jonas, R. Klos, D. Kostin, W. Maschmann, A. Matheisen, U. Mavric, W. -D. Möller, C. Müller, K. Müller, B. Petersen, J. Rothenburg, O. Sawlanski, M. Schmökel, A. Sulimov, E. Vogel, DESY, Hamburg, Germany,
P. Pierini, INFN-LASA & DESY
A. Bosotti, M. Moretti, R. Paparella, D. Sertore, INFN-LASA, Segrate, Italy,
E. Harms, R. Montiel, FNAL, USA, S. Pivovarov, BINP, Russia

Abstract

In order to validate the cavity package concept before the module assembly, one 3.9 GHz cavity, complete with magnetic shielding, power coupler and frequency tuner has been tested in a specially designed single cavity cryomodule in one of the caves of the DESY Accelerator Module Test Facility (AMTF). The cavity was tested in high power pulsed operation at 24 MV/m, above the vertical test qualifications and all subsystems under test (coupler, tuner, waveguide tuners, LLRF system) were qualified to design performances.

INTRODUCTION

The correct operation of a superconducting cavity in an accelerator requires a number of active and passive subcomponents for its proper operation. Among these a cold tuning system is needed to fine tune the cavity frequency, a power coupler needs to deliver the necessary power for the beam, a magnetic shield provides to the superconducting material shielding from the earth magnetic field and HOM antennas extract from the cold region the power possibly generated in the high order modes of the superconducting structure (while properly filtering the main accelerating mode). In addition, the cryomodule mechanical environment around the cavity needs to allow the relative differential contraction of different materials without introducing uncontrolled forces on the cavities that could perturb their frequencies.

Frequently, in order to validate the complete design of the cavity package in its operating environment a complete test of a cavity dressed with all its ancillary components is performed in a short horizontal cryostat, preferably providing a mechanical environment similar to that of its operation in the linac cryomodules.

THE XFEL 3.9 GHz SECTION

The European XFEL injector will host a cryomodule composed of 8 SCRF cavities at 3.9 GHz, for the linearization of the RF curvature experienced by the beam in the first 1.3 GHz accelerating module, before the bunch compressor [1]. The module design has been derived from the FLASH third harmonic section, developed by FNAL [2], with some major modification in the cavity package design, in particular the development of cavities with alternate orientation of couplers with respect to beamline, to compensate coupler dipole kicks [3]. The cavities have been fabricated and vertically tested and the module has been prepared for tunnel installation; as described in several contributions to these Proceedings [4-6].

Figure 1 shows a 3D model of the 3.9 GHz dressed cavities (both orientations), equipped with cold tuners, cold main coupler part, RF antennas for the field probe and the HOM, and the magnetic shield (the top half of the parts connecting the cavities have been removed for better picture clarity).

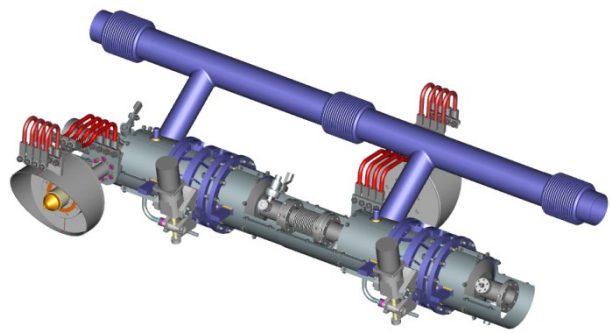

Figure 1: The two 3.9 GHz cavity packages, with opposing couplers.

For the preparation of the regular XFEL 1.3 GHz modules the cavities are individually tested in the AMTF [7], during the module qualification after assembly, before tunnel installation. In order not to interrupt the testing schedule of the 101 modules of the XFEL series, to limit the infrastructure work needed for adapting the AMTF for the testing of 3.9 GHz modules, and in view of the moderate performances needed by the 3.9 GHz cavities [1], the third harmonic system will be commissioned and characterized in the injector building after installation. Due to this fact, the qualification of the cavity package in a horizontal test represents an important verification to perform before the module assembly.

THE AMTF CRYOADAPTERS

Even if no single 1.3 GHz cavity horizontal tests were envisaged for the XFEL construction, two short (~2.2-meter) cryostats fitting the cryogenic connections of the AMTF test caves were delivered by BINP as part of the In

ISBN 978-3-95450-178-6

VERTICAL TESTS OF XFEL 3RD HARMONIC CAVITIES

D. Sertore#, M. Bertucci, A. Bosotti, J. Chen, C. G. Maiano, P. Michelato, L. Monaco, M. Moretti, R. Paparella, P. Pierini, INFN Milano - LASA, Segrate (MI), Italy
A. Matheisen, M. Schmoekel, DESY, Hamburg, Germany
C. Pagani, Università degli Studi di Milano & INFN Milano - LASA, Segrate(MI), Italy

Abstract

The 10 cavities of the E-XFEL 3rd Harmonic Cryomodule have been tested and qualified, before integration in the He-tank, in our upgraded Vertical Test stand. In this paper, we report the measured RF performances of these cavities together with the main features of the test facility.

INTRODUCTION

The 3rd harmonic 3.9 GHz section at the European XFEL (E-XFEL) injector provides linearization of the longitudinal beam phase space after the first accelerating section. To compensate the effect of the space charge, a long bunch is generated in the RF gun. The subsequent RF acceleration in the first 1.3 GHz module produces cosine sinusoidal curvature in the longitudinal phase space of the incoming bunch. To remove this effect, a 3.9 GHz module is placed afterwards to linearize the longitudinal phase space and prepare the beam for the following compression and acceleration stages.

The E-XFEL 3rd harmonic module is an 8-cavity module that provides a maximum voltage of 40 MV, corresponding to an accelerating field of about 15 MV/m per cavity. All the cavities will be operated close to 180° phase with respect to the incoming beam.

INFN Milano–LASA is in charge to provide, as in-kind contribution, the main components of the 3rd harmonic module ready to be installed in the E-XFEL tunnel. An important part of this activity has been the full qualification in Vertical Test of all the cavities (eight plus two spares) produced by the Ettore Zanon S.p.A. under INFN supervision [1]. This paper reports on features of our test facility and results of cavity tests.

VERTICAL TEST FACILITY

Clean Room

The Clean Room is a 9 m^2 ISO4 facility. A High Pressure Rinsing (HPR) system, properly designed for the small bore of the 3.9 GHz cavity, is installed inside the Clean Room. An Ultra Pure Water (UPW) plant supplies a 100 bar LEWA pump (max 170 l/h) which feeds the HPR. The high pressure water is filtered down to 20 nm before entering the HPR wand and impinging on the cavity wall.

The UPW plant operates in two stages. In the first stage, three Millipore Elix devices fill a 6000 litres tank with pure water. On demand, water is taken from the intermediate tank and filtered with a Millipore SuperQ to reach an UPW grade resistivity of 18 MΩ cm and TOC value below 3 ppb.

To clean cavities and large components, we installed an Ultrasound System composed by two tanks: one with Ultrasound Transducers for cleaning and one for rinsing with UPW water.

A slow pumping system is connected directly to the Clean Room for pumping and venting cavities in a controlled way to avoid dust particle movements.

Vertical Insert Support

The Vertical Insert support has been upgraded to host two cavities for increasing the test rate of our facility and it has been routinely used for testing the E-XFEL 3.9 GHz cavities, see Fig. 1.

Figure 1: Vertical Insert with two cavities ready for Vertical Test, fully equipped with thermometers and Second Sound sensors.

Moreover, we improved the UHV vacuum system adding, to the present setup, a Turbo Molecular Pump system and an RGA. The former is used as a backup in case of leak in the cavity vacuum to avoid the SIP pumping He. The latter is generally used to control the vacuum quality before opening the UHV cavity valves towards the Vertical Insert vacuum line and the vacuum composition during test.

Cryogenic Installations

The insert with two cavities to be tested provided with the diagnostic devices, test and feeding cables, piping and all the other ancillaries needed, is transferred inside the vertical cryostat placed in a bunker, to be cooled down to 2K (and below) for the qualification tests.

#daniele.sertore@mi.infn.it

MODE SENSITIVITY ANALYSIS OF 704.4 MHZ SUPERCONDUCTING RF CAVITIES*

K. Papke † [1,2], S. Papadopoulos[1], S. Horvath-Mikulas[1], E. Pilicer[1], F. Pillon[1], F. Gerigk[1] and U. van Rienen[2]
[1]CERN, Geneva, Switzerland
[2]University of Rostock, Rostock, Germany

Abstract

Due to the large variety of beam patterns considered for the superconducting proton linac (SPL) at CERN it is likely that the frequencies of some higher order modes (HOM) are close to machine lines during operation. Hence, in the interest of developing a method to shift HOM frequencies away from machine lines, we study the influence of cavity detuning and retuning (e.g. by field flatness tuning and frequency tuning during operation) on HOMs. The sensitivity of HOMs with respect to the fundamental mode was studied for a mono-cell and for five-cell high-beta SPL cavities operating at 704.4 MHz. First, the variation of the HOMs during the flat-field tuning was measured. In this process, several detuning and retuning cycles were made to estimate the range of residual HOM frequency shifts. Secondly, the effect of the frequency tuner on the HOMs is presented and finally the frequency shifts of all modes due to the cool-down.

INTRODUCTION

The SPL linac [1] is composed of two types of five-cell cavities (geometrical beta = 0.65/1.00) operating at 704.4 MHz in pulsed mode. As the linac allows a large variety of beam patterns, HOMs may easily drive instabilities. Thus, they have to be damped or shifted away from machine lines in order to avoid a resonant build-up. This paper focuses on the latter option and discusses its possibilities and limits for the high beta SPL cavities [2]. We study the influence of cavity detuning and retuning on HOMs as well as their sensitivity with respect to the fundamental mode using the tuning bench shown in Figure 1.

For the sake of simplicity, only the modes with the highest R/Q (Table 1) are shown. The tuning bench allows to compress and to lengthen the SPL mono-cell [2] and each cell of the five-cell cavity individually. In order to lengthen the mono-cell or the end cells of the multi-cell cavity, the setup shown in Figure 1 needs to be changed. One or both tuning wall(s) have to be connected to the beam pipe flanges, which leads to a traction not only of the cell but also of the beam pipe. Thus, the measurements of deformation between compression and traction are not comparable

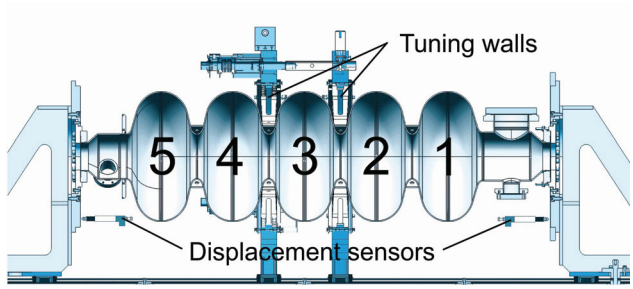

Figure 1: Setup of the tuning bench for a 5-cell SPL cavity.

in these cases as we measure deformations always via the cavity length (see displacement sensors in Fig. 1). A direct measurement of the cell deformation using displacement sensors at the cell irises was not possible.

In the following we present the detuning and retuning tests carried out with a mono-cell made of niobium and a five-cell cavity made of copper. Afterwards the frequency shift of HOMs during a tuner test is discussed and finally the effect of cool-down on the mode spectrum.

Table 1: Modes with High R over Q Values for the High-beta SPL Cavity [3, 4]

Monopole modes			Dipole modes		
Type	f [MHz]	R/Q [Ω]	Type	f [MHz]	$R/Q_\perp$ [Ω]
$TM_{010}\pi$	704.4	566	$TE_{111}3/5\pi$	915	57
$TM_{011}4/5\pi$	1322	39	$TE_{111}4/5\pi$	950	60
$TM_{011}\pi$	1331	140	$TM_{110}3/5\pi$	1014	36
TM_{021}	2087	10	$TM_{110}4/5\pi$	1020	25
TM_{021}	2090	21	Hybrid	1409	20
$TM_{022}\pi$	2449	9			

MONO-CELL CAVITY

The cavity was first compressed plastically by 0.23 mm using the setup in Figure 1 (tuning walls at the irises of the cell). The value of 0.23 mm corresponds to the pressure limit of the tuning bench at that time. Afterwards, the cell was lengthened plastically (tuning walls fixed at the beam pipe flanges) until the original frequency was restored. The results of the complete compression and traction cycle are depicted in Figure 2. Due to the different setup, the deformation is not equal to the cell deformation in the traction

* Work supported by the Wolfgang-Gentner-Programme of the Bundesministerium für Bildung und Forschung (BMBF)
† kai.papke@cern.ch

ISBN 978-3-95450-178-6

ANALYSIS OF THE TEST RATE FOR EUROPEAN XFEL SERIES CAVITIES

J. Schaffran, S. Aderhold, L. Monaco, D. Reschke, L. Steder, N. Walker, DESY, Hamburg, Germany
L. Monaco, INFN Milano - LASA, Segrate, Italy

Abstract

The main part of the superconducting European XFEL linear accelerator consists of 101 accelerator modules each containing eight RF-cavities. Before the installation to a module, all of these cavities will be tested at cryogenic temperatures in a vertical cryostat in the accelerator module test facility (AMTF) at DESY. This paper discusses the average vertical test rate at the present status. It should be 1 in the ideal case, but actually it's observed to be approximately 1.5. Classification and analysis concerning the reasons for this deviation are given as well as suggestions for a reduction of the test rate for future production cycles.

INTRODUCTION

The construction of the European XFEL linear collider is in full, swing. In total, 808 cavities have to be integrated into 101 cryogenic modules. To guarantee an adequate cavity shape, verify the performance and to set up the accelerator in an optimal way, all cavities have to take a comprehensive quality control in the Accelerator Module Test Facility (AMTF) by RF-testing at 2K. Not all cavities pass this test, so that multiple measurements for some are necessary. Since this kind of mass production is unique up to now, it is worth to classify the single tests and calculate the test rate (average tests per cavity). All tests of European XFEL series cavities up to the 31th of July 2015 were taken into account. Reference cavities (RCVs), used for the commissioning at the vendors site, are not included in the calculation, but a brief summary for them is also included. The actual status of the vertical test results is given in [1] and [2].

CAVITY TESTS AND TEST RATE

Vertical cold RF-tests of the superconducting 9-cell niobium cavities play an important role in the construction phase of the European XFEL. More than 800 cavities have to be tested in two vertical cryostats within 3 years. Test results are used for quality control of the performance and RF behavior and also for sorting the cavities into modules. To guarantee a sufficient test rate the cryostats are designed to install four cavities at a time (discussed in [3]). This helps to save worthwhile cool-down time, which is essential to bring the cavities to the module assembly area in time and hold the project schedule. An overview of the test set-up, as it is currently used in the AMTF is given in figure 1. A detailed description of the complete test sequence can be found in [4] and [5].

Figure 1: Vertical support structure for testing at AMTF.

The total number of vertical tests per month, without RCVs, is shown in figure 2. The average delivery rate per month appears to approximately 42 [2]. To get an overview of all cavity tests, the test rate as an expressive value was used. All cavities undergo at least one acceptance test. In order to understand better the evolution of retest rates during the production, we define an average monthly test rate as the average number of tests per cavity arriving in that given month (by definition ≥ 1). Note that the actual vertical tests can occur much later than the arrival date, especially for multiple retesting, but use of the arrival date gives a better indication of the actual production process at the companies. To date 1103 RF tests have been made on 741 cavities. This gives us an average test rate of 1.49 tests per cavity. Due to some vacuum problems (leaks, degasing, etc.) at low temperature, that were too serious for proceeding with the cool down cycle, the number of all cool downs is significantly higher at 1181 and leads to a cool down rate of 1.59. The trend of the test rate as defined above for both cases is given in figure 3. The reference date is the date of arrival at DESY and all tests, without RCVs, are counted in the following. Starting with a test rate around a value of 2 at the beginning of the series production, we have now stabilized at a value of around 1.2, established during a stable cavity delivery rate (see figure 2).

Especially in the beginning of 2014 and at the end of 2014/start 2015 we had a significant deviation between the test rate and the cool down rate, caused by a number of large cold leaks, which forced us to stop the cool down process before the RF-test could be performed. In these cases test results are not available and a transfer to the

ISBN 978-3-95450-178-6

UPDATE AND STATUS OF TEST RESULTS OF THE XFEL SERIES ACCELERATOR MODULES

Mateusz Wiencek, Karol Kasprzak, Agnieszka Zwozniak, IFJ-PAN, Kraków, Poland
Denis Kostin, Detlef Reschke, Nicholas Walker, DESY, Hamburg, Germany

Abstract

The European X-ray Free Electron Laser is under construction at DESY, Hamburg. During preparation for tunnel installation 100 Cryomodules are tested in a dedicated facility on the DESY campus. Up to now around 50 cryomodules have been measured at 2K. This paper describes the current status of the measurements, especially single cavity limitations. In addition we present a comparison between the vertical test results of the individual cavities and the corresponding performance measurements of the cavities once assembled into the accelerator string inside the cryomodule.

INTRODUCTION

The linac part of the XFEL consists of 101 SRF cryomodules. Before installation into the linac tunnel all of the cryomodules are tested in a dedicated Hall AMTF (Accelerator Module Test Facility) on the DESY campus. The AMTF Hall is equipped with three horizontal test benches, which allows three cryomodule tests in parallel.

At the end of August 2015, more than 50 % of the cryomodules have been tested.

STATUS OF TESTED CRYOMODULES

Currently 52 cryomodules have been successfully tested. Some of the cryomodules delivered to the AMTF were not tested due to problems encountered before or during the test procedure.

The testing rate of the cryomodules was planned as one cryomodule leaving the AMTF test benches per week. With three test benches, the number of days foreseen for one cryomodule test is 21 calendar days. Within this time all necessary corrections have to be made as well. To be able to keep this schedule, works at AMTF are performed on two shifts. Current testing rate of the cryomodules is greater than planned (see Fig. 1). After improvements made to the existing testing procedure (see [1], [2]) after June 2015 the testing rate has significantly increased.

SINGLE CAVITIES PERFORMANCE IN THE CRYOMODULES

One of the most important cryomodule parameters measured at AMTF is the single cavity performance. During this so-called "flat - top" test, individual cavity limits are measured. There are two main threshold for the cavities: Maximum gradient and operating gradient.Maximum gradient is the gradient just below the cavity quench. However, at the AMTF with the given XFEL [3] pulse parameters, the maximum gradient which can be achieved is 31 MV/m.

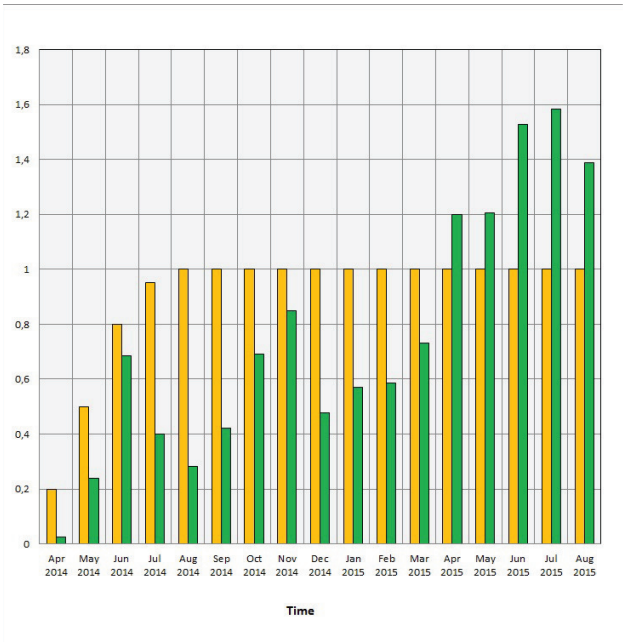

Figure 1: Cryomodule testing rate. Yellow bars represent planned quantity per week. Green one represents real quantity.

Infrastructure limitation causes a situation where some of the tested cavity have power limitation instead of real quench value of the accelerating field.

Operating gradient for a single cavity is a value of the usable acceleration field which is foreseen for the cavity during operation. It is defined as the minimum value of:

- BD (Break Down) Limit - Cavity gradient just before the quench reduced by 0.5 MV/m
- X-ray Limit - Gradient when the radiation level measured at one of the ends of the cryomodule is equal to 10^{-2} mGy/min
- PWR (Power) Limit - is equal to 31 MV/m.

XFEL specification for a single cavity operating gradient has been set to 23.6 MV/m . However, if some of the cavities do not fulfil this criteria, compensation by cavities with higher acceleration field is possible. As shown on Fig. 2, almost 25 % of the tested cavities have operating gradient below the XFEL goal. Despite this fact, the average operating gradient for all of the tested cavities is equal to 27.2 MV/m.

In the Fig. 3, the number of the cavities which did not meet XFEL goal in the cryomodules is shown. There is one of the cryomodules with 7 cavities below the XFEL specification

ISBN 978-3-95450-178-6

COOLING FRONT MEASUREMENT OF A 9-CELL CAVITY VIA THE MULTI-CELL TEMPERATURE-MAPPING SYSTEM AT CORNELL UNIVERSITY

M. Ge#, R. Eichhorn, F. Furuta,
Cornell University, Ithaca, NY 14853, USA

Abstract

Cooling speed significantly affects flux trapping of a SRF cavity, which will determine the residual resistance and the quality factor of the cavity. We measured the temperature distribution of a 9-cell cavity at different cooling speeds by the multi-cell T-map system of Cornell University. This paper proposed a method to evaluate the formation of a normal conducting island at different cooling speed. The fast cool-down and slow cool-down has been compared. We conclude that the slow cool-down freezes less normal conducting islands.

INTRODUCTION

For the future accelerators, the high quality factor of SRF cavities will reduce the cryogenic cost and operation cost. Hence the surface resistance should be kept as low as possible. Resent tests of cavities suggested that the cooling speed impacts the quality factor significantly when the cavity transits from normal conducting state to superconducting. The first observation was reported by HZB in 2011[1]. They stated that the slow cool-down can do the better external magnetic field expulsion. Cornell University observed quite similar results from ELR 7-cell horizontal test by several thermal cycles [2]. The Q-value had been increased by factor 2 due to the slow cool-down. However, the nitrogen-doped cavities can achieve high-Q benefited from the fast cool-down [3-4], which is contradict to the observation in [1-2]. The discussion was focus on how the cooling speed affects the cooling uniformity of a cavity. As Cornell's multi-cell temperature-mapping system has unique capabilities, we started investigating cool-down dynamics of multi-cell cavities to get an understanding how the transition region between the normal and the superconducting state moves along the cavity.

THE EXPERIMENT SET-UP

The Cornell multi-cell Temperature-map system [5, 6] has nearly two thousand thermometers. The temperature sensor is a 100Ω carbon Allen-Bradley resistor (5% 1/8 W). The sensors are pushed tightly to against cavity exterior surface by Pogosticks and springs. APIEZON type N grease, which has good thermal conductivity at low temperature, is applied to fill the gap between the sensors and the surface. The T-map system is consisted of two sets of 3-cell boards and one set of 1-cell boards. One set has 24 boards attached azimuthally in every 15 degree on a cavity. Thus the system is capable to measure up to seven cells of a multi-cell SRF cavity. In this experiment, we mounted the T-map on the middle seven cells of a TESLA-shape 9-cell cavity which is shown in Fig. 1. The 9-cell cavity in Fig. 1 has been vertically mounted on an insert. The main coupler port is on bottom side; the board number 1 in every set has same angle with the main coupler port. In this paper, we only consider the T-map covered cells and define the cell numbers 1 to 7 from top to bottom. The T-map system has 5 channels to connect electronics (depicted in Fig. 1 (Right)); the channel 1 and 2 scan the top three cells, the channel 3 scans the middle cell, and the channel 4 and 5 scan the bottom three cells. The T-map electronic scans 5 channels simultaneously; it takes one minute for the electronics to scan all the T-map sensors. A Matlab program records the resistance value of each T-map sensor. The T-map was continuously running during the cavity cool down and warm up, therefore the T-map can capture the temperature variation versus time.

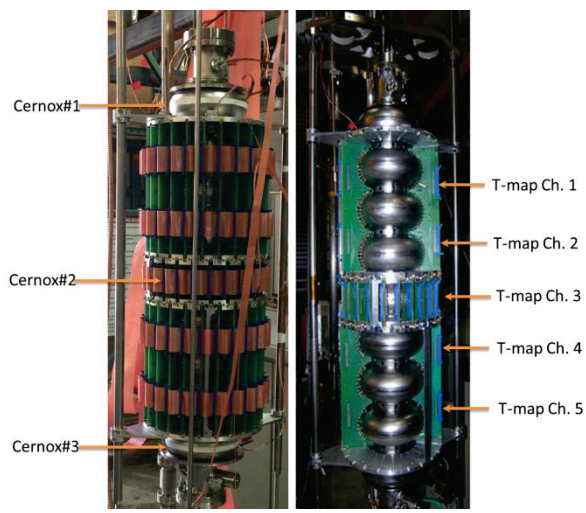

Figure 1: (Left) The multi-cell temperature-mapping system mounted on a TESLA-shape 9-cell SRF cavity, (Right): Several T-map boards have been removed to expose the cavity.

Calibration

As the T-map can only record the resistance value of each sensor, it needs to convert it into temperature value. In a calibration, we change ambient temperature surrounding the T-map sensors recording the resistance of each T-map sensor and the ambient temperature simultaneously. Hence the relation between the resistance and the temperature is possible to be established. The key

#mg574@cornell.edu

ISBN 978-3-95450-178-6

PERFORMANCE OF NITROGEN-DOPED 9-CELL SRF CAVITIES IN VERTICAL TESTS AT CORNELL UNIVERSITY*

M. Ge#, R. Eichhorn, B. Elmore, F. Furuta, D. Gonnella, T. Gruber, G. Hoffstaetter, J. Kaufman, M. Liepe, T. O'Connell, J. Sears, E. Smith, Cornell University, Ithaca, NY 14853, USA

Abstract

Cornell University treated five LCLS-II 9-cell cavities by nitrogen-doping recipe. In this paper, we reported the performance of these 9-cell cavities. In the treatments, the nitrogen recipes are slightly different. The cavities have been firstly doped under high nitrogen pressure; after the vertical tests some of the cavities has been reset the surface and re-doped under light nitrogen pressure. The detail of the cavity preparation and test results will be shown. The comparison of the different recipes will be discussed.

INTRODUCTION

The LCLS-II project [1] requires its Superconducting RF (SRF) cavities working at accelerating gradient (E_{acc}) 16MV/m with intrinsic quality factor (Q_0) 2.7×10^{10} at temperature 2K. The quality factor of a standard electro-polished (EP) cavity can achieve $1.5\text{-}2.5\times10^{10}$ at temperature 2K [2]. Therefore the EP'd cavities cannot reliably meet the requirement of LCLS-II. The nitrogen-doping recipe has been developed and applied for the LCLS-II project, which can reliably produce Anti-Q-slope for cavities [3-5]. Cornell University treated five 1.3GHz 9-cell SRF cavities for the LCLS-II project by the nitrogen-doping recipe. Both the light-doping and heavy-doping recipe has been applied to these cavities. The details of the treatments and vertical test results will be shown and discussed in the following sections.

CAVITY TREATMENTS

The cavities were received as a brand new cavity from Advanced Energy Systems, Inc. (AES), shown in Fig. 1 (a). The cavities have been vertical electro-polished (VEP) about 120μm by Cornell VEP system [6] (Fig. 1 (b)).

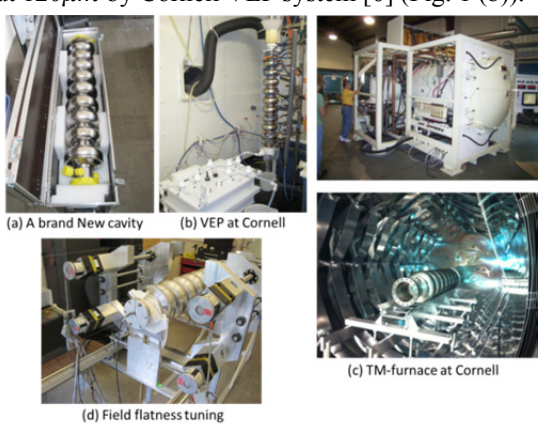

Figure 1: The photographs of the cavity treatments.

Then the cavities were baked in Cornell TM-furnace [7] (displayed in Fig. 1 (c)) at 800°C to degas hydrogen. Figure 2 shows the curves of the partial pressure versus time for the cavity TB9AES018. In total this cavity had been baked about 3 days. However, the curves manifest that the hydrogen can be degassed within 10 hours. Therefore we reduced the baking time to 3 hours for the rest cavities, because long time baking will soften the material and deform the cavities.

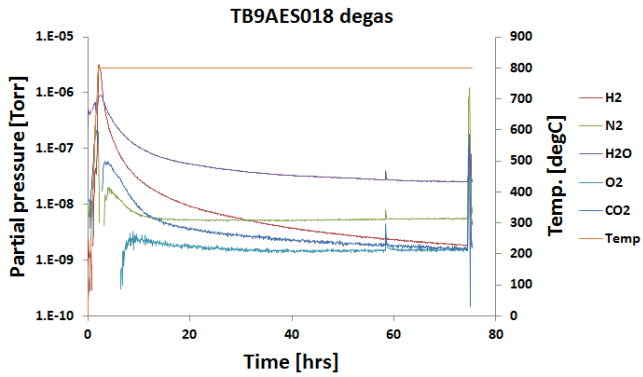

Figure 2: 800°C degassing curves of the cavity TB9AES018; On left scale: the partial pressure versus time curves; On right scale: the temperature versus time curve.

At the end of the baking, high pure nitrogen gas had been injected into the chamber of the furnace for doping; after the doping, the nitrogen gas was pumped out, and the cavity was kept 800°C under good vacuum for a while.

We treated the cavities in two runs: All five cavities had been doped with the heavy doping recipe and tested. After the first run two cavities had been reset the surface by bulk VEP, doped with light-doping recipe, and re-tested. The nitrogen pressure of the heavy and light recipes are listed as follow,

- The heavy doping: nitrogen pressure 40-60mTorr;
- The light doping: nitrogen pressure 20-30mTorr.

Figure 3 shows an example of the relation of nitrogen pressure versus time of the heavy doping recipe for the cavity TB9AES018. During the doping, the nitrogen pressure was difficult to be maintained at a constant level. Hence in our case, the pressure was oscillated in about 20mTorr ranges for both recipes. When the doping was completed, the cavities were tuned to keep field flatness better than 90%, shown in Fig. 1 (d).

*Work supported by the US DOE, the LCLS-II High Q0 Program, and NSF Grant NSF-PHY-1416318.
#mg574@cornell.edu

EFFORTS OF THE IMPROVEMENT OF CAVITY Q-VALUE BY PLASMA CLEANING TECHNOLOGY: PLAN AND RESULTS FROM CORNELL UNIVERSITY

M. Ge#, F. Furuta, G. Hoffstaetter, M. Liepe, J. Sears, V. Veshcherevich,
Cornell University, Ithaca, NY 14853, USA

Abstract

We reported the plasma works at Cornell University. The plasma has been generated for 1) surface cleaning to reduce field emission; 2) the cavity quality factor improvement. The experiment design, including RF design, the gas type and pressure selection, the external DC magnetic field calculation, had been discussed. The plasma experiment set-up by using a 1.3GHz single-cell cavity is shown. Argon and helium plasma was successfully ignited in the cavity; the results of the plasma processing will be displayed.

INTRODUCTION

Experience with larger SRF installations shows that occasionally SRF cavities have substandard performance, and an in-situ cleaning mechanism would be highly desirable to recover the performance. Plasma cleaning was successful in reducing field emission in cavities with poor performance [1]. Potentially, it might also be able to improve the quality factor Q_0 not only by reducing field emission, but also by removing bad oxides or other surface contamination. Within this proposal we would study if in-situ plasma cleaning can be effective in recovering or even improving the medium field Q_0 of SRF cavities.

DESIGN OF THE PLASMA EXPERIMENT

RF Design

As the plasma project has two goals: 1) reducing the field emission; 2) The Q-value improvement. The selection of RF modes has been considered, because the plasma only concentrates in E-field region but not in B-field region. For the Q-improvement purpose, the plasma should treat the surface on the cavity equator region; hence the RF modes should have E-field distribute on the equator region. The fundamental mode of a 1.3GHz cavity is TM010 which has E-field concentrating on the iris region but not the equator. Therefore the TM010 can be only used for the cleaning purpose. Several higher-order-modes have been considered as candidates for the Q-improvement: TM011, TE111, and TE211modes. They have E-field components on the equator.

The couplers of those modes have been designed to transfer the RF power into the cavity without causing RF break-down in the transmission line. Sine we have several modes to excite, both the hook antenna and straight antenna have been designed, shown in Fig. 1.

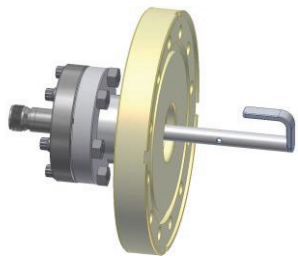

(a) The hook antenna for TE111 and TM011 mode

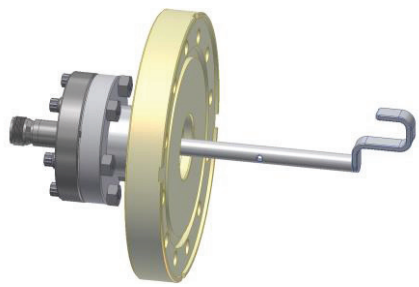

(b) The hood antenna for TE211 mode

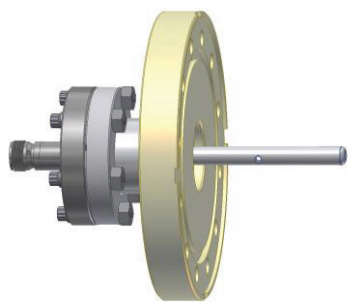

(c) The straight antenna for TM010 mode

Figure 1: Hook antenna and straight antenna designed for TE111, TE211, TM010, and TM011 modes.

The external Q versus antenna length curves for three types of couplers is displayed in Fig. 2. Since we treated the cavities at room temperature, the Q_0 of the cavity was around 5000. The plasma will consume RF power as well; hence the Q-value of the whole system could be even low to 1000. The external Q should match the system Q keeping the reflection power minimum. For our works, we selected the Q_e is about 7e3 marked by the red rectangular in Fig. 2, because the antenna should not be too close to the cell.

#mg574@cornell.edu

ISBN 978-3-95450-178-6

UPDATE AND STATUS OF VERTICAL TEST RESULTS OF THE EUROPEAN XFEL SERIES CAVITIES

N. Walker*, D. Reschke, J. Schaffran, L. Steder, DESY, Hamburg, Germany
M. Wiencek, IFJ-PAN, Kraków, Poland
L. Monaco, INFN Milano, LASA, Milano, Italy

Abstract

The series production by two industrial vendors of the 808 1.3-GHz superconducting cavities for the European XFEL has been on-going since the beginning of 2013 and will conclude towards the end of this year. As of publication some 740 cavities (~93%) have been produced at an average rate of ~7 cavities per week. As part of the acceptance testing, all cavities have undergone at least one vertical RF test at 2K at the AMTF facility at DESY. The acceptance criterion for module assembly is based on the concept of a "usable gradient", which is defined as the maximum field taking into account Q_0 performance and allowed thresholds for field emission, as well as breakdown limits. Approximately 18% of the cavities have undergone further surface treatment in the DESY infrastructure to improve their usable gradient performance. In this paper we present the performance statistics of the vertical test results, as well as an analysis of the limiting criteria for the usable gradient, and finally the impact of the surface retreatment on both usable gradient and Q_0.

INTRODUCTION

The 17.5 GeV superconducting linac for the European XFEL is currently under construction at DESY by a European consortium [1]. The linac consists of 101 cryomodules each containing eight 1.3-GHz TESLA-shape niobium cavities, with a design average operational gradient of 23.6 GeV with $Q_0 \geq 10^{10}$. The 808 cavities are being entirely manufactured by industry. Performance testing (vertical test at 2K) is performed at DESY [2]. After vertical testing, accepted cavities are sent to the string and cryomodule assembly facility at CEA Saclay [3], while low-performing cavities are retreated using the DESY infrastructure.

As of publication, the production and testing of the cavities has been in full swing for over 20 months and is now almost complete. This report presents an update of [4] which presented the vertical test results of the first half of the production. In addition to the overall statistics for the "as received" performance, further analysis of the limiting criteria for the usable gradient are reported. Finally the impact of surface retreatment (at DESY) for the low performance cavities (approximately 18% of the total) on both usable gradient and low-field Q_0 will be given.

* nicholas.walker@desy.de

CAVITY PRODUCTION AND TESTING OVERVIEW

Industrial Cavity Production

The series production of 808 TESLA-type cavities is equally divided between two vendors: E. Zanon Spa. (EZ) in Italy, and Research Instruments GmbH (RI) in Germany. The cavities are delivered to DESY complete with helium tank, pick-up probe, High-Q input coupler (fixed coupling), and are ready for vertical testing. The achieved average production rate is 6.6 cavities per week (slightly lower than the original target of 8 per week). DESY provides the niobium material (semi-finished products). The vendors perform the mechanically fabrication and subsequent surface treatment, both of which must confirm to strict specifications provided by DESY (so-called "build to print"). No final performance guarantee is required, for which DESY accepts the risk: hence DESY is responsible for any remedial action required should the cavity fail to meet gradient and/or Q_0 performance goals.

The cavities produced by EZ and RI differ in the final chemical treatment (final polishing), with EZ applying a final chemical surface removal ("Flash-BCP"), while RI have opted to use a light electro-polishing (EP), both treatments being within the specification. Flash-BCP has the advantage that it can be applied with the cavity already mounted in the helium tank, while for EP, the tank must be mounted post treatment.

Vertical Acceptance Testing

Once delivered to DESY, the cavity undergoes acceptance testing at the purpose built Accelerator Module Test Facility (AMTF), which includes a full performance RF test suite at 2K [5]. To achieve the relatively high testing rates (~10–15 tests per week including retests) two vertical cryostats are employed, each capable of simultaneously cooling down four cavities. The test infrastructure has been in full operation since October 2013 (see Fig. 1). The vertical acceptance tests follow a standardised and automated procedure, which includes the measurement of the unloaded Q-value (Q_0) versus the accelerating gradient E_{acc} at 2 K, as well as the frequencies of the fundamental modes. For each point of the $Q_0(E_{acc})$-curve, X-rays are measured inside the concrete shielding above and below the cryostat. Cavities are always tested to their limiting gradient, generally

ISBN 978-3-95450-178-6

INTEGRATED HIGH-POWER TESTS OF DRESSED N-DOPED 1.3 GHz SRF CAVITIES FOR LCLS-II

N. Solyak#, T. Arkan, B. Chase, A. Crawford, E. Cullerton, I. Gonin, A. Grassellino, C. Grimm, A. Hocker, J. Holzbauer, T. Khabiboulline, O. Melnychuk, J. Ozelis, T. Peterson, Y. Pischalnikov, K. Premo, A. Romanenko, A. Rowe, W. Schappert, D. Sergatskov, R. Stanek, G. Wu,
FNAL, Batavia, IL 60510, USA

Abstract

New auxiliary components have been designed and fabricated for the 1.3 GHz SRF cavities comprising the LCLS-II linac. In particular, the LCLS-II cavity's helium vessel, high-power input coupler, higher-order mode (HOM) feedthroughs, magnetic shielding, and cavity tuning system were all designed to meet LCLS-II specifications. Integrated tests of the cavity and these components were done at Fermilab's Horizontal Test Stand (HTS) using several kilowatts of continuous-wave (CW) RF power. The results of the tests are summarized here.

INTRODUCTION

The LCLS-II 4 GeV superconducting linac [1] is based on XFEL/ILC technology intensively developed over the last couple of decades. A major difference however is that LCLS-II operates in the CW regime, whereas the XFEL/ILC will operate in pulsed mode. This required modifications to or complete re-design of some of the basic components: cavity Helium vessel, tuner, power coupler, and other cryomodule parts in order to accommodate the much higher cryogenic loads expected in the CW regime. To accelerate the production of two pre-production cryomodules, it was decided to use existing ILC bare cavities and fundamental power couplers, which led to some constraints.

The major LCLS-II modifications of the dressed cavity and auxiliaries are as follows:

- Nitrogen doped cavity to reduce losses in CW regime. LCLS-II requirements: $Q_0 > 2.7 \times 10^{10}$ at the nominal gradient of 16 MV/m.
- Helium vessel with a larger diameter two-phase connection to accommodate higher heat flux, and two helium supply inlets to provide more uniform thermal gradients during cooldown, which are crucial to effective magnetic flux expulsion, and hence low surface resistance.
- Two layers of magnetic shielding to reduce residual magnetic field at the cavity below 5mG.
- New end-lever tuner design which had to remain compatible with the "short-short" version of the ILC cavity adopted for the pre-production cryomodule. This design must also fit the "short-long" XFEL version of the cavity, which was adopted for production cryomodules.
- Design of the fundamental power coupler (FPC) was modified to fulfil LCLS-II requirements: loaded Q=4 x 10^7 and average power up to 6.4kW (includes 1.6kW of reflected power). Major modifications include reduction of the antenna length by 8.5mm and increase in the thickness of copper plating on the inner conductor of warm section to reduce coupler temperature.

To minimize the risks to the project all technical solutions and new designs have to be prototyped and tested in a cryomodule. Testing was focused on the most critical components and technical solutions, and performed in the Horizontal Test Stand cryostat (HTS) under conditions approximating the final cryomodule configuration. An integrated cavity test was the last stage of the design verification program. In this test a nitrogen doped cavity (AES021), previously qualified in a vertical cryostat, was dressed and fully assembled with all components (fundamental power coupler, two-layer magnetic shielding, XFEL-type feedthroughs, end-lever tuner). All components were previously individually tested in the HTS with cavities, but not as a complete integrated system. One major goal of this integrated test was to demonstrate that high Q_0 values demonstrated in vertical test can be preserved even when additional sources of heating from the power coupler and tuner and potential additional external magnetic fields from auxiliary components are present.

Other important studies related to design verification included thermal performance and power handling of the power coupler, heating of HOM couplers and tuner components, tuner performance, sensitivity to microphonics, and frequency control. Data from this test program allows component design to be verified and certain other aspects of cryomodule design (e.g., component thermal anchoring) to be finalized.

TEST PREPARATION AND CAVITY CONFIGURATION

Dressed cavity AES021 was tested previously in a vertical test stand (VTS) without HOM feedthroughs. HOM feedthroughs were later installed in a clean room and after a brief high pressure water rinse, a pumping manifold was installed, the cavity evacuated, and successfully leak checked. The cavity field probe was not removed or replaced. The cavity was transported to a different clean room for installation of the coupler cold section. No additional cleaning of the cavity surfaces took place either as part of or subsequent to coupler installation. HOM feedthroughs were later installed in a clean room and after brief high pressure water rinsing, a pumping manifold was installed and cavity was leak tight. Cavity was transported to assembly clean room for

solyak@fnal.gov

HOM MEASUREMENTS ON THE ARIEL eLINAC CRYOMODULES

P. Kolb, R.E. Laxdal, Y. Ma, Z. Yao, V. Zvyagintsev
TRIUMF, 4004 Wesbrook Mall, V6T 2A3 Vancouver, BC, Canada

Abstract

The ARIEL eLINAC is a 50 MeV, 10 mA electron LINAC designed for the creation of rare isotopes via photo-fission. Future upgrade plans include the addition of a re-circulating beam line to allow for either further energy increase of the beam beyond 50 MeV or to operate a free electron laser in an energy recovery mode. For both recirculating LINAC and ERL the higher order modes (HOM) have to be sufficiently surprised to prevent beam-break-up. The design of the 1.3 GHz nine-cell cavity incorporated this requirement by including beam line absorbers on both ends of each cavity and an asymmetric beam pipe configuration on the cavity to allow trapped modes to propagate to the beam line absorbers. Measurements of the higher order modes on the completed injector cryomodule and the first cavity in the accelerating cryomodules will be shown and compared to simulations.

INTRODUCTION

ARIEL will complement the existing accelerator complex at TRIUMF with its rare isotope program. With the addition of the eLINAC up to three out of ten experimental stations (currently one out of ten) can receive rare isotope beams (RIBs). The production of the RIBs is done via photo fission that utilizes the 50 MeV 10 mA continuous wave (cw) e^- beam from the eLINAC. In the finished eLINAC three cryomodules house five 1.3 GHz nine cell cavities. The cryomodules are split into one injector cryomodule (ICM) with one cavity and two accelerator cryomodules (ACM) with two cavities each. In the first phase only one ACM is available and recirculating the beam to use the first ACM a second time is an attractive option to reach 50 MeV. After the eLINAC is completed the recirulating beam line can be used to excite an FEL and run the eLINAC in an energy recovery LINAC (ERL) mode which layout can be seen in fig. 1. Both operation modes, recirculating and ERL, are vulnerable to multi-pass BBU [1]. Therefore it is necessary to study the HOM spectrum of the cavities.

Beam dynamic calculations have shown a limit in dipole shunt impedance $R_{Sh,d}$ (as defined as in Ref. [2]) of 10 MΩ to have a high enough threshold current. A fabrication tolerance study showed uncertainties of up to a factor of two in shunt impedance [3] therefore a lower limit of 1 MΩ is set as goal. Simulation with ACE3P [4] show that this can be reached using the TRIUMF cavity design [5] which utilizes beam line absorbers to reduce the quality factor Q of the HOMs. The damping material CESIC has been tested for its RF properties in a cryogenic environment [6] and found adequate to reach the goal.

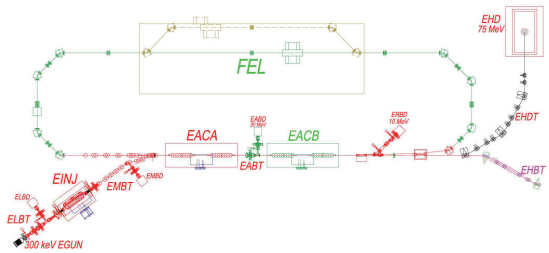

Figure 1: Proposed layout of the ARIEL accelerator with future recirculating beam lines for additional energy gain or ERL operation.

HOM MEASUREMENTS

Figure 2: Injector cryomodule of the ARIEL eLINAC.

HOM beadpulling measurements on a copper model of the ARIEL nine-cell cavity have agreed reasonable well with simulations [7]. For measurements on the cryomodules (fig. 2 shows the ICM), transmission measurements between the main power coupler and the pick-up probe are fitted to a Lorentz-function to extract the frequency and bandwidth. For the data acquisition a Labview program was written to automatically collect the transmission data from a network analyzer for a narrow frequency band and after the signal is sufficiently stable, move on to higher frequencies. This way the resonant frequencies were identified. To improve the resolution on high Q modes, high precision measurements of each resonance followed with a narrower frequency span to improve on resolution. Since the frequency is in the range of 1 to 3 GHz, the bandwidth for modes with Qs of 10^7 and higher is of the order of 100 Hz and lower. This makes measurements difficult as the resolution of the network analyzer is limited and frequency fluctuations cause by small Helium pressure changes or physical vibrations broaden the resonance. This sets the limitations

ISBN 978-3-95450-178-6

1.3 GHz CAVITY TEST PROGRAM FOR ARIEL

P. Kolb[1], P. Harmer[1], J. Keir[1], D. Kishi[1], D. Lang[1], R.E. Laxdal[1], H. Liu[1], Y. Ma[1], B.S. Waraich[1], Z. Yao[1], V. Zvyagintsev[1], E. Bourassa[2], R.S. Orr[2], D. Trischuk[2], T. Shishido[3], and T. Shishido[3]

[1]TRIUMF, Vancouver, B.C., Canada
[2]University of Toronto, Toronto, ON, Canada
[3]High Energy Accelerator Research Organization (KEK), Tsukuba, Ibaraki 305-0801, Japan

Abstract

The ARIEL eLINAC is a 50 MeV 10 mA electron LINAC [1]. Once finished, five cavities will each provide 10MV of effective accelerating voltage. At the present time two cavities have been installed and successfully accelerated been above specifications of 10 MV/m at a Q0 of 1010. The next cavities are already in the pipeline and being processed. In addition, one additional cavity has been produced for our collaboration with VECC, India. This cavity has been tested and installed in a cryomodule identical to the eLINAC injector cryomodule.

New developments for single cell testing at TRIUMF are a T-mapping system developed in collaboration with UoT and vertical EP for single cells in collaboration with KEK.
The progress of the performance after each treatment step has been measured and will be shown.

INTRODUCTION

ARIEL will complement the existing accelerator complex at TRIUMF with its rare isotope program. With the addition of the eLINAC up to three out of ten experimental stations (currently one out of ten) can receive rare isotope beams (RIBs). The production of the RIBs is done via photo fission that utilizes the 50 MeV 10 mA continuous wave (cw) e^- beam from the eLINAC. In the finished eLINAC three cryomodules house five 1.3 GHz nine-cell cavities. The design gradient for each cavity is 10 MV/m. The cryomodules are split into one injector cryomodule (ICM) with one cavity and two accelerator cryomodules (ACM) with two cavities each. At the time of writing the injector cryomodule is completed and accelerated a low intensity beam successfully to about 12 MeV, surpassing the design gradient. The first ACM was initially installed with only one cavity due to time constrains. As soon as the second cavity is ready, the cryomodule will be removed from the beam line and outfitted with the second cavity.

Since the last time reported, two nine-cell cavities have been fully tested and installed into cryomodules. One additional cavity has passed the vertical testing phase and its helium jacket is being dressed with its helium jacket. A fourth cavity is in the vertical testing phase and showed a good performance.

VERTICAL CAVITY TESTS

All vertical tests use a similar self excited loop to control the RF frequency and amplitude as the ISAC-II system. A frequency mixer down- and upconverts the 1.3 GHz signal to the ISAC-II high-β cavity frequency of 140 MHz, so that the the signal is in a useful range. The cryostat is equipped with several temperature sensors spread out over the cavity, LHe level probes, heaters, and pressure sensors for operation at 2 K. A variable coupler is attached to the nine-cell cavity, providing a coupling range from 10^7 to 10^{11} [2]. This allows for critical coupling at 4.2 K (expected $Q_0 \sim 4 \cdot 10^8$) and 2 K ($Q_0 \sim 1 \cdot 10^{10}$) and at the same time a useful overcoupling for pulsed conditioning if needed. The cryogenic system is limited to about 20 W of active load at 2 K before the He vapor pressure regulation system cannot compensate. A background magnetic field of about 1 μT inside the cryostat was measured, leaving only a small contribution to the surface resistance in the measured cavities.

ARIEL1

In [2] the first vertical tests of the first nine-cell cavity, ARIEL1, were shown. The cavity showed a Q_0 of $5 \cdot 10^9$ at low gradient with moderate slope to $3 \cdot 10^9$ at 10 MV/m. After degassing (800° C, 10 hours, no additional chemistry) at FNAL the Q_0 increased to $6.5 \cdot 10^9$ all the way up to 11 MV/m (see fig. 1). While the Q_0 does not fully meet the goal of $\geq 1 \cdot 10^{10}$, it is sufficient for operation in the ICM.

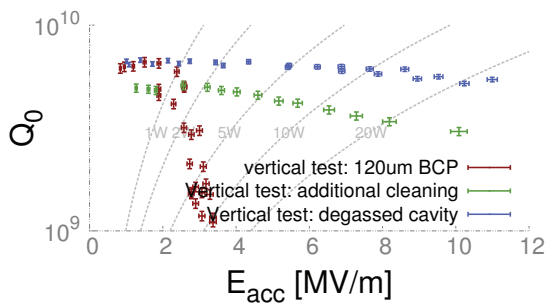

Figure 1: ARIEL1 vertical performance test showed improvements in Q_0 after 800° C degassing.

ANALYSIS OF DEGRADED CAVITIES IN PROTOTYPE MODULES FOR THE EUROPEAN XFEL

S. Aderhold*[1,2], D. Kostin[1], A. Matheisen[1], A. Navitski[1], D. Reschke[1]
[1]Deutsches Elektronen Synchrotron DESY, Hamburg, Germany
[2]Fermi National Accelerator Laboratory, Batavia, USA

Abstract

In-between the fabrication and the operation in an accelerator the performance of superconducting RF cavities is typically tested several times. Although the assembly is done under very controlled conditions in a clean room, it is observed from time to time that a cavity with good performance in the vertical acceptance test shows deteriorated performance in the accelerator module afterwards. This work presents the analysis of several such cavities that have been disassembled from modules of the prototype phase for the European XFEL for detailed investigation like optical inspection and replica.

INTRODUCTION

The assembly of superconducting RF cavities to the string for an accelerating module follows established procedures and is done under controlled conditions in high class clean rooms. This effort routinely demonstrates very good results. At times the good performance of a cavity is not preserved and when operated in the module its maximum achievable gradient is lower, it shows field emission or its losses are higher than expected. Diagnostic methods for a cavity in a module are very limited and if the module is assembled to an accelerator the origins of the deterioration remain unclear. Several modules from the preparatory and prototyping phase for the European XFEL [1] and the S1-global module [2] provided the unique advantage that they were disassembled after the test on the module test bench. This offered the opportunity to study such deteriorated cavities in detail.

Z108 AND Z109

The cavities Z108 and Z109 already have a pretty long history and have been assembled to an accelerating module twice. Both have been part of Module 8 and the S1-global module.

A part of the RF test history of Z108 is shown in Table 1. Prior to string assembly for Module 8 it reached 33.0 MV/m in vertical test number 3. In the module it deteriorated to 25.7 MV/m with field emission. The second test in the same module (test number 5) was done after a transport test of the whole module without any modification to the string. Z108 reached a slightly higher gradient while still exhibiting field emission. After being disassembled from the module string, Z108 was high pressure rinsed and vertically tested again. The performance in test number 6 improved to 31.3 MV/m with no more detectable field emission.

When tested in the string of the S1-global module, Z108 once again showed decreased performance. The accelerating gradient was limited at 19.5 MV/m with some field emission and high cryogenic losses. Disassembly from the string was again followed by high pressure rinsing and additional vertical tests. While test number 7 was not successful due to a vacuum leak, test number 8 demonstrated restored performance, reaching an accelerating gradient of 32.6 MV/m without field emission.

Table 1: Part of the RF Test History of Z108

Test No.	Date	Type	E [MV/m]	FE
3	11.07.2007	Vertical	33.0	no
4	02.07.2008	Module	25.7	yes
5	08.12.2008	Module	28.0	yes
6	25.06.2009	Vertical	31.3	no
S1-G	30.09.2010	Module	19.5	yes
7	16.08.2012	Vertical	vacuum leak	
8	29.08.2012	Vertical	32.6	no

Table 2: Part of the RF Test History of Z109

Test No.	Date	Type	E [MV/m]	FE
5	22.05.2007	Vertical	30.1	no
6	02.07.2008	Module	21.8	no
7	08.12.2008	Module	21.8	no
8	03.08.2009	Vertical	30.7	no
S1-G	01.10.2010	Module	29.5	yes
9	23.08.2012	Vertical	31.7	yes

Vertical test number 5 of cavity Z109 was limited at an accelerating gradient of 30.1 MV/m without field emission (see Table 2). After assembly to the string the performance in Module 8 was decreased to 21.8 MV/m with field emission being comparable to the zero level (test number 7 and 8). The second module test is after the transport test as in the case of Z109 and the performance remains unchanged. High pressure rinsing recovered the gradient to 30.7 MV/m in test number 8, following the removal from the string.

In the S1-global module Z109 did not suffer from significant performance deterioration (29.5 MV/m), although some field emission was detected.

* aderhold@fnal.gov

ISBN 978-3-95450-178-6

ECONOMICS OF ELECTROPOLISHING NIOBIUM SRF CAVITIES IN ECO-FRIENDLY AQUEOUS ELECTROLYTES WITHOUT HYDROFLUORIC ACID*

E.J. Taylor, M. Inman, T. Hall, S. Snyder, Faraday Technology, Inc., Englewood, OH 45315, USA
A. Rowe, Fermilab, Batavia, IL 60510, USA
D. Holmes, Advanced Energy Systems, Inc., USA

Abstract

A major challenge for industrialization of SRF cavity fabrication and processing is developing a supply chain to meet the high production demands of the ILC prior to establishment of a long term market need. Conventional SRF cavity electropolishing is based on hydrofluoric-sulphuric acid mixtures. In comparison, FARADAYIC® Bipolar EP applies pulse reverse electrolysis in dilute sulphuric acid-water solutions without hydrofluoric acid and offers substantial savings in operating and capital costs. Based on an economic analysis conducted with AES on the cavity processing requirements associated with the ILC, we project the cost of FARADAYIC® Bipolar EP to be about 27% that of the Baseline EP. In terms of tangible cost savings, the cost per cavity for the FARADAYIC® Bipolar EP and Baseline EP are $1,293 and $4,828, respectively. A major operating cost saving for Bipolar EP is associated with low sulphuric acid concentration and the absence of hydrofluoric acid. A major capital cost saving for Bipolar EP is associated with vertically oriented stationary cavity. Additional intangible cost savings are expected in terms of worker safety as well as less material degradation and maintenance requirements. Continued development and validation of FARADAYIC® Bipolar EP on lengths equivalent to nine cell cavities will contribute greatly to the industrialization of SRF accelerator technology.

INTRODUCTION

Electropolishing (EP) is used for final surface finishing of niobium SRF cavities to achieve high accelerating gradients and quality factors. Conventional EP for SRF cavities is based on anodic electrolytic dissolution under the influence of direct current (DC) electric fields in an electrolyte consisting of a mixture of sulphuric acid (95-98%) and hydrofluoric acid (49%) in a 9:1 volume ratio [1]. The presence of hydrofluoric acid in the conventional EP process presents considerable challenges in terms of worker safety in terms of compliance with Occupational Safety and Health Administration (OSHA) regulations and environmental considerations in terms of compliance with Environmental Protection Agency (EPA) regulations. Cavity processing facilities world-wide are expected to have similar concerns [2]. Hydrofluoric acid is used industrially for chemical milling or through mask etching and cases of serious worker injury and even fatality associated with hydrofluoric acid accidents have been documented [3]. The use of hydrofluoric acid significantly impacts the cost of cavity processing and is an important consideration in terms of "industrialization" of SRF cavity processing.

With funding from the Department of Energy (DOE) Small Business Innovation Research (SBIR) program, Faraday received Phase I funding to demonstrate the feasibility of electropolishing niobium coupons using pulse reverse current (PRC), in contrast to DC, to enable use of eco-friendly electrolytes. The pulse reverse current approach was based on previous successes in enabling simple electrolytes for surface finishing of a wide variety of materials and components [4-7].

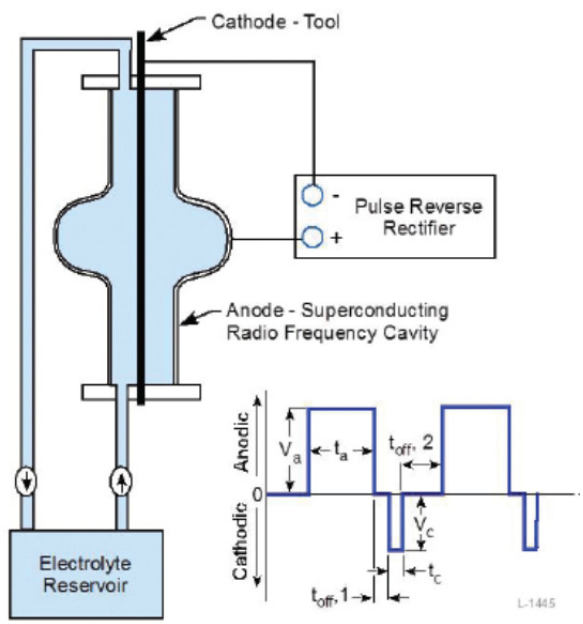

Figure 1: Schematic representation of electropolishing of SRF cavity using pulse reverse current in an aqueous electrolyte without hydrofluoric acid.

During this feasibility study, we successfully demonstrated the ability to electropolish niobium coupons in 5 to 10 wt% aqueous sulphuric acid electrolyte using PRC. The electrolyte did not contain hydrofluoric acid and the surface roughness measured at Thomas Jefferson National Accelerator Facility (TJNAF) were equivalent to that obtained using the conventional sulphuric acid/hydrofluoric acid electrolyte with DC (0.5 to 3 nm)

*Work supported by DOE Grant Nos. DE-SC0011235 and DE-SC0011342, and DOE Purchase Order No. 594128.
jenningstaylor@faradaytechnology.com

ISBN 978-3-95450-178-6

VERTICAL ELECTROPOLISING STUDIES AT CORNELL*

F. Furuta†, B. Elmore, M. Ge, T. Gruber, G. Hoffstaetter, D. Krebs, J. Sears,
Cornell University, Ithaca, NY 14850, USA
E. J. Taylor, M. Inman, Faraday Technology, Inc., Englewood, OH 45315, USA,
H. Hayano, T. Saeki, KEK, High Energy Accelerator Organisation, Oho, Tsukuba, Japan,
Y. Ida, K.Nii, Marui Galvanizing Co., LTD., Himeji 672-8023, Japan

Abstract

Vertical Electro-Polishing (VEP) has been developed and applied on various SRF R&Ds at Cornell as primary surface process of Nb. Recent achievements had been demonstrated with nitrogen doped high-Q cavities for LCLS-II. Five 9-cell cavities processed with VEP and nitrogen doping at Cornell showed average Qo value of 3.0e10 at 16MV/m, 2K, which satisfied the required cavity specs of LCLS-II. We will report the details of these achievements and new VEP collaboration projects between Cornell and companies.

INTRODUCTION

Cornell has leaded the development of VEP and processed many single-/multi-cell cavities [1,2]. The benefits of vertical EP compared with standard horizontal EP are: 1) No rotary aids seal on sleeve joint; 2) No sliding electrical contact; 3) No cavity vertical/horizontal position control fixtures for the rinsing post process; 4) active DI water cooling on the outside of cavity which provides better temperature control during the process; and 5) lower capital equipment cost on simplified system components. In this paper, we will describe about system, details of procedures, RF test achievements, and recent updates of Cornell VEP studies.

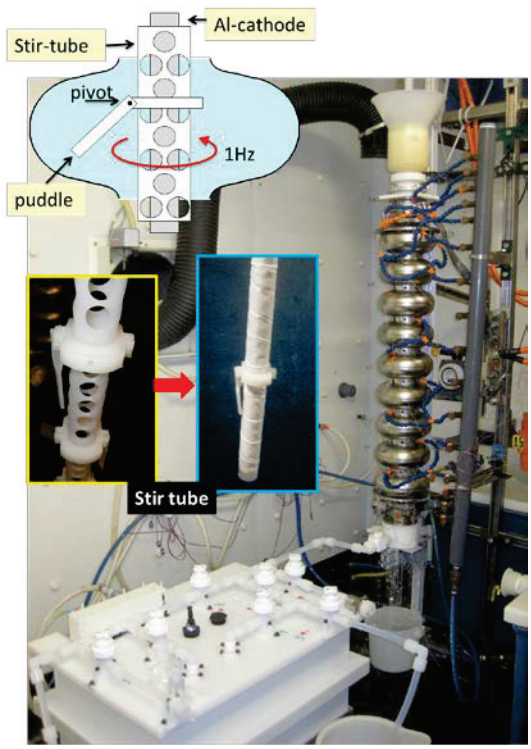

Figure 1: Cornell's VEP system.

CORNELL'S VEP SYSTEM

Figure 1 shows the images of Cornell's VEP system with 9-cell cavity. The system is designed to process 1.3GHz single-/multi-cell Nb SRF cavities. The system could process various shapes of cavities with TESLA/re-entrant/low lows shape.

Table 1: VEP Parameters at Cornell

Parameters	
Cathode	Aluminium > 99.5%
Stir-tube, puddles	PVDF
End group	PVDF, HDPE
Electrolyte volume	24 litres / 9-cell
Electrolyte composition	10:1 (H_2SO_4:HF)
Maximum use	9 g/L dissolved Nb
Current-voltage source	500 A – 20 V max.
Ave. current for 9-cell	80-120 A
EP voltage	12 V
Temp. (cavity outside wall)	15~19 deg. C
Stir frequency	0~3 Hz
EP removal rate (ave.)	~0.3 microns/min.

VEP Process and Parameters

EP electrolyte was mixed in the mixing tank (a big white tank with plumbing shown in Figure 1) and transferred into cavity via bottom sleeve joint. After filling the electrolyte, the valve on bottom sleeve joint was closed. No electrolyte circulation was made during the process. The circulation system has been added into the system, but it is under development. EP process was performed by turning the cathode voltage on. Typical EP process voltage was 12 volts. EP acid agitation was controllable with puddle on stir tube during the process. The temperature during EP process was controlled by sprayed DI water from cavity outside and kept around 15 deg. C. Total current was monitored via I-V supply source. Total removal was calculated from current integration. This calculated removal showed the average surface removal of cavity. Once the removal reached the half of target removal, process was stopped. Cavity was rinsed with DI water, and fully disassembled from the system. Quick eye inspection was done on inner RF

*Work supported by the U.S. DOE, the LCLS-II High Q0 Program, and NSF Grant NSF-PHY-1416318.
†ff97@cornell.edu

INSPECTION AND REPAIR TECHNIQUES FOR THE EXFEL SUPERCONDUCTING 1.3 GHz CAVITIES AT ETTORE ZANON S.P.A: METHODS AND RESULTS

G. Massaro#, N. Maragno, G. Corniani, Ettore Zanon S.p.A, Schio, Italy
C A. Matheisen, A. Navitski, DESY, Hamburg, Germany
P. Michelato, L. Monaco, INFN Milano-LASA, Segrate, Italy

Abstract

The quality control of the inner surface of superconducting RF cavities is essential in order to assure high accelerating gradient and quality factor.

Ettore Zanon S.p.A. (EZ) has implemented in the serial production an optical system that use an high-resolution camera, in order to detect various types of defects. This system is added to a grinding machine, that was specifically designed and built to repair imperfections of the cavities inner surface.

This inspection and repair system is applied to recover performance limited cavities of the 1.3 GHz European EXFEL project, where surface irregularities are detected, either by the Obacht inspection system at Desy or the optical system at EZ.

The optical system and the grinding procedure are qualified using two series cavities limited in gradient and showing different types of surface defects. The performances of these cavities have been recovered to reach the specifications of the project. Until now, all the series EXFEL cavities built by EZ, repaired with this technique, have shown an accelerating gradient well above the EXFEL goal.

The paper describes the equipment installed in the grinding machine and it analyzes the performance of the cavities that have been repaired using this system.

INTRODUCTION

The Ettore Zanon S.p.A. (EZ) company was founded far in 1919. It is located in the northeastern area of Italy 90 km from Venice.

The company works on two different fronts:

- "Standard" production for chemical industry (reactors, heat exchangers, etc.),
- "Special" production of components for research institutes and laboratories (ultra-high vacuum, cryogenics, fusion, superconductivity, etc.).

Since 2011, EZ company is involved in the European X-ray Free-electron Laser (EXFEL) project, constructed at the Deutsches Elektronen-Synchrotron (DESY), for the production of 420 1.3 GHz superconducting cavities, and it is expected to complete the entire production later this year.

Optical inspections and possibilities to remove defects on the inner surface play an important role in the improving of the production-yield of high performance cavities. For this purpose, EZ has developed a system consisting of an optical tool and a grinding machine to investigate the quality of inner surface of cavities and to remove defects, which can cause of performance-limitations of the cavities. Systems for this purpose have already present in the literature [1-4].

To qualify the technical inspection and repair procedure, EZ has used two series cavities; for both cavities the method has been successfully implemented.

Details of the system and the obtained results will be presented and discussed.

OPTICAL SYSTEM AND GRINDING MACHINE

Optical Inspection

Two types of cameras are used for optical inspections, one with fast response time and one with high resolution.

For inspections during the grinding operations, a video boroscope Extech HDV600 is used. This inspection device consists of a camera mounted on a rotating probe and connected to a monitor. Despite of a limited resolution of 640x480 pixels, it has a quick response and makes easy monitoring during the grinding operation thanks to the rotating probe.

The other camera is See3CAM_80 (8 megapixels) from e-con System. It allows obtaining a higher-resolution image of 3264 x 2448 pixels. However, the response time is slower due to the large amount of data to be transmitted to the PC. The camera is mounted at the end of rod for inspection tools (see Fig. 1) and connected to the PC. This camera is mainly used to verify a complete removal of the defect.

For both cameras described, the lighting is provided by two LED strips, mounted on the sides of the camera.

Grinding Machine

The system of grinding machine, consists of the following components (see Fig. 1):

#gmassaro@zanon.com

SRF CAVITY PROCESSING AND CHEMICAL ETCHING DEVELOPMENT FOR THE FRIB LINAC*

I. Malloch#, M. LaVere, E. Metzgar, L. Popielarski, Facility for Rare Isotope Beams (FRIB), Michigan State University, East Lansing, MI 48824, USA

Abstract

In preparation of a rigorous superconducting RF (SRF) cavity processing and test plan for the production of the Facility for Rare Isotope Beams (FRIB) driver linac, a state-of-the-art chemical etching tool has been installed in the FRIB coldmass production facility. This paper seeks to summarize the etching equipment design, installation, and validation program and subsequent etching results for a variety of SRF cavity types and etching configurations. Bulk etching, light etching, and custom (frequency tuning) etching results for different FRIB cavities are discussed. Special emphasis is placed on the etching removal uniformity and frequency tuning reliability of these processes.

INTRODUCTION

The chemical etching of SRF cavities with buffered chemical polish (BCP) has been performed at NSCL/FRIB for fifteen years, and recently, the next step in the evolution of this process was realized with the installation of an automated, recipe-based etching tool. This tool has been used in a preproduction capacity for approximately one year to validate not only the equipment design and functionality, but also to finalize the etching fixtures and procedures that will be used in the processing of all SRF cavities for the FRIB linac.

All four of the FRIB cavity types (beta=0.041 and beta=0.085 quarter-wave resonators (QWR), and beta=0.29 and beta=0.53 half-wave resonators (HWR)) have been etched during this development phase, and these etching procedures have provided valuable data on niobium removal rates, etching uniformity, and cavity frequency shift. These data have been, and will continue to be, applied to the etching of cavities for FRIB coldmasses to improve process throughput and cavity performance.

ETCHING INFRASTRUCTURE

Design and Installation

The NSCL/FRIB chemical etching facility constructed in the year 2001 was designed for the etching of small, elliptical style SRF cavities for research and development purposes. During the processing of large quarter-wave and half-wave SRF cavities for the ReA3, ReA6, and FRIB test cryomodules, the design constraints of the equipment became more apparent, and it was clear that the facility had outlived its useful life expectancy. This facility was demolished in July 2015 to make way for other project needs. In the SRF Highbay building erected to house technical infrastructure necessary for the FRIB project, a new and more technically advanced chemical etching facility was constructed to accommodate the cavities and processing throughputs necessary for the timely and high-quality production of FRIB SRF cavities [1, 2] (Fig. 1).

Figure 1: FRIB production chemical etching facility.

This etching facility includes a chemical storage fume hood with a maximum capacity of 200 L of BCP, a cavity etching cabinet equipped with custom mechanized fixturing for manipulating cavities during etching procedures, and a parts etching fume hood used for processing cavity subassemblies. All aspects of this system are controlled by means of a programmable logic controller (PLC) with an integrated touch-screen operator interface. To neutralize chemical vapors and gaseous etching by-products, and to maintain negative pressure in the etching facility, a gas scrubber with a maximum flowrate of 57 m^3/min is installed and ducted directly into the etching equipment (Fig. 2). Automated louvers are installed in each of the ducting branches to maximize the ventilation in any workstation actively being used by an operator.

Figure 2: Toxic gas scrubber unit.

*This material is based upon work supported by the U.S. Department of Energy Office of Science under Cooperative Agreement DE-SC0000661, The State of Michigan, and Michigan State University.
#malloch@frib.msu.edu

ISBN 978-3-95450-178-6

VERTICAL ELECTRO-POLISHING AT TRIUMF

J.J. Keir*, P.R. Harmer, D. Lang, R.E. Laxdal, T. Shishido, R. Smith, TRIUMF, Vancouver, Canada
T. Shishido, KEK, Tsukuba, Japan

Abstract

A set-up for electro-polishing (EP) of a superconducting niobium (Nb) single-cell cavity has been installed at TRIUMF. A vertical method was selected to make the setup compact. To increase removal speed at the equator and remove hydrogen bubbles at the iris surface, 4 cathode paddles were rotated in the cavity cell during EP. The interest in Vertical EP (VEP) of elliptical cavities in the Superconducting Radio Frequency (SRF) community has lead TRIUMF to begin its own VEP program to determine if the lessons learned at other institutions would be able to yield a positive result with TRIUMF's unique methodology and expertise.

Working with experts from KEK, TRIUMF began to develop its own solution to the VEP problem. We are reporting on our first EP results.

INTRODUCTION

Electro-polishing (EP) is a tool that has been used in the SRF community to remove and polish the inner surface of niobium (Nb). EP is now the process that has been used to a smooth inner surface of an SRF cavity, which has lead these cavities, that were EP processed, being able to achieve higher gradients [1,3]. The current method of EP processing an elliptical cavity is by using the Horizontal EP (HEP) process. In these systems the cavities are mounted in the horizontal plane. These systems are extremely complex, requiring a large foot-print, as well as having sophisticated rotating fluid coupling and electrical connectors and a large dumping apparatus.

This is why many labs including TRIUMF and KEK have been looking at VEP as a simpler solution that can be used more widespread. VEP bring with it many challenges that are directly related cathode shape and operation. The major obstacles encountered when developing any EP system are uniform material removal and surface quality. But this becomes especially difficult in the vertical orientation due to the hydrogen bubbles and cathode shapes.

SYSTEM OVERVIEW

The VEP set-up that was used at TRIUMF incorporated many of the components used in the current Buffered Chemical Polishing (BCP) facilities used at TRIUMF. The system includes Perfluoroalkoxy alkane (PFA) tubing and fittings, with Polytetrafluoroethylene (PTFE) manual valves from the BCP program, with the addition off a rotary electrical contact that was produced in-house, and a 12 V-100 A DC switching power supply as the source of the electrical power needed for the process. The cathode assembly is driven by a 12 V reduction motor that turns at 30 rpm. The overall system diagram for the VEP system is shown in Fig. 1.

The VEP system currently has 34.5 L of H_2SO_4 HF electrolyte. The electrolyte has the same composition as the one used by many labs [1,2]. With a flow rate of 3.1 L/min through the cavity during etching the temperature was stable with passive cooling at approximately 30.6° C

During the last trial the voltage and current were 3.1-3.7 V and 55.1 A with the power supply set to constant current.

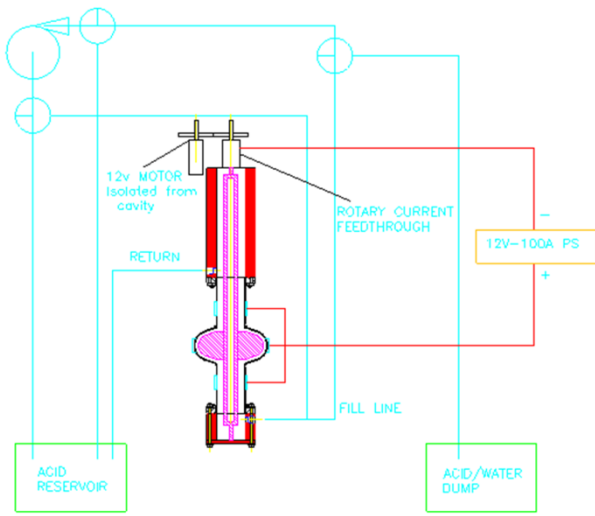

Figure 1: VEP system diagram.

EXPANDING CATHODE

To increase the chances of producing a uniform etch rate an expanding cathode was developed that increase the surface area inside the cell as well as decrease the electrical path length. This cathode has been nick-named D'Sonoqua. The major design requirement was to use pure aluminum for any part of the cathode that is in contact with the EP electrolyte.

It was decided to use 1100-H14 series aluminum for our cathode as that was the most readily available in our region. 1100 series aluminum is 99.0% pure at a minimum and it was decided that the increased availability would out weight the decrease in performance from the more pure 1050 series aluminum with a purity of 99.5%.

Interleaving Blade System

The system that was used to create the larger surface area inside the elliptical cell was by using a four blade system. The blades are able to be nested together to form

*jkeir@triumf.ca

IMPROVEMENT OF TEMPERATURE CONTROL DURING Nb 9-CELL SRF CAVITY VERTICAL ELECTRO-POLISHING (VEP) AND PROGRESS OF VEP QUALITY

K. Nii#, V. Chouhan, Y. Ida, T. Yamaguchi, Marui Galvanizing Co., Ltd., Himeji, Japan
K. Ishimi, Marui Galvanizing Co., Ltd., Kashiwa, Japan
H. Hayano, S. Kato, H. Monjushiro, T. Saeki, M. Sawabe, KEK, Tsukuba, Japan

Abstract

Marui Galvanizing Co.,Ltd. has been developing Nb 9-cell SRF cavity vertical electro-polishing (VEP) facility and technique for mass production in collaboration with KEK. Our first 9-cell cavity VEP facility was not enough to control temperature during VEP, so the polishing quality was not so high. In this article, we will report the progress of temperature distribution and polishing quality due to the improvement of temperature control system of electrolyte and cavity during VEP.

INTRODUCTION

International linear collider (ILC) will require around 16000 niobium 9-cell SRF cavities. In order to meet such requirement mass production of cavities with higher efficiency and lower cost is desired. To solve this problem, worldwide development for mass-production is performed. Electropolishing (EP) is considered as a final surface treatment of these cavities to improve the surface quality for their high performance and high mass-productivity, high performance EP method and facility are also required. Marui Galvanizing Co., Ltd. has been developing Nb SRF cavity EP technology in collaboration with KEK based on experience of various materials and shapes parts EP. In this collaboration, we focused on vertical electropolishing (VEP) technique which was considered more suitable to mass-production and have been developing original cathode named "i-cathode Ninja" to improve polishing quality [1], performing VEP parameter investigation and surface analysis after VEP using 1-cell coupon cavity [2-6], preparing VEP facility for ILC 9-cell SRF cavity [7]. In previous work, we prepared 9-cell cavity VEP facility and performed VEP. Though high quality VEP couldn't be performed because of high cavity temperature (around 50 ^{0}C) during VEP (Usually 20 – 30 ^{0}C is required to perform high quality Nb EP.). To solve this problem, we developed cavity temperature control system during VEP. In this article, we report VEP results using this system.

9-CELL CAVITY VEP WITH HEAT EXCHANGER FOR EP SOLUTION

From the viewpoint of cavity temperature control, babble removal, operation system, following points were improved.

(1) Improvement for cavity temperature control during VEP
  (a) A heat exchanger is injected in EP solution tank and coolant is circulated in it by a chiller.
  (b) Enclosing cavity by acrylic plates and injecting cooler wind into enclosed space (air cooling).
(2) Improvement for bubble removal
  (a) Ninja rotation speed is increased to enhance mixing effect.
  (b) Setting a bubble removal filter.
(3) Improvement for facility usability
  (a) Preparing a control box including all operation controllers.
  (b) Preparing PVC pipes and valves to change flow direction of waste fluid.

Pictures of facility and parts after improvement are shown in Fig. 1.

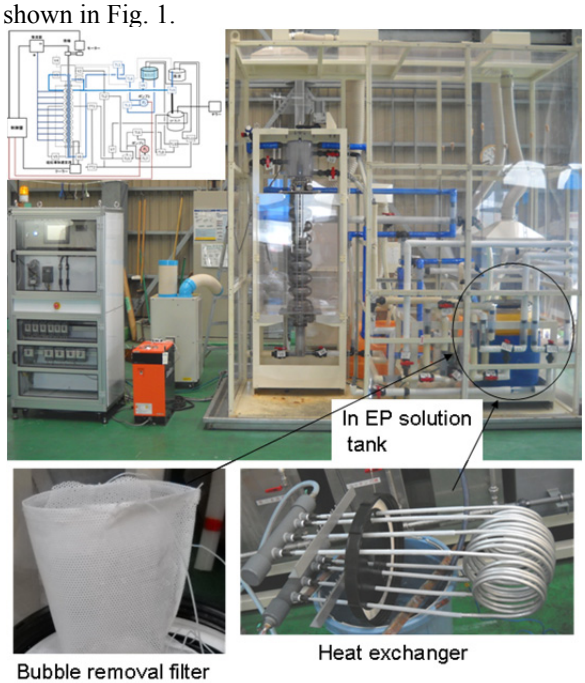

Figure 1: Pictures of facility and parts after improvement.

#keisuke_nii@e-maui.jp

ISBN 978-3-95450-178-6

CATHODE GEOMETRY AND FLOW DYNAMICS IMPACT ON VERTICAL ELECTROPOLISHING OF SUPERCONDUCTING NIOBIUM CAVITIES

Leonel Marques Antunes Ferreira#, CERN, Geneva, Switzerland

Abstract

CERN has now a fully operating vertical electropolishing installation, which has been used for the processing of 704 MHz high-beta five-cell Superconducting Proton Linac (SPL) niobium cavities. This installation relies only on the electrolyte circulation (HF/H2SO4) for power dissipation, evacuation of gases and homogeneous finishing; thus, parameters like cathode geometry, electrolyte flow and temperature become even more crucial when compared with horizontal electropolishing installations. Based on computational simulations performed with Comsol Multiphysics® and on a methodology developed at CERN, it is possible to assess the impact of the different cathode geometries as well as of the flow on the etching rate distribution. The data obtained with two different cathode geometries are presented: electrolyte velocity distribution, etching rate distribution, average current density and minimum working potential. One geometry was defined through a purely electrochemical approach while the second was defined to minimise the difference between the maximum and the minimum electrolyte speed inside the cavity; in both cases, the influence of the electrolyte flow was taken into account.

INTRODUCTION

The most interesting electrochemical characteristic of the Siemens bath formulation [1] is the absence of a transpassivation behaviour in the anodic branch of its polarisation curve, see Figure1. The main outcome is that for a very large range of anodic overpotential, the anodic dissolution yield is 100%; in other words there are no secondary reactions taking place other than the dissolution of niobium. Unlike many other electropolishing (EP) bath formulations, there is no formation of molecular oxygen at the surface and thus, pinholes and related surface defects are less prone to appear and surely not related to anodic oxygen evolution.

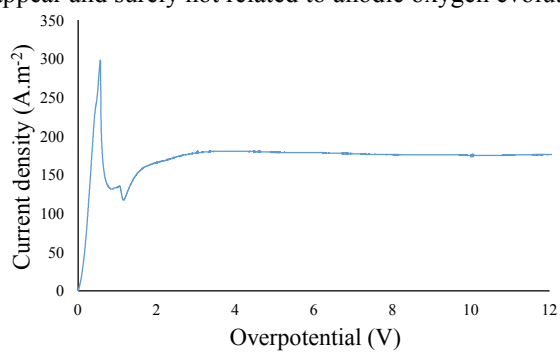

Figure 1: Anodic polarisation curve measured at 25 °C.

#leonel.ferreira@cern.ch

The described bath property plus the possibility to fully simulate the electrochemical polishing has guided CERN to exploit the processing of niobium SRF cavities in a vertical installation [2]. The objective, is to achieve the same performances as of horizontal installations, but with the advantage of a simplified set-up. CERN vertical EP installation relies only on the electrolyte circulation for power dissipation, gases evacuation and homogeneous finishing; thus, making it very simple to operate, but on the other hand, more difficult to tune up. With this constraint, the main optimisation parameters are the cathode geometry and the bath flow. The data and results achieved so far on SPL 704 MHz 5 cell cavities are presented hereafter.

CATHODE GEOMETRY

Two cathode geometries were used so far to process SPL 5 cell cavities. The first geometry was designed taking into account only electrochemical parameters and it'll be referred as the electrochemical cathode (EC); a detailed explanation can be found elsewhere [3]. The surface finishing achieved with this cathode was bright and smooth, but macrostructures were apparent and could be related both to the bath flow and gas bubbles in the circulating bath; see Figure 2. From this experimental result, a reassessment of the cathode geometry was undertaken; laboratory trials and simulation work were developed to understand better the bath velocity distribution inside the cavity as well as to its impact on the polishing rate; the latter was already presented for the EC geometry [4].

Figure 2: Macrostructures on cavity SPL #1.

The SPL cavity geometry cannot be modified and it implies already significant bath velocity differences between the equator (wider section) and the iris (narrower section); the cathode geometry cannot improve the bath velocity distribution, but its impact can be minimised. Taking this principle into account, a second cathode geometry was defined: cylindrical hollow shape, the hollow cathode (HC); this approach is still able to provide sufficient cross section for the total applied current and minimises its impact on the bath velocity distribution

ISBN 978-3-95450-178-6

ELECTROPOLISHING OF NIOBIUM SRF CAVITIES IN ECO-FRIENDLY AQUEOUS ELECTROLYTES WITHOUT HYDROFLUORIC ACID

M. Inman, E.J. Taylor, T. Hall, S. Snyder, S. Lucatero, Faraday Technology, Inc., Englewood OH 45315, U.S.A.
A. Rowe, Fermilab, Batavia, IL 60510, U.S.A.
F. Furuta, G. Hoffstaetter, Cornell University, Ithaca, NY 14853, U.S.A.
J. Mammosser, Oak Ridge National Laboratory, Oak Ridge, TN 37831, U.S.A.

ABSTRACT

Electropolishing of niobium cavities is conventionally conducted in high viscosity electrolytes consisting of concentrated sulfuric and hydrofluoric acids. The use of dangerous and ecologically damaging chemicals requires careful attention to safety protocols to avoid harmful worker exposure and environmental damage. We present an approach for electropolishing of niobium materials based on pulse reverse waveforms, enabling the use of low viscosity aqueous dilute sulfuric acid electrolytes without hydrofluoric acid, or aqueous near-neutral pH salt solutions without any acid. Results will be summarized for both cavity and coupon electropolishing for bulk and final polishing steps. With minimal optimization of pulse reverse waveform parameters we have demonstrated the ability to electropolish single-cell niobium SRF cavities and achieve at least equivalent performance compared to conventionally processed cavities. Cavities are electropolished in a vertical orientation filled with electrolyte and without rotation, offering numerous advantages from an industrial processing perspective. Shielding, external cooling and high surface area cathodes are adaptable to the bipolar EP process.

INTRODUCTION

Electropolishing (EP) is used for final surface finishing of niobium SRF cavities to achieve acceptable performance. EP is a surface finishing process whereby surface asperities are preferentially removed by anodic electrolytic dissolution under the influence of a direct current (DC) electric field in an appropriate electrolyte. Conventional EP for SRF cavities is based on a viscous electrolyte consisting of a mixture of sulphuric acid (95-98%) and hydrofluoric acid (49%) in a 9:1 volume ratio [1]. The need for a viscous electrolyte for effective EP is mechanistically understood in terms of the "viscous salt film theory" proposed by Jacquet [2] and is generally applicable to all metal-electrolyte systems [3]. Hydrofluoric acid completely removes the oxide from the surface [4]. A recent study of niobium EP reports diffusion limited access of fluoride ion to the surface and is generally consistent with the viscous salt film theory [5]. In collaboration with Fermi National Accelerator Laboratory (Fermilab) and Cornell University, we are addressing the need for an eco-friendly EP process.

Work supported by DOE Grant Nos. DE-SC0011235 and DE-SC0011342, DOE Purchase Order No. 594128, and ORNL Purchase Order No. 4000136566.
mariainman@faradaytechnology.com

TECHNICAL APPROACH

In contrast to EP using DC electric fields, our approach is based on pulse reverse pulse waveforms (i.e. bipolar EP). Fig. 1 presents a generalized pulse reverse waveform. The anodic pulse is tuned to enhance mass transport, control current distribution, focus the current on the asperities and eliminate the need for a high viscosity electrolyte. To depassivate the surface, we intersperse cathodic pulses within the anodic pulses, in place of or in conjunction with off-times [6,7,8,9]. The off-times are generally inserted between the anodic and cathodic pulses to facilitate replenishment of reacting species and removal of by-products and heat. The cathodic pulse eliminates the need for hydrofluoric acid to remove the surface oxide. The exact mechanism of depassivation is unknown at this stage. The amplitude of the cathodic pulses required for depassivation is material specific and appears to be based on the strength of the passive film. While a priori determination of the on-times and peak voltages is not currently known, guiding principles based on single pulse transient studies have been presented previously [10].

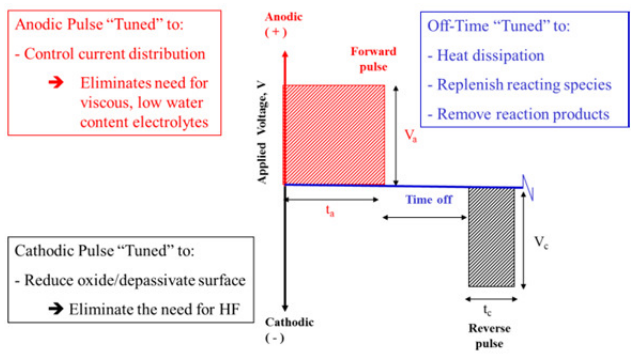

Figure 1: Generalized pulse reverse waveform for surface finishing of passive materials.

We have reported on the application of pulse reverse electropolishing of niobium coupons in 5 to 50 wt% H_2SO_4 in water [11]. We observed a current transient in the anodic current that we attributed to a transition from oxide film formation/growth to oxygen evolution. We speculated that our polishing mechanism occurred by removal of the niobium oxide during the cathodic pulse, and termed this process termed "cathodic electropolishing." We observed that the presence of the anodic current transition is important to effectively

COMMENTS ON ELECTROPOLISHING AT ETTORE ZANON SpA AT THE END OF EXFEL PRODUCTION

M. Rizzi#, G. Corniani, Ettore Zanon SpA, Schio, Italy
A. Matheisen, DESY, Hamburg, Germany
P. Michelato, INFN, Milano, Italy

Abstract

In 2013 a new horizontal Electropolishing facility was developed and implemented by Ettore Zanon SpA (EZ) for the treatment of cavities for the European XFEL series production. More than 300 cavities have been treated. Electropolishing has been used for two applications: bulk removal and recovering of cavities with surface defects. Treatment settings have been analysed and compared with cavities performances to verify possible influences of the various parameters. Main parameters considered are treatment time, voltage and current, that together define average thickness removal. We present here the results of these investigation.

The facility and process in use are also presented, together with possible next upgrade of the system, facing the new production of cavities for the LCLSII project.

INTRODUCTION

Since beginning of 2012, Ettore Zanon SpA has produced 420 1.3 GHz cavities for the EXFEL facility at DESY - Hamburg. At the present time, only final treatments for few cavities are missing before end of production.

BCP Flash Scheme

Cavities with outstanding and stable performances are required for the EXFEL, in order to be acceptable for the accelerator. Minimum goal is 23.6 MV/m with Q_0 = $1x10^{10}$ and low field emission. Almost all cavities prepared up to now are well above the acceptance level required for module installation at CEA France.

To reach high gradients on a stable basis a surface treatment like electropolishing is required [1]. The inner surface of the cavities must be as smooth as possible, without defects or contaminants.

Two different chemical treatment have been developed for preparation of a cavity surface: Electropolishing (EP) and Buffered Chemical Polishing (BCP) [2] .

For the EXFEL cavities two possible options are considered: BCP flash scheme (140 µm main EP + 10 µm final BCP) or final EP scheme (110 µm main EP + 40 µm final EP). Ettore Zanon SpA followed the BCP flash production scheme. After welding, cavity is degreased in a ultrasonic bath and rinsed with ultrapure water inside a clean room of ISO7 standard.

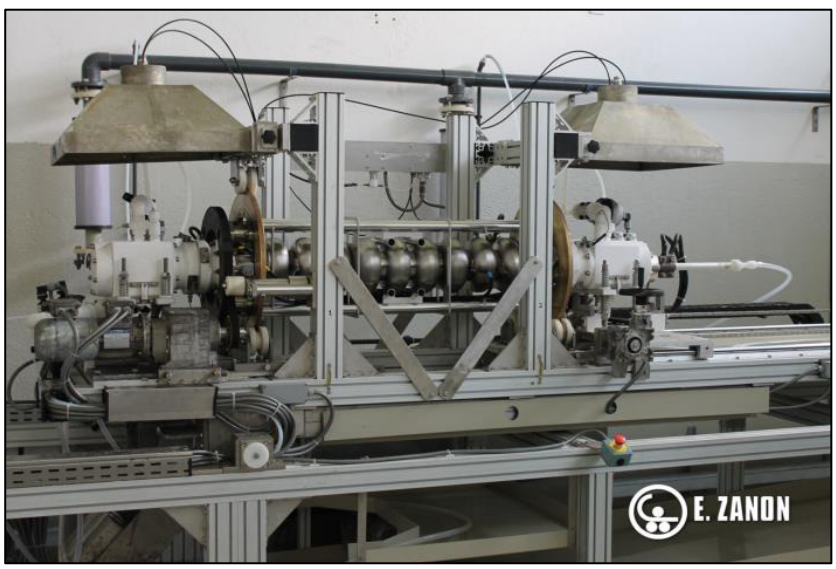

Figure 1: EP bench developed by E. Zanon.

#mrizzi@zanon.com

VERTICAL ELECTRO-POLISHING AT DESY OF A 1.3 GHz GUN CAVITY FOR CW APPLICATION

N. Steinhau-Kühl; A. Matheisen; R. Bandelmann; M. Schmökel, J. Sekutowicz; D. Kostin, DESY Hamburg Germany

Abstract

Superconducting gun cavities for cw operation in accelerators are under study. In 2003 a three-and-a-half cell gun cavity was chemically treated with buffered chemical polishing and tested successfully in a collaboration between Helmholtz-Zentrum Dresden-Rossendorf and DESY. For several years a 1.3-GHz 1.6-cell resonator has been under study, which has been built and tested at DESY and elsewhere. For further studies and optimization the gun cavity needed to be electro-polished, which was conducted at DESY for the first time using vertical electro-polishing. The technical set-up for the vertical electro-polishing and high pressure rinsing as well as the processing parameters applied and the adaptation of the existing infrastructure to the 1.6-cell geometry at DESY are presented.

INTRODUCTION

For CW accelerators several activities are ongoing to develop also superconducting (s.c.) gun cavities for CW application [1,2]. The Rossendorf 3.5 cells gun was prepared at DESY in 2003 by using buffered chemical polishing (BCP) acid in the chemical etching stand of the DESY cleanroom [3,4].

Another s.c. CW gun cavity under study now is the 1.6 cell, DESY Gun 2 16G2, developed in collaboration with TJNL. This 1.6 cells gun cavity has been surface treated by BCP and tested before at TJNL [5]. To study the benefit of EP the DESY horizontal electro polishing infrastructure [6] should be used for this test sequence.

EP SET UP FOR GUN CAVITY

The DESY EP facility is designed for horizontal electro polishing of single and 9 cell 1.3 GHz resonators of Tesla /XFEL type [6]. For horizontal EP the acid is injected into the cavities by nine holes in the centered aluminum electrode and exits on the two beam tubes of the cavity with nearly equal amount of volume. This allows having a homogenous distributed acid flow.

The gun 16G2 is made from one standard TESLA type end cell with beam tube with HOM coupler, power coupler port and a 0.6 cell of middle cell geometry. The 0.6 cell ends with a welded on back plate, made from RRR 300 Niobium. A center hole of 5 mm ID in this back plate allows inserting plugs with different surface coating for study. The inner surface of this 1.6 cell gun is about 10 dm².

The hydrodynamic resistivity of the five millimeter ID hole for the acid flow prevents any nearly homogenous flow distribution in horizontal position like for the single- and nine cell geometries polished so far at DESY. In addition the large back plate needs to be polished homogenously like the cells. Only in vertical position a well-defined acid flow and polishing of the end plate during the EP treatment could be realized for this application.

Modification on EP Bench

The beam tube geometry of gun 16G2 beam is of stand XFEL and TESLA end- cell geometry. This allows connecting the gun cavity at the reference ring of the beam tube to an existing single cell frame for cavity processing in the cleanroom. To realize vertical EP a frame work was build that can be positioned on the EP bench and allows turning the cavity by 180 degrees. The cavity frame is connected to the new frame work for vertical electro polishing (Fig. 1).

After EP the frame can be removed from the frame work and serves for handling, assembly of accessories and high pressure rinsing (HPR) of the cavity inside the cleanroom.

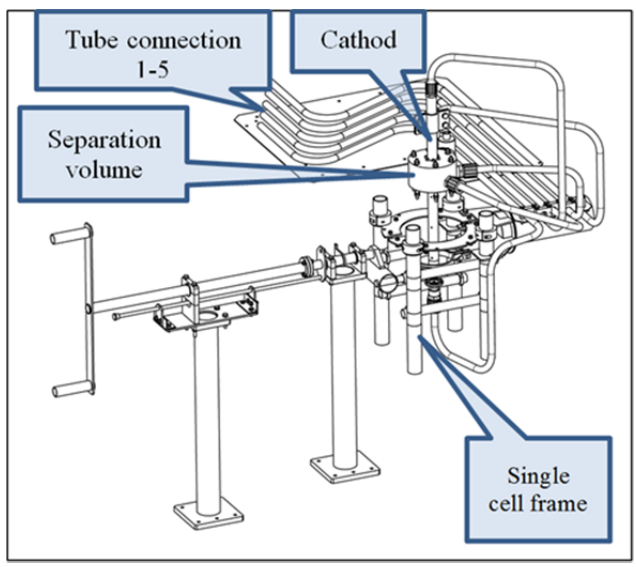

Figure 1: Design drawing of frame work for vertical EP.

Cables from the power supply are connected to the electrode on one side (cathode) and by a copper clamp (anode) directly to the stiffening ring between the cells. No current flows over the rotating bearings of the frame work. All piping's of the horizontal EP for acid charge and discharge, rinsing water and draining as well as exhausted gases of the horizontal EP set up are connected to the gun cavity as well. This allows using the same safety and processing software like qualified for horizontal EP.

ISBN 978-3-95450-178-6

FLUX EXPULSION VARIATION IN SRF CAVITIES *

S. Posen†, A. Grassellino, A. Romanenko, O. Melnychuk,
D. A. Sergatskov, M. Martinello, M. Checchin, and A. C. Crawford
Fermi National Accelerator Laboratory, Batavia, IL 60510, USA

Abstract

Treating a cavity with nitrogen doping significantly increases Q_0 at medium fields, reducing cryogenic costs for high duty factor linear accelerators such as LCLS II. N-doping also makes cavities more sensitive to increased residual resistance due to trapped magnetic flux, making it critical to either have extremely effective magnetic shielding, or to prevent flux from being trapped in the cavity during cooldown. In this paper, we report on results of a study of flux expulsion. We discuss possible ways in which flux can be pinned in the inner surface, outer surface, or bulk of a cavity, and we present experimental results studying these mechanisms. We show that grain structure appears to play a key role and that a cavity that expelled flux poorly changed to expelling flux well after a high temperature furnace treatment. We further show that after furnace treatment, this cavity exhibited a significant improvement in quality factor when cooled in an external magnetic field. We conclude with implications for SRF accelerators with high Q_0 requirements.

BACKGROUND

In the last several years, there has been rapid progress in technology for high Q_0 applications. Nitrogen doping was discovered and recipes were developed to dramatically reduce both BCS and residual surface resistances (R_{BCS} and R_{res}) at peak fields on the order of 70 mT [1]. Furthermore, researchers observed the importance of cooldown on residual resistance in the bulk dressed niobium cavity prepared by BCP [2], attributing the effect to additional magnetic fields generated by thermocurrents [3]. Subsequently, the importance of the cooldown conditions on the amount of trapped flux even for the same ambient field was discovered in bare cavities of various surface treatments [4] showing the dramatic impact of spatial temperature gradient at transition on the residual resistance. Studies showed that N-doping increases the sensitivity of the residual resistance to trapped magnetic flux [5]. In addition, the effect of material preparation on tendency to trap flux (i.e. percent of external flux not expelled during cooldown) was studied in bulk niobium samples [6, 7].

Building on these studies, in this paper we study the effect of preparation and cooldown conditions on the tendency to trap flux in single cell 1.3 GHz cavities.

FLUX EXPULSION

Cooling N-doped bulk niobium cavities through transition with a spatial temperature gradient reduces residual resistance from external magnetic fields. This has been shown both in vertical test [4] and in horizontal test [8]. The exact mechanism is not well understood, but it is likely that thermal forces on pinned vortices play an important role. We offer a picture of how this could work in Fig. 1.

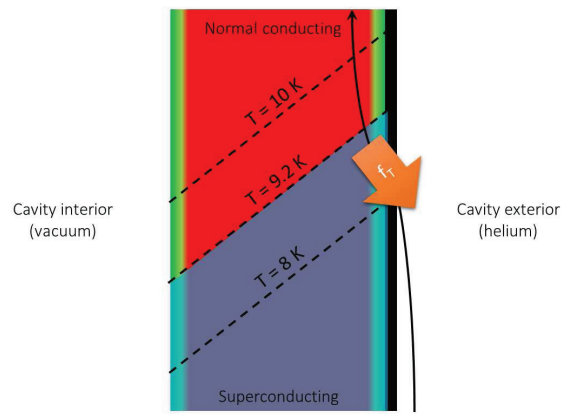

Figure 1: Schematic of a cross section of a bulk N-doped cavity wall, showing layers of different materials: N-doped niobium at the inner surface, high purity niobium in the bulk, N-doped niobium at the outer surface, and NbN compounds at the outer surface. Isotherms during cooldown are also indicated schematically, along with the corresponding thermal force f_T on a vortex.

During cooldown, a temperature gradient will be present not just from the bottom to top of the cavity, but also from outside wall to inside. It has been shown that spatial temperature gradients create a force on vortices, pushing them towards cooler regions [9] (see [10] for another SRF cavity application of this). In the geometry from Fig. 1, there is a component of the force pushing the vortices away from the RF surface and out of the cavity. If the force is large enough, it can depin flux and expel it.

The required depinning force—and hence the required thermal gradient—would depend on the strength with which magnetic field lines were pinned. Sample studies suggest that grain boundaries and dislocations act as pinning centers [6, 7]. In addition to these bulk properties, surface properties may play a role. A N-doped cavity will have a thin layer of nitrogen-rich material at its interior and exterior surfaces. Immediately after doping, it can also have a layer of poorly superconducting niobium nitride phases on its interior and exterior surfaces, though the interior nitrides

* This work was supported by the US Department of Energy
† sposen@fnal.gov

SYMMETRIC REMOVAL OF NIOBIUM SUPERCONDUCTING RF CAVITY IN VERTICAL ELECTROPOLISHING

Vijay Chouhan#, Yoshiaki Ida, Kiyotaka Ishimi, Keisuke Nii, Takanori Yamaguchi
Marui Galvanizing Co., Ltd., Japan
Hitoshi Hayano, Shigeki Kato, Hideaki Monjushiro, Takayuki Saeki, Motoaki Sawabe
High Energy Accelerator Research Organization, KEK, Japan

Abstract

Vertical electropolishing (VEP) leads several advantages over horizontal EP in respect of easy operation and mechanism of an EP system resulting in lower cost. However, till yet VEP always resulted inhomogeneous removal of a niobium (Nb) cavity along its length and bubble traces especially on the top iris of a vertically set cavity. In this work we performed lab EP and VEP experiments in order to study and solve these two problems. A coupon cavity which contains 6 disk type Nb coupons positioned at beam pipes, irises and equator was vertically electropolished to optimize VEP parameters so as to get almost uniform removal of Nb and a smooth surface of the cavity without bubble traces. Our patented unique i-Ninja cathode having 4 wings was used with an optimized rotation speed to get homogeneous removal of Nb. The homogeneous removal and the surface without bubble traces might be result of a uniform thickness of a viscous layer on the surface of the cavity cell and no accumulation of hydrogen bubbles on the top iris surface. The surfaces of the coupons were studied in detail with surface analytical tools.

INTRODUCTION

Electropolishing (EP) has been adopted as a promising method for final surface treatment of superconducting RF cavities. In order to carry out EP, horizontal EP (HEP) is used to get smooth surface and almost similar polishing rate for irises of a cavity cell. However EP rate for equator usually remains less than that on the irises. Vertical EP (VEP) has many advantages over HEP in respect of an EP setup. The VEP requires a simple setup compared to HEP setup since a HEP setup is built with complicated mechanism for cavity rotation and to make it vertical for drainage of acid. In spite of the advantages VEP has some drawbacks which includes inhomogeneous polishing of upper and lower half cells and bubble traces on the upper half-cell. Asymmetric removal might result in degradation of field flatness [1] while bubble traces enhance surface roughness of the upper half-cell of a cavity. To minimize the asymmetry a cavity is flipped to repeat the VEP as shown by other researcher. The flipping method is time consuming and makes cavity surface treatment expensive. In order to solve these issues we have developed Ninja cathodes, VEP setups [2-6] and are further improving cathode and EP parameters. Here we report lab EP experiments to understand and solve the problem of asymmetric removal and apply similar technique in VEP of a cavity.

#vchouhan@e-marui.jp

EXPERIMENTS

Lab EP Experiment

In order to understand the problems appeared in VEP and to solve them, three lab EP experiments, namely lab EP#1, 2 and 3, were performed. In Lab EP#1, four niobium (Nb) square samples in a size of 20×14 mm^2 were prepared for electropolishing. The samples were set horizontally at different positions near to a horizontally set aluminum (Al) cathode. Two Nb samples were set just above and below the cathode while both the samples were facing to the cathode. Other two samples were set aside to the cathode while both were facing downwards. A schematic and a photograph of a set of 4 samples in Fig. 1 show positions of Nb samples and Al cathode, and electrical connections for EP process.

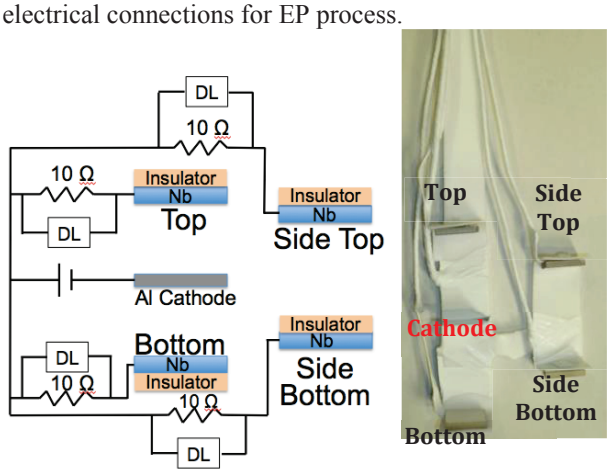

Figure 1: Schematic (left) for arrangement of Nb samples around an Al cathode and electrical connections to measure EP currents from individual sample. Photograph (right) of the samples and cathode.

As shown in the schematic, EP current can be measured for individual sample using data logger. The top/side top and bottom samples were set to simulate with top and bottom irises, respectively, of a cavity in VEP. The top and bottom samples were used to observe and compare effect of hydrogen (H_2) bubbles generated from Al cathode during EP. The side top sample was set to observe indirect hitting of H_2 bubbles. The bottom side

ISBN 978-3-95450-178-6

ANALYSIS OF HIGH PRESSURE RINSING CHACTERISTICS FOR SRF CAVITIES*

Yoochul Jung†, Mijoung Joung, Myung Ook Hyun, RISP, IBS, Daejeon, South Korea
Jiwon Seo, Jeongha Kim, Vitzrotech, Ansan, South Korea

Abstract

High pressure rinsing (HPR) treatment has been widely used in the SRF cavity fabrication. This well- known process helps remove effectively undesirable emission tips from the inner surface of cavities, which are responsible for a different level's multipaction and hellium quenching. Also, the HPR treatment can clean or polish the RF (Radio Frequency) surface, which is critically sensitive to an applied magnetic field, by removing contaminants such as an organic oil, a remnant metal debris and dirty etchants from the cavity surface. Consequently, the HPR treatment contributes to improve quality factor during the cavity operation both by decreasing various field emission sites and by removing defects from the cavity surface. In this paper, we performed HPR experiments by using a simplified cavity structure, intentionally painted with a pattern on the inner surface. Therefore, we report how the surface treatment by HPR was carried out visually as functions of the distance between a target to be cleaned and a nozzle, and a water pressure.

INTRODUCTION

The fabrication of a superconducting cavity requires diverse and complicated processings: a cavity part forming by using a pressing machine [1], a part welding by electron-beam welding [2], a chemical polishing the inner surface of a cavity [3], and a heat treatment by using a high-vacuum furnace [4]. High pressure rinsing by using a high purity water having the resistance of 18 MΩ is also very important processing in the cavity fabrication. A surface state of a superconducting cavity determines a final cavity performance because a superconductivity changes depending on the surface state. The superconductivity tends to disappear when a critical temperature or a critical magnetic field is induced in a superconductor, and various defects, if any, on the surface of a superconductor, will break the superconductivity by inducing a critical temperature or a critical magnetic field [5]. Thus, it is important to keep the surface of a superconductor clean state having defects as less as possible to achieve high performance. We fabricated a prototype high pressure rinsing machine to clean the inner surface of a cavity. And we performed cleaning experiments with a prototype HPR in order to check out its functionality. HPR experiments were carried out with a simplified structure resembling a real cavity in order to observe indirectly how water rinsing treatment was being performed inside the simulated structure. The results by HPR treatment will be discussed as a function of a treatment time and a water pressure.

* This work was supported by the Rare Isotope Science Project of Institute for Basic Science funded by the Ministry of Science, ICT and Future Planning (MSIP) and the National Research Foundation (NRF) of the Republic of Korea under Contract 2013M7A1A1075764
† sulsiin@ibs.re.kr

EXPERIMENTAL

Equipment Setup

The specifications of a prototype HPR equipment fabricated by rare isotope science project (RISP) are listed in Table 1. And a picture of the fabricated HPR machine is shown in Fig. 1. For a simplicity, we will notate a HPR machine (or a HPR tool) as HPR in followings unless we need to distinguish them, because "HPR" itself can signify the meaning of an equipment and the operation performed by HPR machine at the same time. We designed the prototype HPR that can load two types of cavities, a half-wave resonator (HWR) and a quarter-wave resonator (QWR). Another prototype HPR for a single spoke resonator (SSR) is planning to be fabricated. Two types of nozzles are applicable in HPR: 0.5 mm and 0.6 mm in diameter, respectively. The part of nozzle can be classified into three areas: a top, a middle, and a bottom. This is shown in Fig. 2. Each area of the nozzle has equally 6 holes and they are evenly distributed through the entire nozzle. As one can see in Fig. 2, the six sprays of water from the top area have a positive 45 angle and another six sprays from the bottom area have a negative 45 angle with regard to an imaginary horizontal plane consisted of the middle sprays. The pressure of water was measured near an exit from a pump (P@Pump) and near an entrance to the HPR (P@HPR). Table 2 and Table 3 show the results. Thus, the actual pressure of water sprays is less than the pressure measured at the entrance to the HPR (P@HPR). We used deionized water having the resistance of 18 MΩ to operate the HPR.

Table 1: Specifications of High Pressure Rinsing Machine

Items	Specification	Values	Unit
Dimension	W×L× H	1 × 1 × 3	M
Nozzle	Size, Diameter	0.5, 0.6	mm
	Number of Nozzle	6 × 3	EA
Pressure	Water Pressure	Up to 140	bar

Painting the Simplified Cavity Structure

In order to observe visually how HPR works inside an cavity, we simplified an actual niobium (Nb) cavity. We separated only outer-conductor made of oxygen free high conductivity copper (OFHC) form the cavity, and this is shown in Fig. 3. The surface of the simplified structure was

THE TRANSFER OF IMPROVED CAVITY PROCESSING PROTOCOLS TO INDUSTRY FOR LCLS-II: N-DOPING AND ELECTROPOLISHING*

C. E. Reece#, F. Marhauser, and A. D. Palczewski
Thomas Jefferson National Accelerator Facility, Newport News, VA 23606, USA

Abstract

Based on the R&D efforts of colleagues at FNAL, Cornell, and JLab, the LCLS-II project adopted a modification to the rather standard niobium SRF cavity surface processing protocol that incorporates a high temperature diffusion doping with nitrogen gas. This change was motivated by the resulting higher Q_0 and the prospect of significantly lower cryogenic heat load for LCLS-II. JLab is responsible for managing the cavity procurement for the LCLS-II project. The first phase of the procurement action is to transfer the nitrogen-doping protocol to the industrial vendors. We also seek to exploit improvements in understanding of the niobium electropolishing process as part of the production processing of the TESLA-style LCLS-II cavities. We report on the technology transfer activities and progress toward the envisaged performance demonstration of vendor-processed cavities.

N-DOPING REQUIREMENTS

Based on the multi-lab R&D effort that validated the discovery from FNAL of the beneficial effects of nitrogen doping of niobium cavities and explored its sensitivity to process variations, the LCLS-II project selected a particular protocol for cavity preparation that has consistently yielded higher Q_0, and thus lower cryogenic losses, than has previously been accessible. This R&D effort has been documented [1-5], and the subsequent preparation of cavities for the two LCLS-II prototype cryomodules are reported at this conference.[6-11]

By conference time the cavity vendors for the LCLS-II project have been selected. Both vendors visited JLab and FNAL to consult regarding modifications to the cavity treatment protocols compared with prior experience. Furnace gas flow control requirements were discussed. Procedures for controlled cavity electropolishing were discussed. Vendors observed application of both processes to cavities at JLab. Vendors are now in the process of adapting their own facilities to accomplish the modified processes. First commissioning runs are anticipated soon after the conference. Per the terms of the contract, JLab staff will advise and assist. Vendors are required to pass a qualification test by successfully processing two cavities supplied by the project, success being demonstrated by documented process control and acceptable high-Q performance of cavities delivered to JLab under vacuum for cryogenic test.

*Authored by Jefferson Science Associates, LLC under U.S. DOE Contract No. DE-AC05-06OR23177 with partial support from the LCLS-II project, U.S. DOE Contract No. DE-AC02-76SF00515.
#reece@jlab.org

The cavity preparation protocol is a relatively minor, but controlled variation on the now rather standard niobium cavity surface preparation methods developed by the community over the past decades. It involves low-pressure nitrogen gas exposure at the end of a 800 °C vacuum bake, followed by a light electropolish (EP) removing a few microns from the cavity surface. The control parameters associated with the heat treat cycle issued to the vendors are listed in Tables 1 and 2.

Table 1: Vacuum Heat Treatment and Nitrogen Doping

Step	Temperature (°C)	Duration (min)	P_N (mTorr)
Hydrogen degassing	800 ± 10	180 ± 5	0
Nitrogen doping	800 ± 10	2 ± 0.1	26 ± 15%
Vacuum annealing	800 ± 10	6 ± 0.1	0

Table 2: Range of Doping Parameters

P_N	22-30 mTorr (2.9 – 4.0 Pa) P_{avg} = 26 mTorr (3.5 Pa)
T_N (doping)	2 min ± 6 sec
T_A (annealing)	6 min ± 6 sec

This doping by thermal diffusion is followed by controlled electropolishing of the cavity interior surface, to remove 5 µm on average with nominally uniform removal, or 5 µm from the cell equator region.

The vendors have flexibility regarding the particular implementations used to meet these requirements. The lab R&D effort adequately demonstrated that cavity loss characteristics are not highly sensitive to protocol details, so that successful realization of project requirements appears confident. Nevertheless, as reported elsewhere in this conference, research continues into the basic material dynamics of the beneficial effects of nitrogen doping, and there are prospects that further refinements may yet be accessible.

In order to build assurance with vendor N-doping facilities and processes, metallographically smooth niobium samples are being provided for doping simultaneously with initial cavities. These will be returned to JLab for controlled bench EP and dose analysis via SIMS and compared with similar samples treated in the lab facilities.[12]

After successful doping has been demonstrated, the vendors will proceed with fabrication of new cavities and then finish them with the monitored doping and subsequent light EP, delivering completed production

FURNACE N_2 DOPING TREATMENTS AT FERMILAB *

M. Merio†, A.C. Crawford, A. Grassellino, A. Rowe, M. Wong, Fermilab, Batavia, IL, USA
M. Checchin, M. Martinello, Fermilab, Batavia, IL, USA and IIT, Chicago, IL, USA

Abstract

The Fermilab SRF group regularly performs Nitrogen (N_2) doping heat treatments on superconducting cavities in order to improve their Radio Frequency (RF) performances. This paper describes the set up and operations of the Fermilab vacuum furnaces, with a major focus on the implementation and execution of the N_2 doping recipe. The cavity preparation will be presented, N_2 doping recipes will be analyzed and heat treatment data will be reported in the form of plot showing temperature, total pressure and partial pressures over time. Finally possible upgrades and improvements of the furnace and the N_2 doping process are discussed.

INTRODUCTION

High temperature Nitrogen (N_2) doping baking activities for Superconducting Radio Frequency (SRF) cavities are performed on a regular basis in the SRF Department at Fermilab as a mean to improve Q_0 at medium gradients. Q_0 values increase as much as a factor of three at 18 MV/m accelerating gradient [1]. The SRF group owns two vacuum furnaces similar in design but of different size in order to accommodate various types of resonators. This paper will describe in detail how the N_2 doping process is executed, with a particular focus on the furnace operation and how a low pressure atmosphere of N_2 can be maintained in the furnace; finally bake data will be discussed.

FERMILAB VACUUM FURNACES

Two vacuum furnaces manufactured by TM Vacuum [2] are used for baking SRF cavities: the smaller one is represented in Figure 1. They are known as *Small TM* and *Big TM* and are comparable in their characteristics and design, but have a different working volume. Both have a base vacuum of 1×10^{-8} Torr and their maximum operating temperature is 1000°C (under vacuum or backfilled to 1 Torr). Heating is achieved by means of low voltage 2 inches molybdenum (Mo) strips and the hot zone is thermally insulated by six layers of Mo reflective shields, backed by a stainless steel containment. The vacuum chamber and door are double walled for the circulation of cooling water. The chamber is evacuated by a dry roughing pump and high vacuum is achieved by 2 cryopumps. A SRS RGA100 [3] Residual Gas Analyzer (RGA) is mounted on each system and is used to qualitatively follow the evolution the the vacuum atmosphere during a bake. If the pressure raises above 5.5×10^{-5} Torr during a bake cycle, the furnace goes into a *hold* mode: it maintains a constant temperature and lets the pressure drop down below 5.5×10^{-6} Torr; after that, the bake cycle is continued. The furnace also allows for the introduction of a process gas with the flow manually regulated by a metering valve. Once the bake is completed, the chamber is backfilled to atmospheric pressure with boil-off Argon or Nitrogen.

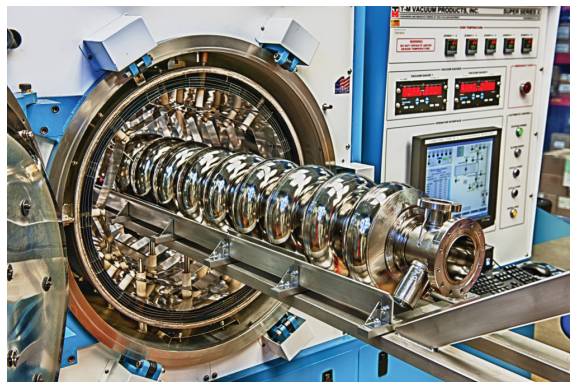

Figure 1: Super Series Vacuum Furnace SS 12/72-10 MCX from TM Vacuum, *Small TM*. Hot zone 12 x 12 x 72 inches. Mainly used for 1.3 GHz single and 9-cell cavities.

Gas Bleed Setup

Fermilab furnaces allow for the introduction of a process gas into the chamber at any temperature.

Figure 2 shows a schematic of the gas bleed setup. The metering valve (Swagelock SS-4MG [4]) is manually adjusted, while the isolation control valve is operated by the furnace PLC: its status (open or closed) is reported on the computer user interface in Figure 3 and it is identified by the name *bleed valve*. The metering valve is not leak tight which means that when the control valve is closed there will always be a trapped volume full of the process gas (N_2 for SRF cavities) between the two valves as shown in Figure 2. This volume of gas will be injected in the furnace as soon as the isolation control valve opens. After that, while the control valve stays open, the gas continues to flow in the chamber at the rate that is set by the metering valve. The optimal position of the metering valve to ensure the desired average chamber pressure of 25±2 mTorr was determined by trial and error during the initial development of the doping recipe.

A more precise setup can be obtained substituting the manual metering valve with a Mass Flow Controller (MFC) which allows a more accurate control of the flow. The size of the MFC orifice should be designed to rapidly bring the furnace from Ultra High Vacuum (UHV) to 25 mTorr and to maintain this average pressure compensating for the N_2 absorbed by the cavity. A MFC could also allow for detailed studies on the N_2 absorption of resonators and it would be

* Work supported by United States Department of Energy under contract DE-AC02-07CH11359
† merio@fnal.gov

ISBN 978-3-95450-178-6

SRF QUALITY ASSURANCE STUDIES AND THEIR APPLICATION TO CRYOMODULE REPAIRS AT SNS*

J. Mammosser†, B. Hannah, R. Afanador, D. Barnhart, B. Degraff, J. Saunders,
P. Tyagi, M. Doleans, S-H. Kim, M. Campbell, D. Hensley*
Oak Ridge National Laboratory, Spallation Neutron Source, Oak Ridge, TN 37831, USA
* Oak Ridge National Laboratory, Center for Nanophase Material Science, Oak Ridge, TN 37831, USA

Abstract

Many of the SRF activities involve interactions with cryomodules which presents risk for particulate contamination to RF surfaces. In order to understand and reduce contamination in cryomodules during maintenance activities such as vacuum pumping and purging, and in-situ cryomodule repairs, a Quality Assurance (QA) study was initiated to evaluate these activities and improve them where possible. This paper covers the results of these activities including procedure development for in-situ cryomodule repairs, investigations on particulate control during pumping and purging and the study of particulate generation during beam line valve actuation and discussion of further improvement in these areas.

INTRODUCTION

The Superconducting Linac (SCL) group at SNS has as its main responsibility to maintain the SCL performance and reliability from both an acceleration and cryogenic operational point of view. To date, the SCL group has not fully disassembled a single linac cryomodule for repairs and has relied on performing in situ repairs on cryomodules which reduces cost and downtime [1]. The repairs to these cryomodules are performed through existing access ports located at each cavity to cavity location as well as the ends of the cryomodule [2]. Repairs so far have been completely successful, with little or no performance degradation but are very difficult to perform and present a high risk of increasing field emission, a main performance limitation of the SCL [3]. Additionally, first time repairs present new challenges and one cannot rely on past experience so the risk is even higher. To reduce these risks, a quality assurance effort was started to measure the performance of the critical tasks required for typical cryomodule repair procedures and to make improvements based on experimental data.

THE MOCK CRYOMODULE

In order to perform these measurements a mock cryomodule was designed and fabricated which utilizes existing string tooling to save cost. This mock cryomodule, allows for development and testing of new and existing procedures as well as for training of staff on procedures prior to the actual cryomodule repair. The mock cryomodule will help build confidence that repair procedures will have minimal impact to cryomodule performance, it will allow for the further development of tooling and procedures and increased the reproducibility of performing the tasks. The mock cryomodule hardware is not fully representative of the real cryomodule but presents the same physical challenges and access limitations as the real thing. One key factor in the mock cryomodule design was to accurately represent the physical limitation repair personnel would be faced with, which is the most challenging part of these repair tasks. Some of the repairs require distortion of ones arms to achieve the task or are better performed facing away from the cryomodule. The first focus of the quality assurance effort was to use the mock cryomodule to test existing techniques for the removal of HOM can probes, a standard maintenance procedure for SNS cryomodules that have not had them removed already, and to develop improvements to the existing procedures where possible. The results of this effort were implemented on a repair (summer 2015) of a high beta cryomodule, CM12.

The mock cryomodule (see Fig. 1) consists of the assembly string rail with a dressed cavity mounted on modified cavity support posts which are used for string assembly.

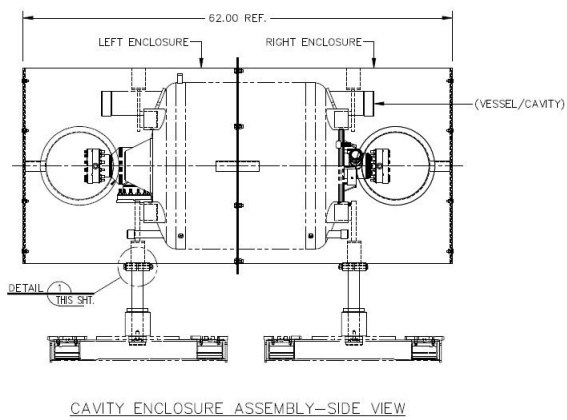

Figure 1: Schematic of the mock cryomodule side view.

A stainless steel shell made to the thermo-shield inner diameter was designed to be split in the center, allowing for insertion from the cavity ends and the two half's are then bolted together in the center. The weight of the structure is carried by rail support posts and the shell half's are aligned to the cavity by plugs which insert into the helium vessel nitronic rod support posts . Ends of the structure are sealed with Lexan covers which are see through and can be remov-

* This work was supported by SNS through UT-Battelle, LLC, under contract DE-AC05-00OR22725 for the U.S. DOE.

STUDY OF THE EVOLUTION OF ARTIFICIAL DEFECTS ON THE SURFACE OF NIOBIUM DURING ELECTROCHEMICAL AND CHEMICAL POLISHING

L. Monaco#, P. Michelato, INFN Milano - LASA, Segrate, Italy
C. Pagani, Università degli Studi di Milano & INFN, Segrate, Italy
A. Navitski, J. Schaffran, W. Singer, DESY, Hamburg, Germany
A. Prudnikava, Y. Tamashevich, Unversity of Hamburg, Hamburg, Germany

Abstract

The presence of defects on the inner surface of Nb superconducting RF structures might limit its final performance. For this reason, strict requirements are imposed during mechanical production of the cavities, specifically on the quality control of the inner surface of components, to avoid the presence of defects or scratches. Nevertheless, some defects may remain also after control or can arise from the following production steps. Understanding the evolution of the defect might shine new insight on its origin and help in defining possible repair techniques.

This paper reports the topographical evolution of defects on a Nb sample polished with the standard recipe used for the 1.3 GHz cavities of the EXFEL project. Various artificial defects of different shape, dimensions, and thicknesses/depths, with geometrical characteristics similar to the one that may occur during the machining and handling of cavities, have been "ad hoc" produced on the sample of the same material used for the cell fabrication. Analysis shows the evolution of the shape and profile of the defects at the different polishing steps.

INTRODUCTION

One meaningful aspect in the niobium cavities production is the quality of the inner surface that must be treated with particular care. Indeed, it is well known that the presence of contaminants, dusts, inclusions and surface defects (scratches, bumps, holes, etc.) on the RF inner Nb surface can limit the cavities performances during their operation [1].

Hence, for the EXFEL cavities production, a strict quality control is applied not only to the row material used for the fabrication of the resonators [2], but also during all preparation steps of the inner surface of Nb cavities [3].

However, despite the strict quality control, mechanical defects can be introduced during the cavity production cycle. Scratches, bumps or holes may occur during the mechanical production of subcomponents, or can be originated by not proper handling or caused by accident during the various treatment steps. The understating of these defects evolution during the following electrochemical (Electro Polishing, EP) and chemical (Buffered Chemical Polishing, BCP) treatments is important to evaluate which kind of defects could be critical for the final resonator performances and which one can be considered as a low risk.

Different equipment developed and built at the laboratories and at the industries are in operation for the quality control of inner surface of the resonators. For EXFEL, inspections are performed not only during the cavity production but also after their cold test if the cavity is not performing as expected [4]. Even if these systems allow detecting and also curing defects with good result (i.e. [5]), the evaluation of the defect evolution is not yet well studied and can be a powerful tool to limit this kind of "cure" only to defects that represent a real high risk for the performance of cavities.

In this paper, we present preliminary results of a study of the evolution during EP/BCP treatments of artificial defects mechanically produced on a Nb sample that are representative of the ones that could be found on the inner surface of resonators. The analysis was started few years ago [6] and is still ongoing with an improved diagnostic. Those measurements gave information on the evolution of main geometrical parameters of defects (i.e. diameter, height) with a rough estimation of their profiles.

This year, in collaboration with DESY, we started a new series of measurements on a new Nb sample, prepared with artificial defects as done in the past. All operation concerning the preparation of the sample and the production of artificial defects, as well as all etching treatments have been performed at LASA, while scanning, images of defects and also profile and roughness measurements before and after each treatment steps have been done at DESY. The aim of these new measurements is to have a complete analysis of defect evolution under EP and BCP treatments, with particular care on the profile evolution, of the smoothness of the edges of the defects and precise measurements of the depth and roughness evolution.

EXPERIMENTAL SET-UP

Sample Preparation and Production of Artificial Defects

A sample (50mm x 85mm x 3mm) machined from a Nb sheet used for the production of cavities has been cleaned with pure ethanol, dried and BCP (1:1:2, HF, HNO_3, H_3PO_4) etched with a total removal of 25 µm, before producing the artificial defects. Figure 1 (left) shows a map of different defects produced on the sample surface.

#laura.monaco@mi.infn.it

ISBN 978-3-95450-178-6

SURFACE STUDIES OF PLASMA PROCESSED Nb SAMPLES*

P. V. Tyagi#, M. Doleans, B. Hannah, R. Afanador, C. McMahan, S. Stewart, J. Mammosser, M. Howell, J. Saunders, B. Degraff, S-H. Kim, SNS, ORNL, Oak Ridge, TN, USA

Abstract

Contaminants present at top surface of superconducting radio frequency (SRF) cavities can act as field emitters and restrict the cavity accelerating gradient. A room temperature in-situ plasma processing technology for SRF cavities aiming to clean hydrocarbons from inner surface of cavities has been recently developed at the Spallation Neutron Source (SNS). Surface studies of the plasma processed Nb samples by Secondary ion mass spectrometry (SIMS) and Scanning Kelvin Probe (SKP) showed that the NeO_2 plasma processing is very effective to remove carbonaceous contaminants from top surface and improves the surface work function by 0.5 to 1.0 eV.

INTRODUCTION

Field emission (electron emission) is one of the prime factors to limit the performance of superconducting radio frequency (SRF) cavities during operation at high accelerating gradient [1]. Many of the SNS (spallation neutron source) SRF cavities are also limited by the field emission and operating below their design accelerating gradient [2]. Surface contaminants (e.g. hydrocarbons) located at top surface of high E-field regions of the SRF cavities (e.g. iris) are believed to be one of the main culprits for the field emission. These contaminants can act as field emitters during the cavity operation at high E-field. Many times, good cavities working at high accelerating gradient tend to degrade over the time during operation and start to show field emission. In order to recover the cavity performance while they are installed in the accelerator tunnel, currently rf conditioning and/or He processing are the most common in-situ processes employed on the cavities and sometimes cavities performance is recovered. However, these processes are not effective all the times and there is no clear understanding of the cleaning mechanism of these processes developed so far.

Therefore an effective in-situ processing is the most demanding for the cleaning of cavity surface to recover cavity performance while they are installed in the accelerator tunnel. Recently, a room temperature in-situ plasma processing [3] for cleaning of the hydrocarbon residues from cavity surface has been successfully developed at SNS for high beta (HB) SRF cavities. A couple of plasma processed cavities have shown significant improvement in the accelerating gradients with reduced electron activities during the cold tests [4].

At SNS, plasma ignition in a desired cell of the SNS HB cavity (6-cells) is achieved utilizing the combination of different modes of the cavity under a continues flow of fundamental gas. Ne gas is the choice of fundamental gas to ignite the plasma and tune in a desired cell of the cavity. After plasma is tuned in a desired cavity cell, O_2 is introduced as a cleaning agent to oxidize hydrocarbons from cavity surface. The oxidized hydrocarbons (volatile) are continuously pumped through the cavity pumping system. The cavity pumping system is equipped with a residual gas analyser (RGA) which is used to monitor the gases coming out of the cavity during the plasma processing.

In order to understand plasma chemistry at cavity surface, we have carried out detailed experimental studies on Nb samples. Surface characterizations of Nb samples were carried out by secondary ion mass spectrometry (SIMS) for chemical analysis at top surface and scanning kelvin probe system (SKP) for workfunction (WF) measurements. In this article, we report the results from these surface studies.

INCREASE WF TO REDUCE FIELD EMISSION

WF measurements of Nb surface are not yet very common in the SRF community to evaluate Nb surface quality after various surface processing. However, WF of Nb surface plays an important role for field emissions in the SRF cavities as it is directly related to the field emission via Fowler-Nordheim law (eq.1).

$$j \propto \frac{E_s^2}{\varphi} \exp\left(\frac{-a \times \varphi^{\frac{3}{2}}}{E_s}\right) \qquad (1)$$

Where, j is current density, φ is the surface WF and E_S is surface enhanced electric field; $E_S = \beta E$ ($\beta > 1$), where β is known as field enhancement factor. It is believed that the onset of field emission at lower than expected field (for constant β) may be associated with the low work function contaminants present at top surface. Hence, higher WF is desirable to lower the field emission after the plasma processing of Nb surface.

NeO_2 PLASMA PROCESSING TO REMOVE HYDROCARBONS AND INCREASE WF

Plasma Processing of Nb Samples

Sample preparation

Nb samples used for studies were prepared from a Nb sheet of similar residual resistance ratio (RRR) as of SNS HB cavities are fabricated. Disc type samples were first EDM wire cut out from the Nb sheet followed by mechanical polishing using a grinder polisher [5]. SiC grinding papers of different grit sizes were used to obtain coarse grinding to fine polishing. After the mechanical

* Work supported by SNS through UT-Battelle, LLC, under contract DE-AC05-00OR22725 for the U.S. DOE.
#tyagipv@ornl.gov, pvtyagi@gmail.com

DEVELOPMENTS OF HORIZONTAL HIGH PRESSURE RINSING FOR SUPERKEKB SRF CAVITIES

Y. Morita#, K. Akai, T. Furuya, A. Kabe, S. Mitsunobu, and M. Nishiwaki
Accelerator Laboratory, KEK, Tsukuba, Ibaraki 305-0801, Japan

Abstract

The Q factors of the eight superconducting accelerating cavities gradually degraded during the long-term operation of the KEKB accelerator. Since we will re-use those SRF cavities for the SuperKEKB, the performance degradation will be a serious problem. Several cavities degraded their performance significantly at high accelerating fields. The Q degradation is still acceptable for the 1.5 MV operations at SuperKEKB. However, further degradation will make the operation difficult. In order to recover the cavity performance, we developed horizontal high pressure water rinsing (HHPR). This method uses a horizontal high pressure water nozzle and inserts it directly into the cavity module. We applied this method to two degraded cavities and their degraded Q factors recovered above 1×10^9 at around 2 MV. In this paper we will present the HHPR method, high power test results after the HHPR and the residual gas analysis.

INTRODUCTION

An asymmetric energy electron-positron double-ring collider accelerator for B-factory, KEKB was shut down in 2010 and its upgrade machine, SuperKEKB [1] is now under construction. The luminosity will be increased up to 8×10^{35} $cm^{-2}s^{-1}$, 40 times the KEKB peak luminosity. The beam current of the high energy electron ring (HER) is 2.6 A with a beam size of 10×0.04 μm^2 and bunch length of 5 mm, while that of the low energy positron ring (LER) is 3.6 A with the bunch length 6 mm. The construction is almost completed and its commissioning will start in January 2016.

In the HER ring, eight SRF cavities [2] will be re-used for the electron beam acceleration. Expected beam-induced HOM power per cavity is more than 30 kW. This issue will be discussed elsewhere [3]. Another issue is cavity performance degradation during the KEKB operation. Q factors of several cavities degraded significantly at around 2 MV with intense X-rays after air exposure of the cavity at the coupler gasket adjustment or at the repair of indium sealed joints. Those degradations are mainly due to particle contamination. It is still acceptable for the SuperKEKB operation because the Q factors are still above 1×10^9 at 1.5MV. However, further degradation will make the operation difficult. Therefore performance recovery is desired.

The high pressure water rinsing (HPR) is effective to clean the cavity surface contaminated by micro-particles. To apply the HPR to degraded cavities, their cavity cells have to be dismounted from cryomodules. This procedure will make the risk of helium leakage at indium sealed joints. If we apply this method directly to the cavity in the cryomodule, we can save a lot of time and costs of re-assembly, and furthermore we can avoid the risk of leakage at the indium joints. Therefore we have developed a horizontal HPR (HHPR) [4] that can be applied to the cavity in a cryomodule. This method uses a horizontal insertion pipe with a water jet nozzle and an evacuation pipe for wasted water. We applied this method to two degraded cavity cryomodules. Their Q factors successfully recovered to 1×10^9 at 2 MV.

Since the cavity is not baked after the HHPR, H_2O contamination on the inner surface of the cavity might cause serious discharge. We studied a H_2O contamination effect not only during the high power test of the cavity but also in a coupler conditioning before cooldown. We also studied desorption gases during warm-up and at the baking of ion pumps to analyse H_2O contamination. The study showed that the H_2O contamination enhanced multipacting discharge in a coaxial structure of the coupler. However, a voltage bias conditioning effectively processed those multipacting levels.

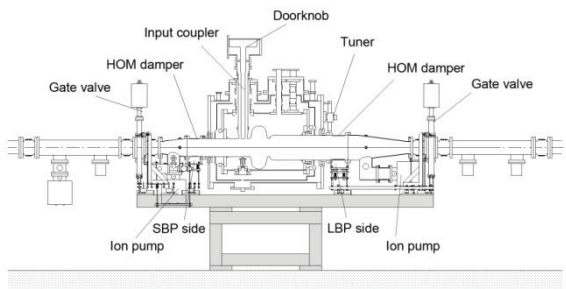

Figure 1: Cross-section of the SRF cavity module.

KEKB SRF CAVITY

Eight SRF cavities were installed in the KEKB tunnel to accelerate the electron beam together with ARES normal conducting cavities. A schematic diagram of the KEKB SRF cavity is shown in Figure 1. The cavity is a 509 MHz single cell cavity optimized for KEKB. Ferrite HOM dampers attached on both beam pipes heavily damp HOM modes to suppress the beam instability. A coaxial type power input coupler [5] attached on the beam pipe feeds RF powers to the beam. The external Q factor of coupling was first set at 7×10^4 then adjusted to 5×10^4 as the beam current was increased. Each cavity provided the cavity voltage of 1.2~1.5 MV and the beam power of 350~400 kW.

#yoshiyuki.morita@kek.jp

ISBN 978-3-95450-178-6

IDENTIFICATION AND EVALUATION OF CONTAMINATION SOURCES DURING CLEAN ROOM PREPARATION OF SRF CAVITIES*

L. Zhao#, K. Davis, T. Reilly, Thomas Jefferson National Accelerator Facility, Newport News, VA 23606, USA

Abstract

Particles are one possible cause of field emission issues in SRF cavity operations. During clean room cavity preparation, several processes could contribute to the generation of particles. One of them is friction between hardware during assembly and disassembly. It is important to understand the behaviours that generate and propagate particles into cavities. Using a single cell cavity, particle shedding between flanges and other materials have been tested. The number of particles is recorded with an airborne particle counter, and the generated particles are examined with microscope. The migration of particles into a cavity due to different movements is studied. Suggestions are made to reduce particle generation and prevent contamination of the cavity interior area.

BACKGROUND

The preparation process of an SRF cavity can significantly influence its performance. Chemical polishing, mechanical polishing, thin film deposition, and the most recent trend of heat treatment while carefully introducing foreign materials are all methods to establish a surface condition that provides satisfying quality factor and accelerating gradient. To make the most out of these surface conditions, it is important to prevent other factors, such as field emission due to contamination, from degrading cavity performance. Field emission has been reported in some circumstances to be caused by micro particles inside the cavity [1]. Various cleaning techniques have been explored and introduced to avoid or reduce particles during cavity production [2, 3]. Exanimation of particle existence at different stages, from surface preparation [4], cleaning [5], storage [6], and cleanroom assembly [7], to vacuum component operation [8], has received wide attention. In this study, we aim to identify and understand the nature of micro particles during clean room preparation, especially assembly and disassembly, of SRF cavities.

EXPERIMENT

Preparation of Cavity and Components

A Tesla shaped 1.3 GHz single cell cavity made from large grain niobium was used for this study. The cavity was cleaned in an ultrasonic tank filled with detergent solution for about an hour. It was then rinsed thoroughly with ultrapure water and dried in air. The cavity was transferred to clean room and received high pressure rinse with ultrapure water. It was then dried in the clean room and ready for assembly.

Hardware to be assembled onto the cavity was cleaned separately in another ultrasonic tank with detergent solution. Then they were thoroughly rinsed with ultrapure water, dried in air, bagged, and transferred into clean room for assembly.

Assembly and Disassembly

Only one of the two beam pipe flanges was assembled in this study; the other one was used for holding the particle counter. A Lighthouse Solair 3100 airborne particle counter was used to monitor particle counts inside the cavity. It detects particle sizes from 0.3 μm to 10 μm. The accumulation mode was used in the experiment. The stainless steel collector and rubber hose connecting the collector was supported by a cleaned PVC tube inserted into the cavity along the beam pipe. One end of the PVC reached the middle of the assembly side of beam pipe. The other end of the PVC tube was mounted onto a PVC flange and fixed to the other beam pipe flange with spring clamps.

Assembly and disassembly at both horizontal and vertical orientations were studied. For vertical assembly, the bottom beam pipe flange was assembled. Before assembly, the stainless steel flange was blow-cleaned with ionized nitrogen gun; the aluminum magnesium alloy gasket was wiped with alcohol and blow-cleaned with ionized nitrogen gun. The particle counter was started and kept running until the particle counts reached zero, which means any particle counts detected later was caused by assembly movements. After the experiment, data from the particle counter were exported for analysis.

Particle Sampling and Characterization

Before assembly, surfaces of flange, gasket, bolt, nut, and washer were sampled with clean carbon tape. During the assembly and disassembly, carbon tape was attached near the particle counter collector as well as the interior of the cavity beam tube. After disassembly, the carbon tape was covered up to prevent exposure to the atmosphere, until the time they were transferred into scanning electron microscope (SEM) for analysis. Energy dispersive spectroscopy (EDS) was used for elemental analysis of the particles.

RESULTS AND DISCUSSION

Figure 1 shows particles collected from surfaces of different assembly hardware, including stainless steel bolt, stainless steel washer, silicon bronze nut, aluminum

*Work supported by Jefferson Science Associates, LLC under U.S. DOE Contracts DE-AC05-06OR23177 and DE-AC02-76SF00515 for the LCLS-II Project.

#lzhao@jlab.org

CLEANLINESS AND VACUUM ACCEPTANCE TESTS FOR THE UHV CAVITY STRING OF THE XFEL LINAC

S. Berry, C. Boulch, C. Cloué, C. Madec, O. Napoly, T. Trublet, B.Visentin, CEA/DSM/irfu/SACM, Saclay, France,
D. Henning, L. Lilje, M. Schmoekel, A. Matheisen, DESY, Hamburg, Germany

Abstract

The main linac of the European XFEL will consist of 100 accelerator modules, i.e. 800 superconducting accelerator cavities operated at a design gradient of 23.6 MV/m.

In this context CEA-Saclay built an assembly facility designed to produce one module per week, ready to be tested at DESY. The facility overcame the foreseen production rate to one cryomodule each 4 days.

We would like to highlight and discuss the critical fields: cleanliness and vacuum.

A new assembly method to protect final assembly against particulates contamination has been implemented on the production line. Modules RF tests results are compared.

Particle transport measurements on components used for the European XFEL accelerator module are presented. The results indicate that the nominal operation of the automated pumping and venting units will not lead to particle transport.

Vacuum acceptance tests are of major interest: leak tests and residual gas analysis (RGA) is used to control the absence of contamination and air leak. The RGA specifications have been slightly relaxed.

INTRODUCTION

The assembly of the beam vacuum string of the XFEL accelerator modules needs to be made under clean room conditions [1]. Particle contaminations of the superconductor surface of the cavities for beam acceleration must be avoided to prevent deterioration of the cavity gradient. Apart from particle cleaning of components and avoiding the generation of particulates it is mandatory not to transport particles with the gas stream. It has been shown that turbulent flow supports transport of particles [2]. As Ultra High Vacuum with associated pump down and venting cycles for assembly of components is a requirement for the successful operation of the superconducting accelerating structures, a setup for venting and pump-down attached to a turbomolecular pump station has been developed [3]. The system (SVPS) is able of slow venting and pumping. Their operation is briefly described in [3]. Six of these pump stations are in operation at CEA.

NEW ASSEMBLY METHOD IN ISO4 CLEANROOM

Environment and Nominal Work Flow

The first week of work consist of cold coupler parts assembly to the 8 cavities on the so called “cold coupler” workstation (CC). The next week the cavities with coupler (CCC) and quadrupole package are assembled in a string on so called “string assembly” workstation (SA). Both workstations are in a ISO4 clean room with laminar flow of air.

For the last connection of the cavity string to the pumping system before the final leak check while in the vacuum vessel (CO workstation), special care has to be taken to maintain the same cleanliness level even if in mobile clean room.

Control of the Parts

Control of all the parts in contact with the cavity RF surfaces is required. This process is strongly operator dependent and well trained operators are required [4]. The control of the inside of the angle valve closing the device under test (DUT) is crucial. This last point is one of the many points raised in the audit of the module XM26*.

Control of the Vacuum Pumping Lines

After each change in the piping configuration or cleanroom maintenance (twice per year), the vacuum pumping lines including nitrogen flushing are systematically qualified by a leak check, a RGA [5], and a particle counting. The criteria threshold is “not more than 10 particles per minute of size bigger than 0.2 µm compare to reference measurement for detail see [6].

New Assembly Method: Solution n°3

The conservative assembly method n°3 proposed in [1] to has been qualified by steps: test part, cavity alone then a complete module. The goal is to maintain cavity performance from vertical test to module test.

The key improvement is the reduction of the risk of contamination by avoiding close and open steps of the angle valve which isolate the cavity. The main difference between nominal and solution n°3 is summarized in the fact that cavities with cold part of the coupler are vented on CC workstation instead of being vented in SA. First

* XM*i* refers to XFEL module n°*i*,

ISBN 978-3-95450-178-6

COMMISSIONING OF THE SRF LINAC FOR ARIEL

V. Zvyagintsev, Z. Ang, T. Au, S. Calic, K. Fong, P. Harmer, B. Jakovljevic, J. Keir, D. Kishi, P. Kolb, S.R. Koscielniak, A. Koveshnikov, C. Laforge, D. Lang, R.E. Laxdal, M. Laverty, Y. Ma, A.K. Mitra, N. Muller, R. Nagimov,
W.R. Rawnsley, R.W. Shanks, R.L. Smith, B. Waraich, L. Yang, Z. Yao, Q. Zhen,

TRIUMF Canada's National Laboratory for Particle and Nuclear Physics, Vancouver, BC V6T 2A3

Abstract

This paper is reporting commissioning results for the SRF linac of ARIEL facility at TRIUMF. The paper is focused on the SRF challenges: cavity design and performance, ancillaries design and preparation, cryomodule design and performance, RF system and final beam test results.

INTRODUCTION

The ARIEL project [1] will allow increase in the RIB delivery hours with the addition of a new electron linac driver of 50 MeV (0.5 MW) and new target stations.

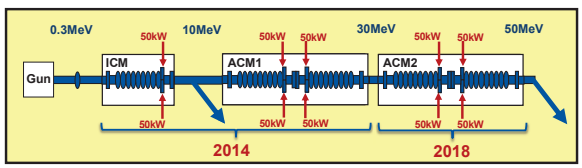

Figure. 1: The stages of the e-Linac project.

Accelerated electrons can be used to generate RIBs via the photo-fission process [2]. The electrons are stopped in a converter to generate bremsstrahlung photons for fission in actinide target material. 10 mA/50 MeV electron beam is required for a goal rate of 10^{13} fissions/sec.

The electron linac is housed in a pre-existing shielded experimental hall adjacent to the TRIUMF 500 MeV cyclotron that has been re-purposed as an accelerator vault. The e-linac is being installed in a phased way with stages shown schematically in Fig. 1.

A first phase consisting of a 300 kV 16 mA electron gun, an injector cryomodule, ICM, containing one 1.3 GHz nine-cell cavity and an accelerating cryomodule, ACM1, that contains two 1.3 GHz nine-cell cavities plus associated beamlines is now installed and is in various stages of commissioning. This first phase is designed to accelerate cw up to 10 mA of electrons at 30 MeV but the initial beam dumps and production targets will only be compatible with 100 kW operation. A second phase, dependent on funding, will see the addition of a second accelerating module, ACM2, and a ramp up in beam intensity to the full capability of 50 MeV 0.5 MW.

The electron linac is housed in a pre-existing shielded experimental hall adjacent to the TRIUMF 500 MeV cyclotron that has been re-purposed as an accelerator vault.

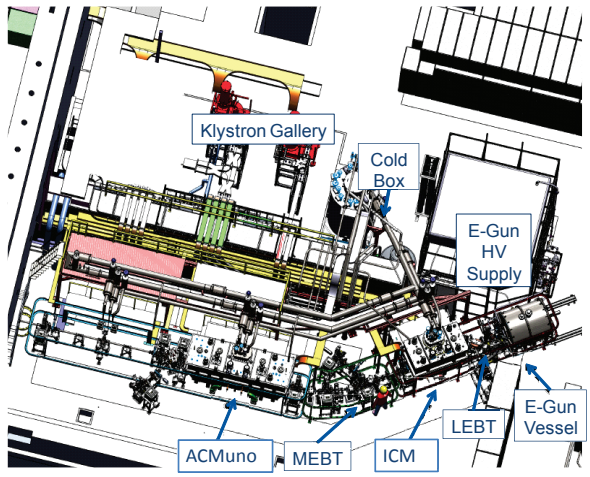

Figure 2: The phase I configuration of the e-Linac.

ARIEL E-LINAC DESIGN

An RF frequency for accelerating cavities of 1.3 GHz is chosen to take advantage of the considerable global design effort at this frequency both for pulsed machines (ILC) but also for CW ERL applications (KEK, Cornell, BerlinPro). The linac architecture was determined by final CW beam power 500 kW (10 mA/50 MeV electron beam) and the available commercial CW RF couplers at 1.3 GHz. The CPI produced coupler VWP3032 developed with Cornell for the ERL injector cryomodule is capable of operation up to 75 kW CW. In order to provide reliable operation it was decided to set a safety factor for power of 1.5 that is 50 kW CW RF power per coupler. To deliver 500 kW of RF power to the beam requires 10 such couplers. The cavity design allows two couplers per cavity arranged symmetrically around one end delivering a total of 100 kW of beam loaded power. This sets the number of cavities at 5 with a maximum gradient per cavity of 10 MV/m. It is our intention to install a future ERL ring with injection and extraction between 5-10 MeV and so a single cavity off-line injector cryomodule was chosen plus two 2-cavity accelerating modules. The electron hall is shown in Fig. 2 as it would appear at the end of Phase I.

Electron Gun

The electron source [3] provides electron bunches with charge up to 15.4 pC at a repetition frequency of 650 MHz. The main components of the source are a gridded dispenser cathode in a SF_6 filled vessel, and an

ISBN 978-3-95450-178-6

BESSY VSR: A NOVEL APPLICATION OF SRF FOR SYNCHROTRON LIGHT SOURCES

A.Vélez, P.Goslawski, A.Jankowiak, J.Knobloch, A.Neumann, M.Ries, H.W.Glock, G.Wüstefeld
Helmholtz-Zentrum Berlin, 12489 Berlin, Germany

Abstract

CW SRF Cavities have been used very successfully in the past in synchrotron light sources to provide high power acceleration. Here we present a novel application of higher harmonic systems of two different frequencies (1.5 GHz and 1.75 GHz) to generate a beating of accelerating voltage. With such a system it is possible to store "standard" (some 10 ps long) and "short" (ps and sub-ps long) pulses simultaneously in the storage ring. This opens up new possibilities for light source users to perform picosecond dynamic and high-resolution experiments at the same facility. The demands on the SRF system and RF control are substantial and a new design, based on waveguide damping, is currently being developed. This system will be used for a major upgrade of the BESSY II facility to the BESSY Variable Pulse length Storage Ring (BESSY VSR) for a next-generation storage-ring light source. We will discuss the concept, challenges and designs for BESSY VSR from the SRF point of view.

INTRODUCTION

Storage ring sources represent very useful and reliable tools for scientist due to the broad spectrum of photon beam parameters available when designing a dedicated experiment: wavelength, flux, peak and average brilliance, coherence, and pulse length. Regarding this last parameter storage rings like BESSY II dedicate most of their beam time to produce long bunches while short bunch operation is provided only during a few days per annum to all beam lines. During the years, BESSY II has been developing a broad community of users working in the THz to hard X-RAY range interested in performing dynamic measurements by means of short pulses (ps to fs). For this reason BESSY has implemented 2 different modes of operation able to satisfy the short pulse demand (low α mode and femto-slicing facility). Nevertheless, short pulses can only be provided to all beam-lines during dedicated low α mode (12 days/year). Although the femto-slicing facility can be operated along the whole year only 1 beam-line is available. In addition, both techniques offer limited flux capabilities. Motivated by this fact HZB's presents the upgrade project of BESSY II by offering the possibility to supply all users simultaneous operation with short (ca. 1.7 ps rms) and long (ca. 15 ps rms) bunches while maintaining a high average brilliance at 300 mA bunch current. Opposite to the upgrade plans in the direction of reducing transverse beam emittance (Difraction Limited Storage Rings, DLSRs) for many facilities like ERSF or Spring-8, BESSY VSR presents a complimentary facility able to supply shorter bunches by an increase in the RF focusing. This RF gain compensates the expected flux reduction due to bunch shortening and a factor 100 increase in bunch current can be potentially obtained with no change in the machine optics. Thus users will be then able to choose the required photon beam for the individual experiments by implementing the proper bunch separation technique in a dedicate beamline. Therefore this paper presents the currents status of the BESSY II SCRF upgrade in order to address the needs of increasingly diverse users community.

BESSY VSR, THE CONCEPT

The original concept of BESSY VSR was proposed in 2006 [1] and further developed in 2011 [2]. It relies on 1.5 GHz CW superconducting RF (SRF) cavities to provide 80 times more longitudinal focusing than from the normal-conducting RF system in BESSY II. The additional installation of a second 3.5 harmonic SRF system (1.75 GHz) leads to a beating of the induced cavity voltages while bunches can be compressed by roughly a factor of √80 into the low picosecond range. Therefore a combination of long and short buckets can be simultaneously generated. Then, long bunches can be then stored to provide the high photon flux while only a few short-bunch buckets are populated with high charge for short-pulse experiments. This procedure successfully avoids eventual impedance and Touschek lifetime problems. Figure 1 shows the voltage beating created by the three cavity system in time domain for a factor 10 bunch shortening. The long bunches are placed within the low gradient buckets, while the short bunches appear 2 ns shifted.

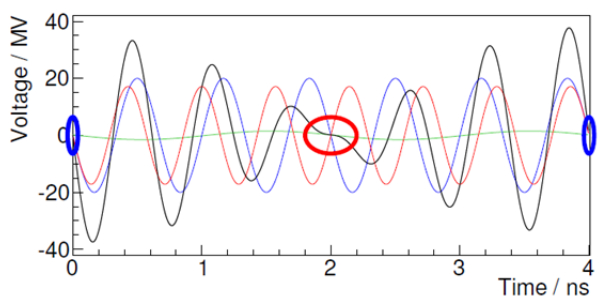

Figure 1: Representations of the 3 cavity system BESSY-VSR concept showing the voltage beating in time domain for a factor 10 bunch shortening. The sum voltage is shown in black. Short bunches are placed at t = 0 and t = 4 ns, long bunches at t = 2 ns.

ISBN 978-3-95450-178-6

RAPID GROWTH OF SRF IN INDIA

D. Kanjilal
Inter University Accelerator Centre, New Delhi - 110067, India

Abstract

The rapid growth of the superconducting radio frequency (SRF) activities at various research centres in India for the development of modern accelerators are summarized. The SRF related activities at Inter-University Accelerator Centre (IUAC) at Delhi, Raja Ramanna Centre for Advanced Technology (RRCAT) at Indore, Bhabha Atomic Research Centre (BARC) and Tata Institute of Fundamental Research (TIFR) both located at Mumbai, and Variable Energy Cyclotron Centre (VECC) at Kolkata are reviewed. The design, fabrication and test facility of niobium quarter wave resonator (QWR) were developed at Inter University Accelerator Centre (IUAC), Delhi at the beginning of this century. The expertise in development of fabrication of niobium cavities, and the availability of fully operational electron beam welding facility along with the various welding parameters developed during more than a decade have been utilized by other laboratories in India and abroad for the development and fabrication of various types of niobium resonators. The SRF related programs at RRCAT, BARC, TIFR and VECC are discussed.

INTRODUCTION

The development of niobium quarter wave resonators (QWRs) was initiated in late ninety eighties by IUAC. Subsequently IUAC developed the collaboration with Argonne National Laboratory (ANL) in early ninety nineties for fabrication and test of initial batch of a new type of bulk 97 MHz two-gap niobium QWRs. The first set of facilities in India for niobium SRF fabrication, surface preparation and tests for the development of superconducting linear accelerator (linac) booster accelerator were developed at the beginning of this century. The superconducting linac booster has been delivering energetic heavy ions regularly for scheduled experiments using the various cavities fabricated at ANL and later at IUAC.

The SRF facility at IUAC became the first fully functional niobium based superconducting resonator design, fabrication and test facility in India. The QWRs developed using these facilities are being used routinely for boosting the energy of the heavy ion beams from the 15 UD Pelletron Tandem Accelerator at required energies to a large number of researchers to carry out scheduled experiments in nuclear physics, materials sciences and atomic physics. The initial batch of QWRs were developed and fabricated in collaboration with Argonne National Laboratory (ANL) in the nineties. Scientists and engineers of IUAC got an excellent opportunity to collaborate with and get trained at ANL. The majority of the niobium resonators of the three superconducting linear accelerator (linac) modules of IUAC were built by the in-house niobium resonator fabrication facilities.

A superconducting lead plated QWR based linac accelerator has been indigenously developed by Tata Institute of Fundamental Research (TIFR) Mumbai and Bhabha Atomic Research Centre (BARC) Mumbail at TIFR to boost the energy of heavy ion beams delivered by the 14 MV Pelletron tandem accelerator. The superconducting booster linac consisting of three accelerating modules in phase I was commissioned in 2002 as first functional superconducting linac in the country. In July 2007, Silicon ions were accelerated using all seven modules. They were transported to the experimental stations in the first user hall. Most of the critical components of the linacbooster have been designed, developed and fabricated indigenously.

There are three major national level projects undertaken in three laboratories of Department of Atomic Energy (DAE). They are: (a) Accelerator Driven sub-critical System (ADS) at Bhaba Atomic Research Centre (BARC), Mumbai; (b) Indian Spallation Neutron Source (ISNS) at Raja Ramanna Centre of Advanced Technology (RRCAT), Indore; and (c) Advanced National facility for Unstable and Rare Isotope Beam (ANURIB) at Variable Energy Cyclotron Centre, Kolkata. In these projects, different types of niobium resonators e.g. half wave, spoke, elliptical resonator in the frequency range of ~ 150 MHz to 1.3 GHz are being developed. Simultaneously the cryostats, power couplers, frequency tuners, RF and, control systems are also being developed.

Fermi National Accelerator Laboratory (FNAL) has proposed the construction of a High Intensity Superconducting Proton Accelerator (HISPA) also known as Proton Improvement Plan (PIP-II). Due to the similar accelerator goal of FNAL, USA and the DAE institutions of India and IUAC Delhi, a collaboration named as Indian Institutes and Fermilab Collaboration (IIFC) has been established to design and develop the superconducting radio frequency accelerators for both the Indian and Fermilab programs [1]. Presently, the R&D activities are going on in Fermilab and Indian institutions including IUAC with the goal of joint preparation towards the construction of the accelerators for the respective domestic programs.

ISBN 978-3-95450-178-6

RECENT PROGRESS OF ESS SPOKE AND ELLIPTICAL CRYOMODULES*

G. Olry, IPN, Orsay, France
on behalf of the ESS collaboration

Abstract

The ESS accelerator high level requirements are to provide a 2.86 ms long proton pulse at 2 GeV at repetition rate of 14 Hz. This represents 5 MW of average beam power with a 4% duty cycle on target. In a framework of collaboration between IPN Orsay, CEA Saclay and ESS, prototype spoke and medium and high beta elliptical cavities and cryomodules have been studied, constructed and tested. After a description of the ESS project and the accelerator layout, this paper will focus on the recent progress towards realization of the detailed design, the manufacturing of the first components of the prototype cryomodules and the first test results of some of the main critical elements such as SRF cavities and cold tuning systems.

ESS PROJECT

The European Spallation Source (ESS) project is a neutron-scattering facility, currently under construction by a partnership of at least 17 European countries, with Sweden and Denmark as host nations [1,2]. Construction started in July 2014, aiming at the source producing first neutrons around 2020. The ESS was designated a European Research Infrastructure Consortium (ERIC) by the European Commission in October of 2015.

The ESS is an accelerator-based facility producing neutrons for a large array of advanced instruments. Once constructed, in Lund, Sweden, it will provide new opportunities for researchers in a broad range of scientific areas including life sciences, energy, environmental technology, cultural heritage and fundamental physics.

The ESS accelerator will deliver to the target a time averaged proton beam power of 5 MW at the completion with a nominal current of 62.5 mA.

The superconducting linear accelerator lattice redesign [3] has permitted to optimize the layout of the linear accelerator using transition energy of 90 MeV with the normal conducting linac and reaching 2 GeV at the target.

The Superconducting Radio-Frequency (SRF) linear accelerator is composed of one section of Spoke-type cryomodules (352.21 MHz) and two sections of elliptical cavity cryomodules (704.42 MHz) [4]. Figure 1 shows the layout of the ESS linac, Optimus +, with emphasize on the SRF sections. The spoke section is being designed by and tested in IPN Orsay before being tested at high power in Uppsala University [5]. The design and test of the elliptical section is led by CEA Saclay and distributed in a SRF collaboration composed of CEA Saclay, INFN-LASA and STFC-Daresbury. LASA and STFC are providing the medium-beta and high-beta elliptical cavities, respectively. The elliptical cavities will be installed in their cryomodules in Saclay, using the experience learned from the X-FEL project.

COLLABORATION OF FRANCE TO THE ESS LINAC CONSTRUCTION

France is one of the major partners of the ESS collaboration, in particular with an important involvement in the accelerator construction under the form of in-kind contributions. Thru the two research organizations CEA and CNRS, France will provide key parts of the ESS accelerator, and is the major contributor to the SRF linac. The IRFU Institute of CEA-Saclay will provide the RFQ, beam diagnostics for the LEBT, all medium and high beta cryomodules (except for the SC cavities), and also controls for the proton source and LEBT. The IPN-Orsay Institute of CNRS has the responsibility to deliver all spoke cryomodules with their associated cryogenic valve boxes and cryogenic lines, and the cryogenic controls for all cryomodules (elliptical and spoke).

Both laboratories are participating to the ESS accelerator design since the early hours of ESS in 2009, and their contribution was reinforced with the signature in 2010 of a French-Swedish cooperation agreement, giving the framework for the design and development of prototype components such as spoke, medium beta and high beta elliptical cavities and cryomodules which are currently under fabrication and tests.

SPOKE CRYOMODULE

Since 2009, IPN Orsay is intensively involved in ESS project by leading the design of the whole Spoke section of the linac. The final aim is to deliver to Lund, 13 Spoke cryomodules, their associated valve boxes and cryogenic transfer lines. This chapter will described the status of the cryomodule, spoke cavities, cold tuning systems and power couplers prototypes developments.

As presented before, the Spoke section will be composed of cryomodules housing two Double-Spoke, beta 0.50, 352.21 MHz resonators with their cold tuning systems and capacitive power couplers (Fig. 2). IPN Orsay has designed a fully equipped prototype cryomodule and its valve box which are intended first to be validated cryogenically at IPN Orsay, then to be fully qualified, at high power, at Uppsala University.

#olry@ipno.in2p3.fr

ISBN 978-3-95450-178-6

STATUS OF THE SRF SYSTEMS AT HIE-ISOLDE

W. Venturini Delsolaro, L. Arnaudon, K. Artoos, C. Bertone, J. A. Bousquet, N. Delruelle, M. Elias, J. A. Ferreira Somoza, F. Formenti, J. C. Gayde, J. L. Grenard, Y. Kadi, G. Kautzmann, Y. Leclercq, M. Mician, A. Miyazaki, E. Montesinos, V. Parma, G. J. Rosaz, K. M. Schirm, E. Siesling, A. Sublet, M. Therasse, L. Valdarno, D. Valuch, G. Vandoni, L. R. Williams, P. Zhang

CERN, Geneva, Switzerland

Abstract

The HIE-ISOLDE project has been approved by CERN in 2009 and gained momentum after 2011. The final energy goal of the upgrade is to boost the radioactive beams of REX-ISOLDE from the present 3 MeV/u up to 10 MeV/u for A/q up to 4.5. This is to be achieved by means of a new superconducting linac, operating at 101.28 MHz and 4.5 K with independently phased quarter wave resonators (QWR). The QWRs are based on the Nb sputtering on copper technology, pioneered at CERN and developed at INFN-LNL for this cavity shape. Transverse focusing is provided by Nb-Ti superconducting solenoids. The cryomodules hosting the active elements are of the common vacuum type. In this contribution we will report on the recent advancements of the HIE-ISOLDE linac technical systems involving SRF technology. The paper is focused on the cavity production, on the experience with the assembly of the first cryomodule (CM1), and on the results of the first hardware commissioning campaign.

INTRODUCTION

At the end of 2014 the HIE-ISOLDE project [1] was well launched into its construction phase, with all the main components being procured or assembled. The phasing of the project had been revised at the beginning of the year; yet the schedule was tight with the target of delivering the first beams for physics in October 2015. While the technical infrastructure work was progressing well, the cryogenics facilities had still to be installed and commissioned. The cavity series production had just started and was delayed by issues with the quality of the copper substrates produced in industry. The first assembly of a cryomodule in the new clean room was just then starting and the actual assembly time was only known with a large uncertainty. The status of the project at this stage is documented in [2]. At that time it was still foreseen to proceed with a full characterization of the assembled cryomodule in a dedicated cold test facility, before shipping it to the HIE-ISOLDE linac. However, at the end of the year it became clear that this was incompatible with a physics run still in 2015. The decision was then taken to test the cryomodule directly in the linac. The plan for 2015 was to complete the cavity production and the assembly of the first cryomodule, in parallel with the installation of the cryogenics facilities at HIE-ISOLDE, and then to commission the whole complex altogether. The High Energy Beam Transfer lines would also be installed and commissioned in the same lapse of time. All going well, a physics run could be envisaged for the end of 2015.

This paper is centred on the aspects of the HIE-ISOLDE project which are related to SRF technologies. A more general status report on the project is given in [3].

SCRF CAVITY PRODUCTION

After a development phase ended in 2013 [4], the series production of HIE-ISOLDE SRF cavities started in 2014. Copper cavity substrates are manufactured in industry, whereas all the subsequent work needed to produce the Nb/Cu QWR and qualify them for installation is carried out at CERN. The workflow, shown in Fig. 1, comprises 12 steps, traced within the CERN standard manufacturing and travelling folder system (MTF). The whole process takes about 7 weeks.

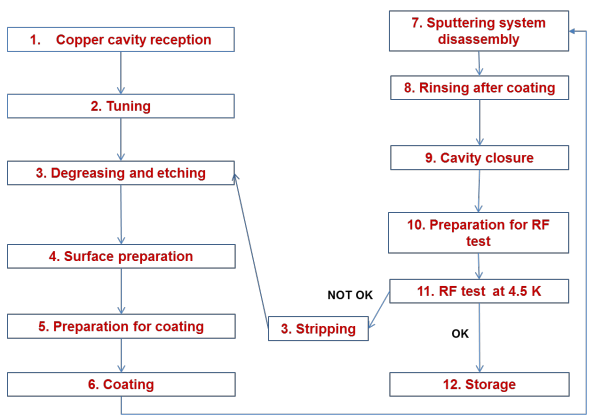

Figure 1: Nb/Cu QWR production workflow.

Acceptance Tests of the Copper Substrates

Upon arrival at CERN, the copper cavities are visually inspected with a portable microscope, in particular around the electron beam weld joining the inner and outer conductors of the QWR, located in the high magnetic field region. This first visual inspection is done before any chemical treatment; therefore it is only useful to spot gross defects. The helium volume inside the cavity inner conductor is also leak tested as a part of the cavity acceptance step. Dimensional checks in the metrology lab are carried out on a sample of cavities or in case of doubts.

ISBN 978-3-95450-178-6

THERMAL CONTACT RESISTANCE AT THE NB-CU INTERFACE

V. Palmieri*[1] and R. Vaglio[2]

[1]Legnaro National Laboratories - Istituto Nazionale Fisica Nucleare (INFN), Legnaro (PD) Italy
[2]Dipartimento di Fisica, Università di Napoli Federico II, CNR SPIN e INFN- Napoli (NA) Italy

Abstract

Niobium thin film sputtered copper cavities are strongly limited for the application in high field accelerators by the unsolved "Q-slope" problem. In the present paper, we examine the different contributions of the niobium film, the copper substrate, the Helium-Copper interface and the Niobium-Copper Interface, proposing the hypothesis that main cause of losses is due to an enhanced thermal boundary resistance $R_{Nb/Cu}$ at the Nb/Cu interface, due to poor thermal contact between film and substrate. So, starting from different Q vs E_{acc} experimental curves from different sources, and using a typical "inverse problem" method, we deduced the corresponding distribution functions generating those curves. Assuming that only a small fraction of the film over the cavity surface is in poor thermal contact with the substrate (or even partially detached), due to bad adhesion problems, we propose as a possible solution of the problem, the possibility to use higher temperatures of deposition and the adoption at the interface of a buffer layer of a material that alloys both with Copper and with Niobium.

INTRODUCTION

Superconducting Niobium sputtered Copper cavities were successful in nineties at CERN for the construction of the Large Electron Collider (LEP), and then at Legnaro National Laboratories of the INFN for the Quarter Wave Resonators (QWRs) of the ALPI heavy ion accelerator [1-2]. Recently the Nb/Cu technology has been retrieved again at CERN for the QWRs fabrication of the ISOLDE ion beam Facility [3].

Unfortunately, the use of Nb sputtered Copper Cavities in particle accelerators is not as common as desired, because, if compared to bulk Nb cavities, Nb thin film sputtered Cu cavities present a severe *Q* decay problem as a function of the RF accelerating field, as displayed in Fig. 1.

The Q-slope affecting thin film cavities prevents their use in any accelerator, where high fields are required.

The reason underlying the strong decay of the Q-factor versus the accelerating field in thin film cavities is still unknown and, the understanding of the reasons under the Q-drop would be the first step to solve the problem and in this way to access at low cost, high performance thin film cavities.

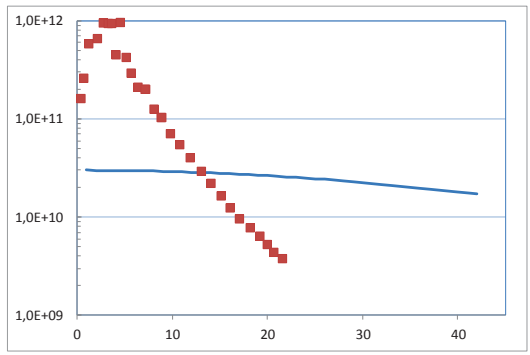

Figure 1: Typical behaviour of Q-factor versus the accelerating field for bulk Niobium cavities compared to Nb film sputtered cavities. The Q factor displayed by red squares is referred to a 1.5 GHz Nb Sputtered Cu cavity measured at 1.7 K [4]. The Q factor displayed by the blue line, is referred to 1.3 GHz bulk Niobium cavities measured at 1.8 K.

A *Q* decay effect is also present, at a lower extent, in bulk niobium cavities and many researchers have proposed several models in order to explain the Q-slope (or Q-drop) mechanism [5], mostly trying to justify the difference between the film and bulk cavities on the basis of the lower film *RRR* [6].

One of the main mechanism on which the Q-slope effect is based is the so called "thermal feedback model" [7]. In few words, the model writes the surface resistance in Taylor expansion:

$$R_s(T) = R_S(T_o) + \left(\frac{\partial R_s}{\partial T}\right)\Big|_{T_o} \Delta T + O(\Delta T^2) \qquad (1)$$

ΔT is the temperature difference between the inner superconducting cavity surface and the Helium bath, and it is proportional to the overall thermal boundary resistance R_B and to the rf power P_d dissipated in the cavity to sustain the accelerating field. The dissipated power depends on $R_S(T)$, being

$$P_d = \frac{1}{2} R_s(T) H_{RF}^2, \qquad (2)$$

where H_{RF} is the peak amplitude of the surface magnetic field. This induces a thermal feedback, since, fixed the H_{RF} value, the power leads to a temperature increase followed by a surface resistance increase and by a further power increase. The overall effect is a moderate Q-slope at low fields rapidly increasing approaching the thermal

*E-mail: palmieri@lnl.infn.it

ON THE UNDERSTANDING OF THE Q-SLOPE OF NIOBIUM THIN FILMS

S. Aull*, CERN, Geneva, Switzerland and Universität Siegen, Germany
T. Junginger, A. Sublet, W. Venturini Delsolaro, P. Zhang, CERN, Geneva, Switzerland
A.-M. Valente-Feliciano, Jefferson Lab, Newport News, VA, USA
J. Knobloch, Helmholtz-Zentrum Berlin and Universität Siegen, Germany

Abstract

The Q-slope of niobium coated copper cavities at medium fields is still the limiting factor for the application the Nb/Cu technology in accelerators. This paper presents a dedicated study of a niobium coating with bulk-like characteristics which shows a Q-slope comparable to bulk Nb at 400 MHz and 4 K. Combining the bulk like film with recent findings of the HIE Isolde indicates that the film microstructure and the Nb/Cu interface are the key aspects to understanding the Q-slope.

INTRODUCTION

The proposal of building superconducting RF cavities from copper and coat the inner surface with a 1 µm to 2 µm thin niobium film goes back to 1984 [1]. The niobium film technology benefits from several advantages over bulk niobium: The copper substrate provides excellent thermal stability which not only prevents the cavity from thermal runaway but also allows to increase the wall thickness to mitigate microphonics. Moreover, the film parameters can be tuned to optimize the BCS resistance which has a minimum for a residual resistance ration (RRR) between 10 and 30 and increases towards higher and lower RRR values [2]. In contrast to the low RRR Nb/Cu films, bulk Nb cavities require high (bulk) RRR as the thermal conductivity is proportional to it. Nb/Cu films are also known to have a low sensitivity to trapped flux. Hence, coated cavities allow reducing the complexity of cryomodules as they do not require magnetic shielding [3]. In addition to physical advantages, Nb/Cu technology allows reducing raw material costs.

Nevertheless, Nb/Cu cavities suffer from a strong, usually exponential, increase of the surface resistance with increasing RF field. This *Q-slope* currently limits the application of Nb/Cu technology to accelerating gradients as low as 10 MV/m. Although the Q-slope is present throughout all Nb/Cu projects, from big (352 MHz) four cell elliptical cavities like LEP2 through small single cell elliptical cavities like CERN's 1.3 GHz/1.5 GHz R&D programme to the quaterwave resonators at 101 MHz of the HIE-Isolde project, the cause is still not well understood and subject to recent research activities.

In the 1990's, CERN launched a vigorous R&D programme for coating single cell 1.5 GHz cavities with dc magnetron sputtering. The study focussed on the influence of coating parameters such as type and mixtures of the working gas(es) and the surface preparation on the BCS and residual surface resistance and the Q-slope [4]. The Nb/Cu research was put on hold in 2001 and relaunched in 2008 for the development of Nb coated quaterwave resonators for the HIE-Isolde project [5].

Until today, several laboratories around the world have (re-)joint the efforts on improving the Nb/Cu technology and on understanding and curing the Q-slope. Based on the work done in the 90's, the community pushes for denser films and improved Nb/Cu interfaces [6–10]

MICROSTRUCTURE OF THE HIE ISOLDE COATINGS

The Nb/Cu technology was chosen for the superconducting cavities for the High Intensity and Energy (HIE) upgrade of the Isolde facility at CERN [5].

The quater-wave resonators are made from bulk OFE copper and are coated using DC-bias diode sputtering. Details on the coating technique can be found elsewhere [11]. The HIE Isolde cavity *Q*4 is a mockup cavity of the same geometry as the RF cavities which allows coating small samples in various positions throughout the cavity surface [12]. The coatings on these samples represent the coating on the RF cavity and are used for dedicated studies on correlating the microstructure of the film with the RF performance.

A focussed ion beam (FIB) can be used to cut a crate into a coating and investigate the cross-section of the film with a scanning electron microscope (SEM) [13]. Figures 1(a) and 1(b) show two FIB-SEM images of a typical HIE Isolde coating according to the standard recipe with a bias of −80 V. Both images show the microstructure of the coating close to the top of the cavity. The geometry and the vicinity to the elctron beam weld make this region the most delicate to coat: Figure 1(a) corresponds to the position *e9* on the outer conductor, close to the electron beam weld and shows intergranular porosity and a rough surface. In contrast to that Figure 1(b) shows the film microstructure in position *TBi*, on the top band on top of the cavity. No porosity in the RF exposed layer is visible, but the film shows voids at the interface with the copper substrate.

In order to reduce the porosity, the bias was increased to −120 V. The RF performance of the cavity coated with this high bias was however poor. Figure 2 compares the surface resistance as function of RF field for a standard coating with the high bias coating. The measurements are done at 4.5 K at resonance frequency of 101 MHz. FIB-SEM images on the high bias coating revealed that the coating was indeed

* sarah.aull@cern.ch

ISBN 978-3-95450-178-6

Nb_3Sn CAVITIES: MATERIAL CHARACTERIZATION AND COATING PROCESS OPTIMIZATION*

D.L. Hall, T. Gruber, J.J. Kaufman, M. Liepe, J.T. Maniscalco, S. Posen†, B. Yu
Cornell Laboratory for Accelerator-Based Sciences and Education (CLASSE),
Ithaca, NY 14853, USA
T. Proslier
Argonne National Laboratory, Argonne, Illinois 60439, USA

Abstract

Recent progress on vapour diffusion coated Nb_3Sn SRF cavities makes this material a very promising alternative for CW medium field SRF applications. In this paper we report on several systematic studies to determine the sources currently limiting the performance of Nb_3Sn cavities to determine improved coating parameters to overcome these limitations. These include a detailed study of the sensitivity of Nb_3Sn to trapped ambient magnetic flux, a first measurement of the field dependence of the energy gap in Nb_3Sn and detailed measurements of the stoichiometry of the obtained Nb_3Sn coatings with synchrotron x-ray diffraction and STEM. Initial results from a study on the impact of the coating process parameters on energy gap, Q-slope, and residual resistance, show clear dependencies, and thus directions for process optimization.

INTRODUCTION

Cornell's cutting-edge program on the development of Nb_3Sn-on-Nb cavities as an alternative to bulk niobium has produced cavities that do not suffer from the Q-slope endemic to previous attempts [1–3]. Recent work on improving the quality factor of these cavities, as well as their susceptibility to ambient magnetic flux has resulted in a $Q_0 \approx 2 \times 10^{10}$ at 16 MV/m at 4.2 K [4]. Contemporarily, recent material studies [5] of the Nb_3Sn produced by the vapour deposition method have shown that the current limitations are non-fundamental, and are instead related to the fabrication process of the thin-film layer. In this paper we present the initial results of a systematic study that will attempt to connect the parameters utilised in the fabrication process to material characteristics and RF performance, with the ultimate objective of creating a map between the two that can be used to tailor the fabrication process to achieve the desired RF performance.

THE COATING PROCESS

The Cornell Nb_3Sn Furnace

Although a more in-depth description of the coating furnace and associated process is given in Ref. [1], a short summary will be given here: The coating furnace consists of a niobium insert, into which the tin crucible, nucleation agent, and any items to be coated, are placed, as seen in Fig. 1. This insert is installed into a vertical UHV furnace chamber. Located at the base of the coating insert is a small cylinder, whose mouth is open to the interior of the insert, in which the tin crucible is placed. Mounted around this location is a second set of heating elements, which allow the temperature of the tin crucible – hereafter referred to as the *source* – to be maintained at an equal or higher temperature than that of the cavity or samples that are to be coated (whose location will hereafter be referred to as the *chamber*). This difference in temperature between the source and the chamber, ΔT, is a crucial element of the coating process.

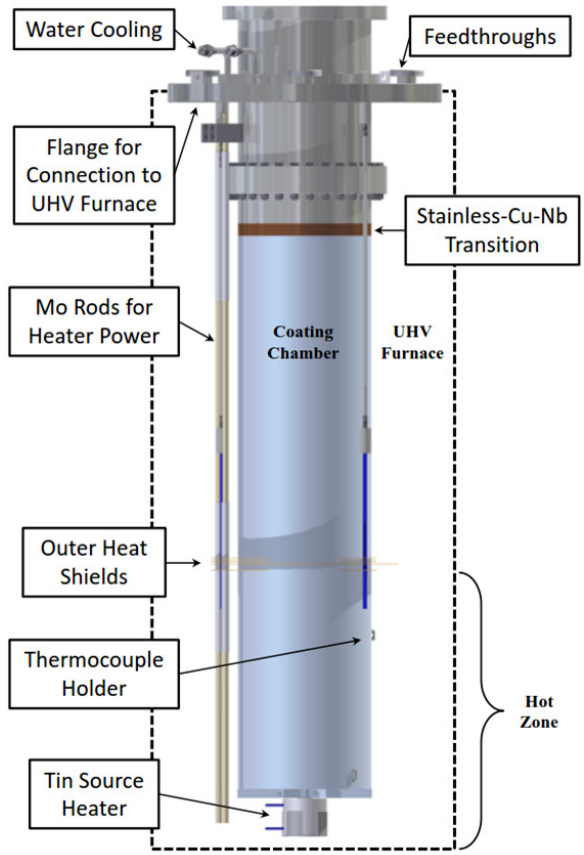

Figure 1: Diagram of the Cornell Nb_3Sn furnace coating insert from Ref. [1], highlighting the major elements.

* Work supported by DOE grant DE-SC0008431 and NSF grant PHY-141638. This work made use of the Cornell Center for Materials Research Shared Facilities which are supported through the NSF MRSEC program (DMR-1120296)
† Now at Fermi National Laboratory, Batavia, Illinois

ISBN 978-3-95450-178-6

PROGRESS WITH MULTI-CELL Nb_3Sn CAVITY DEVELOPMENT LINKED WITH SAMPLE MATERIALS CHARACTERIZATION*

G. Eremeev[1†], C. E. Reece[1], M. J. Kelley[1,2,3], U. Pudasaini[2], J. R. Tuggle[3]
[1]Thomas Jefferson National Accelerator Facility, Newport News, VA 23606, U.S.A.
[2]Applied Science Department, College of William and Mary, Williamsburg, VA 23185, U.S.A.
[3]Materials Science and Engineering Department, Virginia Tech, Blacksburg, VA 24061, U.S.A.

Abstract

Exploiting both the new Nb_3Sn coating system at the Lab and the materials characterization tools nearby, we report our progress in low-loss Nb_3Sn films development. Nb_3Sn films a few micrometers thick were grown on Nb coupons as well as single- and multi-cell cavities by the Sn-diffusion technique. Films structure and composition were investigated on coated samples and cavity cutouts with characterization tools including SEM/EDS/EBSD, AFM, XPS, SIMS towards correlating film growth and RF loss to material properties and deposition parameters. Cavity coating efforts focused on establishing techniques for coating progressively more complicated RF structures, and understanding limiting mechanisms in coated cavities. Nb_3Sn coated 1.5 GHz 1-cell and 1.3 GHz 2-cell cavities have shown quality factors of 10^{10} at 4.3 K, with several cavities reaching above E_{acc} = 10 MV/m. The dominant limiting mechanisms were low field quenches and quality factor degradation above 8 MV/m. The surface data indicates a near-stoichiometric Nb_3Sn consistent with the transition temperature and gap measurements. The Nb_3Sn layer is covered with Nb_2O_5 and SnO_2 native oxides and has little memory of the pre-coating surface.

INTRODUCTION

Nb_3Sn is one of the Nb-Sn compounds that forms when niobium is annealed in the presence of Sn. This phase occurs for Sn concentrations between 18 and 25 % and annealing temperatures between 930 °C and 2130 °C [1]. The phase is superconducting, but the superconducting transition temperature varies from 6 K for the low Sn content to about 18 K for 25 % of Sn [2]. The transition temperature of 18 K for Nb_3Sn is almost twice higher than that of niobium, which implies larger energy gap and, hence, lower dissipation in RF fields that of niobium surfaces. As the consequence of larger energy gap, Nb_3Sn also has a higher thermodynamic critical field, which leads to a higher superheating field. The lower RF dissipation and higher critical field are the advantages that can be exploited in accelerating structures, which benefit from low dissipation at high fields.

These benefits to SRF cavities were recognized early and already in early 70's several labs pursued Nb_3Sn coating for superconducting accelerator cavity applications [3, 4, 5, 6, 7, 8]. The most sustained effort spanned over a decade at Wuppertal University, where several coating chambers were built and coatings under different conditions were explored. These efforts resulted in quality factors above 10^{11} and accelerating gradients above 15 MV/m, limited by a strong Q-slope [9]. The cause of the Q-slope was not completely understood, but subsequent investigation showed that the effect is not local and hence could be a fundamental property of Nb_3Sn [10].

More recently, Cornell University pursed Nb_3Sn coating on Nb cavities in an attempt to replicate and explain Wuppertal results. While the first coated cavity had a high residual resistance, the coating on the second cavity resulted in a high quality factor without significant degradation up to a quench field of E_{acc} = 17 MV/m! [11] This result demonstrates the potential for high fields in Nb_3Sn cavities without Q_0 degradation.

In 2012 Jefferson Lab was funded to pursue R&D of SRF technologies for high-efficiency 4 K compact accelerating modules. Quality factors of 10^{10} at 4 K in 1.5 GHz accelerating cavities shown at Wuppertal suggested potential for high-efficiency 4 K compact accelerating modules. While originally we planned a two heater system exploited by Wuppertal [9] along with a vapor guide [8], we established a coating procedure following the approach explored at Siemens, where researchers coated superconducting structures using Nb cavities as the coating chamber, and Sn and $SnCl_2$ were placed inside the cavity and exposed to the same temperature during coating as the cavity [3]. It is worth noting that some of the 9.5 GHz cavities coated at Siemens had quality factors of $2.3{\cdot}10^9$ at B_{peak} = 101 mT at 1.5 K [3]. Assuming quadratic frequency dependence of the surface resistance, one could speculate that there is potential for quality factors of above 10^{11} at E_{acc} = 25 MV/m in 1.3 GHz accelerating structures for such a coating configuration.

The paper is organized as the following : the next section describes the coating setup. The RF results section presents test results from the coated cavities. Then, the material studies section shows the surface properties gleaned from the coated surface with analytical instruments.

* Authored by Jefferson Science Associates, LLC under U.S. DOE Contract No. DE-AC05-06OR23177.
† grigory@jlab.org

ISBN 978-3-95450-178-6

INCREASE IN VORTEX PENETRATION FIELD ON NB ELLIPSOID COATED WITH A MgB_2 THIN FILM*

T. Tan#, M. A. Wolak, and X. X. Xi, Temple University Department of Physics, Philadelphia, PA 19122, USA
T. Tajima, L. Civale, Los Alamos National Laboratory, Los Alamos, NM 87545, USA

Abstract

The magnetic vortex penetration field (H_{vp}) is an important property of superconducting radio frequency (SRF) cavities. However, measuring H_{vp} of an SRF cavity directly is usually a difficult task. As an alternative, a superconducting ellipsoid in an axial magnetic field would have a similar but inversed field geometry of an SRF cavity and would allow for the characterization of H_{vp}. In this work, we deposited a uniform MgB_2 layer on Nb ellipsoids and used those ellipsoids to mimic the behavior of MgB_2 coated Nb SRF cavities. The H_{vp} of such a structure was measured via zero-field-cool (ZFC) magnetization method. At 1.8 K, the H_{vp} for a coated Nb ellipsoid is 100 Oe higher than H_{vp} for a bare Nb ellipsoid.

INTRODUCTION

Particle accelerators are one of the most powerful tools for physicists. The pursuit for higher accelerating gradients and lower operating power dissipation is an ongoing endeavor. Superconducting radio frequency (SRF) cavity technology is the most promising candidate for creating next generation linear accelerators.[1] Total expulsion of the magnetic field initiated by the Meissner effect can significantly reduce the power dissipation caused by E-M induction, thus allowing to reach a higher accelerating gradient. The thermal breakdown of SRF cavities happens when the magnetic field near the cavity's inner surface surges beyond the threshold at which vortices start to penetrate into the SRF cavity. The vortex penetration field (H_{vp}) is affected by a number of factors, such as cavity geometry, surface roughness, and critical field of the superconductor. In the past decade, great efforts have been made to perfect bulk Nb SRF cavities. However, the maximum gradient is currently approaching the theoretical limit of the material. [2]

In 2001, the superconductivity of magnesium diboride (MgB_2) was discovered.[3] This material soon attracted significant attention in the SRF community. Its high T_c (39 K), high H_c (> 3500 Oe), lower residual resistivity (~ 0.1 μΩ·cm)[4-7] indicated that MgB_2 coated SRF cavity would potentially have a higher gradient and lower dissipation than bulk Nb cavities.

In this work, we used MgB_2 coated ellipsoids to mimic MgB_2 coated SRF cavities and measured their magnetic vortex penetration field (H_{vp}).

* Work supported by US DOE under grant No. DE-SC0011616.
#phys.tan@temple.edu

COATED ELLIPSOID AS AN INVERSED SRF CAVITY

Field Similarities

In an SRF cavity, the magnetic field is parallel to the cavity surface, while no magnetic field is present on the outside. Such kind of a field distribution is different in comparison to the traditional lower critical field (H_{c1}) measurement of type-II superconductors,[8-10] in which samples are submerged in a uniform magnetic field. Simply measuring MgB_2 coated Nb slabs and deriving H_{c1} does not lead to a precise estimate of H_{vp} of an SRF cavity with a similar structure.

A better approach for H_{vp} measurements is a superconducting ellipsoid in the Meissner state (see Fig. 1), which lies in a magnetic field parallel to its long axis. For such an ellipsoid, the magnetic field remains zero at the center while the expelled field is parallel to its surface. The field distribution along the ellipsoid surface is similar but inversed in comparison to the inner surface of an SRF cavity. Therefore a coated ellipsoid is an ideal structure to study the vortex penetration in SRF cavities.

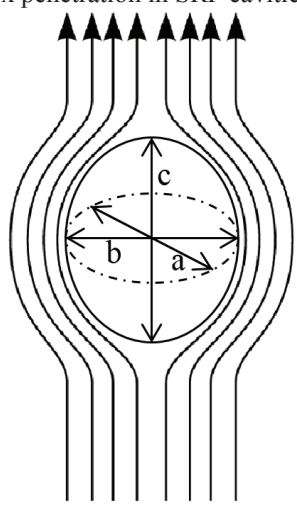

Figure 1: Schematic of a prolate ellipsoid in Meissner state.

Field Non-uniformity Caused by Meissner Current

Because of the existence of a superconducting current, the magnetic field will be equal to the applied field at the ellipsoid zenith but stronger at the equator of the ellipsoid, based on the following equation:

GROWTH AND CHARACTERIZATION OF MULTILAYER NbTiN FILMS*

A-M. Valente-Feliciano†, J.K. Spradlin, G. Eremeev, C.E. Reece, JLab, Newport News, VA 23606, USA
M.C. Burton, R.A. Lukaszew, College William and Mary, Williamsburg, VA 23230, USA

Abstract

Theoretical interest has stimulated efforts to grow and characterize thin multi-layer superconductor/insulator/superconductor (SIS) structures for their potential capability of supporting otherwise inaccessible surface magnetic fields in SRF cavities. The technological challenges include realization of high quality superconductors with sharp, clean, transition to high quality dielectric materials and back to superconductor, with careful thickness control of each layer. Choosing NbTiN as the first candidate material, we have developed the tools and techniques that produce such SIS film structures and have begun their characterization. Using DC magnetron sputtering, NbTiN and AlN can be deposited with nominal superconducting and dielectric parameters. H_{c1} enhancement is observed for NbTiN layers with a T_c of 16.9 K for a thickness less than 150 nm. The optimization of the thickness of each type of layers to reach optimum SRF performance is underway. This talk describes this work and the RF performance characteristics observed to date.

SIS MULTILAYER APPROACH FOR SRF CAVITIES

Theoretical Proposal

A few years ago, a concept was proposed by A. Gurevich [1–3] which would allow taking advantage of high-T_c superconductors without being penalized by their lower H_{c1}. The idea is to coat superconducting radio-frequency (SRF) cavities with alternating superconducting and insulating layers (SIS structures) with a thickness d smaller than the penetration depth λ (Fig. 1). If the superconducting film is deposited with a thickness d «λ, the Meissner state can be retained at a magnetic field much higher than the bulk H_{c1}. The strong increase of H_{c1} in films allows utilization of RF fields higher than the critical field H_c of Nb but lower than those at which the flux penetration at grain boundaries may create a problem. The thin higher-T_c layers provide magnetic screening of the bulk superconducting cavity preventing vortex penetration. The BCS resistance is also strongly reduced because the superconducting materials used have higher gap Δ (Nb_3Sn, NbTiN ...) than Nb. With such structures, Q-values at 4.2 K could be increased two orders of magnitude above Nb values.

If a 50 nm Nb_3Sn layer is coated on a bulk Nb cavity with an insulating interlayer and if the Nb cavity can sustain fields up to 150 mT, this structure could potentially sustain external magnetic fields of about 320 mT and therefore reach accelerating gradients without precedent.

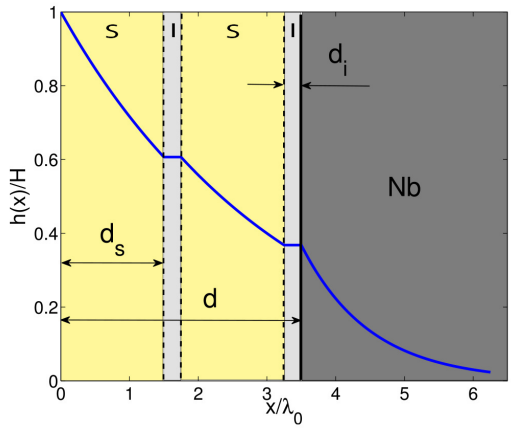

Figure 1: SIS multilayer concept with the magnetic field distribution adapted from [2].

Choice of Materials

Superconductor Although A15 compounds such as Nb_3Sn have a higher T_c and higher superheating field, the Nb B1-compounds are less sensitive to radiation damage and crystalline disorder. B1-compounds have a NaCl structure where metallic atoms form a face centered cubic (fcc) lattice and non-metallic atoms occupy all the octahedral interstices. These compounds are characterized by the fact that they always have a certain amount of vacancies, usually distributed randomly throughout the lattice [4]. The superconducting properties of B1 compounds are very sensitive to deviation from stoichiometric composition. The phase diagram of the binary system Nb-N up to N/Nb=1 includes many different phases, characterized by different T_c. The B1-NbN superconducting phase of interest (cubic δ-phase, a=4.388 Å) is only thermodynamically metastable at room temperature. T_c is very sensitive to the nitrogen (N) stoichiometry and NbN suffers from a high resistivity due to the presence of both metallic and gaseous vacancies randomly distributed in both sub-lattices, in amount of 1.3% respectively. The equi-atomic composition is $Nb_{0.987}N_{0.987}$ [4]. The ternary nitride NbTiN is the B1-compound with the highest critical temperature, 17.3 K. It presents all the advantages of NbN and exhibits increased metallic electrical conduction properties with higher titanium (Ti) percentage [5]. Ti is a good nitrogen getter, so the higher the Ti composition, the lower the number of vacancies. In contrast with NbN, the B1-TiN phase is stable at room temperature (T_c=5K, a=4.24Å). The two nitride phases are completely miscible resulting in a superconducting ternary NbTiN cubic phase which re-

* Authored by Jefferson Science Associates, LLC under U.S. DOE Contract No. DE-AC05-06OR23177 and by DTRA (Grant No. HDTRA12010072).
† valente@jlab.org

PROGRESS ON SUPERCONDUCTING RF CAVITY DEVELOPMENT WITH UK INDUSTRY

A.E. Wheelhouse, R.K. Buckley, L. Cowie, P. Goudket, A.R. Goulden, P.A. McIntosh, ASTeC, STFC, Daresbury Laboratory, Warrington, UK
J. Everard, N. Shakespeare, Shakespeare Engineering, South Woodham Ferrers, Essex, UK

Abstract

As part of a STFC Industrial Programme Support (IPS) Scheme grant, Daresbury Laboratory and Shakespeare Engineering Ltd have been developing the capability to fabricate, process, and test a 9-cell, 1.3 GHz superconducting RF cavity. The objective of the programme of work is to achieve an accelerating gradient of greater than 20 MV/m at an unloaded quality factor of 1.0 x 10^{10} or better. Processes such as the high pressure rinsing and the buffer chemical polishing are being developed at Daresbury Laboratory and the manufacturing of the cavity half-cells and beam-pipes are being optimised by Shakespeare Engineering to enable this target to be achieved. These are discussed in this paper.

INTRODUCTION

ASTeC (Accelerator Science and Technology Center) Department at Daresbury Laboratory and Shakespeare Engineering Ltd [1] are developing the capabilities to produce and test a 9-cell, 1.3 GHz Tesla style superconducting RF (SRF) cavity as part of a 3-year Industrial Programme Support (IPS) Scheme grant [2].

The IPS grant is a follow-up grant from a MINI-IPS [3], in which 3 single-cell 1.3 GHz niobium SRF cavities were successfully produced. The aim of the MINI-IPS was to set the foundations for the development of 9-cell cavity and with a target objective of 15 MV/m at 1.0 x 10^{10} at 2 K, initial tests performed on the first single-cell cavity in collaboration with Jefferson Laboratory, PIPSS #01 achieved a gradient of 15.7 MV/m at 2K prior to processing. After processing, buffer chemical polishing (BCP) and high pressure rinsing (HPR), a gradient of 22.9 MV/m with a Q_0 of 1.06 x 10^{10} at 2K was achieved, as shown in Fig. 1. Qualification tests performed at FermiLab on PIPSS #03 an accelerating gradient of 40 MV/m with a Q_o of 1.0 x 10^{10} was achieved and was limited by a quench at 41 MV/m, as shown in Fig. 2.

These results provided great confidence in the forming of the cell shape and the techniques developed, to progress the knowledge gained toward the manufacture of a 9-cell cavity. Thus expanding on this original programme of work, the aim of the IPS is to develop the ability to produce and test a 9-cell, 1.3 GHz Tesla style SRF cavity. The programme of work is being progressed in a number of stages:

- Development of the design and the drawings
- Fabrication of a prototype 2-cell copper cavity
- Fabrication and vertical testing of a 2-cell niobium cavity
- Fabrication and vertical testing of a 9-cell niobium cavity.

It is planned to firstly perform BCP processing and then electro-polishing processing (EP) on the 9-cell cavity. To verify the quality of the design and the fabrication an accelerating gradient of greater than 20 MV/m at an unloaded quality factor, Q_o better than 1.0 x 10^{10} after BCP is targeted and a gradient greater than 30 MV/m after EP.

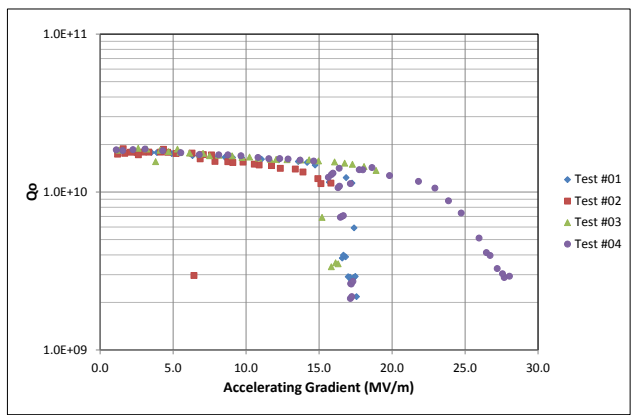

Figure 1: Performance results for PIPSS cavity #01 tested in the vertical test stand at Jefferson Laboratory after BCP processing.

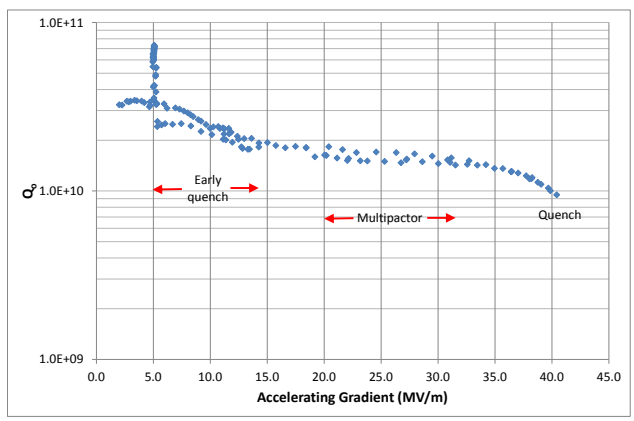

Figure 2: Performance results for PIPSS #03 tested at Fermilab after CBP and a 120ºC vacuum bake.

CAVITY DESIGN

The design of the cavity is based on the Tesla cavity design, but does not include any coupling ports. The beampipe design is seamless, which reduces the need of performing an electron beam (EB) weld process. The design of the equator and iris interfaces incorporates a step joint to ensure the ease of parallelism, in particular

ISBN 978-3-95450-178-6

ELIMINATION OF HIGH FREQUENCY NOISE FROM THE BEAM IN THE DIAMOND LIGHT SOURCE STORAGE RING

C. Christou, A. Bogusz, P. Marten, Diamond Light Source, Oxfordshire, U.K.

Abstract

High frequency beam motion has been identified as a source of noise in infrared beamlines in a number of synchrotron light sources. Diamond is a third generation synchrotron light source with storage ring current maintained by two superconducting CESR-B cavities powered by IOT-driven RF amplifiers. In our case, undesirable beam motion in the kilohertz range is predominantly driven by spectral content in the voltage across the IOTs arising from the switched mode nature of the high voltage power supply. Spectral noise on the amplifiers and beam has been identified and characterised and efforts to eliminate this noise are described. Care has been taken to maintain the overall stability of the RF at Diamond and tests have been carried out on an infrared beamline to investigate the degree to which beam noise impacts beamline operation in its different operating configurations.

HIGH POWER AMPLIFIERS FOR THE STORAGE RING RF SYSTEM

Diamond is a 3 GeV third-generation light source. The SR RF straight is designed to accept up to 3 superconducting 500 MHz cavities similar to those used on CESR [1]. Currently two cavities are installed each connected to a 300 kW amplifier [2] and an analogue LLRF system.

The high-power amplifier system was supplied by Thales Broadcast and Multimedia, now Ampegon, and generates the maximum power of 300 kW in each amplifier by the combination of four IOTs in a waveguide combiner system similar to that used for very high power TV transmitters [3]. A schematic drawing of the IOT combination is shown in Figure 1.

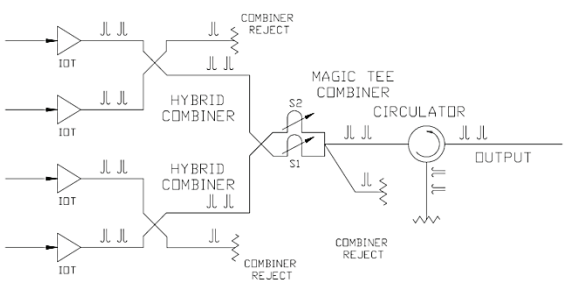

Figure 1: IOT combination scheme used in each of the Diamond 300 kW amplifiers.

The IOTs used are 80 kW IOTD2130 tubes from E2V Technologies. All four IOTs for each amplifier are fed from a single High Voltage Power Supply (HVPS). The HVPS is based on Ampegon Pulse Step Modulation (PSM) technology in which multiple series-connected switched mode power supply modules are switched by IGBT transistors in a process of Coarse Step Modulation (CSM) of multiple modules and Pulse Width Modulation (PWM) of individual modules in order to maintain a constant voltage across the IOTs [4]. There are 64 modules in each Diamond HVPS, each configured to generate 750 V, ensuring redundancy of modules at the Diamond operating voltage of 35 kV. This redundancy allows the amplifier to continue operating in the event of a failure of one or more modules, and the rotation between the multiple modules is designed to load each module equally to ensure maximum component lifetime.

The output of the HVPS is filtered to reduce the PSM switching noise on the IOTs, but nevertheless traces of the modulation can be seen on the beam, and this has been found to pollute beamline measurements at other synchrotrons operating with similar HVPS systems, particularly on the infrared beamlines at the Swiss Light Source, which operates with klystron tubes and normal conducting cavities with much lower quality factor than the CESR cavities at Diamond [5].

MEASUREMENT OF BEAM NOISE

The fundamental frequency of the module rotation noise is dependent on the PWM frequency, and can be defined as a multiple of the internal reference frequency of 3125 Hz by a user-defined parameter, N, and by the number of operating power supply modules, M according to

$$f_{rot} = \frac{N+1}{M} \times 3125\,\mathrm{Hz}.$$

Transverse beam motion in Diamond can be monitored using any one of the Libera Electron Beam Position Monitors (BPMs) located around the storage ring [6]. A simple FFT of the horizontal beam position taken over an extended period of user operation, shown in Figure 2 shows a surprisingly rich spectral content in the accessible range from zero to 5 kHz.

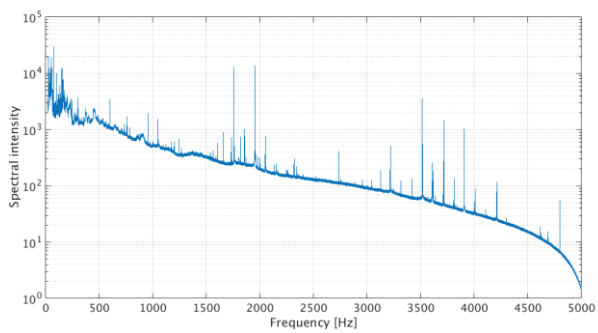

Figure 2: Noise on beam during routine operation with module rotation on.

ISBN 978-3-95450-178-6

CAVITY PROCUREMENT AND QUALIFICATION PLAN FOR LCLS-II*

F. Marhauser#, E.F. Daly, J.A. Fitzpatrick
Thomas Jefferson National Accelerator Facility, Newport News, VA 23606, USA

Abstract

LCLS-II will incorporate a new 4 GeV superconducting linear accelerator. This paper describes the plans for the industrial procurement of the dressed accelerating cavities and the prerequisites for vendor qualification, which aims to transfer the technology of cavity Nitrogen-doping, developed at US laboratories, to the commercial partners in its initial phase.

INTRODUCTION

The Linac Coherent Light Source (LCLS)-II project at the SLAC National Accelerator Laboratory (SLAC) requires a 4 GeV continuous-wave (CW) superconducting radio frequency (SRF) linear accelerator in the first kilometer of the SLAC tunnel. The aim is to operate a high repetition rate X-ray free-electron laser, i.e. with electron pulses at rates approaching 1 MHz delivered to two new undulators covering the spectral ranges of 0.2-1.2 keV and 1-5 keV, respectively. The collaborative project brings together six US institutions, which in alphabetical order are Argonne National Laboratory (ANL), Cornell University, Fermi National Accelerator Laboratory (FNAL), Thomas Jefferson National Accelerator Facility (JLab), Lawrence Berkeley National Laboratory (LBNL), and SLAC [1].

As part of their responsibilities FNAL and JLab will build the 1.3 GHz accelerating cavity cryomodules (CMs) concurrently at two assembly lines. The procurement of CM components are distributed among FNAL and JLab, with the exception of SLAC acquiring the main RF power couplers [2]. In preparation of the CM assembly, FNAL has been leading the LCLS-II CM and cavity design efforts, while JLab is directing the procurement of the production cavities. Engineering designs heavily borrow from the mature TESLA technology utilized at the European XFEL at DESY to leverage the vast experience. Similarly to the EU-XFEL strategy, LCLS-II relies on 'build-to-print' SRF cavity manufacturing. This implies that vendors have to follow precise technical specifications and procedures. Each cavity will be delivered welded into a helium vessel and shipped under vacuum assembled with RF qualification hardware ready for high power acceptance testing in a vertical dewar. The project bears the risk of cavity performance. Qualifying cavities proceed immediately to CM string assembly.

Currently, activities concentrate on building two prototype CMs, one at each laboratory. This consumes 16 project-owned ILC-type nine-cell cavities that were built by AES, Inc. [3]. The near-future cavity large-scale fabrication comprises 266 production LCLS-II cavities for the assembly of additional 33 CMs (16 at FNAL, 17 at JLab) leaving two cavities as spares. This will complete the required 35 CMs for the envisioned 4 GeV energy gain, which can be achieved at an accelerating field (E_{acc}) of 16 MV/m in average accounting for 18 (~6%) unpowered cavities with ~1 % reserved for energy feedback systems, while two third-harmonic (3.9 GHz) decelerating CMs are employed for phase-space linearization housing 16 nine-cell cavities.

The procurement of the dressed accelerating LCLS-II cavities is divided into three phases:

Phase I: Vendor Qualification (VQ)
Phase II: First Article Production (16 cavities)
Phase III: Full Production (250 cavities).

The project reserves the option for a Phase IV to acquire additional cavities depending on upgrade needs.

COMMERCIAL VENDORS FOR SERIES FABRICATION

Following the public request for proposals of LCLS-II production cavities announced early October 2014, bidders' proposals were collected in December. Technical evaluations were conducted in compliance with JLab's standard 'Best Value' source selection process, which has been approved by the US Department of Energy (DOE). The Buy American Act applied to non-domestic vendors. Members of the source selection team, comprising technical experts from both FNAL and JLab, evaluated the proposals independently based on experience, past performance, resources, understanding of requirements and quality assurance. The findings were comprised in a final technical evaluation report for procurement recommendation. The DOE followed the teams' recommendation for a dual award. Subcontract awards were executed by end of May 2015. The awardees are RI Research Instruments, GmbH (Germany) [4] and Ettore Zanon, S.p.A. (Italy) [5] with each vendor producing half of the required quantity of cavities (8+125) in Phases II and III.

* Authored by Jefferson Science Associates, LLC under U.S. DOE Contract No. DE-AC05-06OR23177 with supplemental funding from the LCLS-II Project U.S. DOE Contract No. DE-AC02-76SF00515. The U.S. Government retains a non-exclusive, paid-up, irrevocable, world-wide license to publish or reproduce this manuscript for U.S. Government purposes.
# marhause@jlab.org

ISBN 978-3-95450-178-6

VERTICAL CAVITY TEST FACILITY AT FERMILAB*

O. Melnychuk†, A. Grassellino, F. Lewis, J. Ozelis, R. Pilipenko, Y. Pischalnikov,
O. Pronitchev, A. Romanenko, D.A. Sergatskov, B. Squires
Fermi National Accelerator Laboratory, Batavia, IL 60510, USA

Abstract

After a recent upgrade, the vertical cavity test facility (VCTF) for SRF cavities at Fermilab features a low level RF system capable of testing 325MHz, 650MHz, 1.3GHz, and 3.9GHz cavities, helium liquefying plant, three test cryostats, and the interlock safety system. The cryostats can accommodate measurements of multiple cavities in a given cryogenic cycle in the range of temperatures from 4.2K to 1.4K. We present a description of VCTF components. We also discuss cavity instrumentation that is used for diagnostics of cavity ambient conditions and quench characterization.

INTRODUCTION

Typically characterization of superconducting radio-frequency (SRF) cavity involves measuring intrinsic quality factor Q_0 as a function of accelerating field E_{acc} in a vertical test stand (VTS) [1]. Fermilab's VCTF was commissioned in 2007 [2] with a single cryostat referred to as Vertical Test Stand 1 (VTS-1). VCTF was originally designed for vertical testing of bare ILC 1.3 GHz superconducting RF cavities Between 2007 and 2012 the facility was mainly used for qualification of 1.3GHz 9-cell cavities for the ILC program, PIP-II and developing new cavity processing techniques. Starting from 2012, when effect of nitrogen doping was discovered at this facility [3] cavity testing was more focused on new cavity processing R&D as well as magnetic field expulsion studies. In 2014, two additional test stands (VTS-2 and VTS-3) were commissioned. These newer test stands were designed with testing of production cavities in mind. They are larger in diameter and longer than VTS-1. The larger cryostats contain about twice the volume of VTS-1. Since December 2014 regular cavity testing has been performed in two dewars, VTS-1 and VTS-2. Using two dewars routinely allows to minimize downtime due to warmup and to accommodate more efficiently testing of LCLS-II, PIP-II, and R&D cavities. With the start of LCLS-II project in 2014, Fermilab vertical test facility became the main location for qualifying cavities for this project. Qualification of a full set of cavities for Fermilab's LCLS-II prototype cryo-module is nearing completion. Cavity testing for LCLS-II production cryo-module is planned to commence in 2016.

CRYOGENIC SYSTEM

VCTF as well as other cryogenically cooled test stands located the same building are supplied from a 1500 watt helium refrigerator/liquefier. The vertical test stands are fed liquid helium from the liquid helium storage dewar. When only feeding the vertical test stands, the helium plant has a liquefaction rate of 350 Liter/hour (design value). This mode of operation of the helium plant will be addressed in this paper.

Helium Liquefier

There are four major components of the helium liquefier:

1. Compressor Skid
2. Cold Box
3. Liquid Helium Storage Dewar
4. Gas Helium Storage (Buffer Tanks)

A simplified block diagram of the helium liquifier is shown in Figure 1. The compressor skid contains two compressors,

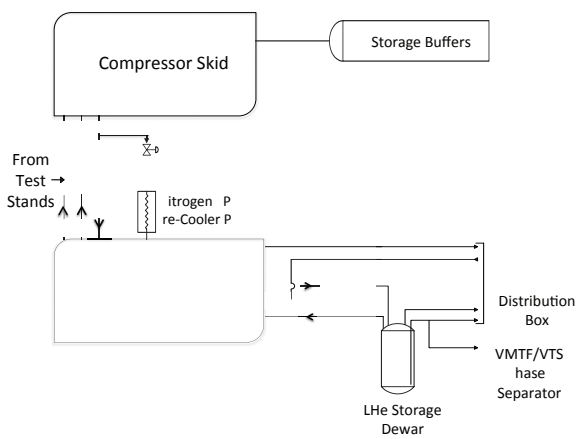

Figure 1: Simplified block diagram of the helium plant.

200 Hp and 1000 Hp, in series. These compress the gas from roughly atmospheric pressure to 38 psia and 150 – 300 psia, respectively. The heat due to compression is removed by cooling water on the compressor skid. The Cold Box is a series of heat exchangers, turbines and expansion valves. There are up to 3 flow paths in the heat exchangers: 1) High pressure helium inlet gas, 2) Medium pressure helium return gas and 3) Low pressure helium return gas. There is also a liquid nitrogen cooled helium pre-cooler that cools a portion of the high pressure helium inlet gas. Liquid helium from the Cold Box is stored in the 10,000 liter liquid helium storage dewar. Due to operational constraints, the current usable liquid capacity of this dewar is approximately 7,000 liters. Excess warm helium gas is stored in the Buffer Tanks until it can be processed into liquid. There are six 4,000 cu.ft. storage tanks in the Buffer Tank system. Due to the nature of

* Operated by Fermi Research Alliance, LLC under Contract No. De-AC02-07CH11359 with the United States Department of Energy
† alexmelnitchouk@gmail.com

THE CLS SRF CRYOGENIC SYSTEM UPGRADE

C. Regier, Canadian Light Source Inc., Saskatoon, Canada

Abstract

The Canadian Light Source currently makes use of a 500 MHz CESR-B type SRF cavity in its storage ring. While the performance of this cavity has generally been good, the reliability of the cryostat and cryogenic system has suffered a few setbacks over 10+ years of operation. The position of CLS as a user facility requires reliable beam to be consistently delivered. For this reason CLS is undertaking an upgrade project to improve system reliability and reduce downtime due to planned and unplanned maintenance. The upgrade is to include a redundant helium compressor, and new cryogenic infrastructure. In addition, the spare CESR-B cryomodule will be installed and operating in the storage ring. This paper reviews the problems with the current system to date, and discusses the proposals for the upgrade of the system.

INTRODUCTION

The Canadian Light Source (CLS) is a third-generation synchrotron facility located in Saskatoon, Canada. CLS has been using a single 500 MHz CESR-B [1] superconducting radio-frequency (SRF) module in the storage ring for over a decade. The CESR-B module was developed at Cornell University in the 1990s, and has been licensed to various private companies for construction. CLS has two CESR-B modules, one operating and one spare.

While system reliability has not been poor, there are issues that have come up over the 10+ years of operation of the SRF system at CLS. To further improve reliability CLS is currently working on a system upgrade that would see a spare compressor added to the system and the second CESR-B unit installed in the storage ring. This will give CLS operational capabilities similar to those at NSLS-II [2] and Diamond Light Source [3].

EXISTING SYSTEM

Figure 1 shows a schematic of the current storage ring system at CLS. This system contains one CESR-B type 500 MHz installed in straight 12 of the CLS storage ring. This SRF cavity is fed with liquid helium by a Linde TCF-50 cryoplant, consisting of a 200 kW Kaeser helium compressor, an oil removal system (ORS), a gas management panel (GMP), a coldbox, and a 2000 L Cryofab dewar. The original load specification for this plant was 284 W at 4.4 K, and the plant was tested to 313 W during commissioning.

To reduce the impact of compressor vibrations on the storage ring and beamlines, the cryoplant is located off of the experimental floor. A 52 m long multi-channel transfer line (MCTL) connects the cryoplant to a valve box located on top of the storage ring radiation shielding near the SRF cavity location. This MCTL supplies both liquid helium and liquid nitrogen to the CESR-B module, and also returns the cold helium gas to the cryoplant. A view of the system layout is given in Fig. 2. The valve box controls the flow of cryogens to and from the SRF cavity, which is connected to the valve box by three single-channel vacuum-jacketed (VJ) transfer lines approximately 4 m in length.

Figure 3 shows a simplified cutaway of the CESR-B module. The helium vessel has a volume of roughly 500 L, and is typically filled to around 490 L when operating. The helium vessel is suspended inside a vacuum vessel, along with two magnetic shields and a liquid nitrogen shield to reduce heat transfer to the helium. A HEX circuit siphons off a small amount of cold helium gas from the helium vessel, and circulates it around the thermal transition section of the input waveguide. The liquid nitrogen exhausted from the shield also coils around the waveguide before being exhausted to atmosphere. This provides a stable thermal transition from 4 K to room temperature. The single cavity is around 60 cm in diameter at the equator, and has a fluted beam tube on one side to help remove HOMs. CLS owns two of these cryomodules, and one is used as an off-line spare in the event of a cryomodule or cavity failure.

SYSTEM PROBLEMS

While the CLS SRF cryosystem has generally performed reliably, there have been a few issues that have created unexpected downtime for the facility. Two MCTL failures on the cold gas return line caused a total of 6 weeks of unplanned downtime on 2007 and 2008. A series of compressor airend failures also resulted in around 2 weeks of lost time. These compressor failures were eventually traced to an incorrect maintenance procedure, which was due to a combination of inexperience in maintenance technicians combined with a misprint in the operating manual.

The compressor issues eventually caused oil to be forced into the return (low pressure) side of the coldbox. This resulted in three more weeks of unplanned downtime in autumn of 2012 while the coldbox was flushed with acetone and then warm dry nitrogen. Around 15 L of oil was removed from the return side of the coldbox heat exchangers during this procedure.

In January 2013 the cryomodule began to leak helium into the cavity vacuum. This forced a three week shutdown as the cryomodule was removed and the spare cryomodule was installed in the storage ring. Conditioning of the spare cryomodule took longer than expected after eight years of storage, and it was almost six months before a full beam current of 250 mA was again

ISBN 978-3-95450-178-6

PROGRESS IN THE ELLIPTICAL CAVITIES AND CRYOMODULE DEMONSTRATORS FOR THE ESS LINAC

F. Peauger, C. Arcambal, S. Berry, N. Berton, P. Bosland, E. Cenni, J.P. Charrier, G. Devanz, F. Eozenou, F. Gougnaud, A. Hamdi, X. Hanus, P. Hardy, V. Hennion, T. Joannem, F. Leseigneur, D. Loiseau, C. Madec, L. Maurice, O. Piquet, J. Plouin, J.P. Poupeau, B. Renard, D. Roudier, P. Sahuquet, C. Servouin, CEA Saclay, Gif-sur-Yvette, France
G. Olivier, IPN, Orsay, France
C. Darve, N. Elias , ESS-AB, Lund, Sweden

Abstract

The European Spallation Source (ESS) accelerator is a large superconducting linac under construction in Lund, Sweden. A collaboration between CEA Saclay, IPN Orsay and ESS-AB is established to design the elliptical cavities cryomodule of the linac. It is foreseen to build and test two cryomodule demonstrators within the next two years.

We present the design evolution and the fabrication status of the cryomodule components housing four cavities. The latest test results of two prototype cavities are shown. The cryomodule assembly process and the on-going testing infrastructures at CEA Saclay are also described.

INTRODUCTION

ESS is a large scientific instrument under construction in Sweden aiming at producing the most powerful neutron source in the world [1]. This new facility is composed of a 5 MW proton linear accelerator, a tungsten target to produce neutrons by spallation reaction and experimental neutron beam lines for multidisciplinary users. The proton linac is a long pulse machine with 2.86 ms beam pulse length and 14 Hz pulse repetition rate giving a duty cycle of 4%. It accelerates a high intensity proton beam of 62.5 mA using a 50 meter long warm linac which increases the beam energy up to 90 MeV and a 312 meter long cold linac to reach the final energy of 2 GeV. This cold section works at a cryogenic temperature of 2 K in a saturated Helium bath and contains three families of superconducting resonators: 26 Spoke cavities working at 352.2 MHz, 36 medium beta elliptical cavities and 84 high beta elliptical cavities working at 704.4 MHz. The elliptical cavities are grouped four by four in 6.6 meter long cryomodules, designed to be similar for both cavity types. The fabrication and power testing of two Elliptical Cavities Cryomodule Technology Demonstrators (ECCTD) are planned before launching the series production of 30 cryomodules. The first one is equipped with medium beta cavities (M-ECCTD) and the second one with high beta cavities (H-ECCTD).

This paper describes the design evolution and fabrication status of the elliptical cavities and cryomodule demonstrators already presented in this workshop [2]. It also presents the cryomodule assembly strategy and the testing infrastructures being developed at CEA Saclay.

CRYOMODULE OVERVIEW

The design of the cavities, the cryomodule and its auxiliary components has been reported in [3] and [4]. Fig. 1 shows a 3D view of the cryomodule installed in the ESS tunnel and Fig. 2 gives a detailed description of the cryomodule composition.

The cavity package design and procurement are under the responsibility of CEA Saclay. It is composed of a bulk niobium multi-cell resonator welded to a titanium helium vessel, a vertical power coupler equipped with a single coaxial ceramic window and a WR1150 doorknob transition, a Cold Tuning System (CTS) with two piezo stacks allowing fast and slow adjustment of the resonant frequency, and a cold magnetic shield with high permeability. The four cavities are connected together by three 140 mm diameter hydroformed bellows and are ended by 100 mm diameter cold-warm transitions. This arrangement constitutes a cavity string and is connected to the focusing unit placed outside the vacuum vessel and at warm temperature. The connection is isolated by two DN 100 type Ultra-high vacuum gate valves at each extremity.

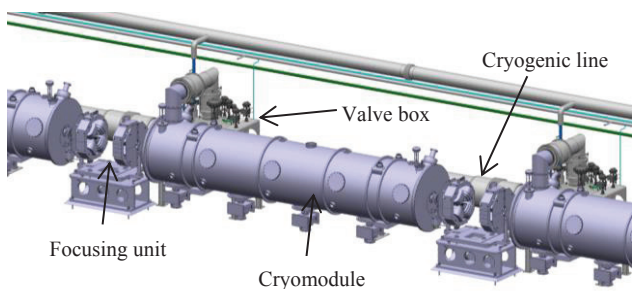

Figure 1: 3D view of the Elliptical cavities cryomodule installed inside the ESS linac tunnel.

The development and procurement of the cryostat components for the M-ECCTD is under the responsibility of IPN Orsay. CEA Saclay will be in charge of this procurement for the H-ECCTD. A common module design for medium (6 cells) and high beta (5 cells) cavities has been possible thanks to the small difference in length (56 mm) between the two cavity types. This allows flexibility in the linac layout and a cost reduction of the cryomodule components manufacturing.

ISBN 978-3-95450-178-6

A NEW CRYOGENIC CONTROL SYSTEM FOR THE VERTICAL TEST AREA AT JEFFERSON LAB *

K. Davis, T. Goodman, P. Kushnick, T. Powers, C. Wilson, JLab, Newport News, VA 23606, USA

Abstract

The Vertical Test Area at Jefferson Lab (JLAB), consisting of eight vertical dewars, recently received a major upgrade by replacing the original (1995) cryogenic control system. A new, state-of-the-art, distributed control system (DCS) based on Programmable Logic Controllers (PLCs) was installed and commissioned. The new system increases facility throughput, reliability and cryogenic efficiency, while improving safety. The system employs a touchscreen graphical user interface and a highly redundant architecture on an Ethernet backbone.

JLAB VTA FACILITY

A significant component of JLab's SRF R&D activities is cavity testing and characterization. This is performed in the Vertical Test Area (VTA): a unique facility designed for testing and measurement of SRF cavities in superfluid helium. The VTA consists of eight dewars, six are fitted with movable radiation shields, which permits high power testing of cavities without personnel exposure to ionizing radiation, see Fig. 1. Cavities can be tested in the VTA at frequencies from 325 MHz to over 2 GHz, and at input power levels up to 500W. In addition to cavity testing, the VTA also supports other cryogenic tests of SRF-related components such as vacuum feed-throughs, mechanical and piezo-electric tuner mechanisms, and material electrical and thermal characterization (e.g., thermal conductivity, RRR, and T c measurements).

The VTA dewars are supplied with liquid Helium (LHe) from the Cryogenic Test Facility (CTF), which can supply 4K LHe at the rate of about 150 L/hr continuously and up to 3 times that rate transiently. Dewars are pumped to sub-atmospheric pressures in order to achieve temperatures as low as 1.9K, using a vacuum pump with a capacity of about 7 g/sec. Lower temperatures can be reached (at correspondingly lower mass flow rates) using dedicated low-pressure vacuum pumps. Multiple dewars can be pumped down simultaneously, in accordance with system capabilities (defined by vacuum pump mass flow limits). All Helium used in the VTA is returned to the CTF where it is purified of any contaminants (most notably nitrogen) and re-liquefied.

The VTA dewars are instrumented with thermometers, LHe level sensors, and pressure transducers, and are controlled via interlocked electro-mechanical valves, which prevents damage to or contamination of the CTF Helium supply. Some functions, such as dewar LHe filling, pumpdown, and warmup, are computer controlled, while others are performed manually. A complete test cycle for the larger (850 liter capacity) dewars can be accomplished (warm-to-warm) in 36 hours or less. Smaller dewars (100-200 liter capacity) can be cycled in 8 hours (one shift). The combination of automated and interlocked control, along with efficient cryogen and thermal management, yields a facility with an SRF cavity test throughput unequalled anywhere in the world [1][2].

Figure 1: JLab Vertical Test Area (VTA).

CONTROL SYSTEM OVERVIEW

The existing control system has over 20 years of successful operations. The availability of parts for maintenance and the difficulties encountered when planning seemingly simple system improvements led to the decision to replace the original custom-built electronics with modern PLCs using touch-screen user interface.

Upgrade Goals

The following goals guided development of the new control system:

1. VTA downtime during the upgrade to be minimized.
2. A graphical display of the time history (temps, pressure, LHe level) for each dewar to be provided for the operator.

*Authored by Jefferson Science Associates, LLC under U.S. DOE Contracts DE-AC05-06OR23177 and DE-AC02-76SF00515 for the LCLS-II Project.

ISBN 978-3-95450-178-6

PLUG TRANSFER SYSTEM FOR GaAs PHOTOCATHODES

P. Murcek, A. Arnold, J. Teichert, R. Xiang, HZDR, Dresden, Germany
P. Lu, H. Vennekate, HZDR & Technische Universität, Dresden, Germany
A. Burrill, K. Martin, Helmholtz-Zentrum Berlin, Germany

Abstract

The transport and exchange technology of Cs_2Te photocathodes for the ELBE superconducting rf photoinjector (SRF Gun) has been successfully developed and tested at HZDR. The next goal is to realize the transport of GaAs photocathodes into the SRF Gun, which will need a new transfer system with XHV 10^{-11} mbar. The key component of the setup is the transfer chamber and the load-lock system that will be connected to the SRF Gun. In the carrier, four small plugs will be transported, one of them will be put on the cathode-body and inserted into the cavity. The new transport chamber allows the transfer and exchange of plugs between HZDR, HZB and other cooperating institutes. In HZDR this transfer system will also provide a direct connection between the SRF Gun and the GaAs preparation chamber inside the ELBE-accelerator hall.

INTRODUCTION

The Rossendorf superconducting RF photo injector (SRF Gun), developed within a collaboration of the institutes HZB, DESY, MBI and HZDR, has been put into operation in 2007. It is designed for medium average beam current and operation in CW mode [1]. The superconducting cavity, the main part of SRF gun, consists of three TESLA cells and one optimized half-cell. The Cs_2Te photocathode is inserted in the half cell isolated by a 1mm vacuum gap.

CATHODE SYSTEM UPDATE

The design of the new transfer system for the SRF gun is shown in Fig. 1.

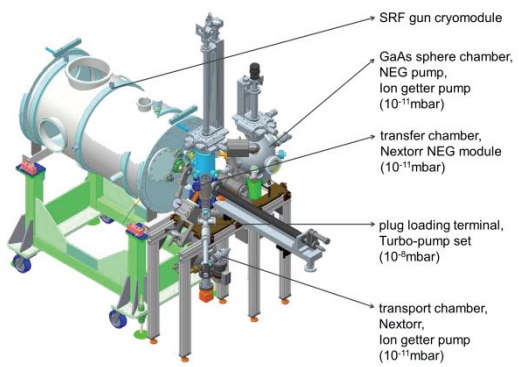

Figure 1: View of new transfer system on the cryomodule.

Figure 2: Photocathode of the new Transfer system.

The main difference of the new transfer system to that of the present one is, that the moving object is only the plug and not the entire cathode (Fig. 2).

- ELBE SRF Gun has been operated with Cs_2Te for medium current up to 400μA
- for high current operation in the future GaAs(Cs,O) is considered to be combined with the SRF Gun technology.
- SRF Gun is supposed to serve as a test bench for GaAs(Cs, O)

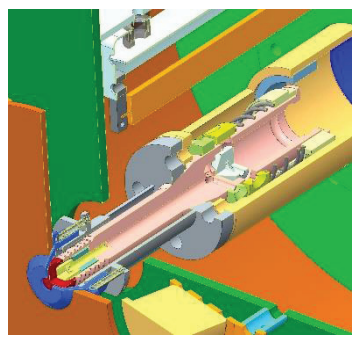

Figure 3: Arrangement in the coating chamber.

Cs_2Te (Fig. 3).

- driven by UV light
- UV laser shaping complicated
- medium current
- 10^{-9} -10^{-10} mbar

NEA-GaAs (Cs, O) [2]

- high QE in the visible light
- laser pulse shaping easier
- polarized electron source
- critical vacuum requirement

GaAs (Cs,O) will be in-situ activated before the transport into SRF gun through a new transfer system. XHV of less than 1×10^{-11} mbar is required.

ISBN 978-3-95450-178-6

HPRF TRANSMISSION COMPONENTS STUDY AND DISTRIBUTION IN TRUMF E-LINAC

Z. Ang. TRIUMF, Vancouver, Canada

Abstract

In September 2014, the first stage of the TRIUMF e-linac was commissioned and the high power rf systems were running in stable operation [1]. Two 300 kW klystrons, along with the key waveguide components were tested before feeding rf power into 1.3 GHz 9-cell superconducting cavities. The rf high power divider and the 360 degrees variable waveguide phase shifters were working successfully. The simulations on different waveguide structures for the power dividers, phase shifters have been studied. The comparisons of the calculation results and rf signal level tests of the both the rf components and waveguide distribution systems are presented in this paper.

INTRODUCTION

A 500 kW electron linear accelerator (e-linac) is under construction at TRIUMF. One 9-cell superconducting niobium cavity is in injection cryomodule. A 150 kW klystron will drive the cavity via two 50 kW rf couplers in phase [2]. There are two accelerating cryomodules, each housing two 9-cell superconducting niobium cavities operating at 1.3 GHz and at 2 degrees Kelvin. Another 300 kW cw klystron is employed to drive two 9-cell cavities in one cryomodule. In order to rf condition each cavity, a Variable Power Divider (VPD) is envisaged. During the rf conditioning, the power divider is set to deliver the rf power to one of the two cavities being conditioned and provide the minimum rf power to the another cavity. After rf conditioning both cavities, the VPD is set to the 3 dB position (equal power to both the cavities) for normal operation of the high power rf system to accelerate electron beams in the e-linac.

Traditionally people have employed the symmetric waveguide structure VPD to realize the operational requirements [3]. However, an asymmetric structure was considered as feasible design to meet our operation requirements. Both structures are based on the hybrids and phase shifter(s). HFSS simulations results for both structures are shown in following paragraphs. The comparisons of the calculation results help us to choose the asymmetric VPD over the symmetric VPD structure for the e-linac high power rf transmission systems. All S-parameters of the calculation and signal level rf tests are presented in this paper.

One klystron feeds rf power into the two cavities and each cavity is powered via two rf high power couplers. Therefore, at least three variable phase shifters must be installed in the waveguide distribution system to meet the operation requirements. There are three ways to reach the phase tuning requirement to operate e-linac for beam and the considerations of choosing the phase shifters in e-linac are presented in the next chapter.

300 KW VARIABLE POWER DIVIDER

This chapter gives a mechanical description for the VPD in details. General views of the symmetric and asymmetric structures of the VPD are shown in Fig. 1 and Fig. 2. TRIUMF e-linac basic operation requirements for the device are presented in Table 1.

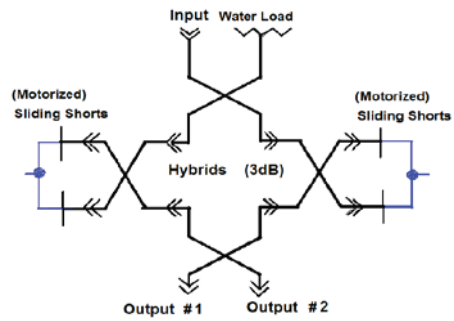

Figure 1: Symmetric waveguide structure VPD.

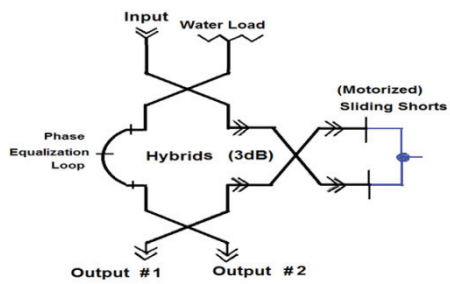

Figure 2: Asymmetric waveguide structure VPD.

Table 1: Specification of the Variable Power Divider

Frequency	[MHz]	1300 ±10
Average power	[kW]	300
Peak rf Power (full Reflected)	[kW]	>1200
Insertion Loss (maximum)	[dB]	0.3
VSWR (Max.), return loss 28.3dB		1.08 : 1
Continuously variable attenuation, with resolution better than 1.0% (0.01 dB)	[dB]	0 - 30
Operation at null position	[dB]	3 ± 0.05

ISBN 978-3-95450-178-6

LCLS-II HIGH POWER RF SYSTEM OVERVIEW AND PROGRESS*

A.D. Yeremian#, C. Adolphsen, J. Chan, G. DeContreras, K. Fant and C. Nantista
SLAC National Accelerator Laboratory, Menlo Park, CA, USA

Abstract

A second X-ray free electron laser facility, LCLS-II, will be constructed at SLAC. LCLS-II is based on a 1.3 GHz, 4 GeV, continuous-wave (CW) superconducting linear accelerator, to be installed in the first kilometer of the SLAC tunnel. Multiple types of high power RF (HPRF) sources will be used to power different systems on LCLS-II. The main 1.3 GHz linac will be powered by 280 1.3 GHz, 3.8 kW solid state amplifier (SSA) sources. The normal conducting buncher in the injector will use four more SSAs identical to the linac SSAs but run at 2 kW. Two 185.7 MHz, 60 kW sources will power the photocathode dual-feed RF gun. A third harmonic linac section, included for linearizing the bunch energy spread before the first bunch compressor, will require sixteen 3.9 GHz sources at about 1 kW CW. A description and an update on all the HPRF sources of LCLS-II and their implementation is the subject of this paper.

INTRODUCTION

The Linac Coherent Light Source II (LCLS-II) is being designed and constructed at SLAC due to the high user demand of the successful operation of the first LCLS at SLAC, the only light source of its kind in the world to date [1]. LCLS-II will use a 4 GeV continuous wave (CW) superconducting 1.3 GHz linac [2]. Figure 1 shows the basic layout of LCLS-II, consisting of a dual-feed photocathode RF gun; a normal conducting double cavity 1.3 GHz buncher, each cavity fed by two RF sources; 280 superconducting 1.3 GHz linac cavities, each fed by its own solid state amplifier (SSA) and grouped into cryomodules (CM) of eight cavities that form each of the linac regions: L0 consisting of one CM, L1 consisting of two CM, L2 consisting of twelve CM and L3 consisting of twenty CM; a laser heater (LH) after L0; two magnetic bunch compressors BC1 and BC2 after L1 and L2 respectively; and sixteen 3.9 GHz superconducting cavities, also fed by individual RF sources and grouped in two cryomodules of eight cavities each to form the Harmonic Linearizer between L1 and BC1 to linearize the beam energy spread prior to the first magnetic bunch compressor.

Table 1 lists all the RF systems in LCLS-II. LCLS-II is currently in the design phase in partnership with FNAL, JLAB, LBNL, ANL and Cornell University. A wider status report is given in [3], while this report focuses on the high power RF (HPRF) system. The initial thrust of the HPRF systems tasks has been to specify the RF sources for the L-band linac, lay out the source rack and waveguide configurations, specify the various waveguide components such as isolator and directional coupler, and resolve any space co-occupancy conflicts such as with low level RF (LLRF) racks, cable conduits and penetration shields. Some preliminary design for the S-band linearizer RF and considerations about the gun and buncher RF and non-ionizing radiation protection (NIRP) are also in progress, but a more substantial report about these systems will be presented in the future.

Table 1: LCLS II HPRF Sources

Region RF Source	Frequency (MHz)	Power (kW)	Quantity
Gun TBD, likely SSA	185.7	60	2
Buncher SSA	1,300	3.8	4
Linac (L0– L3) SSA	1,300	3.8	280
Harmonic Linearizer TBD, likely SSA	3,900	~1	16

L-BAND SOLID STATE AMPLIFIERS

A total of 284 L-band SSAs will power the L-band systems on LCLS-II. The SSAs need to supply up to 3.8 kW of RF power with a 10 dBm or less (preferably ≤ 5 dBm) RF drive signal. The small signal, 1 dB bandwidth should be ≥ 1 MHz, amplitude flatness < 5%, and phase deviation < 5° within 100 kHz of the nominal frequency. The nominal maximum power must be achieved at 1 dB compression, and the harmonic power output must be < -30 dBc. The overall efficiency of the SSA from wall AC to output power must be > 40%, the SSA power supply efficiency should be > 90% and its power factor should be > 0.9 to meet the electric company's requirement for harmonics returned to the power lines.

The SLAC facility requirements for each L-band SSA are 11 KVA of 480 V power, 250 VA of 120 V power, and low conductivity water (LCW) of 30 °C at 40–70 psi, with ≤ 30 psi pressure drop across the SSA. In case of accidental failures of the LCW controls upstream, the SSA should be able to withstand an LCW pressure of as high as 150 psi. All RF connections inside the SSA are to be RF tight so as to comply with NIRP requirements for

*Work supported by DoE, Contract No. DE-AC02-76SF00515
#anahid@slac.stanford.edu

FERMILAB CRYOMODULE TEST STAND DESIGN AND PLANS*

E. Harms#, C. Baffes, K. Carlson, B. Chase, A. Klebaner, M.Kucera, J.Leibfritz, M. McGee, P. Prieto, J. Reid, R. Stanek, D. Sun, M. White, Fermilab, Batavia, IL 60510, USA

Abstract

A facility dedicated to SRF cryomodule testing is under construction at Fermilab. The test stand has been designed to be flexible enough to cool down and power test full length TESLA-style 8-cavity cryomodules as well cryomodules for low-β acceleration. We describe the design considerations, status, and near future plans for utilization of the test stand.

INTRODUCTION

The Cryomodule Test Facility (CMTF) at Fermilab is a research and development facility for accelerator science and technology, in particular, the testing and validating of Superconducting Radio Frequency (SRF) components. CMTF provides the necessary test bed to measure and characterize the performance of SRF cavities in a cryomodule. CMTF was designed to be a flexible test facility, configurable in different ways to meet the needs of current as well as future projects at Fermilab and abroad.

CMTF consists of two new adjoined buildings (as pictured in Fig. 1) located adjacent to the existing NML building, and together with NML comprises a world-class facility for testing SRF components with and without beam [1]. The smaller (4000 square foot/371.6 m^2) Compressor Building houses the warm compressors, vacuum pumps, water cooling system and utilities for the entire facility. The larger building depicted in Fig. 5 consists of a (15,000 square foot/1,394 m^2) high-bay with a 20-ton overhead crane and contains two liquid helium refrigerators, two Cryomodule Test Stands, a test area for RF components and electrical systems, a cleanroom area for particle-free preparation of SRF components, and a control room/office area.

The facility houses a large state of the art cryogenic plant capable of providing a total of 500W of cooling capacity at 2 Kelvin that can provide simultaneous operation of the two independent test stands.

The goal of the first test stand, CMTS-1, is to test cryomodules of various frequencies in pulsed or continuous wave mode. It is currently being prepared to support the testing of cryomodules for the LCLS-II project being built at Stanford Linear Accelerator (SLAC). It will test both 1.3 and 3.9 GHz cryomodules in Continuous Wave (CW) mode for LCLS-II.

The second test stand currently houses PXIE, the R&D program to test the front-end of the proposed PIP-II accelerator.

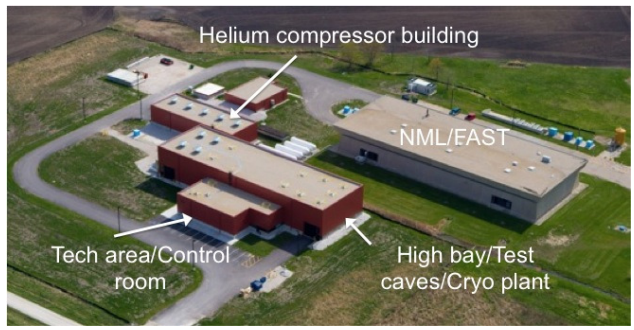

Figure 1: CMTF building adjacent to NML.

The beginning portions of the PIP-II accelerator are being installed and commissioned at PXIE and will eventually contain two different types of cryomodules [2].

TEST CAVE

The CMTS-1 test cave is a shielded enclosure sized to house cryomodules as large as TESLA-style 8 cavity 1.3 GHz ones. Inner dimensions are 64' 9" (19.74 m) long by 15 feet (4.57 m) wide with a height of 10-1/2 feet (3.2 m) as shown in Fig. 2. The walls are composed of shielding blocks and are 3 feet (0.914 m) thick with integrated penetrations for RF waveguide, cabling, etc. The roof is removable in order to move cryomodules in and out of the cave and is similarly composed of blocks with a total thickness of 3 feet (0.914 m).

Interlocked radiation detectors will be situated both within the cave and on the roof of the cave to ensure that safe levels are maintained during cryomodule testing. The cave will be considered an Oxygen Deficient Hazard (ODH) area thus monitoring and ventilation schemes are being implemented based on experience at similar test areas at Fermilab.

Cryomodule Support Girders

The fundamental design of the cryomodule support girders is based on that by INFN, Milan and used at DESY for FLASH. This design was later modified slightly to accommodate using available English structure steel shapes and standard AISC sections [3] while maintaining important metric standard features such as feed/end cap interface hole placement as was applied at Fermilab for CM-1 and currently CM-2 [4] at the NML/FAST facility.

The recent emphasis on reducing stray magnetic fields to maintain high Q_0 in SRF cavities has led to an appreciation of the need to maintain good 'magnetic hygiene' [5]. Given their bulk, composition and proximity to the cryomodules under test, the design and fabrication of the support girders has been given special scrutiny.

* Operated by Fermi Research Alliance, LLC under Contract No. DE-AC02-07CH11359 with the United States Department of Energy
# harms@fnal.gov

FIRST OPERATION OF A SUPERCONDUCTING RF ELECTRON TEST ACCELERATOR AT FERMILAB*

E. Harms#, R. Andrews, C. Baffes, D. Broemmelsiek, K. Carlson, D. Crawford, N. Eddy, D. Edstrom, J. Leibfritz, A. Lumpkin, S. Nagaitsev, P. Piot, P. Prieto, J. Reid, J. Ruan, J. Santucci, V. Shiltsev, W. Soyars, D. Sun, R. Thurman-Keup, A. Valishev, A. Warner, Fermilab, Batavia, IL 60510, USA

Abstract

A test accelerator utilizing SRF technology recently accelerated its first electrons to 20 MeV at Fermilab. Foreseen enhancements will make acceleration to 300 MeV possible at a maximum beam power of 80 kW. A summary of commissioning steps and first experiments as well as current beam parameters compared to design is presented. Plans for expansion and the future physics program are also summarized.

INTRODUCTION

The Fermilab Accelerator Science and Technology (FAST) facility was originally conceived to serve as, "a system test, with beam, of a complete ILC RF unit" [1]. Over time the purpose has changed, but the fundamental design of the injector section has remained more or less the same and is still envisioned to be a facility providing a high-brightness, high-intensity electron beam. The accelerator and its intended purposes have been extensively described [2, 3].

The FAST injector as shown in Fig. 2 consists of

- A normal conducting photoinjector gun
- Two 'booster' SRF cavities
- A 50 MeV beam transport line including a bunch compressing chicane
- A Spectrometer magnet which bends the beam down by 22.5° into a
- Low energy beam absorber.

When fully completed, the electron accelerator will consist of the low energy section described above, one ILC-type cryomodule, accelerator R&D beamlines, and a high energy beamline able to inject up to 300 MeV electrons into the Integrable Optics Test Accelerator (IOTA) [4].

PHOTOINJECTOR GUN

The RF photocathode electron gun is identical to the guns developed at DESY Zeuthen (PITZ) for the FLASH facility [5]. It is a normal conducting 1-½ cell 1.3 GHz RF cavity operated in the TM010 π-mode, with a Q_L of 11,700, and driven by a 5 MW klystron. The gun is capable of average DC power dissipation of 20 kW, and a temperature feedback system will regulate cooling water temperature to less than ±0.02° C for good phase stability. The gun is routinely operated at peak gradients of 40-45 MV/m with an output beam kinetic energy of 4.5 MeV.

The RF Gun cavity is immersed in two solenoid magnets each capable of a peak field of 0.28 T at 500 A. The main solenoid provides the appropriate field for focusing the electron beam to the booster cavities while the bucking solenoid cancels the magnetic field from the main solenoid at the photocathode surface in order to minimize beam emittance.

The photocathode is a 10 mm diameter molybdenum disk coated with Cs_2Te with a 5 mm diameter photosensitive area. It is illuminated by 263 nm wavelength laser light which is directed onto the photocathode by a 90° off-axis mirror downstream of the RF coupler. A complete description of the gun and its early operation is previously documented [6].

SUPERCONDUCTING RF SYSTEMS

Two single cavity Superconducting RF Cryomodules comprise the accelerating section of the FAST injector. These are located immediately downstream of the gun as depicted in Fig. 1 and together will provide an accelerating voltage of order 50 MV.

Capture Cavity 1

The history and recent upgrade of Capture Cavity 1 (CC1) has been previously documented [7, 8]. Based on horizontal tests it is expected to operate at gradients up to 29 MV/m. With the upgrade work now completed, the cryomodule has been installed on the FAST beam line. Vacuum and cryogenics connections are being made and full integration into FAST is now in process. In anticipation of its resumption of operation, the 300 kW klystron previously used to drive it at has been relocated to FAST and is being re-commissioned there. CC1 re-commissioning and operation is expected to occur in late 2015 to early 2016.

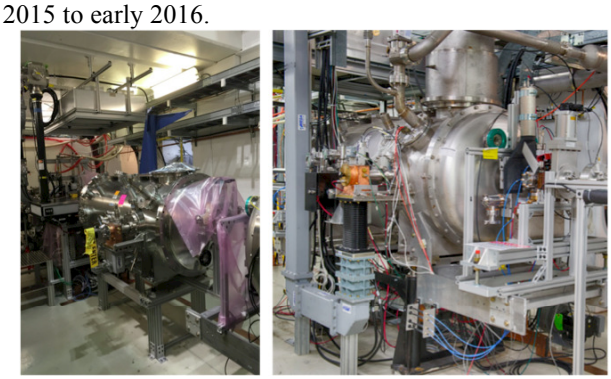

Figure 1: CC1 (left) and CC2 (right) installed in FAST.

* Operated by Fermi Research Alliance, LLC under Contract No. DE-AC02-07CH11359 with the United States Department of Energy

harms@fnal.gov

ISBN 978-3-95450-178-6

A NEW CLEANROOM WITH FACILITIES FOR CLEANING AND ASSEMBLY OF SUPERCONDUCTING CAVITIES AT HELMHOLTZ-INSTITUT MAINZ

F. Schlander*, R. Heine, KPH JGU, Mainz, Germany
K. Aulenbacher, KPH JGU, Mainz, HIM, Mainz, Germany
W. Barth, S. Mickat, GSI, Darmstadt, HIM, Mainz, Germany
V. Gettmann, M. Miski-Oglu, HIM, Mainz, Germany

Abstract

The Helmholtz-Institut Mainz HIM will operate a clean room facility for the assembly and possible re-treatment of superconducting cavities. This is mandatory for several SRF accelerator projects, like the advanced demonstrator for a dedicated sc heavy ion cw-linac at HIM or other projects pursued by research facilities or universities close by. While the installation of the clean room is in progress, the procurement of the appliances is ongoing. The present equipment planned and the current status of the installation will be presented.

INTRODUCTION

Superconducting radio frequency technology is already in use in the Rhine-Main metropolitan area and several further accelerator projects are in progress. A new building for the Helmholtz-Institut Mainz (founded in 2009) - on the campus of Johannes Gutenberg-Universität Mainz is under construction and will be available for moving in in 2016. One of the six research sections is ACID (ACcelerator Design and Integrated Detectors), which deals with accelerator and detector development. The infrastructure for superconducting cavities at Helmholtz-Institut Mainz is mainly dedicated to a new superconducting heavy ion cw-linac [1], but will also provide excellent conditions for assembly and testing of other cavities and cryomodules. Besides a radio frequency performance test bunker and an area for testing of accelerator components, e.g. magnets, a large clean room with staged clean areas up to ISO 4 quality will be available, which will be described in the next section. To allow cleaning and mounting of cavities and cryomodules, devices for cleaning, assembly and quality control must be at hand. The devices to be used and the workflow will be described in the subsequent sections.

CLEAN ROOM

The clean room is located within the experimental hall in the HIM building, including a mounting rail allowing the assembly and sealing of full cavity strings under clean conditions in ISO 4, and to move it outside for further installations. In total, the clean room covers an area of about 155 m^2, including grey room for built-in appliances, air locks for personnel access and to load single cavities and equipment into the ISO 6 and ISO 4 clean room. An overview of the clean room is displayed in Fig. 1.

It is designed to allow cleaning in stages from regular environmental pollution up to the cleanliness required - as has been proven to be sufficient for SRF - in the ISO 4 area. Air locks and an air shower ensure the boundaries for the staff between the different areas, while the cavities have to pass the HPR system to enter the ISO 4 level sufficiently cleaned. The maximum size of the cavities to be treated is approximately 1400 mm in length and 700 mm in diameter, which is sufficient for the largest type of cavities required for the heavy-ion cw linac project [2]. A summary of the dimensions is given in Table 1.

Table 1: Dimensions of the Clean Room

total length	19.5 m
total width	8 m
ISO 6 area	42 m^2
ISO 4 area	44 m^2

CLEAN ROOM INSTALLATIONS

The clean room will be equipped with all appliances to clean and to assemble superconducting cavities. During the earlier planning and approval phase, it has been refrained from installing a chemical polishing facility due to the high safety requirements. For wet pre-cleaning of the cavities a high pressure washer will be installed in the air lock between grey room and the ISO 6 area. To remove any kind of grease and contaminants, a cleaning station including an ultrasonic bath and a second bath for measuring the water conductance is foreseen to ensure a proper cleaning progress. In particular for the relatively heavy and bulky CH-type cavities, an automated lifting device will be included. A high pressure rinsing cabinet between ISO 6 and ISO 4 allows thorough cleaning of the inner cavity surface, as has been proven to be the treatment of choice to avoid field emission [3]. A furnace designed to either dry the cavity or to do the 120 °C bake, is available.

WORKFLOW

The workflow for cavity handling and the accessories is described separately. A flow chart is given in Fig. 2.

* schland@uni-mainz.de

ISBN 978-3-95450-178-6

PROGRESS ON SUPERCONDUCTING LINAC FOR THE RAON HEAVY ION ACCELERATOR

H. J. Kim* representing the RAON, IBS, Daejeon, Korea

Abstract

The RISP (Rare Isotope Science Project) has been proposed as a multi-purpose accelerator facility for providing beams of exotic rare isotopes of various energies. It can deliver ions from proton to uranium. Proton and uranium ions are accelerated upto 600 MeV and 200 MeV/u respectively. The facility consists of three superconducting linacs of which superconducting cavities are independently phased. Requirement of the linac design is especially high for acceleration of multiple charge beams. In this paper, we present the RISP linac design, the prototyping of superconducting cavity and cryomodule.

INTRODUCTION

The RISP accelerator has been planned to study heavy ions in nuclear, material and medical science at the Institute for Basic Science (IBS). It can deliver ions from protons to uranium atoms with a final beam energy, for example, 200 MeV/u for uranium and 600 MeV for protons, and with a beam current range from 8.3 pμA (uranium) to 660 pμA (protons) [1,2]. The facility consists of three superconducting linacs of which superconducting cavities are independently phased and operating at three different frequencies, namely, 81.25, 162.5 and 325 MHz.

SUPERCONDUCTING LINAC

Lattice Design

The configuration of the accelerator facility within the RISP is shown in Fig. 1. An injector system accelerates a heavy ion beam to 500 keV/u and creates the desired bunch structure for injection into the superconducting linac. The injector system comprises an electron cyclotron resonance ion source, a low-energy beam transport, a radio-frequency quadrupole, and a medium-energy beam transport. The superconducting driver linac accelerates the beam to 200 MeV/u. The driver linac is divided into three different sections, as shown in Fig. 2: a low-energy superconducting linac (SCL1), a charge stripper section (CSS) and a high-energy superconducting linac (SCL2). The SCL1 accelerates the beam to 18.5 MeV/u. The SCL1 uses two different families of superconducting resonators, i.e., a quarter wave resonator (QWR) and a half wave resonator (HWR). The SCL11 consists of 22 QWR's whose geometrical β is 0.047 and 22 qudruopole doublets. The resonance frequency of the QWR is 81.25 MHz. The cryomodule of the SCL11 hosts one superconducting cavity. The SCL12 consists of 102 HWR's whose geometrical β is 0.12 and 62 quadrupole doublets. The resonance frequency of the HWR

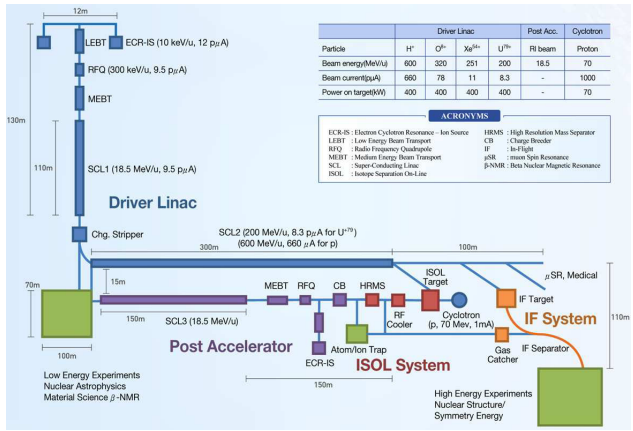

Figure 1: Layout of the RISP accelerator.

is 162.5 MHz. This segment has two families of cryomodules: one type of cryomodule hosts two superconducting cavities, and the other hosts four superconducting cavities. The CSS accepts beams at 18.5 MeV/u. The charge stripper strips electrons from the heavy-ion beams to enhance the acceleration efficiency in the high-energy linac section. The charge stripping section consists of normal conducting quadrupoles and room-temperature 45-degree bending magnets. The quadrupole magnets provide adequate transverse focusing and beam matching to the SCL2, and the bending magnet provides momentum dispersion for charge selection. The SCL2 accepts a beam at 18.5 MeV/u and accelerates it to 200 MeV/u. The SCL2 uses two types of single spoke resonators, i.e., SSR1 and SSR2. The SCL2 consists of the SCL21 and the SCL22, each with geometric β 0.30, resonance-frequency 325-MHz SSR and a geometric β 0.51, resonance-frequency 325-MHz SSR. The single-spoke-resonator type is chosen mainly because it can have a larger bore radius compared with the half-wave-resonator type, which is very important for reducing the uncontrolled beam loss in the high-energy linac section. The numbers of cavities in the SCL21 and the SCL22 is 69 and 138 respectively. The cryomodules of the SCL21 and SCL22 host 3 and 6 cavities, respectively. The SCL2 provides a beam into the in-flight fragmentation (IF) system via a high-energy beam transport (HEBT).

The post accelerator (SCL3) is designed to accelerate the rare isotopes produced in the ISOL (Isotope Separation On-Line) system. The SCL3 is, in principle, a duplicate of the driver linac up to low energy linear accelerator. The accelerated rare isotope beams are reaccelerated in the SCL2. Hence, the RISP accelerator provides a large number of rare isotopes with high intensity and with various beam energies.

* hjkim@ibs.re.kr

ISBN 978-3-95450-178-6

1.3 GHz SRF TECHNOLOGY R&D PROGRESS OF IHEP

J.Y. Zhai#, Y.L. Chi, J.P. Dai, X.W. Dai, J. Gao, R. Ge, D.Y. He, T.M. Huang, X.F. Huang, S. Jin, H.Y. Lin, S.P. Li, B.Q. Liu, Z.C. Liu, Q. Ma, Z.H. Mi, W.M. Pan, X.H. Peng, L.R. Sun, Y. Sun, Z. Xue, S.W. Zhang, Z.J. Zhang, H. Zhao, T.X. Zhao, H.J. Zheng, Z.S. Zhou,
IHEP, Beijing 100049, China

Abstract

IHEP started the 1.3 GHz SRF technology R&D in 2006 and recently enters the stage of integration and industrialization. After successfully making several single cell and 9-cell cavities of different shape and material, we designed and assembled a short cryomodule containing one large grain low-loss shape 9-cell cavity with an input coupler and a tuner etc. This module will perform horizontal test in 2016 with the newly commissioned 1.3 GHz 5 MW klystron and the 2 K cryogenic system. Beam test with a DC photocathode gun is also foreseen in the near future. We report here the problems, key findings and improvements in cavity dressing, clean room assembly, cryomodule assembly and the liquid nitrogen cool down test. A fine grain TESLA 9-cell cavity is also under fabrication in a company as the industrialization study.

INTRODUCTION

IHEP started to build a 1.3 GHz superconducting accelerator cryomodule in 2009 and completed the design, prototyping and testing of all the key components (9-cell cavity, input coupler, tuner, cryomodule) in late 2013 [1]. Then the cavity was dressed with the helium vessel and magnetic shielding, and assembled with cold part of the input coupler, gate valves and beam tubes etc. in the clean room. First-time cryomodule assembly was done in July 2014 and 2 K line cold leak was found during the liquid nitrogen cool down test. After solving the cold leak problem and improving the related vacuum system, the reassembled cryomodule finally met the requirement for the high power horizontal test. The newly commissioned 2 K cryogenic plant and 1.3 GHz RF power source are ready to use for the test. A fine grain TESLA-like 9-cell cavity has been fabricated. Two fine grain TESLA 9-cell cavities are under fabrication as industrialization study.

CAVITY DRESSING AND CLEAN ROOM ASSEMBLY

Cavity Dressing

After processing and vertical test in Fermilab [2], the large grain low-loss 9-cell cavity (IHEP-02) was filled with nitrogen gas and shipped back to IHEP. TA2 transition rings were electron-beam welded to the NbTi55 end plates of the cavity, and then the TA2 helium vessel was TIG welded to the transition rings in a glove box. An adapter ring and the bellow on the helium vessel were used to avoid cavity deformation during welding. The upper, lower and lateral surfaces of the four supporting legs were milled to final dimensions after welded on the vessel. The magnetic shield cylinder was inserted between the helium vessel and the cavity (Fig. 1).

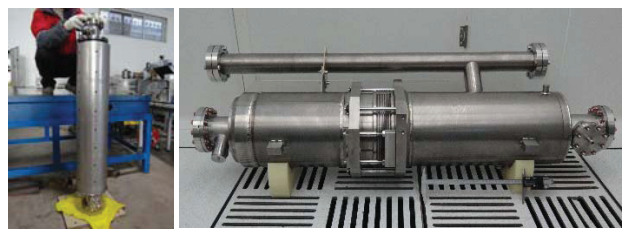

Figure 1: Cavity dressing with magnetic shield and helium vessel.

Clean Room Assembly

The 9-cell cavity in the helium vessel was assembled with the gate valves, field pick-up, HOM coupler feedthroughs, cold part of the input coupler, beam pipes, bellows and angle valves etc. (Fig. 2, 3). Particle free flange assembly method was used to guarantee no contamination.

Very careful components, tools, consumables, fixtures and environment etc. cleaning and quality control were performed before assembly. Components were cleaned and blown-off to Class 10.

Slow pump down (130 ml/min) with a mass flow control and slow venting (0.2 L/min) with high purity nitrogen gas were routinely used in leak check, back filling and flushing. Beam pipe assemblies were baked out for 12 hrs at 120 °C before assembled to the cavity.

During assembly, the seat side of the two gate valves was assembled opposite to the cavity flange by mistake. The allowable differential pressure of the valve is 2 bar in either direction. The leak rate will be a little higher, but tolerable. The cleanness is considered to be OK. The cavity has been always kept in vacuum by the two gate valves since the final leak check of the clean room assembly to avoid any contamination.

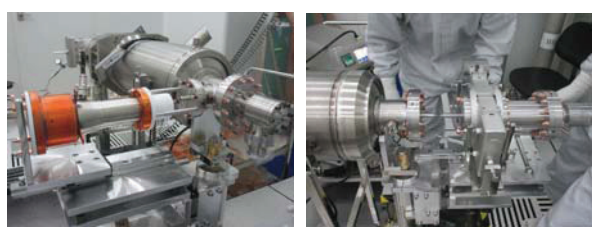

Figure 2: Input coupler cold part and gate valve assembly.

#zhaijy@ihep.ac.cn

ISBN 978-3-95450-178-6

PREPARATION OF THE 3.9 GHZ SYSTEM FOR THE EUROPEAN XFEL INJECTOR COMMISSIONING

P. Pierini (INFN - LASA, Segrate (MI) & DESY, Hamburg)
C. Albrecht, N. Baboi, S. Barbanotti, J. Branlard, T. Büttner, L. Butkowski, T. Delfs, H. Hintz, F. Hoffmann, M. Hüning, K. Jensch, R. Jonas, R. Klos, D. Kostin, L. Lilje, C. G. Maiano, W. Maschmann, A. Matheisen, U. Mavric, W.-D. Möller, C. Müller, J. Prenting, J. Rothenburg, O. Sawlanski, M. Schlösser, M. Schmökel, A. Sulimov, E. Vogel (DESY, Hamburg)
E. R. Harms, C. R. Montiel (Fermilab, Batavia, Illinois)
M. Bertucci, M. Bonezzi, A. Bosotti, J. Chen, M. Chiodini, P. Michelato, L. Monaco, M. Moretti, R. Paparella, D. Sertore (INFN-LASA, Segrate (MI))
C Pagani (Università degli Studi di Milano & INFN-LASA, Segrate)

Abstract

The 3.9 GHz cryomodule and RF system for the XFEL Injector is being assembled and delivered to the underground building in summer 2015, for the injector commissioning in Fall 2015. This contribution outlines the status of the activity and reports the preparation stages of the technical commissioning of the system.

INTRODUCTION

The European XFEL (E-XFEL) injector hosts a cryomodule composed of 8 SCRF cavities at 3.9 GHz, for the linearization of the longitudinal phase space distortions experienced by the beam in the first 1.3 GHz accelerating module, before the bunch compressor stages [1]. The module design was derived from the FLASH third harmonic section, developed by FNAL [2], with some major modifications in the module and cavity package design, in particular the development of a cavity string with alternate coupler orientation with respect to the beamline, for coupler dipole kick compensation [3]. The cavities have been fabricated and vertically tested as described in other contributions to these Proceedings [4-6], here we describe the module preparation for the tunnel installation.

RF COMPONENTS

The procurement of E-XFEL third harmonic cavities started in 2012, after the fabrication of three prototypes in order to set the industrial production and treatment steps. Long procedures were however required to qualify the design and the fabrication procedures before the cavity production in order to achieve conformance to the European Pressure Equipment Directive (PED) norms, as required by the E-XFEL Project. As a consequence of this, , the first 8 cavities fully qualified in the INFN Vertical Testing (VT) facility reached DESY in the period from mid-December 2014 to mid-March 2015, and the last two at the end of May 2015, in conditions ready for starting the string and module installation.

Power Couplers (PC) are of the same FNAL design as the ones installed in FLASH ACC39, with the antenna length adapted to the different E-XFEL beam structure.

Couplers were industrially procured and processed after fabrication at FNAL. The 8 couplers necessary for the string installation were sent in pairs in their conditioning boxes from FNAL and were available at DESY from mid-February to Mid-June 2015.

CAVITY PACKAGE QUALIFICATION

Early in the development of the E-XFEL 3.9 GHz system planning the possibility to perform a complete cold module characterization before installation in the injector was ruled out. Both the Accelerator Module Test Facility (AMTF) infrastructure for the 1.3 GHz module testing and the smaller Cryomodule Test Bench (CMTB, which was used for the ACC39 2m module) at DESY would have required significant time and work for the adaptation to the nearly 6 m E-XFEL 3.9 module, incompatible with the tight operation schedule of these facilities for the preparation of the main linac components. The decision was taken to characterize the module in the injector commissioning phase, which is planned during the main linac installation, and almost a year before its commissioning.

In the original plans, individual cavity tests in horizontal cryostats (at DESY or elsewhere) were foreseen to achieve cavity qualification in conditions similar to their operation before installation in the accelerating module. As cavities and couplers were delayed the plan was amended and a single horizontal cavity test was performed to qualify the cavity package (including all ancillaries like coupler, tuner, shielding, HOMs) and the assembly procedures. The test was successfully performed in March 2015 and is described in another contribution in these Proceedings [7].

X3M1 MODULE ASSEMBLY

The preparation of RF components was performed at their arrival in DESY: Coupler cold parts were installed on available cavities in order to return the transport and conditioning boxes to FNAL for the successive shipments of further items. With the installation of the last pair of cold coupler parts the preparation of the E-XFEL module string could start at the end of June 2015.

ISBN 978-3-95450-178-6

RECENT STATUS NEW SUPERCONDUCTING CW HEAVY ION LINAC@GSI

V. Gettmann[*,2], M. Amberg[2,3], M. Miski-Oglu[2], W. Barth[1,2], K. Aulenbacher[2,4], M. Heilmann[1], S. Mickat[1], S. Yaramyshev[1], M. Basten[3], D. Bänsch[3], F. Dziuba[3], H. Podlech[3], U. Ratzinger[3]
[1]GSI Helmholtzzentrum, 64291 Darmstadt, Germany
[2]HIM, Helmholtzinstitut, 55099 Mainz, Germany
[3]IAP, Goethe University, 60438 Frankfurt, Germany
[4]KPH, Johannes Gutenberg-University, 5099 Mainz

Abstract

The demonstrator is a prototype of the first section of the proposed cw-LINAC@GSI, comprising a superconducting CH-cavity embedded by two superconducting solenoids. The sc CH-structure is the key component and offers a variety of research and development. The beam focusing solenoids provide maximum fields of 9.3 T at an overall length of 380 mm and a free beam aperture of 30 mm. The magnetic induction of the fringe is minimized to 50 mT at the inner NbTi-surface of the neighboring cavity. The fabrication of the key components is still in progress and is near to completion. After cold performance testing of the RF cavity, the helium jacket will be welded on. The cryostat is partly assembled and will be finished in the next weeks. The test environment is completely prepared. Advanced emittance measurement is foreseen to prepare for best matching of the heavy ion beam from the injector. Integration of the cryostat into the beam line, the first cool down of the module and commissioning of the RF elements will be performed as next steps towards a complete testing of the demonstrator.

CW LINAC DEMONSTRATOR

The Demonstrator project kick-off at GSI was in 2010, which was followed by design studies for the 217 MHz CH cavity, two sc solenoids, and the cryostat. Meanwhile the fabrication is near completion. The main parameters are listed in Table 1.

The concept of a suspended support frame, which carries the cavity embedded by two sc solenoids, was chosen (Fig.1) [1]. The support frame as well the accelerator components are suspended each by eight tie rods in a cross-like configuration (nuclotron suspension) balancing the mechanical stress during the cooling-down and warm up (Fig.2). This way the components will stay always within the tolerance limits related to the beam axis (longitudinal ±2 mm, transversal ±0.2 mm).

Cryogenic Limited (UK), assembled already the cryostat, the solenoids, the support frame, and the helium supply. After mounting and cool down tests, the cryostat will be delivered to GSI in end of 2015 (Table 2).

Table 1: Main Parameters

CH-Cavity		
β		0.059
max A/Q		6
Resonance Frequency	MHz	217
Gap number		15
Total length	mm	690
Cavity Diameter	mm	409
Aperture	mm	20
Effective gap voltage	kV	225
Accelerating gradient	MV/m	5.1
Cryostat		
Inner length	mm	2200
Inner diameter	mm	1120
Material		Al
Operating temperature	°K	4.4
Operating pressure above atmosphere	bar	< 1
Solenoids		
Aperture	mm	30
Total length	mm	380
Max. field	T	9.3
Nominal current	A	110

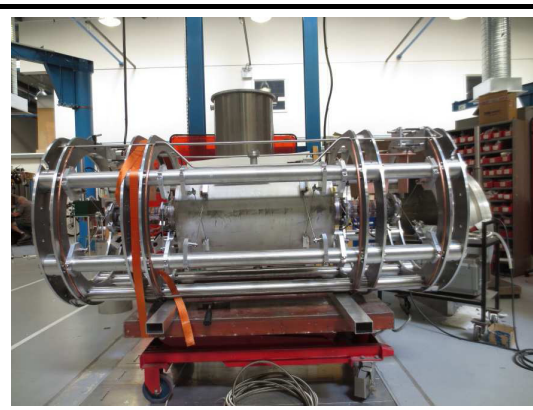

Figure 1: The cw Demonstrator comprising, a CH-cavity embedded by two solenoids supported by a frame, inside the cryostat.

ISBN 978-3-95450-178-6

MEASUREMENT OF THE CAVITY PERFORMANCES OF COMPACT ERL MAIN LINAC CRYOMODULE DURING BEAM OPERATION

H. Sakai#, M. Egi, K. Enami, T. Furuya, S. Michizono, T. Miura, F. Qiu, K. Shinoe, K. Umemori
KEK, Tsukuba, Ibaraki, Japan
M. Sawamura, JAEA, Tokai, Naka, Ibaraki, Japan

Abstract

We developed ERL main linac cryomodule for Compact ERL (cERL) in KEK. The module consists of two 9-cell 1.3 GHz superconducting cavities, two 20 kW high power coupler, two mechanical tuner and three HOM dampers. After construction of cERL recirculation loop, beam operation was started in 2013 Dec. First electron beam of 20 MeV successfully passed the main linac cavities. After adjusting beam optics, energy recovery operation was achieved. Main linac cavity was enough stable for ERL beam operation with digital LLRF system and energy recovery was successfully done with CW 90 μA beam. However, field emission was a problem for long term operation. In this paper, we express the measurement of the cavity performances during long term beam operation.

COMPACT ERL PROJECT

Compact ERL (cERL)[1, 2] is a test facility, which was constructed on the ERL Test Facility in KEK. Its aim is to demonstrate technologies needed for future multi GeV class ERL. One of critical issues for ERL is development of the superconducting cavities.

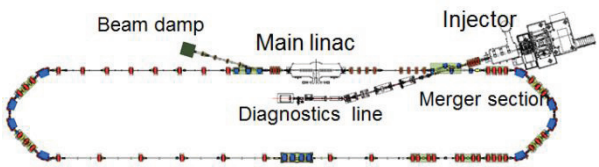

Figure 1: Conceptual layout of the cERL project.

Conceptual layout of the cERL is shown in Figure 1. The cERL main linac cryomodule was assembled and placed inside cERL radiation shield at fall of 2012. First high power test of cryomodule was carried out at December of 2012.

After commissioning of injector parts, recirculation ring was constructed during the summer and fall of 2013. Following the second high power test of main linac cryomodule, beam commissioning was started from December of 2013.

Its main parameters are shown in Table 1. Although the target beam parameters are 35 MeV and 10 mA for the first stage of cERL, current operation is limited to 20 MeV and 10 μA. The beam energy was restricted because of severe field emission of main linac cavities. The beam current was limited due to safety reason. In this paper, we present performance of main linac cryomodule under the cERL beam operation.

#hiroshi.sakai.phys@kek.jp

Table 1: Main Parameters for cERL Project

Beam energy	35 MeV
Beam current	10 – 100 mA
Normalized emittance	0.1 – 1 mm mrad
Bunch length	1 – 3 ps (usual) 100 fs (bunch compression)

MAIN LINAC CRYOMODULE

The left of figure 2 shows a schematic view of the main linac cryomodule [3], which contains two 9-cell KEK ERL model-2 cavities [4] mounted with He jackets. Beampipe-type ferrite HOM absorbers [5] are connected at both sides of cavities, to strongly damp HOMs. The HOM absorbers are placed on 80K region. Coaxial input couplers [6] with double ceramic windows feed RF power to the cavities. Frequency tuners [7] control cavity resonant frequencies. Cooling pipes of 80K, 5K and 2K are extended throughout the cryomodule. The 80K line was cooled by Nitrogen, and 5K and 2K lines were cooled by Helium. After filling with 4K liquid He, insides of the He jackets were pumped down and the cavities were cooled down to 2K.

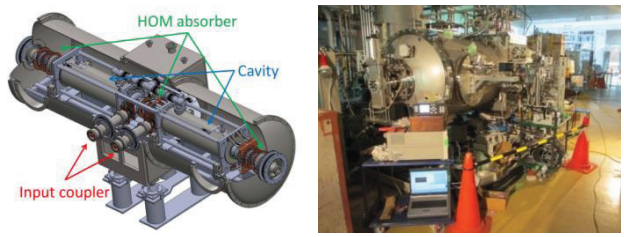

Figure 2: Schematic view of ERL main linac cryomodule (left) and the one placed inside the cERL radiation shielding room (right).

CERL BEAM OPERATION

Main Linac Cryomodule Performance

Main linac cryomodule was connected to He refrigerator system and cooled down to 2K. Figure 3 shows typical example of cryogenic operation, at December of 2013. The cryomodule was cooled down with cooling rate of less than 3K/hour, in order to avoid thermal stress to the ferrite HOM absorbers.

ISBN 978-3-95450-178-6

LOW-BETA SRF CAVITY PROCESSING AND TESTING FACILITY FOR THE FACILITY FOR RARE ISOTOPE BEAMS AT MICHIGAN STATE UNIVERSITY *

L. Popielarski#, B. Barker, C. Compton, K. Elliott, I. Malloch, E. Metzgar, J. Popielarski, K. Saito, G. Velianoff, D. Victory, T. Xu
Facility for Rare Isotope Beams, Michigan State University, East Lansing, MI, 48824, U.S.A.

Abstract

Major work centers of the new SRF Highbay are fully installed and in use for FRIB pre-production SRF quarter-wave and half-wave resonators, including inspection area, high temperature vacuum furnace for cavity degassing, chemical etching facility and processing and assembly cleanrooms. Pre-production activities focus on optimizing workflow by reducing process time, tracking part status and related data, and identifying bottlenecks. Topics discussed may include; buffered chemical polish (BCP) etching for cavity frequency control, degassing time reduction, automated high pressure rinse, particle control against field emission, pre-production cavity test results and implementation of workflow status program.

INTRODUCTION

The FRIB project is now in pre-production cryomodule fabrication and assembly phase. A new low beta cavity processing and testing facility has been installed to support building 48 coldmasses that contain a total of 332 cavities [1]. The first pre-production coldmass consists of eight β =0.085 quarter-wave resonators (QWR) and three 50 cm 8 Tesla solenoids. The second pre-production coldmass consists of eight β =0.53 half-wave resonators (HWR) and one 50 cm 8 Tesla solenoid. The baseline workflow has been established (Fig. 1) however, feedback from pre-production is valuable to optimize workflow and techniques for production.

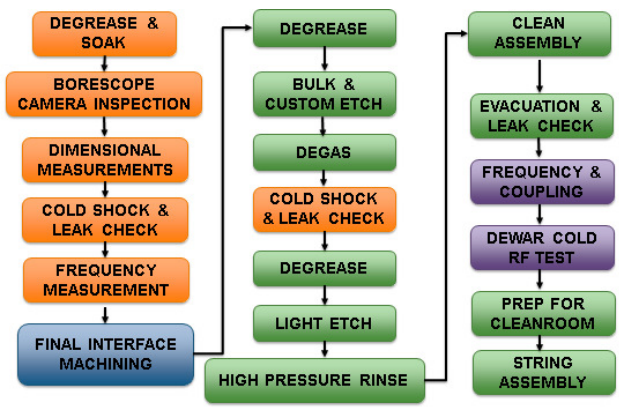

Figure 1: Production cavity workflow.

FACILITY GENERAL OPERATIONS

The SRF Production Floor is fully implemented and in use. The facility includes a receiving and tagging station, rack storage and kitting area to support production inventory control and assembly. Individual work center boards and a main electronic dashboard are installed and actively used to track cavity work flow through the facility work stations.

The SRF staff complete a comprehensive SRF Production Floor training which includes FRIB Leak Detector and Vacuum Equipment Standardization, SRF Coldmass Workflow, Coldmass Component Handling, SRF Department Quality Control Workflow, 5S Training, E-Traveler System, and General Cleanroom Training. Shoe covers are donned upon entering the SRF Production Floor to reduce contamination.

CAVITY ACCEPTANCE PROCESS

An SRF Cavity Vendor Risk Management and Quality Assurance Plan has been documented. The plan defines the strategic cavity workflow prioritization. The Acceptance Criteria Listing (ACL) is immediately performed upon cavity delivery (built-to-print procurement acceptance). The strategic priority rank on cold vertical tests is listed below:

1. Vendor qualification: first cavity of each type and first cavity delivered from each new vendor
2. Vendor mass production needs: cavities used for frequency validation
3. Critical path needs: cavity tests needed to meet FRIB master schedule near or on critical path
4. Quality monitoring: at least every 1 of 8 incoming cavities from each vendor

If a cavity fails a certification test a root cause must be identified, and prioritization made to continue sequential cavity tests from the same material lot and/or fabrication lot. All cavities (100%) are planned to be cold vertical tested before coldmass assembly, and 100% of cryomodules tested before tunnel installation.

As of September 1st 2015, a total of 43 FRIB cavities have been received [2]. The cavity status dashboard is updated each morning and allows personnel to easily see router status and cavity location. All β=0.041 cavities have

*Work supported by the U.S. Department of Energy Office of Science under Cooperative Agreement DE-SC0000661.
#lpopiela@frib.msu.edu

ISBN 978-3-95450-178-6

TUNING THE LINAC WITH SUPERCONDUCTING RESONATOR USED AS A PHASE DETECTOR

Nikolai R. Lobanov#, Peter Linardakis and Dimitrios Tsifakis, The Department of Nuclear Physics, Research School of Physics and Engineering, The Australian National University, Canberra, Australia

Abstract

The ANU Heavy Ion Facility is comprised of a 15 MV electrostatic accelerator and superconducting linac booster. The beam is double terminal stripped to provide high charge states at the entrance to the linac, which consists of twelve β=0.1 Split Loop Resonators (SLR). Each SLR needs to be individually tuned in phase and amplitude for optimum acceleration efficiency. The amplitude and phase of the superbuncher and time energy lens also have to be correctly set. The linac set up procedure developed at ANU utilises a beam profile monitor in the middle of a 180 degree achromat and a new technique based on a superconducting resonator operating in a beam bunch detection mode. Both techniques are used to derive a full set of phase distributions for quick and efficient setting up of the entire linac. Verification of the superconducting phase detector is accomplished during routine linac operations and is complemented by longitudinal phase space simulations. The new technique allows better resolution for setting the resonator acceleration phase and better sensitivity to accelerating current. In addition, it is faster to perform, independent of energy and atomic number of the incident beam and less sensitive to beam steering and de-focusing introduced by accelerating resonators.

INTRODUCTION

The ANU Heavy Ion Facility (HIAF) is comprised of a 15 MV electrostatic accelerator followed by a superconducting linac booster. A pulsed beam is obtained using a single frequency, single gap grid buncher operating at the 1/16th sub-harmonic of the linac frequency of 150 MHz and positioned at the low energy (LE) of the 14UD accelerator. The beam bunches have a typical pulse width of 1.5 ns FWHM with a bunching efficiency ~25%. The beam is further compressed to ~ 100 ps wide by the superconducting buncher made up of a β=v/c=0.1 Quarter Wave Resonator (QWR).

The setting of the bunching and acceleration phase of the resonators is achieved by two complemtary techniques. The first technique interprets a Beam Profile Monitor (BPM) trace in the middle of a 180 degree achromat [1, 2]. A special large bore BPM83 by National Electrostatic Corporation (NEC) is used for this procedure. The energy dispersion at this location allows observation of the beam energy affected by each successive resonator. The second technique employs a superconducting resonator to detect the arrival time of a beam bunch and it is described in this contribution.

This paper has been organised into three main sections. The first section outlines the general concept of the linac tuning procedure based on superconducting cavity as a phase detector at very low, sub-nA beam intensities. The second section presents key experimental results based on the new technique of utilising a superconducting phase detector to set up linac resonators for effective acceleration. Finally, the third section presents interpretation of linac tune results and defines limitations of the technique.

METHODS

Phase detection based on rf cavities similar to [3] has been developed for a low intensity tandem operating with a linac booster accelerator. The use of superconducting SLRs, normally employed for ion beam acceleration, to detect the arrival phase of the bunch results in very high sensitivity due to the very high shunt impedance when compared to room temperature resonators. The unloaded quality factor Q_0 of the electroplated SLRs used is just above 10^8, resulting in a very low frequency bandwidth of about Δf_{BW}=1 Hz at an eigenfrequency of 150 MHz. The simplest technique to minimise the effect of microphonics is overcoupling of the rf pick up port, which in turn results in a widening of the loaded bandwidth and a lower sensitivity. For example, in order to widen the loaded bandwidth to an acceptable band Δf_L=100 Hz, the coupling constant should be set to a value $\beta=\Delta f_l/\Delta f_{bw}+1=101$.

A HP Model 8405A Vector Voltmeter is the main building block of the experimental setup. The instrument has sensitivity of 100 μV full scale with phase resolution of 0.1°. The two probes are ac-coupled. Loading of the SLR is acceptable because of the high input impedance of the probes (0.1 MΩ shunted by 2.5 pF). The Vector Voltmeter measures the magnitude of a reference and resonator voltage and the difference in phase between the voltages. The SLR is overcoupled to a loading constant β~101 by driving its coupler to a predefined position with the stepper motor. The channel "A" probe is connected to output of linac master oscillator while the channel "B" probe is connected to the SLR inductive variable coupler. The phase recorder output provides a DC voltage proportional to phase in the range ±180 degrees. Both amplitude and phase outputs are routed to a data logger.

The linac tunes are arbitrated by estimating the beam transmission through the linac up to the target devices, the optimum energy gain, transverse dimension and pulse

*Work supported by Heavy Ion Accelerators Education Investment Fund
#Nikolai.Lobanov@anu.edu.au

TUNING THE SUPERCONDUCTING LINAC AT LOW BEAM INTENSITIES*

N. R. Lobanov#, P. Linardakis and D. Tsifakis, The Department of Nuclear Physics, Research School of Physics and Engineering, The Australian National University, Canberra, Australia

Abstract

The ANU Heavy Ion Accelerator Facility (HIAF) is comprised of a 15 MV electrostatic accelerator followed by a superconducting linac booster. Employment of double terminal stripping allows the system to accelerate beams with mass up to 70 amu. The disadvantage of double terminal stripping is low beam intensity of few particle nanoamps delivered to the linac. One of the linac set up procedures developed at ANU utilises a U-bend at the end of the linac. One special wide Beam Profile Monitor (BPM) is installed after the 90 degree magnet. The technique allows correct setting of phase by observing the displacement of beam profile versus phase shift of the last phase locked resonator. In this paper, a simple method has been proposed to improve sensitivity of a commercially available BPM for efficient operation with low beam intensities. Verification of BPM with enhanced sensitivity is accomplished during routine linac operations and it is supplemented by longitudinal phase space simulations.

INTRODUCTION

The ANU Heavy Ion Facility (HIAF) is comprised of a 15 MV electrostatic accelerator followed by a superconducting linac booster as shown in Fig. 1 [1]. A pulsed beam is obtained using a single frequency grid buncher operating at 1/16th sub-harmonic of the linac frequency of 150 MHz and positioned at low energy (LE) of the 14UD accelerator. The beam bunches have a typical pulse width of 1.5 ns FWHM with a bunching efficiency ~25%. The beam is further compressed to ~ 100 ps wide by the superconducting buncher "C1" made up of a β=v/c=0.1 Quarter Wave Resonator (QWR).

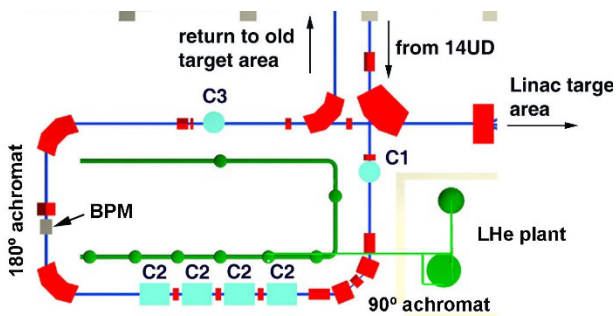

Figure 1: Layout of the ANU superconducting linac booster. The main components are: the superbuncher C1; split loop resonator modules C2 and the time-energy lens C3. Bending radius of 180° achromat dipole is $R_{180°}$ = 1100 mm. The distance from exit of 180° achromat dipole to large bore BPM is L=1608 mm.

*Work supported by Heavy Ion Accelerators Education Investment Fund
#Nikolai.Lobanov@anu.edu.au

The twelve, β=0.1, lead tin electroplated resonators currently installed in module cryostats "C2" mean that only double terminal stripped ions from the 14UD with mass below ~70 amu match adequately the resonator gap separation. Heavier ions have velocity at injection into the linac of β < 0.06, limiting its performance due to TTF mismatching. The Time-Energy Lens (TEL), a β=0.1 QWR, "C3", serves as the energy homogenizer for return of the beam to the old target area or as rebuncher for optimal time resolution. Two main factors limit 14UD performance due to double terminal stripping operation: limited beam intensity and range of beams available from the ion sources and restriction on transmission and significant loading associated with heavy beams. For example, the beam loading limits the maximum intensity of injected beams to 1.5 μA at LE end. Typically, with double terminal stripping and single frequency bunching, one can produce nanoamp beams injected into the linac. Specialised, sensitive equipment is required to tune linac with such low intensity beams.

The setting of the bunching and acceleration phase of the resonators can be achieved by a few different techniques. First, it can be done by interpreting the BPM trace in the middle of the 180 degree achromat [2]. The energy dispersion at this location allows observation of the beam energy affected by each successive resonator. The second technique employs a fast Faraday cup, which provides a direct view of the time structure of the beam [3]. More sophisticated application employs a superconducting resonator to detect the arrival time of a beam bunch [4].

This paper has been organised into three main sections. The first section outlines the general concept of a BPM with factor of 2.5 increased sensitivity and describes resonator set up procedures. The second section presents key experimental results based on new techniques, including using a high sensitivity BPM to set up linac resonators for effective acceleration. Finally, the third section presents interpretation of linac tune results and defines technique limitations.

METHODS

A beam profile is generated by collecting secondary electrons that are produced when rotating wire intersects the beam. The scanner element is made of 1.5 mm diameter molybdenum wire. With the axis of rotation of the wire inclined at 45° to the vertical, it scans the beam twice in each cycle at 19 Hz in the horizontal and vertical directions. An isolated cylindrical electrode mounted coaxially with the housing collects secondary electrons released from the wire. The collector is coupled electrically

ISBN 978-3-95450-178-6

CRYOGENIC PERFORMANCE OF THE HNOSS TEST FACILITY AT UPPSALA UNIVERSITY

R. Santiago Kern, L. Hermansson, K. Gajewski, R. Ruber
Uppsala University, Sweden
T. Junquera, J.P. Thermeau, Ph. Bujard
Accelerator and Cryogenic Systems AS, Orsay, France

Abstract

The FREIA Laboratory at Uppsala University, Sweden, is developing part of the RF system and testing the superconducting double spoke cavitites for ESS. During 2014 it was equipped with HNOSS, a versatile horizontal cryostat system for testing superconducting cavities. HNOSS is designed for high power RF testing of up to two superconducting accelerating cavities equipped with helium tank, fundamental power coupler and tuning system. In particular it will be used to characterise the performance of spoke cavities like used in the accelerator for the ESS project. HNOSS is connected to a cryogenic plant providing liquid helium and a sub-atmospheric pumping system enabling operation in the range 1.8 to 4.5 K. We present a brief description of the major components, installation and results from the recent operation and tests.

INTRODUCTION

The FREIA Laboratory at Uppsala University was created in 2011 to continue the expertise in accelerator science and technology initiated with the construction of a cyclotron in the late 1940's. FREIA was inaugurated in 2013 [1]. Its first major project is to be a test environment for the superconducting spoke cavities and develop their high power RF amplifiers to be used in the ESS accelerator. In addition the laboratory provides cryogenic fluids such as liquid nitrogen and helium to experimental groups at the university. The global layout of the FREIA Laboratory is shown in Figure 1. The main equipment consists of a horizontal test cryostat (HNOSS), a helium liquefier, high power RF transmitters and several concrete bunkers. The infrastructure of the FREIA Laboratory has been designed to accommodate modest future extensions for other test facilities and experiments.

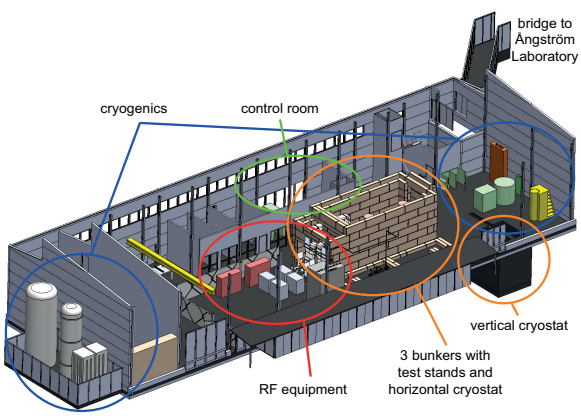

Figure 1: Layout of the FREIA Laboratory.

The main project for the FREIA Laboratory at present is the development of the ESS accelerator while a THz-FEL study has been started for the longer term future. Among the critical elements of the ESS proton accelerator are the superconducting accelerating cavities and their RF power stations. FREIA is concentrating on the spoke linac part of the accelerator and in specific on the development of the RF power station and high power test of the spoke resonators.

The ESS accelerator will contain 26 double spoke resonators which are being developed by IPN Orsay [2]. The prototype spoke resonators will be tested first at the SupraTech vertical test stand at IPN Orsay. One resonator has been brought to FREIA where it is being tested in HNOSS: first at low power with a high-Q antenna to verify vertical test stand results, then fully dressed with the high power coupler and tuning systems at nominal power. This testing programme will continue until mid-2016, after which the first prototype cryomodule, with a pair of spoke resonators, also will be tested at FREIA.

INSTALLATION

Last year the cryostat and its cryogenic system were installed at FREIA. First the liquefier with gas recovery system, then the cryostat and the sub-atmospheric pumping system.

The HNOSS Horizontal Cryostat

FREIA has constructed a versatile horizontal cryostat called HNOSS (Horizontal Nugget for operation of Superconducting Systems[1]) for test of superconducting accelerator cavities, magnets or other devices. With an internal length of 3.3 m, up to two accelerating cavities can be installed and tested simultaneously in order to investigate possible coupling between the two devices. The design of HNOSS has been described elsewhere [3–5]. HNOSS has an available internal diameter of 1.2 m and full size access doors on each side to facilitate installation work. Its total height is 4 m with the central horizontal axis line at 1.7 m. HNOSS is designed to accommodate TESLA type 1.3 GHz and ESS type 704 MHz elliptical cavities as well as ESS type 352 MHz double-spoke resonators. HNOSS has an integrated internal magnetic shield and a valve box located on top as shown in Figure 2. The 1 mm thick, room temperature, mu-metal magnetic shield is installed between the warm vacuum vessel and the thermal radiation shield.

[1] In Norse mythology, Hnoss is one of Freia's daughters.

ISBN 978-3-95450-178-6

DEVELOPMENTS ON SRF COATINGS AT CERN

A. Sublet#, S. Aull, B. Bartova, S. Calatroni, T. Richard, G. Rosaz, M. Taborelli, M. Therasse, W. Venturini Delsolaro, P. Zhang
CERN, Geneva, Switzerland

Abstract

The thin films techniques applied to Superconducting RF (SRF) have a long history at CERN. A large panel of cavities has been coated from LEP, to LHC. For the current and future projects (HIE-ISOLDE, HL-LHC, FCC) there is a need of further higher RF-performances with focus on minimizing residual resistance Rres and maximizing quality factor Q_0 of the cavities.

This paper will present CERN's developments on thin films to achieve these goals through the following main axes of research:

The first one concerns the application of different coating techniques for Nb (DC-bias diode sputtering, magnetron sputtering and HiPIMS). Another approach is the investigation of alternative materials like Nb_3Sn.

These lines of development will be supported by a material science approach to characterize and evaluate the layer properties by means of FIB-SEM, TEM, XPS, XRD, etc.

In addition a numerical tool for plasma simulation will be exploited to develop adapted coating systems and optimize the coating process, from plasma generation to thin film growth.

MOTIVATIONS

The technical and financial challenges set by the next generation of accelerators rely on the availability of the SRF thin film technology for the acceleration of the particles.

Superconductive thin film materials on copper remain one of the best options in terms of thermal stability, material cost, potential for higher T_c coatings and low sensitivity to Earth's magnetic field, the latter allowing simpler and cheaper cryostat design [1].

The main drivers for the SRF thin film developments at CERN are:

- Short term: HIE-ISOLDE high-beta Nb/Cu Quarter Wave Resonators (QWR) cavities (100 MHz), 20 cavities in total [2].
- Medium term: HL-LHC Crab Nb/Cu Wide Open Waveguide (WOW) cavities (400 MHz), 16 cavities [3]
- Long term: LHC upgrade, ERL, FCC elliptical cavities (400/800 MHz) [4]

The bottleneck of the Nb thin films is the strong increase of R_s with RF-field [1].

R_s is composed of the BCS surface resistance (R_{BCS}), the residual resistance (R_{res}) and the fluxon-induced surface resistance.

#alban.sublet@cern.ch

R_{BCS} is a material property, which is found to depend both on temperature and frequency. Factors governing R_{res} are still not well understood.

To reduce the R_s increase with RF-field different paths related to the choice of the superconductive (SC) material or its treatment or the substrate treatment are under investigation at CERN.

The thin film developments at CERN are oriented along three axes referring to the different coating process steps:

1. Substrate preparation, surface and interface
2. Thin film production
3. Top layer surface properties

The target is to grow a smooth, pure, defect free, dense layer of uniform thickness.

SUBSTRATE PREPARATION, SURFACE AND INTERFACE

The first axis concerns the substrate properties, its surface preparation and the resulting interface with the thin film. These parameters will influence the way the layer grows, its purity and composition. The surface preparation will influence the adhesion of the layer and its thermal contact with the copper substrate.

Substrate Preparation

The substrate chemical preparation by electropolishing or chemical polishing are currently used at CERN. Understanding of the key parameters, beyond the roughness, towards the ideal surface conditions is still in progress. The duration and uniformity of the chemical polishing in complex substrate geometry can affect the resonant frequency of the cavity [5]. The surface etching map will be characterized in the case of HIE-ISOLDE cavity geometry for further understanding and optimization of the process.

Substrate assembly in the coating system in a dust free environment is mandatory to guarantee reproducible and reliable coatings conditions. These actions are well controlled at CERN using ultra-pure high pressure rinsing of the substrate and assembly in an ISO 5 clean room. An upgrade of these facilities is foreseen in the next future to match the new substrate shapes and dimension requirements.

Surface and Interface

Thermal annealing at 650°C of the copper substrate is done in between two chemical polishing steps as it was observed that this thermal cycle combined with the chemical surface etching helps to reduce the sulphur content and its segregation at the surface of the copper [6]. XPS surface analysis of OFE copper samples chemically

ISBN 978-3-95450-178-6

MATERIAL QUALITY & SRF PERFORMANCE OF Nb FILMS GROWN ON Cu VIA ECR PLASMA ENERGETIC CONDENSATION*

A-M Valente-Feliciano†, G. Eremeev, C. Reece, J. Spradlin, JLab, Newport News, VA 23606, USA
S. Aull, CERN, Geneva, Switzerland
T. Proslier, ANL, Argonne, IL 60439, USA

Abstract

The RF performance of bulk Nb cavities has continuously improved over the years and is approaching the intrinsic limit of the material. Although some margin seems still available with processes such as N surface doping, long term solutions for SRF surfaces efficiency enhancement need to be pursued. Over the years, Nb/Cu technology, despite its shortcomings, has positioned itself as an alternative route for the future of superconducting structures used in accelerators. Significant progress has been made in recent years in the development of energetic deposition techniques such as Electron Cyclotron Resonance (ECR) plasma deposition. Nb films with very high material quality have then been produced by varying the deposition energy alluding to the promise of performing SRF films. This paper presents RF measurements, correlated with surface and material properties, for Nb films showing how, by varying the film growth conditions, the Nb film quality and surface resistance can be altered and how the Q-slope can be eventually overcome.

INTRODUCTION

RF fields have a very shallow penetration depth in SRF materials (~40 nm for Nb). Instead of the commonly used bulk Nb, one can then envision using a thin layer of Nb deposited on the inner surface of a castable cavity structure made of copper (Cu) or aluminum (Al). This opens the possibility to dramatically change the cost framework of SRF accelerators by decoupling the active SRF surface from the accelerating structure definition and cooling. The viability of SRF Nb films on Cu (Nb/Cu) technology has been demonstrated with pioneer studies at CERN on 1.5 GHz cavities [1–3] and the successful implementation in LEP-2 with 352 MHz cavities. Due to defects inherent to the magnetron sputtering technique used for Nb deposition, the 1.5 GHz Nb/Cu cavities suffered a significant reduction of Q at accelerating gradients above 15 MV/m [4]. Several material factors, highly dependent upon the surface creation conditions, may contribute to degraded SRF performance by the reduction of the electron mean free path and enabling early flux penetration. Fundamental work is thus required to determine the functional dependence of film-grown niobium crystal texture, intragrain defect density, and grain boundary characteristics on the resulting SRF performance (surface resistance, lower critical field H_{c1}...).

The understanding of the dependence of the final RF surface for Nb and multilayer films on the characteristics of the films produced, the nucleation, the diverse deposition parameters, substrate nature, temperature and morphology is of primary importance. The quality of the resultant thin film is heavily influenced by the chosen deposition technique. With the recent developments in deposition techniques via energetic condensation [5], films with a wide range of structure and features potentially relevant to RF performance can be produced. In this context, JLab is using an ECR plasma as a Nb ion source in ultra-high vacuum (UHV) [6, 7] for careful investigations into the film growth dynamics. The main advantages are the production of a high flux of singly charged ions with controllable kinetic energy and the absence of macro-particle production.

NB/CU FILM STRUCTURE

The challenge is to develop an understanding of the film growth dynamics from its nucleation to the final exposed surface. The defect density within the RF penetration depth determines the electron mean free path in that layer. It is certainly affected by impurities incorporated during the final stage of film growth, but it is also strongly affected by the underlying crystal structure developed from the initial film nucleation and the substrate nature. One can approach SRF Nb film growth in three phases: film nucleation on the substrate, growth of an appropriate template for subsequent deposition of the final RF surface and deposition of the final surface optimized for minimum defect density. The development of every phase can be expected to depend strongly on the kinetic energy of the arriving Nb ions. Films are produced by ECR at different bias voltages, bake and coating temperatures on Cu substrates (single crystal and polycrystalline), as well as a variety of crystalline and amorphous insulator substrates which serve as controlled systems for analysis. As anticipated, it is found that the substrate properties and the initial growth conditions — ion energy and substrate temperature — strongly influence the final properties of the Nb film [8]. The on-going studies show that hetero-epitaxy of Nb on Cu single crystal substrates is easily achievable with high crystalline character and at temperatures low enough to maintain the mechanical integrity of the Cu substrate [9]. Films coated on polycrystalline Cu substrates are hetero-epitaxial, with grain size comparable to the underlying substrate. The substrate crystal quality is shown to have a strong influence on the final quality and structure of the Nb film.

* Authored by Jefferson Science Associates, LLC under U.S. DOE Contract No. DE-AC05-06OR23177 and by DTRA (Grant No. HDTRA1-20-1-0072).
† valente@jlab.org

RECENT RESULTS FROM THE CORNELL SAMPLE HOST CAVITY*

J. T. Maniscalco†, B. Clasby, T. Gruber, D. L. Hall, M. Liepe

CLASSE, Cornell University, Ithaca, NY, 14853, USA

Abstract

Many novel materials are under investigation for the future of superconducting radio-frequency accelerators (SRF). In particular, thin-film materials such as Nb3Sn, NbN, SIS multilayers, and also thin-film niobium on copper, may offer improvements in cost efficiency and RF performance over the standard niobium cavities. To avoid the difficulties of depositing thin films on full cavities, Cornell has developed a TE-mode sample host cavity which allows for RF measurements of large, flat samples at fields up to and over 100 mT. We present recent performance results from the cavity, reaching record high fields and quality factor using a niobium calibration plate. We also discuss plans for future collaborations.

INTRODUCTION

In the field of superconducting radio-frequency accelerators (SRF), research groups are investigating many novel materials which may offer improvements over the performance of niobium, the standard material used in cavity fabrication. Thin-film materials are of particular interest; however, manufacturing RF cavities with these thin film materials can be expensive and challenging due to the complex geometry and size of traditional accelerator cavities. Thus it is ideal to find another way to measure the RF performance and properties of these materials in more easily-fabricated configurations.

To solve this, Cornell has developed a cavity that supports a removable sample plate of the material under investigation [1–4]. Now in its third generation, the TE-mode sample host cavity takes a five inch disk, clamped to the face of the cavity with an indium seal (Table 1). The cavity also features a temperature-mapping system (T-map) on the sample plate to locate quenches and hot spots. Figure 1 shows the cavity mounted on the test insert with the T-map as well as external bath temperature sensors. Figure 2 shows a 3D CAD representation of the cavity, without sample plate or dressing; Figures 3 shows the normalized magnetic field profile on the RF-active portion of the sample plate.

In recent tests over the past year, several issues resulting in a low-field quench of the cavity have been considered and addressed, and the cavity has now reached a peak magnetic field on the sample plate of 106 mT, higher than ever before in the history of this cavity. The cavity operates at a quality factor Q_0 reaching a maximum of 4.1×10^{10} at a temperature of 1.6 K. Figure 4 shows the Q_0 vs. H_{sample} for this test.

Figure 1: Third-generation Cornell TE sample host cavity with temperature map and external temperature sensors installed.

Table 1: Sample Host Cavity Parameters

Parameter	Value
Frequency	3.96 GHz
Geometry factor G	309 Ω
$H_{\text{sample}}/H_{\text{peak}}$	0.892
RF mode	TE_{011}
Sample plate diameter	5 in (12.7 cm)
Sample plate diameter exposed to RF	4 in (10.2 cm)
Pct. of losses on sample plate (Nb)	13.2%

PERFORMANCE IMPROVEMENTS

In late 2014, during a calibration test, the sample host cavity reached a peak field of 105 mT, limited by quench. Since then, we have made a number of improvements to the cavity, testing equipment, and testing procedures. These included replacing a faulty traveling-wave-tube amplifier with a new, 100 W solid-state system; disassembling and thoroughly cleaning the coupler; "resetting" the cavity surface with first a nitric acid soak, followed by an electropolishing (EP) treatment to remove 10 μm of material, and ending with a 120° C bake for 48 hours; replacing the sample plate clamp with a new design that applies azimuthally symmetric pressure to the plate; improving the cavity assembly process and inspecting and replacing most of the components in the RF circuit (mixers, directional couplers, etc.).

* This work was supported by NSF Career grant PHY-0841213 awarded to Matthias Liepe.

† jtm288@cornell.edu

ENERGETIC CONDENSATION GROWTH OF Nb ON Cu SRF CAVITIES*

K. M. Velas#, S. F. Chapman, I. Irfan, M. Krishnan, AASC, San Leandro, CA 94577, USA

Abstract

Alameda Applied Sciences Corporation (AASC) grows Nb thin films via Coaxial Energetic Deposition (CED) from a cathodic arc plasma. The plasma from the cathode consists exclusively of 60-120eV Nb ions (Nb^+ and Nb^{2+}) that penetrate a few monolayers into the substrate and enable sufficient surface mobility to ensure that the lowest energy state (crystalline structure with minimal defects) is accessible to the film. AASC is coating 1.3 GHz SRF cavities using a graded anode to ensure uniform film thickness in the beam tube and elliptical regions. Copper cavities are centrifugal barrel polished and electropolished (done for us by the Fermilab Technical Division, Superconducting RF Development Department and by Thomas Jefferson National Accelerator Facility (JLAB)) before coating, to ensure good adhesion and improved film quality. The Nb coated copper cavities will undergo RF tests at JLAB and at Fermilab to measure Q_o vs. E.

INTRODUCTION

The goal of replacing bulk niobium with niobium films for SRF accelerator cavities and resonators has been pursued since the 1980's [1] and remains an attractive though elusive goal. LEP-II used 256 niobium coated copper cavities that operated with gradients up to 7 MV/m [2]. However, present research employs accelerating gradients of 20 MV/m. To replace bulk Nb in future SRF applications, thin film Nb cavities must achieve the same operating parameters of $Q_o > 10^{10}$ out to 20 MV/m. AASC is developing and implementing a technique called Coaxial Energetic Deposition (CED) to grow a film using a cathodic arc plasma. Demonstration of superconducting properties of a Nb film comparable to the properties of bulk Nb will allow for a cost reduction in SRF accelerator fabrication. This paper covers advancements made in the CED coating process with regard to copper elliptical cavities. Fermilab and JLAB are providing AASC with welded copper 1.3 GHz SRF cavities that have been centrifugal barrel polished (CBP) and electropolished (EP). Our partners will test the niobium coated copper cavities.

ENERGETIC CONDENSATION

The CED process uses a 30–100 V arc discharge to generate a highly ionized plasma made exclusively from the cathode material. A Nb cathode produces 60–120 eV ions (Nb+ and Nb2+) bombarding the substrate and undergoing subplantation [3]. The ions deposit their energy a few monolayers beneath the surface, bringing the local area to the melting point. This promotes film growth with excellent adhesion and crystallinity. Heating the substrate promotes defect free crystal growth.

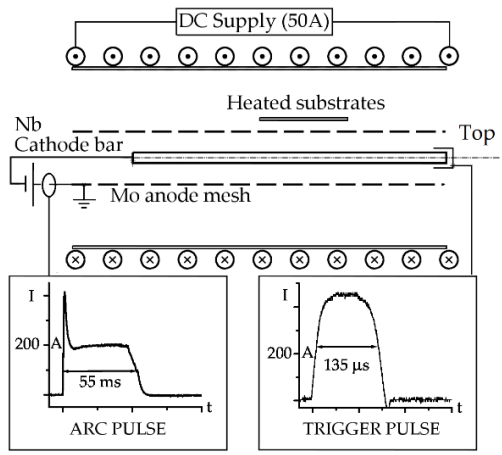

Figure 1: Schematic drawing of CED showing coaxial geometry and typical current pulses to run the vacuum arc.

A schematic drawing of the CED process in shown in Fig. 1. A cathode rod is surrounded by an anode mesh made of stainless steel or a refractory metal. A vacuum arc is triggered and sustained using a 100 V, 200 A power supply. In the presence of a magnetic field, the cathode spots traverse a stochastic helical path along the length of the cathode. The CED chamber is oriented vertically such that the arc is triggered at the top and travels down the length of the cathode. Each arc pulse deposits a monolayer of Nb and a multi-micron film is built up over thousands of pulses.

While the RF penetration is on the order of 50 nanometers, previous work has found that a thicker film may have better crystalline properties, which may lead to better RF performance [4]. However, internal stresses can cause a thick film to buckle and delaminate. To adequately coat an SRF cavity with the desired thickness, we need to characterize our coating process by accounting for the average arc spot behaviour and niobium deposition rate.

Global Axial Arc Velocity

To ensure we fully coat the entire length of a cavity, we measured the apparent axial velocity of the cathodic arc. This is a measure of the time it takes the initial plasma breakdown to travel from the trigger location, down the length of the cathode, and run past the bottom of the substrate that is to be coated.

To characterize the average axial velocity of the cathodic arc as a function of ambient magnetic field, multiple loops of copper wire were placed concentric with the cathode and anode at various axial locations. Figure 2 shows the experimental arrangement.

*Work supported by DOE SBIR Grant #DE-SC0011371
#kvelas@aasc.net

ISBN 978-3-95450-178-6

BULK NIOBUM POLISHING AND ELECTROPOLISHING STEPS FOR THINFILM COATED COPPER SRF CAVITIES*

Mahadevan Krishnan#, Irfan Irfan, Steve Chapman and Katherine Velas,
Alameda Applied Sciences Corporation, San Leandro, CA, USA
Joshua Spradlin and Hui Tian, Jefferson National Accelerator Facility, Newport News, VA

Abstract

Alameda Applied Sciences Corporation (AASC) grows Nb thin films via Coaxial Energetic Deposition (CED) from a cathodic arc plasma. The plasma consists of 60-120eV Nb ions (Nb+ and Nb++) [1] that penetrate a few monolayers into the substrate [2] and enable sufficient surface mobility to ensure that the lowest energy state (crystalline structure with minimal defects) is accessible to the film [3]. One limitation of CED thinfilms is the presence of Nb macroparticles (~0.1-10 microns) that could be deleterious to high field performance of the SRF cavity. One way to remove such macroparticles [4] is to grow a thick film (~3-5 microns), followed by mechanical polishing (MP) using the finest media as might be applied in Centrifugal Barrel Polishing (CBP) to achieve a 0.4 micron surface figure, and an electropolishing (EP) step to remove ~1 micron of Nb that also removes all traces of embedded media in the film. The residual 2-4 micron Nb film should more nearly resemble the surface of a bulk Nb cavity that has been subjected to the same steps. This paper describes experiments conducted on Cu coupons as a prelude to an SRF Cu cavity coating.

INTRODUCTION

In the early 1980s, researchers at CERN [5] explored the concept of sputtered films of Nb on copper cavities as a potential replacement for bulk Nb SRF cavities. Q_0 values in excess of $2x10^9$ at 5 MV/m were reproducibly achieved on single cell 500 MHz cavities and a Q_0 value of $6.2x10^9$ was reached at 5 MV/m on a 4 cell 352 MHz cavity. These excellent results were tempered by the sporadic appearance of blisters in the Nb film and a rapid decrease of Q_0 with increasing field (called Q-slope). Papers published in the 1990s [6,7] suggested that impurities in the film were responsible for the drop in Q with higher field. In the early 2000s, Langner [8] Russo [9] and others proposed the use of cathodic arcs to grow the Nb thin films. This pioneering work was motivated by the fact that cathodic arcs naturally generate ions that are energetic (60-120eV) as compared to the ~1eV ions from magnetron guns. The more energetic ions would presumably lead to denser (less porous) films with better adhesion. Furthermore, the source of ions from an ultrahigh vacuum might also be conducive to purer films with better SRF properties. Residual Resistivity Ratio (RRR) of up to 100 was measured in Nb films grown at substrate temperatures of ~100 °C. RF cavity cells were coated using various configurations of cathodic arcs. These early attempts did not demonstrate high Q_0 either due to poor surface preparation or impurities in the film.

There are three types of plasma sources that use energetic ions to grow thin films: cathodic arcs, Electron Cyclotron Resonance (ECR) plasmas and High Power Impulse Magnetron Sputtering (HiPIMS). All three sources produce dense, well adhered films and have therefore been actively pursued for better SRF cavity coating applications. This paper presents results using cathodic arcs. Our earlier work on coupons of a-sapphire and MgO [1] motivated coating of Nb films on Cu coupons and has recently progressed to coating 1.3 GHz RF cavities.

This paper focuses on the problem of macroparticles in the thin films that are grown using cathodic arc deposition. Macroparticles are neutral droplets ranging in size from ~0.1-10 µm in all cathodic arcs, ejected from molten craters [10] as cathode spots extinguish. With regard to the magnetic field, these macroparticles could allow vortex penetration if the thermal conductivity from the macroparticle to the underlying Nb thinfilm is poor. With regard to the electric field, the protrusion of the macroparticles from the thinfilm surface could cause field enhancement and cavity breakdown at lower fields than required. Figure 1 shows a cross-section SEM of a typical Nb macroparticle on a 2.43 µm thick Nb film grown using CED.

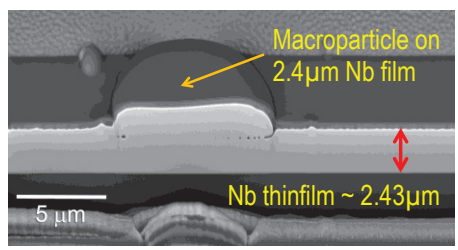

Figure 1: Cross-section SEM of Nb thinfilm showing an embedded macroparticle.

XRD analysis of the film showed that the film was a Nb crystal with {100} orientation. The macroparticle also showed the same crystalline structure and is obviously well adhered to the film. The macroparticle is ejected from the crater of the cathode spot and is at the melt temperature when it lands on the film (the flight time from cathode to substrate is short enough

Work supported by DOE SBIR
Grant #DE-SC0011371
#krishnan@aasc.net

ISBN 978-3-95450-178-6

SUPERCONDUCTING NBN-BASED MULTILAYER AND NBTIN THIN FILMS FOR THE ENHANCEMENT OF SRF ACCELERATOR CAVITIES

M. C. Burton, M. R. Beebe, K. Yang, J. Riso, A. Lukaszew
The College of William and Mary, Williamsburg, VA 23188, USA
A. M. Valente-Feliciano, C.E. Reece
Thomas Jefferson National Accelerator Facility, Newport News, VA 23606, USA

Abstract

Current superconducting radio frequency (SRF) technology, used in various particle accelerator facilities across the world, is reliant upon utilizing bulk superconducting cavities, usually made of bulk Nb. Due to technological advancements in the processing of bulk Nb cavities, the facilities have reached accelerating fields very close to material-dependent limits, ~50 MV/m for bulk Nb. One possible solution to improve upon this fundamental limitation was proposed a few years ago by A. Gurevich and it consists of the deposition of alternating thin layers of superconducting and insulating materials on the interior surface of the cavities. Some candidate superconducting materials proposed for this multilayer scheme are NbN, NbTiN and Nb3Sn. Here we present our recent results on NbN-based trilayers in coupon samples in order to further advance the multilayer approach. Since NbTiN has higher lower critical field (Hc1) and higher critical temperature (Tc) than Nb and increased conductivity compared to NbN, it is a more promising candidate material for this new method. Thus, we also present experimental results correlating film microstructure with superconducting properties on NbTiN thin film coupon samples while also comparing films grown with targets of different stoichiometries. It is worth mentioning that we have achieved thin films with bulk-like lattice parameters and transition temperatures while also achieving Hc1 values larger than bulk for films thinner than their London penetration depths.

INTRODUCTION

Linear particle accelerator facilities like the Thomas Jefferson National Accelerator Facility (JLab) in Newport News, VA rely on superconducting radio frequency (SRF) cavities made of bulk niobium. These SRF cavities benefit from their ability to be continuously operated with low power dissipation, have lower microwave surface resistance and achieve higher maximum accelerating fields than conventional copper cavities. Recent advances in Nb cavity technology have increased the maximum breakdown field (~50MV/m) approaching the theoretical limit given by the thermodynamic critical field Hc(0) = 200mT, at which the RF field induces the depairing current density at the surface of the cavity. Thus, further enhancements require a new approach.

Due to the fact that the SRF phenomenon is active a short distance into the superconducting material close to the surface, one can feasibly exploit thin films with the goal of improving cavity performance. Thin films offer several advantages over current bulk materials, since their microstructure can be tailored and have the ability to be employed in a multitude of material combinations that can result in cavities that could surpass current individual bulk properties. Therefore, in order to push the accelerating fields of SRF cavities beyond the current material limitations it is possible to utilize thin film deposition on the interior of cavities using various new materials and combinations, as well as improved deposition conditions compared to previous attempts [1].

A possible model to achieve field enhancement utilizes alternating layers of superconducting-insulating-superconducting (SIS) thin films deposited on the interior of cavities to shield the innermost surface from magnetic field vortex penetration thus enabling the possibility to even double the maximum field gradient achievable [2]. In such model, it is predicted that shielding of the inner surface is possible using layered superconducting materials, with higher critical temperatures (Tc) and lower critical field (Hc1) values than bulk Nb, such that magnetic field vortex penetration and propagation is reduced or even suppressed resulting in enhanced cavity quality factor, Q. Here, the insulating layers (I) are needed between the superconducting layers (S) to (i) suppress the Josephson currents between the screening superconducting layers so that magnetic field (H) at the interior surface of the Nb cavity is smaller than the bulk Hc1 ≅ 150 mT of clean Nb and (ii) to impede propagation of magnetic field vortices that might form to decrease losses resulting from such vortex propagation near the interior surface of the cavity. Proposed candidate superconducting materials for this system include: NbN, NbTiN, Nb_3Sn, MgB_2 and possibly other more exotic materials. The ultimate goal of the SIS structures is to reduce or even eliminate strong dissipation of vortices in a thin film geometry for which no thermodynamically stable position of a single vortex exists up to $H \approx H_{sh}$. An important feature to take into account is that it is well known that superconducting films thinner than their London penetration depths exhibit enhanced Hc1 values in the parallel field geometry compared to bulk, but – concerning screening ability, this enhanced Hc1 would be relevant primarily for the special metastable state in which the trapped field in the insulating layer is equal to the applied field H; more importantly a thermodynamically stable vortex situation with strong RF

*Work supported by the Defense Threat Reduction Agency HRDTA1-10-1-0072
mcburton@email.wm.edu

SUPERCONDUCTING COATINGS SYNTHETIZED BY CVD/PECVD FOR SRF CAVITIES

P. Pizzol[1,4], A. Hannah[1], R. Valizadeh[1], O.B. Malyshev[1], S. Pattalwar[1], G. B. G. Stenning[2], T. Heil[3], P. R. Chalker[4]
[1] ASTeC, STFC Daresbury Laboratory, Warrington, UK
[2] ISIS, STFC Rutherford Appleton Laboratory, Didcot, UK
[3] Nanoinvestigation Centre at Liverpool, University of Liverpool, Liverpool, UK
[4] Department of Material Science, University of Liverpool, Liverpool, UK

Abstract

Finding a way to overcome the acceleration gradient limits that bulk niobium cavities can provide is a major challenge, fundamental to allow the accelerator science field to progress.

In order to overcome the accelerating gradient limits of bulk niobium and reduce manufacturing and operation costs, the idea of using thin layers of niobium deposited on a copper cavity is being explored. This approach has lower material cost with higher availability and more importantly higher thermal conductivity.

Physical vapour deposition (PVD) method is currently the preferred method to coat superconducting cavities, but its lack of conformity renders complicated shapes such as crab cavities very difficult to coat. By using chemical vapour deposition (CVD) and plasma enhanced chemical vapour deposition (PECVD) it is possible to deposit thin Nb layers uniformly with density very close to bulk material. This project explores the use of PECVD / CVD techniques to deposit metallic niobium on copper using $NbCl_5$ as precursor and hydrogen as a coreagent. The samples obtained were then characterized via SEM, XRD, and EDX as well as assessing their superconductivity characteristics (RRR and T_c) The samples deposited are superconductive and polycrystalline; the sample obtained with PECVD exhibited RRR=9 and T_c= 9.4 K. The film grew in a (100) preferred orientation.

A successful preliminary deposition of NbN has also been performed and analyzed via EDX.

INTRODUCTION

SRF niobium cavities are used in particle accelerators to provide accelerating gradients with low power dissipation than traditional copper cavities. Bulk niobium has been exploited to its technological limit [1], leading the research to explore alternative ways to progress. Since the SRF requires less than 1 micron of material, it could be possible to obtain the same properties of niobium bulk with niobium thin films [2]. Thin films are a considerably cheaper option than bulk materials for the following reasons, firstly less material is being used and secondly, since SRF cavities operate at temperatures below 10 K, the films can be deposited on high thermal conductivity materials such as copper making it easier to cool and maintain the low temperatures than with bulk superconductors [3]. Theoretical studies [4] have also suggested that the use of Superconductor / Insulator / Superconductor thin films (ISI) can lead to an increase in the accelerating gradient, surpassing the limits of bulk niobium. These superconductor thin films could then be chosen from a range of alloys with a higher H_c and T_c, such as NbN, Nb_3Sn or MgB_2. CVD [5] is a chemically driven technique that allows the coating of large areas with great control over the produced film. This technique is therefore being explored to verify the feasibility of depositing metallic niobium nitrate with a homogeneous and uniform structure.

The purpose of the present study is to deposit thin films of Nb using CVD and plasma enhanced CVD (PECVD) techniques, and to deposit thin films of NbN using plasma enhanced CVD (PECVD) techniques. The use of plasma enables the creation of N radicals, the reduction of the deposition temperature and allows coating of shapes with a high degree of complexity, such as cavities [6]. After microstructural evaluation, the films have then been assessed for their superconducting properties showing their suitability for use in SRF cavities.

EXPERIMENTAL SETUP

A steel spherical chamber is kept at a base pressure of 10^{-6} mbar and constantly heated to 120 °C. The carrier gas (argon) and the reducing gas (hydrogen) are purified through a heated filters system to ensure that the presence of residual contaminants in the deposition chamber is kept as low as possible.

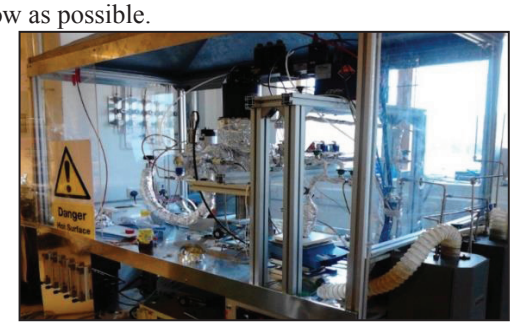

Figure 1: Deposition facility.

The chemical precursor ($NbCl_5$) is placed under controlled atmosphere in a two-legged steel bubbler. The bubbler is then connected to the deposition rig and

ISBN 978-3-95450-178-6

HIGH POWER IMPULSE MAGNETRON SPUTTERING OF THIN FILMS FOR SUPERCONDUCTING RF CAVITIES*

S. Wilde[1,6], R. Valizadeh[1], O.B. Malyshev[1], N.P. Barradas[2], E. Alves[3,4] G.B.G. Stenning[5], A. Hannah[1], S. Pattalwar[1], B. Chesca[6]

[1] ASTeC, STFC Daresbury Laboratory, Warrington, UK
[2] C²TN, Centro de Ciências Tecnológicas e Nucleares, Portugal
[3] IPFN, Instituto de Plasmas e Fusão Nuclear, Portugal
[4] Laboratório de Aceleradores e Tecnologias de Radiação, Portugal
[5] ISIS, STFC Rutherford Appleton Laboratory, Didcot, UK
[6] Department of Physics, Loughborough University, Loughborough, UK

Abstract

The production of superconducting coatings for radio frequency cavities is a rapidly developing field that should ultimately lead to acceleration gradients greater than those obtained by bulk Nb RF cavities. The use of thin films made from superconductors with thermodynamic critical field, $H_C > H_C^{Nb}$, allows the possibility of multilayer superconductor – insulator – superconductor (SIS) films and also accelerators that could operate at temperatures above the 2 K typically used. SIS films theoretically allow increased acceleration gradient due to magnetic shielding of underlying superconducting layers [1] and higher operating temperature can reduce cost [2]. High impulse magnetron sputtering (HiPIMS) and pulsed DC magnetron sputtering processes were used to deposit NbN and NbTiN thin films onto Si(100) substrate. The films were characterised using scanning electron microscopy (SEM), x-ray diffraction (XRD), Rutherford back-scattering spectroscopy (RBS) and a four point probe.

INTRODUCTION

Superconducting radio frequency (SRF) cavity technology in particle accelerators is now reaching the limit of performance achievable with bulk Nb cavities [3]. Since superconducting properties for SRF are confined to a penetration depth of less than one micron [4] then superconducting thin-films offer an alternative to bulk Nb with the advantage of Cu substrates which have a factor of three higher thermal conductivity than Nb [5]. Multilayer SIS films have been suggested as a way to increase accelerating voltages further by utilising an increased first critical field (B_{c1}) for superconducting layers with $H_C > H_C^{Nb}$ and thickness (d) less than λ, to shield an underlying Nb layer (Fig. 1). Equation 1 shows that as film thickness and coherence length, ξ, get smaller then B_{c1} increases in the overlying superconducting layers [1]:

$$B_{C1} = \frac{2\phi_0}{\pi d^2} ln \frac{d}{1.07\xi} \quad d < \lambda \,. \qquad (1)$$

Another use of superconducting materials other than Nb is to reduce the surface resistance (R_s) of SRF cavities which allows for higher Q factors. Superconductors with $T_C > T_C^{Nb}$ have been shown to have a lower R_s than Nb at 4.2 K due to the fact that $R_S \propto e^{-T_C/T}$ [6]. It is also possible to reduce R_s further by combining higher T_C with as small a normal state low temperature resistivity as possible [7]. Operation at 4.2 K can provide reduced operational costs.

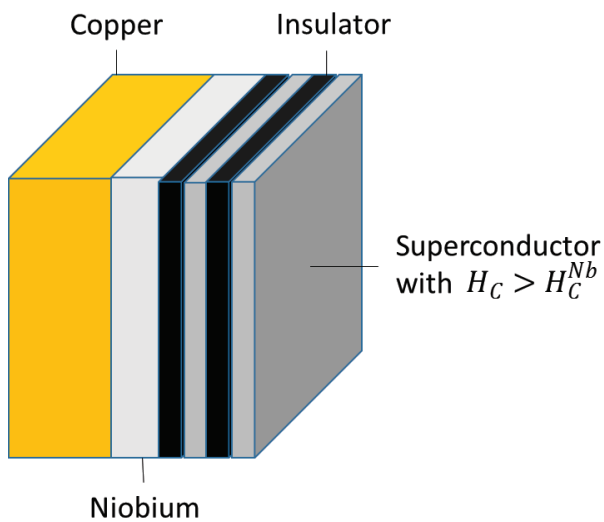

Figure 1: A schematic representation of an SIS multilayer film deposited on to Cu substrate.

The purpose of the present study is to deposit and then characterise a selection of NbN and NbTiN thin films that would be suitable for use in both SIS multilayer coatings or for operation in accelerators at 4.2 K. NbN was chosen for to its H_C of 0.23 T which is higher than the 0.2 T of Nb. NbN also has a high T_C of 17.3 K, small ξ of 2.9 nm and λ of 375 nm [6]. One drawback of NbN is its high normal state resistivity. NbTiN was therefore considered due to its smaller resistivity than NbN [2], higher T_C of 18 K, ξ of 3.8 nm [8] and λ of 150 nm. Films were deposited by reactive sputtering in a mixture of Kr and N_2 gas using three inch planar magnetrons utilising either an Ionautics

ISBN 978-3-95450-178-6

TESTING Nb3Sn COATING USING μSR

R.E. Laxdal, T. Buck, TRIUMF, Vancouver, Canada
M. Liepe, S. Posen*, Cornell, Ithaca, USA
R. Kiefl, S. Gheidi, UBC, Vancouver, Canada

Abstract

The SRF group at TRIUMF has tested samples relevant for SRF application since 2010 using the TRIUMF μSR facility. In this study collaborators at Cornell coat a Nb coin and a Nb ellipsoid sample with Nb3Sn for characterization using μSR at TRIUMF. Field of first flux entry measurements are performed at M20 on both samples. Measurements include the vortex nucleation field $H_{nucleate}$ and T_c of both Nb3Sn and Nb. Interestingly the Nb3Sn increases the vortex nucleation field at 2K over standard Nb samples.

INTRODUCTION

μSR (muon spin rotation) is a powerful condensed matter technique to characterize superconductors in terms of their magnetic-phase diagram. Since 2010 the SRF group at TRIUMF has been using the μSR technique to characterize materials and processing techniques typical for the SRF community using the TRIUMF surface muon beam [1][2]. Typical samples have been prepared from RRR Nb either as coins or in a machined ellipsoid geometry. In this paper we present results on measurements of a Nb coin and ellipsoid each coated with a 2 μm layer of Nb3Sn.

The performance of niobium as an SRF material is reaching critical limits in terms of surface resistance and peak surface field. Alternative superconductors to niobium are being developed to offer a way to push performance beyond Nb. One very promising material is Nb3Sn, a Type-II superconductor with a relatively high Kappa (~40) as opposed to 1.4 for Nb. Nb3Sn has a relatively high critical temperature, 18K, double that of Nb which allows for example to operate 1.3GHz cavities at 4.2K with the same losses as for Nb at 2K. Although H_{c1} for Nb3Sn is relatively low, 38mT, as opposed to 170mT for Nb, Nb3Sn has a high superheating field, 400mT, compared to 220mT for Nb and an extended mixed phase with an H_{c2} of ~30T.

A Nb3Sn SRF program began at Cornell University in 2009. The program has achieved some significant milestones with a 1.3GHz single cell cavity: (1) reproducible high Q0 on the order of 10^{10} at 4.2 K, (2) reproducible sustaining of this high Q0 to useful gradients ~14 MV/m, and (3) reproducible H_{pk} significantly higher than H_{c1} with no strong degradation, showing that it is not a limit [3].

A comparison of the main superconducting properties of Nb and Nb3Sn (close to stoichiometric) is presented in Table 1 [4] at T = 0. The goal of this experiment is to characterize the performance of Nb3Sn in terms of its ability to repel magnetic field as a function of temperature.

Table 1: Superconducting Properties of Nb and Nb3Sn

Property	Nb	Nb3Sn
Tc [K]	9.2	18
$\mu_0 H_{c1}$ [T]	0.17	0.038
$\mu_0 H_c$ [T]	0.2	0.52
$\mu_0 H_{c2}$ [T]	0.4	30
$\mu_0 H_{sh}$ [T]*	0.24	0.43
ξGL(0) [nm]	29	3.3
λeff(0) [nm]	41	135
κ(0)	1.4	41
Δ(0) [meV]	1.4	3.4

*All values quoted from [4] except H_{sh} which is computed from [5]

$$H_{sh} = H_c \cdot \left(\frac{\sqrt{20}}{6} + \frac{0.55}{\sqrt{\kappa}} \right) \quad (1)$$

EXPERIMENTAL METHOD

μSR Technique

In a μSR experiment, 100% spin polarized muons are implanted one at a time into the sample, stop in interstitial sites and precess with characteristic Larmor frequencies determined by the local magnetic field. The geometry of the TF measurement is illustrated in Fig. 1. The muons travel down the beam line and pass through an initial muon counter that starts an electronic clock. The muons then pass through a silver mask with an 8mm diameter hole in the centre used to restrict the measured muons to the centre of the sample. The muons will decay with a

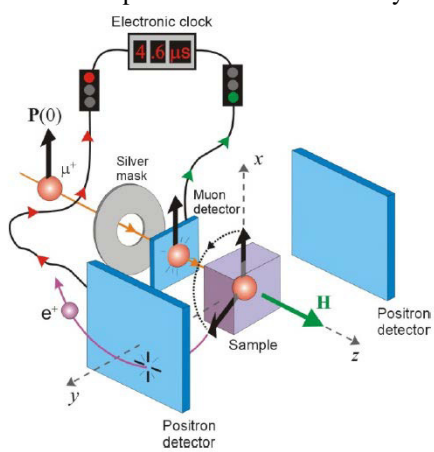

Figure 1: TF-μSR setup with the initial muon spin polarization perpendicular to the magnetic field. The silver mask in front of the sample restricts the muon implantation to the central region of the sample.

*now at FNAL

ISBN 978-3-95450-178-6

LOW ENERGY MUON SPIN ROTATION AND POINT CONTACT TUNNELING APPLIED TO NIOBIUM FILMS FOR SRF CAVITIES

T. Junginger *[1,2], S. Calatroni[3], T. Proschka[5], T. Proslier[6], Z. Salman[5], A. Suter[5], G. Terenziani[3,4], and J. Zasadzinski[7]

[1]TRIUMF Canada's National Laboratory for Particle and Nuclear Physics, Vancouver
[2]Helmholtz-Zentrum Berlin fuer Materialien und Energie (HZB), Germany
[3]European Organisation for Nuclear Research (Cern), Geneva, Switzerland
[4]Sheffield University, UK
[5]Paul Scherrer Institut (PSI), Villigen, Switzerland
[6]Argonne National Lab (ANL), USA
[7]Illinois Institute of Technology, Chicago, USA

Abstract

Muon spin rotation (μSR) and point contact tunneling (PCT) are used since several years for bulk niobium studies. Here we present studies on niobium thin film samples of different deposition techniques (diode, magnetron and HIPIMS) and compare the results with RF measurements and bulk niobium results. It is consistently found from μSR and RF measurements that HIPIMS can be used to produce thin films of high RRR. Hints for magnetism are especially found on the HIPIMS samples. These could possibly contribute to the field dependent losses of superconducting cavities, which are strongly pronounced in niobium on copper cavities.

CURRENT LIMITATIONS OF NIOBIUM ON COPPER CAVITIES

Superconducting cavities prepared by coating a micrometer thick niobium film on a copper substrate enable a lower surface resistance than bulk niobium at 4.5 K the operation temperature of several accelerators using this technology, like the LHC or the HIE-Isolde project. Additionally Nb/Cu cavities have lower material cost, and do not need to be shielded against the earth's magnetic field [1]. Thermal stability is enhanced avoiding quenches [1].

Despite these advantages, the Nb/Cu technology is currently not considered for accelerators requiring highest accelerating gradient E_{acc} or lowest surface resistance R_S at temperatures of 2 K and below, because R_S increases strongly with E_{acc}. The origin of this field dependent surface resistance has been the subject of many past and recent studies [2–5], but is still far from being fully understood. The film thickness of about 1.5 μm is large compared to the London penetration depth λ_L of about 32 nm. Differences in the performance (apart from thermal conductivity issues) should therefore be correlated to the manufacturing procedure and the resulting surface structure. Since no single dominant source can be expected, several hypotheses need to be addressed individually to identify their origin and possibly reduce their extent.

Surface Magnetism, a Possible Cause of Dissipation

A possible source of dissipation could be surface magnetism in the oxide layer. Surface magnetism has been found on bulk niobium samples by point contact tunneling [6]. Especially samples cut out from cavity hot spots show strong hints for surface magnetism [7]. This can be correlated to ferromagnetism of nanoparticles in the metal oxides. In Ref. [8] several metal oxid layers were found to have magnetic impurities and ferromagnetism. It was suggested that ferromagnetism is a universal feature of nanoparticles in otherwise nonmagnetic oxides. It is interesting to note that only nanoparticles in the oxides with a size of about 10 nm showed ferromagnetism. If the material was pressed into a bar and sintered the sample became diamagnetic. By sputtering Nb one usually obtains a grain size of several 10 nm, about 2-3 orders of magnitude smaller than fine grain bulk niobium. Nanoparticles could possibly be formed along/between grain boundaries. If they are responsible for dissipation the effect could therefore be a lot stronger for Nb/Cu cavities.

LE-μSR MEASUREMENTS

Direct Measurement of the London Penetration

Low energy muon spin (LE-μSR) rotation enables the measurement of the magnetic field inside a sample as a function of depth. An external magnetic field with a value below H_c can be applied to probe the London penetration depth of a superconductors as has been done first in 2010 [9] and recently for bulk niobium samples prepared for superconducting cavities [10]. If no external magnetic field is applied LE-μSR can be used as a local probe for surface magnetism.

The aim of the μSR experiment presented here was to test whether there are spatial variations in the penetration depth as found in Ref. [10] and/or surface magnetization of niobium thin films on copper substrates prepared by sputter

* tobi@triumf.ca

ISBN 978-3-95450-178-6

HIGH QUALITY FACTOR STUDIES IN SRF Nb_3Sn CAVITIES*

Daniel Leslie Hall†, Brian Clasby, Holly Conklin, Ralf Georg Eichhorn,
Terri Gruber, Georg H. Hoffstaetter, John Julian Kaufman, Matthias Liepe
Cornell Laboratory for Accelerator-Based Sciences and Education (CLASSE),
Ithaca, NY 14853, USA

Abstract

A significant advantage of Nb_3Sn coated on niobium over conventional bulk niobium is the substantial reduction in the BCS losses at equal temperatures of the former relative to the latter. The quality factor of a 1.3 GHz Nb_3Sn cavity is thus almost entirely dictated by the residual resistance at temperatures at and below 4.2 K, which, if minimised, offers the ability to operate the cavity in liquid helium at atmospheric pressure with quality factors exceeding 4×10^{10}. In this paper we look at the impact of the cooldown procedure – which is intrinsically linked to the effect of spatial and temporal gradients – and the impact of external ambient magnetic fields on the performance of a Nb_3Sn cavity.

INTRODUCTION

Recent work on Nb_3Sn cavities fabricated at Cornell University [1–3] has focused understanding sources of RF losses in these cavities. In particular, since Nb_3Sn cavities must be cooled slowly through T_c to avoid the creation of excessive flux-generating thermal currents between the Nb_3Sn layer and the niobium substrate, the sensitivity of the cavity to trapped flux must be determined. This is because previous studies in niobium [4] have shown that cooling a cavity slowly through T_c traps more external flux, which will cause an increase in the residual resistance. In this paper we present results on the impact on the cavity surface resistance of both the thermal gradient across the cavity during cooldown as well as the sensitivity of Nb_3Sn cavities to trapped magnetic flux. We also present the first results of a measurement of the change in the superconducting energy gap as a function of the RF magnetic field on the surface of the cavity. It has been theorised [5] that the spectral gap may close as the applied RF magnetic field is increased. The effect of this should be two-fold: firstly, the BCS resistance should increase with the accelerating gradient in the cavity, and secondly, the ultimate quench field can be reduced to lower than that expected by the superheating field H_{sh} of the material in the clean limit.

EXPERIMENTAL PROCEDURE

These studies were performed on the Nb_3Sn coated 1.3 GHz single-cell cavity designated ERL1-4, which has shown the best performance to date in a cavity coated at Cornell. The cavity was coated with tin for 3 hours, following which it was annealed for 30 minutes; a more in-depth description of the coating apparatus and procedure is given in Ref. [1]. The cavity was tested on a vertical test stand inserted in a cryostat that is magnetically shield with a mu-metal lining, resulting in an ambient magnetic field of 2-3 mG. To cool the cavity in a controlled manner, a specially designed heater is used to control the temperature of the helium that is introduced into the cryostat. The procedure is described more completely in Ref. [1]; recently, however, the procedure has been improved to allow a reduced temperature gradient across the cavity – by approx. a factor of 5 – while maintaining the same cooling rate.

The studies on the effects of trapped flux were performed using the method described in Ref. [4]. An external Helmholtz coil surrounding the cavity is used to apply an external magnetic field that is then trapped in the cavity as it transitions through T_c. The impact on the residual resistance is then measurement to gauge the cavity's susceptibility to trapped flux.

To measure the dependence of the superconducting energy gap on the surface RF magnetic field, a measurement of surface resistance against accelerating gradient was performed at different temperatures between 2.0 and 4.2 K when no external magnetic field was applied. The BCS fitting was then used to determine the value of the gap at different values of RF surface field based on the change in surface resistance between 2.0 and 4.2 K.

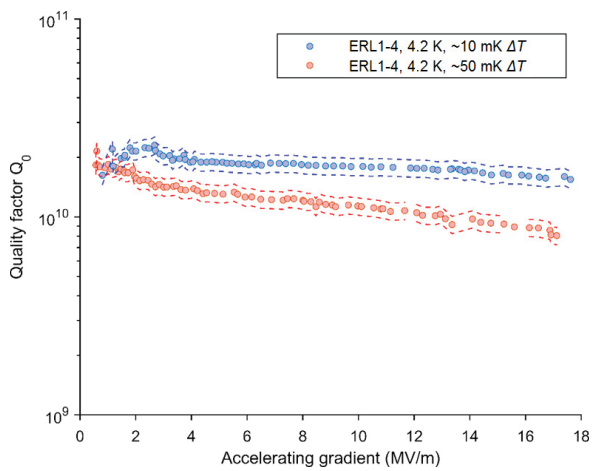

Figure 1: Two separate tests of the 1.3 GHz Nb_3Sn cavity designated ERL1-4, taken at a bath temperature of 4.2 K. The cooldown procedure was improved between the tests, with the thermal gradient across the cell, ΔT having been reduced by a factor of ≈ 5, which results in a significantly reduced Q-slope.

* Work supported by DOE grant DE-SC0008431 and NSF grant PHY-141638
† dlh269@cornell.edu

ISBN 978-3-95450-178-6

SURFACE ANALYSIS AND MATERIAL PROPERTY STUDIES OF Nb_3Sn ON NIOBIUM FOR USE IN SRF CAVITIES*

D.L. Hall, H. Conklin, T. Gruber, J.J. Kaufman, M. Liepe, J.T. Maniscalco, B. Yu
Cornell Laboratory for Accelerator-Based Sciences and Education (CLASSE),
Ithaca, NY 14853, USA
T. Proslier
Argonne National Laboratory, Argonne, Illinois 60439, USA

Abstract

Studies of superconducting Nb_3Sn cavities and samples at Cornell University and Argonne National Lab have shown that current state-of-the-art Nb_3Sn cavities are limited by material properties and imperfections. In particular, the presence of regions within the Nb_3Sn layer that are deficient in tin are suspected to be the cause of the lower than expected peak accelerating gradient. In this paper we present results from a material study of the Nb_3Sn layer fabricated using the vapour deposition method, with data collected using AFM, SEM, TEM, EDX, and XRD methods as well as with pulsed RF testing.

INTRODUCTION

Nb_3Sn cavities fabricated at Cornell University have shown good performance without suffering from the Q-slope seen in cavities coated previously [1–3]. In this paper we present results aimed at characterising the material properties of the Nb_3Sn fabricated at Cornell, with an aim to understand current CW quench fields of approx. 65-70 mT seen in the majority of these cavities. Measurements of the surface topology, flux entry field, and phase content are presented here.

FLUX ENTRY FIELD

Measurements of the flux entry field, which at its theoretical limit would be the superheating field H_{sh}, were performed on two separate cavities using Cornell's 1.3 GHz high power pulsed klystron. The 1.3 GHz, single-cell cavities received the same coating recipe, consisting of a 3 hour coating and a 6 hour annealing stage; an in-depth description of the coating apparatus and proces is given in Refs. (CITE TALK AND THESIS). Both showed similar behaviour in vertical tests. A plot of the flux entry field against the square of the bath temperature is shown for the most recently tested cavity is shown in Fig. 1. The results from the previously tested cavity can be found in Ref. [2].

The cavities both show similar behaviour, with two evidently separate linear regions appearing above and below 15-16 K. These have been fitted with the empirically expected approximate temperature dependence of the superheating field,

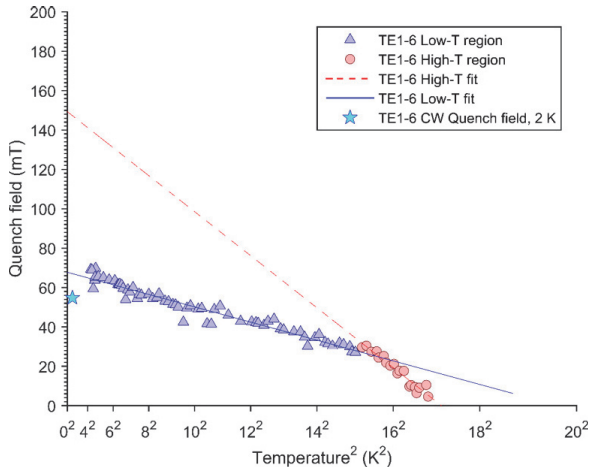

Figure 1: Results from the high pulsed power RF test, showing the flux entry field as a function of bath temperature squared. Both this cavity and that shown in Ref. [2] show two distinct slopes when going from 2^2 to 18^2 K^2.

$$H_{sh}(T) = H_{sh}(0)\left(1 - \left(\frac{T}{T_c}\right)^2\right) . \quad (1)$$

In both of the high temperature cases, the fit gives a zero-temperature flux entry field, H_{fe}, 150-250 mT, lower than the expected $H_{sh} \approx 400$ mT. Below $15^2 - 16^2$ K^2, the extrapolated H_{fe} is further reduced. This behaviour suggests that two superconductors are in effect, one dominating the RF performance near T_c and the other below 15 – 16 K.

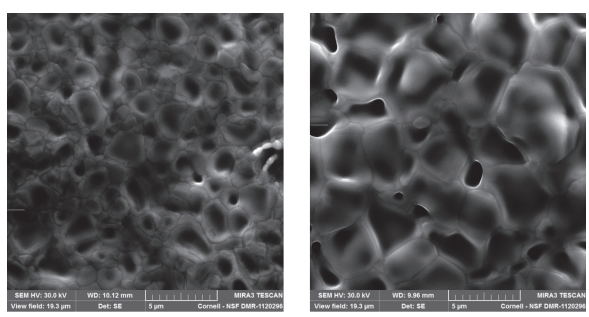

Figure 2: An SEM image of the Nb_3Sn layer for samples from two different coatings which were annealed at different temperatures, a) 1100°C and b) 1200°C.

* Work supported by DOE grant DE-SC0008431 and NSF grant PHY-141638. This work made use of the Cornell Center for Materials Research Shared Facilities which are supported through the NSF MRSEC program (DMR-1120296)

ISBN 978-3-95450-178-6

STRUCTURE AND COMPOSITION OF Nb_3Sn DIFFUSION COATED FILMS ON Nb*

Jay Tuggle, Virginia Tech, Blacksburg, VA 24061, USA
Grigory Eremeev, Charles E. Reece, Jefferson Lab, Newport News VA 23602, USA
Hanyang Xu, Michael J. Kelley#, College of William & Mary, Williamsburg VA, 23187, USA

Abstract

The structure and composition of Nb_3Sn films obtained by diffusion coating niobium coupons and SRF cavities were investigated by x-ray photoelectron spectroscopy (XPS), secondary ion mass spectroscopy (SIMS) and scanning electron microscopy (SEM) with energy-dispersive x-ray spectroscopy (EDS) and electron back-scatter diffraction (EBSD), including native surfaces, depth profiles and cross-sections. We find that the native surface oxide is significantly tin-rich, we have measured depth profiles. We find that the grains apparent in the SEM images are individual crystallites having no evident relationship to the substrate or each other.

INTRODUCTION

Advanced particle accelerators are a critical tool for frontier science. Superconducting radio frequency (SRF) technology continues to grow as the choice for high-end machines because of cost and performance advantages over warm copper. Nonetheless, the initial cryoplant and ongoing electric powers costs of the presently-required 2 K operation are a significant burden for today's niobium cavity machines. Operation at 4.2 K instead would be a major benefit.

More than 40 years ago, accelerator science researchers exploring alternatives to pure niobium settled on Nb_3Sn as the most promising alternative. Their preferred embodiment was a few-micron thick layer formed by diffusion coating. Extensive R&D programs at Siemens and at the University of Wuppertal into the 1990's sought to achieve a readily deployable Nb_3Sn SRF cavity technology. Despite aggressive efforts to the contrary, the best and typical cavity performance featured quality factors in the mid 10^{10} to low 10^{11} range at few MeV/m gradients, which fell sharply with increasing gradient. Meanwhile, the performance of pure niobium cavities continued to improve. While the cause was never clearly identified, the consensus view was that the slope is something inherent to Nb_3Sn and research activity declined.

Recently, however, performance results obtained by researchers at Cornell were essentially free of the slope, achieving gradients in excess of 10 MeV/m with diffusion-coated cavities.

*Partially authored by Jefferson Science Associates, LLC under U.S. DOE Contract No. DE-AC05-06OR23177. College of William & Mary supported by U.S. DOE Office of High Energy Physics under grant DE-SC-0014475.
#mkelley@jlab.org

The prospect of success has thus re-emerged. Further, during the years since Wuppertal, the needs of microelectronics technology have driven development of an arsenal of powerful materials characterization tools that can wrest new insights from systems like Nb_3Sn diffusion coatings. Accordingly, Jefferson Lab and its university partners were motivated to undertake a research program aimed at diffusion coating. A diffusion coating facility, described elsewhere in these proceedings [1], was constructed to provide materials for research and coated cavities for performance studies. A goal for the present research was to explore what modern characterization tools might reveal about Nb_3Sn diffusion coatings, choosing the most effective for extensive investigation in the next program phase.

EXPERIMENTAL STUDIES

The material for the present study was 10 mm square coupons cut by electrical discharge machining from trimmings of the 3 mm thick niobium sheet used to make SRF cavities ("RRR grade"). Typical grain size was in the 50 µm to 100 µm range ("polycrystals"). The availability of large-grained sheet made possible to cut some coupons consisting of two grains with a single grain boundary lying side-to-side at the center ("bicrystals"). Coupons were prepared into conditions typical of cavity production: buffered chemical polishing (BCP), centrifugal barrel polishing (CBP) and electropolishing (EP). They were diffusion coated along with specially metallographically polished coupons ("nanopolished", NP). The details of the diffusion coating facility and its operation, the topography of the resulting coatings and its investigation by atomic force microscopy (AFM) are described in a companion paper in these proceedings.

The most widely applied surface analysis technique is X-Ray Photoelectron Spectroscopy (XPS), revealing the elemental composition and chemical state of the first few nanometers of a solid surface down to roughly a part per thousand [2]. Lateral resolution is 10 – 20 µm, somewhat depending on the sample. The XPS measurements were carried out in an ULVAC-PHI "Quantera SXM" instrument equipped with a monochromated aluminum anode. Surface analyses were collected at 50 W/15 kV using a 200 µm spot size, 45° take off angle. Survey scans were done using a pass energy of 280 eV, while high resolution scans used a pass energy of 26.00 eV. For depth profiles, sputtering was accomplished via an argon ion source at 5 kV over a 3 mm^2 area. Depth profile data was collected at 50 W/15kV with a spot size of 200 µm, 45^o take off angle and 140 eV pass energy. Data were

ISBN 978-3-95450-178-6

NEXT GENERATION OF SRF-GUNS: LOW SECONDARY ELECTRON YIELD BASED ON A THIN FILM APPROACH

C. Schlemper#, M. Vogel, X. Jiang, University of Siegen, Germany

Abstract

Multipacting is a common issue in the context of cathode units of superconducting radiofrequency photoinjectors (SRF-guns) utilized in linear accelerators under resonant conditions. In this study, Titanium Nitride (TiN) and Carbon thin films have been prepared by DC and RF magnetron sputtering in a Nitrogen and Argon plasma discharge, respectively. Films featuring a thickness of about 600 nm were produced under various deposition conditions on substrates such as Copper, Molybdenum, and Silicon. Materials characterization was carried out utilizing SEM, Raman and FTIR spectroscopy, XRD and AFM. In order to evaluate the secondary electron yield (SEY) a new device is introduced, which is capable of quasi in-situ measurements. The latter is realized by connecting the coating-, the SEY- and a contamination chamber into one setup allowing sample transfer under UHV conditions. Even after an exposure to air, carbon shows SEY values down to 0.69. These values, however, turn out to be quite sensitive with respect to the actual surface morphology. Clean TiN surfaces, on the other hand, displayed SEY values as low as 1.4. In this case the SEY value is strongly affected by potential surface contamination.

INTRODUCTION

In electron or particle accelerators, which are for instance operated at CERN or Helmholz-Zentrum Dresden-Rossendorf (HZDR), undesirable electron clouds arise which limit the accelerator operation. This phenomenon of multipacting frequently occurs at the cathode unit of superconducting radiofrequency photoinjectors (SRF guns) in linear accelerators under resonant conditions. Electrons, for example caused by field emission at the surface of a RF component, get accelerated by the RF-field and trigger an avalanche of secondary electrons which limits the beam lifetime and causes power loss. To suppress such multipacting and to prevent a deterioration of accelerator performance, a material with a correspondingly low secondary electron yield is required.

Surfaces of metal typically feature a SEY value of 1.3, whereas contaminations like air exposure usually lead to much higher SEY values up to 2.4. Consequently, a material is required that, in spite of air exposure, shows a stable SEY value below one. In this context carbon is a promising candidate which does not require bake-out and is robust against air exposure. It was demonstrated that carbon films prepared by magnetron sputtering deposition potentially fulfill these requirement [1,2]. Another promising coating candidate is TiN which also offers very low SEY values on the order of one and which can easily be deposit using RF-Magnetron-Sputtering [3]. Based on this work the goal of this paper is the preparation and analysis of these coating systems in particular, the influence of process parameters on the film properties and structure with reference to the SEY. To improve the adhesion of carbon films, especially on copper substrates, the applying of intermediate layers is also investigated.

christoph.schlemper@uni-siegen.de

EXPERIMENTAL

The films were deposited on polished Copper-plates with a diameter of 2.5cm using a CC800 PVD coating system by CemeCon (Figure 1). Prior to deposition the samples were cleaned with ethanol and distilled water to avoid contamination. High purity Krypton (99.999%) and Argon (99.999%) were used as inert sputtering gases. The carbon source was setup by two 99.9% pure graphite targets with a dimension of 40 cm x 15 cm. This setup allows for the coating of large samples such as a complete SRF-cathode. For film deposition, a target power of 3500 W was used at each graphite target leading to a power density of 5.8 W/cm². The deposition pressure varied between 500 mPa and 850 mPa depending on the gas flow ratio. Due to a rotation of the sample holder there was no constant distance between targets and sample. However, the minimum distance was 3 cm. The samples were deposit at temperatures between 60 and 630 °C, respectively, which were measured at the heating source itself. During the whole process the sample holder was biased with a medium-frequency voltage of 80 V (240 kHz). With this setting, film thicknesses of 600 nm were achieved.

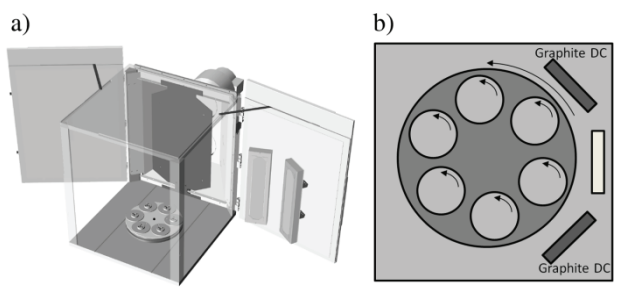

Figure 1: a) Scheme of the CC800-PVD coating system a) opened view from the side, b) closed view from the top with rotating substrate table and Graphite-DC-cathodes.

Titanium-Nitride films were produced using a different setup. The whole system is shown in Figure 2. To replace the samples, without venting the whole chamber, a load

ISBN 978-3-95450-178-6

FERMILAB Nb_3Sn R&D PROGRAM *

S. Posen†, A. Romanenko, M. Merio, and Y. Trenikhina
Fermi National Accelerator Laboratory, Batavia, IL 60510, USA

Abstract

A substantial program has been initiated at FNAL for R&D on Nb_3Sn coated cavities. Since early 2015, design, fabrication, and commissioning has been ongoing on a coating chamber, designed for deposition via vapor diffusion. The volume of the chamber will be large enough to accommodate not just R&D cavities, but full production-style cavities such as TeSLA 9-cells. In this contribution, we overview the development of the chamber and we introduce the program planned for the coming years. We discuss research paths that may yield increased maximum fields and reduced residual resistances as well as new applications that could be explored with larger coated cavities.

BACKGROUND

Nb_3Sn is a very promising alternative material to niobium for SRF cavities. Its predicted superheating field H_{sh} is approximately twice that of niobium [1], giving it the potential to offer up to double the accelerating gradients used in accelerators today. Because of its high critical temperature T_c, Nb_3Sn also can offer higher quality factors Q_0 as a function of temperature than niobium. In 1.3-1.5 GHz cavities, Q_0 of 2×10^{10} has been demonstrated at 4.2 K [2] and Q_0 of 10^{11} has been demonstrated at 2 K [3]. These qualities would make it possible to reduce the number of cavities necessary to reach a given energy, reduce the infrastructure required for a cryogenic system, and reduce the power consumption of the cryogenic system. The resulting decrease in costs would make it feasible to build large new accelerators to answer questions on the frontiers of modern physics and to operate small scale accelerators for industrial applications. These applications could include medical accelerators in hospitals, scanners for border security, transmutation devices for nuclear waste, and treatment plants for flue gas and wastewater.

Pioneering work was performed in the 1970s to 1990s at various labs to develop Nb_3Sn as an SRF material [4–10]. By the end of this period, very high Q_0-values had been observed in Nb_3Sn accelerator cavities at low fields, and peak surface magnetic fields of up to 80 mT were reported. However, strong Q-slope was observed in these cavities above 5 MV/m limited their utility in real applications [3]. Recently, additional development at Cornell led to an important performance advance: single cell 1.3 GHz cavities were produced that did not suffer from strong high field Q-slope, as shown in Fig. 1. They maintained Q_0 on the order of 10^{10} at 4.2 K out to quench fields as high as 70 mT [11].

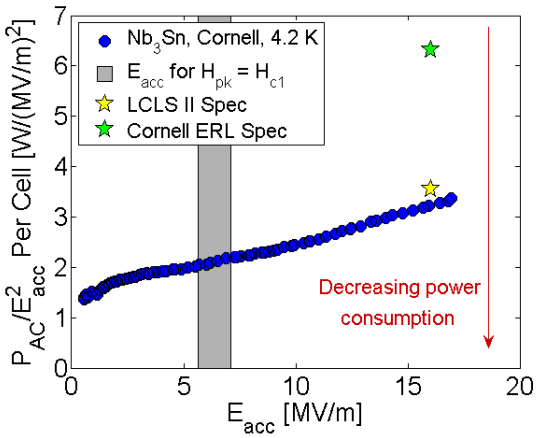

Figure 1: Recent promising results from a single cell 1.3 GHz Nb_3Sn cavity that exceeded the cryogenic efficiency and accelerating gradient specifications of LCLS II.

The proof of principle has been established: a Nb_3Sn cavity that met the cryogenic efficiency and accelerating gradient specifications of state the art high-Q_0 accelerator LCLS II [12]. Already this material is useful for industrial accelerators operating at 4.2 K. With additional development to find ways to further reduce residual resistance, Nb_3Sn could far outperform Nb for future high-Q_0 accelerators. With sustained development, preparation methods may be found that allow this material to significantly exceed the maximum fields obtained in niobium cavities.

To work towards realization of these possibilities, a substantial research and development program has begun at Fermilab on Nb_3Sn for SRF. With funding from the Laboratory Directed R&D (LDRD) program, the goals of the program include establishing Nb_3Sn fabrication facilities at Fermilab, material research and development, and coating of production-style cavities.

Nb_3Sn FACILITIES AT FERMILAB

A CAD model of the planned Nb_3Sn fabrication apparatus is shown in Fig. 2. A niobium coating chamber will be fabricated to hold the cavity and tin source, and an existing ultra-high-vacuum (UHV) furnace will be modified to host it. The coating chamber will be large enough to hold production-style cavities, including 9-cell TeSLA cavities and 650 MHz PIP-II cavities.

Having flexibility in cavity type to coat was planned when designing this coating chamber. Possible applications for Nb_3Sn cavities include a future multi-MW proton accelerator, the Future Circular Collider at CERN [13], an upgrade to the ILC, and industrial accelerators [14]. The chamber

* This work was supported by the US Department of Energy
† sposen@fnal.gov

CUTOUT STUDY OF A Nb_3Sn CAVITY *

S. Posen†, A. Romanenko, Y. Trenikhina, O. Melnychuk, and D. A. Sergatskov
Fermi National Accelerator Laboratory, Batavia, IL 60510, USA
D. L. Hall‡, M. Liepe
Cornell Laboratory for Accelerator-Based Sciences and Education, Ithaca, NY 14853, USA

Abstract

The first 1.3 GHz single cell Nb_3Sn cavity coated at Cornell was shown in RF measurements at Cornell and FNAL to have poor RF performance. Though subsequent cavities showed much higher quality factors, this cavity exhibited Q_0 on the order of 10^9 caused by strong heating concentrated in one of the half cells. This paper presents an investigation into the source of this excess heating, for the purpose of process improvement, so that similar degradation can be avoided in future coatings. Through the use of temperature mapping both at Cornell and at FNAL, locations with high and low surface resistance were located, cut out from the cavity, and studied with microscopic tools. We present the RF measurements and temperature maps as well as the microscopic analyses, then conclude with plans for continued studies.

BACKGROUND

Nb_3Sn is a promising alternative material for SRF cavities, with the potential to increase both accelerating gradients and quality factors at a given temperature compared to niobium, reducing the cost of large accelerators and making feasible new applications for small industrial accelerators. Pioneering work was performed on this SRF material in the 1970s to 1990s at various labs [1–7], and, recently, additional development at Cornell led to 1.3 GHz Nb_3Sn cavities with Q_0 on the order of 10^{10} at accelerating gradients above 15 MV/m [8, 9].

The development effort of Nb_3Sn continues at Cornell and Fermilab, and in this paper, we present a collaborative effort between these two labs to understand a limitation that was observed in a Nb_3Sn cavity, ERL1-5. This was a 1.3 GHz single cell cavity, the first coated under Cornell's program, and it showed considerably poorer performance than cavities coated afterwards. After the first coating, it showed an unusual appearance: looking into the surfaces of the cavity visible from the beamtubes, one half-cell appeared a matte gray as expected, while the other appeared shiny, as shown in Fig. 1.

After coating, the cavity was treated only with high pressure water rinse (HPR), followed by testing, where it showed a Q_0 of 10^9 at low field, with significant Q-slope above 5 MV/m, with the accelerating gradient eventually being RF power-limited, as shown in Fig. 2. The cavity was then

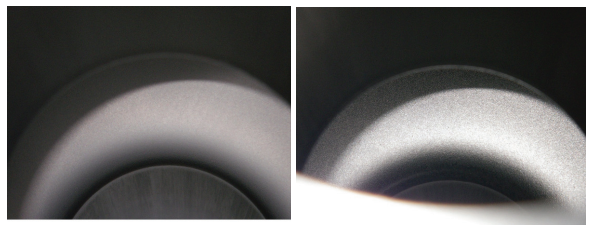

Figure 1: After coating, one half cell showed expected matte gray appearance (left) and the other showed unusually shiny appearance (right).

oxypolished and tested again, with poorer performance. Following this test, the coating was removed with BCP, and the cavity was recoated in the same orientation. Again, the same half cell appeared shiny, so a method was devised to coat the cavity in the flipped orientation, and the coating cycle was run again in this manner. Though the same half cell again appeared shiny, the cavity was tested again, and showed similar performance. The cavity was finally given two cycles of HF rinse and retested, with similar results.

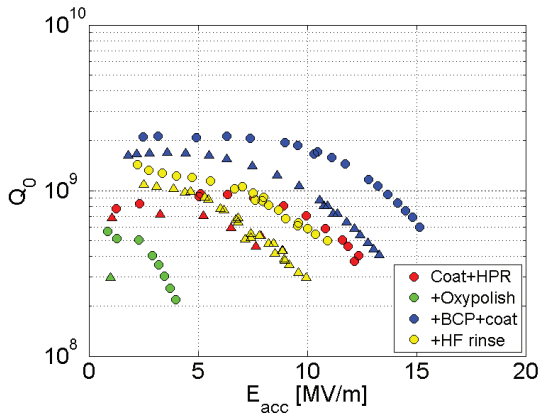

Figure 2: Q vs E curves for the cavity with unusual appearance. Curves were measured at each stage of treatment at 4.2 K (triangles) and 2 K (circles).

OPTICAL INSPECTION

An optical inspection was performed on the cavity before the BCP to remove the first coating. After optical inspection, the cavity was anodized to attempt to distinguish between niobium and tin during optical inspection. The procedure from [4] was followed, which is expected to cause niobium to turn blue and Nb_3Sn to turn purple. However, the procedure specifies that the process should be current limited

* This work was supported by the US Department of Energy and the National Science Foundation
† sposen@fnal.gov
‡ dlh269@cornell.edu

ISBN 978-3-95450-178-6

SECONDARY ELECTRON YIELD OF SRF MATERIALS

S. Aull*, CERN, Geneva, Switzerland and Universität Siegen, Germany
T. Junginger, H. Neupert, CERN, Geneva, Switzerland
J. Knobloch, Helmholtz-Zentrum Berlin and Universität Siegen, Germany

Abstract

The secondary electron yield (SEY) describes the number of electrons emitted to the vacuum per arriving electron at the surface. For a given geometry, the SEY is the defining factor for multipacting activity. In the quest of superconducting RF materials beyond bulk niobium, we studied the SEY of the currently most important candidates for future SRF applications: Nb_3Sn, NbTiN and MgB_2. All studies were done on clean but technical surfaces, i.e. on clean surfaces exposed to air and with their native oxides as it would be the case for SRF cavities.

INTRODUCTION

In the late 1970's multipacting was the main limitation for SRF cavities in terms of accelerating gradient. For multipacting to occur, free electrons need to be accelerated by the RF field, the emission and the arrival point have to meet certain symmetry criteria and the secondary electron yield (SEY) has to be greater than one [1]. Multipacting activity is suppressed as soon as one of the criteria is not fulfilled, which was achieved by optimizing the cavity geometry towards an elliptical shape. However, multipacting is still an issue for non-elliptical cavities, couplers and waveguides. The development of materials beyond niobium requires the evaluation of the secondary electron yield as a material parameter in order to avoid the return of multipacting as a performance limitation for elliptical cavities.

SECONDARY ELECTRON EMISSION

The SEY describes the number of (secondary) electrons emitted to the vacuum per arriving (primary) electron at the surface. Upon arrival the primary electron travels through the material elastically scattering with the lattice ions and inelastically scattering with electrons. The latter produce secondary electrons along the travelling path of the primary. With increasing incident energy the maximum penetration depth of the primary electron increases. Although secondary electrons are generated along the whole path the majority of secondaries is created at the end of the primary's path and the total number of secondary electrons increases with the energy of the primary electron. The secondaries diffuse into the material and get emitted if they reach the surface with a remaining energy high enough to overcome the surface-vacuum barrier [2]. The probability to escape decreases exponentially on a characteristic escape length. These two mechanisms define the typical bell shape of the SEY curve as function of primary electron energy: In the low energy regime more and more secondary electrons are produced and since they are produced close to the surface, they are likely to escape. For high primary energies, many secondary electrons are produced but they are less likely to reach the surface as they are produced deeper in the material. Both effects compensate each other leading to a maximum of the SEY curve when the penetration depth of the primary electron is comparable to the characteristic escape length. Is a SEY value reported for a given material or sample, it usually refers to this maximum.

SEY of Conductors and Insulators

The number of emitted electrons is given by the minimum energy to overcome the surface-vacuum barrier and the interaction of the secondaries with the material, i.e. the energy loss until reaching the surface. If an internal secondary electron passes through a metal, it mainly scatters on electrons in the conduction band which results in high energy loss. Once it reaches the surface it can only be emitted to the vacuum if its remaining energy exceeds the minimum escape energy which is the sum of the work function and the Fermi level and is in the order of 10 eV [3]. As a result, pure, oxide and contamination free metals have low secondary electron yields, ranging from 0.5 for lithium to 1.8 for platinum [3] while alloys range between 1.5 and 3. In contrast to metals, an internal secondary electron passing through an insulating material scatters with phonons and defects and might excite valence electrons into the conduction band if its energy is higher than the band gap. All three contributions are small compared to the scattering in metals so that the kinetic energy of many secondaries exceeds the electron affinity which is usually as low as 1 eV. As a consequence, many generated secondaries are emitted and insulators have typically SEY values $\gtrsim 4$.

MEASURING THE SEY

At CERN, there is a dedicated set-up for SEY measurements which is combined with an XPS[1] setup. This allows coupled SEY and XPS measurements at room temperature and without breaking the vacuum which results in altering the surface conditions. The SEY part is schematically shown in Figure 1 and a thorough description of the setup including a description of the electron gun and the vacuum system can be found in [4]. Primary electrons emitted from an electron gun with a certain energy bombard the sample under test. Secondary electrons as well as scattered primary electrons leave the sample surface and will be absorbed by the surrounding collector.Reemission from the collector is suppressed by positively biasing the collector. In order to

* sarah.aull@cern.ch

[1] X-ray photoelectron spectroscopy

ISBN 978-3-95450-178-6

DEVELOPMENT OF Nb_3Sn COATINGS BY MAGNETRON SPUTTERING FOR SRF CAVITIES

G. Rosaz#, S. Calatroni, F. Leaux, F. Motschmann, Z. Mydlarz, M. Taborelli, W. Vollenberg,
CERN, Geneva, Switzerland

Abstract

This paper presents the first results obtained on DC magnetron sputtering of Nb_3Sn thin films dedicated to superconducting radio frequency cavities (SRF). Nb/Sn ratio of 3.76 and 3.2 have been obtained for Ar coating pressures of respectively 1.10^{-3} mbar and 5.10^{-2} mbar. According to XRD analyses both coating pressures lead to amorphous Nb_3Sn layers that are not superconducting. Afterward, one coating has been annealed at 700°C, 750°C and 800°C under vacuum for 24h and exhibited for the three different temperatures the A15 cubic phase.

INTRODUCTION

Very low losses SRF accelerating systems, together with high-efficiency cryogenics systems, have the potential of low running costs. Nb coated Cu cavity technology used for LEP [1], LHC [2] and HIE ISODLE [3] starts to show limited performances in terms of Q-slope and quench limit. The use of A15 materials is very promising as they exhibit higher T_c value than pure Nb, allowing to reach better quality factor for a given working temperature. Recent work [4] has demonstrated the possibility to use such materials in bulk Nb cavities showing good performances. The present investigation proposes to combine the efficiency of such A15 materials with the good thermal performances of copper accelerating cavities.

The study considers the possibility to coat a copper resonator with an Nb_3Sn layer by means of DC magnetron sputtering using an alloyed target. The influence of the process parameters on the as-deposited layer stoichiometry is presented. The latter is in good agreement with previous results reported in the literature and can be fine-tuned by acting on the process gas pressure. The effect of post-coating annealing temperature on the morphology and crystallinity of the film is being also investigated.

EXPERIMENTAL PROCEDURE

A 150 mm diameter magnetron sputtering source was used to deposit Nb_3Sn from a 3 mm thick stoichiometric Nb-Sn target. All samples were coated at 150°C using a cathode-substrate distance of 100 mm with an average power of 200 W and using Ar as the sputtering process gas for 60 min. Before coating, a 135°C bakeout of the entire coating chamber was performed for at least 10 h allowing reaching a base pressure of 7.10^{-8} mbar at room temperature.

The coating pressure was tuned by modifying the process gas flow through a mass flow controller.

The substrates used in this study were:

- High purity quartz with OH content lower than 1ppm dedicated to DC superconducting properties measurements;
- OFE copper;
- Standard borosilicate glass for thickness measurements.

Film annealing was carried out in a separate furnace over 24 h under vacuum with a constant ramp-up of 200°C/hour up to three different temperatures, 700°C, 750°C and 800°C. The furnace temperature was monitored by two thermocouples showing a maximum temperature deviation within the chamber of 3°C, over the entire process. The typical maximum pressure value reached during the annealing was around 2.10^{-6} mbar.

Characterization was carried out using SEM for morphology, EDX for composition (at 10 KeV incident electron beam), XRD (θ-2θ, fixed source and rotatable sample and detector, Cu anode) for crystal structure, and profilometry for thickness measurements. Superconducting DC (Tc, RRR) properties were evaluated using a 4-probes setup cooled down to 4K using liquid He. The measures were performed at a constant current of 100 mA.

RESULTS

As Deposited Films

It is well known that the critical temperature of the Nb_3Sn phase is strongly coupled to the Sn content of the film [5]. Controlling such stoichiometry is thus compulsory to tune the film properties.

In order to modify the film stoichiometry, two different coating pressures were used, 1.10^{-3} mbar and 5.10^{-2} mbar. The resulting coating thickness were 1.6 µm and 2.1 µm respectively

Figure 1 shows that the composition depends on process pressure and is in good agreement with the previous results reported by C.T. Wu et al [6] using the same coating method. This effect is directly linked to the modulation of the mean free path of sputtered atoms leading to a change in their transmission ratios.

#guillaume.rosaz@cern.ch

ISBN 978-3-95450-178-6

HTS COATINGS FOR IMPEDANCE REDUCTION OF BEAM-INDUCED RF IMAGE CURRENTS IN THE FCC

S. Calatroni#, CERN, Geneva, Switzerland

Abstract

The FCC-hh presently under study at CERN will make use of 16 T superconducting dipoles for achieving 100 TeV p-p center-of-mass collision energy in a 100 km ring collider. A copper coated beam screen, like in the LHC, is envisaged to shield the 1.9 K dipole cold bores from the 28 W/m/beam of synchrotron radiation. Operating temperature should be in the 50 K range, as best compromise temperature in order to minimize the wall-plug power consumption of the cryogenic system. However, preliminary studies indicate that copper at 50 K might not provide low enough beam coupling impedance in the FCC-hh. It has then been proposed to reduce the beam impedance by a thin layer of a High-Temperature Superconductor (HTS), which will thus effectively shield the beam-induced RF image currents. Purpose of this paper is to define the basic requirements for an HTS film in the RF field induced by beam image currents and exposed to a high magnetic field, and to identify the best candidate materials and coating processes.

INTRODUCTION

The FCC-hh is a study for a next-generation large p-p collider aiming for a 100 TeV center-of-mass collision energy in a 100 km circumference ring [1]. Superconducting magnets at 16 T cooled at 1.9 K will steer the beam which will emit 28 W/m/beam of synchrotron radiation. A beam screen held at around 50 K will shield the magnets from it, thus allowing for a better overall cryogenic efficiency and power consumption. A similar screen in the presently running LHC makes use of a copper coating to minimize impedance for beam image currents. However the surface resistance of copper at 50 K might not be sufficiently low for the FCC-hh beam stability. The goal of this paper is to study the feasibility [2] of using High-Temperature Superconductor (HTS) coatings in order to minimize the surface impedance.

The operating conditions of HTS in the proposed FCC-hh beam screen are extremely challenging. The beam screen of about 30 mm diameter would operate in a temperature window between 40 K and 60 K, and the coatings will have to remain superconductive (in the mixed state) up to a field of 16 T. Although the beam average current is of the order of 1 A, the 8 cm long bunches of 10^{11} protons would induce in the HTS film peak currents of the order of 25 A, with a frequency spectrum extending from DC up to well above 1 GHz (Fig. 1) [3]. Assuming a thickness of 1 µm which is typical in thin films technology, this would mean that the HTS material should have a critical current density J_c of about 25 kA/cm^2 at 50 K and 16 T, of course with a reasonable safety margin, and have surface resistance in these conditions better than copper.

Several HTS have been discovered in the last 25 years having a critical temperature much larger than the classical technological superconductors. Two main families have been identified as having the highest potential for applications: the REBCO family, thus called to include several Rare Earths such as Y, Gd, Sm; and the BSCCO family, which includes not only the Bi- but also the Hg- and Tl-based compounds. Key properties of the most commonly used YBCO and BSCCO compounds used for SC cable manufacturing are listed in table 1 [4], compared to classical LTS materials.

In the following, we will analyse the RF behaviour of superconductors in such extreme conditions, identify what are the required performances and possible benefits for the FCC-hh making use of YBCO as an example, and finally underline the research needed for identifying the best possible material and ways to characterize it.

RF PROPERTIES OF A SUPERCONDUCTOR

The field and temperature dependent surface resistance of a superconductor is usually experimentally described in the following form [5]:

$$R_s(H_{rf},T,B) = R_{BCS}(H_{rf},T,0) + R_{res}(H_{rf},0,0) + R_{fl}(H_{rf},T,B) \quad (1)$$

where $R_s(H_{rf},T,B)$ indicates the total surface resistance as a function of the RF field H_{rf}, the temperature T and the external applied flux density B. In our case H_{rf}

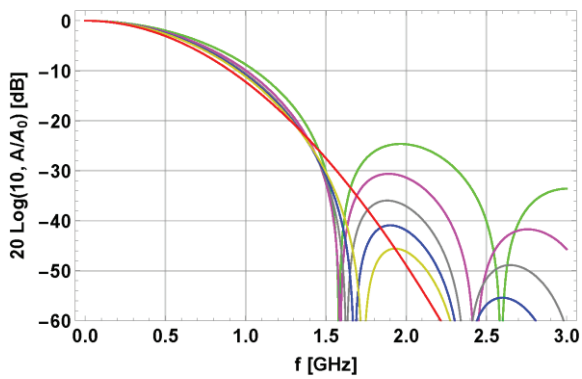

Fig. 1: frequency spectrum for 8 cm long bunch of 10^{11} p$^+$ of various shapes. Peak bunch current is about 25 A. [3]

#sergio.calatroni@cern.ch

ISBN 978-3-95450-178-6

RESEARCH ON MgB_2 AT LANL FOR THE APPLICATION TO SRF STRUCTURES*

T. Tajima#, L. Civale, R.K. Schulze, LANL, Los Alamos, NM 87545 USA

Abstract

This paper is focused on the development of MgB_2 coating technique at LANL. Using boron film samples obtained at a large furnace system, we succeeded in obtaining superconducting MgB_2 films (T_c of up to 37 K so far) by reacting them with Mg vapor. The major improvements were 1) confinement of the Mg vapor in a hot zone to mitigate the insufficient Mg pressure due to condensation on low temperature surfaces of the connected vacuum pipes and 2) reduction of cooldown time, i.e., ~13 minutes instead of ~1 day with the large system to prevent MgB_2 from decomposing.

INTRODUCTION

We have constructed and used a large coating system in a building at Technical Area 35 (TA-35) in LANL. This system has a furnace capable of coating up to a 9-cell 1.3 GHz elliptical cavity [1]. We have been unsuccessful, however, in obtaining superconducting MgB_2 films stably. The identified causes include 1) insufficient Mg vapour pressure due to the condensation on cooler surfaces on the pipes and 2) a long cooling time (~1 day). Since it was difficult to modify the current large system to address these issues, we used a small system in the SRF lab at TA-53 to verify these.

EXPERIMENTAL SETUP

While the large coating system described in Ref. [1] consisted of a hood with air venting to outside and the pressure in the room was kept slightly negative relative to outside as well as with gas monitors for hydrogen and diborane (B_2H_6 toxic) gases for safety, the small setup described here is very simple because of little concern on safety, i.e., reacting Mg vapour with the boron films obtained using the large coating system.

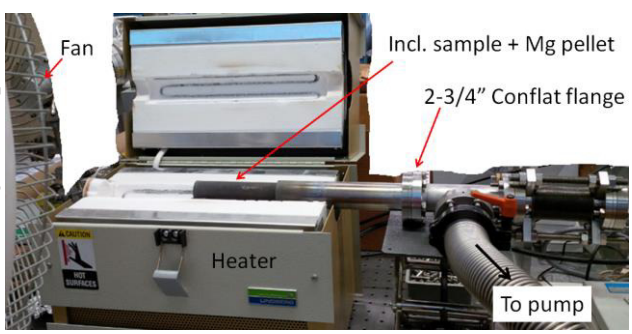

Figure 1: Experimental setup

The system consists of a tube heater (Lindberg type 55035 max. temp. 1100 °C), a turbo pump, a, diaphragm pump and vacuum gauges. Figure 1 shows a photo of the setup.

Figure 2 shows a schematic showing the inside of the stainless steel tube. A plug to confine the zone with a sample and a Mg pellet was used to keep sufficient Mg vapor pressure.

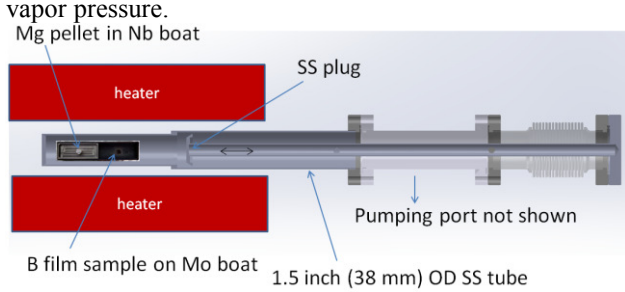

Figure 2: Inside the SS tube. The Mg pellet is on a Nb boat in a Mo boat and the B sample is in the same Mo boat. This Mo boat is confined in a smaller diameter tube after the plug closes this tube.

PROCEDURE TO GET MgB_2

At first, we tried the reaction without Ar gas, i.e., pumping down the pipe and plugged the hot zone and raised temperature, but we did not get any stoichiometric MgB_2, only got B rich films. We might not have had a good sealing of the plug, but we decided to use Ar gas to mitigate the issue of leaking of the Mg vapor since Hanna et al. were successful in obtaining clean MgB_2 films by annealing CVD-deposited B films in Mg vapor in Ar atmosphere [2].

While we need more parameter optimization to get better films, the following procedure was used to get MgB_2 films successfully.

- Bake the system at ~150 °C under vacuum for ~20 min
- Fill the system with UHP Ar gas up to 1/3 psi
- Plug the hot zone with a Mg pellet and a B film
- Raise the temperature to a planned value
- Hold it for 50 min
- Quench it to ~40 °C in ~13 min

CHARACTERIZATION OF THE FILMS

The elemental composition and their depth profile were obtained using XPS and Auger electron spectroscopy. The superconductivity transition temperature T_c was determined with magnetization measurements using a SQUID magnetometer. Figure 3 shows a summary of 3 successful samples that showed superconductivity. Figures 4 through 6 show the depth profile of B (red), Mg (green) and O (purple) for the 3 samples. Although we have not fully optimized the parameters yet, so far, the sample (c) that was annealed at

*Work supported by the US Department of Energy (DOE).
#tajima@lanl.gov

LOCAL COMPOSITION AND TOPOGRAPHY OF Nb_3Sn DIFFUSION COATINGS ON NIOBIUM *

U. Pudasaini[1], G. Eremeev[2], Charles E. Reece[2] and M. J. Kelley[1,2]
[1] Applied Science Department, College of William and Mary, Williamsburg, VA 23187, USA
[2]Thomas Jefferson National Accelerator Facility, Newport News, VA 23606, USA

Abstract

The potential for energy savings and for increased gradient continues to bring attention to Nb_3Sn-coated niobium as a future SRF cavity technology. We prepared these materials by vapor diffusion coating on polycrystalline and single crystal niobium. The effect of changing substrate preparation, coating parameters and post-treatment were examined by AFM and SEM/EDS. The AFM data were analyzed in terms of power spectral density (PSD). We found little effect of pre-coating topography on the result. The PSD's show some surprising kinship to those obtained from BCP-treated surfaces. SEM/EDS revealed no composition non-uniformities at the micron scale.

INTRODUCTION

Nb_3Sn is a superconducting material with a critical temperature and predicted superheating field nearly twice that of niobium. Accordingly, Nb_3Sn has the potential to achieve superior performance both in terms of quality factor and accelerating gradient resulting in significant reduction in both initial and operating costs.

Research on Nb_3Sn started in 1970's as a promising alternate material for SRF application. Siemens AG and University of Wuppertal took the lead.They developed a diffusion coating recipe, and successfully fabricated Nb_3Sn cavities. Operating at 4.2K, these cavities exhibited a quality factor more than 10^{10} up to an accelerating gradient approaching 5 MV/m, but then suffered a precipitous drop [1]. The reason was never firmly established, but it was speculated that it might be an implicit property of Nb_3Sn. Continuous improvement of niobium cavity performance and discovery of high temperature superconducting materials diverted attention from Nb_3Sn research. All the research activities fell off by the end of 1990's until Cornell started a Nb_3Sn development program in 2009. Their recent results from diffusion coated cavities are free from sharp drop of quality factor for accelerating gradient more than 10 MV/m. [2]. It revived hope of Nb_3Sn application for future accelerators once again.

A research program was initiated at Jlab recently to develop Nb_3Sn coated cavities. It is based on tin diffusion coating of niobium, which is the method of choice of most research institutions so far [1–3]. The goal is to determine the process parameters to obtain high-performing Nb_3Sn coated niobium cavities by materials and RF studies.

It is known that Nb_3Sn is the equilibrium phase within its composition range, 18%-25%, and that the superconducting properties degrade with decreasing tin content. It is very important to obtain a deeper understanding of how the coating process controls the coating's structure and composition, and how these control performance, showing the path to better performance. Nb_3Sn samples were prepared via tin diffusion to validate the prepared coatings. Results from a study of Nb_3Sn coated samples are presented here. The focus is to examine the composition and topography of prepared coatings and its variation.

SAMPLE PREPARATION

Materials

The substrate samples used here were 10 mm × 10 mm niobium coupons produced by EDM cutting 3 mm thick, high RRR sheet material of the type used for cavity fabrication at Jlab. These were further processed.

- The first set of samples was prepared by metallographic polishing, also known as nanopolishing (NP) at Micron Analytical Inc.
- The second set of samples was subjected to buffered chemical polishing (BCP) using a solution of 49% HF, 70% HNO_3 and 85% H_3PO_4 in the ratio of 1:1:2 by volume for 14 minutes at room temperature, expected to remove about 30-40 μm.
- The third set of samples received electropolishing (EP) using a 1:9 mixture of 49% HF and 96% H_2SO_4 for one hour at room temperature, removed about 30-40 μm. Some of the samples in this set had been subjected to centrifugal barrel polishing (CBP) prior EP.
- Other samples were only degreased with Micro90 for 15 minutes and then rinsed with deionized water.

Some samples obtained by cutting a Nb_3Sn-coated cavity were also examined. It was the same cavity coated for commissioning of the Nb_3Sn cavity vapor deposition system at Jlab [3].

Nb_3Sn Coating

The Nb_3Sn cavity deposition system commissioned recently was used for coupon coating. A detailed description of deposition system is available in [3]. We fabricated a new sample chamber for sample coating. Required tin and tin chloride were packaged in niobium foils. One package (1 gm) of tin and two packages (2×0.5 gm) of tin chloride were placed on the floor of the sample chamber on the niobium foil

* Partially Authored by Jefferson Science Associates, LLC under U.S. DOE Contract No. DE-AC05-06OR23177. College of William & Mary supported by U.S. DOE Office of High Energy Physics under grant DE-SC-0014475.

ISBN 978-3-95450-178-6

CHARACTERIZATION OF Nb_3Sn COATED Nb SAMPLES

Y. Trenikhina*, S. Posen, FNAL, Fermilab, Batavia, IL, USA
D. Hall, M. Liepe, Cornell University, Ithaca, USA

Abstract

Nb_3Sn has great potential to replace traditional Nb for the fabrication of SRF cavities. The higher critical temperature of Nb_3Sn potentially allows for an increased operational temperature in SRF cavities, which could save tremendous funding and effort. We present preliminary characterization of a Nb_3Sn layer grown on flat a Nb sample prepared by the same chemical vapor deposition method that is used for the cavity coating. XRD, SEM, STEM/EDS, TEM imaging and diffraction characterization was used in order to evaluate any chemical and structural defects that could be responsible for the limited quench field and high residual resistance. Variation of local stoichiometry was found in the Nb_3Sn layer, which is in line with previous studies. Regions of decreased Sn content can have a lower Tc in comparison to the stoichiometric composition, which may be responsible for the limited performance. AES investigations of the Nb_3Sn surface after HF-rinse were done in order to explore the mechanism that is responsible for the performance degradation of HF-rinsed Nb_3Sn coated cavities.

INTRODUCTION

Growing demand for higher SRF cavity performance at higher accelerating gradients brings traditional niobium to it's theoretical limits. Nb_3Sn alloy is one of the primary alternative materials for SRF cavity production. Being a type II superconductor with maximum T_c of 18K and superheating field of 400 mT, Nb_3Sn offers a much broader parameter space for new SRF performance records. An optimized chemical vapor deposition method adopted at Cornell university for the production of Nb_3Sn coating on Nb cavities has shown the great potential of Nb_3Sn for SRF applications. However early quenching and elevated residual resistance were found to limit SRF performance of Nb_3Sn coated Nb cavities [1].

In order to understand and overcome performance limitations for Nb_3Sn cavities, intrinsic properties of Nb_3Sn coating need to be evaluated at microscopic scale. Understanding the connections between Nb_3Sn material defects and RF performance of the cavities will help to optimize the coating process. Such an optimization could improve the design of the future Nb_3Sn coating facility at Fermilab [2]. In order to build up a toolset for routine evaluation of Nb_3Sn coating, structural and chemical evaluation of Nb_3Sn coated Nb samples was initiated. The samples were prepared at Cornell University by chemical vapor deposition of Sn vapor into Nb surface in the temperature range of 1000C to 1200C [1]. This paper discusses the results of structural and analytical characterization with X-Ray Diffraction (XRD), Auger Electron Spectroscopy (AES), Scanning Electron Microscopy (SEM), Transmission Electron Microscopy (TEM), Scanning Transmission Electron Microscopy (STEM) and Energy Dispersive Spectroscopy (EDS).

EXPERIMENTAL METHODS

TEM Sample Preparation

Cross sectional TEM samples were prepared from Nb_3Sn coated Nb flat sample by Focused Ion Beam (FIB) using a Helios 600 FEI instrument at the Materials Research Laboratory (MRL) at the University of Illinois at Urbana-Champaign (UIUC). The FIB lift-out technique allows one to prepare and mount a small rectangular cross sectional sample onto a standard copper TEM half-grid using an Omniprobe micromanipulator. Before FIB milling, the top surface of each cross sectional cut was covered by a protective layer of platinum, in order to protect the native surface from Ga ions.

Characterization Techniques

A JEOL JEM 2100 LaB_6 thermionic gun TEM at MRL/UIUC was used for nano-area electron diffraction (NED) and scanning electron nano-area diffraction (SEND). The beam size of approximately 100 nm was used to obtain NED patterns.

The JEM 2010F Schottky FEG TEM at MRL/UIUC operated at 197kV was used for NED and HRTEM imaging. An approximately 80nm sized parallel beam was used to record NED patterns onto the Fuji imaging plates.

A Hitachi HD 2300 Dual EDS STEM at Northwestern University was used for STEM imaging and EDS chemical analysis. STEM images were taken with a high angle annular dark field detector (HAADF) with an incident electron beam energy of 200 kV.

A Pananalytical/Philips X'pert^2 Material Research Diffractometer (with crossed-slit collimator, parallel plates collimator, flat graphite monochromator and proportional detector) at MRL/UIUC was used for XRD. AES was performed with Physical Electronics PHI 660 instrument.

RESULTS AND DISCUSSION

Structural and Chemical Characterization

Two flat Nb_3Sn coated Nb samples were provided by Cornell University for the material characterization. One of the samples had been anodized at Cornell in order to test the surface composition [3]. Pink-purple oxide which had been grown during the anodization indicated Nb_3Sn surface under the oxide. Anodized sample had been used for structural and chemical evaluation of the coating.

XRD was initiated to evaluate composition of the sample. As expected, the XRD patten in Fig.1 shows the presence

* yuliatr@fnal.gov

CHARACTERIZATION OF THIN FILMS USING LOCAL MAGNEOMETER

Katyan N, Antoine C Z. CEA, Irfu, SACM, Centre d'Etudes de Saclay,
91191 Gif-sur-Yvette Cedex, France

Abstract

SIS nanocomposite (Superconductor/Insulator /Superconductor) could improve the efficiency of bulk Nb accelerating cavities as proposed in 2006 by A. Gurevich [1]. The SRF multilayers concept takes advantage of the enhancement of H_{C1} of thin layers with thickness d~λ. The use of thin layers makes it easier to prevent avalanche penetration of vortices in case of local defects that could promote early penetration. The external field is not fully attenuated in such configuration, so several layers are necessary in order to screen the external field down to values below Nb H_{C1}, decoupled from each other with a dielectric layer. Many deposition techniques exist that can allow the deposition of such multilayers but a few of them are adapted for accelerating cavities shapes. Moreover we do not know yet how the predicted properties evolve in realistic deposition conditions. It seems reasonable to start the optimization of such structure on samples. Two parameters need to be measured to predict their behavior in conditions close to cavity operation: H_{C1} (or at least the penetration field for vortices) and surface resistance, in particular the residual resistance part value of which cannot be predicted by the current superconductivity models.

For that purpose a local magnetometer was developed at Saclay.

A local magnetometer allows measuring the vortices penetration on samples without the common orientation and edge effects encountered in classical SQUID magnetometers. Its operating conditions range from 2 to 40 K, with field up to 150 mT, and possible upgrade to higher field.

INTRODUCTION

In this paper, the working principle of local magnetometry, which is a tool of choice to characterize and optimize new superconductors dedicated to SRF application. In particular it allows measuring unambiguously the field at which vortices start to enter the superconducting samples, namely H_{C1}. Conventional Magnetometer (SQUID) give ambiguous results for very thin film samples because of demagnetization effects (field on the back and sides, alignment issues). With Squid measurement, the samples exhibit a strong transverse moment because, due to misalignment and very high demagnetization factor, the perpendicular field component is sufficient to let vortices enter the material. The local field B is then a combination of the uniform external applied field and the transverse moment. Hence even if the penetration field can be determined, the exact local field configuration is not known, it can be far from the cavities configuration. Moreover its physical meaning is difficult to establish. Indeed Squid magnetometry shows that thin layers/multilayers exhibit a strong enhancement of the penetration field H_P (which is expected to be close to H_{C1})[2-6]

It is shown in [3,7] that the misalignment should be $<0.005^0$ to avoid demagnetization and edge effects. To overcome these issues there is a mandatory need to measure H_{C1} with another technique.

So, a local magnetometer specifically dedicated to measure thin films and multilayer samples is being developed at Saclay, the details of which will be described in this paper.

Local magnetometry is based on infinite slab approximation (Figure 1): when the field is generated in a coil which diameter is small compared to the size of the sample, the field becomes negligible about four to five diameter away from the center of the coil. So if one takes a sample with diameter larger than this dimension, it can be approximated like an infinite slab. This last condition makes negligible any demagnetization or edge effect.

Local measurement based ac third harmonic (V_3) analysis was proposed in ref. [8-10]. This technique depends on the hysteretic behavior of the magnetization in the critical state, which gives rise to none zero odd harmonics in the spectrum of the electrodynamic response of superconductors an AC magnetic field $b_0\cos\omega t$ is applied to a zero field cooled sample, where b_o is the amplitude of the ac magnetic field and ω_o is the frequency. As b_o equals H_{C1}, vortices start to penetrate into the superconducting sample. Under these conditions, a nonlinear power law $J \propto E_n$ in the current-voltage curve applies, where the exponent $n\rightarrow\infty$ in the Bean limit, n>1 in the flux creep regime, n=1 in the flux flow linear regime. Thus odd harmonic components are produced in the spectrum of the sample response signal when it enters into a region of field and temperature in the magnetic phase diagram delimited by H_{C1} and the irreversibility field H_{irr}. Out of all the odd harmonics present, the 3rd harmonic is the most intense.

In other words, the coil provides excitation as well as detection; as long as the sample keeps in the Meissner state, the sample acts as a perfect magnetic mirror, the current (and voltage) in the coil keeps linear. Once vortices start to enter the sample (upon rising temperature and/or rising the current in the coil), the electrons experience a dragging force and this gives rise to non-linearity in the current/voltage inside the coil.

ISBN 978-3-95450-178-6

A FACILITY FOR MAGNETIC FIELD PENETRATION MEASUREMENTS ON MULTILAYER S-I-S STRUCTURES

Oleg B. Malyshev[1,3], Lewis Gurran[1,2,3], Shrikant Pattalwar[1,3], Ninad Pattalwar[1], Keith D. Dumbell[1,3], Reza Valizadeh[1,3] and Alex Gurevich[4]

[1] ASTeC, STFC Daresbury Laboratory, Warrington, Cheshire WA4 4AD, UK
[2] Lancaster University, Lancaster, UK
[3] Cockcroft Institute, Warrington, Cheshire, UK
[4] Old Dominion University, Norfolk, VA 23529, USA

Abstract

The best-performing superconducting RF cavities made of bulk Nb have reached breakdown fields which sometimes exceed 200 mT and are close to the superheating field for Nb. As it was theoretically shown [1], a multilayer coating can be used to enhance the breakdown field of SRF cavities. In the simplest case, such multilayer may be a superconductor-insulator-superconductor (S-I-S) coating, for example, bulk niobium (S) coated with a thin film of insulator (I) followed by a thin layer of another superconductor (S) which could also be a dirty niobium [2]. To verify such an enhancement under a DC magnetic field at 4.2 K an experimental facility was designed, built and tested in ASTeC. The details of experimental setup and first results of the measurements are presented here.

METHOD

A number of well-known techniques such as RRR measurements, DC magnetization in parallel and perpendicular magnetic field and AC susceptibility studies have been used to study the superconducting properties of thin films. These methods are useful for the characterization of the films; however, they are not very suitable to select the best coating material in the superconductor-insulator-superconductor (S-I-S) coating, which would provide the higher breakdown field in the SRF cavities. There are several reasons for that:

(1) The most interesting case corresponds to the magnetic field parallel to the surface; however, as the film samples are usually small, then their alignment parallel to the magnetic field is difficult.
(2) These small samples would only represent a small fraction of total surface area of a larger sample, not representing the whole area.
(3) The samples are exposed to the magnetic field from both sides of the film, so in the case of S-I-S coating the magnetic field can easily penetrate between the layers from the open edges.

To address the problems listed above, the following method was suggested by A. Gurevich and implemented by ASTeC at STFC Daresbury Laboratory to study and compare various superconducting materials under DC magnetic field. A short superconducting magnetic coil is placed in the middle of a relatively long sample tube made of or coated with superconducting material with a large aspect ratio. Two magnetic field strength sensors (e.g. Hall-effect sensor/probe) are placed in on the central plane of the magnet: one inside the tube and the other outside as shown in Figure 1.

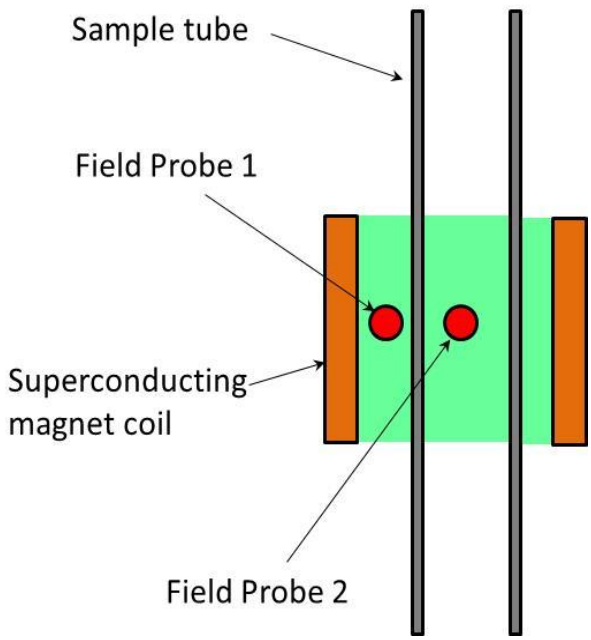

Figure 1: A schematic layout of magnetic measurements with tubular superconducting samples.

In this geometry the maximum magnetic field in the middle plane of the coil is uniform over the cross section of the bore. In the middle of the magnet, the magnetic field is the strongest and tangential to the sample tube walls. The magnetic field decreases with a distance from the middle plane of the coil and is no longer tangential. So, when Hall probes are placed in the middle of the

ISBN 978-3-95450-178-6

MEASUREMENTS OF RF PROPERTIES OF THIN FILM Nb_3Sn SUPERCONDUCTING MULTILAYERS USING A CALORIMETRIC TECHNIQUE

S. Sosa-Guitron*, A. Gurevich, J. Delayen
Center for Accelerator Science, Old Dominion University, Norfolk, VA 23517, U.S.A.
G. Eremeev
Thomas Jefferson National Accelerator Facility, Newport News, VA 23606, U.S.A.
C. Sundhal, C.-B.Eom
University of Wisconsin, Madison, WI 53706, U.S.A.

Abstract

Results of RF tests of Nb_3Sn thin film samples related to the superconducting multilayer coating development are presented. We have investigated thin film samples of $Nb_3Sn/Al_2O_3/Nb$ with Nb_3Sn layer thicknesses of 50 nm and 100 nm using a Surface Impedance Characterization system. These samples were measured in the temperature range of 4 K - 19 K, where significant screening by Nb_3Sn layers was observed below 16-17 K, consistent with the bulk critical temperature of Nb_3Sn.

INTRODUCTION

Progress in the superconducting radio-frequency (SRF) science and technology has pushed the Nb cavities close to their theoretical limits of operation, this limitation coming mainly from the superheating magnetic field. A further enhancement of SRF breakdown fields by using superconducting multilayer coating was proposed in [1]. As part of an ongoing project towards the multilayer development, we report here the results of investigation of two Nb_3Sn thin films which were fabricated at University of Wisconsin-Madison and characterized at Jefferson Lab using the Surface Impedance Characterization (SIC) system.

SAMPLE PREPARATION

Three superconducting film samples investigated in this work were grown at the University of Wisconsin, Madison. Two of them were Nb_3Sn films deposited onto a 0.3 mm thick sapphire wafer which had the diameter of 5 cm. A thick 0.2 mm Nb film was grown on the opposite side of the wafer to fully screen the RF field applied to the thin Nb_3Sn film. The structure of both Nb_3Sn film samples is shown in Figure 1. The thicknesses of Nb_3Sn films were 50 nm and 100 nm, respectively. The third sample was a 0.2 mm thick Nb film on sapphire without Nb_3Sn. This sample was used to evaluate the contribution of dielectric losses in the sapphire wafer.

Nb_3Sn Film Growth

The Nb_3Sn film was grown by magnetron sputtering followed by annealing. For the 50 nm film, 6 alternating layers of Nb and 5 of Sn were grown, whereas the 100 nm film had 12 layers of Nb and 11 of Sn on the Al_2O_3 substrate. Each layer was grown under controlled Argon atmosphere pressure and the parameters summarized in Table 1, except for the first Sn layer, which was grown at 3 mTorr. Layer thickness corresponds to a growth time of 53.4 s for Nb layer and 52.4 s for Sn layer. [2] After sputtering, the structures were annealed at about 950°C for 15 mins. The 100 nm thick Nb_3Sn film attached to the SIC sample holder is shown in Figure 2.

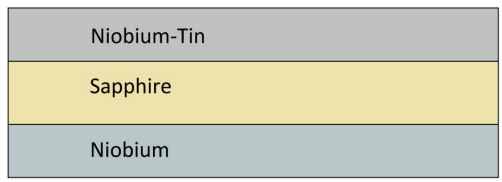

Figure 1: Sketch of the Nb_3Sn film sample. Nb_3Sn thickness is 50 nm and 100 nm, correspondingly. Sapphire substrate is 0.3 mm thick and Nb film is ~ 0.2 mm.

Table 1: Nb and Sn sputtering parameters for 50 nm and 100 nm Nb_3Sn films.

	W. Pressure	Current to Target	Thickness
Nb	3 mTorr	0.1 A	5.6 nm
Sn	100 mTorr	0.07 A	3.3 nm

MEASUREMENT

SIC system has been widely used for the measurements of loaded cavity quality factor Q_L and surface resistance R_s of superconducting materials for particle accelerator applications [3] [4]. In this work the SIC system was used for the measurements of Q_L and R_s as functions of temperature. Specific details of SIC setup have been described elsewhere, for example, in [4], [5], [6] and [7]. Figure 3 shows SIC cavity with the 100 nm thick Nb_3Sn film sample loaded for the SRF measurements.

Superconducting samples were attached to SIC calorimeter under clean room conditions, using cryogenic-rated, N-

* salvaisg@jlab.org

EVALUATION OF SC PROPERTY COATED ON A SURFACE

Y. Iwashita, Y. Fuwa, ICR, Kyoto U., Kyoto, Japan
M. Hino, KURRI, Kyoto U., Osaka, Japan
T. Kubo, T. Saeki, KEK, Ibaraki, Japan

Abstract

Depositions of thin superconducting materials on a substrate are investigated for improvements of performance on superconducting cavity such as higher accelerating field gradients. Some trial depositions of thin superconducting material on a substrate are performed by ion sputtering method. In order to evaluate the deposition method, surface properties are measured. Some results on measurements at DC and a preparation status toward RF measurement are reported.

INTRODUCTION

Multilayer coating techniques of thin superconducting (sc) films seem promising to enhance sc cavity performances [1]. Recently, a guide to investigate the idea becomes available by the self-consistent analysis of such configurations [2]. In order to start the experimental study, the thin film deposition technique had to be established.

Two sets of deposition trials have been performed so far, where each trial is followed by a measurement at DC.

Next section describes the deposition technique and the following sections describe the trial results at DC.

PHYSICAL VAPOR DEPOSITION

As the physical vapour deposition, we adopted the ion beam sputtering method that was developed for supermirror for neutrons [3]. A supermirror has a structure of multilayers to reflect neutrons with smaller incident angles. There are two kinds of PVD coating systems for fabrication of such neutron optical devices at the KURRI. One is based on a vacuum deposition technique [4], and the other is ion beam sputtering (IBS) [5]. The IBS technique enables us to fabricate smooth layer structures with sharp boundaries. In addition, the adhesion force to the substrate for the case of IBS deposition is much larger than that of vacuum deposition.

Figure 1 shows the schematic structure of the KUR-IBS coating system, in which the outlet of the ion gun is 12 cm in diameter. The outer size of the process chamber is 1.2 m wide, 0.9 m long and 1.1 m high. Because of the space for the ion gun system, vacuum pumps, stand, load-lock chamber, etc., the interior volume of the process chamber itself is thus not large (see Figs. 2-3). The system is a specially modified version of the Veeco IBD-350. The ion gun generally generates Ar^+ ions. The accelerating voltage and current of Ar^+ ions can be controlled with the resolution of 1 V and 1 mA, and typical values are from 120 to 240 mA, respectively. The deposition rate is proportional to the current, and a high current is better for high throughput. Our typical current,

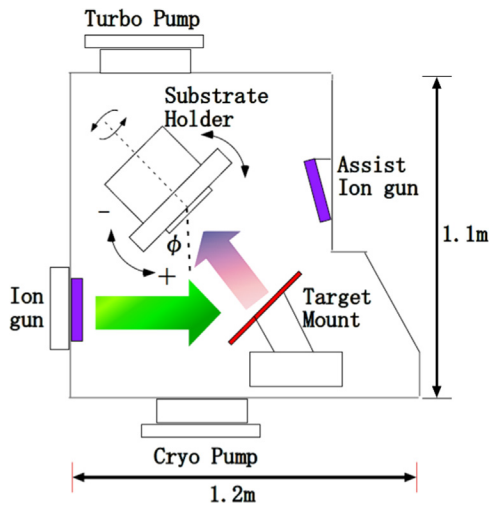

Figure 1: Schematic view of the Ion Sputtering System.

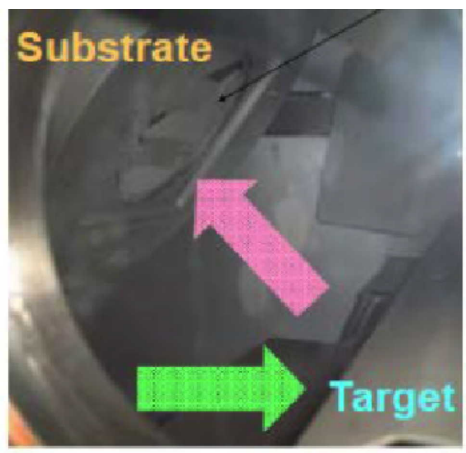

Figure 2: Sputtering target and the substrate.

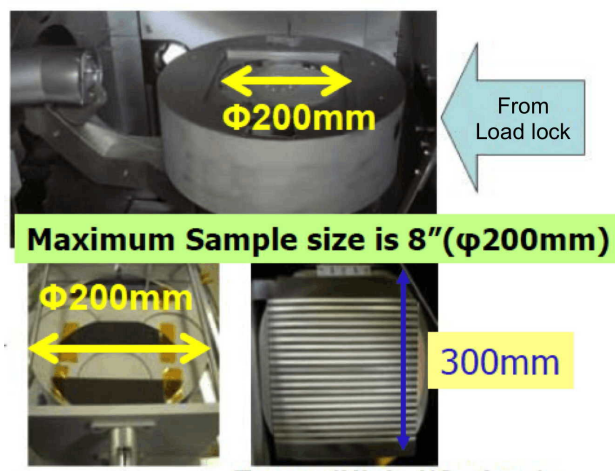

Figure 3: Sample (substrate) holder and sputtering target.

ISBN 978-3-95450-178-6

A MULTI-SAMPLE RESIDUAL RESISTIVITY RATIO SYSTEM FOR HIGH QUALITY SUPERCONDUCTOR MEASUREMENTS*

J. K. Spradlin#, A.-M. Valente-Feliciano, and C. E. Reece
Thomas Jefferson National Accelerator Facility, Newport News, VA 23606, USA

Abstract

For developing accelerator cavity materials, superconducting transition temperature (T_C), transition width (ΔT_C), and residual resistivity ratio (RRR), are useful parameters to correlate with SRF performance and fabrication processes of bulk, thin film, and novel materials. The RRR gauges the purity and structure of the superconductor based on the temperature dependence of electron scattering in the normal conducting state. Combining a four point probe delta pulse setup with a switch allows multiplexing of the electrical measurements to 32 samples per cooldown cycle. The samples are measured inside of an isothermal setup in a liquid helium (LHe) dewar. The isothermal setup is required for a quasistatic warmup of the samples through T_C. This contribution details the current setup for collecting RRR and T_C data, the current standard of throughput, measurement quality of the setup, and the improvements underway to increase the system's resolution and ease of use.

INTRODUCTION

Superconducting materials have two convenient DC figures of merit associated with superconducting RF performance, the transition temperature and the residual resistivity ratio. The transition temperature marks the onset of the superconducting state. T_c and ΔT_c, are the parameters used to characterize the phenomena. RRR is a comprehensive gauge of the quality of the material. The conduction of electrons includes several scattering mechanisms with one mechanism usually dominating at a given temperature [1]. The RRR for Nb is determined according to equation 1 by dividing the averaged measured values of resistivity at 300 +/- 0.1 K and at 10 +/- 0.1 K to create a unitless figure of merit [2,3].

$$RRR = \frac{R_{300K}}{R_{10K}} = \frac{V_{MEASURED\ 300K}/I_{DRIVE}}{V_{MEASURED\ 10K}/I_{DRIVE}} = \frac{V_{300K}}{V_{10K}} \qquad (1)$$

Jefferson Lab Superconducting Radio Frequency Process and Materials Group has developed a residual resistivity ratio system capable of measuring up to 32 samples per cooldown cycle with a temperature resolution of less than 50 mK through Nb T_c range. The samples are measured inside of an isothermal setup in a liquid helium dewar in the JLab vertical test area [4]. Systematic quick feedback on superconducting character is instrumental in process development of thin films and novel materials.

MEASUREMENT SYSTEM

The RRR system is capable of measuring bulk and thin film samples of various shapes and sizes. The high throughput RRR system is capable of meeting the demands of a multitude of projects in the lab and the sample volumes associated with concurrent research programs. The sample's resistivity is measured in a four point probe setup as a function of temperature. This method eliminates sources of error that are intrinsic to two wire measurements, such as thermal EMF and line resistances. Figure 1 depicts the four point probe setup, and equation 1 details how RRR is calculated from the resistivity data.

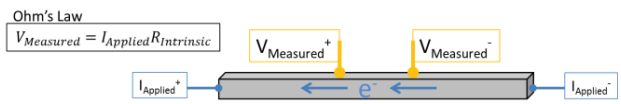

Figure 1: Four point probe measurement scheme.

There have been numerous methods developed for determining RRR, adopting a simple unambiguous method is essential to reproducibility, technique equivalency for different materials, and rapid communication of results [5]. A slight discrepancy is presented where NIST has chosen the room temperature resistance at 273 K, while the accelerator community had previously chosen the room temperature resistance at 300 K.

A calculation of a sample's expected voltage is based on the sample's geometry, RRR seat design, and the material's resistivity. For novel materials, such as MgB_2, NbTiN, and Nb_3Sn, the resistivity is selected slightly above the literature value for pure specimens. An expected sample RRR projects the low temperature voltage that will be measured and then is compared to the systems noise floor to anticipate the low temperature signal quality. If the voltage is too low, the sample's voltage will not be observable above the noise floor of the system, making the data set unusable.

For high quality data, it is essential for the setup to have a reliable representation of the samples' temperature with a thermal measurement device. Temperature uniformity in a vertical dewar is challenged by the stratification of the helium gas within the dewar. The thermal latency of the setup in the LHe dewar dictates the temperature rise of the system which is compounded by the number of samples and the amount of time it takes to

*This material is based upon work supported by the U.S. Department of Energy, Office of Science, Office of Nuclear Physics under contract DE-AC05-06OR23177.

#spradlin@jlab.org

SUPERCONDUCTING THIN FILM TEST CAVITY COMMISSIONING

Lewis Gurran[1,2,3], Philippe Goudket[1,3], Shrikant Pattalwar[1,3], Oleg B. Malyshev[1,3], Ninad Pattalwar[1], Thomas J. Jones[4], Edward S. Jordan[4], Keith Dumbell[1,3], Graeme Burt[2,3] and Reza Valizadeh[1,3]
[1] ASTeC, STFC Daresbury Laboratory, Warrington, Cheshire WA4 4AD, UK
[2] Lancaster University, Lancaster, UK
[3] Cockcroft Institute, Warrington, Cheshire, UK
[4] TD, STFC Daresbury Laboratory, Warrington, Cheshire, WA4 4AD, UK

Abstract

A radiofrequency (RF) cavity and cryostat dedicated to the measurement of superconducting coatings at GHz frequencies was designed to evaluate surface resistive losses on a flat sample. The test cavity consists of two parts: a cylindrical half-cell made of bulk niobium (Nb) and a flat Nb disc. The two parts can be thermally and electrically isolated via a vacuum gap, whereas the electromagnetic fields are constrained through the use of RF chokes. Both parts are conduction cooled hence the cavity halves are suspended in vacuum during operation. The flat disc can be replaced with a sample, such as a Cu disc coated with a film of niobium or any other superconducting material. The RF test provides simple cavity Q-factor measurements as well as calorimetric measurements of the losses on the sample. The advantage of this method is the combination of a compact cavity with a simple planar sample. The paper describes the RF, mechanical and cryogenic design, and initial commissioning of the system with notes on how any issues arising are to be addressed.

CAVITY DESIGN

A use of a double-choked pillbox-type cavity for surface resistance measurements was described in [1].

Figure 1: A three-choked 8 GHz test cavity.

The main advantage of this setup is that is it not harmful to the sample or cavity as there is no need to provide a good electrical contact between the pillbox-like cavity and the studied surface because the electromagnetic field leakage is mitigated through use of RF chokes. A new three-choked cavity with improved leakage mitigation was used for this work and can be seen in Figure 1.

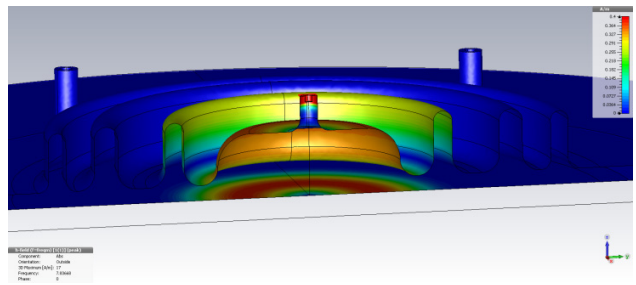

Figure 2: H-field distribution on the surface of the three choke cavity (top) and sample plate (bottom) simulated using CST [2].

The H-field distribution in the cavity can be seen in Figure 2. Final optimization of the chokes was done via measurement across the cavity diameter of the electric field in the cavity/sample gap (Figure 3.). The cavity was manufactured by Niowave Inc. [3].

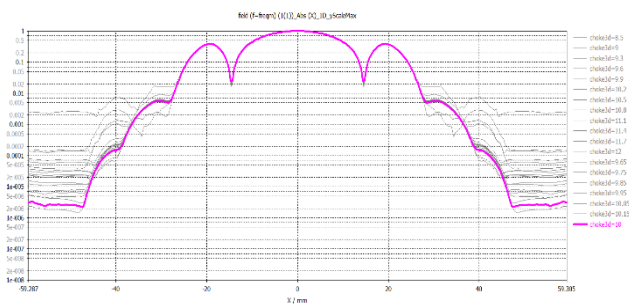

Figure 3: Optimisation of the 3rd choke depth using the normalised E-field amplitude as measured across the gap.

CRYOSTAT DESIGN AND ASSEMBLY

Cooling is provided by concentric LHe and LN_2 chambers, suspended from the steel top plate by thin-walled tubes (as shown on Figure 4). The 'cradle assembly' holding the test cavity and sample is bolted onto the bottom face of the LHe chamber, and covered by a steel vacuum can. A long neck passes through the centre of the LHe chamber, leading to warm ports for the RF cables and thermometry wiring. An aluminium thermal shield is attached to the LN_2 chamber, and both are covered with 30-layer aluminised Mylar MLI. The whole

ISBN 978-3-95450-178-6

CRYOGENIC RF CHARACTERIZATION OF SUPERCONDUCTING MATERIALS AT SLAC WITH HEMISPHERICAL CAVITIES*

Paul B. Welander#, Matt Franzi, Sami Tantawi
SLAC National Accelerator Laboratory, Menlo Park, CA 94025, USA

Abstract

For the characterization of superconducting radio-frequency (SRF) materials, SLAC has commissioned a second-generation, X-band cavity cryostat for the rapid analysis of either thin-film coatings or bulk samples. With this test cryostat one can measure the sample's surface resistance, critical temperature, and magnetic quenching field. The system operates at a frequency of 11.4 GHz, at temperatures between room temperature and 4 K, and utilizes two interchangeable hemispherical cavities (one copper, one niobium) that can accommodate 2"-diameter (50.8 mm) samples on the flat surface. With the niobium cavity one can resolve surface resistances down to 0.7 $\mu\Omega$ (about one tenth of bulk niobium), while with the copper cavity one can measure quenching fields up to 360 mT (about twice that of bulk niobium).

INTRODUCTION

Bulk niobium SRF technology has reached a sufficient level of maturity such that it is being employed in a number of accelerators currently under construction [1]. Despite recent advances in niobium surface preparation, it still falls short of its theoretical potential. Thin films are an appealing alternative for a number a reasons (e.g. more materials options, reduced cost, better heat dissipation), but are yet to outperform bulk niobium in terms of both their quenching field or their RF surface loss. Extensive research efforts have been made in the area of SRF materials, both in bulk niobium and in thin-film coatings. The goal of these studies is to develop new materials with a) higher RF quenching field for higher accelerating gradient; b) higher T_c for higher operating temperature; and c) lower surface resistance for reduced dynamic loss. To support these efforts, SLAC has commissioned a new cryostat with two test cavities for the RF characterization of superconducting materials.

Researchers at SLAC have been developing this test bed over the past decade, beginning with the copper "mushroom"-shaped cavity [2-4]. About five years ago we switched to a hemispherical cavity design that provides for higher magnetic fields on the sample surface [5-6]. More recently we have added a niobium-coated cavity to our arsenal, with an intrinsic surface loss two orders of magnitude lower than our bare copper cavity. These two hemispherical cavities operate at 11.4 GHz and, along with a 50 MW SLAC XL-4 klystron, allow us to measure a sample's critical temperature, T_c, surface resistance, R_s, and magnetic quenching field, H_{quench}.

* Work supported by the U.S. Department of Energy
# welander@slac.stanford.edu

CRYOSTAT & CAVITY DESIGN

The SLAC cryostat is built around a commercially-available pulse-tube cryorefrigerator from Cryomech (model no. PT415-RM). The remote-motor design of this model provides for reduced vibration levels and permits cavity measurements while actively cooling. Implemented in our system, the second stage of the cryorefrigerator has a base temperature of 3.6 K, with about 0.7 W of dynamic cooling power at 4.2 K. The entire cryostat can be cooled from room temperature to base in less than four hours. A complete measurement cycle in one of our cavities (including sample loading, pump-down, cool-down, and warm-up) can take less than 24 hours.

The key components of our measurement system are the hemispherical cavities (see Fig. 1). Both are machined in two parts (sample plate and dome) from high-purity copper. The niobium cavity has a thin-film coating applied to these parts (deposited by Sergio Calatroni's group at CERN) and a smaller-diameter choke to achieve critical coupling at 4 K. X-band operation permits a small sample size and compact cavity design – the sample diameter is 2.0 in. (50.8 mm) and the cavity base plate has an outer diameter of 5.6 in. (142 mm). Utilizing a variety of mounting plates, our cavities can accommodate sample thicknesses from 0.017"–0.250" (430 μm – 6.35 mm). By

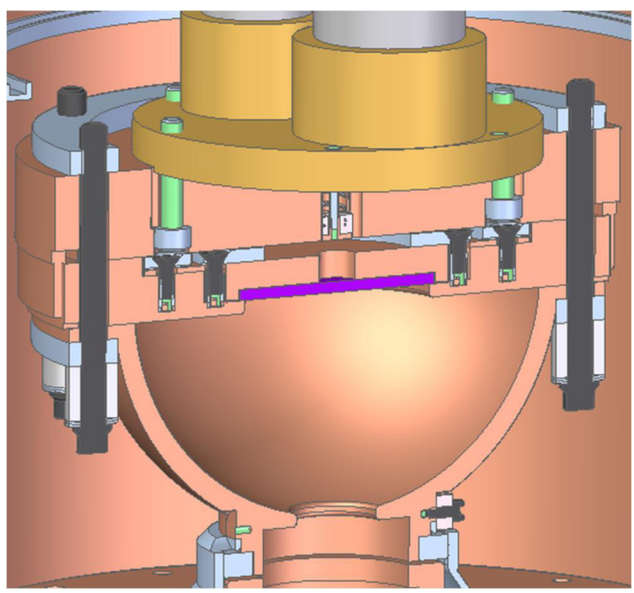

Figure 1: Rendering of SLAC's hemispherical test cavity. The cavity is mounted to the second stage of a pulse-tube cryorefrigerator, with RF power fed from the bottom. The sample under test (purple) is mounted on the flat surface of the cavity. SLAC has two such test cavities: one bare copper, and a new niobium-coated one.

ISBN 978-3-95450-178-6

DESIGN AND FIRST MEASUREMENTS OF AN ALTERNATIVE CALORIMETRY CHAMBER FOR THE HZB QUADRUPOLE RESONATOR

S. Keckert*, R. Kleindienst, J. Knobloch, O. Kugeler
Helmholtz-Zentrum Berlin, Germany

Abstract

The systematic research on superconducting thin films requires dedicated testing equipment. The Quadrupole Resonator (QPR) is a specialized tool to characterize the superconducting RF properties of circular planar samples. A calorimetric measurement of the RF surface losses allows the surface resistance to be measured with sub nano-ohm resolution. This measurement can be performed over a wide temperature and magnetic field range, at frequencies of 433, 866 and 1300 MHz. The system at Helmholtz-Zentrum Berlin (HZB) is based on a resonator built at CERN and has been optimized to lower peak electric fields and an improved resolution.

In this paper the design of an alternative calorimetry chamber is presented, providing flat samples for coating which are easy changeable. All parts are connected by screwing connections and no electron beam welding is required. Furthermore this design enables exchangeability of samples between the resonators at HZB and CERN.

First measurements with the new design show ambiguous results, partly explainable by RF losses at the indium gasket.

INTRODUCTION

In order to measure the RF surface resistance of circular planar samples the Quadrupole Resonator (QPR) was invented at CERN [1, 2]. In 2014 a second resonator was commissioned at HZB which is improved mainly towards a higher magnetic field on the sample surface and a lower peak electric field [3].

The QPR consists of a pillbox-like screening cavity with four vertical rods inside which are connected pairwise by crescent-shaped pole shoes (see Fig. 1). These pole shoes are placed at small distance (0.5 mm) above the sample surface and provide focusing of the RF magnetic field to that area. The length of the rods is adjusted to λ/2 of the baseline operation frequency of 433 MHz. Higher harmonics at 866 MHz and 1.3 GHz can be excited as well. For operation the resonator is cooled down to liquid helium temperature using a helium bath cryostat. The quadrupole rods are hollow, allowing liquid helium to cool these regions of high magnetic field.

The cylindrical calorimetry chamber is inserted into the resonator from below. The outside planar face of the calorimetry chamber facing the bottom of the rods is the sample. The calorimetry chamber itself acts as inner conductor of a coaxial structure which provides thermal decoupling of sample and resonator. Local heating of the sample using a DC heater attached to its bottom is used to set/change the temperature of it without changing the properties of the remaining resonator. All operation frequencies of the QPR are below the cut-off of the coaxial structure, hence significant RF heating of the calorimetry chamber is only located on the sample surface.

*sebastian.keckert@helmholtz-berlin.de

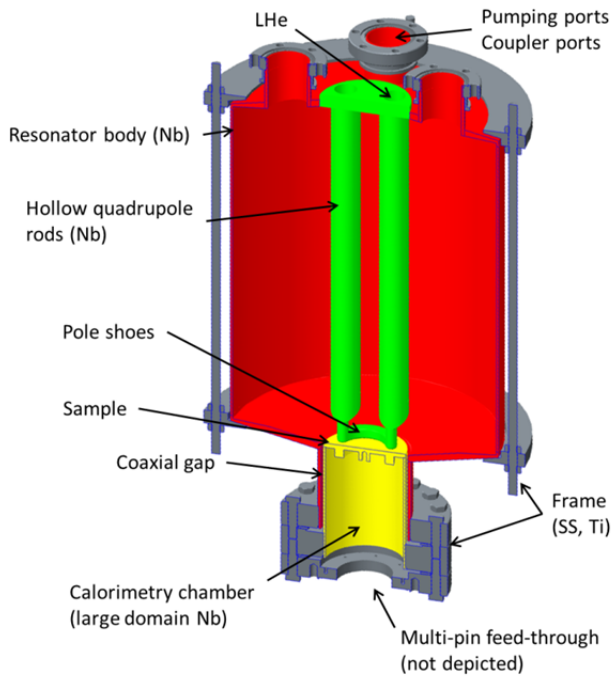

Figure 1: Schematic view of the Quadrupole Resonator in the plane of mirror. Each pole shoe connects two quadrupole rods (green colored) and focuses the RF magnetic field onto the sample surface (yellow) [4].

This enables the calorimetric measurement of the RF surface resistance. A direct RF measurement is less precise due to the strong coupling of the input coupler. Using the DC heater the sample is heated up to the temperature of interest and the heater power is measured. For temperature measurement calibrated Cernox™ sensors are attached to the sample at the regions of high magnetic field. In thermal equilibrium the RF is switched on and the heater power is reduced such, that the temperature of the sample again reaches the initial value. In steady state the heater power is measured again and the RF dissipation is given by the difference of DC heater power. Using a weakly coupled field probe the magnetic field strength is measured and the surface resistance is calculated according to

$$R_S = \frac{2\mu_0^2(P_{\mathrm{DC1}} - P_{\mathrm{DC2}})}{\int_{\mathrm{Sample}} |B|^2 dS} = \frac{2c\omega\mu_0^2(P_{\mathrm{DC1}} - P_{\mathrm{DC2}})}{Q_t\, P_t}$$

ISBN 978-3-95450-178-6

DEVELOPMENT AND TESTING OF A 325 MHZ $\beta_0 = 0.82$ SINGLE-SPOKE CAVITY*

C. S. Hopper†‡, HyeKyoung Park, and J. R. Delayen
Center for Accelerator Science, Department of Physics,
Old Dominion University, Norfolk, VA, 23529, USA and
Thomas Jefferson National Accelerator Facility, Newport News, VA 23606, USA

Abstract

A single-spoke cavity operating at 325 MHz with optimum beta of 0.82 has been developed and tested. Initial results showed high levels of field emission which limited the achievable gradient. Several rounds of helium processing significantly improved the cavity performance. Here we discuss the development process and report on the improved results.

INTRODUCTION

High-velocity single- and multi-spoke cavities are being investigated for a number of applications [1–4]. A single-spoke cavity operating at 325 MHz with $\beta_0 = 0.82$ has been designed, fabricated, and cryogenically tested. Figure 1 shows the fabricated cavity with the stiffening structure attached.

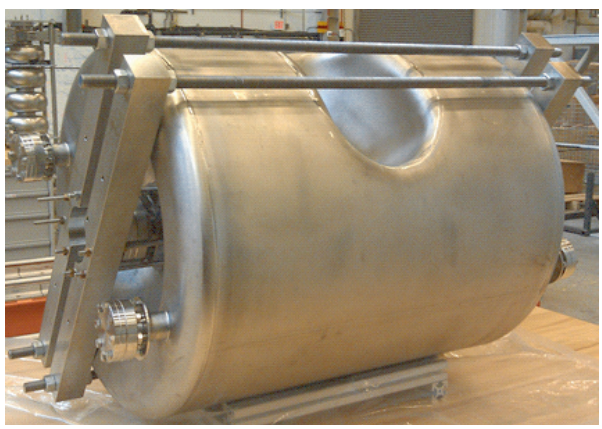

Figure 1: 325 MHz, $\beta_0 = 0.82$ single-spoke cavity with stiffening bars.

ELECTROMAGNETIC OPTIMIZATION

The primary goals of electromagnetic optimization are to reduce the peak surface electric and magnetic fields while increasing the shunt impedance. However, it is important to point out that there is no “optimal" design for all applications [5]. For this particular cavity, minimizing the peak surface fields was a priority [6]. Table 1 shows some of the geometric and rf properties for this cavity. The reference length used to define E_{acc} is $\beta_0\lambda$ = 757 mm and E_{acc} = 1 MV/m.

Table 1: Geometric and RF Properties

Parameter	325 MHz	Units
Frequency	325	MHz
Cavity diameter	609	mm
Cavity length	717	mm
Aperture diameter	60	mm
β_0	0.82	-
E_p/E_{acc}	3.6	-
B_p/E_{acc}	6.0	[mT/(MV/m)]
R/Q	449	[Ω]
$Q \cdot R_s$	182	[Ω]

There are a number of other analyses which are typically performed prior to fabrication. Multipacting reduction, particularly with the complex geometry of the spoke cavity [7] is one of the most important. Doing so resulted in minor modifications to the geometry which are reported elsewhere [6, 8]. It is also necessary to understand how the cavity will respond under various pressure scenarios. ANSYS [9] was used to evaluate the von-Mises stress under 1 and 1.4 atm vacuum load. It was determined that the cavity would experience plastic deformation even at 1 atm if not properly stiffened. Figure 2 shows the location of the high stress areas on the end caps. Even with the stiffening structure shown in Fig. 1, there was additional support which needed to be introduced. When the beam pipe is fixed, a great deal of stress appears on the curvature where the beam pipe meets the end cap. For this reason, that area was made of thicker material. This was also necessary for the spoke; the large flat areas perpendicular to the beam line experience significant bowing which can be alleviated with 4 mm thick niobium and stiffeners.

CAVITY FABRICATION AND PROCESSING

The 325 MHz single-spoke cavity was designed and optimized at Old Dominion University’s Center for Accelerator Science. The fabrication and chemical processing were carried out at Niowave, Inc. The chemical processing involved a 120 μm bulk BCP and 30 μm light etch. In between these processing steps, a 600 °C, 10 hour heat treatment was preformed at FermiLab.

* Work supported by U.S DOE Award No. DE-SC0004094
† chopper@anl.gov
‡ Now at Argonne National Laboratory

REPORT OF VERTICAL TEST OF THE $\beta = 0.12$ HALF WAVE RESONATOR (HWR) AT RISP*

Gunn Tae Park†, Woo Kang Kim, Heetae Kim,
Hyuckjin Cha, Rare Isotope Science Project, Daejeon, Korea
Zhongyuan Yao, TRIUMF, Vancouver, Canada

Abstract

The $\beta = 0.12, f = 162.5$ MHz half wave resonator (HWR) has been developed for the low-to-medium energy acceleration in RAON, the proposed heavy ion accelerator at rare isotope science project (RISP). Its first prototype was fabricated by Vitzro tech, and was sent to TRIUMF for a surface processing and vertical test. Despite some field emission, the cavity achieved the target value of $Q_0 = 2 \times 10^9$ at $E_{acc} = 6.3$ MV/m.

INTRODUCTION

A $\beta = 0.12, f = 162.5$ MHz half wave resonator (HWR) accelerates uranium beam in low-to-medium energy in RAON, the proposed heavy ion accelerator at rare isotope science project (RISP). The cavity is made to accelerate various ions ranging from proton to uranium in high intensity current of about 1 mA. In particular, the cavity will accelerate uranium beam from 2.5 MeV/u to 18.5 MeV/u. To accommodate high intensity current, the aperture was made as big as possible, reaching 40 mm. The first prototype was manufactured by Vitzro tech. with high purity $RRR \sim 330$ niobium. The fabrication of its first prototype by standard deep drawing and electron beam welding was complete (See Fig. 1) and the cavity was sent to TRIUMF for surface processing and vertical test. The detailed description of the design and fabrication are reported in [1], [2]. At TRIUMF, it was decided that high temperature baking at 800 °C will not be done and instead do "Q-disease test" to check if there is hydrogen leftover after BCP. The cavity will be operated at 2 K minimizing the helium press fluctuations, which is major cause for frequency shift.

In this paper, we report on the surface processing and the vertical test for the prototype HWR in detail.

SURFACE PROCESSING

The cavity was given a standard procedure of surface processing, i.e., buffered chemical polishing (BCP) followed by high pressure rinsing before the vertical test.

Buffered Chemical Polishing

Before BCP, cavity was degreased and cleaned with ultrasound for about 40 minutes (20 minutes in 1 % Liquinox, another 20 minutes in DI water). In BCP as shown in Fig. 2(a), the cavity was etched about 120 μm in total.

Figure 1: HWR delivered from the vendor Vitzrotech.

(etching was done in 4 different treatments, 30 μm etching each treatment) The composition of an acid is as follows.

$$HF : HNO_3 : H_3PO_4 = 1 : 1 : 2 \quad \text{(volume ratio)} \qquad (1)$$

Being kept near 12 °C, the etching rate was maintained around 1 μm per minute. The rate drops rapidly when the concentration of acid exceeds 10 g/L. The frequency check before and after the etching gave frequency shift about 660 kHz/mm.

After etching, the cavity is immediately low pressure rinsed with DI water. The inner surface of the cavity was visually inspected after BCP, which is shown in Fig. 3

High pressure rinsing (HPR)

The cavity was rinsed in high pressure with DI water to clean the surface and eliminate possible field emitters. The pressure was controlled to be around 40 bar and the rinse was through 4 ports and took 325 minutes for each port .

After HPR, the cavity was kept for dry in class10 clean room over 48 hours.

Low Temperature Baking

Before the 2nd cool down, low temperature baking was done to see if there is any improvement on Q_0, high field slope in particular. The baking was done at 120 °C for 48 hours. The vacuum was in the range of 10^{-6} torr. There was some outgassing and one spike around 100 °C. It is known that low temperature baking decreases BCS resistance, while increases residual resistance.[3]

* Work supported by ICT, MSIP, NRF
† gunnpark@ibs.re.kr

ISBN 978-3-95450-178-6

COLD TESTS OF SSR1 RESONATORS MANUFACTURED BY IUAC FOR THE FERMILAB PIP-II PROJECT*

L. Ristori #, A. Grassellino, O. Melnychuk, A. Sukhanov, D. A. Sergatskov, Fermilab, Batavia, IL 60510, USA
P. N. Potukuchi, K. K. Mistri, A. Rai, J. Sacharias, S. S. K. Sonti, Inter University Accelerator Centre, New Delhi - 110067, India

Abstract

In the framework of the Indian Institutions and Fermilab Collaboration (IIFC) within the PIP-II project, two Superconducting Niobium Single Spoke Resonators were manufactured at the Inter-University Accelerator Centre (IUAC) in New Delhi and tested at Fermilab. The resonators were subject to the routine series of inspections and later processed chemically by means of Buffered Chemical Polishing, heat-treated at 600°C and cold-tested at Fermilab in the Vertical Test Stand. In this paper we present the findings of the inspections and the results of the cold-tests.

INTRODUCTION

The design of the SSR1 resonator was developed at Fermilab [1] within the scope of the Project X R&D program [2]. A production batch of 10 SSR1 resonators was initiated by Fermilab in US industry [3]. Through the IIFC collaboration, it was possible to develop the manufacturing process and fabricate two additional SSR1 resonators at IUAC. In Figure 1, the two SSR1 niobium resonators developed by IUAC are shown.

Figure 1: The two SSR1 niobium resonators developed by Inter University Accelerator Centre (IUAC), New Delhi.

MANUFACTURING

The fabrication of the SSR1 resonators was carried out using the model adapted by IUAC for constructing superconducting niobium cavities. The rolling, cold-forming and machining of the major sub-assemblies (e.g. the shell, the spoke and the end wall), along with the RF tuning, associated dimensional measurements and trimming, were all performed at an outside vendor, who has been working with IUAC in the development of niobium resonators. The design, development and fabrication of the dies, punches and of the various fixtures required for machining, chemical treatment and EBW of the resonator parts were done by the outside vendor in consultation with IUAC personnel. The validation of the dies and punches was done on copper material.

Material

All Niobium material was procured from a qualified vendor, inspected at Fermilab and provided to IUAC. The material was subject to visual inspection and immersed in water for 24 hours to reveal any iron contamination. Coupons from different annealing batches were subject to eddy current scanning and RRR measurements.

All brazed joints necessary for the SSR1 flanges were designed and manufactured at ANL [4] and provided to IUAC in the stock condition.

Electro-Polishing of Sub-Assemblies

The chemical treatment, which primarily consisted of electro-polishing of individual sub-assemblies to remove ~125-150 μm of material, was accomplished using the in-house facilities at IUAC.

A standard electro-polishing recipe was used. An electrolytic mixture of HF (48%) and H2SO4 (98%) was used in the ratio of 1:9 (Vol./Vol.). The mixture was maintained at a temperature of 30 ± 2°C and a current density of ~60 mA/cm2 at 18 V was achieved during the process. In Figure 2 the electro-polishing setup for the niobium shell is shown.

Electron-Beam Welding

A substantial amount of effort was put in developing the EBW parameters for the different weld joints. The starting point in these developments was the parameters used for constructing niobium resonators for the in-house programs. Some of the critical welds, like the spoke to

* Operated by Fermi Research Alliance, LLC under Contract No. DE-AC02-07CH11359 with the U.S. Department of Energy.
# leoristo@fnal.gov

HIGH-VACUUM SIMULATIONS AND MEASUREMENTS ON THE SSR1 CRYOMODULE BEAM-LINE*

D. Passarelli†, M. Parise, T. H. Nicol, L. Ristori, FNAL, Batavia, IL 60510, USA

Abstract

In order to guarantee an effective cool-down process for the SSR1 cryomodule, a high-vacuum level must be achieved at room temperature in the beam-line before introducing gaseous and liquid helium. The SSR1 cavities in the beam-line have a small beam aperture compared to the size of their internal volume. To avoid unnecessary complications for the vacuum piping of the cryomodule cold-mass, a pilot study was conducted on the string prior to processing and qualification of the components to investigate the vacuum level achievable by pumping only through the beam-line. To estimate the pressure distribution inside the cavity string we used a mathematical model implemented in a test-particle Monte-Carlo simulator for ultra-high-vacuum systems.

INTRODUCTION

The SSR1 cryomodule [1] will be part of the 800 MeV linear accelerator complex that Fermilab is planning to build in the framework of the Proton Improvement Plan-II (PIP-II) project. The cavity string assembly of this cryomodule which constitutes the beam-line volume, contains eight superconducting Single Spoke Resonators type 1 (SSR1) with their cold-end input couplers and four solenoids, see Fig 1. The connections along the beam-line are made using aluminum diamond seals and stainless steel flanged joints and bellows. At each end, the beam-line is terminated with ultra-high-vacuum gate valves through which the beam-line will be pumped down. The planned pumping system for the cryomodule consists of two turbo pumps with a pumping speed of $S = 300\,\mathrm{L/s}$ and an ultimate pressure of $1 \cdot 10^{-8}$ Torr at the pump inlet.

The cavity string will be assembled in a class 10 cleanroom to minimize particle contamination in the beam-line known to cause field emission and therefore degrading cryomodule performance. Limiting the number of beam-line components and sub-assemblies from the initial stages of design simplifies greatly the installation procedure promoting a cleaner assembly approach. The goal for this study was to prove that a vacuum level of $5 \cdot 10^{-5}$ Torr or lower can be achieved in each section of the beam-line by pumping down the cavity string simply through the beam aperture without any additional manifold connected to the cavities. The pressure threshold of $5 \cdot 10^{-5}$ Torr was chosen to avoid negative effects such as increased field emission [2] and residual resistance due to condensed gases [3]. This level of vacuum must be reached in less than 12 hours to minimize the down-time associated with thermal cycles for the cryomodule.

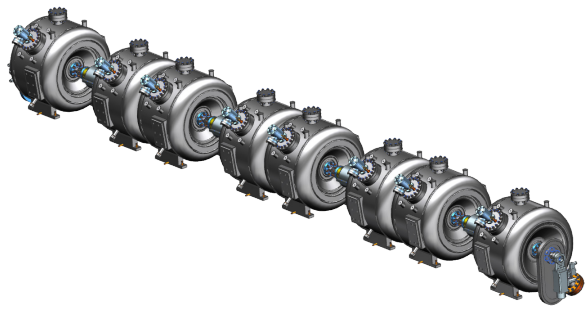

Figure 1: SSR1 cavity string assembly.

PILOT STUDY

A series of measurements was performed on the cavity string to evaluate the feasibility of pumping down the SSR1 string assembly from the beam-pipe ports only.

Vacuum Test

The test was performed on a half-string (four cavities) thanks to the symmetry of the problem. A turbo pump with cold trap was connected to the first cavity. Two pressure gauges (gauge 1 and gauge 2), calibrated for UHV, were installed on the first and last cavity to monitor the trend of pressure as function of time, see Fig. 2.

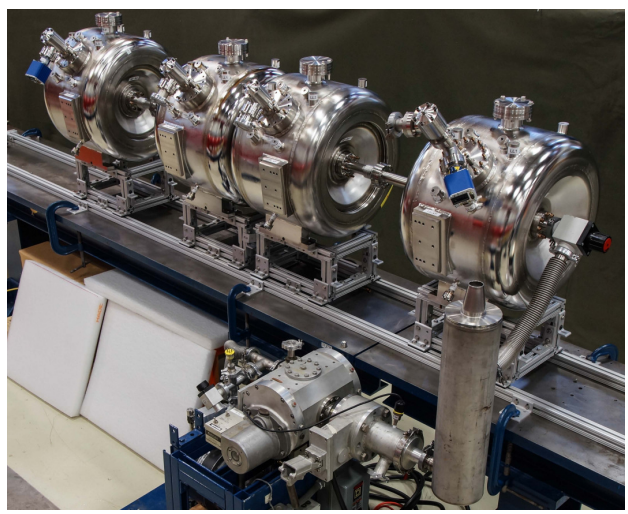

Figure 2: Half-string setup for the vacuum test.

The study is conservative for several reasons:

- niobium cavities were exposed to atmosphere and not yet baked;

* Work supported by Fermi Research Alliance, LLC under Contract No. DEAC02- 07CH11359 with the United States Department of Energy
† donato@fnal.gov

MEASUREMENTS ON THE SUPERCONDUCTING 217 MHz CH CAVITY DURING THE MANUFACTURING PHASE*

F. Dziuba†,[1], M. Amberg[1,3], K. Aulenbacher[3,4], W. Barth[2,3], M. Basten[1], M. Busch[1], H. Podlech[1], S. Mickat[2,3]

[1]IAP University of Frankfurt, 60438 Frankfurt am Main, Germany
[2]GSI Helmholtzzentrum, 64291 Darmstadt, Germany
[3]Helmholtz Institute Mainz (HIM), 55099 Mainz, Germany
[4]KPH Mainz University, 55128 Mainz, Germany

Abstract

Since in future the existing UNILAC (Universal Linear Accelerator) will be used as an injector for the FAIR (Facility for Antiproton and Ion Research) project, a new superconducting (sc) continuous wave (cw) linac at GSI is proposed to keep the Super Heavy Element (SHE) program at a competitive high level. In this context, a sc 217 MHz crossbar-H-mode (CH) cavity [1] has been designed at the Institute for Applied Physics (IAP), Frankfurt University, and was built at Research Instruments (RI) GmbH, Germany. The cavity serves as a first prototype to demonstrate the reliable operability under a realistic accelerator environment and its successful beam operation will be a milestone on the way to the new linac. In this contribution measurements during the production process of the cavity as well as corresponding simulations will be presented.

INTRODUCTION

Presently, the fabrication of the sc 217 MHz CH cavity [2] (see Fig. 1) is finished except for the helium vessel. The cavity has a design gradient of 5.5 MV/m which will be achieved by 15 equidistant accelerating cells at an effective length of 612 mm. It is equipped with nine static and three dynamic frequency tuners, a 10 kW cw power coupler and several flanges for surface preparation. The related beam dynamics concept is based on EQUUS (EQUidistant mUlti-gap Structure) [3]. Presently, the cavity is prepared for the high pressure rinsing (HPR) process. Hence, first performance tests on the cavity at 4 K with low rf power are expected at the end of 2015. Since the cavity consists of niobium sheets with 4 mm wall thickness its resonace frequency is very sensitive to external influences. Already small mechanical deformations can change the frequency of the cavity significantly. Static changes of the cavity's resonance frequency will be caused by the manufacturing accuracy, the evacuation process and the cool-down procedure to 4 K. These effects have to be compensated by the static tuners during the production phase. On the other hand, dynamic frequency changes during the operation can be adjusted accordingly by the dynamic tuning system of the cavity [4]. Several measurements have been performed

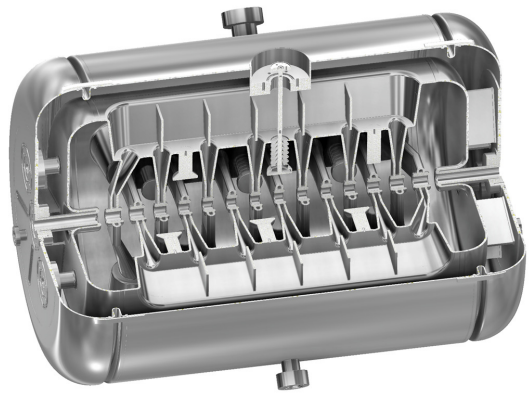

Figure 1: Layout of the sc 217 MHz CH cavity.

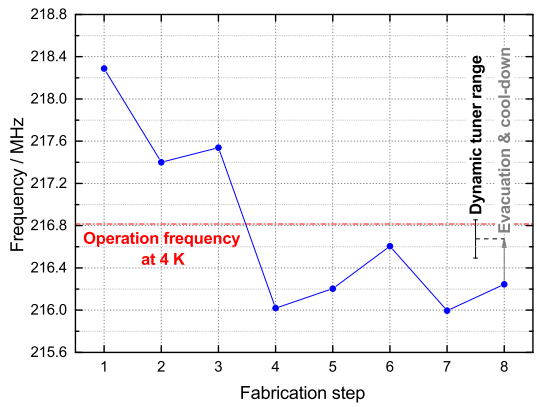

Figure 2: Measured frequency of the sc 217 MHz CH cavity during each fabrication step: (1) temporarily attached end caps with oversize, (2) four static tuners welded in, (3) left end cap welded on, (4) three static tuners welded in, (5) right end cap welded on, (6) 50 μm BCP, (7) two static tuners welded in, (8) 25 μm BCP.

during each fabrication step in order to compensate static variations, thus the frequency of the cavity is finally in the range of the dynamic tuners which provide ±180 kHz/mm (see Fig. 2). Initially, the frequency was designed higher than the operating value and lowered successively by reducing the end cap length, inserting static tuners and by preparing the cavity's surface with standard BCP (Buffered Chemical Polishing) treatment. In principle, an additional BCP

* Work supported by GSI, HIM, BMBF Contr. No. 05P12RFRBL
† dziuba@iap.uni-frankfurt.de

ISBN 978-3-95450-178-6

THE MULTIPACTING STUDY OF NIOBIUM SPUTTERED HIGH-BETA QUARTER-WAVE RESONATORS FOR HIE-ISOLDE

P. Zhang* and W. Venturini Delsolaro
CERN, Geneva, Switzerland

Abstract

Superconducting Quarter-Wave Resonators (QWRs) will be used in the superconducting linac upgrade in the frame of HIE-ISOLDE project at CERN. The cavities are made of bulk copper with thin niobium film coated. They will be operated at 101.28 MHz at 4.5 K providing 6 MV/m accelerating gradient with 10 W maximum power dissipation. Multipacting (MP) has been studied for the high-beta (β=10.9%) QWRs and two MP barriers have been found: Eacc at around 0.05 MV/m and 1.5 MV/m. We have used both CST Microwave Studio & Particle Studio and the parallel codes Omega3P & Track3P developed at SLAC. The results from the two codes are consistent and are in good agreement with cavity vertical cold test results. Both MP barriers can be conditioned by RF processing.

INTRODUCTION

The ISOLDE project at CERN is under a major upgrade to boost both the energy and intensity of the radioactive beam [1]. This includes replacing part of the existing normal conducting linac with superconducting quarter-wave resonators (QWRs). The QWRs are made of bulk copper (Cu) coated with thin niobium (Nb) film [2]. They will be operated with a frequency of 101.28 MHz at 4.5 K. Each QWR will provide an accelerating gradient of 6 MV/m on beam axis with a maximum of 10 W power dissipation on the cavity inner surface. Two types of QWRs, low-β (6.3%) and high-β (10.3%), are planned to be installed in 3 phases to cover the entire energy range [1]. Since the linac upgrade started from the high energy section, all R&D efforts have been focussed on the high-β QWRs [3]. A CAD model of the cavity is shown in Fig. 1(a) and its main RF parameters are listed in Table 1.

The electromagnetic field distribution in the cavity simulated with CST Microwave Studio® [4] is shown in Fig. 1(b)(c). The peak electric field is at the tip of the inner conductor and can go up to 30 MV/m during normal operation. The magnetic field, on the other hand, peaks at the top part of the cavity and can reach 57 mT when Eacc=6 MV/m.

Cavity RF cold tests have shown multipacting (MP) at various field levels requiring dedicated processing time. Therefore MP simulations have been carried out in order to improve the understanding of this phenomena in these cavities. The simulations are in good agreement with results from cavity RF cold tests.

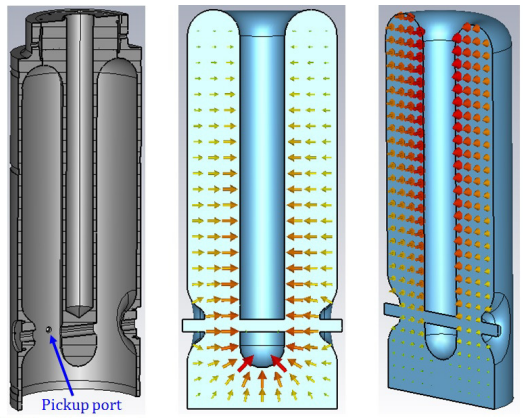

(a) Cavity geometry (b) E-field (b) H-field

Figure 1: The cavity geometry and its electromagnetic field distribution simulated using CST Microwave Studios®.

Table 1: The main RF Parameters of the High-β QWR

Parameter	Value
f_0 at 4.5 K [MHz]	101.28
$\beta_{optimum}$ [%]	10.9
E_{peak}/E_{acc}	5.0
B_{peak}/E_{acc} [mT/(MV/m)]	9.5
geometry factor G=R_sQ_0 [Ω]	30.8
nominal gradient E_{acc} [MV/m]	6
max power dissipation at 6 MV/m [W]	10
Q_0 at E_{acc}=6 MV/m	4.7×10^8

MULTIPACTING STUDIES BY SIMULATIONS

Two sets of codes have been used to study the MP phenomena: CST Microwave Studio® & Particle Studio® [4] and SLAC Omega3P & Track3P [5]. These will be described in the following sections.

Multipacting Study by CST Code Suite

A typical secondary electron yield (SEY) curve for Nb is shown in Fig. 2. The SEY is greater than 1 when the energy of the electron impacting on the Nb surface falls into

* pei.zhang@cern.ch

THE INFLUENCE OF COOLDOWN CONDITIONS AT TRANSITION TEMPERATURE ON THE QUALITY FACTOR OF NIOBIUM SPUTTERED QUARTER-WAVE RESONATORS FOR HIE-ISOLDE

P. Zhang*, G. Rosaz, A. Sublet, M. Therasse, W. Venturini Delsolaro
CERN, Geneva, Switzerland

Abstract

Superconducting quarter-wave resonators (QWRs) are to be used in the ongoing linac upgrade of the ISOLDE facility at CERN. The cavities are made of niobium sputtered on copper substrates. They will be operated at 101.28 MHz at 4.5 K providing 6 MV/m accelerating gradient with maximum 10 W power dissipation. In recent measurements, we found the thermal gradient along the cavity during the niobium superconducting transition has an impact on the cavity quality factor. On the other hand, the speed of the cooling down through the superconducting transition turned out to have no influence on the cavity quality factor.

INTRODUCTION

The High Intensity and Energy (HIE) ISOLDE project is a major upgrade to the current radioactive beam facility at CERN [1, 2]. The main focus is to boost the beam energy from 3 MeV/u to 10 MeV/u for a mass to charge ratio of 2.5<A/q<4.5. Superconducting quarter-wave resonators (QWRs) will be used to replace part of the existing normal conducting linac. Each QWR is made of OFE copper (Cu) as a substrate sputtered with thin layers of niobium (Nb). They will provide an accelerating gradient of 6 MV/m on beam axis with a maximum of 10 W power dissipation on the cavity inner surface. A total number of 32 QWRs, 12 low-β (6.3%) and 20 high-β (10.3%), are planned to be installed to complete the energy upgrade. According to the project schedule, all R&D efforts have been focused on the high-β QWR, thus is the focus of this paper. Its main RF parameters are listed in Table 1.

Table 1: The main RF Parameters of the High-β QWR.

Parameter	Value
f_0 at 4.5 K	101.28 MHz
$\beta_{optimum}$	10.9 %
E_{peak}/E_{acc}	5.0
B_{peak}/E_{acc}	9.5 mT/(MV/m)
geometry factor G=R_sQ_0	30.8 Ω
nominal gradient E_{acc}	6 MV/m
max power dissipation at 6 MV/m	10 W
Q_0 at E_{acc}=6 MV/m	4.7×10^8

The influence of cooldown conditions on the cavity performance has become a hot topic in SRF community in recent years. Many labs have done dedicated experimental studies mainly on bulk Nb cavities and several theories have been developed aiming to explain the results in terms of thermal current induced flux trapping and the efficiency of flux expulsion due to cooldown dynamics. These can be refered to [3–5]. In this paper, we present our experimental studies on cooldown conditions in Nb-sputtered-on-copper quarter-wave resonators.

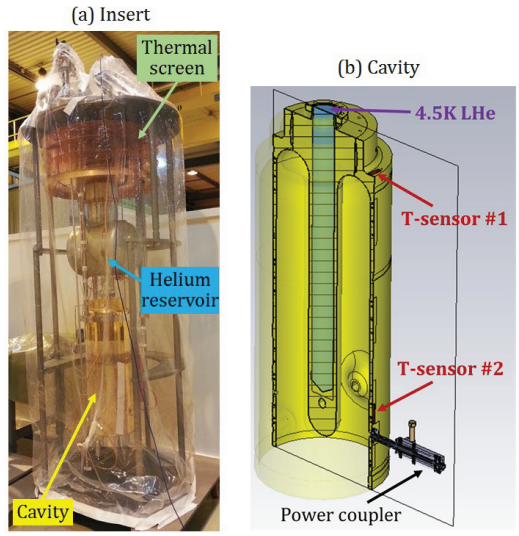

Figure 1: The insert for the vertical test at 4.5 K and the cavity geometry with temperature sensors.

After frequency tuning, substrate surface treatment and Nb sputtering [6, 7], all QWRs are tested in the vertical cryostat at 4.5 K at CERN before assembling into the cryomodule. The insert for the vertical test is shown in Fig. 1(a) [8]. The liquid helium (LHe) is delivered to the cryostat where its level is kept constant in the reservoir. The cavity inner conductor is hollow and filled with LHe from the reservoir as shown in Fig. 1(b). The rest of the cavity is cooled by conduction. During the cooldown process, a temperature gradient can be built up along the cavity with the bottom of the outer conductor is warmer than the top part. Temperature sensors (T-sensors) are mounted on the cavity outer wall at various locations and two of them, one on the top and the other close to the bottom as shown in Fig. 1(b), are used for the following study to characterize the thermal gradient and the cooldown speed. The quality factor (Q_0) at different accelerating gradient in the cavity

* pei.zhang@cern.ch

ISBN 978-3-95450-178-6

DEVELOPMENTS ON A COLD BEAD-PULL TEST STAND FOR SRF CAVITIES

A.Vélez, A. Frahm, J. Knobloch, A. Neumann, Helmholtz-Zentrum Berlin, 12489 Berlin, Germany

Abstract

Final tuning and field profile characterization of SRF cavities always takes place at room temperature. However, important questions remain as to what happens when the cavity is cooled to LHe temperature, in particular with multi-cell systems. To enable the characterization of cavities in the cold, we have designed and commissioned a "cold bead-pull" test stand at HZB. The present test-stand is designed to be integrated in HoBiCaT (Horizontal bi-cavity testing facility) [1] with the ability to provide electric field profile measurements under realistic superconducting conditions (T=1.8K). In this paper mechanical and operational details of the apparatus will be described as well as future plans for the development and usage of this facility.

INTRODUCTION

Cavity tuning is the final process step after the fabrication of a new SRF cavity. This process will lead to the achievement of the field flatness specification and therefore to the final acceptance of the cavity. Valuable information such as the field profile and R/Q can be accurately determined and compared to electromagnetic simulations in order to determine the fabrication accuracy and cavity performance. In order to perform this test a so called bead-pull test stand is needed. The theory of the system is based on the Slater´s perturbation theory and takes advance of the frequency deviation induced by the pass of a perturbing object through a cavity in order to determine the induced field profile. To this end, many different mechanical systems have been developed and serve as a cavity analysis and commissioning tool for many very different cavities in several labs [2,3]. Nevertheless, this test is always performed at room temperature even for Niobium based cavities, which superconducting physical characteristics substantially differ from the warm state to [4]. As it is known once the cavity is at 1.8K the natural frequency shifting due to thermal shrinkage can be easily measured. Nevertheless, after the last tuning is performed at room temperature and the cavity is taken to a S.C. state there is no measured evidence of the conservation of its field profile. To investigate this problem HZB presents a first prototype of a test-stand able to perform bead-pull measurements under superconducting conditions. The system has been successfully tested in HoBiCaT [1] for a 1.3GHz 9-cell Tesla cavity and the results obtained are presented on this paper.

BEAD-PULL TEST STAND

HZB's cold bead-pull test-stand is designed to be allocated in the horizontal tests of superconducting cavities (HoBiCaT [1]). Due to the reduced available space inside the cryo-module the design is required to be as compact as possible. Therefore, an aluminium frame sustaining the cavity structure and the bead-pull equipment at the same time has been fabricated. Also due to the limited space, the system is design to slide over a 2K cooled table in order to allow cavity preparation and bead mounting outside of the module. In addition the typical weigh-hanging structure [3] has been replaced by a winding/releasing threaded wheel system directly connected to the motor axis (Fig. 1). Therefore the system is bi-directional in a closed loop. The motor used consists on a VSS52 with transmission gear typically used for tuner actuation and suitable for low temperature operation. In order to supply the proper tension needed on the wire, a tension pulley has been implemented (see Fig. 2a). This pulley is attached to the aluminium frame by means of a metal spring providing the tension needed.

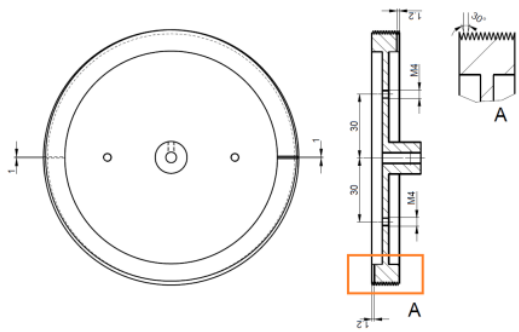

Figure 1: Winding threaded wheel.

Due to the tension needed and the low temperature operation (1.8K) there is a material selection limitation on the wire to be used. Titanium based wires would represent a perfect choice in terms of strength at low temperatures. Nevertheless its metallic characteristics will change boundary conditions and therefore disturb field characteristics inside the cavity. Thus a Kevlar based string has been chosen. A material validation successful initial cold-stress test for the wire was performed by immersing a sample into liquid Nitrogen and applying tension to it.

A layout of the aluminium test-stand frame holding the cavity is depicted in Fig. 2. As it can be seen three extra pulleys have been added in order to handle the pass of a plastic tube though the cavity. This tube will serve as a

ISBN 978-3-95450-178-6

SECOND SOUND QUENCH DETECTION OF DRESSED TESLA-SHAPE SRF CAVITIES

Y. Tamashevich*, University of Hamburg, Hamburg, Germany
E. Elsen, A. Navitski, DESY, Hamburg, Germany

Abstract

A compact detector and numerical algorithm for second sound measurements has been developed. The detector allows precise 3D quench localisation within a single unit and can be used even for cavities with mounted helium tank. The compact device is easily mounted and requires minimum space. It can be used as a part of the standard cold test of cavities. The results obtained with the new detector and a 3D algorithm have been cross-checked by optical inspection and resistor-based temperature mapping. The resolution of the detector is seen to be limited by the sampling rate and the lateral extent of the quench induced heated area on the Nb superconductor.

MOTIVATION

Sudden heat deposits such as induced in a quench of a superconductor produce a second sound wave in the surrounding helium bath when operated below the λ-point. The second sound propagates at velocities of $\approx$20 m/s which makes it conveniently accessible to measurements of propagation delays [1]. The second sound wave propagates without much attenuation over distances of several meters.

An additional challenge arises in restricted areas such as the 9-cell cavities used for the European XFEL. The helium tank of the E-XFEL cavity has one opening with a diameter of 56 mm with the two-phase gas return pipe attached. So the sensors can be placed only in this opening (Fig. 1).

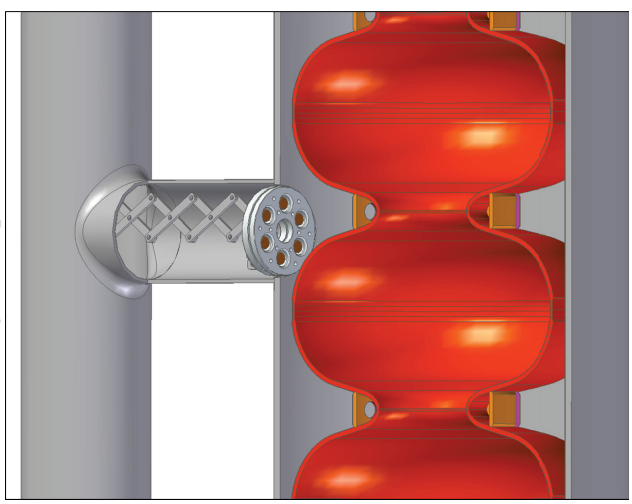

Figure 1: MultiOST detector installed inside the helium pipe.

* yegor.tamashevich@desy.de

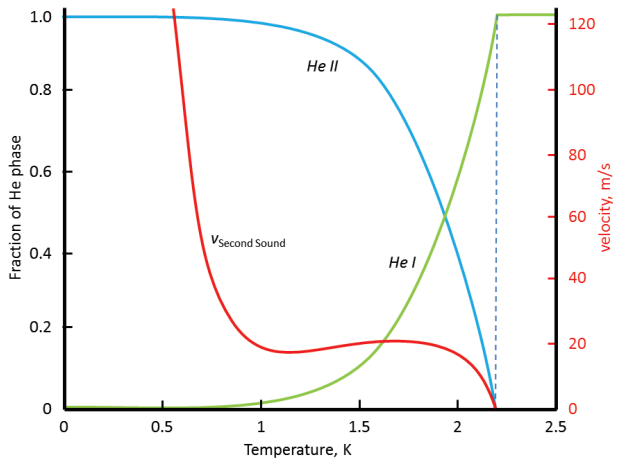

Figure 2: Helium phases and second sound velocity [1, 2].

This limitation significantly increases the complexity for measurements and algorithms for calculations.

EXPERIMENTAL SETUP

In the setup second sound oscillations are detected by oscillating superleak transducers (OST) [3, 4]. Within the OST the electrical capacity changes due to oscillation of the ratio of the fractions of helium phases. Typically second sound tests are performed at 1.8 K as the ratio of He I and He II phases is close to 1:1 and the capacitance change is maximal (see Fig. 2). The corresponding velocity of the second sound is 19.9 m/s [1].

While the OST is biased, its capacitance change leads to voltage changes on the measuring resistors. The voltage oscillations on this resistor can be easily measured after amplification (see Fig. 3).

For testing of dressed cavities a special Multi-OST sensor was developed. It consists of 6 OSTs placed in a single housing (see Fig. 4 for following details). Each OST consists of a copper anode of 7 mm diameter (2), which is biased with 120 V DC, and the porous membrane with golden layer (4), which serves as cathode. Anodes are isolated from the housing (1) by dielectric epoxy (3). Each OST has independent readout. A retractable mounting allows quick installation of the Multi-OST into the nozzle tank tube of a standard E-XFEL cavity with precise (ca. 1 mm) positioning accuracy (see Fig. 1).

The signal amplifier is in-house built and based on a simple operational amplifier circuit (see Fig. 3). Noise level demands require full cable shielding and the positioning of the ADC inside the amplifiers box. It is also necessary to stabilize the power buses for operational circuits, which

ISBN 978-3-95450-178-6

DIAGNOSTIC DEVELOPMENTS AT CERN'S SRF TESTING FACILITY

A. Macpherson*, K. Hernandez Chahin, S.Aull, A. Benoit, P. Fernández López, C. Jarrige, P. Maesen, K.-M. Schirm, R. Torres-Sanchez, R. Valera Teruel, CERN, Geneva, Switzerland
T. Junginger, TRIUMF, Vancouver, Canada

Abstract

As part of CERN's re-establishment of an SRF cold testing facility for bulk niobium cavities, diagnostic instrumentation and testing procedures on our vertical cryostat have been upgraded, with particular attention given to quench location, ambient magnetic field control, thermometry and thermal cycling techniques. In addition, preparation and measurement procedures have been addressed, allowing for improved measurement of cavity properties and detailed study of transient effects during the course of cavity testing.

INTRODUCTION

As part of CERN's R&D programme on bulk Niobium cavities [1], considerable effort has been invested in the refurbishment of the vertical cryostat test stand at our SRF test facility [2]. Included in this refurbishment has been an upgrading of measurement hardware and the addition of a full suite of diagnostic tools. For the measurement infrastructure, the setup is as shown in Fig. 1, with the test stand operating at 2K in CW mode with a fixed input coupler, and a maximum input power of 260W.

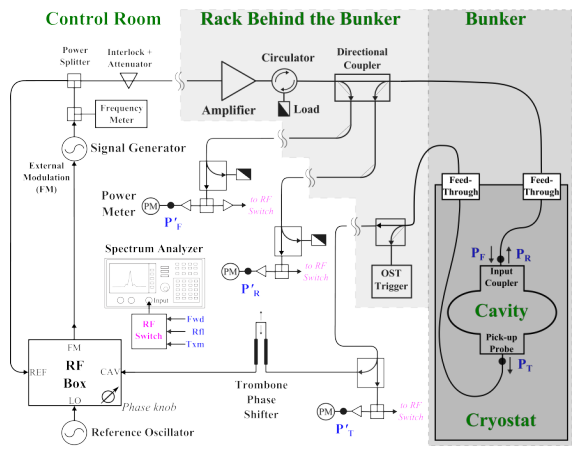

Figure 1: Schematic of the vertical test cryostat setup.

MEASUREMENT TEST STAND

As part of the refurbishment, the test stand software has been completely re-written in LabView, and now uses an underlying queue-based manager handler structure. This has resulted in significant improvement in data taking capabilities, with data acquisition rates of 3 Hz for Q_0 vs E_{acc} scans. This permits detailed semi-automated power scans with small incremental input power steps (typically 0.05 dBm), which in turn allows us to clearly scan and identify multipacting sub-structure of the cavity, as can be seen in Fig. 2. Data sets for a typical detailed scan contains about six thousand data points, where each data point is a data object containing both measurement and environmental data. Also seen in Fig. 2 is the transient behaviour of the cavity on increment of the input power, which can be used to estimate the cavity filling time, and hence give a cross-check of the test stand calibration.

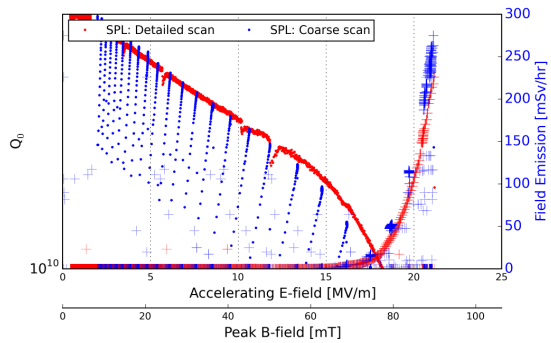

Figure 2: A detailed Q_0 vs E_{acc} scan for a cavity. The scan with a coarse incremental power step is in blue, while the red points show the same cavity scanned with 0.05 dBm increments. The detailed scan reveals a sub-structure most likely small multipacting barriers. Radiation data from the field emission is shown as a "+".

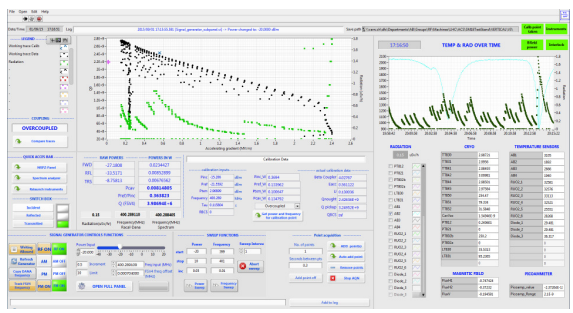

Figure 3: Front panel display of the LabView software framework used for the SRF test stand. Scan results are on the left and environmental monitoring data on the right.

For the cavity environment monitoring, on-line diagnostics have been installed and validated. These include contact resistors used as cavity temperature sensors, fluxgate magnetic field probes for ambient field measurements, and standard monitoring of field-emission induced radiation, cavity vacuum, and the full monitoring of the cryo process and operation. All monitoring data is available at the top level of the data taking application for real-time display (see Fig. 3), and is time stamped and stored. Due to the large increase in measurement and environmental data, a hierarchical data storage

* alick.macpherson@cern.ch

MULTI-CELL TEMPERATURE MAPPING AND CONCLUSIONS

Fumio Furuta, Ralf Eichhorn, Mingqi Ge, Daniel Gonnella, Don Hartill, Georg Hoffstaetter, John Kaufman, Matthias Liepe, Eric Smith, Cornell University, Ithaca, NY 14850, USA

Abstract

Multi-cell temperature mapping (T-map) system for 1.3GHz SRF Nb cavities has been developed at Cornell. T-map system consists of nearly two thousand thermometers array positioned precisely on an exterior cavity wall and is capable of detecting small increases in temperature. It has achieved a 1mK resolution of niobium surface temperature rinsing in superfluid liquid helium. We have upgraded the system to be capable of monitoring the temperature profiles of quench spot on cavity. The recent results of T-map during cavity tests and details will be reported.

INTRODUCTION

T-mapping history can be traced back to the 1980s. Cornell University was a pioneer in developing a 1-cell T-map system for 1.5GHz SRF cavity research [1, 2, and 3]. Now Jefferson Lab and Fermilab also have 1-cell or 2-cell T-map systems. These systems are used for fundamental SRF research via single-cell cavities. Due to the requirement on further understanding of multi-cell cavities, the development of a multi-cell T-mapping system becomes more necessary and ultra-important. DESY and Los Alamos have multi-cell T-mapping systems for ILC 9-cell cavities [4, 5]. Those systems are mainly used to detect quench location.

The Cornell multi-cell T-mapping system, by virtue of its high sensitivity, is able to detect heating levels much lower than those required to cause a quench. The hot-spots normally start in the medium accelerating gradient region and cause a Q-drop. Increasing the accelerating gradient of cavity, the heating at a hot-spot will grow as well, and eventually quench the cavity. Therefore it is important to discover not only the quench location but also the original location of heating as well as the growth of the heating rate versus accelerating gradient. This information would help to unveil the loss mechanism of superconductivity under medium RF field, and address fundamental physics..

MULTI-CELL TEMPERATURE MAPPING SYSTEM

Cornell multi-cell T-map system has been developed for the 7-cell cavities of Cornell ERL project. This system could also fit onto 1.3GHz TESLA shape 9-cell cavities, and covers the centre 7-cells of 9-cell. We did several trials of T-map with 9-cell cavity to confirm the performance of system. The details of them will be described later. The additional boards are under fabrication for the full 9-cell T-map system. The cavity specification values of Cornell ERL 7-cells are quality factor (Qo) of 2×10^{10} at accelerating field gradient of 16MV/m in 1.8K [6]. The temperature rise of ~20mK on the exterior wall is estimated against a 1.3GHz SRF cavity with Qo of 2.0e10 at 16MV/m in 2.0K helium bath [7]. The sensor is able to detect the temperature rise of the cavity wall with 25% efficiency [3]. Thus the resolution of this T-map is required to be approximately 1mK.

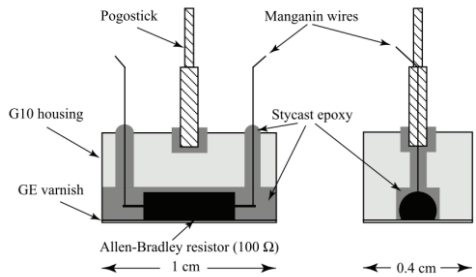

Figure 1: Thermometer schematic [3].

Thermometers and Boards

The temperature sensors are a 100Ω carbon Allen-Bradley resistor (5% 1/8 W). Carbon is a semiconductor, its resistance increases exponentially when temperature drops. Figure 1 shows the schematic of sensor and its picture. The system consists of two sets of 3-cell boards and one set of 1-cell boards, so it covers 7-cells in total. The sensor boards are spaced azimuthally every 15° around the cavity; totally it has 24 boards per cell around the azimuth. Each board has 11 thermometers per cell, so each cell is covered by an 11×24 thermometer array. The quantity of thermometers for the whole 7-cell cavity is 1848. Dow Corning vacuum grease was applied on the varnished side of the thermometers prior to inserting the boards in cages. Silicone-based Dow Corning grease has similar thermal conductivity to traditional APIEZON grease in superfluid helium, but much cheaper than APIEZON grease. When the thermometers press to the cavity wall, the grease spreads into remaining gaps and

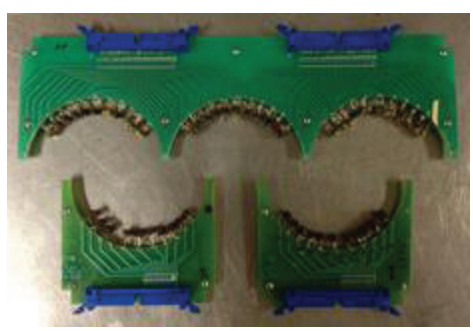

Figure 2: A 3-cell board and 1-cell boards.

*This work has been supported by NSF award PHY-0969959 and DOE award DOE/SC00008431

ISBN 978-3-95450-178-6

AUTOMATIC SURFACE DEFECT DETECTION AND SIZING FOR SUPERCONDUCTING RADIO FREQUENCY CAVITY USING HAAR CASCADES*

D. Iriks, Santa Rosa Junior College, Santa Rosa, CA, U.S.A.
G. Eremeev†, Jefferson Lab, Newport News, VA, U.S.A.

Abstract

Serious albeit tiny surface defects can remain on the surface of superconducting radio frequency (SRF) cavities after polishing and cleaning. These defects reduce the efficiency of cavities and often limit the maximum attainable fields. We applied a Haar cascade artificial vision technique for automated identification, counting, and sizing of defects induced on niobium surface by Nb-H precipitates formed at cryogenic temperatures. The defects were counted and sized by a computer program and also counted and measured manually to estimate detection rate and accuracy of sizing. The overall detection rate was 53%, and the overall false positive rate was 29%. The technique that was used to automatically size the features was found to oversize the features, but oversize them consistently, resulting in a size histogram that represents the defect size distribution on the sample. After scaling the histogram data, the average defect area was found to be 90 μm^2 with the standard deviation of 70 μm^2.

INTRODUCTION

Superconducting RF structures made of sheet metal niobium are widely used around the world to accelerate particle beams [1]. Being cooled to liquid helium temperatures, they provide an efficient way to deliver electric energy to particle beams. While very efficient, the cavities are still prone to limitations such as multipacting, field emission, Q-slopes, and defects. For the best cavities to date, the two main gradient limitations are defects and field emission. Larger defects left on the cavity surface after cavity preparation lead to higher dissipation and eventually quench, while smaller defects contribute to dissipation and reduce the quality factor, which is the measure of cavity efficiency.

A number of tools have been developed for internal inspection of cavity surface for small surface imperfections. The tool most widely used presently is the so-called KEK system [2] and its modifications. The tool is capable of capturing images of the cavity surface at the equator and iris regions. The modifications to this tool include imaging of 9-cell cavity equator regions with automatic cavity positioning and focusing [3, 4]. The pictures captured by these imaging systems still need to be reviewed in order to identify, count, and record defects on the inner surface. To achieve full automation of cavity inspection process, defects need to be identified automatically. Hence, there is an interest in exploring different techniques for automated defect identification.

METHOD

Sample pictures were captured with a HIROX KH-7700 digital microscope. The MXG-2500REZ lens was used at high-range (x1000), as was an angular light filter. The samples were made out of high residual resistivity ratio (RRR 300) niobium. The defects on the samples surface were formed by hydrogen precipitates formed in the bulk at about 100 K. More details about these defects can be found in [5]. The photographing procedure was to take a picture, move the stage so that there was a small overlap between frames, adjust the lens focus, take another picture, move the stage a little again, and so on. About 2000 negative pictures and 1000 positive pictures were taken. An attempt was made to seek negative pictures generally with backgrounds similar to those in the positives, however some with less similar backgrounds were also intentionally taken. Of the pictures taken, a certain number of positives and negatives were reserved for testing only.

For defect recognition, a C++ program was written in Visual Studio C++ 2008 that uses the OpenCV 2.1. library and a Haar cascade [6, 7]. Instructions and materials for training the cascade can be found online, e.g. [8]. In total, 731 positive pictures were taken for training, and the total count of training defect samples obtained from these images was 1148. The total number of the negative training pictures was 1917.

For testing, four folders of images that were not used in cascade training were assembled. Every test image was a jpg image with dimensions of 1600 by 1200 pixels. One was a folder of 90 negatives. The other three were folders of positives which were separated according to how difficult it was thought it would be for the program to detect the defects. There was an easy folder with 8 images and medium and hard folders with 21 images each. The assignment of positives into these folders was based on personal judgment of the quality of surface cleanliness and de-

* Authored by Jefferson Science Associates, LLC under U.S. DOE Contract No. DE-AC05-06OR23177.
† grigory@jlab.org

TEST CHARACTERIZATION OF SUPERCONDUCTING SPOKE CAVITIES AT UPPSALA UNIVERSITY

H. Li, V.A. Goryashko, A. Bhattacharyya, R. Santiago Kern, L. Hermansson,
Roger Ruber and Dragos Dancila, Uppsala University, Sweden,
G. Olry, IPN Orsay, France

Abstract

As part of the development of the ESS spoke linac, the FREIA Laboratory at Uppsala University, Sweden, has been equipped with a superconducting cavity test facility. The cryogenic tests of a single and double spoke cavity developed by IPN Orsay have been performed in the new HNOSS horizontal cryostat system. The cavities are equipped with a low power input antenna and a pick-up antenna. Different measurement methods were investigated to measure the RF signal coupling from the cavity. Results from the tests confirm the possibility to transport the cavities from France to Sweden without consequences. We present the methods and preliminary study results of the cavity performance.

INTRODUCTION

After decades of studies, spoke cavities are considered compact structures at low frequencies and having an excellent RF performance in both low and medium velocity regimes. These advantages make them attractive for modern accelerator facilities, including the ESS proton accelerator where double-spoke resonators (DSR) will be used for the medium energy section [1].

The Facility for Research Instrumentation and Accelerator Development (FREIA) is developing the RF system for ESS superconducting spoke cavities. This project contains three phases: (1) test of the first RF source, (2) test of the prototype cavity and (3) test of the prototype cryo-module [2]. In the second phase, the bare spoke cavity is tested at low power-level to confirm its vertical test performance at IPN Orsay. Then, a spoke cavity equipped with an RF power coupler will be tested at high power with the tetrode-based RF system from phase 1. Since self-excited loops have a lot of advantages for testing high gradient, high-Q cavities, FREIA developed a test stand based on a self-excited loop for demonstrating the performance of superconducting cavities at low power-level.

Table 1: Main Parameters of Spoke Cavities

Parameter	Hélène (SSR)	Germaine (DSR)
Frequency (MHz)	360	352.2
Beta (optimal)	0.2	0.5
R/Q_0 (Ω)	117	426
E_{pk}/E_{acc}	6.56	4.33
B_{pk}/E_{acc} $(mT/MV/m)$	13.4	6.89
G (Ω)	89	130

We received a single spoke cavity (Hélène) and a double spoke cavity (Germaine) from IPN Orsay, and performed cold tests at FREIA to validate our test protocol, hardware and cryo system. Test results in FREIA are consistent with the ones obtained at IPN Orsay [3]. Table 1 shows the main RF properties of the two spoke cavities [3,4].

CRYOGENIC TESTING

The cryogenic testing of both cavities was carried out at FREIA using the self-excited loop test stand shown in Fig. 1. In the loop, the cavity is a narrowband filter and starts from noise to oscillate by itself. In this way, the cavity field amplitude is unaffected by the ponderomotive instability and there is no need for an external frequency source and tracking feedback. Therefore, the self-excited loop is ideally suited for high gradient, high-Q cavities operated in continuous wave (CW) mode [5].

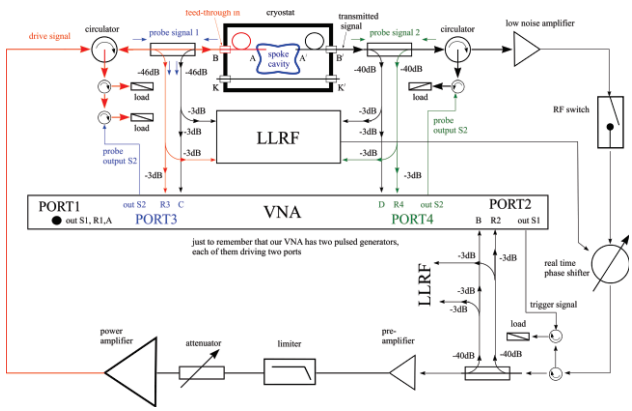

Figure 1: Schematic of the FREIA self-excited loop.

With this test stand, the loop can be tuned by 40 dB variable attenuation and 270 degree trombone phase shifter, and can reach up to 100 W CW power and 100 dB maximum gain. A digital phase shifter is under development. Also a new high-precision measurement of super-conducting cavities quality factor has been studied [6].

Two cavities are set inside the new HNOSS horizontal cryostat system at the same time [7]. Six identical cryo-cables are installed inside the cryostat; four of which connect the cavity ports with RF feedthroughs on a cryostat flange, while the other two cables connect back to back with a RF through as reference. The warm part of the system is calibrated using a vector network analyser (VNA) with two-ports S parameters, together with a power meter for power calibration. By connecting the

ISBN 978-3-95450-178-6

CHARACTERIZATION OF OPTICAL SURFACE PROPERTIES OF 1.3 GHz SRF CAVITIES FOR THE EUROPEAN XFEL*

M. Wenskat†, L. Steder, DESY, Hamburg, Germany

Abstract

The optical inspection of the inner surface of superconducting RF cavities is a well-established tool at many laboratories. Its purpose is to recognize and understand field limitations and to allow optical quality assurance during cavity production. Within the ILC-HiGrade program at DESY, as part of the XFEL cavity production, an automated image processing and analysis algorithm has been developed that recognizes structural boundaries. The properties of these boundaries can be used for characterization. The potential of this framework for automated quality assurance as an integral part of large-scale cavity production will be outlined.

OBACHT

A fully automated robot for optical inspection has been continuously used at DESY. It is equipped with a high-resolution camera, which resolves structures down to 12 µm for properly illuminated surfaces. The mechanical details of OBACHT, the optical system and the control are described in [1–3]. Figure 1 shows an image of the inner cavity surface taken with OBACHT.

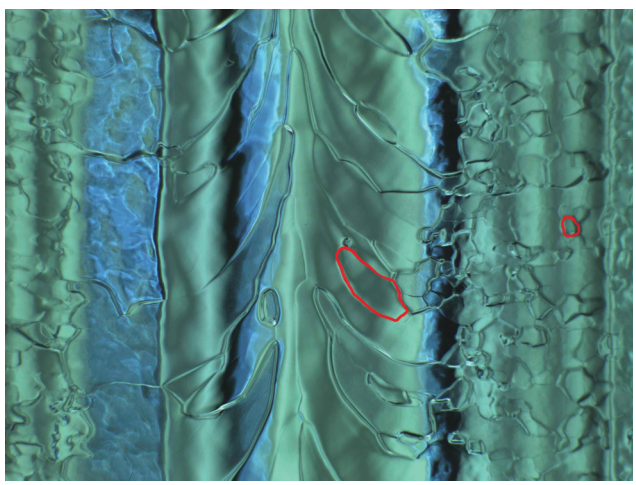

Figure 1: Image of the inner cavity surface with the equatorial welding seam in the image center taken with OBACHT. The image size is 9×12 mm^2. The red contours are examples of grain boundaries identified with the image processing algorithm.

* Work is funded from the EU 7th Framework Program (FP7/2007-2013) under grant agreement number 283745 (CRISP) and "Construction of New Infrastructures - Preparatory Phase", ILC-HiGrade, contract number 206711, BMBF project 05H12GU9, and Alexander von Humboldt Foundation.

† marc.wenskat@desy.de

The objects of interest within an image of the inner cavity surface are grain boundaries. In order to identify and quantify those boundaries, an image processing and analysis algorithm has been developed.

IMAGE PROCESSING AND ANALYSIS

The main goal of the image processing algorithm is to identify grain boundaries, regardless of their position within the image which is exposed to varying illumination, as can be seen in Figure 1. The approach of this algorithm is, by applying a sequence of high-pass filter and local contrast enhancements, to project pixels which belong to grain boundaries onto a uniform gray scale range, which is distinct to the background. After this projection, a histogram based segmentation of the image is performed. This segmentation assumes, that the image contains two classes of pixels (grain boundary and background), where the intensity values follow a bi-modal distribution, and calculates the optimum threshold separating the two classes. The output is a binary image with the same size as the input image. It will contain grain boundary pixels in white (logical one) and background pixels in black (logical zero). As a last step, group of connected white pixels which form a grain boundary have to be classified as a single object and a labeled binary image is obtained. For more details on the image processing algorithm see [3]. An example of such a binary image is given in Figure 2.

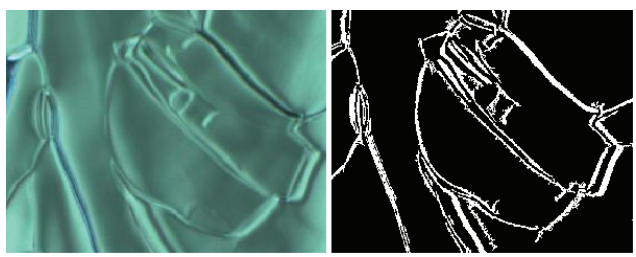

Figure 2: Left: a detail of an OBACHT image is shown. Right: the same detail after the image processing algorithm is shown. Features like grain boundaries (white) are visible.

Features can be identified in the binary image. Those are grain boundaries with varying width, so that an area can be ascribed, as well as an eccentricity, a centroid and an orientation. The grain boundary area is the total amount of pixels, of which a boundary consist of. This number is retrieved from the binary image and then multiplied by the *pixel size*, which is a property of the optical system. At OBACHT, this value is 12.25 µm^2. Other variables, such as a measure for the surface roughness based on the intensity gradient, include information from the original image.

ISBN 978-3-95450-178-6

DEVELOPMENT OF AN X-RAY FLUORESCENCE PROBE FOR INNER CAVITY INSPECTION

M. Bertucci*, P. Michelato, L. Monaco, M. Moretti, INFN Milano - LASA, Segrate (MI), Italy
C. Pagani, Università degli Studi di Milano & INFN Milano - LASA Segrate, Italy
A. Navitski , DESY, Hamburg, Germany

Abstract

The development of an x-ray fluorescence probe for detection of foreign material inclusions of the inner surface of 1.3 GHz tesla-type Niobium cavities is here presented. The setup dimensions are minimized so to access the inner cavity volume and focus on the surface of equator. Preliminary tests confirmed the system capability to detect and localize with good precision small metal inclusions of few micrograms. The results obtained from the inspection of some 1.3 GHz XFEL series production cavities are also pointed out.

INTRODUCTION

The ability to detect performance-limiting defects on the inner surface of superconducting radiofrequency (SRF) niobium cavities, which lead to low quality factor Q_0 factor, thermal breakdowns (especially at the equator welding seams and the surrounding area), and X-ray radiation (mainly due to sharp geometric defects on the irises) provides a tool of quality control (QC) and failure reason clarification. Detection of failures and defects, especially in early production steps, would significantly reduce repetition of quite expensive cryogenic RF tests and retreatments of the cavities. Inspection of the inner cavity surface by an optical system is an inexpensive and useful means for surface control and identification of dangerous or suspicious features [1, 2]. It does not provide, however, information about material content in the defect region, which is required for sorting out the cavities with foreign inclusions and for the localisation of a contamination source in the production cycle. Preliminary diagnostic is usually performed during the QC of niobium sheets resorting to several non-destructive techniques, e.g. eddy current scanning [3].

X-ray fluorescence (XRF) analysis is widely used for elemental and chemical analyses, particularly in the investigation of metals. This technique, already employed during the QC of niobium sheets [4], appears to be entitled for development of a diagnostic tool for the detection of trace element inclusions on the cavity surface. Preliminary feasibility tests [5] performed with a low-performance XRF setup, demonstrated that low amounts (some μg) of different metals could be easily detected when embedded in the niobium matrix. These encouraging results have been the first step towards the development of an XRF tool for the QC of the inner surface of 1.3 GHz SRF cavities. The complicated shape of the cavities and hidden inner surface require, however, development of a special device.

* michele.bertucci@mi.infn.it

CHARACTERISTICS OF XRF SPECTROSCOPY TECHNIQUE

XRF spectroscopy is well known non-destructive elemental analysis technique based on the detection of characteristic X-ray radiation emitted from a material that has been excited by a high-energy primary X-ray source. It allows simultaneous acquisition of the whole sample spectrum in a very short time, detecting low concentration values up to a part per million. The fluorescence spectrum lines offer an unequivocal determination of sample elements. The XRF setup consists of an X-ray tube for primary excitation of the material to be investigated and a detection unit for energy dispersive spectroscopy. The excitation spectrum of the tube is given by bremsstrahlung radiation produced by electron-bombardment of the target along with characteristic fluorescence line of the target material. The X-ray tube radiation in its turn excites the characteristic radiation of sample elements (X-ray fluorescence spectrum). A schematic overview of an XRF setup is shown in Fig. 1.

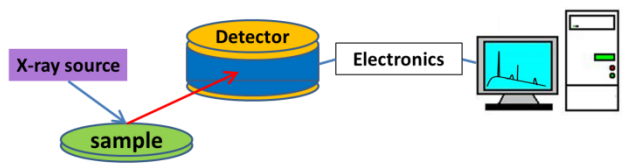

Figure 1: Schematic overview of an XRF setup.

Typical benchtop XRF instruments do not require a specific sample preparation, although both X-ray source and detector must be as close as possible to the sample surface to maximize detection efficiency and avoid spurious signals in the detected spectrum. Aiming to develop an inspection tool for the cavity inner surface, the X-ray source and detector must enter the inner cavity space.

Detection Depth

Since the niobium X-ray absorption cross section is high for energies below 100 keV, the excitation radiation will penetrate inside the bulk for a depth of about 68 μm when employing an X-ray tube with the molybdenum anode. The penetration depth corresponds to an inverse of attenuation linear coefficient of niobium μ_{Nb} of 146 cm^{-1} at the energy of Mo K_α characteristic line of 17.4 keV [6].

ISBN 978-3-95450-178-6

ON QUENCH PROPAGATION, QUENCH DETECTION AND SECOND SOUND IN SRF CAVITIES

R. Eichhorn# , D. Hartill, G. Hoffstaetter, and S. Markham
Cornell Laboratory for Accelerator-Based Sciences and Education, Cornell University
Ithaca, NY 14853-5001, USA

Abstract

The detection of a second sound wave, excited by a quench, has become a valuable tool in diagnosing hot spots and performance limitations of superconducting cavities. Several years ago, Cornell developed an oscillating super-leak transducer (OST) for these waves that nowadays is used world-wide. In a usual set-up, several OSTs surround the cavity, and the quench location is determined by trilateration of the different OST signals.

Convenient as the method is, there is a small remaining mystery: taking the well-known velocity of the second sound wave, the quench seems to come from a place slightly above the cavity's outer surface. We will present a model based on numerical quench propagation simulations and analytic geometrical calculations that helps explain the discrepancy.

INTRODUCTION

Many future linear accelerators rely on superconducting radio frequency (SRF) cavities to accelerate the particles. During the last decade, the advantages of SRF technology compared to normal conducting RF systems based on copper resonators have been broadly recognized. Early SRF cavities had low accelerating gradients, high RF losses and, being the most serious issue, a very unreliable performance reproducibility. State of the art SRF cavities have overcome these limitations: they reach high gradients and low losses, very close to the theoretical limit. Many of the advances in the field are due to a better understanding of the surface effects in SRF cavities, quench limits and contamination.

Today's SRF cavities undergo a sophisticated fabrication scheme which ensures a smooth and uniform surface. Despite precautions taken, it is still common for cavities to bear small (sub-millimeter) surface defects that impede cavity performance. These defects cause localized excess heating, eventually causing a quench to normal conductivity and limiting the cavity's performance.

One method of locating a defect involves using oscillating superleak transducers (OSTs [1]) to detect second sound waves emitted from the cavity. Second sound is a phenomenon observed in superfluid helium [2] wherein heat propagates as a wave with properties comparable to that of a classical sonic wave. The speed of the second sound depends somewhat on the parameters of the fluid, but is almost a constant of 20 m/s, within the temperature range of 1.6 to 2 K.

By measuring the time of arrival of the 2nd sound wave-front at the detectors relative to the time of the RF field collapse, the distance between each transducer and the defect heated region may be calculated. This information is used in trilateration the defect location using the well-know propagation velocity of the sound wave. A common problem in the trilateration is that the source of the second sound wave seems to be located above the cavity surface, giving rise to various theories as the propagation speed of the wave would have to be larger than published data if it propagated from the defect through helium, starting at the time of field-collapse[3-5].

Within this paper we will elaborate on two mechanisms that explain the early arrival of the wave. We will present results from dynamic heat transport calculation through the niobium which includes the ring-down of the RF field inside the cavity after the onset of the quench. Furthermore, this paper will describe how heat propagation in the niobium can contribute to the quench signal propagation and to the misinterpretation of the quench location.

MODEL SPECIFICATION

A MATLAB computational model is used to investigate the time dependent dynamics of the SRF cavity with a known defect under medium RF field conditions. We were particularly interested in the potential disparity between the time of the excitation of a second sound wave on the Nb-HeII interface and the time where losses in stored energy of the SRF system become significant. Our model has two arbitrarily chosen parameters: one being the heat flux level at which a significant and detectable amplitude of the second sound wave is generated and the other being the drop in RF power at which a quench is realized. We will discuss our choice of parameters below and allow the readers to draw conclusions using different values for these parameters.

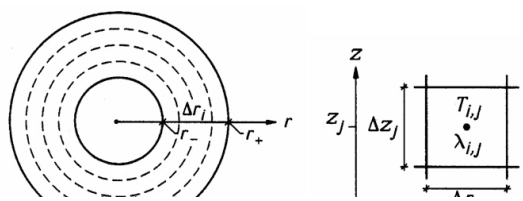

Figure 1: Discretization used for calculating the heat propagation through the niobium. The coordinate system is centred around the defect, reducing the calculations to a quasi-2D problem.

#r.eichhorn@cornell.edu

ISBN 978-3-95450-178-6

HIGH-PRECISION MEASUREMENTS OF THE QUALITY FACTOR OF SUPERCONDUCTING CAVITIES AT THE FREIA LABORATORY

V.A. Goryashko*, Han Li, H. Nicander, S. Teerikoski, K. Gajewski, L. Hermansson,
R. Santiago Kern, R. Ruber and Dragos Dancila, Uppsala University ,Uppsala ,Sweden

Abstract

The dependence of cavity quality factor Q_0 on accelerating gradient gives insight into the intrinsic limit of RF surface impedance that determines the cavity performance. In this paper we propose a high-precision method of measuring Q_0 of SRF cavities. A common way to study the performance of an SRF cavity is to build an oscillator around it that is referred to as a self-excited loop. In the standard approach, by tuning the loop phase for a maximum field level in the cavity and measuring forward and reflected waves, one finds the cavity coupling. Then, performing a time-decay measurement and finding the total quality factor, one gets Q_0. However, this approach suffers from a deficiency originating from a single data-point measurement of the reflection coefficient. In our method by varying the loop phase shift, one obtains amplitudes of the reflection coefficient of the cavity as a function of its phases. The complex reflection coefficient describes a perfect circle in polar coordinates. Fitting the overdetermined set of data to that circle allows more accurate calculation of Q_0 via the least-squares procedure. The method has been tested at the FREIA Laboratory [1] on two cavities from IPN Orsay: a single spoke and a prototype ESS double spoke.

INTRODUCTION

The quality of accelerated beams and overall efficiency of a superconducting (SC) linear accelerator depend on the performance of SC cavities and an extensive research and development program on the cavities has been undertaken during last decades. However, some aspects of the physics of SC RF cavities remain unclear and even controversial such as the so-called low-field Q-slope [2]. According to the classical BCS theory, the cavity quality factor, Q_0, is a monotonically decreasing function of the field created in the cavity whereas experimental observations strongly indicate that in the low-field region between a few mT and a few tens of mT, Q_0 increases as the field is raised, see [2] and references herein. A recent field-dependent model [3] of the RF surface impedance based of Mattis-Bardeen theory suggests that the positive low-field Q slope continues up to 100 mT. That has an important implication on the intrinsic limit of RF surface impedance that determines the performance of SC RF cavities.

Accurate measurements of intrinsic cavity characteristics such as the quality factor are indispensable for facilitation of understanding of the physics of SC RF cavities and the low-field Q-slope effect, in particular. In this paper we propose a high-precision method of measuring Q_0 of SC RF cavities. The method can also be used at accelerator test facilities for studying the cavity performance needed to ensure the proper dynamics of accelerated beams. Measurements of the pressure sensitivity, Lorentz force detuning and microphonics are presented in the conference proceedings, TUPB083.

There is a number of accurate methods of measuring Q_0 developed for normal conducting cavities [4–9]. However, these methods fail to work for SC cavities because of their ultra-narrow bandwidth, which is in the order of a Hz or even less, and large variations of the cavity frequency on a time scale required for measurements. The cavity walls are made thin for good heat transfer so that fluctuations in pressure of helium – the cavity is immersed to – can detune the cavity by many times of the cavity bandwidth.

A common way to circumvent the problem is to build an oscillator around the cavity that is referred to as a self-oscillating loop [10]. The loop tracks the cavity frequency and the field excited remains constant in time provided that the system reached a steady-state equilibrium. By tuning the loop phase for a maximum field level in the cavity and measuring forward and reflected waves, one finds the cavity coupling [11]. Then, performing a time-decay measurement [12] and finding the total quality factor, we can find Q_0. However, this approach suffers from a deficiency originating from a single data point measurement of the reflection coefficient. Here, we propose an extension of a high-precision method developed for normal conducting cavities to SC counterparts. By varying the loop phase, one obtains amplitudes of the reflection coefficient as a function of its phases. This overdetermined set of data allows more accurate calculation of the cavity coupling coefficient via the uncertainty minimization procedure.

THE CAVITY MODEL

An electromagnetic (EM) field of a closed metallic cavity is represented by a set of TE and TM eigenmodes corresponding to different spatial field distributions and being solutions to the source-free Maxwell equations. Each eigenmode is characterised by a quality-factor, Q_0, and a frequency of temporal oscillations, ω_c. In the presence of a source, the general solution for a field excited in the cavity can be represented as an expansion over the eigenmodes with unknown *scalar* field amplitudes [13]. If the modes are not degenerated, then the amplitudes in question evolve in time according to the second-order differential equation of the oscillator-type. The effective excitation source (driving force) in this equation is given by the overlap integral of the spatial distributions of a physical excitation source, for example, such as an antenna and the eigenmode. The over-

* vitaliy.goryashko@physics.uu.se; vitgor06@gmail.com

ISBN 978-3-95450-178-6

SYSTEMATIC UNCERTAINTIES IN RF-BASED MEASUREMENT OF SUPERCONDUCTING CAVITY QUALITY FACTORS*

W. Schappert#, J.P. Holzbauer, Yu. Pischalnikov, D.A. Sergatskov, FNAL, Batavia, IL 60510, USA

Abstract

Q_0 determinations based on RF power measurements are subject to at least three potentially large systematic effects that have not been previously appreciated. Instrumental factors that can systematically bias RF based measurements of Q_0 are quantified and steps that can be taken to improve the determination of Q_0 are discussed.

INTRODUCTION

The intrinsic quality factor, Q_0, of a superconducting cavity is an important measure of its performance. If the coupling factor, β, is close to unity, Q_0 can be determined from RF losses in the cavity. If the coupling is far greater than unity, cryogenic heat load measurements must be employed. Only RF measurement techniques will be considered here.

RF-based quality factor measurements commonly compare the power incident on the cavity, P_F, to the power reflected by the cavity, P_R, to determine the cavity coupling factor:

$$\beta^* = \left(\frac{\sqrt{P_F}+\sqrt{P_R}}{\sqrt{P_F}-\sqrt{P_R}}\right)^{\pm 1}.$$

The sign of the exponent in this equation is chosen to be positive (negative) if the cavity is over-coupled (under-coupled). The loaded cavity quality factor, Q_L, can be determined from the decay time, τ, of the stored energy when power to the cavity is shut off.

$$Q_L = \omega\tau.$$

The intrinsic quality factor is related to the cavity coupling and loaded quality factor:

$$Q_0 = (1+\beta^*)Q_L.$$

RF power levels and cavity decay times can typically be determined with an accuracy of a few percent. These uncertainties limit the accuracy of RF based quality factor measurements to 5% or more, even under the best conditions [1,2,3].

Implicit in this approach are three assumptions:

1. The forward and reflected waveforms are perfectly separated during the coupling factor measurement.
2. No power is incident on the cavity during the decay time measurement.
3. The cavity is precisely on resonance during the measurement of the coupling factor.

Each of these three assumptions is violated in practice.

1. The imperfect directivity of the directional coupler used to separate the waveform incident on the cavity from the reflected waveform inevitably introduces some degree of cross-contamination between the signals.
2. Energy emitted into the reflected waveform from the cavity during the decay can re-reflect back from the circulator commonly used to isolate the RF power amplifier as energy incident on the cavity. The re-reflected energy may interfere constructively or destructively with the cavity field. Constructive interference will systematically bias measured decay times to values longer than the true cavity decay time. Destructive interference will systematically bias the measured decay times to shorter values.
3. Energy re-reflected from the circulator will also systematically shift the resonance frequency of the cavity-waveguide system from the true resonance of the cavity leading to systematic biases in the measured coupling factor.

DIRECTIVITY UNCERTAINTIES

Dual directional couplers are commonly used to separate the voltage incident on the cavity from the voltage in the waveform reflected from the cavity. Perfect separation of the forward and reflected waves within the coupler is not possible. Some degree of cross-contamination will always be present. The level of cross-contamination that may be expected is specified by the directivity of the coupler. The directivity of the forward port can be determined from the S-parameters of the coupler.

$$D = 20\,log_{10}\frac{S_{31}}{S_{41}}$$

Poor directivity couplers may have directivities as low as 10 dB. Couplers with directivities of 20 or 30 dB are commonly employed for cavity testing. Ultra-high directivity couplers may have values as high as 60 dB.

While a directivity of 20 dB implies that less than one percent of the power is leaking into the other port, depending on the relative phases of the direct signal and the contamination, interference effects can lead to systematic power mismeasurements of up to ±10 percent. If the contamination adds constructively with the direct signal the measured power may be systematically larger than the true power by up to $10^{D/20}$. If the contamination

*This manuscript has been authorized by Fermi Research Alliance, LLC under Contract N. DE-AC02-07CH11359 with U.S. Department of Energy.

#jeremiah@fnal.gov

INITIAL COMMISSIONING EXPERIENCE WITH THE SPALLATION NEUTRON SOURCE VERTICAL TEST AREA RF SYSTEM*

M. Crofford, J. Ball, T. Davidson, M. Doleans, S-H. Kim, S-W. Lee, J. Mammosser, J. Saunders, S. Whaley, ORNL, Oak Ridge, TN 37831, USA

Abstract

The Spallation Neutron Source (SNS) has developed a vertical test area (VTA) for the testing and qualification of superconducting radio frequency cavities. The associated RF System successfully supported the initial commissioning of the VTA system and has been utilized for cavity testing at both 4 and 2 K. As operational experience was gained, improvements to the RF system were implemented to better utilize the dynamic range of the system, and software updates and additions were made to meet operational needs. The system continues to evolve as we gain better understanding of the testing needs.

INTRODUCTION

The Spallation Neutron Source (SNS) project was completed in 2006 and is now routinely operating at power levels of 1.3 MW on target. Our Linac consists of both normal conducting structures and superconducting cavities to generate the nominal 1000 MeV H- ion beam. To maintain our operational readiness we have invested significant effort in the infrastructure of the Radio Frequency Test Facility (RFTF) to include a vertical test area (VTA) for the qualification of superconducting radio frequency cavities [1]. The RF systems utilized in the VTA are based on the systems developed at both Jefferson Lab (JLAB) and Fermi National Accelerator Laboratory (Fermilab).

The RF system shown in Figure 1 is a combination of commercial-off-the-shelf (COTS) equipment and custom designed hardware to implement a self-excited loop style control system. This design process was chosen due to experiences at other laboratories and the time constraints for system implementation. The custom hardware functions have been separated into five modules consisting of a cavity input/PLL module, a VCO/RF drive module, a power monitoring module, and two signal conditioning modules. The hardware is controlled via a National Instruments PXIe 8133 quad-core controller running LabView to support the processing requirements. Data acquisition and control of the custom hardware is accomplished with a PXI-6229 multifunction data acquisition card. Standard test equipment is used as part of the system where possible and includes two dual channel power meters, two single channel power meters, a frequency counter, and a signal generator [2].

Figure 1: VTA RF Control System.

*This manuscript has been authored by UT-Battelle, LLC under Contract No. DE-AC05-00OR22725 with the U.S. Department of Energy. The United States Government retains and the publisher, by accepting the article for publication, acknowledges that the United States Government retains a non-exclusive, paid-up, irrevocable, world-wide license to publish or reproduce the published form of this manuscript, or allow others to do so, for United States Government purposes. The Department of Energy will provide public access to these results of federally sponsored research in accordance with the DOE Public Access Plan (http://energy.gov/downloads/doe-public-access-plan).

ISBN 978-3-95450-178-6

JEFFERSON LAB VERTICAL TEST AREA RF SYSTEM IMPROVEMENT*

T. Powers# and M. Morrone, Jefferson Lab, Newport News, VA, USA

Abstract

RF systems for testing critically coupled SRF cavities require the ability to track the cavity frequency excursions while making accurate measurements of the radio frequency (RF) signals associated with the cavity. Two types of systems are being used at Jefferson Lab. The first, the traditional approach, is to use a voltage controlled oscillator configured as a phase locked loop (VCO-PLL) such that it will track the cavity frequency. The more recently developed approach is to use a digital low level RF (LLRF) system in self excited loop (SEL) mode to track the cavity frequency. Using a digital LLRF system in SEL mode has the advantage that it is much easier to lock to the cavity's resonant frequencies and they tend to have a wider capture range. This paper will report on the system designs used to implement the 12 GeV digital LLRF system in the JLAB vertical test area. Additionally, it will report on the system modifications which are being implemented so that the RF infrastructure in the VTA will be ready to support the LCLS II cryomodule production effort, which is scheduled to begin in calendar year 2016.

INTRODUCTION

The JLAB Vertical test area (VTA) was originally constructed in 1990 [1]. It has eight vertical test dewars capable of being operating at temperatures down to 1.6 K. Six of the dewars have radiation shielding which allows one to safely test SRF structures which are capable of producing radiation. Two of the dewars, which are not shielded are used to test non accelerating structures at low temperatures. The VTA is supported by a helium liquefier, pumping and recovery system, which is dedicated to production testing of superconducting cavities and cryomodules. Over the past 25 years the facility has been used to perform in excess of 5,200 cavity tests on more than 600 different cavities.

The VCO-PLL based, L-band RF systems in the JLAB vertical test area (VTA) were built in the early 1990's and have worked well over the years [2]. An additional UHF system, with capabilities from 500 MHz to 1 GHz, was implemented in 2002 and used for production testing of the SNS cavities. In recent years one of the L-band systems has been dedicated to testing 1497 MHz cavities while the second has been used for testing 1300 MHz cavities. The 1497 MHz system has a high power switching network that routes the drive signals between the different test dewars and provides the appropriate personnel safety interlocks.

* Authored by Jefferson Science Associates, LLC under U.S. DOE Contract No. DE-AC05-06OR23177 with supplemental funding from the LCLS-II Project U.S. DOE Contract No. DE-AC02-76SF00515.
#powers@jlab.org

The first system that was upgraded to a digital LLRF based system was the UHF system. One of the driving factors for this upgrade was the failure of the vector modulator which was used to control the phase and amplitude of the output signal. Unfortunately, this part is no longer available and replacement with an analog input variant suffers from "dead zones" in phase and amplitude space when the attenuation is much above 20 dB. In addition to avoiding future failures of obsolete parts, the L-band systems are being upgraded in order to increase the frequency range to 1.2 GHz to 1.6 GHz as well as to improve the ease to test the cavities. We are also installing a switching network that will allow one to route the RF power to and RF signals from either of the two L-band systems to/from any of 6 shielded vertical test dewars.

RF HARDWARE CONFIGURATION

The L-band RF system consists of a pair of digital low level RF systems which are fed into a high power/low power amplifiers. The output of the amplifier networks are fed into a 2-input, 6-output RF switching network. The RF signals from the cavities are routed back to the measurement network through a set of three 6-input, 2-output low power RF switching networks. The overall block diagram is shown in Figure 1.

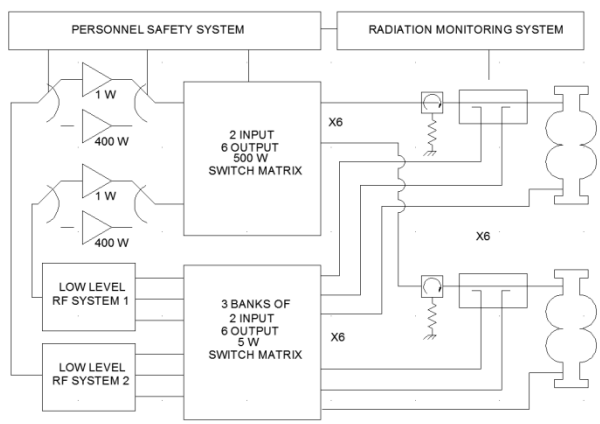

Figure 1: System level block diagram of a the L-Band system.

RF-Switching Networks

Two modified commercial off-the-shelf switching networks were procured for this system. Rather than a standard USB interface the coil signals and the high power RF-switch position read-back contact closures were brought out to connectors. This was done so that the system could be integrated into the personnel protection system which is implemented in a PLC. Had we used the USB interface there would have been issues with certification of the system to safety system standards. An

ISBN 978-3-95450-178-6

RESONANCE CONTROL FOR NARROW-BANDWIDTH, SUPERCONDUCTING RF APPLICATIONS*

W. Schappert, J. Holzbauer#, Yu. Pischalnikov, FNAL, Batavia, IL 60510, USA
D. Gonnella, M. Liepe, Cornell University, Ithaca, NY 14853, USA

Abstract

Fast, active resonance stabilization has been attempted in several recent accelerator complexes, but has so far been unsuccessful. The next generation of superconducting accelerators will require both precise control of the gradient and active stabilization of the resonance frequency. Advanced techniques are being developed at Fermilab to monitor and correct for cavity detuning using fast piezo electric mechanical tuners. Results from recent cold cavity tests at Fermilab and Cornell University are presented.

INTRODUCTION

Many of the next generation of particle accelerators (ERLs, XFELs) are designed for relatively low, or even ideally zero beam loading. This leaves the ideal RF power requirement for the cavities dominated by wall losses and the power required to overcome detuning in operation. This smaller requirement means the cavities can operate with narrow bandwidths, minimizing capital and base operational costs of the RF plant. With such narrow bandwidths, however, cavity detuning from microphonics becomes a significant factor, and in some cases can drive the cost of the machine, see Figure 1.

Smaller bandwidths increase the fractional power increase for a given increase in detuning, and detuning environment is a very challenging thing to predict. Unlike beam loading, detuning spectrum can vary from cavity to cavity and hour to hour in an operational machine in a relatively unpredictable way. Additionally, mitigation/ improvement of the detuning spectrum is a very technical challenging task, requiring holistic approaches. Even if efforts at passive environmental detuning reduction are as successful as the best efforts of previous machines, active resonance stabilization will likely be required. Piezo actuators have been used with some success to actively stabilize cavity resonant frequencies in the past. This paper will present the results of ongoing detuning compensation efforts at FNAL using prototype 325 MHz SRF single spoke resonators (SSR) designed for the PIP-II project at Fermilab [1, 2] as well as 1.3 GHz 9-cell SRF cavities designed for the LCLS-II project at SLAC .

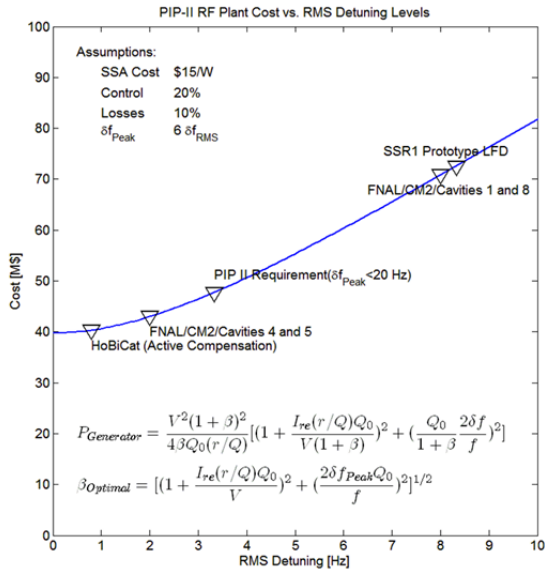

Figure 1: RF Generation Cost vs. Detuning Environment Example.

This work was done at the HTS and STC test stands at Fermilab as well as the HTC test stand at Cornell University.

PREVIOUS EFFORTS

Active compensation of both Lorentz Force Detuning and microphonics had been previously studied using an earlier SSR1 prototype with two different power couplers. An adaptive feedforward algorithm developed for pulsed 1.3 GHz 9-cell elliptical cavities [3] was able to reduce detuning in the spoke resonator from several kHz to 50 Hz or better during pulsed operation with a 150 Hz bandwidth power coupler [4].

SSR1 SPOKE RESONATOR

A dressed SSR1 cavity (SSR1-107) was installed in the Spoke Test Cryostat (STC) in May 2015. The cavity was equipped with a production coupler (60 Hz bandwidth), which was later reduced to 30 Hz with the addition of an air-side reflector in the drive circuit. The cavity was equipped with a production style tuner, including two piezoelectric actuators to provide dynamic tuning. This cavity had been the focus on an active design effort to reduce and minimize pressure sensitivity [2]. During

*This manuscript has been authorized by Fermi Research Alliance, LLC under Contract N. DE-AC02-07CH11359 with U.S. Department of Energy.
#jeremiah@fnal.gov

MECHANICAL DAMPER STUDY FOR ISAC-II QUARTER WAVE RESONATORS

L. Yang, V. Zvyagintsev, R.E. Laxdal, TRIUMF, Vancouver, Canada

Abstract

ISAC-II superconducting quarter wave resonators are equipped with mechanical dampers to supress mechanical oscillations of the cavity structure. The study has been carried out to optimize the damper efficiency.

INTRODUCTION

The mechanical oscillation of inner conductor is an essential cause of instability of superconducting coaxial quarter wave resonators (QWR). Due to its low resonant frequency, the fundamental mechanical mode could be easily excited by helium pressure fluctuation, vacuum pumping system, vibrations coupled into the helium bath and ambient vibrations. Under natural damping, the intrinsic quality factor could be as high as several hundred with large amplitude of oscillation and long decay time once the mode is built up. It could cause significant frequency detuning and finally could trip the cavity from amplitude and phase locked operating regime. The ISAC-II linac at TRIUMF has 40 superconducting QWRs: 20 cavities operating at 106 MHz and 20 at 141 MHz. In order to reduce the detuning effect from mechanical oscillations, a kind of dry friction-based mechanical damper designed in INFN-LNL [1], is employed in all the ISAC-II QWRs [2]. The damper is dissipating oscillation kinetic energy by means of friction. ISAC-II operates with negligible beam loading and to operate in locked amplitude and phase loop regime overcoupling is required to provide loaded cavity bandwidth significantly higher than frequency detuning from mechanical oscillations.106 MHz QWR operates for effective accelerating voltage 1 MV and dissipates about 7 W of RF power at 4 K, forward power in overcoupled regime required for stable operation is about 200 W. Such a way the transmission line operates in standing wave regime; most of the RF power is reflecting from the cavity and dissipates in the circulator RF load outside of the cryomodule, at room temperature. Anyway standing wave regime potentially could develop overheat in high current and RF discharge in high voltage locations of the transmission line and coupler. Consequently, it could cause transmission line failure. To mitigate this problem we need to use more expensive components for transmission line: cables, connectors, feedthroughs. The mechanical damper helps to reduce the required overcoupling and RF forward power for the cavities. Study is motivated with possibly to improve the damper efficiency and further reduction of the RF power, which will increase reliability of cryomodule operation. This paper will present the analytical model and experimental results.

THE LOWEST MECHANICAL MODE

The lowest mechanical mode of a QWR is associated with the first order of transverse vibration mode of its inner conductor. Its eigenfrequency and mode vector, could be approximately predicted by a model known as cantilever beam [3], and given by the analytic formulas:

$$\omega = \frac{\alpha^2}{L^2}\sqrt{\frac{EI}{\rho A}}$$

$$\phi(z,L) = \frac{1}{2}\left[cosh\left(\alpha\frac{z}{L}\right) - cos\left(\alpha\frac{z}{L}\right) - 0.734\left\{sinh\left(\alpha\frac{z}{L}\right) - sin\left(\alpha\frac{z}{L}\right)\right\}\right]. \quad (1)$$

Here, E, L, I, ρ, A, stand for the beam's Young modulus, length, geometrical moment of inertia, mass density, cross area, and α is the mode constant; for the first mode $\alpha = 1.875$. For 106 MHz QWR parameters the formula predicts the result of 83.5 Hz. This model doesn't take into account the shorting plate extension, hence, the eigenfrequency is actually overestimated. The finite element method by using ANSYS is able to do the modal calculation for the entire 3D model [4], and predicts the frequency 68 Hz.

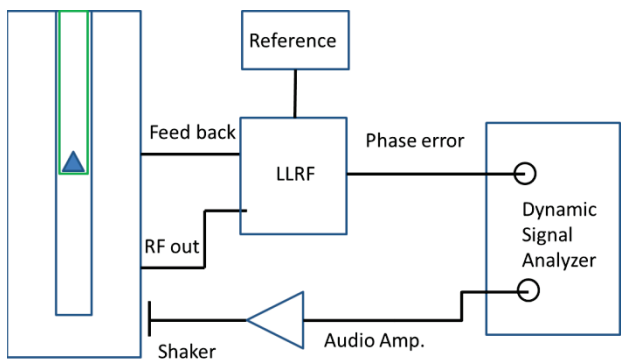

Figure 1: Schematic of setup for mechanical mode measurements.

Measurements at room temperature have been done to verify the simulation results. Figure 1 shows the schematic of setup, which was also used for the later damper measurement. A mechanical shaker driven by an audio amplifier is used to induce the vibration of the 106MHz ISAC-II QWR. The LLRF board operating in the general driven mode provides phase error signal induced by the cavity detuning regarding to reference frequency due to vibration. Reference frequency is tuned for the cavity resonance. The Dynamic Signal Analyzer (DSA) processes the phase error signal by FFT, and provides the spectrum of the cavity's response to the shaker. DSA also provides a sinusoidal drive signal to the

THE STUDY ON MICROPHONICS OF LOW BETA HWR CAVITY AT IMP

Z. Gao#, Y. He, W. Chang, S.H. Zhang, W.M. Yue, Z.L. Zhu, Q. Chen, IMP, CAS, Lanzhou, China
Tom Powers, JLab, Newport News, VA 23606, USA

Abstract

The superconducting linac of China Accelerator-Driven System Injector II will operate at CW-mode. The mechanical vibrations of the superconducting cavity, also known as microphonics, cause shifts in the resonant frequency of the cavity. The microphonics is the main disturbance source of cavity frequency shifts when the cavity running in CW mode. In order to understand the effects, microphonics measurements were performed on the half-wave superconducting cavities when they were operated in the cryostat. And the experimental modal test was also performed to identify noise source and improve the cavity structure optimization. The measurement method and results will be shown and analyzed in this paper.

INTRODUCTION

The superconducting half-wave resonator operated at 162.5 MHz, the geometry parameters and RF parameters were described in ref [1]. And the cavity operating temperature was 4.4 K, the test cryostat design detail can be found in the ref [2]. The test cryo-module was built to verify the performance of cryogenic system and LLRF system, it only contain one HWR cavity which didn't be weld with reinforcing ribs. The cryo-module 6 (CM6) had been installed and operated on the beam line, 6 HWR cavities were assembled in this module, the 6 cavities were weld with reinforcing ribs on the outer surface of the region of electric field to minimize df/dp, which means that the mechanical structure of those cavities is more stable.

THE MICROPHONICS MEASUREMENT

A new digital cavity resonance monitor was developed at Institute of Modern Physics (IMP) [3], which utilizes the NI intermediate frequency transceiver to digitize RF signal and process the digital signal, the IF transceiver contains digital down converter (DDC) and a Virtex-5 field programmable gate array (FPGA), the performance test result indicated that the new measurement system is adequate for measuring microphonics of low beta cavity.

The Measurement Scheme

The experimental measurement scheme of the measurement system with cavity installed in the test cryo-module is shown in Figure 1. The frequency of cavity was tracked by the VCO-PLL loop, the down-converted IF signal was input to the IF transceiver, the ADC in the IF transceiver outputs digitized data stream to FPGA for digital signal processing.

#gaozheng@impcas.ac.cn

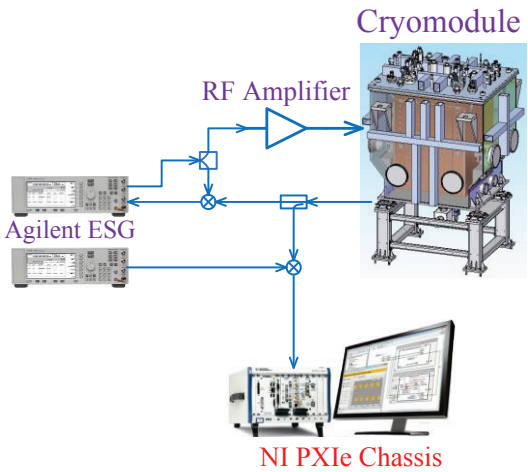

Figure 1: The microphonics measurement setup.

The Experimental Result of Test Cryomodule

The measurement results were shown in Figure 2 and Figure 3, the cavity frequency changed about 25 Hz (peak to peak value) to take no account of the helium pressure fluctuation.

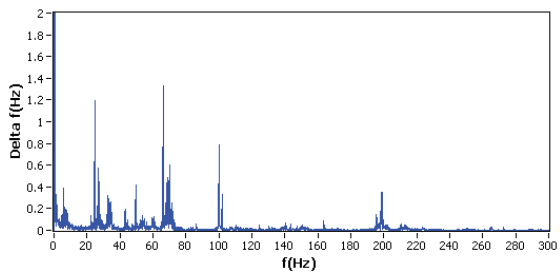

Figure 2: The spectrum of cavity vibration.

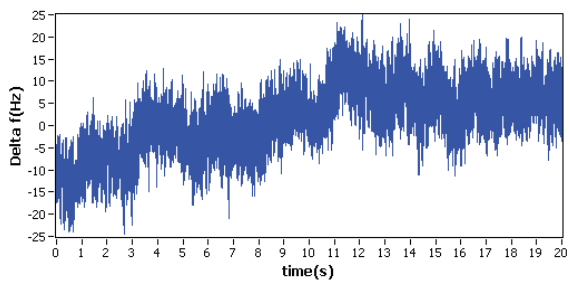

Figure 3: The time domain waveform of cavity frequency shift.

The Microphonics Test Result of CM6

The superconducting cavities in the CM6 were controlled by the LLRF systems which operated in self-excited mode, the function of the self-excited mode is same as VCO-PLL. The measured peak to peak frequency shift of 6 # HWR is about 11.5 Hz as shown in Figure 4, the peak vibration frequency 40 Hz can be found in Figure 5.

ISBN 978-3-95450-178-6

ERROR ANALYSIS ON RF MEASUREMENT DUE TO IMPERFECT RF COMPONENTS *

G. Wu, J. Ozelis, S. Aderhold, M. Checchin, M. Martinello
Fermilab, Batavia, IL 60510, USA

Abstract

An accurate cavity test involves the accurate power measurement and decay time measurement. The directional coupler in a typical cavity test llrf system usually has low directivity due to broadband requirement and fabrication errors. The imperfection of the directional coupler brings unexpected systematic errors for cavity power measurement in both forward and reflect power when a cavity is not considered a matched load as assumed in a cable calibration. An error analysis will be given and new specification of directional coupler is proposed. A circulator with a low voltage standing wave ratio (VSWR) creates a standing wave between the circulator and cavity. As long as the cavity phase is maintained, the standing wave of a non-matched cavity load will only change the input coupler coupling factor (Q_{ext1}), but not to the calculation of the cavity power loss that is independent of the Q_{ext1}.

INTRODUCTION

RF measurement has been used to determine the cavity gradient and unloaded quality factor (Q_0) since very early days in SRF [1,2]. RF measurement is nevertheless subjected to errors of power measurement and rf parameters. The error analysis has been described in earlier studies [2,3]. Lately, the additional errors caused by imperfect RF components have been studied experimentally [4]. The validity of the latest studies has been hotly debated. A careful study of these additional errors has to consider all the equations of the RF calculations and the practical procedures of RF measurement.

Considerable detailed RF measurement circuit diagram can be found in many references and text book [1,2]. A dramatically simplified RF measurement diagram is shown in Figure 1 which consists only a simple phase lock loop involving a RF power source, a circulator, a directional coupler and a RF cavity.

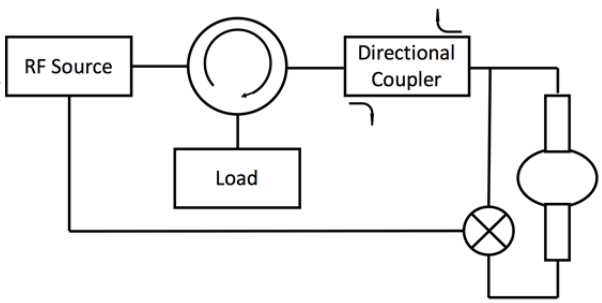

Figure 1: A dramatically simplified cavity test diagram.

The directional coupler allows the measurement of the forward power to the cavity (P_f) and the reflected power from the cavity (P_r). Measuring cavity transmitted power P_t allows one to derive the cavity power loss P_{loss}. Ideally, P_f is only proportional to the forward power from the RF source. However, due to design imperfections associated with broad band requirement and fabrication tolerances, the reflected power from the cavity can be slightly coupled into the P_f measured at the directional coupler forward coupling port. Equally, the P_r measured at the directional coupler's reflected coupling port includes the reflected power plus the coupled power from the forward power. Directivity represents how strong this unwanted coupling is in a directional coupler. Definition and measurement of the directivity is well discussed [5]. The higher the directivity, the weaker the unwanted coupling is. The unwanted coupling is also a function of the phase angle between the reflected power and forward power. The error analysis will be focused on the forward power and reflected power. The transmitted power is not affected by the imperfect directional coupler.

The circulator redirects the cavity reflected power to a RF load. Most commercial circulator does not have fully matched port where all the incoming power was fully cycled out. The standard VSWR is around 1.1-1.2. As such some power will be reflected and forms a standing wave in the line. The standing wave in the transmission line lead to cavity will modify the field at the cavity input coupler and cause the coupling factor of the cavity input coupler to change. This will change the external Q of the cavity (Q_{ext1}) and thus change the loaded Q (Q_L). The cavity decay time will change as the loaded Q changes. A misconception happens from time to time that the decay time changes means the cavity unloaded Q is also affected. In reality, cavity unloaded Q is not much affected by the standing wave in the forward power transmission line in most cases.

DIRECTIONAL COUPLER

Directional coupler is mostly characterized and used under matched load. Unfortunately, the load is mostly reflected or mixed for SRF cavities even with beam loading except the case for energy-recovered linear accelerators. All of the commercially available directional coupler has limited directivity (***D***). Power measured through directional coupler will be affected by its non-ideal directivity. Figure 2 illustrates the power measurement affected by directivity and non-matched load.

*Work supported by DOE Contract # DE-AC02-07CH11359
genfa@fnal.gov

MAGNETIC FOILS FOR SRF CRYOMODULE*

G. Wu#, A. Grassellino, A.C. Crawford, S. Chandrasekaran, S. Aderhold, A. Vostrikov, C. Grimm, D. A. Sergatskov, J. Ozelis, Fermilab, Batavia, IL 60510, USA

Abstract

High quality factor niobium SRF cavities require minimal residual magnetic field around the cavity high RF magnetic field region. Global magnetic shields use more material and provide less effective magnetic screening. On the other hand, local magnetic shields have complex geometries to cover access ports and instrumentation, and need thermal straps for cooling. Local magnetic sources and thermal currents will increase residual fields seen by the cavities regardless of the local magnetic shields. Magnetic foils that are cryogenically compatible could increase shield effectiveness and reduce residual magnetic fields. This paper will describe the evaluation of such magnetic foils in both vertical and horizontal tests.

INTRODUCTION

Record high operational quality factors have been routinely demonstrated in nitrogen doped niobium cavities[1,2]. The residual surface resistance of a nitrogen doped cavity, however, is slightly more sensitive to trapped magnetic flux [3]. As the cavity operational Q and BCS surface resistance are inversely proportional, it is important to reduce the residual resistance.

As magnetic trapped flux is a very important contributor to residual surface resistance, it is highly desirable to use local magnetic shields of single or multiple layers to reduce the magnetic field at the cavity surface when the cavity transitions from the normal to the superconducting state. Due to the mechanical necessity in a cryomodule setting, it is common to have openings in the local magnetic shield to allow access to cavity supports, tuner arms, thermal straps, couplers and instrumentations as illustrated in the LCLS-II magnetic shield design shown in Figure 1.

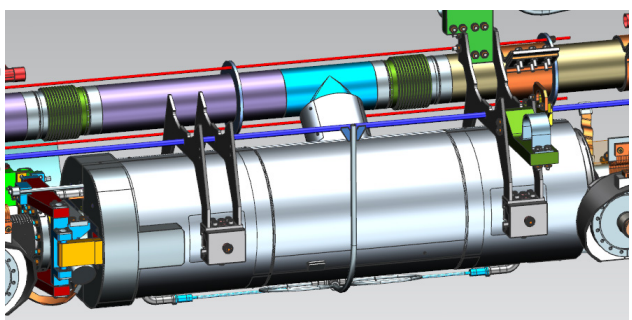

Figure 1: LCLS-II cavity magnetic shielding that leaves openings to coupler, tuner and cavity supports.

*Work supported by DOE Contract # DE-AC02-07CH11359
#genfa@fnal.gov

The openings in the local magnetic shield allow the ambient magnetic field to leak into the shield and increases the possibility of flux trapping during the superconducting transition.

It is not always practical to design a solid magnetic shield that accommodates the penetrating component. Both fabrication cost and assembly complexity have to be considered.

A magnetic foil that is flexible and has high permeability can be used to cover the openings of the solid magnetic shield. It can magnetically reinforce the overlap in the solid shield or can cover gaps that may be present due to fabrication defects of the solid magnetic shield. Magnetic foils can also be used to create a shield extension, like a hat, that provides shielding of the openings. This has been proven to be effective to reduce field penetration through the openings.

Certain METGLAS® foils have been used elsewhere which has demonstrated the relative permeability of greater than 10,000 at liquid helium temperatures [4]. A different but larger size METGLAS® foil called 2605SA-1 was selected for evaluation in SRF applications. METGLAS® SA-1 foil is 22 μm thick and 8-inch wide. It costs significantly lower than other solid cryogenic magnetic shielding material for similar shielding effectiveness. Its magnetic properties were measured and compared to other common cryogenic magnetic shield materials. It was later used in a horizontal test of a LCLS-II 9-cell cavity and has been proven effective as augmentation with solid magnetic shielding.

MAGNETIC PROPERTY MEASUREMENT

Two properties of the magnetic foil were measured; magnetic field attenuation and initial permeability at various temperatures.

A 250 mm long, 55 mm diameter G-10 tube was used as a mandrel to create a simple cylindrical shield. A permanent magnet was placed outside the tube near the longitudinal center of the tube. The magnetic field was measured inside the tube, with and without the foil, as the number of layers of foil wrapped on the outside of the tube was increased. The attenuation factor is plotted in Figure 2.

It is shown that 20 layers of magnetic foil is equally effective compared to a 1 mm Cryoperm® 10 solid magnetic shield. Fifteen layers provided a factor of 100 attenuation, suggesting that the transverse geo-magnetic field could be shielded to below 5 mG.

A small sample of foil was wrapped into a 3 mm diameter open cylinder with a height of 5 mm. The

CEA EXPERIENCE AND EFFORT TO LIMIT MAGNETIC FLUX TRAPPING IN SUPERCONDUCTING CAVITIES

Juliette Plouin#, Nicolas Bazin, Patrice Charon, Guillaume Devanz,
Hervé Dzitko, Philippe Hardy, Fabien Leseigneur, Jérôme Neyret, Olivier Piquet
CEA-Saclay, Gif-sur-Yvette, France

Abstract

Protecting superconducting cavities from the surrounding static magnetic field is considered as a key point to reach very good cavity performances. This can be achieved by both limiting the causes of magnetic flux around the cavity in the cryomodule, and enclosing cavities and/or cryomodules into magnetic shields. We will present the effort made at CEA into this direction: shield design, shield material characterization, at room and cryogenic temperature, and search and attenuation of the magnetic background present in the cryomodule during the cavities superconducting transition. This last point will be especially studied for the IFMIF project where the cryomodule houses the focusing magnets.

INTRODUCTION

In low beta cryomodules with high intensity beams it is generally necessary to have solenoids close to superconducting cavities. When the cryomodule contains more than one or two cavities, the solenoids are usually inside the module, which adds a level of complexity to the cryomodule design considerations [1], because the static magnetic field can degrade the cavities performance. The static field close to a cavity must be lower than the critical field (tens of mT) when it is in the superconducting state. It has to be lower than some μT during the superconducting transition to avoid a significant increase of the surface resistance.

Then it is mandatory to prevent magnetic pollution generated by these solenoids, even when they are switched off.

Moreover the cavities must be protected from the earth magnetic field (~50 μT).

MAGNETIC SHIELD OF THE IFMIF CRYOMODULE

The IFMIF cryomodule contains all the equipment to transport and accelerate a 125 mA deuteron beam from an input energy of 5 MeV up to 9 MeV. It consists of a horizontal cryostat of about 6 m long, 3 m high and 2 m wide, which includes 8 superconducting HWRs (Half Wave Resonators) for beam acceleration working at 175 MHz and at 4.5 K, 8 power couplers to provide RF power to cavities, and 8 Solenoid packages as focusing elements [2].

A warm magnetic shield is installed on the inner walls of the vacuum vessel to protect the cavity from the earth magnetic field. Calculations have shown that with 2 mm thickness and with standard mumetal, the static magnetic field should stay lower than 2 μT inside the cryomodule, which is the design target for the HWR.

Several views (inside, outside the cryomodule, exploded) of this magnetic shield are shown in Figure 1.

The many apertures of the cryomodule are critical for the shielding, and overlap of mumetal sheets are mandatory. The tendering phase of this magnetic shield has started.

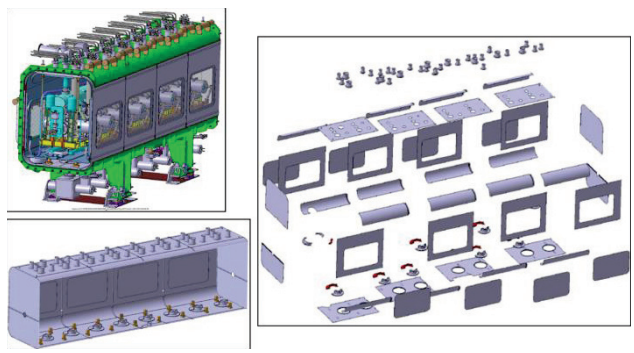

Figure 1: Magnetic shield of the IFMIF cryomodule.

MAGNETIZATION OF CRYOMODULE ELEMENTS

Due to space charge associated to the high intensity beam, a short, but strong, superconducting focusing magnet package is necessary between cavities. During the cryomodule operation, the solenoids will only be switched on once the cavities are in superconducting state. Each magnet package contains one inner solenoid, which can reach 7 T, four steerers, and one outer solenoid connected in series with the inner one with current established in opposite sense, in order to work as an active shielding. The fringe field at the cavity flange is then limited to 20 mT [3]. Figure 2 shows the magnetic field pattern generated by the solenoid package at several places in the cryomodule. Our concern is that some cryomodule components could be magnetized by this fringe field, and be a source of remnant field once the solenoid is switched off. We have focused our attention in particular on the needles bearings, the invar rod, and the magnetic shield itself.

Moreover the supporting frame was initially planned to be made of stainless steel 316L C-beams which are welded together. The large number of welding rims with potentially higher permeability than expected represented

juliette.plouin@cea.fr

ISBN 978-3-95450-178-6

DESIGN OF THE THERMAL AND MAGNETIC SHIELDING FOR THE LHC HIGH LUMINOSITY CRAB-CAVITY UPGRADE

N. Templeton, T. Jones, S. Pattalwar, K. Marinov, A. May, E. Nolan
STFC, Daresbury Laboratory, UK
G. Burt, University of Lancaster, UK
K. Artoos, R. Calaga, O. Capatina, T. Capelli, F. Carra, R. Leuxe, C. Zanoni
CERN, Geneva, Switzerland
A. Ratti, LBNL, Berkley, California, USA

Abstract

Before the High Luminosity (Hi-Lumi) upgrade of the Large Hadron Collider (LHC), two pairs of superconducting compact Crab Cavities are to be tested within separate cryomodules, on the Super Proton Synchrotron (SPS) at CERN in 2018 prior to Long Shutdown 2 [1]. Two novel side-loaded cryomodules, which allow ease of access for assembly, inspection and maintenance, have been developed for the prototype tests. The cryomodule shielding includes a thermal shield and double layer magnetic shield, consisting of a warm-outer shield, and two cold-inner shields (one per cavity). Various constraints and considerations have led to unique cold shielding, mounted inside the cavity helium vessels, resulting in several design challenges. The shielding adopts and utilises the module's side-loaded configuration, for continuity and accessibility, while satisfying tight spatial constraints and requirements to meet the functional specification. This paper outlines the design, analysis, manufacture and assembly of the Hi-Lumi SPS test cryomodule's thermal and magnetic shielding, which are critical to achieving the operational stability [2].

INTRODUCTION

The Double Quarter Wave (DQW) and RF Dipole (RFD) cavities, shown in fig. 1 below, are superconducting compact crab cavities for ultra-precise beam rotation, developed by Brookhaven National Laboratory and Old Dominion University respectively [1].

Figure 1: DQW (left) and RFD (right) prototype crab cavity models.

The cavities feature several ports for the input coupler and High Order Mode (HOM) absorbers, as well as tuner and helium vessel interfaces. A dummy beampipe has been included on SPS tests for compatibility with LHC. The RFD cavity also features stiffening ribs to reduce pressure sensitivity [3]. These features all impact the cold magnetic shield design which is assembled around the cavities.

Two of each cavity will be installed on the SPS ring within separate cryomodules for commission and cold testing prior to the Hi-Lumi LHC upgrade [1]. Figure 2 shows a model of the DQW cryomodule in section, the thermal and outer magnetic shields are represented blue and grey respectively, while the cold magnetic shields are shown within the cavity helium vessel. The image shows a number of cryomodule and cavity string systems which impact on the shield designs [4].

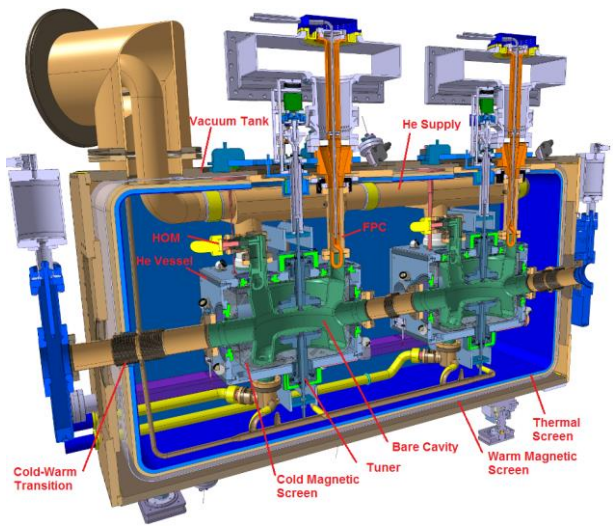

Figure 2: DQW cryomodule section.

The thermal shield serves as a radiative heat barrier and also recycles gaseous helium to intercept and thermalise critical components, such as the fundamental power coupler, ensuring minimal heat leak to the cavities, since there is limited cooling capacity at super-fluid helium level [4]. The design of the magnetic shielding prevents field of more than 1 μT reaching the niobium cavity surface as not to increase the surface resistivity through magnetic field trapping which would limit cavity performance [5].

ISBN 978-3-95450-178-6

VALIDATION OF LOCAL MAGNETIC SHIELDING FOR FRIB USING A PROTOTYPE CRYOMODULE*

S.K. Chandrasekaran#, †, K. Saito§, Facility for Rare Isotope Beams, East Lansing, MI 48824, USA

Abstract

The local magnetic shield design and cryogenic magnetic shielding material for the FRIB QWR cryomodule was validated in a two cavity, one solenoid prototype cryomodule. The magnetic fields were measured inside and outside the magnetic shielding before, during, and after operation of an 8 T superconducting solenoid. The effect of demagnetization cycles of the solenoid was also examined.

The magnetic field at the cavity's high RF magnetic field area, inside the magnetic shield and with the solenoid off, was measured using a single-axis fluxgate to be less than 0.3 μT (3 mG) after cool down of the cryomodule. A 3.07 μT (30.7 mG) residual field was observed at high magnetic field area after conclusion of solenoid operation. This was attributed to the persistent currents circulating in the superconducting solenoid. Demagnetization cycles were therefore determined to be unnecessary for FRIB cryomodules, as long as the solenoid is normal conducting when the cavity is cooled through the superconducting critical temperature.

INTRODUCTION

The Facility for Rare Isotope Beams (FRIB) shall employ local magnetic shielding around the niobium (Nb) superconducting RF (SRF) cavities in its cryomodules (CM). Each CM shall contain at least one 8 T superconducting (SC) solenoid, made of niobium-titanium (NbTi) wire, whose operation could magnetize components in the CM. The quality factors (Q) of the Nb cavities could degrade if they are cooled through the superconducting critical temperature (T_c) in the presence of magnetic fields from either the earth's magnetic field or from magnetized components. To reduce such degradation, FRIB requires the magnetic field at the surface of the SRF cavity to be less than 1.5 μT (15 mG). Historically, demagnetization cycles are performed using the superconducting solenoid to demagnetize components within the CM prior to warming of the CM. If the local magnetic shields used for FRIB are able to attenuate fields from magnetized components, demagnetization cycles will not be required.

The FRIB solenoid design contains bucking coils, beam steering dipole coils, but does not include any iron yoke. The residual magnetic field of the solenoid package, due to hysteresis in the iron, is therefore expected to be small. In addition, the local magnetic shields are expected to attenuate the fields around the cavities further. In the event of a quench of the cavity during solenoid operation, however, the fringe fields of the solenoid may be trapped in the cavity and degrade Q.

Separate cryogenic tests in a vertical Dewar [1] with only the magnetic shields used in this work, without the cavity or any CM components but in the fringe fields of a 2.5 T superconducting solenoid, displayed sufficient shielding of the fringe fields at the quarter wave resonator (QWR) cavity's high RF magnetic field region.

In this work, the magnetic fields before, during, and after operation of a superconducting solenoid at 8 T, inside and outside the 1 mm thick magnetic shielding, within a prototype QWR CM were measured. The effect of demagnetization cycles of the solenoid on the magnetic field distribution were also examined.

PROTOTYPE CRYOMODULE TEST

The Re-Accelerator 6 (ReA6) is a prototype of a FRIB QWR CM, showcasing the bottom-up design and assembly procedure. This CM was populated with two QWR cavities and one superconducting solenoid, with space for six additional cavities and two additional solenoids. The solenoid used in ReA6 is repurposed from the technology demonstration CM (TDCM), and has shielding coils and bucking coils in series with the main coil. In addition, there are horizontal and vertical corrector dipoles, with individual excitation leads. All the coils of the solenoid were manufactured using NbTi wire. The bucking coils operate in series with the main coil of the solenoid, and reduce fringe fields of the main coil in the longitudinal direction. The shielding coils are also in series with the main coil, but help reduce the fringe fields of the main coil in the radial direction. While the TDCM solenoid has the bucking and shielding coils, the FRIB solenoids shall only have bucking coils to limit the fringe fields along the longitudinal direction. The FRIB requirement for the fringe fields of the 25 cm and 50 cm solenoids at the surface of the magnetic shields is to be less than 24 mT (240 G) and 27 mT (270 G), respectively. Due to the differences in the TDCM and FRIB solenoids, there will be some differences in the fringe field distribution in the FRIB CM as compared to the ReA6 CM. These differences will be mainly in the radial direction and should not significantly affect the fringe fields near the cavities.

Solenoid Excitation

The main coil and the corrector dipoles of the solenoid were excited at 4.2 K to 70.4 A (8 T field) at 0.2 A/s and 40 A (0.06 T·m) at 2 A/s, respectively. After several

* Work supported by the U.S. Department of Energy Office of Science under Cooperative Agreement DE-SC0000661, the U.S. National Science Foundation under Grant No. PHY-1102511, Michigan State University, and the State of Michigan.
# saravan@fnal.gov.
§ saito@frib.msu.edu.
† Currently at Fermi National Accelerator Laboratory, Batavia, IL 60510, USA.

ISBN 978-3-95450-178-6

CRYOMODULE PROTECTION FOR ARIEL E-LINAC

Z. Yao#, R.E. Laxdal, W.R. Rawnsley, V. Zvyagintsev, TRIUMF, Vancouver, B.C., Canada

Abstract

The e-Linac cryomodules require high RF power, cryogenics, ultra-high vacuum, and precise mechanical adjustment. They require protection against of failures, like quench in the cavity, bad vacuum or multipacting in power couplers, low liquid helium level or high temperatures. The protection unit should stop RF power in the cryomodule in case of the listed failures. An Interlock Box is developed to implement protection function for the cryomodule. The paper will describe the design of Interlock Box for e-Linac cryomodule protection. As quench protection required, quench evolution analysis with RF transient analysis is investigated. The details of quench detection for e-Linac will also be reported.

INTRODUCTION

The ARIEL e-Linac is a CW 10mA 50MeV electron LINAC [1]. It consists of one injector cryomodule with one 9-cell cavity and two accelerator cryomodules with two 9-cell cavities each. The nominal operating accelerating gradient of the superconducting cavity is 10MV/m at the power dissipation on cavity wall of 10W [2]. As the high intensity beam loading, each cavity requires 100kW RF power. Two 300kW klystrons provide RF power for injector and one accelerator cryomodule. Each cavity has two 50kW CPI RF power couplers.

In general, cryomodule is a cryo-vacuum chamber. Vacuum leak, local high temperature and low helium level should be prevented during operation.

The RF power couplers were conditioned up to 20kW [3] in CW mode with traveling wave on the room temperature power coupler test stand. They to be conditioned to operational power level of equivalent 50kW in-situ. Couplers require protection to prevent damage in case of multipacting, discharge or vacuum activity.

The specification of cavity quality factor is 1×10^{10} at operational gradient of 10MV/m. Due to the 100kW beam power requirement, the external quality factor of pair couplers is 10^6. In case of cavity quench, part of the superconducting cavity wall switches to normal conducting state, and decreases cavity Q_0. More RF power will dissipate on cavity wall, and cryogenic system loading will increase beyond its capability. A reliable fast trip is required to protect cryogenic system due to SRF cavity quench and high beam loading.

To protect cryomodule and cryogenic system in operation, fast hardware interlock boxes are designed and produced for ARIEL e-Linac. This paper will discuss the theoretical analysis of cavity quench detection for ARIEL specification, and the design of cryomodule interlock box.

#zyyao@triumf.ca

QUENCH DETECTION ANALYSIS

Cavity quench in cryomodule can be detected from changes of helium pressure, liquid level, cavity temperature. The limitation of these measurements is a long response time.

When the cavity quenches, the 'defect' area switches to normal conducting state. More RF power is dissipated, and the 'defect' is growing and increasing RF power dissipation. The cavity Q_0 decreases from operation specification 10^{10} to close to coupler Q_{ext} 10^6. The Q_0 of a quenched cavity is assumed to be 10^6. RF power loss on cavity inner surface is 45kW for full beam loading limit, and 100kW for no beam loading limit. The ARIEL e-Linac cryogenic system capability is 100J/s per cavity for RF power consumption. To protect cryogenic system, RF power to the cavity should be stopped in 1ms after cavity quench.

In CW operation, cavities are controlled by feedback system. TRIUMF's LLRF feedback system has a typical cycle time of 1ms. For longer periods than 1ms after cavity quench, LLRF will increase amplitude drive for RF forward power to compensate the reduction of cavity accelerating field. The positive feedback effect limits quench detection and protection in 1ms.

As the fast response requirement, RF signal is proposed for quench detection. Quench evolution and RF transient analyses are developed.

Cavity Quench Evolution Analysis

A quench evolution model has been developed based on COMSOL Multiphysics model, shown in Fig. 1. The upper boundary of each model is helium surface, and lower one is RF surface. The left side is symmetry axis, where a defect exists on RF surface, and right side is unlimited boundary. The model simulates growth rate of the normal conducting zone during a cavity quench.

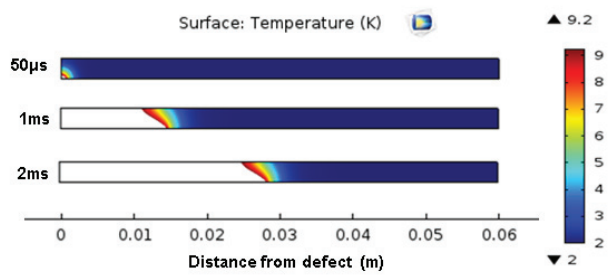

Figure 1: 2D axial symmetry quench evolution model in COMSOL Multiphysics. The plots show temperature distribution in cavity wall during quench at 50µs, 1ms and 2ms. White color shows normal conducting zone.

The simulation result for radius evolution of the normal conducting zone is 14.1mm/ms with e-LINAC specification. Assume that cavity quench is happening at

ISBN 978-3-95450-178-6

SERIES PRODUCTION OF BQU AT DESY FOR THE EU-XFEL MODULE ASSEMBLY AT CEA SACLAY

B.v.d. Horst, A. Matheisen, M. Helmig, S. Saegebarth, M. Schalwat,
DESY Hamburg, Germany

Abstract

Each of the 103 XFEL modules foreseen for the EU-XFEL as well as the 3,9 GHZ injector module is equipped with a combination of beam position monitors, superconducting quadrupole and a gate valve connected to the beam position monitor. The subunits are prequalified by the different work package of the EU-XFEL collaboration and handover to the DESY cleanroom. These subunits are assembled in the DESY ISO 4 cleanroom to unit named BQU, quality controlled in respect of cleanliness and handover in status "ready for assembly in ISO 4 cleanroom" for string assembly to the ISO 4 cleanroom located at CEA France. Series production started with production sequences of one unit per week and needed to be accelerated up to five or six units per month (>=1.25 units per week) in beginning of 2015. Analysis of data taken during production and the optimization of work flow for higher production rates are presented.

INTRODUCTION

In 2013 an assembly line for beam position monitors and quadrupole units (BQU) was set up and commissioned at DESY [1]. This production line was designed for completion of one BQU (Fig. 1) per week in the DESY ISO 4 cleanroom at building 28. During continues flow of module assembly these BQU are handed over to CEA by regular transports circulating weekly between CEA Paris and DESY Hamburg.

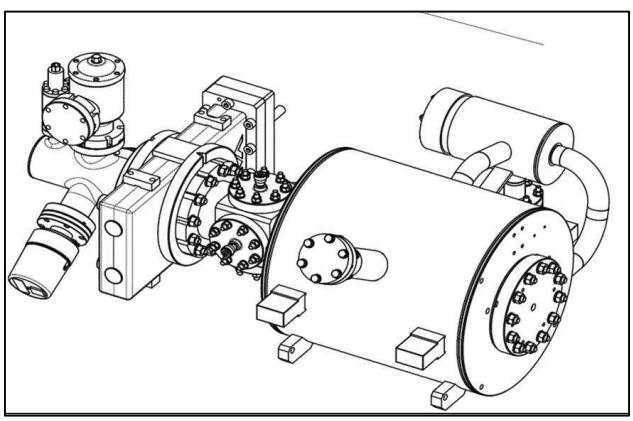

Figure 1: Overview of BQU unit - from left side: vacuum star; gate valve; beam position monitor; s.c. quadrupole; blank off flange.

In autumn 2013 production of modules had to be ramped down due to problems on orbital welds of interconnection between the cavity helium tank service pipes and interconnection bellows of the 2 K helium line [2]. This caused a time delay of several months and had to be compensated by increasing the production rate from 1 to 1.25 or even higher rate of modules per week. Also the BQU production was ramped down and the uprating to 5 BQU per month should be realized without increased man power and avoiding two shifts or week end operations, if possible.

STRATEGY FOR PRODUCTION OF FIVE BQU PER MONTH

The procedures and hard ware for BQU assemblies were analyzed to determine risk and capability for ramp up of production rate. At CEA area a stock of three BQU units had to be ensuring for stable production of modules. During analysis it was found that the existing hard ware, (horizontal assembly device, turn device, wear frame for the HPR system and transport device [1]) can serve for higher production rates than four units per month.

Table 1: Infrastructure Upgrade for BQU Assembly

Workstation	Infrastructure	Units
WS 1	Assembly device	1
WS 2	Turning device + wear frame	1+1
WS 3	Transport tool + vacuum pump	1+1
WS 4	Assembly device + vacuum pump	1+1
WS 5	Transport tool + vacuum pump	1+1
WS 6	Transport box	6+2
WS 7	Transport frame	5+2

Also availability of components and timing for handover of parts for BQU assembly was sufficient for the higher production rate.

Vacuum pumping units and availability of high pressure rinsing stand (HPR) hold the highest risk factor of the analysis.

The number of transport frames and boxes for one BQU per week was not adequate for a stable turn around and the buffer request for module assembly (Table 1).

Each module, when transported from CEA to DESY, is equipped with a vacuum diagnostic system (vacuum star) composed from NW 16 CF angle valve, a venting line with 0.02 µm particle filter integrated and two vacuum gauges (Fig. 2).

This vacuum star is connected to the gate valve and leak checked before handover for BQU assembly. They remain on the units until modules are sent to DESY. After return from module assembly the BQU vacuum stars are

ISBN 978-3-95450-178-6

STRING ASSEMBLY FOR THE EU-XFEL 3.9 GHZ MODULE AT DESY

M. Schmökel, R. Bandelmann, A. Daniel, A. Matheisen, P. Schilling, B. v.d.Horst,
DESY, Hamburg, Germany,
P. Pierini, D. Sertore, R. Paparella, INFN/LASA, Segrate (MI), Italy.

Abstract

For the injector of the EU-XFEL one so-called 3.9 GHz module is required. This special module houses eight 3.9 GHz s.c. cavities, a beam position monitor and a quadrupole package. The cavities were fabricated and vertically tested as an in-kind contribution to the EU-XFEL by INFN Milano collaborators. The power couplers have been fabricated and conditioned by FNAL. The string assembly took place inside the ISO 4 cleanroom at DESY. A seven meter long alignment and assembly girder for this special string assembly has been designed and fabricated at DESY. The girder facilitates the assembly of the 3.9 GHz resonators with alternating power coupler orientation in ISO 4 cleanrooms. For redundancy and fast action on problems during string assembly, the DESY high pressure rinsing system (HPR) has been modified on the basis of the INFN Milano design for this 3.9 GHz application. The HPR has been qualified by four 3.9 GHz resonators, tested at INFN Milano. The integration of the cavities into Helium vessels, power coupler coupling factor and the power coupler assembly at DESY is qualified by one cavity that has been equipped with Helium tank and a power coupler and tested horizontally.

INTRODUCTION

In 2008 a first 3.9 GHz module [1] was set up for the FLASH accelerator at DESY. Also for the EU-XFEL accelerator, currently under installation, the benefit of higher efficient bunch compression should be applied [2]. As an in kind contribution from INFN Milano a 3.9 GHz module, housing 8 resonators, a beam position monitor and quadrupole magnet unit (BQU) was designed. Fabrication and testing of superconducting resonators as well as manufacturing of the module cold mass and vessel took place under responsibility of INFN. The BQU adapted to the 3.9 GHz cryostat geometry, is taken from the XFEL series production [3]. The setup of the 3.9 GHz cavity string and its integration in the module is done at the DESY Hamburg, as a joint collaboration between INFN Milano and DESY Hamburg [4]. The existing DESY infrastructure developed for 1.3 GHz modules was modified and adopted to the needs of the smaller 3.9 GHz resonators and cryostat.

ADAPTATION OF CLEAN ROOM HARDWARE

In the DESY cleanroom the handling of cavities is based on the usage of cavity frames, lifters and manipulators. These components are designed for 1.3 GHz nine cell resonators of TESLA shape. For the 3.9 GHz string and module assembly, this infrastructure needed to be adapted to the different size of the 3.9 GHz resonators. Ensuring a smooth 3.9 GHz string assembly as well as to provide a reprocessing capability for surface treatment and cleaning during the production and during string assembly most of the existing infrastructure needed to be modified.

Frame for Cavity with and without Tank

For 3.9 GHz cavities without helium tank (undressed cavities) the existing frames from 1.3 GHz single and triple cell treatment were modified. Here only the connecting plate between the frame and the reference rings of the 1.3 GHz cavities needed to be redesigned and exchanged (Fig. 1)

Figure 1: Undressed 3.9 GHz cavity in modified frame during high pressure rinsing.

The 3.9 GHz resonators are tuned by blade tuners where the Titanium bellows, needed for the tuning of the resonator, is located in the middle of the Helium vessel [5]. In addition the smaller diameter of the Helium vessels and thereby the shorter distance between the tank brackets as well as the long Helium pipe connection tubes does not allow to make use of the 4 post frames, that are in use for the 1.3 GHz cavity activities. At the HPR 2 system [6] the positioning of frame and HPR is made by four guide pins on a locating plate. A new frame for the 3.9 GHz cavities dressed with the Helium vessel was designed, with two long and two short posts allowing installation on the HPR 2 (Fig. 2).

ISBN 978-3-95450-178-6

FIRST HIE-ISOLDE CRYO-MODULE ASSEMBLY AT CERN

M. Therasse, G. Barlow, S. Bizzaglia, J-A. Bousquet, A. Chrul, P. Demarest, J-B. Deschamps, J-C. Gayde, M. Gourragne, A. Harrison, G. Kautzmann, D. Mergelkuhl, V. Parma, J. Somoza, M. Struik, V. Venturini, L. Williams, P. Zhang, CERN, Geneva, Switzerland
J. Dequaire, Intitek, Lyon, France

Abstract

The first phase of the HIE-ISOLDE project aims to increase the energy of the existing REX ISOLDE facilities from 3 MeV/m to 5 MeV/m. It involves the assembly of two superconducting cryo-modules based on quarter wave resonators made by niobium sputtered on copper. The first cryo-module was installed in the linac in May 2015 followed by the commissioning. The first beam is expected for September 2015. In parallel the second cryo-module assembly started. In this paper, we present the different aspects of these two cryo-modules including the assembly facilities and procedures, the quality assurance and the RF parameters (cavity performances, cavity tuning and coupling).

INTRODUCTION

The HIE-ISOLDE project consist in an increase of the beam energy and intensity of the existing ISOLDE and REX-ISOLDE. This upgrade requires the integration of the existing post acceleration system with a superconducting linac of four high-β (phase 1 and 2) and two low-β (phase 3) cryo-modules (CM) based on quarter wave SRF cavities. The cryo-modules will have to work at 4.5 K in a common vacuum (cavity vacuum and insulation vacuum are the same).

The first phase (CM1 and CM2) started in August 2014 with the assembly of the first HIE-ISOLDE cryo-module (CM1) which was completed in April 2015 and installed on the HIE-ISOLDE beam line in May 2015. CM1 is under full functional testing (vacuum, cool down, cavity alignment, RF conditioning and test) [1].

In parallel, for the second cryomodule, the production of cavities continued and the parts preparation was launched in early April. An upgrade of the tooling and assembly facilities was done. The assembly of the second cryo-module started in June 2015.

THE CRYOMODULE ASSEMBLY

The complete high-β cryo-module assembly (see Fig. 1) is done vertically, suspended to a mobile frame. The assembly process can be divided in 14 main steps:

1-Vacuum vessel- top plate separation and storage.
2-Vacuum vessel (VV) preparation.
3-Thermal shield (TS) assembly and insertion into VV.
4-Chimney assembly and installation on the frame.
5-Top plate assembly.
6-Chimney insertion in the top plate.
7-Support frame installation.
8-Solenoid and cryogenics instrumentation interfaces installation.
9-Cavity insertion test.
10-Intermediate vacuum testing.
11-Cavities installation.
12-RF ancillaries' installation and test.
13-Cryo-module vessel closure.
14-Final assembly and qualification tests.

This sequence is imposed by the cryo-module design and by the tooling characteristics. To minimize the risk of contamination, the RF cavities are installed at the latest possible step. All cryo-module technical specifications and required performance are presented in [2].

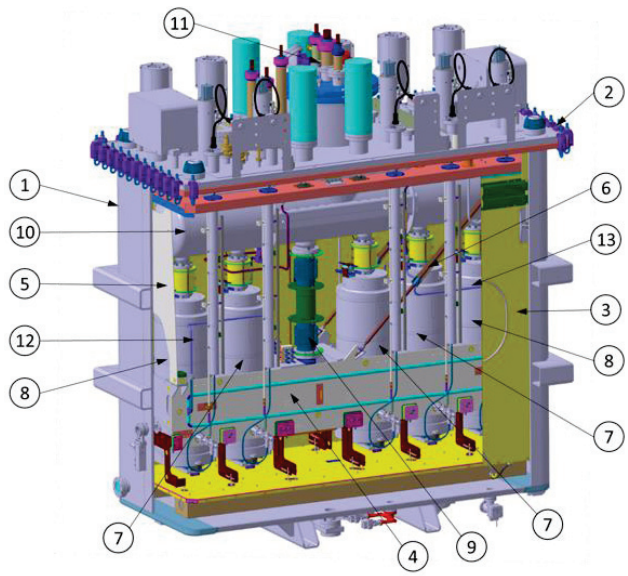

Figure 1: The complete HIE-ISOLDE high-β cryo-module; 1 Vacuum vessel lower box, 2 Vacuum vessel top plate assembly, 3 Thermal shield lower box, 4 Support frame, 5 Suspension end plate, 6 Tie-rod, 7 Inboard cavity, 8 Outboard cavity, 9 Down tube to solenoid, 10 Helium vessel, 11 Chimney assembly, 12 Support frame cooling supply, 13 Support frame cooling return, 14 Mathilde targets, 15 Mathilde viewport.

WORK ORGANIZATION

In order to reduce problems during the cleanroom assembly and to minimize the working time in the cleanroom, the work needs to be carefully organized.

One cryo-module contains more than 10000 parts under more than 500 references, going in size from sub-millimetre dimensions to four cubic meters, and weighing up to 2.5 tonnes. The assembly of CM1 showed that a full

DEVELOPMENT OF A TEST BENCH TO PREPARE THE ASSEMBLY OF THE IFMIF LIPAC CAVITY STRING

N. Bazin#, J. Chambrillon, G. Devanz, H. Dzitko, P. Hardy, J. Neyret, C. Servouin,
CEA/DSM/IRFU, Gif sur Yvette, France
F. Toral, CIEMAT, Madrid, Spain

Abstract

The IFMIF LIPAc cryomodule, whose final design and fabrication status is presented in [1], houses eight half-wave resonators and eight solenoids which will be assembled on a support frame in clean room. Due to the short lattice defined by beam dynamics constraints, there is not much room between two elements for the operators' hands to connect them. In order to test, optimize and validate the clean room assembly procedures and the associated tools, a test bench, consisting of a frame, a little bigger than one eight of the final support has been manufactured. In order to start the tests before the delivery of the actual key components of the cryomodule, a dummy cavity, solenoid and coupler were manufactured and will be used to perform tests outside and inside the clean room to validate the assembly procedure and the tools. The mock-up will then be used to train the operators for the assembly of the whole string.

THE IFMIF LIPAC CAVITY STRING

The cavity string of the IFMIF LIPAc cryomodule, which is depicted in Figure 1, is made of eight 176 MHz half-wave resonators with their power couplers, eight focusing solenoids - each equipped with beam position monitors (BPMs) - two warm/cold transitions with beam valves, and a pumping line connected to the two central cavities [2]. Due to their size and weight, the couplers are mounted vertically and connected to each cavity at their mid-plane. In order to meet the beam dynamics constraints [3], the cryomodule has been designed to be as short as possible: 400 mm space is allowed for the solenoid package – i.e the focusing solenoid, the BPMs and one bellows on each side [4] – and 280 mm for the cavity equipped with its tuning system. This one is a compression mechanical tuner attached to pads welded to the helium tank of the cavity [5]. These pads are close to the cavity / solenoid interface flange and could hinder operators' hands for the connection.

All the elements of the cavity string are placed on a frame made of titanium. Because of the thermal shrinking of the 5.5 meter long frame during the cool down of the cryomodule - about 8.4 mm – it is not possible to directly attach the cavities and the solenoids on this one in order to be compatible with the couplers which are in interface with the vacuum vessel.

To leave the cavities and solenoids longitudinal position independent from the titanium frame, C-shaped elements with needle rollers similar to the ones presented in [6] are used. Each cavity and solenoid is fixed on an invar rod which is attached to the frame in its centre. Because of the low thermal expansion coefficient of invar (0.4 mm/m between ambient temperature and liquid helium temperature to compare to 1.5 mm/m for titanium), this invar rod fixture determines the longitudinal positions of the couplers.

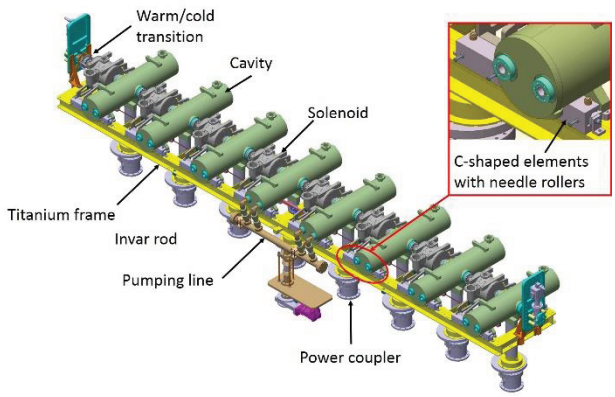

Figure 1: The IFMIF LIPAc cavity string.

The C-shaped elements also assure a fine alignment of the cavities and solenoids around the beam axis with accuracy of ±1 mm and ±10 mrad for the solenoids and of ±2 mm and ±20 mrad for the cavities. The cavity alignment is particularly critical because of its long power coupler. The coupler is connected to the vacuum tank through a flexible bellow and to a RF line. A bellow deformation or a small force in the RF line connection could drive to a resulting moment of rotation, which could perturb the cavity alignment. The spring washer package has been calculated to balance this resulting moment and to keep the cavity alignment.

PRINCIPLES IN THE CAVITY STRING ASSEMBLY

The beam line is a critical part as it must be free of any pollution for the good performance of the SRF Linac. It means that all the components of the beam line – cavities, solenoids, couplers and accessories – must be assembled in an environment free of dust, an ISO 5 clean room.

The Support Frame

Because the titanium frame is a critical part of the alignment system of the cavity string and is used as a reference for the assembly in clean room, it is made of I-

Contact: nicolas.bazin@cea.fr

ISBN 978-3-95450-178-6

CONNECTION OF EU-XFEL CRYOMODULES, CAPS, AND BOXES IN THE EU-XFEL MAIN LINAC AND INJECTOR: WELDING OF CRYO-PIPES AND ASSEMBLY OF BEAM-LINE ABSORBERS UNDER THE REQUIREMENTS OF THE PED REGULATION

S. Barbanotti#, C. Buhr, H. Hintz, K. Jensch, L. Lilje, W. Maschmann, A. de Zubiaurre Wagner
DESY, Hamburg, Germany
P. Pierini, INFN/LASA, Segrate MI, Italy and DESY, Hamburg, Germany

Abstract

The European X-ray Free Electron Laser (EU-XFEL) [1] cold linac [2] consists of 100 assembled cryomodules, 6 feed/end boxes and 6 string connection boxes fixed to the ceiling of the accelerator tunnel; the injector consists of a radio frequency gun, one 1.3 GHz and one 3.9 GHz cryomodule, one feed and one end cap lying on ground supports. The components are connected together in the tunnel, after cold testing, transport, final positioning and alignment. The cold linac is a pressure equipment and is therefore subjected to the requirements of the Pressure Equipment Directive (PED). This paper describes the welding and subsequent Non-Destructive Testing (NDT) of the cryo-pipes (with a deeper look at the technical solutions adopted to satisfy the PED requirements), the assembly of the beam line absorbers and the final steps before closing the connection with a DN1000 bellows. A special paragraph will be dedicated to the connection of the injector components, where the lack of space makes this installation a particularly challenging task.

INTRODUCTION

The EU-XFEL cold linac cryogenic layout is shown in Figure 1. It consists of 100 1.3 GHz accelerating cryomodules divided in 3 linac sections (L1, L2 and L3); between the sections there are 2 warm bunch compressors (BC1 and BC2), where the continuity of the cryogenic distribution is made possible by 2 transfer lines.

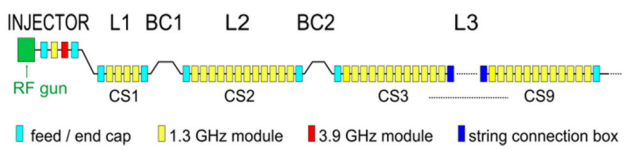

Figure 1: Layout of the EU-XFEL injector and cold linac.

The L1 section (CS1) is composed of 4 cryomodules, one feed (FC) and one end cap (EC); the L2 is section has 12 cryomodules, one feed and one end cap (CS2), while the L3 section is divided in 7 cryo-strings (CS3-9, 12 modules each), divided by string connection boxes (SCB).

A vacuum barrier is installed at the SCBs and at the FCs and ECs, to separate the insulation vacuum of each cryo-string, allowing independent pumping.

The cryogenic circuits at 2.2 K, 5-8 K and 50-80 K flow along the whole linac without interruptions, while the 2-phase circuit and the warm up / cool down line are filled with helium at the beginning of each cryo-string through a Joule-Thompson (JT) valve and a warm up / cool down valve from the 2.2 K circuit (Figure 2).

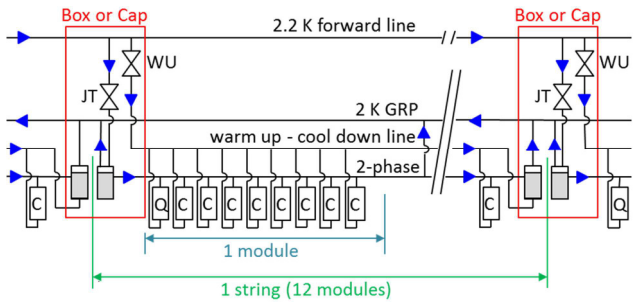

Figure 2: Flow scheme of the 2K circuit: JT = Joule-Thompson valve, WU = warm up – cool down valve, GRP = gas return pipe, C = cavity, Q = quadrupole.

The gas return pipe is connected to the 2-phase pipe at each module connection and flows through the whole linac without interruption, making also the 2 K circuit a unique cryo-circuit for the whole EU-XFEL cold linac.

The EU-XFEL injector is independent from the main linac and has one 1.3 GHz and one 3.9 GHz cryomodule, one feed and one end cap.

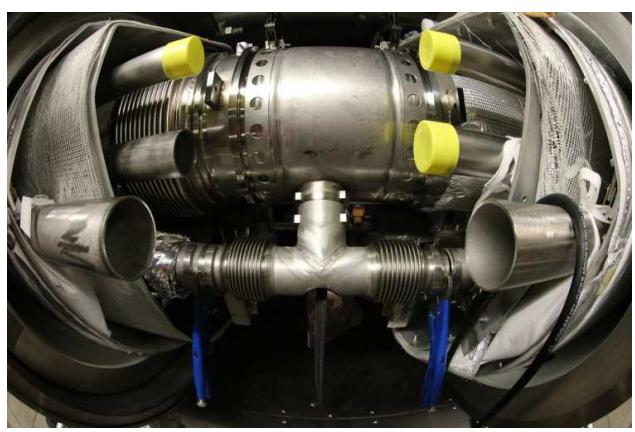

Figure 3: A typical module-module connection, where only the gas return pipe and 2 phase line are positioned for the first weld operations.

All the cryogenic pipes contained in the cryomodules, feed and end caps and string connection boxes are

#serena.barbanotti@desy.de

ISBN 978-3-95450-178-6

ASSEMBLY AND COOL-DOWN TESTS OF STF2 CRYOMODULE AT KEK

Toshio Shishido*#, Kazufumi Hara, Eiji Kako, Yuuji Kojima, Hirotaka Nakai,
Yasuchika Yamamoto,
KEK, High Energy Accelerator Research Organization, Tsukuba, Ibaraki, Japan

Abstract

As the next step of the quantum beam project, the STF2 (STF; Superconducting Test Facility) project is in progress at KEK. Eight 9-cell SC cavities and one superconducting quadrupole magnet were assembled into the cryomodule called CM1. Four 9-cell SC cavities were assembled into the cryomodule called CM2a. These two cryomodules were connected as one unit, and the examination of completion by a prefectural government was performed. The target value of beam energy in the STF2 accelerator is 400 MeV with a beam current of 6 mA. The first cool down test for low power level RF measurements was performed in autumn of 2014. In this paper, the assembly procedure of the STF2 cryomodules and the results of the low-power measurement are reported.

VERTICAL TEST RESULTS

The following cavity surface treatment processes were performed before the vertical test at KEK.

1) Pre-EP 5 μm and EP-I 100 μm for the impurities layer removal
2) Annealing for 3 hours at 750 ˚C for stress relief and degassing
3) Inner surface inspection using Kyoto camera system and local grinding if defects are found
4) Finish electropolishing, EP-II 5~20 μm
5) HPWR for 5 hours with 8 MPa using ultra-pure water
6) Baking for 44 hours at 140 ˚C

Figure 1 and Figure 2 show the final vertical tests results of the cavities MHI#14~MHI#22 [1]. The vertical tests were performed 22 times in total from January, 2011 to November, 2012. MHI#14~MHI#22 cavities except MHI#16 constitute cryomodule 1 (CM1). The average value of the maximum accelerating electric field of the cavities that constitutes the CM1 was 37 MV/m.

Figure 3 shows the final vertical tests results of the cavities MHI#23~MHI#26 [1]. The vertical tests were performed 10 times in total from October, 2013 to January, 2014. MHI#23~MHI#26 cavities constitute cryomodule 2a (CM2a). The main purpose of the cavities from MHI#23 to MHI#26 is the manufacturing cost reduction [2]. The maximum accelerating electric field of the MHI#24 was 12 MV/m due to strong field emission. So, the average value of the maximum accelerating electric field of the cavities that constitutes the CM2a was 28 MV/m.

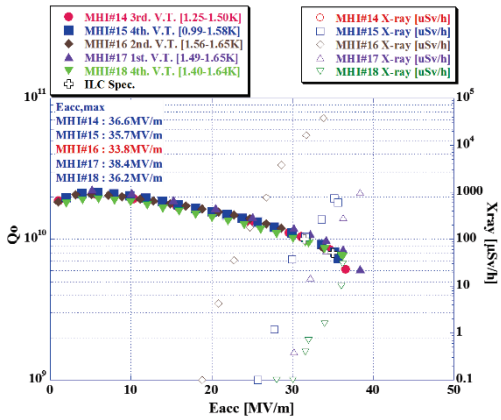

Figure 1: Final results of V.T.: MHI#14~MHI#18.

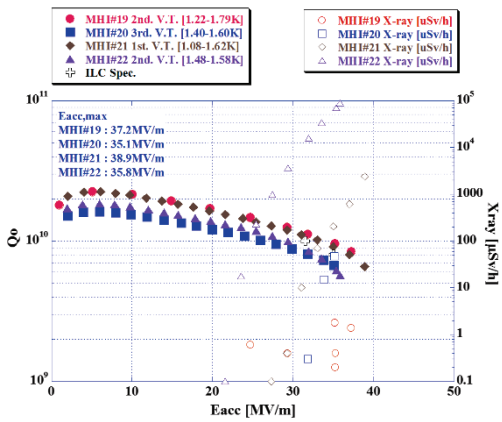

Figure 2: Final results of V.T.: MHI#19~MHI#22.

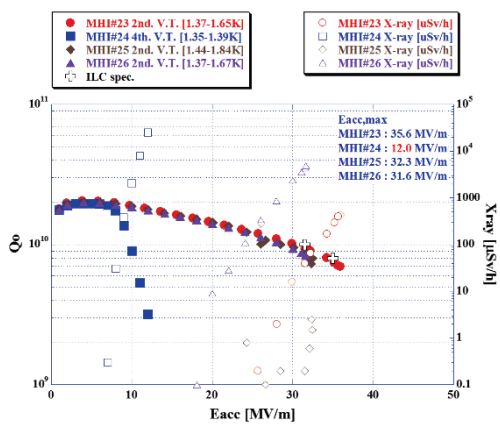

Figure 3: Final results of V.T.: MHI#23~MHI#26.

* Staying in SCRF group of TRIUMF from April, 2015 to March, 2016
#shishido@post.kek.jp

LCLS-II 1.3 GHZ DESIGN INTEGRATION FOR ASSEMBLY AND CRYOMODULE ASSEMBLY FACILITY READINESS AT FERMILAB*

T. Arkan#, C. Ginsburg, Y. He, J. Kaluzny, Y. Orlov, T. Peterson, K. Premo
Fermi National Accelerator Laboratory, Batavia, USA

Abstract

LCLS-II is a planned upgrade project for the linear coherent light source (LCLS) at Stanford Linear Accelerator Center (SLAC). The LCLS-II linac will consist of thirty-five 1.3 GHz and two 3.9 GHz superconducting RF continuous wave (CW) cryomodules that Fermilab and Jefferson Lab will assemble in collaboration with SLAC. The LCLS-II 1.3 GHz cryomodule design is based on the European XFEL pulsed-mode cryomodule design with modifications needed for CW operation. Both Fermilab and Jefferson Lab will each assemble and test a prototype 1.3 GHz cryomodule to assess the results of the CW modifications. After prototype cryomodule tests, both laboratories will increase cryomodule production rate to meet the challenging LCLS-II project installation schedule requirements of approximately one cryomodule per month per laboratory. This paper presents the 1.3 GHz CW cryomodule design integration for assembly at Fermilab, Fermilab Cryomodule Assembly Facility (CAF) infrastructure modifications for the LCLS-II cryomodules, and readiness for the required assembly throughput.

INTRODUCTION

The LCLS-II main linac 1.3 GHz cryomodule is based on the XFEL design, including TESLA-style superconducting accelerating cavities, with modifications to accommodate CW (continuous wave) operation and LCLS-II beam parameters.

Two prototype cryomodules will be assembled between September 2015 and March 2016 at Fermilab and JLab. At Fermilab, Cryomodule Assembly Facility (CAF) will be used to assemble the prototype cryomodule and 16 production cryomodules. For the prototype cryomodule, 8 ILC style bare cavities were processed with High Q0 recipe [1, 2] and then qualified in one of Fermilab's large test dewars, Vertical Test Stand (VTS) [3]. The qualified bare cavities are jacketed with their helium vessel at CAF glove box welding infrastructure [4]. The dressed cavities are tested and qualified for cavity string assembly either in VTS and/or at Horizontal Test Stand (HTS) [5].

For the 16 production cryomodules, the cavities will be fabricated, processed, jacketed with helium vessel and assembled (ready to be tested in vertical test stand) at cavity vendors. The cavities will be shipped from vendors to Fermilab for vertical testing. Qualified cavities will arrive to CAF for string assembly. Procurement responsibilities of the cryomodule components for the prototypes and production cryomodules are divided between Fermilab and JLab. Each laboratory is responsible to procure a specific component for all 35 cryomodules. The half of the components will be drop shipped from vendor(s) to each partner laboratory. The incoming quality control and acceptance of the component will be done by each laboratory before the component is accepted and can be fed to the assembly workflow. The procurement strategy is chosen to eliminate the schedule competition with a specific vendor. JLab developed sub-contracting officer technical representative (SOTR) scheme is being used to manage the procurement. Two SOTRs (one from each partner laboratory) are identified. SOTR from the laboratory who has the main responsibility of a specific procurement oversees the procurement specifications development, assists the preparation of the request for procurement (RFP), reviews the bids, forms a technical evaluation criteria and review team for evaluation of the bids and finally chooses the best value vendor to award the contract. The second SOTR from the other laboratory has the role of helping the main SOTR as needed and two SOTRs have to work closely to ensure qualified components are fabricated and delivered to each laboratory on time and on budget.

DESIGN INTEGRATION FOR ASSEMBLY

The overall structural design of the LCLS-II cryomodule is similar to that of the TESLA-style module [6]. Fermilab has assembled two 1.3 GHz pulsed Tesla type 3+ cryomodules in the last years. CM2, the second cryomodule assembled at CAF, has achieved world record gradient results [7, 8].

LCLS-II CW cryomodule cavity string is very similar to CM2 design, which consists of 8 dressed cavities, a beam position monitor (BPM) with a magnet spool tube and a gate valves at each end of the cavity string. The only difference between CM2 and LCLS-II cavity string is the BPM and magnet package assembly. In the cleanroom, BPM is assembled with a magnet spool tube and downstream gate valve. The conduction cooled split magnet will be assembled later during cold mass assembly; it does not need to be in the cleanroom. A beamline vacuum monitoring manifold will be assembled to the downstream end gate valve in order to monitor the beamline vacuum integrity from CAF to testing of the cryomodule, during shipping to SLAC until cryomodules are installed and interconnected in the linac tunnel. The

*Work supported, in part, by Fermi Research Alliance, LLC under Contract No. DE-AC02-07CH11359 with the United States Department of Energy and the LCLS-II Project
#arkan@fnal.gov

ISBN 978-3-95450-178-6

JLAB CRYOMODULE ASSEMBLY INFRASTRUCTURE MODIFICATIONS FOR LCLS-II*

E. F. Daly#, J. Armstrong, G. Cheng, M.A. Drury, J.F. Fischer, D. Forehand, K. Harding, J. Henry, K. Macha, J.P. Preble, A.V. Reilly, K.M. Wilson
Thomas Jefferson National Accelerator Facility, Newport News, VA 23606, USA

Abstract

The Thomas Jefferson National Accelerator Facility (TJNAF, aka JLab) is currently engaged, along with several other DOE national laboratories, in the Linac Coherent Light Source II project (LCLS II). The SRF Institute at Jefferson Lab will be building 1 prototype and 17 production cryomodules based on the TESLA / ILC / XFEL design. Each cryomodule will contain eight nine cell cavities with coaxial power couplers operating at 1.3 GHz. New and modified infrastructure and assembly tooling is required to construct cryomodules in accordance with LCLS-II requirements. The approach for modifying assembly infrastructure included evaluating the existing assembly infrastructure implemented at laboratories world-wide in support of ILC and XFEL production activities and considered compatibility with existing infrastructure at JLab employed for previous cryomodule production projects. These modifications include capabilities to test cavities, construct cavity strings in a class 10 cleanroom environment, assemble cavity strings into cryostats, and prepare cryomodules for cryogenic performance testing. This paper will give a detailed description of these modifications.

INTRODUCTION

The Linac Coherent Light Source (LCLS)-II project at the SLAC National Accelerator Laboratory (SLAC) requires a 4 GeV continuous-wave (CW) superconducting radio frequency (SRF) linear accelerator in the first kilometer of the SLAC tunnel. The aim is to operate a high repetition rate X-ray free-electron laser, i.e. with electron pulses at rates approaching 1 MHz delivered to two new undulators covering the spectral ranges of 0.2-1.2 keV and 1-5 keV, respectively. The collaborative project brings together six US institutions, which in alphabetical order are Argonne National Laboratory (ANL), Cornell University, Fermi National Accelerator Laboratory (FNAL aka Fermilab), Thomas Jefferson National Accelerator Facility, Lawrence Berkeley National Laboratory (LBNL), and SLAC [1].

As part of shared responsibilities Fermilab and JLab will build the 1.3 GHz accelerating cavity cryomodules (CMs) concurrently in two assembly lines in order to meet the overall project schedule. In preparation for CM assembly, Fermilab has been leading the CM design efforts based on extensive experience with TESLA-style CM design and assembly. The starting point for design is existing models and drawings of similar ILC CMs (e.g. Type III+) with modifications to enable continuous-wave (CW) operation [2]. JLab and Cornell are partners in R&D and design contributing to development activities, design reviews, integration, cost estimation and production. Both Cornell and JLab have valuable CW CM design experience. JLab has directly applicable recent 12 GeV Upgrade production experience. Experienced SRF and cryogenic personnel at ANL are participating in cryostat design beginning with system flow analyses and pipe size verification and may be available for other collaborative tasks. The procurement of CM components is distributed between Fermilab and JLab, with the exception of SLAC who will procure the main RF power couplers [3, 4].

Currently, activities and preparations are underway for assembling two prototype CMs, one at each laboratory. Following the prototyping efforts, thirty-three production CMs are planned - sixteen at Fermilab [5], seventeen at JLab – for a total of thirty-five CMs in order to provide reliable 4 GeV energy gain.

STRATEGY – ONE DESIGN, TWO PRODUCTION LINES

CM designs currently under development for the prototype and production CMs are intended to satisfy LCLS-II Project Requirements [6] as well as the CM Functional Requirements Specification [7]. The two prototype CMs will be identical and utilize as much existing hardware as possible in order to reduce schedule risk and reduce overall cost while achieving the same performance as the production CMs. The production designs will utilize as much of the DESY/XFEL design as practically possible in order to reduce schedule risk and reduce overall cost.

The two partner labs plan to receive identical parts and sub-assemblies based on final drawing packages, requirements and specifications that are well-developed. This is accomplished through concurrent reviews within LCLS-II project. Procurement activities are coordinated between technical leads at Jlab, Fermilab and SLAC who work together during all phases of the procurement process. The interfaces between CM hardware and

* Authored by Jefferson Science Associates, LLC under U.S. DOE Contract No. DE-AC05-06OR23177 with supplemental funding from the LCLS-II Project U.S. DOE Contract No. DE-AC02-76SF00515. The U.S. Government retains a non-exclusive, paid-up, irrevocable, world-wide license to publish or reproduce this manuscript for U.S. Government purposes.

edaly@jlab.org

TRANSIENT STUDY OF BEAM LOADING AND FEED-FORWARD LLRF CONTROL OF ARIEL SUPERCONDUCTING RF e-LINAC

Edward Thoeng[1,2], Robert Edward Laxdal[2]
[1]University of British Columbia, Vancouver, B.C., Canada,
[2] TRIUMF, Vancouver, B.C., Canada

Abstract

ARIEL e-LINAC is a ½ MW-class SRF accelerator operated at 10 mA of average current. In the initial commissioning, e-LINAC will be tested with increasing duty factors from 0.1% up to CW mode. During the pulsed mode operation, beam loading causes cavity gradient fluctuation and therefore transient behaviour of SRF Cavity gradient needs to be studied in order to determine how the Low-level RF (LLRF) should be implemented. Performance of LLRF control system with and without non-adaptive feed-forward are simulated to determine the resulting beam energy spread and experimental measurements are proposed to measure the increase of beam size due to beam loading.

INTRODUCTION

ARIEL e-LINAC will produce a 50 MeV electron beam as the photo-fission driver for Rare Isotope Beams (RIB) production [1]. Electron beam is first accelerated up to an energy of 10 MeV through an injector cryomodule (ICM) containing a single 9-cell SRF cavity, and further accelerated with two accelerating cryomodules (ACM), each containing two 9-cell SRF cavities, up to an energy of 50 MeV. The schematic of the e-LINAC is shown in Fig. 1. Initial commissioning of the e-LINAC will be tested with pulsed beam operation for cavity conditioning and the duty factor will be increased gradually up to CW mode.

The ARIEL e-LINAC is dominated by RF beam loading with ½ MW of beam power. During pulsed operation, beam loading causes cavity voltage to fluctuate and this result to an increase of the beam energy spread at the cavity output as shown in Fig. 2. This cavity voltage fluctuation is usually too fast to be controlled by feedback loop alone. Both feedback and additional feedforward control is needed to minimize voltage fluctuation and it is therefore studied in this simulation.

The effect of the beam loading can be observed directly from the increase in beam size as electron beam passed through a bending magnet. Experiments are proposed at the output of ICM to measure beam size coming out of a single beam loaded cavity. A combination of beam profile monitor (view screen) and BPM (beam position monitor) will be used to measure integrated and time snapshot of the beam energy.

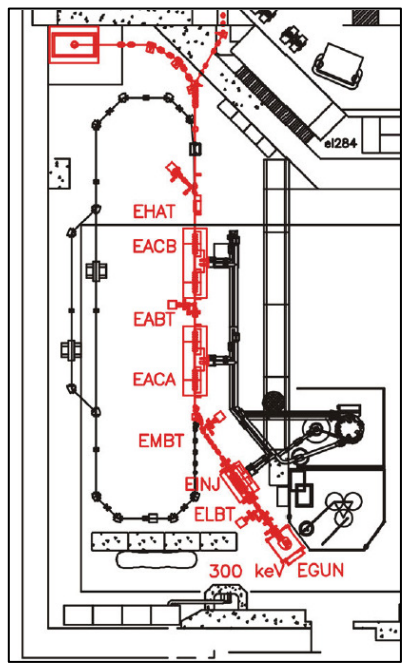

Figure 1: ARIEL e-LINAC layout.

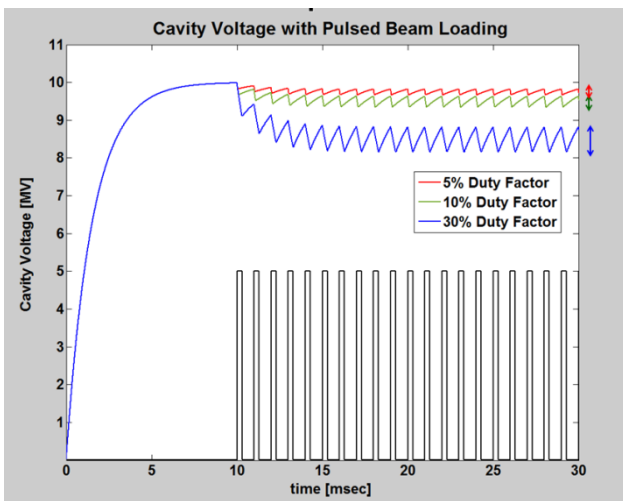

Figure 2: Cavity voltage fluctuation at different pulsed beam duty factor. Shown in black colour is the beam pulse (not drawn to scale) at 30% duty factor and injected 10 msec after RF power is turned on. Double headed arrows illustrate the measure of beam spread.

ISBN 978-3-95450-178-6

IMPROVEMENTS OF THE MECHANICAL, VACUUM AND CRYOGENIC PROCEDURES FOR EUROPEAN XFEL CRYOMODULE TESTING

Jacek Swierblewski, Mikolaj Bednarski, Barbara Dzieza, Wawrzyniec Gaj, Lukasz Grudnik, Pawel Halczynski, Andrzej Kotarba, Artur Krawczyk, Krzysztof Myalski, Tadeusz Ostrowicz, Boguslaw Prochal, Jakub Rafalski, Michal Sienkiewicz, Marek Skiba, Marcin Wartak, Mateusz Wiencek, Jan Zbroja, Pawel Ziolkowski, IFJ-PAN, Kraków

Abstract

The European X-ray Free Electron Laser is under construction at DESY, Hamburg. The linear accelerator part of the laser consists of 100 SRF cryomodules. Before installation in the tunnel the cryomodules undergo a series of performance tests at the AMTF Hall. Testing procedures have been implemented based on TTF (Tesla Test Facility) experience. However, the rate of testing and number of test benches is greater than in the TTF infrastructure. To maintain the goal testing rate of one module per week, improvement to the existing procedures were implemented at AMTF. Around 50 % of the testing time is taken by connection of the cryomodule to the test bench, performing all necessary checks and cool down. Most of the preparation procedures have been optimized to decrease mounting time. This paper describes improvements made to the mechanical connections, vacuum checks and cryogenics operation.

INTRODUCTION

During the planning phase of the XFEL [1] project it was presumed that one Cryomodule should leave AMTF (Accelerator Module Test Facility) Hall per week. The AMTF Hall consists of three separated Cryomodule test benches. This means that presumed time for single Cryomodule test was estimated for around 3 weeks. During this time following operation have to be performed on Cryomodule:

- Installation of the cryomodule on the test bench
- Connection of the Beam Line
- Connection of the cryogenic process pipes
- Integral leak check
- Leak check of the Cryomodule
- Interconnection isolation with MLI (Multi - Layer Isolation)
- Warm coupler conditioning
- Cool - down
- Measurements at 2K (this paper does not cover this part of the testing procedure, see [2])
- Warm - up
- Disconnection of the Cryomodule from the test bench

In the old testing procedure all mentioned steps were split in three weeks. During first week connection of the Cryomodule to test bench and cool - down process was done. Second week was foreseen for measurements at 2K. Third week was foreseen for warm - up and disconnection of the Cryomodule. However, the old procedure has one general problem. It did not cover the problem which could occur during the test procedure. Moreover, there were no time foreseen for any mistakes or Cryomodules reparation inside the test stand. This means that each problem during the test (like leaks on the Cryomodules) causes delay in the general schedule. There was a necessity to improve the procedure to get some extra time needed for some special testing cases, reparation, exchanging of the Cryomodule parts etc.

MECHANICAL PROCEDURES IMPROVEMENTS

Shifting of the Possible Mounting Operations from Test Bench to Preparation Time (eg. GRP Adapters)

After reception of the cryomodule special preparation time is scheduled within incoming inspection checks and preparation of the cryomodule to installation into test bench are performed [3]. After that, the cryomodule can be mounted into test bench and all connections can be performed. One of the task which realization has been shifted from inside to outside of the test bench is mounting of the GRP adapter. GRP complex reductor is used to connect a cryomodule to the test bench. During installation of the cryomodule into test bench all process pipes are connected.

Figure 1: GRP adapter.

One of them is 300 mm of diameter gas return pipe. The test bench gas return pipe has 150 mm of diameter. Therefore to connect a cryomodule to test bench a special reductor (See Fig.1) as well as special indium seal have been designed. The installation of the GRP adapter to the cryomodule has to be performed very attentively according to the special

ISBN 978-3-95450-178-6

CAVITIES AND CRYOMODULES MANAGING SYSTEM AT AMTF

Mateusz Wiencek, Krzysztof Krzysik, Jacek Swierblewski IFJ-PAN, Kraków
Jacek Chodak, DESY, Hamburg

Abstract

800 SRF cavities and 100 SRF cryomodules are under test in the AMTF Hall at DESY, Hamburg. Testing of such a large volume of components requires a management system which can store the measurement data. In addition the system should simplify tasks which are recurrent. In the case of the system developed at AMTF, communication with external databases has also been developed. An added complication is that not all the test procedures are identical for each component, and therefore the management system keeps track of all work done for each of the individual components. In the case of the vertical acceptance tests for the 800 SRF cavities, the management system provides an interface for specifying a decision of the next step each cavity (e.g. send for module assembly or retreatment). This paper describes the most important parts of this system.

INTRODUCTION

Limited time, manpower, capacity of test infrastructure and amount of processed information caused necessity of having a tool, that would make easier to manage available resources effectively and provide space for data required to proceed with tests. The tool should also provide access to common data space from multiple locations at the same time, restricted however by user's permissions. In response for these requirements IFJ team designed and developed a system dedicated for managing tests at AMTF (Accelerator Module Test Facility) [1].

OVERVIEW OF THE SYSTEM

In the managing system test of every object is divided into steps, that have to be performed in defined order. Every following step depends on previous ones – activity connected with the step can be started only if appropriate criteria are met. In case of unexpected events (e.g. cold leak) test sequence may be changed by authorized person. Test progress contains information about past and future steps for selected object and is up-dated according to activities and decisions. The managing system allows also to view summary for AMTF - current status of test infrastructure and all tested objects.

Test of every object provides measurement data, that have to be saved for further analysis and transferred to the external data base. Results of measurements require appropriate representation in the data base, transfer procedures and user interface. The managing system implements all these functionalities. Results of measurement are formatted into XML files and then uploaded to the internal data base (AMTFMEAS). Data are assigned to appropriate test and activity (step) to be easily accessed and avoid an ambiguous situation. In this point results can be viewed and analyzed in dedicated sections, i.e. preparation, vertical test and module test. After approval by authorized persons the data are finally transferred to the external data base (XFELDB).

IT REALIZATION

AMTF managing system is realized as server - side Java application (Tomcat 7). It is implemented on Linux (Ubuntu) server encapsulated in Apache 2 server with jdk connection (see Fig. 1). Java application is connecting with external Oracle database server. Functionality of the system on the clients computers is completely independent from operating system and internet browser used. Clients computers requires only Internet browser with enabled JavaScript. Application have an access control realized in two steps. First is htaccess on the Apache side. Second is a realized in the application. Application have implemented privileges system with special permissions for special groups of users.

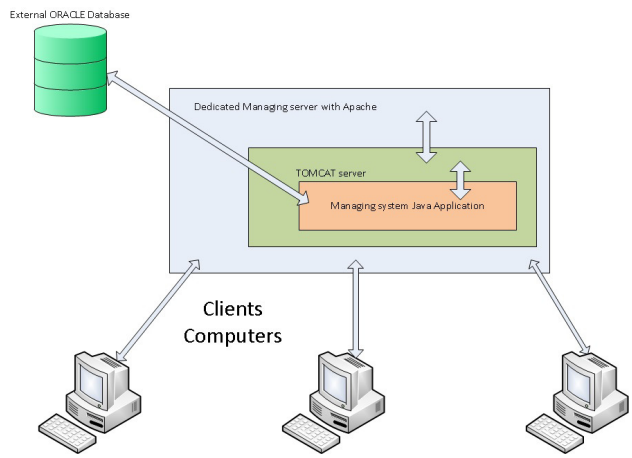

Figure 1: Basics of the IT realization of AMTF Managing system.

AMTF STATUS

From the planning of the works point of view important part of the system is a summary created from all components tested and staying at AMTF. Managing system provides two such summaries. One is directly accessible from the system (see Fig. 2). In this summary view user can find cavities which are during the testing or preparation for the testing (upper part of the view). In addition summary tables for cavities are available. In those tables user can check how many cavities are currently stored at AMTF and how many have been sent to vendors or for assembly of the cryomodules.

Second part of the AMTF status table is so - called "AMTF monitor" (see Fig. 3). In this tool all important parameters

ISBN 978-3-95450-178-6

IMPROVEMENTS OF THE RF TEST PROCEDURES FOR EUROPEAN XFEL CRYOMODULE TESTING

Mateusz Wiencek, Karol Kasprzak, Daniel Konwisorz, Szymon Myalski,
Katarzyna Turaj, Agnieszka Zwozniak, IFJ-PAN, Kraków

Abstract

The testing of the 100 SRF cryomodules for E-XFEL is currently ongoing at the AMTF Hall, located at DESY, Hamburg. Cold tests for the cryomodules have been developed based on TTF (Tesla Test Facility) experience. However, to be able to test the cryomodules with required test rate of one a week, some improvements to the measurements had to be made. The goal of these improvements was to reduce the time needed for testing without losing any of the important data for the cryomodule. Currently, after testing more than 30 % of the cryomodules, gathered experience is now allowing us to skip or combine some of the measurements. This paper describes changes in the cold test procedures which have been made since the testing of the first serial cryomodules delivered by IRFU.

INTRODUCTION

Before installation in the linac part of the European XFEL (X-ray Free Electron Laser), all of the superconducting cryomodules have to be tested to find optimal position in the accelerating string and to exclude failures, which prevents to install them into the accelerator. The measurement in superconducting state (2K) is the crucial parts of those tests. To be able to test all modules according to the schedule improvements were necessary at many stages of module life cycle. Test procedure was also required to be improved in order to meet deadlines and measure the most important module parameters. Time when the module is cold is a critical period during the module test. Cryogenic slots that enables us to cool down or warm up the module are limited and there is a number of measurements that cannot be done in parallel that limits our options.

In this paper we describe most important improvements done up to now. Improvements done at the cold test of the cryomodule can be split into two main parts. First part describes changes in the order of the measurements, skip or combine some of them. Second part describes the improvements in the measurements itself.

TEST PROCEDURE BEFORE IMPROVEMENTS

Test procedure for the XFEL Module includes several low and high power measurements important for determining module parameters and performance before qualifying it to be used in the accelerator. This is an important task, because a module performance can change significantly after subjecting it to high power due to a processing. Detailed information makes it possible to sequence modules in the tunnel in the optimal way, prepare correct waveguide power distributions and set LLRF parameters.

Low Power Measurements

Module test starts with low power measurements. During this step fundamental mode spectra were measured for all cavities (See Fig. 1) using dedicated software developed by IFJ PAN group [1]. This gives an information about pi mode frequencies and deviation from the reference spectra.

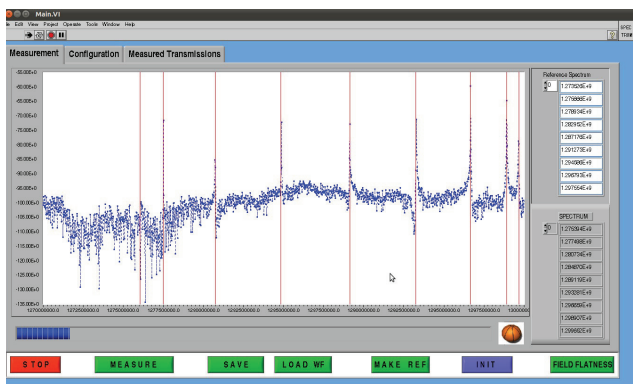

Figure 1: Fundamental mode spectra measurement application.

In addition TM011, TE111, TM110 modes through Higher Order Mode couplers are measured (See Fig. 2) [2]. After those measurements tuner test was performed. Cavities pi-mode frequency was measured after moving the step motor by a fixed number of steps. This gave us information about the relation of frequency change and tuner steps and let us estimate number of steps to tune the cavity to the operating frequency.

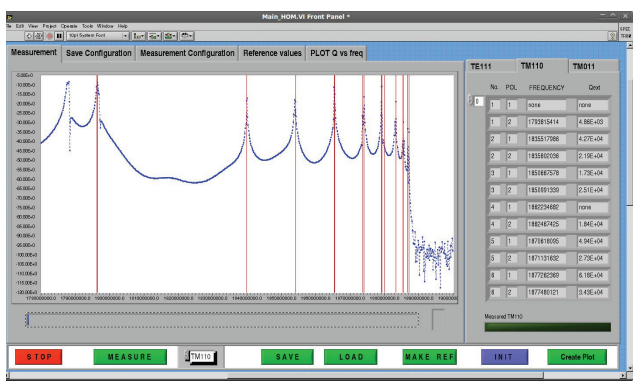

Figure 2: HOM spectra measurement application.

ISBN 978-3-95450-178-6

THE CRYOGENIC INFRASTRUCTURE FOR SRF TESTING AT TRIUMF

R. Nagimov, P. Harmer, D. Kishi, A. Koveshnikov, R. E. Laxdal, H. Liu, N. Muller,
TRIUMF, Vancouver, Canada

Abstract

At the moment TRIUMF operates one superconductive radio-frequency (SRF) accelerator and is building the second one. The superconducting heavy ion linear accelerator of the Isotope Separation and Acceleration (ISAC) facility utilizes medium beta quarter wave cavities cooled down to 4 K. The Advanced Rare IsotopE Laboratory (ARIEL) is a major expansion of the ISAC facility. ARIEL SRF electron linear accelerator (e-linac) operates nine-cell TESLA type cavities at 2 K. Both accelerators have dedicated cryogenic systems including liquid helium plants and distribution systems. In addition to accelerator cryogenic support, ISAC cryoplant provides liquid helium for the SRF testing facility at both 4 K and 2 K temperatures. TRIUMF's SRF development involves both SRF testing facility and accelerators cryogenic support systems. This paper presents the details of the SRF testing cryogenic systems as well as recent commissioning results of the new e-linac cryogenic system.

ISAC FACILITY CRYOSYSTEM ARCHITECTURE

The cryogenic system of ISAC superconducting accelerator facility was installed in two phases. In 2006, the first Linde TCF50 cryoplant was installed and commissioned [1]. Phase-I cryogenic system installation supported five cryomodules with liquefaction rate of ~5 g/s. From the first days of operation the ISAC distribution system allowed for supplying cryogens to SRF test facility for cavities and cryomodule testing. During the Phase-II ISAC facility upgrade the second Linde TCF50 cryoplant was installed and integrated into the existing infrastructure [2]. Liquid helium and liquid nitrogen distribution systems were integrated to the existing lines. At full load both Phase-I (~620 W) and Phase-II (~590 W) cryoplants have enough capacity to handle the entire linac static heat load (in the range of 16 to 23 W per each cryomodule, with additional 95 W for helium distribution lines), allowing minor cryoplants maintenance without warm-up of the cryomodules.

ISAC SRF test facility had been developed in parallel with ISAC linac to support TRIUMF's SRF development. The current state of the SRF test facility includes cavity preparation facility (ultrasound cleaning tanks, high pressure water rinse area, chemical etching facility), cryomodule assembly area and SRF cavities test facility.

Individual cavities and assembled cryomodules undergo set of warm and cold tests at both 4 K and 2 K before the final installation. Individual SRF cavity tests are performed in the test cryostat, designed for the ISAC linac quarter-wave cavity and later upgraded to support 9-cell cavities (Figure 1). Cryomodules went through the cold tests before initial installation, as well as after periodical maintenance operations.

The current ISAC cryogenic system configuration includes the capability to support the following operations:

- ISAC Phase-I and Phase-II cryomodules nominal operation with the support of SRF test facility cryogenic tests using both cryoplants;
- ISAC Phase-I and Phase-II cryomodules maintenance mode (handling static heat load) with the support of SRF test facility cryogenic tests using one cryoplant.

Figure 1: SRF test facility cavity cold test (left), cryostat section view (right).

The SRF testing facility is actively used to perform cryogenic tests of individual cavities for TRIUMF and other laboratories. The tests were performed on a quarter-wave cavities (Legnaro cavities for ISAC Phase-I, TRIUMF-PAVAC cavities for ISAC Phase-II), elliptical cavities (TRIUMF-PAVAC cavities for ARIEL Phase-I and VECC cryomodule). The prototype cavity for ISOLDE facility at CERN was tested at TRIUMF SRF test facility. Currently SRF group is closely involved in R&D efforts testing quarter-wave and half-wave cavities for RISP project in South Korea.

SRF Test Facility

Due to the set of requirements to the cryogenic support of SRF test facility, highly configurable liquid helium supply source is essential. To minimize cavity replacement and cryostat maintenance periods, liquid helium is supplied through the single flexible vacuum-jacketed line with no extra liquid nitrogen or cold return helium gas precooling (Figure 2).

ISBN 978-3-95450-178-6

SURFACE RESISTANCE STUDY ON LOW FREQUENCY (LOW BETA) CAVITIES

D. Longuevergne, F. Chatelet, G. Michel, G. Olry, F. Rabehasy, L. Renard, IPNO, Orsay, France

Abstract

Additional RF tests and temperature treatments (120°C baking, 100K soaking, ...) have been carried out on Spiral2 quarter-wave resonator (QWR) and ESS double spoke resonator (DSR). For each test, residual resistance and BCS resistance have been evaluated by testing the cavities between 4.2K and 1.5K. This talk will summarize the main results and try to highlight the main differences with high frequency cavities.

INTRODUCTION

The analysis of the evolution of the quality factor (noted Q_0) versus the accelerating gradient (noted Eacc) of a superconducting cavity made of bulk Niobium has been in the community very important and fruitful to optimize the surface and heat treatments. This way, three regions of importance have been defined based on general observation of 1.3 GHz elliptical cavities; the Low, Medium and High Field Q-Slope, noted respectively LFQS, MFQS and HFQS. LFQS corresponds to a slight increase of the Q_0, the MFQS to a slow decrease of the Q_0 and finally the HFQS to a fast decrease of the Q_0 [1].

It has to be pointed out that this general behaviour has never been observed at lower frequencies (88 MHz and 352 MHz); the Q-slope is monotonous, progressive and starts already at low field (see Figure 1).

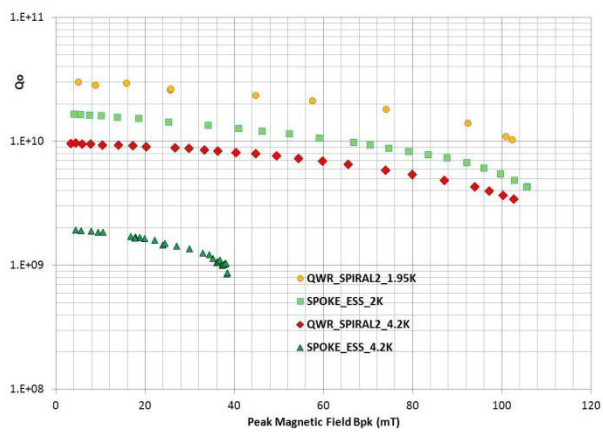

Figure 1: Typical Q-curve of Spiral2 QWR and ESS DSR.

The aim of this paper is to report some typical behaviour of cavities operating at 88 MHz (Spiral2 QWR) and 352 MHz (ESS DSR).

Extensive cold tests between 4.2K and 1.5K in vertical cryostat have been carried out to fully understand the evolution of the residual and BCS resistance (noted R_{res} and R_{BCS}) versus Eacc. By quantifying both the residual and BCS resistances of the cavity versus the accelerating gradient, one can fully assess what is the best procedure to treat the surface of a cavity regarding the specifications of a project. The advantage is that at these low frequencies and at 2K, R_{BCS} is small and even negligible at 88 MHz contrary to 1.3 GHz cavities where R_{BCS} stays comparable to R_{res}. Table 1 summarizes typical values of R_{BCS}.

In order to extract correctly both resistances and their dependences versus Eacc, an empirical model has been built as described in [2], based on the magnetic dependence of the energy gap for R_{BCS}. The field dependence of R_{res} is fitted with a second order polynomial function because of its complexity. It appears that this model is fitting very nicely the Q-slope visible on experimental data at 88 MHz. However, at 352 Mhz, the model can't be used due to a bad cooling of the cavity at 4.2K tested vertically instead of horizontally.

Table 1: Typical BCS Resistance Values Versus Frequency at Different Temperatures

R_{BCS} (nΩ)	4.2K	2K	1.5K
1300 MHz	600	15	1.2
700 MHz	174	4.3	0.35
352 MHz	44	1	9E-2
88 MHz	3	7E-2	6E-3

Finally, the magnetic ambiance around the cavity during cooling down has been monitored. Very interesting but complex behaviour has been observed without surprisingly any consequences on the quality factor of the cavities. Details will be given in this paper.

RS MODEL

The model used to interpret the R_{BCS} increase versus the amplitude of the RF magnetic field is based on the magnetic dependence of the energy gap as detailed in [2]. In other terms, the energy gap, difference of free energies between the normal and superconducting states, is altered by the magnetic energy brought by the RF wave.

We can write the corrected formula of the BCS resistance as in equation 1 :

$$R_{BCS} = \frac{A(\lambda,\xi,l,...)\cdot\omega^2}{T}\cdot\exp\left(\frac{-\Delta(T=0,B=0)}{k_B\cdot T}\cdot\left(1-\left(\beta\cdot\frac{B}{Bc(T)}\right)^2\right)\right) \quad (1)$$

With A and β two parameters, T the temperature, ω the pulsation of the RF wave, Δ the energy gap, k_B the Boltzmann constant, B the amplitude of the RF magnetic field and Bc the critical magnetic field.

ISBN 978-3-95450-178-6

COMMISSIONING RESULTS OF THE HZB QUADRUPOLE RESONATOR

R. Kleindienst*
A. Burrill, S. Keckert, J. Knobloch, O. Kugeler
Helmholtz-Zentrum-Berlin, Albert-Einstein-Strasse 15, 12489 Berlin, Germany

Abstract

Recent cavity results with niobium have demonstrated the necessity of a good understanding of both the BCS and residual resistance. For a complete picture and comparison with theory, it is essential that one can measure the RF properties as a function of field, temperature, frequency and ambient magnetic field. Standard cavity measurements are limited in their ability to change all parameters freely and in a controlled manner. On the other hand, most sample measurement setups operate at fairly high frequency, where the surface resistance is always BCS dominated. The quadrupole resonator, originally developed at CERN, is ideally suited for characterization of samples at typical cavity RF frequencies. We report on a modified version of the QPR with improved RF figures of merit for high-field operation. Experimental challenges in the commissioning run and alternate designs for simpler sample changes are shown alongside measurement results of a large grain niobium sample.

INTRODUCTION

Bulk niobium cavities today can achieve quality factors of over 10^{10} at accelerating gradients of $25-35$ MV/m. These high quality cavities can be produced consistently with a high success rate as the result of decades of research into the material properties of niobium and the required surface finishing and heat treatment techniques.

Three paths are currently being pursued to break beyond bulk niobium cavities:

- Titanium or nitrogen 'doped' niobium
- Different superconductors such as Nb_3Tn, NbN or MgB_2, coated on copper or niobium
- A SIS multilayer structure, described in [1]

For all of these approaches, studying samples as opposed to cavities can be advantageous. Thin films deposition is easier on flat samples as opposed to on curved surfaces. The cost of a small sample and the potentially fast turn-around rate are further benefits. Lastly, cavity testing is typically limited to a narrow temperature range below 4.2 K.

RF Sample Testing Setups

Several systems exist around the world dedicated to testing the RF properties of superconducting samples. At Cornell, a third generation TE host cavity has been commissioned, which at 4 GHz can apply 80 mT onto a flat sample of 10 cm diameter [2, 3] . A temperature mapping system on the back of the sample is used to measure the RF losses. A similar system is in operation at Orsay/Saclay [4]

At JLAB, a sapphire loaded cavity has been used to characterize 5 cm samples at 7.5 GHz. [5]. The sample is thermally decoupled from the cavity, allowing measurements within the temperature range between 2 and 20 K.

The quadrupole resonator was developed at CERN in the late 1990's [6]. Since its upgrade, it can be used to characterize a superconducting sample at 400 , 800 and 1200 MHz [7]. Measurements are possible over a wide temperature range with peak magnetic fields reaching up to 60 mT on the 7.5 cm sample.

The benchmarks of the different systems are summarized in Table 1. At HZB, the decision to build an improved version of the QPR was made due to advantageous measurement frequencies. At the comparatively low frequency, one can not only study the BCS resistance, but also the residual resistance of a sample. Having multiple frequencies also allows measuring scaling factors and provides additional cross checks to the data. The main aims for improvement of the system were identified as raising the peak field on sample, while increasing measurement resolution and the change of sample. The size of the sample was left unchanged, to allow interchangeability between the two systems.

Overview Quadrupole Resonator

Figure 1 shows a cross sectional view of the Quadrupole Resonator (QPR). With the particular geometry of the niobium rods, a set of TE21n modes exist, which all have high magnetic field region on the sample surface.

The sample plate of diameter 75 mm is welded to a hollow niobium tube which is brazed to a double sided stainless steel flange. The coaxial gap between the resonator and the sample chamber causes dipole and quadrupole modes to decay exponentially when penetrating towards the flange.

The coaxial gap separating sample and resonator also decouples them thermally. This allows changing the sample temperature freely while keeping the rest of the resonator at the temperature of the helium bath, typically 1.8 K.

* Email: raphael.kleindienst@helmholtz-berlin.de

ISBN 978-3-95450-178-6

NANOSTRUCTURE OF THE PENETRATION DEPTH IN Nb CAVITIES: DEBUNKING THE MYTHS AND NEW FINDINGS

Y. Trenikhina*, A. Romanenko, Fermilab, Batavia, USA
J. Kwon, J.-M. Zuo, MatSE, UIUC, Urbana, United States

Abstract

Nanoscale defect structure within the magnetic penetration depth of 100nm is key to the performance limitations of niobium superconducting radio frequency (SRF) cavities. Using a unique combination of advanced thermometry during cavity RF measurements, and TEM structural and compositional characterization of the samples extracted from cavity walls at both room and cryogenic temperatures, we directly discover the existence of nanoscale hydrides in SRF cavities limited by high field Q-slope, and show the decreased hydride formation after 120C baking. Crucially, in extended studies, we demonstrate that adding 800C hydrogen degassing - both with AND without light BCP afterwards - restores the hydride formation to the pre-120C bake level correlating perfectly with the observed high field Q-slope behavior. We also show absence of niobium oxides along the grain boundaries and the modifications of the surface oxide upon 120C bake, which contradicts some of the widely used models of the niobium surface.

INTRODUCTION

High Field Q-slope (HFQS) is an outstanding degradation effect which significantly limits performance of niobium SRF cavities. The characteristic signature of HFQS is a rapid decrease of the quality factor (Q) values starting from accelerating gradients of ≈ 25 MV/m. Temperature mapping of the cavities during the RF measurements demonstrates strongly dissipating localized regions to be the cause of HFQS onset. Strong dissipation of those regions stems from a sudden increase in the surface resistance, causing Joule heating of the Nb near-surface. Characterization of intrinsic features of Nb near-surface that are responsible for the increased dissipation, is crucial for understanding HFQS.

Electropolishing (EP), buffered chemical polishing (BCP), and even annealing at 800C with no further chemical treatments, result in cavity performance limited by HFQS. Only mild 120°C baking of Nb fine grain cavities for 12 hours eliminates HFQS. A decade of HFQS research revealed a few potential hypotheses, but failed to find a complete explanation of HFQS and its cure, satisfying all experimental findings. The most recent promising model is based on the formation of lossy niobium nanohydrides in the penetration depth [1]. Nanohydrides may remain superconducting due to the proximity effect up to the breakdown field, which is determined by their size. The model attributes HFQS onset field to such a loss of proximity-induced superconductivity, which manifests as a strong increase in residual resistance and causes HFQS. The presence of a high concentration of interstitial hydrogen in the penetration depth, upon cooling to 2K, may coalesce into lumps of niobium hydrides. A challenging part is that in order to search for such nanohydrides directly, cryo-investigations at < 100K are required as at room temperature no hydrides are present.

Our studies are based on a unique combination of advanced thermometry during cavity RF measurements, and TEM structural and compositional characterization of the samples extracted from cavity walls at both room and cryogenic temperatures. In order to directly correlate different dissipation characteristics with surface nanostructure and to determine the underlying mechanisms of HFQS in Nb SRF cavities, we base our studies on the comparison of cutouts from cavities with and without HFQS, similar to previous studies [2–4]. Comparison of the original cavity cutouts with known heating profiles guarantees the absence of artifacts associated with witness sample preparation.

In this work we present structural and analytic comparison of cross-sectional samples taken from the cavities with and without HFQS. TEM diffraction techniques were performed at room and cryogenic (94K) temperatures. Temperature dependent nano-area electron diffraction (NED) and scanning electron nano-area diffraction (SEND) reveal the formation of stoichiometric, non-superconducting, small niobium hydride inclusions. Mild baking is shown to decrease nanohydride sizes and/or density, which directly correlates with the observed suppression of the high field Q-slope in SRF cavities. Additionally, high resolution TEM (HRTEM) and bright field (BF) imaging show similar surface oxide thickness and lack of any oxidation along grain boundaries. Electron energy loss spectroscopy (EELS) chemical characterization of the surface oxides suggests slight oxygen enrichment just below the oxides after the mild bake.

EXPERIMENTAL METHODS

Preparation of Cavities Cutouts

Our studies are based on the comparison of cutouts from cavities with and without HFQS. Two Nb fine grain (≈50 μm) TESLA shape cavities with resonant frequency f_0 = 1.3 GHz were used. Both cavities were electropolished, and one of them was additionally baked at 120°C for 48 hours. Dependence of the quality factor on peak surface magnetic field at 2 K was measured for both cavities, and both also had temperature maps acquired during rf measurements in order to identify the regions for cutout. As expected, the EP-only cavity that had no final mild bake showed prominent HFQS, while the performance of the EP+120°C baked cavity was free from HFQS.

* yuliatr@fnal.gov

ISBN 978-3-95450-178-6

HIGH-VELOCITY SPOKE CAVITIES

C. S. Hopper*† and HyeKyoung Park
Center for Accelerator Science, Department of Physics,
Old Dominion University, Norfolk, VA, 23529, USA and
Thomas Jefferson National Accelerator Facility, Newport News, VA 23606, USA

Abstract

There are several current and recent projects which explore the feasibility of spoke-loaded cavities operating in the high-velocity region. Spoke cavities have a large number of geometric parameters which often influence multiple rf properties. Fabricating, handling, and processing these cavities presents some unique challenges, not unlike other TEM-class structures. This paper will summarize the current efforts toward the design, fabrication, and testing of spoke cavities with optimum beta greater than 0.8.

INTRODUCTION

The original motivation for spoke cavity development was for medium energy, high current protons and ions [1]. And indeed, over the past several decades, proton and heavy-ion beams have become extremely important tools used in scientific research. Over the past 25 years, many groups around the world have made great progress developing spoke cavities to meet this demand. This progress has resulted in more and more spoke cavities being fabricated and tested [2–7]. Eventually, TEM- and TM-class cavity designs were overlapping in the $\beta_0 = v/c = 0.6$ region [2, 8]. With the advantages that spoke cavities can offer, there has been recent interest in the design and development of these structures for the high-velocity region. One such such example is shown in Fig. 1.

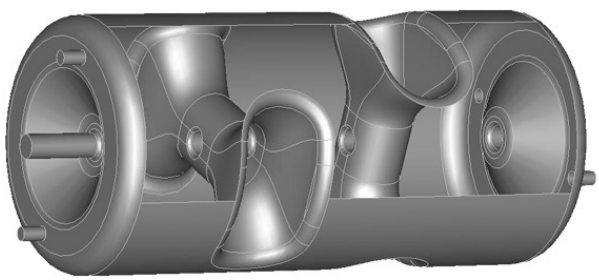

Figure 1: 325 MHz, $\beta_0 = 1$ double-spoke cavity.

FEATURES OF HIGH-VELOCITY SPOKE CAVITIES

Spoke cavities offer a number of attractive features which have been well documented elsewhere [9]. Here, the focus will be on how these features translate to spoke cavities designed for $\beta_0 > 0.8$.

Size

In the fundamental mode, spoke cavities support a TEM mode along the spoke. For a uniformly shaped spoke, this results in the diameter being roughly half the rf wavelength. While this is true at low β_0 and for simple spoke geometries (i.e. uniformly cylindrical), optimized high-β_0 geometries result in this factor of 1/2 being increased, bringing the diameter closer to their TM-class counterparts. Nonetheless, since the BCS surface resistance is proportional to the square of the rf frequency, accelerators can be designed to operate at lower frequencies (and have fewer elements with different fundamental frequencies) where 4 K operation is practical while maintaining cavities of a reasonable size. Furthermore, at half the frequency of a TM cavity of the same β_0, a multi-spoke cavity of the same length would have half the number of cells. This results in a larger velocity acceptance causing the cavity to be useful over a wider range of velocities. Lower frequency would also lead to a higher longitudinal acceptance, which could prove beneficial in high-current applications. Figure 2 shows examples of the velocity acceptance for a single-spoke (2 cell) cavity, a double-spoke (3 cell) cavity, and a 5 cell elliptical cavity.

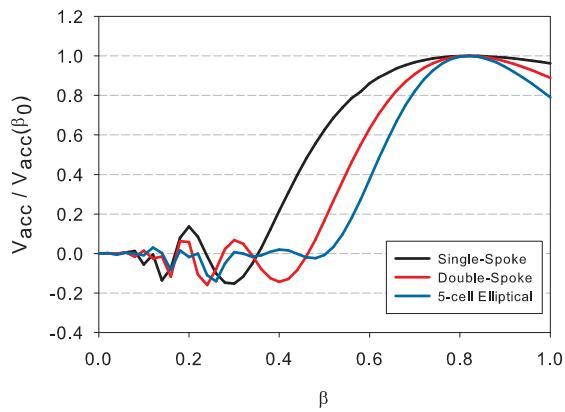

Figure 2: Accelerating voltage as a function of β normalized to the voltage at β_0 for 2 and 3 cell spoke cavities and a 5 cell elliptical cavity.

Cell-to-Cell Coupling

In spoke cavities, the magnetic field encircles the spoke(s) and couples one cell to the next. The result is a strong cell-to-cell coupling, especially in simple geometries. Tuning to achieve field flatness is therefore less important than in a cavity where the cells are coupled through the beam aperture via the electric field.

* Now at Argonne National Laboratory
† chopper@anl.gov

ISBN 978-3-95450-178-6

HIGH GRADIENT TESTING OF THE FIVE-CELL SUPERCONDUCTING RF MODULE WITH A PBG COUPLER CELL*

S. Arsenyev†, Massachusetts Institute of Technology, Cambridge, MA 02139, USA
W.B. Haynes, D.Yu. Shchegolkov, E.I. Simakov, T. Tajima,
Los Alamos National Laboratory, PO Box 1663, Los Alamos, NM 87545, USA
C.H. Boulware, T.L. Grimm, A.R. Rogacki, Niowave, Inc.,
1012 North Walnut Street, Lansing, MI 48906, USA

Abstract

Superconducting radio-frequency (SRF) accelerating structures allow high-gradient operation in continuous-wave mode. These machines can be limited by beam-breakup instability at high currents because higher-order modes with very high Q factors are easily excited by the beam. Photonic band gap (PBG) structures provide a way to strongly damp higher-order modes without compromising the performance of the structure in the fundamental mode.

We first address the design of the structure and issues that arise from incorporating a complex PBG cell into an SRF module. In particular, the module was tuned to have uneven accelerating gradient profile in order to provide equal peak surface magnetic field in every cell. We then cover the fabrication steps and surface treatment of the five-cell niobium structure and report results of the high gradient tests at temperatures of 4 K and 2 K.

INTRODUCTION

Superconducting radio frequency (SRF) cavities are the natural choice for future generations of high energy linacs, especially for high-duty-factor machines where the heat produced in the accelerating structure cannot be effectively extracted [1]. Going to higher frequencies in SRF cavities is desirable in some applications for various reasons. First, it allows lowering the cost of an accelerator and increasing achievable luminosity of an electron beam. Second, it is necessary for harmonic cavities operating at multiples of accelerator frequency. One example of a high-current linac of relatively high frequency is the proposed SRF harmonic linac for eRHIC [2], which would be used to undo nonlinear distortion of the beam's longitudinal phase space induced by the main linac's waveform.

However, going up in frequency makes higher-order-mode (HOM) wakefields increasingly problematic, as their transverse impact on the beam scales as the frequency cubed [3]. In a high-frequency machine, wakefields destroy quality of the beam and cause beam-breakup instability that leads to beam loss. Thus designs of high frequency SRF accelerators incorporate HOM dampers. We propose to replace one of the conventional elliptical cells with a PBG cell that includes HOM couplers and a fundamental power coupler (FPC) (see Fig. 1). PBG cells possess intrinsic property of frequency selectivity and can therefore be designed so that only the accelerating mode is selectively confined. The fundamental mode provides acceleration, and HOMs are coupled out.

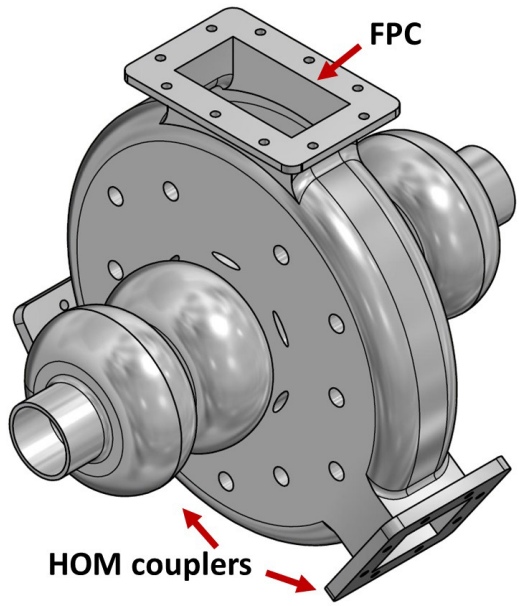

Figure 1: 2.1 GHz 5-cell module with a PBG center cell.

To date, accelerator research has been mostly focused on room temperature PBG cavities. Various designs have been proposed, including metal and dielectric structures [4–6]. In particular, it has been experimentally shown that a room-temperature PBG accelerating module can greatly reduce HOM wakefields [7].

Several tests have previously demonstrated that a high gradient and high Q factor can be achieved in a single superconducting PBG cell [8,9], opening a possibility for building a multi-cell accelerating module. The designed module consists of four elliptical cells and one PBG cell. Using cells of different kinds in one module introduces new challenges such as ensuring that the peak surface magnetic fields in all cells are equal. A niobium 5-cell cavity was made for high gradient testing (see Fig. 3 later).

This paper briefly discusses the design and fabrication of the cavity, and focuses on the high gradient testing. Results of the test are analyzed and discussed. The last section discusses a low Q problem encountered in the first high

* This work is supported by a DOE Office of Nuclear Physics SBIR grant DE-SC0009523 and the U.S. Department of Energy (DOE) Office of Science Early Career Research Program.

† arsenyev@mit.edu

RF MEASUREMENTS FOR QUALITY ASSURANCE DURING SC CAVITY MASS PRODUCTION

A. Sulimov, DESY, Hamburg, Germany

Abstract

The publication will describe the comprehensive program and results of RF measurements taken during the mass production of superconducting cavities for the European XFEL.

INTRODUCTION

The demanding performance requirements coupled with the ability to provide quick and accurate quality control of more than 800 cavities during mass production for the European XFEL gave us an impulse to organize an automatic quality assurance (QA) procedure basing on RF measurements [1].

Mass Production

Cavity life cycle can be divided in three major phases:

1. Pre-production: niobium sheet mechanical and material purity controls [2].
2. Production: mechanical cavity fabrication.
3. Post-production: cavity RF tests and operation.

Many critical RF measurements are necessary from niobium sheet control up to the accelerating module being ready for the linac installation. During the mechanical fabrication the cavity half-cells, dumb-bells and end-groups (Fig. 1) are measured and sorted. The cavity spectrum and field profiles are measured and tuned. The Higher Order Modes (HOM) couplers filter tuning, vertical cavity RF tests, cavity checks during the string assembly and final cavity performance measurements in the module as well as the fundamental mode and HOM RF spectra measurements complete the sequence.

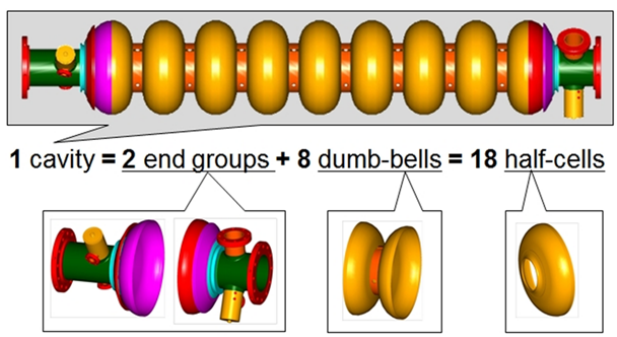

Figure 1: European XFEL cavities subcomponents.

This article will be concentrated on quality assurance during cavity production. Some aspects of post-production control will be mentioned only in case of their importance for mass production.

Purpose of Quality Assurance

The main purpose of the QA, based on RF measurements, is achieving both the RF and the mechanical specifications:

a) fundamental mode frequency at 2 K before adjustment to 1.3 GHz:
F(TM010,pi) = (1299.7 ± 0.1) MHz;
b) flatness of field distribution: FF > 90 %;
c) cavity straightness:
cell and flange eccentricity ECC < 0.4 mm;
d) final cavity length: L = (1059 ± 3) mm;
e) cells shape (inner cavity surface fluctuation):
accuracy = ± 0.2 mm.

Different processes (Final EP and Flash BCP) and infrastructure parameters have to be taken into account during cavity production.

For example, it was noticed that a field amplitude degradation of about 3 % occurred at one end of the cavity after final BCP. This fact is now taken into account during the cavity tuning for this procedure.

The field flatness (FF), eccentricity (ECC) and pi-mode frequency can usually be achieved without any difficulties during cavity tuning [3, 4]. Reducing the time of this operation to 4 hours was very important before starting mass production.

Cell shape is generally checked during subcomponent control with quick RF measurements on HAZEMEMA [5] and precise mechanical 3D inner cavity surface measurements when needed.

Final cavity length depends on the accuracy of sub-component trimming and can be predicted before cavity equator welding with a mean accuracy ±0.4 mm.

RF Measurement Choice

Rf measurements for QA were chosen:

1. to measure and calculate RF characteristics (frequency, field, quality-factors);
2. because they are more flexible than mechanical one and do not require mechanical contact with inner cavity surface;
3. due to very high sensitivity to mechanical deviations.

Accuracy of transverse deviations determination for cavity geometry (cell's diameters) is about 0.1 µm/kHz. This was demonstrated on example of small geometry deviations estimations for TESLA shape cavities arising from inner surface polishing [6].

Sensitivity of the fundamental-mode frequency to longitudinal cavity deformations is 300 kHz/mm, which allows tracking of about 3 µm/kHz.

ISBN 978-3-95450-178-6

PRODUCTION STATUS OF SRF CAVITIES FOR THE FACILITY FOR RARE ISOTOPE BEAMS (FRIB) PROJECT

C. Compton, A. Facco, S. Miller, J. Popielarski, L. Popielarski, A. Rauch, K. Saito, G. Velianoff, E. Wellman, K. Witgen, T. Xu,
Facility for Rare Isotope Beams, Michigan State University, East Lansing, MI, 48824, U.S.A.

Abstract

As the Facility for Rare Isotope Beams (FRIB) project ramps into production, vendor relations, cavity quality, and schedule become critical to success. The driver linac will be constructed of 332 cavities housed in 48 cryomodules and designed with two cavity classes (quarter-wave and half-wave) and four different betas (0.041, 0.085, 0.29, and 0.53). The cavities will be supplied to FRIB from awarded industrial vendors. FRIB's experience with SRF cavity fabrication will be presented including acceptance inspections, test results, technical issues, and mitigation strategies.

INTRODUCTION

The Facility for Rare Isotope Beams (FRIB) at Michigan State University (MSU) is an approved project funded by a cooperative agreement between MSU and The US Department of Energy (DOE) for advancement in the study of rare isotopes. The driver linac for the FRIB project is a 200 MeV/u superconducting linac with final beam power reaching 400 kW.

The FRIB linac will require the fabrication of 332 superconducting radio frequency (SRF) cavities housed in 48 cryomodules. Two classes of cavities at two different operating frequencies will be used; 80.5 MHz quarter-wave cavities and 322 MHZ half-wave cavities, shown in Figure 1. Both cavity classes will have two different operating betas; 0.041 and 0.085 quarter-wave cavities [1,2] will be used in segment one of the linac and 0.29 and 0.53 half-wave cavities[3] will make up the accelerator in both segments 2 and 3.

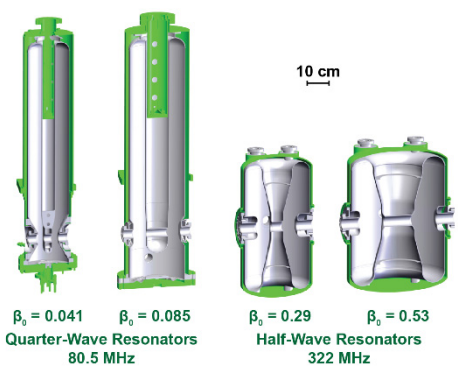

Figure 1: FRIB production SRF cavity designs.

CAVITY PRODUCITON

FRIB has contracted the fabrication of the four cavity types to industrial vendors for production fabrication. Total required cavity counts for the FRIB main driver are provided in Table 1.

Cavities are fabricated from bulk polycrystalline niobium with titanium helium vessels. FRIB manages the procurement, quality, and sequencing of niobium materials to the vendors, including replacement materials. All materials shall be tracked by cavity vendors; managing quantities as well as mapping material serial numbers to cavity components fabricated.

All cavities are sequence through incoming acceptance inspection upon receipt from vendor to FRIB. Cavities are checked against the Acceptance Criteria List or ACL. The ACL criteria for cavity acceptance is:

- Inspection of Vendor required documentation
- Check the cavity is properly labelled with correct serial number
- Dimensional inspection (measuring critical dimenisons)
- Surface inspection (RF surfaces, seal interfaces and welds)
- Frequency check
- Vacuum leak check (both cavity and helium space)

Table 1: Cavity Production Quantity Requirements and Received Cavities to Date (Shown in Red)

Beta	Development	Preproduction	Production	TOTAL
0.041	2(2)		17(17)	19(19)
0.085	2(2)	10(10)	103	115(12)
0.29	2(2)	10(3)	68	80(5)
0.53	2(2)	10(8)	150	162(10)

CAVITY STATUS

FRIB has begun to receive vendor cavities of all four types starting in January 2014. The beta=0.041 contract was completed in April of 2015. Table 1 provides the numerical status of cavities received to FRIB as of September 1, 2015.

All accepted cavities are certified in vertical testing before being accepted for cold-mass assembly. Cavities

ISBN 978-3-95450-178-6

PERFORMANCES OF SPIRAL2 LOW AND HIGH BETA CRYOMODULES

C. Marchand*, P. Bosland, G. Devanz, O. Piquet, CEA, Saclay, France
D. Longuevergne, G. Olry, IPN, Orsay, France
Y. Gómez Martínez, LPSC, Grenoble, France
P.-E. Bernaudin, R. Ferdinand, GANIL, Caen, France

Abstract

All SPIRAL2 cryomodules (twelve with one quarter wave resonator (QWR) at β=0.07 and seven with two QWRs at β=0.12) have been produced and qualified, and are now in installation phase on the LINAC at GANIL. After a general introduction on the LINAC, we will first remember and compare the different design choices taken for the two families of cryomodules. We will then present a summary of the techniques used for the preparation and integration of the cavities in the cryomodules, and compare the achieved performances with design parameters. At last, we describe the status of the LINAC installation as of end of August 2015.

INTRODUCTION

The GANIL's SPIRAL 2 Project [1] aims at delivering high intensities of rare isotope beams by adopting the best production method for each respective radioactive beam. The unstable beams will be produced by the ISOL "Isotope Separation On-Line" method via a converter, or by direct irradiation of fissile material.

The driver will accelerate protons (0.15 to 5 mA –33 MeV), deuterons (0.15 to 5 mA – 40 MeV) and heavy ions (up to 1 mA, Q/A=1/3 14.5 MeV/u to 1/6 8.5 MeV/A). It consists of high performance ECR sources, a RFQ, and the superconducting light/heavy ion LINAC. The driver is also asked to provide all the energies from 2 MeV/u to the maximum designed value (see Table 1).

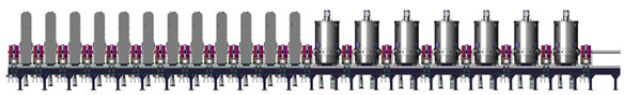

Figure 1: SPIRAL2 LINAC – 2 QWR families.

The SPIRAL2 [1] LINAC is based on superconducting (SC), independently phased resonators (Fig. 1). In order to allow the broad required ranges of particles, intensities and energies, it is composed of two families of short cryomodules developed by CEA/Irfu and IN2P3/IPN-O teams. The first family (CMA) is composed of 12 quarter-wave resonators (QWR) with β_0=0.07 (one cavity/cryomodule), and the second family (CMB) of 14 QWR at β_0=0.12 (two cavities/cryomodule) (see Fig. 4). Resonance frequency is 88.0525 MHz and maximum gradient in operation of the QWRs is $E_{acc} = V_{acc}/\beta\lambda$ = 6.5 MV/m. The exact values of accelerating field used in each cavity for different ion species is illustrated on Fig. 2, which is the result of beam dynamics studies to optimize longitudinal focalization and acceptance of the ion beam [2].

Developed by IN2P3/LPSC (Grenoble), the RF power couplers shall provide up to 12 kW CW beam loading power to each cavity [3]. The transverse focusing is ensured by means of warm quadrupole doublets located between each cryomodule, in so-called "warm sections" also equipped with beam diagnostic and vacuum equipments (see Fig. 3).

Table 1: Beam Specifications

Particles	H^+	$^3He^{2+}$	D^+	ions	ions
Q/A	1	3/2	1/2	1/3	1/6
Max. I (mA)	5	5	5	1	1
Min. energy (MeV/A)	0.75	0.75	0.75	0.75	0.75
Max energy (MeV/A)	33	24	20	15	9
Max. beam power (kW)	165	180	200	45	54

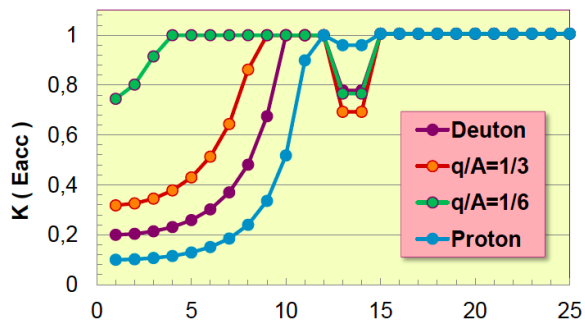

Figure 2: Ratio K = cavity accelerating field/max accelerating field for different beam types in the LINAC.

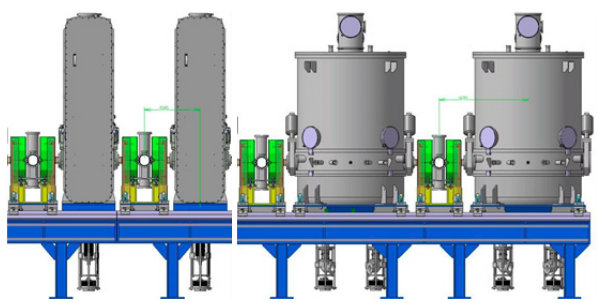

Figure 3: The warm quadrupoles (in green) installed between the cryomodules (left: CMA; right: CMB).

ISBN 978-3-95450-178-6

ACHIEVING HIGH PEAK FIELDS AND LOW RESIDUAL RESISTANCE IN HALF-WAVE CAVITIES*

Z.A. Conway#, A. Barcikowski, G.L. Cherry, R.L. Fischer, S.M. Gerbick, C.S. Hopper, M.J. Kedzie, M.P. Kelly, S-h. Kim, S.W.T. MacDonald, B. Mustapha, P.N. Ostroumov, and T.C. Reid
ANL, Argonne, IL 60439, USA

Abstract

We have designed, fabricated and tested two new half-wave resonators following the successful development of a series of niobium superconducting quarter-wave cavities. The half-wave resonators are optimized for beta = 0.11 ions, operate at 162.5 MHz and are intended to provide up to 2 MV effective voltage for particles with the optimal velocity. Testing of the first two half-wave resonators is complete with both reaching accelerating voltages greater than 3.5 MV with low-field residual resistances of 1.7 and 2.3 nΩ respectively. The intention of this paper is to provide insight into how Argonne achieves low-residual resistances and high surface fields in low-beta cavities by describing the cavity design, fabrication, processing and testing.

INTRODUCTION

Fermi National Accelerator Laboratory (FNAL) is building the front-end of a new 800 MeV accelerator as part of the Proton Improvement Project-II (PIP-II) [1, 2]. The first superconducting cryomodule in this front-end is being built at Argonne. It contains 8 162.5 MHz half-wave resonators (HWRs) and 8 solenoids, one in front of each cavity, for the acceleration of an H^- beam from 2.1 to 10.3 MeV. These cavities will operate at 2.0 K and are designed to provide up to 2.0 MV of effect voltage gain for beta = 0.11 H^- ions with less than 2 W of cryogenic heating per cavity. The first two HWRs are now finished and have been cold tested. The aim of the work presented here is to describe the fabrication, processing and test results for two prototype HWRs to highlight the peak fields and low residual resistance achieved in cold testing. In the following we discuss the design, processing and cold test results for two 162.5 MHz HWRs optimized for particle velocities of $\beta \sim 0.11$. Figure 1 shows the HWR and Figure 2 shows the cold testing results.

CAVITY SPECIFICS

Design and Fabrication

The HWR design was constrained to provide 2 MV per cavity at 162.5 MHz with an optimum $\beta = 0.11$ with a 33 mm aperture. Given these constraints the RF optimization focused on reducing the cryogenic load and the peak electromagnetic surface fields while maximizing the shunt impedance [3]. This was accomplished with an advanced design using conical inner and outer conductors. The conical shape increases the volume over which the magnetic energy is stored decreasing the peak surface magnetic field and increasing the shunt impedance in a manner analogous to re-entrant elliptical-cell resonators [4]. This design is electromagnetically similar to recently commissioned quarter-wave resonators which have excellent online performance [5]. Table 1 gives the RF performance parameters for the HWR.

The RF design described above includes 2 ports on each end of the cavity. These ports are located to ensure that the cavity electropolishing cathodes remove material from the cavity surface as evenly as practical and also provide good drainage with sufficient high pressure water rinse wand access.

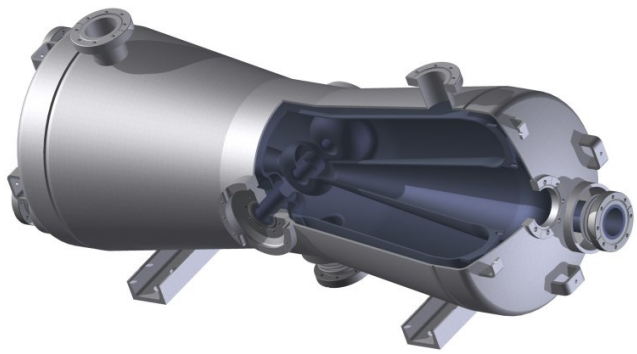

Figure 1: Cut away view of the 162.5 MHz, $\beta = 0.11$, niobium half-wave resonator enclosed in an integral stainless-steel helium vessel. The cavity is 125 cm end-to-end.

Table 1: HWR RF Parameters

Parameter	Value
Frequency	162.5 MHz
Beam Aperture	33 mm
β	0.112
Effective Length ($\beta\lambda$)	20.7 cm
E_{peak}/E_{acc}	4.68
B_{peak}/E_{acc}	5.02 mT/(MV/m)
$G = R_sQ$	48.2 Ω
R_{sh}/Q	271.7 Ω

*This material is based upon work supported by the U.S. Department of Energy, Office of Science, Office of Nuclear Physics, under contract number DE-AC02-06CH11357, and the Office of High Energy Physics, under contract number DE-AC02-76CH03000. This research used resources of ANL's ATLAS facility, which is a DOE Office of Science User Facility.
zconway@anl.gov

ISBN 978-3-95450-178-6

DESIGN STUDIES FOR QUARTER-WAVE RESONATORS AND CRYOMODULES FOR THE RIKEN SC-LINAC

N. Sakamoto*, O. Kamigaito, H. Okuno, K. Ozeki, K. Suda, Y. Watanabe, K. Yamada,
RIKEN Nishina Center, Saitama, Japan
E. Kako, H. Nakai, K. Umemori, KEK, Ibaraki, Japan
H. Hara, K. Okihira, K. Sennyu, T. Yanagisawa,
Mitsubishi Heavy Industries, Ltd., Hiroshima, Japan

Abstract

Recently we proposed a plan to upgrade the intensity of uranium beams at the RIKEN RI-Beam Factory [1] . In this plan, a superconducting linac replaces the existing injector cyclotron. The linac's quarter-wave resonators (QWRs) operate at 73 MHz in the continuous wave mode with $\beta(\equiv v/c)$ as low as 0.055-0.122. A coaxial probe-type RF fundamental power coupler that transmits RF power of 5 kW will be utilized for beam loading at about 1 kW/resonator. Tuning of the resonant frequency will be achieved using a mechanical tuner pressing on the resonator wall in the direction parallel to the beam. In this paper, design studies for a pure Nb QWR and its cryomodule are described. The construction status of the prototype, consisting of a QWR, a coupler, a tuner and a test cryomodule, is also reported.

SC-LINAC FOR RIKEN RI-BEAM FACTORY

Why a Superconducting Linac?

At this time, the RIKEN RI-Beam Factory (RIBF) provides the world's most intense uranium beams with an energy of 345 MeV/u. However, the beam currents of uranium are still not intense enough to reach the goal of 1 pμA. A schematic of the current method for the acceleration of uranium ions is shown in Fig. 1. As reported in Ref. [2], the injector RILAC2 [3, 4] can accelerate uranium ions with a mass-to-charge ratio of 7 up to 0.67 MeV with an intensity greater than a few pμA. However, the transmission efficiency, defined as the ratio of the beam current bombarding the target to the beam current from the ion source is only a few percent. This is partly due to the low efficiency of charge stripping, indicated by CS in Fig. 1, which occurs twice during acceleration at the energies of 11 MeV/u and 51 MeV/u. Furthermore, the succeeding booster RIKEN Ring Cyclotron [5] (RRC) cannot handle such a high beam current because the acceleration voltage of its double gap resonator is too low [6].

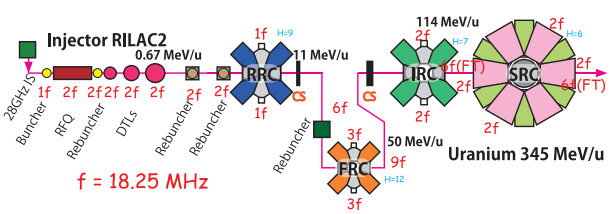

Figure 1: Schematic of uranium acceleration by an accelerator cascade at RIBF.

An upgrade of the RIBF is therefore under discussion, the objective being to significantly increase the uranium beam currents. One candidate is a new injector, with a latter part consisting of superconducting resonators, to replace the RRC, which was not designed to handle very high power beams with a high mass-to-charge ratio. The layout of the new injector is shown in Fig. 2.

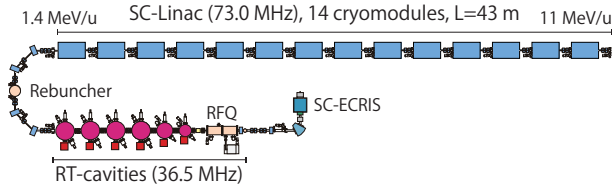

Figure 2: Schematic of a new injector.

RIKEN SC-LINAC

The superconducting part of the proposed RIKEN linac, called SRILAC, consists of 14 cryomodules, each of which contains four quarter-wave resonators (QWRs). It is designed to accelerate 1 mA $^{238}U^{35+}$ from 1.4 MeV/u up to 11 MeV/u. We set moderate goals for the design: The resonator should have a total gap voltage of 1.6 MV with 4.0 W RF power dissipation. The RF of the QWRs will be 73.0 MHz, and a large beam aperture of 40 mm$^{\phi}$ is chosen for the beam pipes of the drift tubes.

The conceptual design of an accelerator cryomodule is shown in Fig. 3. The QWRs, made from Nb sheets with a thickness of 4 mm, are housed independently in a helium vessel made of titanium. The operating temperature of the helium is 4.5 K. The valve box is separated from the cryomodule which contains four QWRs. In this design top loading is adopted so that the QWRs hang from the top lid of the chamber of the cryomodule. The cryomodule is equipped with a single-stage thermal shield and its temperature is 80 K. The thermal shield provides a thermal anchor to the fundamental power couplers (FPCs). The FPC is designed to handle RF power from 5 kW to the maximum required for operation with $Q_{ext} \sim 10^6$. Note that Q_{ext} of the order of 10^6 is set for beam loading of a few kilowatts and for better RF control. Q_{ext} must be chosen carefully taking

* nsakamot@ribf.riken.jp

BEAM COMMISSIONING OF THE 56 MHz QW CAVITY IN RHIC*

Q. Wu#[1], S. Belomestnykh[1,2], I. Ben-Zvi[1,2], M. Blaskiewicz[1], T. Hayes[1], K. Mernick[1], F. Severino[1], K. Smith[1], A. Zaltsman[1]
[1]BNL, Upton, NY 11973, USA
[2]Stony Brook University, Stony Brook, NY, 11790, USA

Abstract

A 56 MHz superconducting RF cavity has been designed, fabricated and installed in the Relativistic Heavy Ion Collider (RHIC). The cavity operates at 4.4 K with a "quiet helium source" to isolate the cavity from environmental acoustic noise. The cavity is a beam driven quarter wave resonator. It is detuned and damped during injection and acceleration cycles and is brought to operation only at store energy. We have observed clear luminosity increase and bunch length reduction in the first operation of the cavity with Au + Au and Au + He3 collisions. The cavity voltage was limited by quenching in the Higher Order Mode coupler. This paper also discusses the cavity beam experiments with no higher order mode coupler in p + p and p + Au RHIC operation.

INTRODUCTION

The 56 MHz superconducting RF cavity has been manufactured and installed in RHIC in January 2014, and started beam operation later in the same year. The cavity is installed in the common section, 1.25λ away from the interaction point 4 (IP4), shown in Figure 1.

The purpose of the cavity is to provide sufficient RF acceptance to long bunches, thus reducing number of particles lost due to intra-beam scattering during rebucketing. Detailed studies have been discussed in previous papers [1][2].

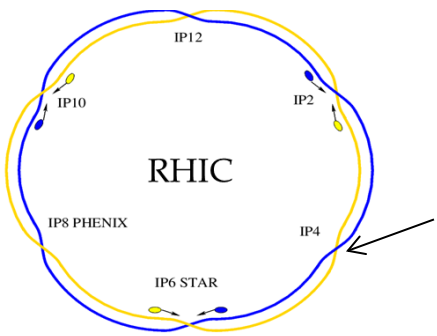

Figure 1: Location of the 56 MHz cavity in RHIC.

The helium supply for the cavity is provided via a quiet helium source, which exchanges the heat of a closed helium bath with the RHIC helium supply pipes. This system prevents big fluctuations of pressure brought by the main cooling pipes. The cryomodule of the cavity with the helium system is shown in Figure 2.

*Work supported by Brookhaven Science Associates, LLC under Contract No. DE-AC02-98CH10886 with the U.S. DOE.
#qiowu@bnl.gov

Figure 2: The 56 MHz cryomodule installed in the RHIC tunnel. Red arrow points to the quiet helium source tank.

CAVITY

The cavity is a quarter-wave resonator with beam traversing its axis. The diameter of the cavity is 50 cm. The acceleration gap is 8.5 cm with a flat end cap, as shown in Figure 3. Frequency tuning of the cavity is achieved via pushing and pulling the beam pipe on the gap side thus deforming the flat cap. The tuning range is listed in Table 1 for both stepper motor coarse tuning and piezo fine tuning. More details of the tuning study can be found in Ref. [3].

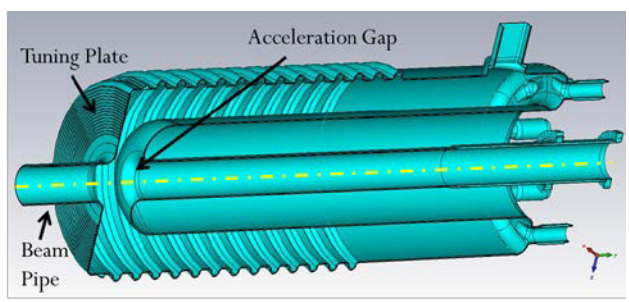

Figure 3: Cross-section view of the 56 MHz SRF cavity.

Table 1: Tuning Parameters of the Cavity

	Coarse tuning	Fine tuning
Frequency range	46.5 kHz	60 Hz
Travel distance	3 mm	3.5 μm
Tuning mechanism	Stepper motor	Piezo

RECENT DEVELOMENTS IN SUPERCONDUCTING DEFLECTING-MODE CAVITIES*

J. R. Delayen#
Center for Accelerator Science, Old Dominion University, Norfolk, VA 23529, USA
Thomas Jefferson National Accelerator Facility, Newport News, VA 23606, USA

Abstract

The last few years have seen significant activities directed towards the development of superconducting cavities operating in the deflecting mode. The stringent requirements imposed by new requirements necessitated the development of new cavity geometries. Proofs-of principle cavities have been fabricated and tested, and have shown excellent properties. Prototype cavities and cryomodules for operation and testing with beam are now under development as part of a world-wide collaboration. The status of these activities is being presented.

INTRODUCTION

While most superconducting cavities for use in accelerators are for accelerating particles, they can also be used for deflecting beams or crabbing bunches. Accelerating cavities provide a longitudinal voltage in order to increase the forward momentum of the particles while deflecting/crabbing cavities apply a transverse voltage. Deflecting and crabbing cavities are identical, the only difference being in the phase between the rf transverse fields and the bunches. Deflecting cavities operate at maximum –or close to maximum– phase so the whole bunch acquires a transverse momentum. Crabbing cavities operate at zero phase so there is no net deflection of the center of the bunch, but the front and back of the bunch are deflected in opposite direction.

Deflecting systems were one of the first applications of superconducting rf to particle accelerators. In the early 1970's an rf separator, shown in Fig.1, was designed and fabricated at KfK Karlsruhe [1]. It was comprised of 104 cells and the frequency of the deflecting mode was 2.865 GHz. The separator was operated at CERN between 1977 and 1981 and is now being resurrected at IHEP.

The first superconducting crabbing system was developed, implemented, and operated at KEK [2-4]. The crabbing system consisted of two cavities, shown in Fig. 2, one for each of the two rings. The cavities operated at 508 MHz in the TM110 mode. In order to remove the degeneracy between the two polarizations of the TM110 mode, the cavity was designed with a race-track shape cross-section. The cavities were installed in the rings in 2007 and were operated until recently. Although there were some difficulties associated with amplitude instabilities and mechanical tuner resolution, luminosity increase using a crabbing scheme was clearly demonstrated.

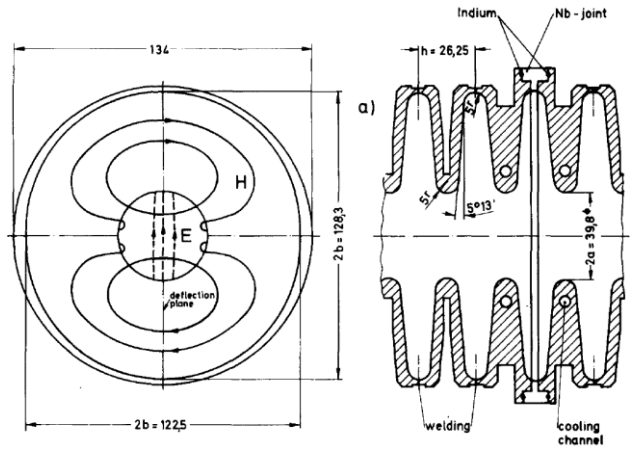

Figure 1: Karlsruhe/CERN superconducting rf separator.

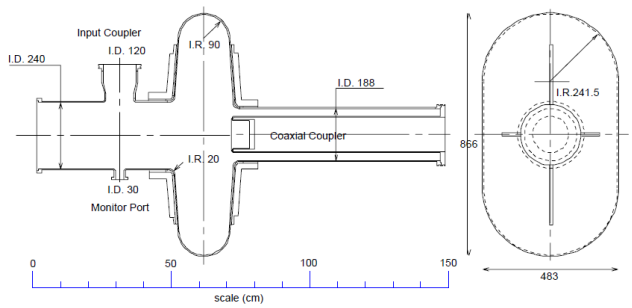

Figure 2: 508 MHz crab cavity used at KEKB.

TM CLASS CAVITIES

Those cavities operated in the TM110 mode, where the deflection results from the interaction with the transverse magnetic field. Because of the mode used, these cavities are larger (by about 30%) than the accelerating cavities of the same frequency that operate in the TM010 mode. For example the 508 MHz KEK crab cavity had a transverse dimension of 87 cm. This would prevent their application when low frequency is needed but there are dimensional constraints

On the other hand, the fact that these cavities are relatively large at a given wavelength can be an advantage when a high frequency is needed. For example a TM010 2.815 GHz cavity, shown in Fig. 3, was developed by JLab and ANL [5]. This can also be an advantage when a large aperture is needed.

*Work supported by DOE via the US-LARP program and by EU FP7 HiLumi LHC - Grant Agreement 284404.
#jdelayen@odu.edu delayen@jlab.org

ISBN 978-3-95450-178-6

SRF GUN DEVELOPMENT OVERVIEW

J. Sekutowicz, DESY, Hamburg, Germany

Abstract

The most demanding component of a continuous wave (cw) operating electron injector delivering low emittance electron bunches is the cw operating RF-gun. RF-guns, both working at room temperature and superconducting, particularly when they generate highly populated low emittance bunches have to operate at high accelerating gradients to suppress space charge effects diluting emittance. Superconducting RF-guns (SRF-guns) are technically superior to normal conducting devices because they dissipate orders of magnitude less power at very high gradients in the cw mode. In this contribution, progress made since the SRF13 conference in R&D programs, designing and operation of the SRF-guns at KEK, HZB, HZDR, PKU and DESY is discussed.

INTRODUCTION

SRF-guns have a potential to generate low emittance electron beams, if required with highly populated bunches, when operating in cw mode at high accelerating gradients. This makes the superconducting RF-guns superior to the room temperature operating devices, which at high gradients, operating in cw mode, would dissipate an enormous amount of RF-power. The main motivation for the development of and application for the SRF electron sources are facilities generating coherent photon beams. In general, the anticipated use is two-fold, Energy Recovery Linacs (ERL) and FEL facilities. In the past years, two directions in R&D programs could be observed. The first is meant for ERLs are SRF sources generating very high current electron beams whose bunches are rather low populated and whose repetition rate is high. The second are low current SRF electron sources, devoted mainly to FELs, whose bunches have higher charge but whose repetition rate is low, as compared to the ERLs electron sources.

The difficult part of all SRF-gun designs is the integration of a cathode into a clean superconducting (sc) cavity. This is especially challenging when a cathode is non-metallic, which is the case for all high quantum efficiency (QE) emitting materials commonly used in high beam current electron sources.

Three SRF-gun design approaches are under investigation since more than a decade:

- DC Pierce gun adjacent to sc cavity.
- Choke filter with a non-superconducting cathode.
- Superconducting cathode integrated into sc cavity.

The main advantage of the first approach is that the cathode does not penetrate the interior of the sc gun cavity, which helps to preserve its SRF performance. The main limitation is that low energy emitted electrons must pass certain distance before they enter the high electric accelerating field of the sc cavity. This constrains emittance of the beam and/or electron population per bunch due to the space charge force. The approach has been investigated for many years at Peking University (PKU).

The second approach is superior to two others when high beam current is required for the cw operation of an accelerator. It utilizes a choke filter allowing employment of high QE, usually alkali cathodes, which are exposed directly to the accelerating field of a gun cavity. This enables achievement of low emittances even though the electron population per bunch is large. High QE makes requirements on the irradiating laser less demanding, permitting operation with lower pulse energy and at longer wavelength (fewer conversion stages). The QE and lifetime of an alkali cathode depend strongly on the vacuum in a gun. When the vacuum is good the best performing cathodes can operate for several months but even these have to be exchanged when QE drops below the spec. Detachable cathode plugs and load lock mechanisms, similar to those used for room temperature RF-guns, are attached to superconducting gun cavities to enable cathode exchange. Unfortunately, this limits RF performance of sc gun cavities and/or very often causes multipacting in the cathode vicinity. This type of SRF-gun operates successfully at HZDR and is there and at HZB and KEK under continuous development.

The third approach, meant for low and very low current beams, employs superconducting cathode material. Since ca. 10 years R&D program is ongoing at DESY with support of other laboratories to integrate into the sc environment and maintaining of QE of Pb-layers deposited on various versions of Nb cathode plugs. The implementation of a sc cathode material significantly simplifies the SRF-gun design but does not make problem-free the integration itself.

In the following, the progress in all above-mentioned projects is discussed in more detail.

R&D AT PKU

The PKU SRF-gun R&D program goal is a cw operating injector for the planned ERL facility, whose final electron energy and beam current will be 30 MeV and 1 mA correspondingly. Figures 1 and 2 show a picture of the 3.5-cell SRF cavity and a drawing of the DC Pierce gun with cavity. Table 1 displays goal and achieved parameter for the PKU electron gun. There was remarkable progress in the project over the last two years demonstrated by the recent results shown in the table. The large grain Nb gun cavity without cathode in the final vertical test has reached E_{acc} of 23.5 MV/m with intrinsic $Qo>1\cdot10^{10}$, after two multipacting barriers had been

ISBN 978-3-95450-178-6

SRF GUN AT BNL: FIRST BEAM AND OTHER COMMISSIONING RESULTS *

Wencan Xu[#,1], Z. Altinbas[1], S. Belomestnykh[1,2], I. Ben-Zvi[1,2],S. Deonarine[1], L. DeSanto[1], D. Gassner[1], R. C. Gupta[1],H. Hahn[1], L. Hammons[1], Chung Ho[1], J. Jamilkowski[1], P. Kankiya[1], D. Kayran[1], R. Kellerman[1], N. Laloudakis[1], R. Lambiase[1], C. Liaw[1], V. Litvinenko[1,2], G. Mahler[1], L. Masi[1], G. McIntyre[1], T. Miller[1], D. Phillips[1], V. Ptitsyn[1], T. Seda[1], B. Sheehy[1], K. Smith[1], T. Rao[1], A. Steszyn[1], T. Tallerico[1], R. Than[1], J. Tuozzolo[1], E. Wang[1], D. Weiss[1], M. Wilinski[1], A. Zaltsman[1], Z. Zhao[1]

[1)] Collider-Accelerator Department, Brookhaven National Lab, Upton, NY 11973, USA

[2)] Physics & Astronomy Department, Stony Brook University, Stony Brook, NY 11794, USA

Abstract

The BNL 704 MHz SRF gun for R&D Energy Recovery Linac (ERL) successfully generated the first photoemission beam in November of 2014, with a copper substrate cathode stalk. A new multipacting-free, Ta-substrate cathode stalk was designed, fabricated and demonstrated as truly multipacting free. With this new cathode stalk, the beam commissioning has been continued to bring the beam to dump, which is called Gun-to-dump commissioning. This paper discusses the first beam commissioning, design and commissioning of multipacting-free cathode stalk. ERL commissioning status will be addressed as well.

INTRODUCTION

The R&D ERL [1] at BNL is an electron accelerator designed for high average current, up to 350 mA. It serves as a test bed for future RHIC projects, such as eRHIC [2], Coherent-Electron-Cooling [3], and Low Energy RHIC Electron Cooler [4]. The 704 MHz half-cell SRF gun is designed to provide 0.5 A, 2 MeV electron beam. Commissioning of the SRF gun is being carried out in stages: (1) without a cathode stalk, (2) with a copper cathode stalk, (3) first beam commissioning and (4) gun to dump commissioning. Without a cathode stalk insertion, the SRF gun cavity reached the design voltage of 2 MV in CW mode. However, strong multipacting in the quarter-wavelength choke-joint occurred during commissioning with a copper-substrate cathode stalk. Multipacting in the choke-joint was later understood with simulations [5]. While the beam commissioning was carried out with Cu-substrate cathode stalk to successfully generate the first beam in November 2014 [6,7], a multipacting-free choke joint with Ta substrate has been designed, tested and showed that it is truly multipacting-free in March 2015. With the Ta-tip cathode stalk [8], the cathode lifetime is very long: from its first use June 1 and three days per week since then, QE is still good for beam commissioning. We are now in the Gun-to-Dump commissioning stage, where the electron beam is transported from SRF gun, through Zig-Zag, and 5-cell main linac (5-cell cavity is not powered) down to the beam dump. This paper discusses the latest commissioning results.

* This work is supported by Brookhaven Science Associates, LLC under Contract No. DE-AC02-98CH10886 with the U.S. DOE.

#wxu@bnl.gov

FIRST BEAM COMMISSIONING

Layout

The first beam commissioning of the SRF gun was done with a straight beam line ending up at a faraday cup. This beam line configuration is shown in Figure 1. The Cs_3Sb photocathode was deposited on the cathode stalk with copper substrate in the cathode deposition system located outside the ERL blockhouse. Then, the cathode stalk was moved to the ERL blockhouse inside a cathode transport cart and inserted into the SRF gun. A load-locked system is used for the connection between the SRF gun and the cathode transport cart. The beam path consists of the 704 MHz half-cell SRF gun cavity, a high temperature superconducting solenoid (HTSS), a room-temperature HOM absorber (Now, in the place of the absorber, a room temperature solenoid was installed there for better beam quality), a laser cross, an Integrated Current transformer (ICT), a Beam Position Monitor (BPM), a vertical and horizontal beam corrector, a beam halo monitor, a pepper pot for beam emittance measurement, a beam profile monitor and a Faraday cup. The dipole magnet for bending electron beams to the Zig-Zag is locked out for the first beam tests.

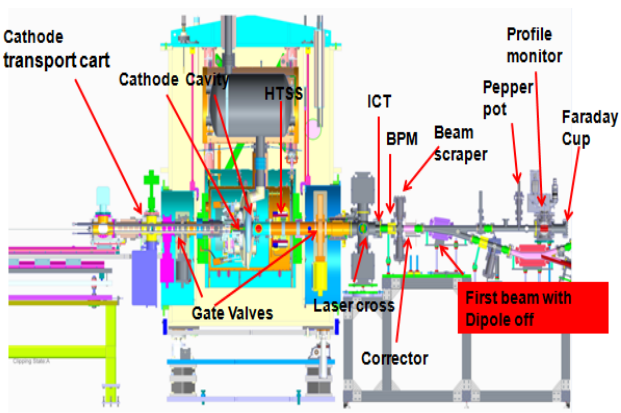

Figure 1: First beam commissioning configuration.

ISBN 978-3-95450-178-6

COMPARISON OF CAVITY FABRICATION AND PERFORMANCES BETWEEN FINE GRAINS, LARGE GRAINS AND SEAMLESS CAVITIES*

K. Umemori#, H. Inoue, T. Kubo, G. Park, H. Shimizu, Y. Watanabe, M. Yamanaka,
KEK, Ibaraki, Japan
A. Hocker, Fermilab, Batavia, Illinois, USA
T. Tajima, LANL, Los Alamos, New Mexico, USA

Abstract

At KEK, L-band superconducting cavity fabrication studies have been carried out. One target of the R&D is investigation of cavity fabrication methods using different Nb materials and applying different cavity fabrication techniques. Different Nb materials are compared, between fine grain Nb and large grain Nb from different vendors including low RRR large grain Nb, from which cavities were fabricated by electron beam welding method. The difficulty with the large grain cavity fabrication comes from the deformation due to stressed grain boundaries. In addition to nominal electron beam welded cavities, hydro-formed seamless cavities have been fabricated. The large amount of expansion required for Nb tubes makes successful full deformation difficult. Good qualified Nb pipes are essential and the control of hydro-forming steps including annealing of materials is also important. In order to evaluate these cavity performances, vertical tests were carried out and they showed good performances. In this paper, fabrication processes, technical difficulties, mitigation strategies and vertical test results are presented.

INTRODUCTION

Techniques of superconducting RF (SRF) cavity fabrication have been developed for several decades. At present, the most popular material and fabrication method used for SRF cavity fabrication are fine grain Niobium (Nb) and electron beam welding (EBW) of deep-drawn half-cells. High gradients of more than 30 MV/m can be achieved with good yield rates, for example for TESLA 9-cell cavities [1]. By applying nitrogen doping technique and / or optimized cooling procedure, high-Q of $3x10^{10}$ is also possible at 2.0 K [2, 3].

KEK also have conducted cavity fabrication R&D studies at CFF (Cavity Fabrication Facility) [4]. KEK-CFF is a facility for SRF cavity fabrication and every machine and equipment, such as a pressing machine, a vertical lathe, and an EBW machine and a chemical polishing (CP) area are located in clean environment. They are shown in Fig. 1. In-house cavity production under clean condition is possible at KEK-CFF.

One aim of our R&D programs is development of cavity fabrication techniques, which include studies on different Nb materials and different cavity fabrication methods. For the material study two kinds of large grain Nb, high-RRR and low-RRR, were used in addition to nominal fine grain Nb disk. For the study on cavity fabrication methods we have been trying seamless cavity fabrication with hydro-forming [5].

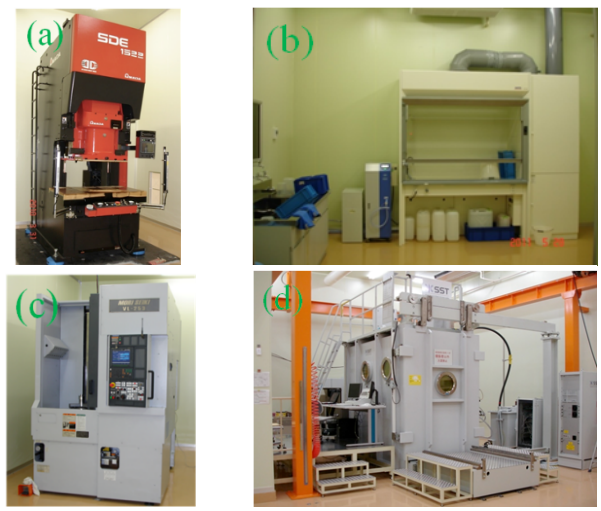

Figure 1: (a) Press machine, (b) CP area, (c) vertical lathe, (d) EBW machine, which are located in KEK-CFF.

MOTIVATION OF STUDY

To investigate cavity fabrication and their performances, a total of six single-cell cavities were produced. Table 1 is a list of cavities. Two fine grain, two large-grain and two seamless 1.3 GHz single-cell cavities were fabricated.

The R-1, R-2 and R-5 cavities are TESLA-like end-cell structure with 80mm diameter beampipes and the R-4, W-1 and U-4 cavities are TESLA-like center-cell structure with 70mm diameter beampipes.

Table 1: List of fabricated single-cell cavities

Cavity type	Nb Material	Vendors	Cavity name
Fine grain single cell	Fine grain Nb sheet	Tokyo Denkai	R-2
		ULVAC	R-4
Large grain single cell	Sliced Nb ingot (large grain)	Tokyo Denkai (RRR = 390)	R-1
		CBMM (RRR = 100)	R-5
Seamless single cell	Fine grain Nb tube	Wah Chang	W-1
		ULVAC	U-4

For the fine grain cavities, two vendors, Tokyo-Denkai and ULVAC, delivered fine grain Nb sheets. Cavities made by fine grain Nb sheets are current standard.

#kensei.umemori@kek.jp

ISBN 978-3-95450-178-6

FIRST RESULTS OF SRF CAVITY FABRICATION BY ELECTRO-HYDRAULIC FORMING AT CERN

S. Atieh, A. Amorim Carvalho, I. Aviles Santillana, F. Bertinelli, R. Calaga, O. Capatina, G. Favre, M. Garlasché, F. Gerigk, S.A.E. Langeslag, K.M. Schirm, N. Valverde Alonso,
CERN, Geneva, Switzerland
G. Avrillaud, D. Alleman, J. Bonafe, J. Fuzeau, E. Mandel, P. Marty,
A. Nottebaert, H. Peronnet, R. Plaut
Bmax, Toulouse, France

Abstract

In the framework of many accelerator projects relying on RF superconducting technology, shape conformity and processing time are key aspects for the optimization of niobium cavity fabrication. An alternative technique to traditional shaping methods, such as deep-drawing and spinning, is Electro-Hydraulic Forming (EHF). In EHF, cavities are obtained through ultra-high-speed deformation of blank sheets, using shockwaves induced in water by a pulsed electrical discharge. With respect to traditional methods, such a highly dynamic process can yield valuable results in terms of effectiveness, repeatability, final shape precision, higher formability and reduced spring-back. In this paper, the first results of EHF on copper prototypes and ongoing developments for niobium for the Superconducting Proton Linac studies at CERN are discussed. The simulations performed in order to master the embedded multi-physics phenomena and to steer process parameters are also presented.

INTRODUCTION

Several projects at CERN require developments of new or spare superconducting RF cavities, in particular for the LHC consolidation, the LHC High Luminosity upgrade (HL-LHC), the Superconducting Proton Linac (SPL) and the Future Circular Collider (FCC) studies. CERN has in recent years increased its effort into SRF technologies R&D as well as the related infrastructure.

SPL is an R&D study aiming at developing key technologies for the construction of a multi-megawatt proton linac based on state-of-the-art RF superconducting technologies, which would serve as a driver in new physics facilities. Amongst the main objectives of this R&D effort, is the development of 704 MHz bulk niobium beta=1 elliptical cavities (see Fig. 1), operating at 2 K with a maximum accelerating gradient of 25 MV/m, and the testing of a string of cavities integrated in a machine-type cryomodule.

HL-LHC relies on the availability of new technologies such as superconducting RF crab cavities, which would be installed in the interaction region (IR) of the upgraded ATLAS and CMS experiments. This requires the development of superconducting RF cavities of complex, non-axisymmetric shapes.

Superconducting RF (SRF) structures are traditionally fabricated from sheet metal formed using a wide range and combination of techniques: spinning, deep drawing, necking and hydroforming.

Figure 1: SPL 704 MHz elliptical cavity.

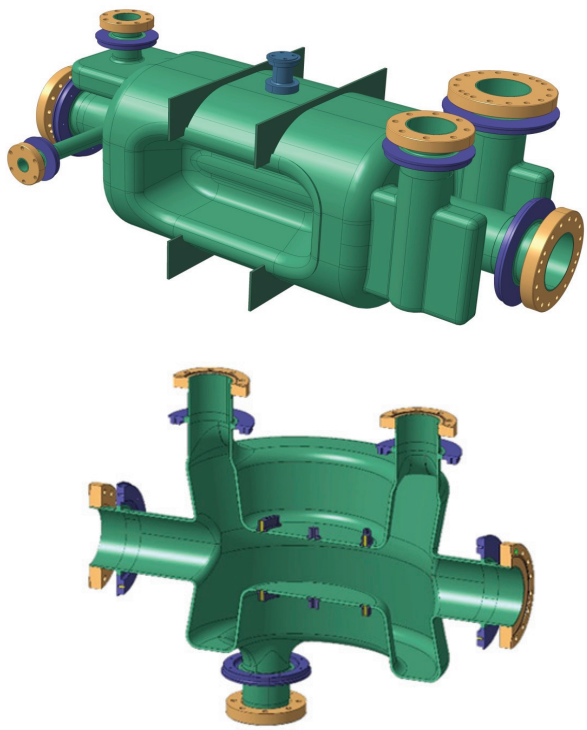

Figure 2: Special shapes 400 MHz crab cavities for HL-LHC upgrade.

The metals involved are pure niobium as well as oxygen free OFE copper typically used for preliminary trials and as substrate for niobium sputtered cavities. Geometries used for SRF cavities can be axisymmetric (e.g. LHC, ILC, SPL) or non-axisymmetric (e.g. HL-LHC crab cavities, Fig. 2). Electron-beam welding is typically

PRECISE STUDIES ON He-PROCESSING AND HPR FOR RECOVERY FROM FIELD EMISSION BY USING X-RAY MAPPING SYSTEM

H. Sakai#, K. Enami, T. Furuya, M. Satoh, K. Shinoe, K. Umemori, KEK, Tsukuba, Ibaraki, Japan
M. Sawamura, JAEA, Tokai, Naka, Ibaraki, Japan

Abstract

We usually met the degradation of superconducting RF cavity on the cryomodule test and beam operation even if the performance of this cavity is good on the vertical test (V.T). Field emission is the most severe problem for this degradation after reassembly work from vertical test. Not only high pressure rinsing (HPR) but also He-processing, which is more suitable method without the reassembly work for recovery, is recommended and tried to recover this degradation. However, we did not investigate the details of how field emission sources were processed and removed after HPR and He-processing. We deeply investigated the processing procedure during He-processing and how many field emission sources removed after HPR by using rotating X-ray mapping system in V.T [1].

INTORODUCTION

The ERL project in Japan was started with an aim to realize 3 GeV class ERLs. Especially, more than 100mA beam current will be expected for the ERL operation. For this aim, nine-cell SC cavities, named as "KEK-ERL model-2 cavity"[2], used for the main linac cryomomoule and were developed to achieve a stable accelerating gradient of 15 - 20 MV/m under the beam of 100 mA. High Q-value of more than 1×10^{10} is also required to realize energy recovery condition with high gradient of 15 - 20 MV/m. In order to know the cavity performance of KEK-ERL model-2, we carried out the vertical tests and achieved 25MV/m gradient in vertical test and satisfied our requirements of more than 1×10^{10} of Q_0 with 15 MV/m as shown in the right figure of Fig. 1 [3]. After vertical test, these two cavities of KEK-ERL model-2 were assembled into Compact ERL(cERL) [4] main linac cryomodule and its cryomodule was placed inside cERL radiation shield at fall of 2012. High power test of cryomodule was carried out at December of 2012. The degradation of Q-values of two cavities were observed from 10 MV/m as shown in the left figure of Fig. 1. We also observed heavy radiations from 9-10 MV/m [5, 6]. We assumed that the field emission sources like small particles inside these cavities were created during string assembly and resulted in the Q-values degradation. Furthermore, degradation was proceeded during beam operation from 2013 [7]. At present, reason why field emission became worse is not clear. It is important to overcome these degradations during string assembly and beam operation.

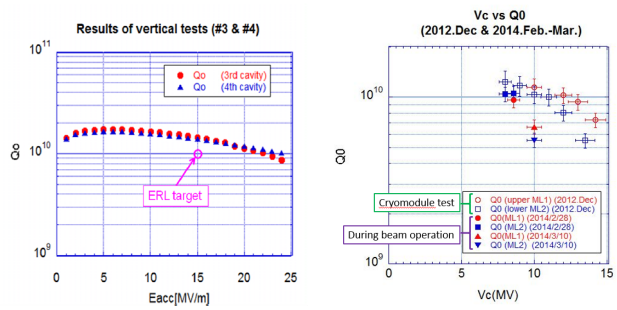

Figure 1: (Left) The results of vertical tests of KEK-ERLmodel-2 cavities. Horizontal and vertical axis shows accelerating field (Eacc) and Unloaded Q-values (Q_0). (Right) Performance degradation due to full-assembly (open circles and squares), and during beam operation (solid circles, squares and triangles).

This degradation of Q-value come from field emission was also appeared in KEKB [8] an CEBAF accelerator in Jlab [9]. So it is crucially important to suppress field emission all over the world [10]. There are some approaches to suppress the field emission. One is the high power pulse processing (HPP) and the other is the He processing. Both approaches can give the recovery from field emission after the cryomodule assembly and during beam operation. HPP is the normally used processing method after cryomoudule assembly and during the beam operation. By applying the higher peak voltage with about 1 ms pulse length compared with the nominal operating voltage, this peak power of higher voltage would burn the field emission source and recover from the degradation. We also applied the HPP to our cryomodule in Compact ERL (cERL) and could suppress the degradation during long term beam operation [7]. He processing is thought as more powerful processing method. By feeding the He gas with $10^{-2} \sim 10^{-4}$ Pa into the cavity in cryomodule with a higher RF voltage, He ion with high energy probably would attack the field emission source and crush it. Actually, this He processing worked in CEBAF cryomodule and recently C100 cryomodule performances of CEBAF, part of which suffered from field emission, were recovered from 9.3 MV/m to 13.1 MV/m in average [11]. HPP is expected that more powerful recovery method compared with pulse processing. However, we did not know the mechanism of He processing in detail. Especially we did not know that how field emission source would be processed while He processing applied.

ISBN 978-3-95450-178-6

RECENT DEVELOPMENT IN VERTICAL ELECTROPOLISHING

*Vijay Chouhan, Yoshiaki Ida, Kiyotaka Ishimi, Keisuke Nii, Takanori Yamaguchi
Marui Galvanizing Co., Ltd., Japan
Hitoshi Hayano, Shigeki Kato, Hideaki Monjushiro, Takayuki Saeki, Motoaki Sawabe
High Energy Accelerator Research Organization, KEK, Japan

Abstract

Horizontal electropolishing (HEP) is being used for final surface treatment of niobium SRF cavities. However a HEP system is equipped with complicated mechanism that makes it expensive and enhances cost of surface treatment of cavities especially when mass production is considered. Vertical electropolishing (VEP) has been introduced by other labs and the research is being carried out to establish the VEP technique. The VEP system requires simple mechanism and has advantages over HEP setup. Positive results have been obtained from the VEPed cavities also as shown by other labs. However further improvement in a VEP setup, cathode and VEP parameters is required. Marui Galvanizing Co., Ltd in collaboration with KEK has been working for development of VEP system, optimization of cathode and VEP parameters to obtain uniform Nb removal with a smooth surface of a cavity. Here we report our recent development of VEP system, unique Ninja cathode and parameter optimization with a 1-cell coupon cavity containing 6 Nb disk coupons at the beam pipes, irises and equator. The coupon surfaces were analyzed to obtain detail of the cavity surface.

INTRODUCTION

Electropolishing (EP) has been carrying out for several materials to obtain smooth surface. In accelerator surface of niobium (Nb) SRF cavities also treated with EP process to achieve a high electric field gradient with high Q_0 value [1]. Rough surface limits cavity performance due to presence of sharp tip like structure which might act as field emitters at a high field. Surface contaminations also degrade performance of Nb cavity as the contaminants might enhance surface resistance and might act as field emitters. In order to reduce roughness of inner surface of an Nb cavity, electropolishing (EP) is being carried out to remove Nb from inner surface in a depth of 100 microns. KEK perform bulk EP for 200 µm removal followed by fine EP for ~20 µm removal of Nb. An optimized EP parameters and adequate temperature can provide a smooth surface and very less amount of contaminants like sulfur and fluorine. Treating a cavity with EP can solve above-mentioned problems.

EP of an Nb cavity is either performed horizontally or vertically. Horizontal EPed cavities have shown consistently good performance and hence HEP is being used for surface treatment of the cavities worldwide. Vertical EP (VEP) has several advantages over horizontal (HEP) in respect of cost effective setup and easy operation [2].

Study on VEP is being carried out at Cornell, JLab, Saclay and other labs to optimize its parameters to establish the VEP method. In VEP polishing rate is usually found to be non-uniform along the length of the cavity. The top iris is strongly polished while the bottom iris shows the lowest polishing rate. A removal thickness on the top iris is usually found to be ~3 times higher than that on the bottom iris [3,4]. The asymmetry can degrade field flatness and therefore more efforts are require to tune the cavity after VEP [5]. Another issue with VEP is bubble traces on upper half-cell of a cavity. When bubbles move on Nb surface with acid flow from bottom to top, bubble leave their footprint on Nb surface. In order to minimize the longitudinal asymmetry, flipping of the cavity to repeat VEP is being used by other groups. In 1-cell cavity symmetry might be obtained by flipping the cavity while achieving symmetry in 9-cell cavity might not be easy even though the cavity is flipped to vertically electropolished twice. The flipping of a cavity upside down for repeating VEP makes VEP process time consuming and expensive. Therefore for industry point of view the flipping process cannot be adopted. Cavity performance was obtained in vertical test at Saclay for 1-cell cavity [4] and at Cornell for a 9-cell cavity [6]. A field gradient of ~35 MV/m was achieved with a Q_0 value of ~10^{10} for the 1-cell cavity and the performance was similar to that obtained with HEP of the same cavity [4]. The 9-cell cavity after VEP at Cornell also showed good performance as required for ILC [6]. The good performances of the cavities encourage us to further optimize VEP parameters. We are optimizing VEP parameters and cathode shape in order to solve issues in VEP and to reduce cost of surface treatment of cavities [3,7-11]. We have joint collaborations with Saclay (Marui-KEK-Saclay) and with Cornell University (Marui-KEK-Cornell University). Cavity performance test is carried out at Saclay while our unique Ninja cathode will be tested at Cornell University.

In this paper we report effect of two types of recently developed Ninja cathodes on surface of a 1-cell Nb cavity.

RECENT DEVELOPMENT AT MARUI

VEP Setups

Two setups were constructed for VEP of 1-cell and 9-cell cavities. However a 9-cell system can also be used

#vchouhan@e-marui.jp

OVERVIEW OF RECENT HOM COUPLER DEVELOPMENT*

Binping Xiao†, Brookhaven National Laboratory, Upton, New York 11973-5000

Abstract

Higher Order Mode (HOM) damping is important for SRF applications, especially for high intensity machines. A good HOM damping design will help to reduce power load to the cryogenic system and to reduce the risk of beam breakup. The design of HOM damping, including antenna/loop HOM couplers, beam pipe HOM absorbers and waveguide HOM couplers, is to solve a multi-physics problem that involves RF, thermal, mechanical, and beam-cavity interaction issues.

In this talk, the author provides an overview on the latest advances of the HOM couplers for high intensity SRF applications.

INTRODUCTION

A charged particle bunch that encounters any cross-section perturbation of the beam pipe (SRF cavity in our case) can generate electromagnetic (EM) fields that might or might not get trapped within the perturbation. The EM fields will interact with, and influence the motion of this specific bunch and the following bunches. It can lead to beam quality degradation, beam energy loss, beam instability, and in the worst case, beam breakup. The EM fields can also interact with the SRF cavity and result in unwanted RF heating, multipacting etc. A good design of HOM damping would help to minimize the above-mentioned problems and allow higher beam intensity operation.

There are three major varieties of HOM couplers: beam pipe absorber, coaxial (loop/antenna) coupler and waveguide coupler. For high intensity application, it is possible that two, or even all three of these couplers to be adopted. This paper will cover the coaxial and waveguide couplers. For beam pipe absorbers, please refer to Eichhorn's talk [1].

The design of HOM damping is to solve a multi-physics problem that involves RF, thermal, mechanical, and beam-cavity interaction issues. Insufficient consideration on either aspect can lead to the failure of the SRF cavity operation. For example, for the 3.9 GHz FNAL/FLASH cavity, insufficient multipacting analysis of the fundamental mode in the HOM filter led to fracture of the coupler [2]; for the TESLA-shape loop HOM coupler, the RF loss on the tip of the HOM Nb antennae can give a limit to the accelerating gradient on CW operations[3-5]; for the 56 MHz Quarter Wave Resonator (QWR), the thermal quench caused by the brazing material at the sapphire-Nb joint limited the cavity performance to 330 kV in CW operation and 550 kV in pulsed operation [6].

In this paper, we will discuss the latest advances of the HOM coupler designs, the lessons learned and the approaches that were taken.

RECENT ADVANCES

DQW HOM Coupler

A Double Quarter Wave (DQW) crab cavity was designed for the Large Hadron Collider (LHC) luminosity upgrade [7]. A compact HOM filter with wide stop band at the deflecting mode is developed for this cavity, as shown in Figure 1 [8].

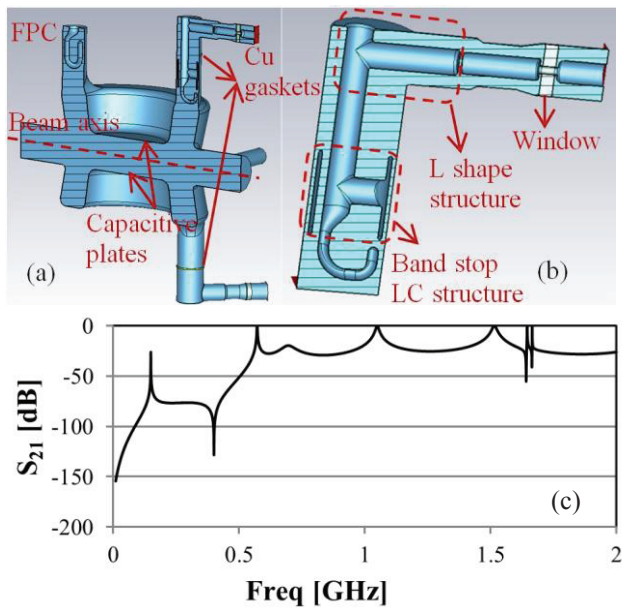

Figure 1: (a) DQW with 3 HOM filters; (b) HOM filter; (c) S_{21} of the HOM filter, with TE_{11} mode on the hook side and TEM mode on the port side. [8]

The HOM filter, shown in Figure 1(b), consists of a band stop LC structure right above the hook to minimize the RF loss on the Cu gasket that will be used to connect the cavity and the filter, shown in Figure 1(a), and an L shape structure on the top to form a pass band starting from 570 MHz, the frequency of the first HOM. There are three HOM filters in each cavity, with one on the FPC side with the pickup port along the beam pipe direction and the other two on the opposite side with the pickup port 60 degrees away from the beam pipe port. This symmetric design is adopted to lower the multipolar components of the fundamental mode field. The S_{21} of this design, with TE_{11} mode on the hook side and TEM mode on the port side, is shown in Figure 1(c). The

* Work partly supported by US DOE through Brookhaven Science Associates LLC under contract No. DE-AC02-98CH10886 and by the US LHC Accelerator Research Program (LARP). This research used resources of the National Energy Research Scientific Computing Center, which is supported by US DOE under contract No. DE-AC02-05CH11231. Research supported by EU FP7 HiLumi LHC - Grant Agreement 284404.

†binping@bnl.gov

ISBN 978-3-95450-178-6

HIGHER ORDER MODE ABSORBERS FOR HIGH CURRENT ERL APPLICATIONS

R. Eichhorn#, J. Conway, Y. He, Y. Li, G. Hoffstaetter, M. Liepe, T. Gruber, M. Tigner,
T. O' Connell, P. Quigley, J. Sears, E. Smith, V.D. Shemelin,
Cornell Laboratory for Accelerator Based Sciences and Education

Abstract

Efficient damping of the higher-order modes (HOMs) of the superconducting cavities is essential for any high current operation. The talk will provide an overview on the latest advances of HOM absorber development for high intensity SRF applications. As the ideal absorber does not exist, the different conceptual approaches will be presented and the associated issues are outlined. Design examples from various labs will be given that help explain the issues and resolutions. Some focus will be given to the Cornell HOM beamline absorber that was designed for high current, short bunch operation with up to 400 W heating. The design will be reviewed and testing results will be reported.

INTRODUCTION

The acceleration of particle inside an accelerator is usually provided by RF cavities and many machines today rely on superconducting cavities. Usually, the accelerating mode inside that cavity is chosen to be the fundamental mode (even so exceptions exists). In this mode, which corresponds to a certain (operation) frequency, power is forwarded to the cavity and eventually transferred to the particle beam. However, cavities have (theoretically) an infinite number of resonant frequencies. They are denoted higher order modes and these frequencies may be excited by the beam, which leads then to a reverse power flow: from the beam to the cavity. Not only exists the drawback of the beam loosing energy via this mechanism, the excited higher order modes correspond to field configurations inside the cavity which can seriously affect the beam. For example, if a higher order mode frequency corresponds to a dipole mode, any excitation of that mode results in a deflection of the beam. For circular machines this can be a limiting factor.

Several strategies to minimize higher order mode effects exists, starting from a carefully designed accelerating cavity to control mode frequencies, to having dedicated coupler antennas or waveguides to extract higher order mode power to absorbing the power directly at the beam pipe using ferrites or lossy ceramics. This paper focusses on the absorbing materials. Widely used materials to absorb RF frequencies are ferrites and (electrically) lossy ceramics, and a variety of materials exist. They differ in their loss tangent (a figure of merit for the absorption) and the frequency range in which they display adequate absorption. Being common to all ferrites, the losses in the material are of magnetic type and display a resonant-like behaviour, which usually leads to absorption characteristics with limited bandwidth (which still can be in the GHz region). Typically, one can find good ferrites for frequencies below 5-10 GHz.

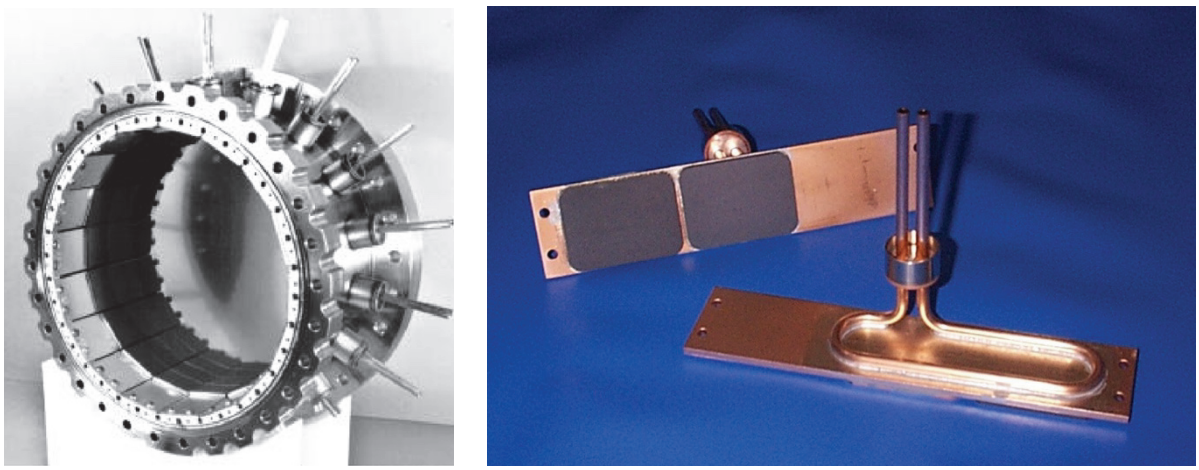

Figure 1: Absorbing tiles of the CESR B-Cell HOM absorber. Three layers are sputtered onto the ferrite (titanium, a mixture of titanium/copper, and a copper layer: total thickness: 1 μm). The ferrite tiles are soldered to a copper plated Elkonite (copper-tungsten sinter metal that fits the thermal expansion of the ferrites) plate. Water cooling tubes are soldered on the backside of the Elkonite. Each HOM panel is designed to absorb up to 600 W RF power. For the delicate soldering of the ferrites to the Elkonite plate inductive brazing under an argon atmosphere is used.

r.eichhorn@cornell.edu

OVERVIEW ON MAGNETIC FIELD MANAGEMENT AND SHIELDING IN HIGH Q MODULES*

G. Wu, Fermilab, Batavia, IL 60510, USA

Abstract

Maintaining very high cavity Q_0 in linac applications creates new challenges for cryomodule design. Magnetic shielding from both external fields and internal fields is required and its importance to thermal gradients during Tc transition is now emerging. This paper will describe the design challenges and possible mitigation strategies with examples from various applications or laboratories including DESY/TTF, FRIB, LCLS-II, Cornell University and KEK.

INTRODUCTION

Superconducting RF (SRF) accelerators have been increasingly adopted in various applications from nuclear physics, high energy physics, basic energy sciences and medical physics, etc. Maintaining high performance while reducing the construction and operational costs have been the forefront of the SRF science and technology. Pushing the limits of high operating quality factor (Q) of SRF cavities results in significant cost savings by reducing cryogenic costs. This is especially significant when considering the fact that continuous wave (CW) SRF accelerators require several tens of million dollar cryogenic plant.

Latest developments of nitrogen doping brings the usable niobium cavity Q_0 to be 5 times higher than previously specified [1]. The residual surface resistance of a nitrogen doped cavity, however, is slightly more sensitive to trapped magnetic flux [2,3]. As the cavity operational Q and BCS resistance are inversely proportional, it is important to reduce the residual resistance.

Many factors contribute to the residual surface resistance of a niobium cavity. Surface contamination, oxides are improved by careful chemical and clean room processes while hydrides are minimized using high temperature hydrogen degassing, low temperature baking, and relatively fast cool down through 100K. Magnetic flux trapping, on the other hand, requires optimal design and operational control to minimize its effect on residual resistance.

Ambient magnetic fields arise from several sources. Environmental magnetic fields consist the combined field of earth's magnetic field, buildings, utility infrastructures, and instrumentation equipment. Cryomodule enclosure shells such as vacuum vessels and end caps, as well as components inside the cryomodule are also potential sources that contribute to the ambient magnetic field at the SRF cavities.

A review of the magnetic field effect on cavity Q shows the importance of the magnetic field management in an actual cryomodule. Many types of materials and engineering solutions are available to reduce the ambient magnetic field in the cavity. Earlier systematic studies have been very thorough during the Tesla Test Facility cryomodule development [4]. The magnetic shield design studies have been spotty since then.

The operational control can further reduce the magnetic flux trapping using high thermal gradient during superconducting transition that can overcome the flux pinning force [5].

Design and practices will be showcased in this paper using LCLS-II prototype cryomodule as an example.

MAGNETIC SHIELDING MATERIALS

There are many types of magnetic shielding materials that provides various levels of magnetic shielding at different temperatures and under different ambient magnetic field. Permeability and the saturation are the two main parameters to consider which material to choose, in addition to the cost of the material. There have been many characterization studies related to the magnetic shielding materials [6,7].

There are two major shielding materials typically used in a cryomodule, depending on the shielding design. Traditional mu-metal has very good permeability at room temperature, but decreases dramatically at cryogenic temperature. Cryogenic magnetic shield has high permeability at cryogenic temperature but cost much more than mu-metal. Cryogenic magnetic shield material is very vulnerable to stress and impact vibration. While stress can be relieved by high temperature annealing, handling can introduce stress to the material again. Potential impact of the material is usually unavoidable during an actual assembly. These practical limitations suggest that the design has to consider the worst case permeability for the cryogenic magnetic shields. Based on past experience, a relative permeability of 7,000 for mu-metal and 12,000 for cryogenic magnetic shield are typically used in designing magnetic shield at cryogenic temperatures [4]. Magnetic design in cERL cryomodule at KEK uses a flat sheet format to minimize the fabrication and assembly stress in order to retain the highest permeability [8].

Both A4K and annealed mu-metal have been considered for the cryomodules of Facility for Rare Isotope Accelerator (FRIB) [9]. Cornell ERL linac cryomodule utilized A4K. Both XFEL linac cryomodule and cERL cryomodule chose Cryophy, a material similar

*Work supported by DOE Contract # DE-AC02-07CH11359
genfa@fnal.gov

ISBN 978-3-95450-178-6

PROPAGATION OF THE HIGH FREQUENCY FIELDS IN THE CHAIN OF THE SUPERCONDUCTING CAVITIES*

A. Novokhatski#, SLAC National Accelerator Laboratory, Menlo Park, CA 94025, USA

Abstract

Combination with the very high repetition rate requires to use the superconducting cavities to accelerate very short bunches for the FEL operation as it planned for LCLS-II. In the cavities these bunches excite very high frequency electromagnetic fields. There are severe concerns, that these fields will remain inside the structure for a long time, bring additional heating or even break up the Cooper pairs. We present results of the simulation of the transient dynamics of wake fields of very short bunches. We show how much of the energy is vanishing through the beam pipes immediately and how much energy is staying in the cavity for a long time.

INTRODUCTION

While passing a cavity a bunch creates electromagnetic fields. A fraction of these fields is staying in the cavity for a very long time (captured modes). After several reflections, another part is leaving the cavity and the rest of the field is chasing the bunch. In a time this field will catch the bunch and take its kinetic energy. The time or the distance, where the bunch is caught, is inversely proportional to the bunch length. It can be very long for a very short bunch.

We may imagine that the spectrum of this part contains mainly high frequency modes. We will try giving the analyses for the TESLA cavity, as it is very important from the point of feasibility of the short bunch acceleration in super conducting cavities.

To give quantitative values, we study the energy distribution of the wake field in a single cell cavity with connected tubes and in multi-cell cavities. In this paper we update the previous study [1]. For wake field calculation we use a computation code NOVO [2]. The algorithm for this code was specially designed for calculation of the wake fields of very short bunches.

ENERGY OF THE WAKE FIELD

To study the fields, which are really acting on particles, it is necessary to split the full field into the wake field, that really acts on the bunch particles and the "self" field, that is moving everywhere together with the bunch, but does not interact with particles (in the relativistic case).

$$E_{full} = E_{bunch} + E_{wake} \quad (1)$$

The energy distribution of the wake field, following the bunch, can be described by the longitudinal energy density $\Lambda(s)$, which is the cross-plane integral over the energy density at a distance s after a bunch center:

$$\Lambda(s) = \int\left(\frac{\varepsilon_0}{2}E^2_{wake}(s) + \frac{\mu_0}{2}H^2_{wake}(s)\right)d\varphi r dr \quad (2)$$

The integral of this density represents the total energy that is following the bunch at a distance s

$$T(s) = \int_{-\infty}^{s}\Lambda(s')ds' \quad (3)$$

Depending on the distance s this integral may include only propagating fields (finite s) or include also trapped modes when s goes to plus infinity. Naturally in this case the integral is approaching the value of the loss factor K_{loss} of a bunch

$$K_{loss} = T(\infty) \quad (4)$$

A SINGLE CELL CAVITY

While decreasing the bunch length, the loss factor is increasing, and more and more high order modes are excited in a cell. The loss factor in one regular cell of the TESLA cavity is shown in Fig. 1 as a function of the bunch length. The integral of energy of the field which is following a bunch is also shown in Fig. 1 for a moment when a bunch left a cell and at distance more than 15 bunch length.

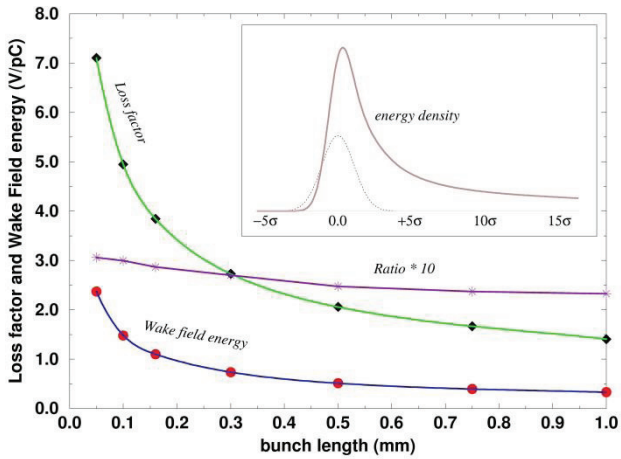

Figure 1: Loss factor and the wake field energy, following the bunch in the tube, after a single cell of the TESLA cavity over the bunch length. Ratio of field energy to the loss factor is multiplied by 10 (to use the same scale).

In this figure, inside a box, one can find the energy density distribution $\Lambda(s)$ in the tube and the bunch charge distribution. At this time there is still some wake fields, which are chasing a bunch but with a slowly vanishing tail. The energy of the following field is defined as $T(s=15\sigma)$. The ratio of the energy integral to the

*Work supported by DOE-AC02-76SF00515
#novo@slac.stanford.edu

ISBN 978-3-95450-178-6

SECOND HARMONIC CAVITY DESIGN FOR SYNCHROTRON RADIATION ENERGY COMPENSATOR IN eRHIC PROJECT

Chen Xu[1], Sergey A. Belomestnykh[1,2], Wencan Xu [1]and Ilan. Ben-Zvi [1,2]
[1] Brookhaven National Laboratory, Upton, New York 11973-5000, USA
[2] Stony Brook University, Stony Brook, New York 11794, USA

Abstract

eRHIC project requires construction of a FFAG ring to accelerate electrons and connect to the existing ion ring of Relativistic Heavy Ion Collider (RHIC) at Brookhaven National Laboratory. This new ring will have the same radius as the RHIC ring. Synchrotron radiation lost in the electron ring should be compensated by a CW superconducting radio frequency (SRF) cavity. Here we propose an 845 MHz single cell harmonic cavity. This cavity will experience a high average current (~0.7 A) passing through it. With this consideration, this cavity design requires optimization to reduce higher order mode power. On the other hand, the cavity will operate at relatively high gradient up to 18 MV/m. Current design requires fundamental couplers to handle 400 kW forward RF power and HOM couplers to extract 2.5 kW HOM power.

INTRODUCTION

eRHIC project is based on a superconducting Energy Recover Linac (ERL). This linac will be built on top of the current RHIC ring. Electrons will be accelerated a certain numbers of passes to reach the final energy to collide with heavy ion beam. Then bunches will be decelerated to pass their energy back to SRF cavities [1]. The accelerating and decelerating electron bunches cruise co-linearly inside SRF cavities in the circulating ring. They will lose energy due to synchrotron radiation. This energy loss would cause phase changes and reduce the energy recovery rate. Second harmonic cavity is needed to accelerate both accelerating and decelerating electron bunches. High gradient operation at high beam loading is required from these cavities. As they will be part of the ERL, they should not produce much wake field power.

CAVITY DESIGN

By designing the second harmonic cavity as a single cell cavity, we can avoid the trapped modes as shown in multi-cell cavity. The maximum power of synchrotron radiation is around 2.4 MW. If we plan to use six single cell cavities, each cavity would deliver 400 kW CW power to the beam. The cavity's fundamental frequency is 844 MHz. and these cavities will operate at a gradient of 18.1 MV/m in high gradient mode and at 9.1 MV/m in high current mode. Thus, the Fundamental Power Coupler (FPC) is retractable. These six cavities will be put in between the two linacs housing fundamental cavities· The total length occupied by the SRF linac is 120 meter, and the affordable length for each second harmonic cavity is 88 cm.

Cavity Design without Couplers

The cavity shape is optimized using 2D code Superfish while its loss factor and impedance are calculated with 2D code ABCI [2]. In Figure 1, 8 major parameters can be optimized to reach the specification. The beam pipe radius is 80 mm, which is also the beam pipe radius of the main ERL cavities. The radius of middle ellipse is critical for peak electric field. The iris radius *r* and radius of top ellipse are critical for the *R/Q* of the fundamental mode and the taper angle is critical for the loss factor.

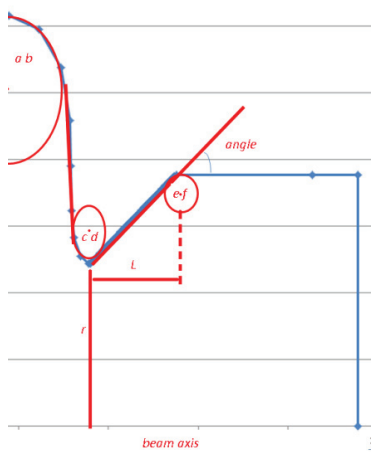

Figure 1: Optimization parameters of the harmonic cavity.

The iris should set a cut-off frequency higher than 844 MHz but the first HOM mode should leak out of the cavity. A large iris radius will reduce *R/Q* of the fundamental mode. Therefore, a taper design will be essential for maintaining high *R/Q* while allowing the first HOM mode to propagate. That determines *r* to be 71 mm.

The taper structure is used to minimize *R/Q* of HOMs, especially the first few modes. An analytical formula for taper's loss factor indicates that a longer taper will generate lower loss factor than a shorter taper [3]. However, due to limited space available for these cavities, we limited the taper length to 20 cm.

The *H* field at both ends should be limited to 100 A/m because of thermal consideration. It also defines the total length of the cavity. The *E* field pattern of the fundamental mode is shown in Figure 2. At both ends of the beam pipe, the *H* field is less than 100A/m at a gradient of 18 MV/m.

This work is supported by Brookhaven Science Associates, LLC under Contract No. DE-AC02-98CH10886 with the U.S. DOE.
#chenxu@bnl.gov

CALCULATIONS FOR RF CAVITIES WITH DISSIPATIVE MATERIAL*

F. Marhauser#
Thomas Jefferson National Accelerator Facility, Newport News, VA 23606, U.S.A.

Abstract

For the design of RF devices like accelerating cavities, feeding and/or extracting RF energy requires antenna/waveguide ports, which present a perturbation to the otherwise closed system. Calculating Eigenmodes requires a numerical solver. The accurate numerical assessment and optimization of the external Q factors at such ports for a specifically excited RF mode or a mode ensemble can be crucial for proper operation of the device. Here a 3D Eigenmode solver technique is presented for the determination of the external Q, which makes use of dissipative material at external ports rather than the more traditional method of resembling matched conditions at external ports via the calculation of waveguide modes. This has advantages since both the external Q factor and the loaded frequency are calculated as part of the Eigenmode solver run (complex solution), while allowing for travelling mode conditions instead of standing waves. The technique does not require the external Q to be evaluated from subsequent runs with magnetically and electrically (closed) boundaries.

INTRODUCTION

With multi-processor and/or multithreaded processor systems becoming the norm, and increase in computer RAM capabilities as well as the improvement of numerical meshing options, comes the opportunity to incorporate complexities into numerical designs for realistic assessments on a reasonable timescale. This makes feasible studying subtle geometrical changes - which yet can have significant influence on the results - and detailed parametric studies allowing for fabrication tolerances. The latter becomes important when more stringent performance goals are imposed on RF devices - like accelerating cavities - that rely on conventional technologies, but make use of improved methods for production, surface treatments or the use of advanced materials to push operational limits to new frontiers.

The numerical determination of the external Q factor (Q_{ext}) has advanced over more than two decades from comparably tedious methods - when computational RF codes had no built-in capability to calculate Q_{ext} [1] - to very user-friendly codes with a 'one-click' option to compute Q_{ext}-values. This does not necessarily come though without significant expenses for commercially available software. Yet, the numerical simulations are often invaluable to meet scientific needs in order to turn a design into a properly operating device with a minimum effort of prototyping and thus development costs. The Q_{ext} calculation with dissipative material is elucidated in this paper by means of three relatively complex superconducting RF (SRF) cavities. For this purpose, capabilities of the frequency domain and Eigenmode solver of the CST Studio Suite [2] have been explored. The investigations has been triggered by software bugs in the CST Eigenmode solver that led to a false arrangement of mode numbers, principally due to sorting modes either in ascending order of the unloaded frequency (f_0) or the loaded frequency (f_l). Since the loaded frequency depends on the Q_{ext}, this can readily lead to ambiguous results, particularly when calculating of a large ensemble of Eigenmodes. The bug has been reported to CST at the time (CST version 2014). Using dissipative material (henceforth: absorber) instead of waveguide ports cured this problem, since the computed frequency is f_l. Furthermore, as part of Q_{ext} optimizations for fundamental power couplers (FPC) of SRF cavities (relatively high Q_{ext}-values), the results have been found to vary significantly depending on symmetry planes and/or the total number of modes used.

CALCULATION METHOD

Note that curved element tetrahedral meshes are employed throughout. This yields an accurate discretization of complex geometries. Each absorber placed in the domain can be optimized individually with respect to its reflection response (S11). Furthermore, each absorber can be placed arbitrary in the calculation domain to best resemble the real boundary conditions. At relatively high frequencies one or more propagating waveguide modes may participate in the external energy absorption depending on the excited Eigenmode in the structure. Waveguide mode conversion is also feasible as a cause of symmetry-breaking components. An advantage over the Q_{ext} determination with waveguide ports is that one does not need to predefine the number of traveling modes for absorption (with unconsidered modes reflected at the boundary, but more modes increasing the calculation time), nor does an external port has to end with a planar boundary. Additionally, waveguide modes are calculated at a center frequency given by the frequency range. This can elevate inaccuracies of matched conditions when a cutoff frequency is present, i.e. the further the Eigenfrequency is apart from the center frequency. The presented method instead can account for

* Authored by Jefferson Science Associates, LLC under U.S. DOE Contract No. DE-AC05-06OR23177. The U.S. Government retains a non-exclusive, paid-up, irrevocable, world-wide license to publish or reproduce this manuscript for U.S. Government purposes.
# marhause@jlab.org

HOM CALCULATIONS FOR DIFFERENT CAVITIES AND BEAM INDUCED HOM POWER ANALYSIS OF ESS

H. J. Zheng#, J. Gao, Institute of High Energy Physics, CAS, Beijing, China
C. Pagani, J. F. Chen, INFN Milano, LASA, Via Fratelli Cervi 201, I-20090 Segrate (MI), Italy

Abstract

For different design of ESS superconducting cavities, the higher order modes (HOMs) of monopoles, dipoles, quadrupoles and sextupoles are found. Their *R*/*Q* values are also calculated at their geometric beta.

Main HOM related issues are the beam instabilities and the HOM induced power especially from TM monopoles. The analysis for the beam induced HOM voltage and power in this paper shows that, if the HOM frequency is a few kHz away from the beam spectrum, it is not a problem.

In order to understand the effects of the beam structure, analytic expressions are developed. With these expressions, the induced HOM voltage and power were calculated by assuming external *Q* for each HOM. Our analysis confirms that, with the beam structure of ESS and a good cavity design, no special tight tolerances are required for cavity fabrication and no HOM couplers in the cavity beam pipes are planned.

INTRODUCTION

A time–averaged HOM power spectrum normalized to the cavity's *R*/*Q* has been calculated by Sangho Kim for the Spallation Neutron Source (SNS) beam time structure (single pass) [1], and Haipeng Wang's paper 'Beam Induced HOM Power Spectrum in JLab 1MW ERL-FEL' [2]. The analysis of ESS beam time structures is explained in this paper. Since the most dangerous HOM monopole is close to 5th harmonic of micro-bunch frequency for ESS median-beta cavity, the HOM induced voltage and power analysis based on the 5th harmonic of micro-bunch frequency is also showed in this paper.

HOMs are found with the CST MW Studio [3], and HOM properties such as frequencies and *R*/*Q* are calculated. We can find the dangerous mode which frequency is close to the beam spectrum from the simulation results. The total HOM induced power can also be calculated by the *R*/*Q* values. These works are showed in this paper.

ESS BEAM& HOM IDUCED VOLTAGE ANALYSIS

Time Structure of ESS

Time structure of ESS (50 mA pulse) is showed in Fig. 1.

HOM induced voltage analysis of ESS based on Sangho Kim's SNS/AP Technical Note No. 10 and Haipeng Wang's paper are showed below.

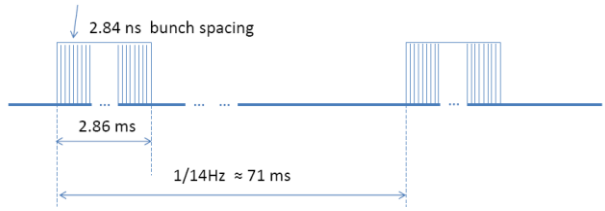

Figure 1: Time structure of ESS beam (bunches at 352.21 MHz).

The parameters used in the calculation are listed as following:

- HOM decay time constant: $T_d = \frac{2Q_e}{\omega} = \frac{Q_e}{\pi f}$
- SRF cavity's fundamental mode frequency: $f_1 = 704.42*10^6$ Hz
- Total numbers of micro-pulse within one macro-pulse: $N = 1.01*10^6$
- Pulse period between each micro-bunch: $T_b = 1/(352.21\ \text{MHz}) = 2.839*10^{-9}$ s
- Bunch period between each macro-pulse: $T_m = 71*10^{-3}$ s
- Macro-pulse length: $T_{mb} = 2.83*10^{-3}$ s
- Macro-pulse spacing: $T_G = T_m - T_{mb} = 68.17*10^{-3}$ s
- Single bunch charge (approximate to a point charge): $q = 1.42*10^{-10}$ C
- *R*/*Q* normalized induced voltage by a point charge: $V_q(\omega) = \frac{\omega}{2}\cdot q$
- At the time just after *k*th macro-pulse:

$$A(k, Q_e, \omega) = V_q(\omega)\cdot \frac{1-\exp(\frac{-NT_b}{T_d} + i\omega NT_b)}{1-\exp(\frac{-T_b}{T_d} + i\omega T_b)}\cdot \frac{1-\exp(\frac{-kT_m}{T_d} + i\omega kT_m)}{1-\exp(\frac{-T_m}{T_d} + i\omega T_m)} \quad (1)$$

- During the gap between *k*th and (*k*+1)th macro-pulse:

$$B(k, Q_e, \omega, t_1) = A\cdot \exp(\frac{-t_1}{T_d} + i\omega t_1),\ 0<t_1<T_G \quad (2)$$

- At the time just after *n*th micro-pulse in (*k*+1)th macro-pulse:

#zhenghj@ihep.ac.cn

ISBN 978-3-95450-178-6

SIMULATIONS OF 3.9 GHz CW COUPLER FOR LCLS-II PROJECT*

Ivan V. Gonin#, Timergali N. Khabiboulline, Andrei Lunin, Nikilay Solyak, Fermilab, Batavia, IL 60510, USA

Abstract

LCLS-II linac is based on XFEL/ILC superconducting technology. Third harmonic cavity of 3.9 GHz is used to compensate nonlinear distortion of the beam longitudinal phase space. The TTF-III fundamental power coupler for the 3.9 GHz 9-cell cavities has been modified to satisfy to LCLS-II requirements and operation in the CW regime. In this paper we discuss the results of thermal analysis for proposed modifications of the power coupler design suitable for various operating regimes of the LCLS-II linac. The results of mechanical study are also presented

INTRODUCTION

The LCLS-II SCRF linac consists of 35 1.3 GHz, 8-cavity Cryomodules (CM), and two 3.9 GHz, 8-cavity CMs. 3.9 GHz third harmonic superconducting cavities are used to increase the peak bunch current and to compensate non-linear distortions in the beam longitudinal phase space due to sinusoidal 1.3 GHz accelerating cavity voltage [1]. The fundamental power coupler (FPC) is an important and complicate component of the third harmonic system developed for the LCLS-II project. Table 1 shows main parameters of the 3.9 GHz cavity and cryomodule.

Table 1: Main 3.9 GHz CM and Cavity Parameters

	Nominal	Min	Max
Average Q_0, 2K	$2.5x10^9$	$2x10^9$	
Average gradient	13.4 MV/m	-	15.5 MV/m
Nominal beam to RF phase	-150deg	-90deg	-180deg
Cavity R/Q	750 Ω	-	-
G factor	273 Ω	-	-
FPC Q_{ext}	$2.5x10^7$	-	-

For a 300 uA beam current, a 15.5 MV/m accelerating gradient and a 180 deg beam-to-rf phase, the RF power induced by a beam and radiated to the power coupler is about 1700 W per cavity. If the cavity is detuned by 30 Hz due to microphonics (nominally is 0 Hz detuning), the required input power to maintain the operating gradient would be about 80 W, so the coupler needs to be rated for at least 1.9 kW of average RF power (in particular, it needs to operate below the peak surface temperature noted below). Therefore in simulations we apply 2 kW of the input RF power in the TW regime.

* Operated by Fermi Research Alliance, LLC under Contract No. DE-AC02-07CH11359 with the United States Department of Energy.

gonin@fnal.gov

POWER COUPLER DESIGN

Fermilab has developed a new 3.9 GHz power coupler for the third harmonic cavities for the TTF3 project after series of simulations and optimizations of different coupler designs [2]. The final design of the 3.9 GHz power coupler is shown in Fig. 1. It consists of a 50 Ohm coaxial line with a 30 mm diameter of the outer conductor.

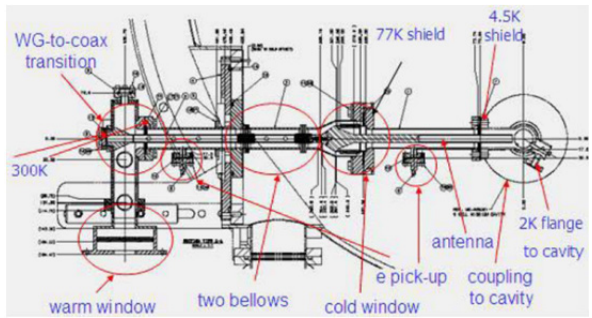

Figure 1: The 3.9 GHz power coupler developed at Fermilab.

Power coupler for the TTF3 project was designed for pulsed operation (Power is 50 kW, duration is ~2ms, repetition rate is 10 Hz). The LCLS-II requirements are CW operation at 2 kW in a traveling wave regime. At first, we performed COMSOL thermal simulations using LCLS-II parameters without any modifications of the 3.9 GHz TTF3 coupler. It is resulted in an overheating of the inner conductor of the warm part of the coupler up to 670 K. Thus, we propose the following modifications of the current design:

- Reducing the length of two inner bellows from 20 convolutions to 10 convolutions.
- Increasing the thickness of a copper plating in the inner conductor from 30 microns to 150 microns.
- Changing the antenna length to fulfil to the LCLS-II coupling requirement.

THERMAL ANALYSIS

Thermally, the power coupler represents a connector from the room temperature (300K) to the superconducting cryogenic environment (2K). Figure 2 shows the thermal analysis model used in COMSOL simulations [3].

IMPROVEMENTS OF BUILDCAVITY CODE

J.F. Chen#, M. Moretti, P. Pierini, INFN Milano-LASA, Segrate (MI), Italy
C. Pagani, Università degli Studi di Milano & INFN-LASA, Italy

Abstract

Recently, we improved the BuildCavity code, which is a graphics interface to SUPERFISH for the study of superconducting cavities of elliptical shape. Now it works with last SUPERFISH 7 and can be installed also on newer Windows systems such as Win 7 and 8. Several improvements have been done in the code. As an example, a design of ESS medium-beta cavity with BuildCavity will also be presented.

INTRODUCTION

BuildCavity (written as BC in abbreviation) is a code devoted to design an elliptical cavity that has been written ten years ago at LASA and has been used widely also in other labs [1, 2]. As a graphics interface to SUPERFISH (SF in abbreviation) [3], BC allows changing interactively the cell geometries on the screen, executing SF and tuning the inner cells of a multicell structure by iterating through a series of SF runs, storing the simulation results for the analysis of the dependence of the cell e.m. performances from the geometrical parameters that define its shape (as described in [1]). Separate tuning routines for the end cells (including the beam tube) are available, and a multicell cavity can be assembled and analyzed automatically from inner and end cells in the database that stores the geometrical and electromagnetic parameters of the cells.

After more than ten years without updating, the old version BC 1.3.4 is still functional, but outdated. This BC version does not work with the later distributions of SF, version 7 and needs version 6, no longer under distribution. In the new version, several instructions have been modified to match with the updates of SF 7.

Besides, several improvements have been performed on the code during the design activities of the ESS medium-beta cavity at INFN. Firstly, we have added the possibility to adjust the equator radius also on the end cell at the Pickup side, which is a very effective to maintain a good end-cell shape without modified the wall angle, thanks to the large frequency sensitivity of the equatorial region. Previous version of the code allowed this option only on the Fundamental Coupler (FC) side. Second, a post-process function allows BC to generate directly an APDL script file for ANSYS to perform mechanical analysis and structural simulations, while originally the cavity model for ANSYS had to be generated by an external auxiliary code. With this function, we can easily combine the RF cavity design by BC with the structural analysis by ANSYS, to perform design iterations to reach the desired e.m. and mechanical specifications.

#jinfang.chen@mi.infn.it

So far, the latest version is BC 1.4.3.

The second section of this paper presents the main improvements on BC, and the third section presents the design of the ESS medium-beta cavity as an example of the BC use.

IMPROVEMENTS ON BUILDCAVITY

The code framework has not been modified, and a few additional functions were added. Figure 1 shows the interface of "Build MultiCell Cavity", in which the main improvements have been added. In the lower-left part of the screen, users can choose different end-cell types from the database. In the lower-right portion, the function "Generate ANSYS mesh file" is available after the cavity has been modelled with RF simulations by running "SuperFish Execution".

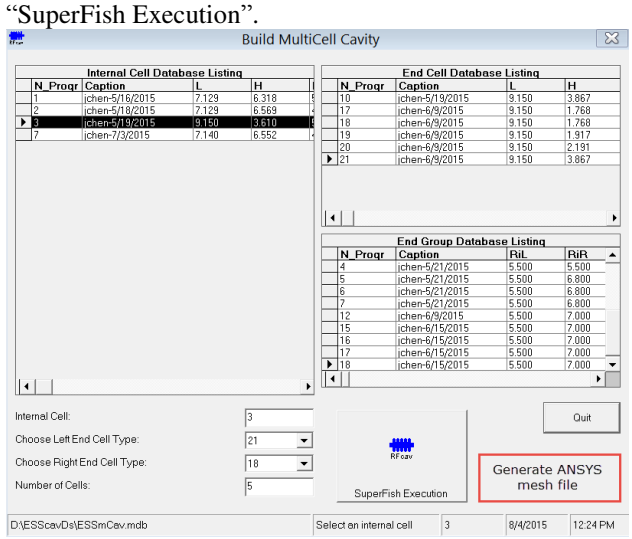

Figure 1: BC interface to generate a multi-cell cavity.

End-cell Types

After the definition of the inner cell geometry of a multicell structure, end-cells need to be tuned separately, with the proper inclusion of the attached beam pipes. The beam-pipe size affects the maximum surface fields, the cavity R/Q and the higher-order-modes (HOMs) propagation. Keeping the same radius of the beam tube as the inner cell irises leads to a high R/Q value, while enlarging the beam pipe is usually necessary at the fundamental coupler (FC) side to provide correct coupling and frequently performed at the opposite side in order to prevent HOM trapping in the structure and for the cavity interconnection.

Enlarging the beam pipe size with respect to the inner cells increases the volume of the capacitive region, therefore the tuning to the correct frequency requires a corresponding increase of its inductive region. There are three ways to accomplish this task according to the cell

A STUDY OF RESONANT EXCITATION OF LONGITUDINAL HOMS IN THE CRYOMODULES OF LCLS-II*

K.L.F. Bane§, C. Adolphsen, A. Chao, Z. Li, SLAC, Menlo Park, CA 94025, USA

INTRODUCTION

The Linac Coherent Light Source (LCLS) at SLAC, the world's first hard X-ray FEL, is being upgraded to the LCLS-II. The major new feature will be the installation of 35 cryomodules (CMs) of TESLA-type, superconducting accelerating structures, to allow for high rep-rate operation. It is envisioned that eventually the LCLS-II will be able to deliver 300 pC, 1 kA pulses of beam at a rate of 1 MHz.

At a cavity temperature of 2 K, any heat generated (even on the level of a few watts) is expensive to remove. In the last linac of LCLS-II, L3—where the peak current is highest—the power radiated by the bunches in the CMs is estimated at 13.8 W (charge 300 pC option, rep rate 1 MHz) [1, 2]. But this calculation ignores resonances that can be excited between the bunch frequency and higher order mode (HOM) frequencies in the CMs, which in principle can greatly increase this number. A. Sukhanov, et al, have addressed this question for the LCLS-II in a calculation—where they make assumptions, including a cavity-to-cavity mode frequency variation (with rms 1 MHz)—to end up with a conservative estimate of 10^{-3} probability of the beam losing an extra watt (beyond the non-resonant 13.8 W) in a CM [3].

In the present work we look at the problem in a different way, and calculate the multi-bunch wakefields excited in a CM of LCLS-II, in order to estimate the probability of the beam losing a given amount of power. Along the way, we find some interesting properties of the resonant interaction. In detail, we begin this report by finding the wakes experienced by bunches far back in the bunch train. Then we present a complementary approach that calculates the field amplitude excited in steady-state by a train of bunches, and show that the two approaches agree. Next we obtain the properties of the 450 longitudinal HOMs that cover the range 3–5 GHz in the CMs of LCLS-II, where we include the effects of the inter-CM ceramic dampers. At the end we apply our method using these modes. More details can be found in Ref. [4].

Selected beam and machine properties in L3 of LCLS-II, some of which we use in calculations, are given in Table I.

MULTI-BUNCH WAKE

Consider a train of equally spaced bunches, each with charge q, moving at the speed of light c and exciting a cavity longitudinal HOM defined by wavenumber k and loss factor $\varkappa$ [$= \frac{1}{4}ck(R/Q)$]. If the quality factor Q is infinitely large, the voltage loss of bunch n to the mode is given by

$$\Delta V_n = 2q\varkappa\left(\frac{1}{2} + \sum_{n'=1}^{n-1} \cos k(s_n - s_{n'})\right), \qquad (1)$$

where s_n is position of bunch n within the train, with a larger number representing a position further toward the back.

If the bunch spacing is an integer multiple of the mode wavelength, then $\Delta V_1 = q\varkappa$, $\Delta V_2 = 3q\varkappa$, ..., $\Delta V_n = 2q\varkappa(n - \frac{1}{2})$, which means that, on resonance, the loss grows linearly with bunch number.

With finite (but large) Q, the loss at bunch n becomes

$$\Delta V_n = 2q\varkappa\left(\frac{1}{2} + \sum_{n'=1}^{n-1} \cos k(s_n - s_{n'})\, e^{-\frac{k(s_n - s_{n'})}{2Q}}\right). \qquad (2)$$

The terms in parenthesis—which we call the *normalized loss*—can be written as

$$h(n) \equiv \frac{1}{2} + \mathcal{R}\mathrm{e}\left[e^{-\alpha}\frac{1 - e^{-(n-1)\alpha}}{1 - e^{-\alpha}}\right], \qquad (3)$$

where $\mathcal{R}\mathrm{e}(z)$ means take the real part of z; and $\alpha = (\frac{1}{Q} - 2i)\pi\nu$, with the tune $\nu \equiv f/f_0 = ck/(2\pi f_0)$ and f_0 is the bunch frequency. For example, with $f \approx 4$ GHz and $f_0 = 1$ MHz, the tune $\nu \approx 4000$. Note that h is normalized so that for the case of no multi-bunch wake effect (the single bunch case), $h = \frac{1}{2}$.

The LCLS-II bunch trains are very long (at $f_0 = 1$ MHz a million bunches pass by per second). For any mode with finite Q the wake eventually settles to a steady-state solution. [This happens for $n \gg 1/\mathcal{R}\mathrm{e}(\alpha)$; with *e.g.* $f = 4$ GHz, $f_0 = 1$ MHz, $Q = 10^7$, this requires only that $n \gg 800$.] Thus we are here really interested in the limiting loss $h_{lim} \equiv \lim_{n\to\infty} h(n)$. Letting $n \to \infty$ in Eq. 3, the normalized loss can be written as (we drop the subscript)

$$h = \frac{1}{2}\left(\frac{\sinh x}{\cosh x - \cos y}\right), \qquad (4)$$

Table 1: Selected beam and machine properties in the LCLS-II. Nominally the bunch charge is 100 pC, and the maximum charge is 300 pC (but with the same peak current).

Parameter name	Value	Unit
Charge per bunch, q	300	pC
Beam current, I	1	kA
Full bunch length, ℓ	90	μm
Repetition rate, f_0	1	MHz
Fundamental mode frequency, f_{rf}	1.3	GHz
TM0 cut-off frequency, f_{co}	2.94	GHz
Non-resonant HOM power loss, P_{sb}	13.8	W
Single bunch total loss factor, $\varkappa_{sb}$	154.	V/pC

* Work supported by the Department of Energy, Office of Science, Office of Basic Energy Science, under Contract No. DE-AC02-76SF00515.
§ kbane@slac.stanford.edu

ISBN 978-3-95450-178-6

RF SIMULATIONS FOR AN LCLS-II 3RD HARMONIC CAVITY CYROMODULE*

L. Xiao, C. Adolphsen, Z. Li, T. Raubenheimer
SLAC National Accelerator Laboratory, Menlo Park, CA 94025, USA

Abstract

The FNAL designed 3.9 GHz third harmonic cavity for XFEL will be used in LCLS-II for linearizing the longitudinal beam profile. The 3.9 GHz SRF cavity is scaled down from the 1.3 GHz TESLA cavity shape, but has a disproportionately large beampipe radius for better higher-order mode (HOM) damping. The HOM and fundamental power (FPC) couplers will generate asymmetric field in the beam region, and thereby dilute the beam emittance. Meanwhile, due to the large beampipe, all but a few of the HOMs are above the beampipe cutoff. Thus the HOM damping analyses need to be performed in a full cryomodule, rather than in an individual cavity. The HOM damping in a 4-cavity cryomodule was investigated to determine possible trapped modes using the parallel electromagnetic code suite ACE3P developed at SLAC. The RF kicks induced by the HOM and FPC couplers in the 3.9 GHz cavity were evaluated. A possible cavity-to-cavity arrangement is proposed which could provide effective cancellation of these RF kicks. In this paper we present and discuss the RF simulation results in the 3.9 GHz third harmonic cavity cryomodule.

INTRODUCTION

LCLS-II is a major upgrade add-on to the Linac Coherent Light Source (LCLS) at SLAC, by which its capabilities as a world-class discovery machine will be greatly advanced by the installation of a 4 GeV superconducting RF (SRF) linac and other instruments in the beamline [1]. The 3.9 GHz third harmonic cavity designed at Fermi National Accelerator Laboratory for the European XFEL will be used in the LCLS-II linac for linearizing the longitudinal beam profile. Two 3.9 GHz 8-cavity cryomodules will be installed between the 1.3 GHz linac segments L1 and L2.

The 3.9 GHz SRF cavity, shown in Figure 1, is scaled down from the 1.3 GHz TESLA cavity shape, but with a disproportionately large beampipe radius [2]. Strong multipacting was found in the curved leg region of the original loop-type HOM coupler design. Therefore, a new HOM coupler design with a probe plus a fundamental mode filter was adopted, illustrated in Figure 2 [3].

The HOM and FPC couplers in the LCLS-II 3.9 GHz linearizer cavities will induce field asymmetry, which will then kick the beam transversely and degrade the beam performance. The RF kicks produced by the HOM and FPC couplers in the original 3.9 GHz cavity design for XFEL have been evaluated [4, 5]. In this paper we will evaluate the RF kicks generated by the current HOM and FPC couplers in the 3.9 GHz cavity with an RF input coupling Q_{ext} of 1.3×10^7 for the FPC.

The HOMs have been studied experimentally and numerically for beam diagnostics in the 3.9 GHz modules [6, 7]. However, the RF simulations have been focused on finding the modes with higher R/Q in a cryomodule without damping information. In this paper, the HOM damping in a cryomodule is investigated to determine possible trapped modes in a 4-cavity cryomodule.

Figure 1: 3.9 GHz third harmonic cavity.

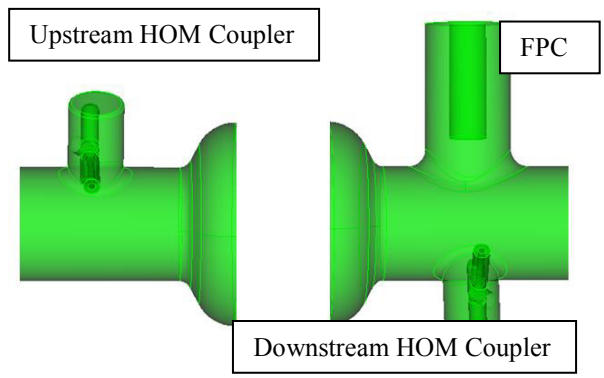

Figure 2: The upstream (left) and downstream (right) HOM/FPC couplers.

RF KICKS

RF field and kick simulations require high numerical solution accuracy to resolve the transverse components on the beam axis, which are usually about 2 or 3 orders of magnitude smaller than the accelerating field. The calculations were performed using the parallel electromagnetic code suite ACE3P, developed at SLAC. ACE3P is based on the high-order finite-element method, so that geometries of complex structures can be represented with high fidelity through use of conformal grids and high solution accuracies can be obtained using high-order basis functions in finite elements [8].

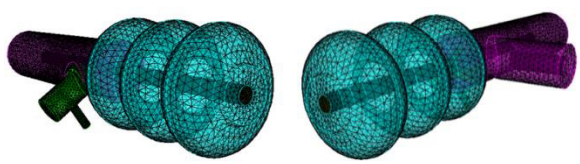

Figure 3: Upstream (left) and downstream (right) HOM/FPC coupler RF kick simulation models. Different colors represent different mesh qualities.

*Work supported by Department of Energy under contract Number DE-AC02-76SF00515.

INFN MILANO - LASA ACTIVITIES FOR ESS

P. Michelato#, M. Bertucci, A. Bignami, A. Bosotti, J. Chen, L. Monaco, M. Moretti, R. Paparella, P. Pierini, D. Sertore, INFN Milano – LASA, Segrate (MI), Italy
H. Zheng, IHEP, Beijing, China
C. Pagani, Università degli Studi di Milano & INFN Milano - LASA, Segrate (MI), Italy

Abstract

INFN Milano – LASA is involved in the development and industrialization for the production of 704.4 MHz medium beta (β = 0.67) cavities for the ESS project. In this framework, we are designing a medium beta prototype cavity exploring both Large Grain and Fine Grain Niobium for its production as well as a high beta (β = 0.86) Large Grain cavity. In the meanwhile, an activity is ongoing for upgrading the LASA test facility to be able to test these kind of resonators.

INTRODUCTION

INFN is involved in the ESS project [1], contributing in kind with the Proton Sources and LEBT (low energy beam transport) system, the Drift Tube Linac and 36 massive Niobium Medium Beta (β=0.67) Superconducting cavities. INFN - LASA, in the framework of the WP5, in collaboration with CEA Saclay, is in charge for the development and industrialization of the 36 medium beta Superconducting Cavities.

The cavities will be fully produced, chemically treated and prepared for RF measurements at the industry, and will leave the company equipped with the He tank, ready to be cold tested in a vertical test facility. The LASA responsibility includes the cold characterization tests that will be performed in a qualified large European infrastructure capable of delivery a suitable test rate. The cavities, after the successful cold test, will be delivered to CEA Saclay for the string assembly and its integration in the cryomodule. The delivery of the first three cavities is scheduled for the end of 2017. The foreseen delivery rate for the series cavities is at least of one cavity per week, in order to comply with the present Project installation schedule.

Our strategy for the ESS medium beta cavities production is based on the design and construction of two "CEA design plug-compatible" medium beta cavity prototypes, employing both Large Grain (LG) [2] and Fine Grain (FG) Niobium. These cavity prototypes will be fully treated by the industry in order to qualify the production and treatment infrastructures for the series. This prototypical activity will allow us to carefully prepare, analyse and optimize procedures and develop tools that will be needed for the series production. In fact up to now no ESS cavity has been ever fully treated in an industrial infrastructure capable of delivery the needed production rate. Moreover, the possibility to compare the performances of the two medium beta cavities, based on the same geometry, but produced with different materials will be of great scientific interest for future superconducting linac based projects.

We intend also to design and build one prototype of a High Beta cavity (β=0.86) for ESS, using the same LG material which is already available for the medium beta cavities. Three prototypes will be then built: two medium beta cavities (one FG and one LG) and one LG High beta.

CAVITY PROTOTYPING

The cavity prototypes we are developing, have to be fully "plug compatible" with the CEA existing design and fulfil the interfaces as defined and documented by ESS. These interfaces are provided in order to fit the cryomodule, power coupler and tuner already developed by CEA for ESS.

For the medium beta superconducting cavities, the strategy, we followed, is based on an integrated approach where the electromagnetic and mechanical design are developed iteratively.

We explored two different possible cavity designs. The first one, identified as "Type 1", is characterized by an asymmetric structure, with beam pipe tubes with two different diameters: a large tube diameter on the coupler side and a smaller diameter tube for the other side. This geometry is inspired by the SNS structures [3]. The second design, identified as "Type 2", is instead a symmetric structure with tubes of the same diameter on both sides of the cavity. Figure 1 shows a sketch of the "Type 2" cavity.

Parameters of the two cavity designs are presented in paper THPB006 [4] while HOM calculations are discussed in paper THPB004 [5], both at this Conference. Mechanical analysis, for the final optimization of stiffening ring position, Lorentz force detuning, vacuum sensitivity, natural frequency evaluation, etc. is currently progressing with the development of the RF design.

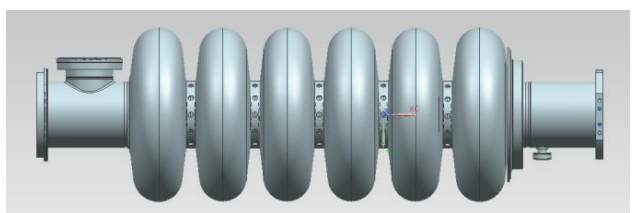

Figure 1: Sketch of the "Type 2" medium beta cavity.

Paolo.Michelato@mi.infn.it

ISBN 978-3-95450-178-6

SUPERCONDUCTING TRAVELLING WAVE ACCELERATING STRUCTURE DEVELOPMENT*

Roman Kostin#, Pavel Avrakhov, Alex Didenko, Alexei Kanareykin,
Euclid Techlabs, LLC, Solon, Ohio, USA
Nikolay Solyak, Vyacheslav Yakovlev, Timergali Khabiboulline, Yuriy Pischalnikov
Fermilab, Batavia, IL 60510, USA

Abstract

The 3 cell superconducting TW accelerating structure was developed to experimentally demonstrate and to study tuning issues for a new experimental device - the superconducting traveling wave accelerator (STWA), a technology that may prove of crucial importance to the high energy SRF linacs by raising the effective gradient and therefore reducing the overall cost. Recently, a STWA structure with a feedback waveguide has been suggested. The structure was optimized and has phase advance per cell of 105° which provide 24% higher accelerating gradient than in SW cavities. Also STWA structure has no strong sensitivity of the field flatness and its length may be much longer than SW structure. With this presentation, we discuss the current status of a 3-cell L-band SC traveling wave along with the analysis of its tuning issues. Special attention will be paid to feedback loop operation with the two-coupler feed system. We also report on the development and fabrication of a niobium prototype 3-cell SC traveling wave structure to be tested at 2°K in fall 2015.

INTRODUCTION

Accelerating gradient in RF cavities is one of the most important parameter of particle accelerator. It determines particle energy and accelerator length which is crucial for multi-kilometres accelerators such as International Linear Collider (ILC) [1,2]. The cost of this project highly depends on it. In order to reduce the cost with determined particle energy one should have a greater accelerating gradient. TESLA style superconducting standing wave (SW) cavity (180 degree phase advance per cell) is considered to be used as a current ILC design. Accelerating gradient shows the efficiency of acceleration and includes the multiplication of electric field gradient in a cavity and transit time factor which is around 0.7 for 180 degree phase advance. Standing wave cavities length is restricted to 1 meter in order have field flatness degradation less than 5% because of strong dependence on the cavity length. Thus, there is a gap between cavities (220 mm) which reduces accelerating rate by 22%. Superconducting traveling wave accelerating structure was proposed before in our previous publications [3, 4]. It requires feedback waveguide (WG) from one end of accelerating structure to another in order to make a closed loop for power distribution. Although, this cavity has more complicated design (additional waveguide) and tuning procedure (two tuners are required to tune operational frequency and compensate reflections along the loop) it has two urgent advantages. Firstly, field flatness has lower dependence on cavity length. If surface treatment and manufacturing process allow to build 10 meter long (cryomodule length) traveling wave cavity it will have better field flatness than 1 meter long standing wave cavity. This fact increases accelerating gradient by 22%. Secondly, traveling wave does not need to have 180 degree phase advance as it is required for standing waves cavities in order to have each cell filled with EM energy. Accelerating wave travels along the cavity together with accelerated particle. The geometry of TW cavity was optimized in order to obtain a higher accelerating gradient. 105 degree phase advance was found to have 24% higher accelerating gradient than in TESLA style SW cavity. The detailed information can be found in the following article [3, 4].

A 3-cell cavity was chosen to demonstrate traveling wave regime. It was optimized and is manufacturing in AES, Ink. This cavity will be processed and tested at Fermilab in the end of autumn 2015. 3-cell tuning studies were presented in publications [5, 6]. They are the following for -30 dB reflections: WG deformation range is 90 um; WG deformation step is 20 nm; longitudinal position range ±4 mm, and longitudinal position step 0.5 um. WG deformation range was extended to 1 mm after some investigations with tuner design and tuning procedure. WG wall deformations were calculated by Ansys and 15 kN force was found to be required for 1 mm wall deformation at 2 K.

3-CELL TRAVELING WAVE CAVITY TUNER DESIGN

As was discussed in [6] 3-cell traveling wave cavity tuner must have the possibility to move the point of force application to the WG. This is the main feature which distinguishes it from conventional SW cavity tuners and the first attempt to make a design became SW tuners review. Cryogenic stepper motor actuator for vacuum application with a reinforced axial load was found in one of Fermilab tuner design. It consists of 200/1 stepper motor, 50/1 gearbox and a shaft with 1 mm thread. That means that 1 step of this actuator produce a 100 nm longitudinal displacement. This motor can withstand 1.3 kN of axial load (Fermilab experience shows 4 kN of

*Work supported by US Department of Energy # DE-SC0006300
r.kostin@euclidtechlabs.com

ISBN 978-3-95450-178-6

A NOVEL DESIGN AND DEVELOPMENT OF 650 MHZ, β=0.61, 5-CELL SRF CAVITY FOR HIGH INTENSITY PROTON LINAC

Sumit Som*, Sudeshna Seth, Pranab Bhattacharyya, Aditya Mandal, Surajit Ghosh, Anjan Duttagupta, Variable Energy Cyclotron Centre (VECC), Kolkata, India

Abstract

DAE labs in India are involved in R&D activities on SRF cavity technology for the proposed high intensity proton linacs for ISNS/IADS and also FERMILAB PIP-II program under IIFC. VECC is responsible for design, analysis and development of a 650 MHz, β=0.61, 5-cell, elliptical cavity. This paper describes the novel design of the cavity, with different aperture and wall angle, having better field flatness and mechanical stability, reliable surface processing facility and less beam loss. The cavity geometry has been optimized to get acceptable values of field enhancement factors, R/Q, Geometric factor, cell-to-cell coupling etc. The effective impedance of transverse and longitudinal HOMs are low enough to get rid of HOM damper for low beam current. 2-D analysis shows no possibility of multipacting. However, 3-D analysis using CST Particle Studio code confirms its presence and it can be suppressed by introducing a small convexity in the equator region. Two niobium half cells and beam pipes for the single cell cavity have been fabricated. Measurement and RF characterisation of half cells, prototype 1-cell and 5-cell and also 1-cell niobium cavities have been carried out.

CAVITY DESIGN

The 650 MHz 5-cell elliptical cavities with geometric velocity factors $\beta_G = 0.61$ have been designed to optimize acceleration efficiency. The cavities are required to operate in superfluid helium at a temperature of around 2K, with accelerating gradient (E_{acc}) of 17 MV/m. The cell shape has been designed to minimize the peak surface magnetic (B_{peak}) and peak surface electric field (E_{peak}), to achieve the required gradient and minimum field emission, and also to minimize the effect of multipacting and to maximize R/Q and geometric factor (G) to have less RF power dissipation in the cavity wall and smaller heat load on the cryogenic system. RF design of the cavity has been carried out using 2-D Superfish and 3-D CST Microwave Studio [1]. Multipacting analysis of the cavity has been carried out for 650 MHz, β=0.61, superconducting elliptical cavity using 2-D code MultiPac2.1 [2] and 3-D CST particle studio code[1].

RF Design

The electromagnetic (EM) design parameters [3] of the optimized cavity geometry at 2K are summarized in Table 1 and electric field lines for five fundamental modes of the cavity have been shown in Figure 1 to Figure 3. The geometry of end cell of the cavity is optimized to have good field flatness over the five cells.

Table 1: Cavity EM Parameters

Parameters	Values
Frequency	650 MHz
Shape, No. of Cells	Elliptical, 5
Geometric beta (β_G)	0.61
Effective Length = 5*(βg.λ/2)	703.4 mm.
Iris Aperture	96 mm.
Wall angle for midcell	2.4^0
Wall angle for endcell	4.5^0
E_{peak}/E_{acc}	3
B_{peak}/E_{acc}	4.84
R/Q	296
G	200
Cell-to-cell coupling, K_{cc}	1.24%

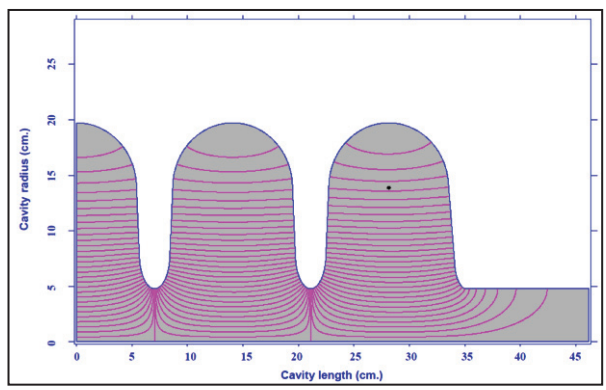

Figure 1: Accelerating mode (π-mode) at 649.99896MHz.

The 5-cell cavity structure has been analysed for transverse and longitudinal higher order modes and their effective impedances have been obtained as very low. No trapped modes with high effective impedance (as shown in Figure 4 and Figure 5) is observed for beam current up to a few mA.

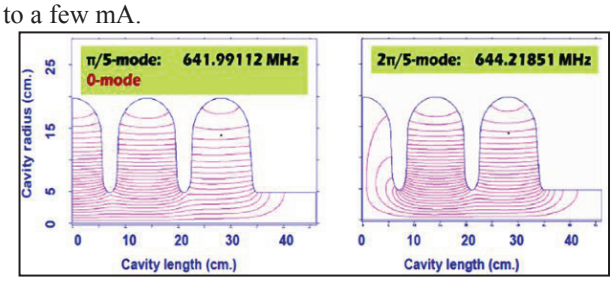

Figure 2: E-Field Profile at π/5-mode and 2π/5-mode.

*E-mail: ssom@vecc.gov.in

ISBN 978-3-95450-178-6

MECHANICAL OPTIMIZATION OF HIGH BETA 650 MHZ CAVITY FOR PULSE AND CW OPERATION OF PIP-II PROJECT*

Timergali N. Khabiboulline#, Ivan V. Gonin, Chuck Grimm, Andrei Lunin, Thomas H. Nicol, Vyacheslav P. Yakovlev, Fermilab, Batavia, IL 60510, USA
Pankaj Kumar, RRCAT, Indore, India

Abstract

The proposed design of the 0.8 GeV PIP-II SC Linac employs two families of 650 MHz 5-cell elliptical cavities with 2 different beta. The β=0.61 will cover the 185-500 MeV range and the β=0.92 will cover the 500-800 MeV range. In this paper we will present update of RF and mechanical design of dressed high beta cavity (β=0.92) HB650 optimized for pulse regime of operation at 2 mA beam current. In previous CW version of PIP-II project the mechanical design was concentrated on minimization of frequency shift due to helium pressure fluctuation. In current case of pulse regime operation the main goal is Lorentz force detuning minimization. We present the scope of coupled RF-Mechanical issues and their resolution. Also detailed stress analysis of dresses cavity will be presented.

INTRODUCTION

HB650 cavity originally was developed for CW operation. Current cryogenic power deficiency forced to consider switching of operation regime from CW to pulse mode in order to reduce cryogenic losses. During pulsed operation electromagnetic field energy stored in the cavity change with time and RF filed pressure to cavity walls also change causing resonance frequency modulation. Low beam current of 2 mA require relatively low RF power, therefore operating loaded Q of the cavity is high and operating frequency bandwidth 60 Hz is very narrow. Requirements for accelerating field amplitude 0.1% and phase 0.1° are very tight [1]. Lorenz force detuning (LFD) factor became a critical factor for cavity design optimization [2]. We introduce some modifications to dressed cavity design in order to reduce LFD coefficient. Also we need to keep very low sensitivity of operating mode resonance frequency to Helium pressure variations. Some modifications were added to simplify cavity tuner installation.

Cavity Mechanical Design Optimization

As mentioned above, the original design of the cavity and Helium vessel has been done for CW version of PIP-II project. For original design "as is" LFD~-1.33 Hz/(MV/m)^2 [3] i.e. 530 Hz of detuning for E_{acc}=20 MV/m. Fig. 1 shows the cavity wall deformation corresponded to E_{acc}=20 MV/m.

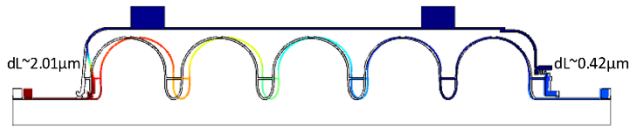

Figure 1: Wall deformation in original design.

On Fig. 1 are shown also 2 μm deformation of "coupler end" (left) and 0.42 μm of "tuner end" (right). Cavity sensitivity is ~ 160 Hz/μm. It means that Helium vessel walls deformations have 70% impact on the LFD value. Having the goal to minimize the Helium vessel modifications, the obvious way to significantly reduce the LFD value is to strengthen its walls. Also to reduce LFD coefficient, reducing process included optimization of position and number for stiffening rings of the cavity. One and two rings were considered with radius of rings as a parameter for optimization. Low sensitivity to helium pressure variations and external vibrations is still necessary parameter during optimization.

One of the possible solution to reduce the LFD is adding the second stiffening ring in the cavity. Figure 2 shows the 3D view of COMSOL solid model. Two rings with radiuses R1 and R2 used in optimization process. Radius of stiffening ring in the end groups are the same as in original design. In these simulations we keep beam pipe flanges fixed.

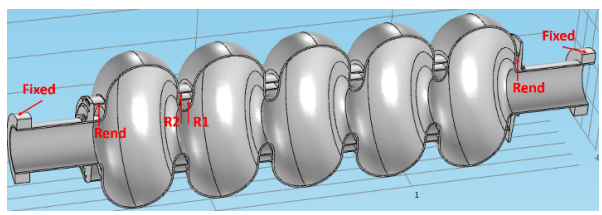

Figure 2: 3D view of COMSOL model with 2 rings.

In 2 rings option the cavity stiffness only depend on the position of the ring R2. Figure 3 shows the dependence of the stiffness vs. R2 radius. We decided to keep radius R2 not higher than 120mm to avoid the cavity over stiffening.

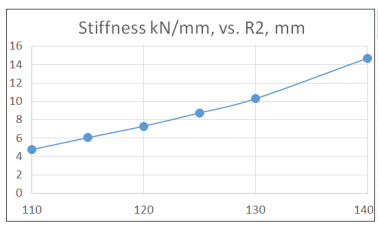

R2,mm	Stiffness kN/mm
110	4.75
115	6.2
120	7.3
125	8.75
130	10.3
140	14.7

Figure 3: Cavity stiffness vs. position if the ring R2.

* Operated by Fermi Research Alliance, LLC under Contract No. DE-AC02-07CH11359 with the United States Department of Energy.
# khabibul@fnal.gov

ISBN 978-3-95450-178-6

DESIGN OF A MEDIUM BETA HALF-WAVE SC PROTOTYPE CAVITY AT IMP*

A.D. Wu#, S.H. Zhang, W.M. Yue, Y.M. Li, T.C. Jiang, F.F. Wang, S.X. Zhang, L.J. Wen, R.X. Wang, C. Zhang, Y. He, H.W. Zhao,
Institute of Modern Physics, Chinese Academy of Sciences, Lanzhou, Gansu 730000, China

Abstract

A superconducting half-wave resonator has been designed with frequency of 325 MHz and beta of 0.51. The geometry parameters and the three shapes of inner conductors (racetrack, ring-shape and elliptical-shape) were studied in details to decrease the peak electromagnetic fields to obtain higher accelerating gradients and minimize the dissipated power on the RF walls. To suppress the operation frequency shift caused by the helium pressure fluctuations and maximize the tuner ranges, the frequency shifts and mechanical characters were simulated in the electric and magnetic areas separately. At the end, the helium vessel was also designed to keep stability as possible. The fabrication and test of the prototype will be complete at the beginning of 2016.

INTRODUCTION

Low beta superconducting Half-wave resonators have developed for Chinese Accelerator Driven Sub-critical System (C-ADS) at Institute of Modern Physics [1]. The production development of the 162.5 MHz half-wave resonators (squeezed) with the optimal beta of 0.101 have achieved great success and revealed excellent performance on the High Current Proton Superconducting Linac for C-ADS Injector II [2, 3]. Because of its simple structure, easy to fabrication and surface preparation, it attracts people to research the application on the medium beta section for the high power and continuous wave mode linear accelerators for the ADS [4].

RF DESIGN

The main task of RF design aims at reducing the normalized magnetic field and dissipated RF power. The RF property simulations were complete by the CST Microwave Studio Software [5].

An elliptical inner conductor was proposed to optimize the distribution of surface field, the Epeak/Eacc of 4.03 and Bpeak/Eacc of 7.08 mT/MV/m were achieved, where Eacc is accelerator gradient defined by the voltage gain over the efficient length of $\beta\lambda$.

EM Characters

The geometry of half wave transmission lines resonator, with TEM class structure, consists of the inner conductor and out conductor. The electric field concentrates on the center of inner conductor near the beam pipe, and magnetic field encircles around the inner conductor of two short dome areas, as illustrated in Figure 1.

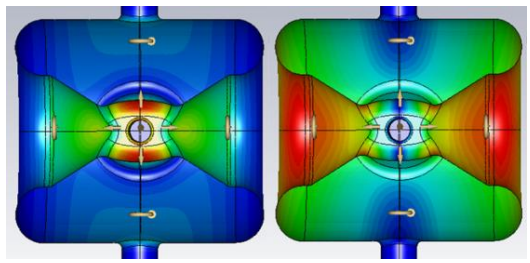

Figure 1: The surface electromagnetic field distribution of elliptical shaped center inner conductor HWR, the left for electric field and the right for magnetic field. The field strength decrease as the color changes from red to green to blue.

The RF property mainly depends on the shape of inner conductor and geometry parameters. In order to identify a proper shape which can obtain uniform distributed fields and higher shunt impedances effectively, three types of inner conductors, named after the cross profiles of inner center conductors as ring shaped (RS), race track (RT) and elliptical shaped (ES), were taken into optimizations, as shown in Figure 2. Additionally, the cavity aperture radius is 25 mm for the beam dynamic consideration.

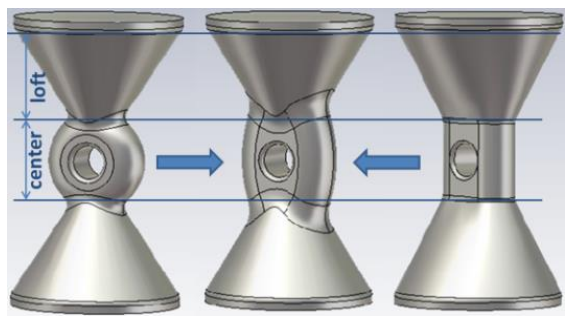

Figure 2: Three types of inner conductor, ring shaped (left), elliptical shaped (medium) and race track (right).

Effect of Inner Conductors

The effects of quadrupole asymmetry on the variously of inner conductor are analyzed for the low energy coaxial resonators, especially the compassion between the racetrack and ring shaped inner centre conductors [6, 7]. Beside the advantages of better acceleration field symmetry as the results of symmetrical geometry along with the beam axial line, the center conductor with ring shaped can also provide higher R/Q and lower

*Work supported by the Important Directional Program of the Chinese Academy of Sciences (Y115210YQO), 973 Project (Y437030KJO).
#antonwoo@impcas.ac.cn

ISBN 978-3-95450-178-6

A HIGHER HARMONIC CAVITY AT 800 MHz FOR HL-LHC

T. Roggen*†, P. Baudrenghien, R. Calaga, CERN, Geneva, Switzerland

Abstract

A superconducting 800 MHz second harmonic system is proposed for HL-LHC. It serves as a cure for beam instabilities with high beam currents by improving Landau damping and will allow for bunch profile manipulation. This can potentially help to reduce intra-beam-scattering, beam induced heating and e-cloud effects, pile-up density in the detectors and beam losses. An overview of the 800 MHz cavity design and RF power requirements is given. In particular the design parameters of the cavity shape and HOM couplers are described. Some other aspects such as RF power requirements and cryomodule layout are also addressed.

INTRODUCTION

For HL-LHC a mechanism to provide Landau damping is useful to increase the instability threshold of the future high intensity beams [1]. A superconducting (SC) 800 MHz second harmonic RF system, operating in conjunction with the existing 400 MHz accelerating LHC cavities (ACS) suits these requirements. In addition longitudinal bunch profiles can be flattened [2] or shortened [3, 4], and beam induced heating, e-cloud effects [5], Intra-Beam-Scattering (IBS), beam losses on the flat bottom [6] and pile-up density in the detectors can all be reduced. Each 800 MHz cavity is equipped with a proper Fundamental Power Coupler (FPC) and proper Higher Order Mode (HOM) couplers. An initial design study of the higher harmonic system was carried out in [7]. This paper summates on the 800 MHz cavity design and RF power requirements, notably the cavity shape design parameters and HOM coupler characteristics. RF power requirements and cryomodule layout are also addressed.

GENERAL CONSIDERATIONS

The SC 400 MHz ACS cavity cell and FPC were developed to handle 300 kW CW at 400.8 MHz. Two types of dedicated HOM couplers damp excited HOMs in the system: A narrow-band hook-type coupler and a broad-band probe-type coupler [8, 9]. The 400 MHz ACS system has proven its functionality and reliability during LHC run I, operating from 2008 onward with 1/2 the nominal LHC beam current. It therefore serves as an 800 MHz design reference by scaling the geometry with a factor 1/2. Subsequently the model is iteratively refined and verified to comply with the specifications. Substantial beam loading due to beam intensities of $2.2e^{11}$ p^+ and operation of the 400 MHz ACS system in full detuning mode will require a large amounts of 800 MHz RF power. 300 kW CW has to be considered as an upper boundary. It is therefore mandatory to keep the Fundamental Mode (FM) R/Q low and the voltage levels at a rather moderate 2 MV/cavity, in contrast with today's trend to reliably increase SC cavity voltage levels to 10 MV/m.

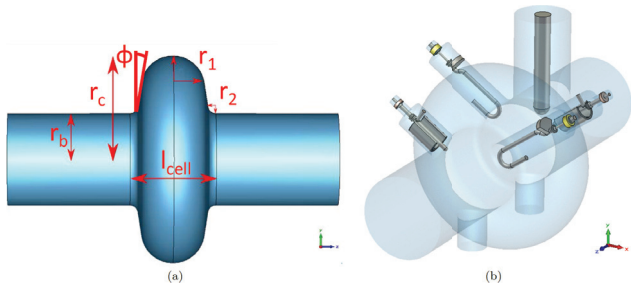

Figure 1: HL-LHC 800 MHz cavity: (a) Design parameters: cell length l_{cell}, beam pipe radius r_b, cavity height r_c, cavity cell radius r_1, iris radius r_2 and cavity wall angle ϕ. (b) RF cavity with installed HOM couplers and FPC.

Table 1: HL-LHC 800 MHz Cavity Design Parameters and Characteristics [7]

Parameter	Value [mm]	Spec	Value [unit]
l_{cell}	140	f	801.4 [MHz]
r_b	75	$R/Q^{(2)}$	45 [Ω]
r_c	169.3	E_p/V_{acc}	14.6 [m^{-1}]
r_1	52	H_p/V_{acc}	28.2 [mT/MV]
r_2	12.5	K	14.3 [kN/mm]
Φ	10°		

RF CAVITY

To ensure sufficient separation between the FM and first two HOM frequencies TE_{111} and TM_{110} (important for FM rejection in the HOM couplers) but simultaneously guarantee sufficient margin for mechanical tuning, the 800 MHz cavity wall inclination was reduced to 10° by shortening the cavity length l_{cell} from 160 mm to 140 mm. The fully parametrised model in CST Studio Suite (Fig. 1a) preserves the 400 MHz cavity wall thickness of 2.9 mm to withstand similar liquid helium pressure, including pressure fluctuations. The choice of l_{cell} originates from the sensitivity studies performed in [7], ensuring separation of the HOM frequencies and a more pronounced R/Q increase with respect to B_p/V_{acc}. Finally r_c was adjusted to have the FM resonating exactly at 801.4 MHz (Table 1). The R/Q analysis is performed along the central beam line within a 4 cm^2 area and shows increased $R/Q_\perp$ for the TE_{111} mode (2.34 Ω) and TM_{110} mode (13.6 Ω), two polarisations each. Their frequencies (1047 MHz and 1087 MHz respectively) are sufficiently separated from the FM to allow appropriate damping using dedicated narrowband hook-type couplers. In the beam pipe

* Fellowship co-funded by the European Union as a Marie Curie action (Grant agreement PCOFUND-GA-2010-267194) within the Seventh Framework Programme for Research and Technological Development.
† toon.roggen@cern.ch

[2] Circuit definition

BEAD-PULL MEASUREMENTS OF THE MAIN DEFLECTING MODE OF THE DOUBLE-QUARTER-WAVE CAVITY FOR THE HL-LHC *

M. Navarro-Tapia†, R. Calaga, CERN, Geneva, Switzerland

Abstract

A full-scale model of the double-quarter-wave (DQW) cavity towards the High-Luminosity Large Hadron Collider (HL-LHC) upgrade was built in aluminum to characterize the deflecting mode. Field strength measurements have been carried out for both the transverse and longitudinal electromagnetic fields, by using the bead-pull technique. A reasonably good agreement was found between numerical simulation and measurements, which confirm the reliability and accuracy of the measurements done.

INTRODUCTION

The novel machine configuration of the LHC, called High-Luminosity LHC (HL-LHC) [1], will rely on a number of innovative technologies, such as the use of superconducting deflecting cavities for beam rotation (crab cavities). These cavities are designed to deflect/crab the beam at 400 MHz [2], where the transverse kick results from the interaction of the particle with both the transverse electric and magnetic fields. The double-quarter-wave (DQW) cavity [3] is one of the candidates to be considered.

In order to assess the manufacturing process and validate the tolerances after fabrication, comprehensive radio-frequency (RF) measurements will be needed. This article reports the first RF tests that have been carried out on a full-scale aluminum prototype of the DQW cavity. The RF characterization of the fundamental deflecting mode, for both the transverse and longitudinal electromagnetic fields, has been done by means of bead-pull measurements.

PROTOTYPE DESCRIPTION

Geometry

Figure 1 is a schematic showing the cavity geometry, which can be seen as a double $\lambda/4$ line with symmetric poles –also referred to as "domes"– to create a transverse electric field and cancel any longitudinal field. The deflection in this case is mainly due to the strong transverse electric field between these parallel domes. The aperture of the domes is equal to the diameter of the incoming and outgoing beam pipes ($\varnothing$42 mm).

Figure 1 also shows the definition of the reference coordinate system that will be used in this paper. The beam-pipe axis is oriented along the $\hat{z}$-direction, so that the kick takes place in the $\hat{x}$-direction, following the orientation of the electric field lines there.

* The research leading to these results has received funding from the European Commission under the FP7 project HiLumi LHC (Grant agreement no. 284404), and under a Marie Curie action (Grant agreement PCOFUND-GA-2010-267194).

† maria.navarro-tapia@cern.ch

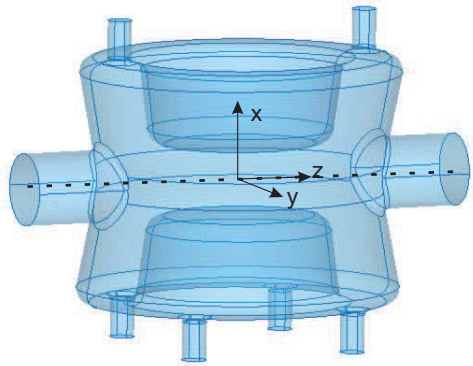

Figure 1: Schematic of the DQW cavity geometry and coordinate system definition.

The first higher-order mode is resonating at ~578 MHz, around 180 MHz apart from the fundamental mode. This mode only has a longitudinal component of the electric field on axis, which will be useful when calibrating the longitudinal form factor of any needle-like perturbing object.

A full-scale prototype of the DQW cavity –made out of aluminum– has been built at CERN to carry out the first RF measurements. Figure 2 shows a picture of the prototype, with the beam-pipe axis lying vertically. The drawings with the exact dimensions of this prototype can be found in [4].

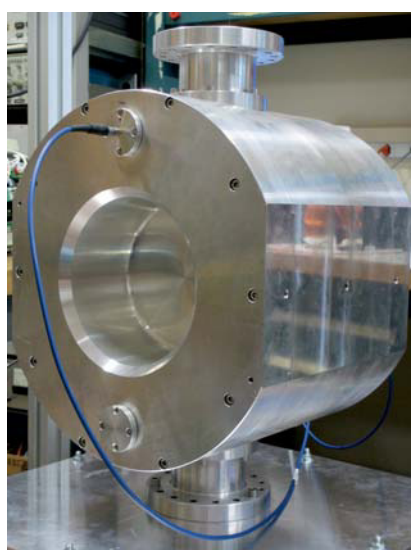

Figure 2: Full-scale aluminum prototype of the DQW cavity. The beam-pipe axis is lying vertically.

ISBN 978-3-95450-178-6

BALLOON VARIANT OF SINGLE SPOKE RESONATOR

Z. Yao#, R.E. Laxdal, V. Zvyagintsev, TRIUMF, Vancouver, B.C., Canada

Abstract

Spoke resonators have been widely proposed and optimized for various applications. Good performance has been demonstrated by many cold tests. Accompanying the great progress, the adverse impact of strong multipacting (MP) is also noted by recent test reports, consistent with modern 3D simulations. This paper will discuss MP behaviors in the single spoke resonator. In particular a phenomenological theory is developed to highlight the details of the geometry that affect MP. The analysis leads to an optimized geometry of a single spoke resonator defined here as the 'balloon geometry'.

INTRODUCTION

Spoke resonators have been wildly proposed as the accelerating cavity type of the low-medium energy section in several proton and ion LINAC projects like PIP-II [1], ESS [2], MYRRHA [3], CADS [4] and RAON [5]. Recently, the application of the spoke resonators is extended to electron LINACs like the compact ERL-LCS [6]. The additional focus on the spoke resonator has prompted further optimized geometries with low Epeak/Eacc values around 4 and Bpeak/Eacc values around 6 mT/(MV/m) [5, 7-12]. With these optimizations higher accelerating gradients are predicted to be achieved. To date an accelerating gradient of 22MV/m was demonstrated by Fermilab [13] in a low β resonator.

Despite the successes spoke resonators have a reputation as being sensitive to MP. Strong MPs during cavity cold tests were reported by ODU[14], IHEP[12], and Fermilab[15]. As spoke cavities are pushed to higher accelerating gradients and quality factors a deeper understanding of MP issues is required to avoid reduced performance during operation. MP is dependent on secondary electron resonance and the surface secondary electron yield (SEY) properties of niobium. In this paper we analyze the MP phenomenon and demonstrate the relationships between the local electro-magnetic (EM) field distributions and MP. A phenomenological theory is proposed that is then used to develop an optimized geometry for a single spoke resonator with regards to MP suppression.

CHARACTERISTICS OF MULTIPACTING

The common features of MP in the single spoke resonator are studied with CST [16]. For the generic study, we consider the simple spoke model shown in Fig. 1. The model is not optimized for any application or geometry β range. The cavity voltage excluding the transient time factor is used to define the RF field level. The resonance frequency is in the range 325…350MHz, a common frequency range for spoke resonator applications.

#zyyao@triumf.ca

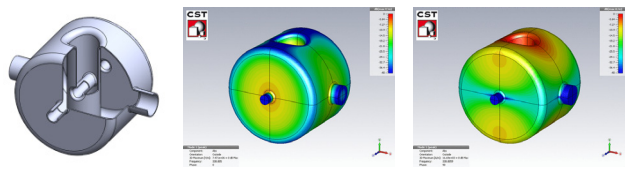

Figure 1: A simplified single spoke resonator model for a generic MP study with surface electric and magnetic field distributions.

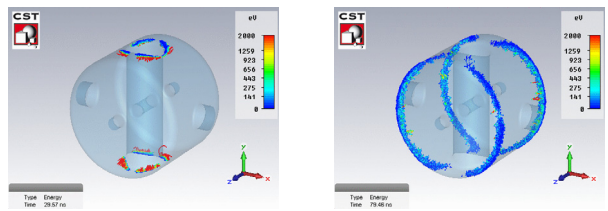

Figure 2: Typical secondary electron trajectories and resonance position of 1st order (left) and higher order (right) MPs in single spoke resonators.

Particle trajectories of various orders of MP are shown in Fig. 2. The secondary electron number will grow exponentially if MP happens in a stable resonance path. The exponential fit parameter is defined as growth rate of that certain order MP. The impact-varying growth rate is shown in Fig. 3 by solid lines as a function of cavity voltage for various orders. A positive rate indicates potential MP trajectories exist.

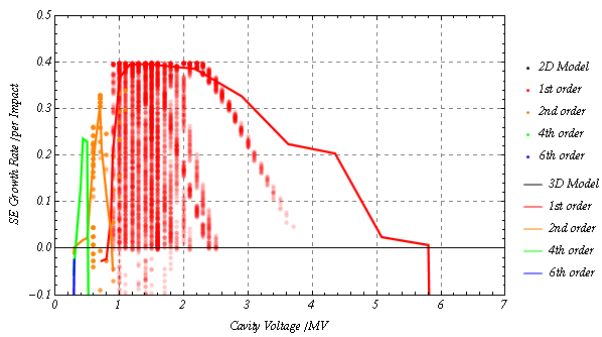

Figure 3: The comparison secondary electron growth rate diagram for the 3D CST simulation results (solid lines) and the 2D simplified single particle tracking model results (dots).

Some common features of MP in the single spoke resonators can be summarized: 1. Single spoke resonators have MP barriers in a wide range of field levels. (Fig. 3) 2. Higher order MP barriers exist at lower field levels, while lower order ones are at higher field levels. (Fig. 3) 3. Lower order MP has wider barriers. (Fig. 3) 4. 1st order MP locates at the spoke roots, while higher order ones locate at the joints of the end shells and the body cylinder.

A PRELIMINARY DESIGN OF A SUPERCONDUCTING ACCELERATING STRUCTURE FOR EXTREMELY LOW ENERGY PROTON WORKING IN TE210 MODE*

Z. Q. Yang, X. Y. Lu#, J. F. Zhao, D. Y. Yang, W. W. Tan
State Key Laboratory of Nuclear Physics and Technology, Peking University, Beijing, China

Abstract

For the application of high intensity continuous wave (CW) proton beam acceleration, a superconducting accelerating structure for extremely low β proton working in TE210 mode has been proposed at Peking University. The cavity consists of eight electrodes and eight accelerating gaps. The cavity's longitudinal length is 368.5mm, and its transverse dimension is 416mm. The RF frequency is 162.5MHz, and the designed proton input energy is 200keV. A peak field optimization has been performed for the lower surface field. The accelerating gaps are adjusted based on KONUS beam dynamics. Numerical calculation shows that the transverse defocusing of the KONUS phase is about three times smaller than that of the conventional negative synchronous RF phase. The beam dynamics of a 10mA CW proton beam is simulated by the TraceWin code. The simulation results show that the beam's transverse size is under effective control, while the increase in the longitudinal direction is more serious. The reason is that the minend gap is not a 0.5βλ structure, and the input phase should be carefully chosen, so that the beam can timely get re-bunched at the end of the minend gap. The EM design and dynamics simulation is under further optimized.

INTRODUCTION

The radio frequency quadrupole (RFQ) has been applied with great success to a variety of ion accelerators as a low energy front end [1-4]. Also, the crossbar H mode (CH) cavity, which is a multi-gap drift tube accelerating structure, has been demonstrated to be possible for superconducting operation [5-8]. By combining the advantages of the RFQ and the CH cavity, a accelerating structure working in TE210 mode, which is designed to operate in a superconducting state and to allow the acceleration of an intense proton beam with extremely low β at relatively high effective accelerating gradient, is proposed at Peking University. As can be seen from Fig. 1, the 4 vanes connected to the cavity wall are cut by elliptical cylinders, which results in longer electrical length to reduce the cavity's transverse dimension. The electrodes are connected by two stems with the vanes of the same electrical potential. The cavity consists of eight electrodes and eight accelerating gaps, including the gap between the first electrode and the cavity end plate, which is called the minend gap. Also, the electrodes are perpendicular to one another, so there is no quadrupole asymmetry effect, which may have an impact on the transverse beam envelope. The RF frequency of the cavity is 162.5MHz, and the designed proton input energy is 200keV. The cavity's longitudinal length is 368.5mm, and its transverse diameter is 416mm. By this arrangement, the TE110 mode, which may cause the problem of strong mixing between the quadrupole modes, is short circuited along the whole cavity. Overall, the cavity is topologically equivalent to a coaxial transmission line, terminated by a short at both ends. The magnetic field bunches up and down along the cut-vanes, while the electric field is mainly concentrated in the interelectrode capacitance area.

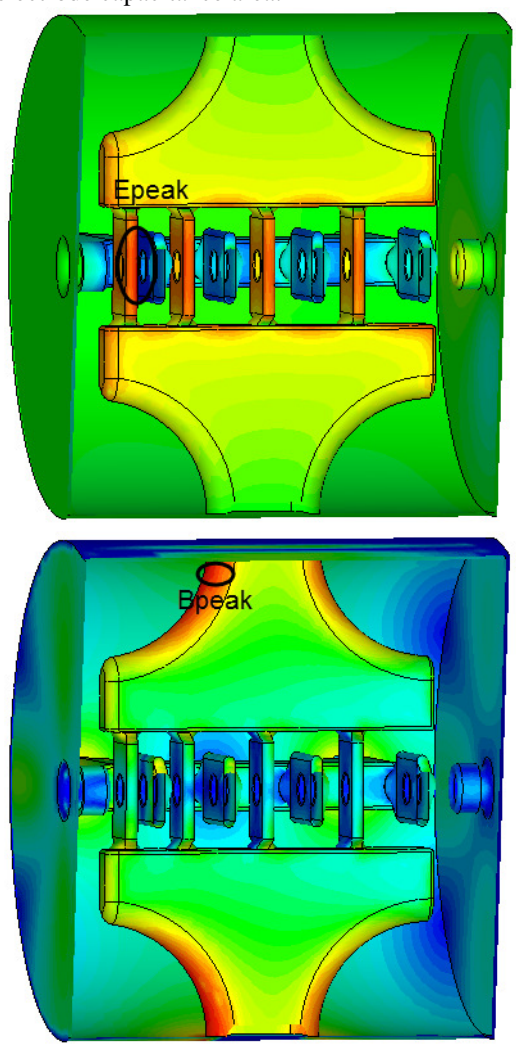

Figure 1: The surface EM fields of the cavity.

*Work supported by Major Research Plan of National Natural Science Foundation of China (91026001)
#E-mail: xylu@pku.edu.cn

ISBN 978-3-95450-178-6

THE STATISTICS OF INDUSTRIAL XFEL CAVITIES FABRICATION AT E. ZANON

M. Giaretta, A. Gresele, A. Visentin, E. ZANON SpA, via Vicenza 113, 36015 Schio, Italy,
A. Sulimov, J.-H. Thie, DESY, Notkestrasse 85, 22603 Hamburg, Germany

Abstract

Serial production of superconducting cavities for European-XFEL will be completed at E.ZANON by the end of 2015. For that reason we can summarize the results and present the statistics of industrial cavity fabrication. Many parameters have been traced during different steps of cavity production. The most interesting of them, as cavity length, frequency, field flatness and eccentricity, are presented and discussed.

INTRODUCTION

We will concentrate our attention on RF aspects of the statistics for XFEL cavities fabricated at E.ZANON, separating them to mechanical and RF characteristics. The idea of the RF measurements procedure and first results for XFEL cavities production were already published in [1, 2].

The results of all measurements are collected in XFEL DB [3] and were used for analyzes.

MECHANICAL CHARACTERISTICS

The shrinkage welding parameter (see figure 1) depends on the characteristics of niobium sheets from different suppliers: Plansee, Tokyo-Denkai and Ningxia. It has to be taken into account for estimation of final length, before cavity welding.

The mean shrinkage values for Tokyo-Denkai material is 0.43 mm, for Plansee and Ningxia is 0.41 mm.

The average shrinkage for all produced cavities is (0.419 ± 0.015) mm. It overlaps the average values for all materials supplier.

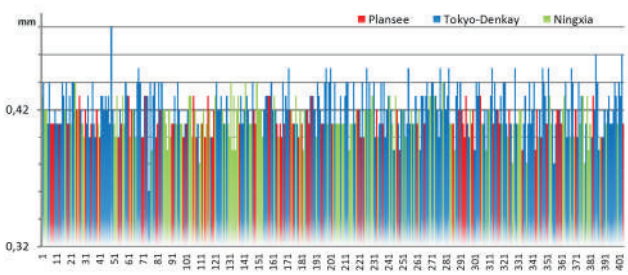

Figure 1: Shrinkage of equator welding for different materials.

The predicted lengths for cavities with helium tank and real values are compared on figure 2.

The difference between them should be 224.4 mm. It corresponds to: 2 mm length reduction during planned tuning and 222.4 mm (lengths of cavity tubes) due to different measurements (predicted length – between connecting flanges, real – between reference rings).

Average deviation relative planned difference is ± 0.4 mm. It's less than 15 % of the length tolerance.

Average length between reference rings of produced cavities is 1058.24 mm, as required by XFEL specification (1059 ± 3) mm.

One can see the average length reduction about 1 mm for the most part of the cavities, according the additional requirements from DESY.

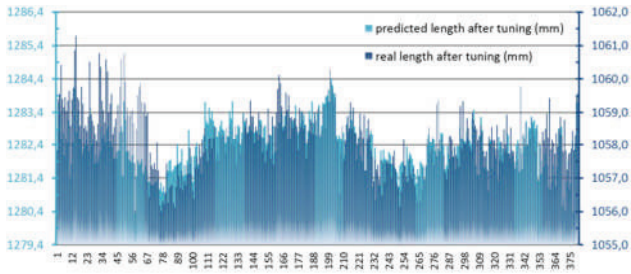

Figure 2: Predicted and real cavity lengths.

The next important mechanical characteristic for beam dynamics is cavity cell's eccentricity. It's used for cavity assembling into the accelerating module. The maximal from 11 eccentricity values (9 for cells and 2 for flanges) for each cavity are presented on figure 3.

Average maximal eccentricity value for cavities is 0.2 mm. So the cavities are twice straighter than it's required by XFEL specification.

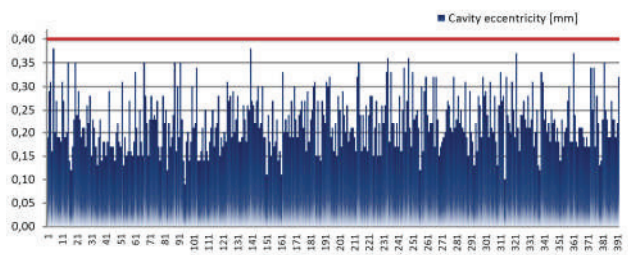

Figure 3: Maximal value of cavity eccentricity before welding in helium tank.

RF CHARACTERISTICS

The main RF characteristics for cavity production (TM010 pi-mode frequency and field flatness) are presented on figures 4 and 5.

After the cold measurements results for pre-series cavities the pi-mode frequency was increased, correcting the target values during the tuning. The further control and correction are planned.

ISBN 978-3-95450-178-6

EXCHANGE AND REPAIR OF TITANIUM SERVICE PIPES FOR THE EXFEL SERIES CAVITIES

M. Schalwat, A. Matheisen, A. Daniel, S. Saegebarth, P. Schilling; H. Hintz, K. Jensch, S. Barbanotti, DESY Hamburg, Germany
A.Schmidt, XFEL.EU GmbH, Hamburg, Germany

Abstract

Longitudinally-welded 72 mm ID service pipes (HSP) made from titanium grade 2 is used by the two suppliers of the helium tanks for the EU-XFEL accelerator. From the perspective of the PED DESY is legally designated as the manufacturer and is responsible for conformity to all relevant codes. During module assemblies at CEA Saclay the orbital welds of the interconnection bellows between cavities showed pores with dimensions outside the specifications, set by DESY. These welds needed to be redone which caused a project delay of several months. The X-ray examination of the HSP showed that the pipes already exhibited many pores in the longitudinal welds out-of- DESY spec and some also out of PED spec. These pores were most likely the main cause of the problems in the orbital welds. It was decided to replace the extremities of the service pipes with seamless titanium tubes both on "naked" helium tanks as well as on tanks with cavities already welded in. At DESY more than 750 service pipes were exchanged over a period of 2 years. The qualification of the repair line according to PED regulation and the prove with RF test at 2 K that the repairs do not influence the high performance of the s.c. cavities were done.

INTRODUCTION

Each of the 800 superconducting cavities, ordered at industry for the EU-XFEL cold Linac, is installed into an individual helium tank, made of titanium and built under the regulations of the Pressure Equipment Directive (PED).

The helium tanks (HT), for the EU-XFEL cavities are manufactured by two companies. One half is made by E. Zanon SpA in Italy for their in house cavity fabrication. The second half of tank production, with slightly different weld geometry at the connection to the conical disk, were made by the companies CSC and E. Zanon SpA, both located in Italy. These HT were welded to EU-XFEL cavities at Research Instrument [1].

The 2 phase helium pipe, named helium service pipe (HSP), is one part of the helium tank. At the beginning of HT production only one supplier of pipes was available for this the required diameter of the HSP. During module assembly at the EU-XFEL partner institute CEA-IRFU in Saclay (France) [2] the HSP were welded to an interconnecting titanium bellow. The Titanium interconnecting bellows, manufactured according to the PED regulations as well, are welded between each pair of consecutive cavities to form the helium supply line for the cavity string [3].

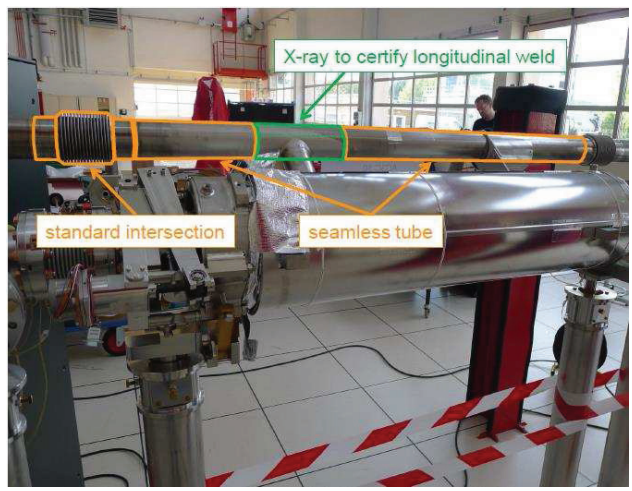

Figure 1: Sketch of the repair work, green part (Chimney) not exchanged during HSP repair.

All interconnection welds, made during module assembly, need to be X-rayed exanimated, since a pressure test cannot be applied any more to the cavity string at that stage of assembly.

During the first X-ray investigations (Fig. 2) it was found that many of the HSP longitudinal welds contained pores bigger than acceptable according to the DESY specifications. DESY took the decision to X-ray all the longitudinal welds of the HSP and remove all the pores bigger than 0.4 mm. These pores might be the origin of the problem for the pores, which were seen in the round welds at CEA. It was found that this required the exchange of all the pipe extremities (Fig. 1) with seamless pipes for about 620 already produced tanks. The exchange of the complete HSP with a seamless pipe was possible for about 180 tanks still under production.

ISBN 978-3-95450-178-6

UPDATE ON SRF CAVITY DESIGN, PRODUCTION AND TESTING FOR bERLinPro*

A. Neumann†, W. Anders, A. Burrill‡, A. Frahm, H.-W. Glock, J. Knobloch, O. Kugeler
Helmholtz-Zentrum Berlin, 12489 Berlin, Germany
G. Ciovati, W. Clemens, C. Dreyfuss, D. Forehand, T. Harris, P. Kneisel, R. Overton, L. Turlington
JLab, Newport News, Virginia, USA
K. Brackebusch, T. Galek, J. Heller, U. van Rienen
Rostock University, 18059 Rostock, Germany
E. Zaplatin
Forschungszentrum Jülich, 52425 Jülich, Germany

Abstract

The bERLinPro Energy Recovery Linac (ERL) is currently being built at Helmholtz-Zentrum Berlin in order to study the accelerator physics of operating a high current, 100 mA, 50 MeV low emittance ERL utilizing all SRF cavity technology. For this machine three different types of SRF cavities are being developed. For the injector section, consisting of an SRF photoinjector and a three two cell booster cavity module, fabrication is completed. The cavities were designed at HZB and manufactured, processed and vertically tested at Jefferson Laboratory. In this paper we will review the design and production process of the two structures and show the latest acceptance tests at HZB prior to installation into the newly designed cryo-module. For the Linac cavity the latest cavity and module design studies are being shown.

CAVITY TYPES FOR bERLinPro

Helmholtz-Zentrum Berlin is currently designing and building a high average current all superconducting CW driven energy recovery linac (ERL) as a prototype to demonstrate low normalized beam emittance of 1 mm·mrad at 100 mA and short pulses of about 2 ps [1]. The injector section (see Figure 1) consists of a 1.4-cell photo-injector cavity [2] using a high quantum efficiency normal conducting multi-alkali cathode and three high power 2-cell booster cavities of Cornell type [3]. The photo-injector will deliver 2.3 MeV kinetic energy, two booster cavities 2.1 MeV each whereas the third is operated in zero crossing to impose an energy chirp for bunch compression. This beam is fed via the merger section into the recirculator consisting of a string of three linac cavities, where the beam is accelerated to 50 MeV and in a second pass its energy is recuperated. According to their role in this machine the requirements and such the SRF properties of these three cavity types vary:

- **The Gun** cavity needs to deliver high on axis fields close to the cathode within the half-cell to suppress beam emittance dilution by space charge. Further an effective RF power to beam energy conversion at a field level as high as possible is required, as the cavity will experience the full beam-loading of 100 mA and the foreseen transmitters power and coupler power handling will be limited to 230 kW [4]. To achieve this, a high beam emission phase between laser pulse and RF field is mandatory and was achieved by having a $0.4\times\lambda/2$ half cell. This was optimized for low peak fields to avoid field emission, especially from the cathode area, as here emitted electrons have the highest probability to leave the structure.

- **The Booster** cavity design relies on the proven concept of Cornell's 2-cell injector cavity. The design was altered in order to house a pair of modified KEK c-ERL couplers since higher power than in the Cornell case and stronger coupling than in the KEK case were needed. This was achieved by introducing a golf tee shaped antenna tip which also helps in mitigating coupler kicks and related emittance deterioration [5] and by also increasing the one beam tube diameter to 88 mm.

- **The Linac** cavity needs to operate at high CW fields of E_{acc} of 20 MV/m, at best experiences no net beam-loading and can thus be operated at a narrow bandwidth, but experiences still the Wakes of two high current with respect to the $TM_{010\text{-}\pi}$ mode by π shifted beams. Thus this design needs to be a very good compromise with respect to both, low peak field ratios, a high impedance for the fundamental mode and maximum higher order mode (HOM) propagation and damping. Often these design features have opposite requirements with respect to the geometry. The cavity is thus a combination [6] of Cornell's mid-cell shape and the waveguide based HOM damping approach of JLab. Here, one port is sacrificed to install a variable coaxial coupler of TTF-III type.

Table 1 summarizes all RF design properties of the three structures and first measured properties in vertical (VTA) or horizontal (HTS) set up already after welding the helium vessel (HV) for the gun and booster cavities. The two latter were both fabricated and processed at JLab and delivered

* Work supported by German Bundesministerium für Bildung und Forschung, Land Berlin, and grants of Helmholtz Association
† Axel.Neumann@helmholtz-berlin.de
‡ Now at SLAC

ISBN 978-3-95450-178-6

WELDING A HELIUM VESSEL TO A 1.3 GHz 9-CELL NITROGEN DOPED CAVITY AT FERMILAB FOR LCLS-II*

C. Grimm, J. Kaluzny, D. Watkins
Fermi National Accelerator Laboratory, Batavia, IL 60510, U.S.A.

Abstract

Fermilab has developed a TIG welding procedure that is used attach a nitrogen doped 1.3 GHz 9-cell niobium (Nb) cavity to a titanium (Ti) helium vessel. These cavities will be used in the two prototype cryomodules for the Linac Coherent Light Source upgrade (LCLS-II) at SLAC National Accelerator Laboratory. Discussion in further detail will include setting up TIG welding parameters and tooling requirements for assembly and alignment of the cavity to the helium vessel. The weld designs and glovebox environment produce the best quality TIG welds that meet ASME Boiler and Pressure Vessel Code. The cavity temperature was monitored to assure the nitrogen doping is preserved, and RF measurements are taken throughout the process to monitor the cavity for excessive cell deformation due to heat loads from welding.

INTRODUCTION

The procedure for dressing a 1.3GHz cavity with a Ti helium vessel entails five steps with three welds in the following sequence: (1) Alignment of cavity and helium vessel on the assembly fixture, (2) Tack weld assembly in fixture and load into the welding glovebox, (3) circumferential TIG weld of the cavity to the helium vessel at the fundamental power coupler (FPC) end of the cavity, (4) circumferential TIG weld of the bellow cuff to the helium vessel at the tuner/field pick-up end of the cavity, (5) circumferential TIG weld of the bellow cuff to the Nb55Ti conical disk at the field pick-up/tuner end of the cavity. The welding procedure is followed by a vacuum leak check of the helium circuit, a pressure test to slightly above the maximum allowable working pressure (MAWP), and a follow-up vacuum leak check. The weld joint geometry is shown in Figure 1. Backing rings/ledges were incorporated on all TIG welds to avoid weld vapor deposition on the exterior surfaces of the cavity cells that could potentially degrade cavity performance.

TIG WELD QUALIFICATION

In order to qualify our TIG welding process, welders, and weld joints for ASME conformity, exact weld samples of each joint were fabricated. These samples were welded using the same process and environment as the real cavity/helium vessel. Upon completion, the samples were sent to an independent company for radiograph inspection and were processed in accordance with ASME Section VIII. Once the "Golden Sample" of each joint was achieved the next step in the assembly process was approved.

*Work supported by FRA under DOE contract DE-AC02-07CH11359.

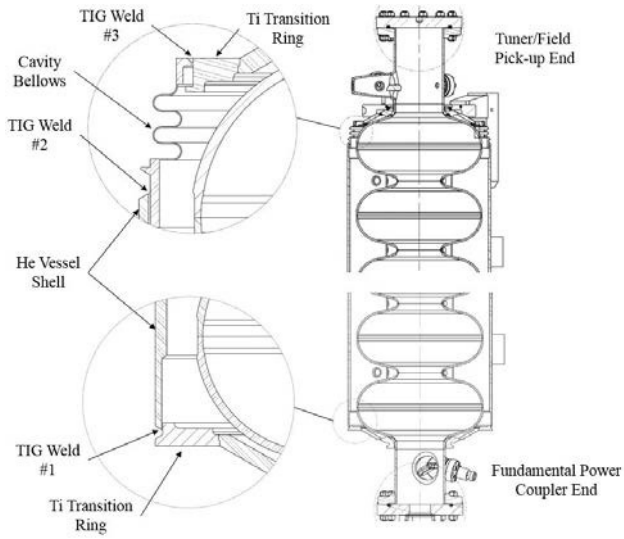

Figure 1: Section view of dressed cavity showing the weld joint geometry.

CAVITY TO HELIUM VESSEL ALIGNMENT

After all of the components are properly cleaned the cavity, helium vessel, and bellows are mounted in the assembly fixture shown in Figure 2. The assembly fixture function is similar to the design used to insert a coldmass into a vacuum vessel. The cavity is positioned on a long arm and is attached to the survey rings on the end groups.

The fundamental power coupler port on the cavity is aligned in the horizontal position and parallel to the moving cart using a bracket that engages the coupler flange. The helium vessel is mounted to the cart supported by the bearing lugs and travels along the rail track with bearing rollers. This design enables us to achieve the perpendicularity requirement of the coupler flange to the helium vessel bearing support lugs.

The helium vessel is rolled over the cavity until there is engagement of the vessel to the titanium transition ring on the FPC end of the cavity. The bellows at the tuner/field pick-up end (installed over arm prior to mounting the helium vessel) is then slid into place. Once the weld roots are established the fixture is locked to prevent the parts from shifting.

TIG WELDING

Before the aligned cavity and helium vessel can be moved into the glovebox, tack welds are added at the helium vessel joints to further lock the alignment. The

ESS MEDIUM BETA CAVITY PROTOTYPES MANUFACTURING

Enrico Cenni#, Christian Arcambal, Pierre Bosland, Guillaume Devanz, Xavier Hanus, Philippe Hardy, Vincent Marie Hennion, Fabien Leseigneur, Franck Peauger, Juliette Plouin, Dominique Roudier, CEA Saclay, Gif-sur-Yvette, France
Christine Darve, ESS-AB, Lund, Sweden
Gabriele Costanza, Lund University, Lund, Sweden

Abstract

The ESS elliptical superconducting Linac consists of two types of 704.42 MHz cavities, medium and high beta, to accelerate the beam from 216 MeV (spoke cavity Linac) up to the final energy at 2 GeV. The last Linac optimization, called Optimus+, has been carried out taking into account the limitations of SRF cavity performance (field emission). The medium and high-beta parts of the Linac are composed of 36 and 84 elliptical cavities, with geometrical beta values of 0.67 and 0.86 respectively. We describe here the procedures and numerical analysis leading from half-cells to a complete medium cavity assembly, which take into account not only the frequency of the fundamental accelerating mode but also the higher order modes near the machine line. The half-cell selection process to form dumb bells will be described, as well as the reshaping and trimming procedure.

INTRODUCTION

ESS [1] aim to be the most powerful neutron spallation source. It will be equipped with a 5MW proton linear accelerator [2] composed by a 50m long warm section (up to 90MeV of energy) and a 312m long cold section to reach 2GeV. In the cold section will be inserted spoke cavities and elliptical cavities, the former operating at 352.2MHz the latter at 704.4MHz. The elliptical cavities are present in two different families, one installed just after the spoke cavities section and designed to operate with proton at β=0.67 (medium beta) followed by a second group designed to operate at β=0.86 (high beta).

In this paper we will focus on the manufacturing of the medium beta cavities as designed to be installed in the Elliptical Cavities Cryomodule Technology Demonstrator (M-ECCTD) [3]. We are currently manufacturing 6 medium beta cavities, 4 of them will be installed in the cryomodule demonstrator.

Figure 1 shows a 3D drawing of the medium beta cavity model housed in the helium tank. The cavity has 6 cells, with two specific geometries, one for the central part (5 dumbbells) and one for the end groups. In table 1 are shown parameters relative to the designed cavity parameters obtained from RF calculations (COMSOL).

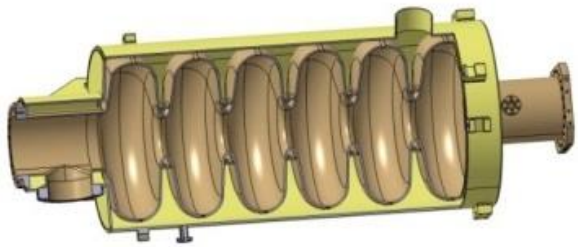

Figure 1: Medium beta elliptical cavity with helium tank.

Table 1: Medium Beta Cavity Design Parameters

Parameter	Value
Frequency	704.4 MHz
Length	1258.8 mm
# of dumbbells	5
Dumbbells length	142.8 mm
DB Trimming sensitivity	907 KHz/mm
Cavity tuning sensitivity	211 KHz/mm
Cell to cell coupling	1.2%

DIMENSIONAL & RF MEASUREMENTS SETUP

During the manufacturing the cavity components were controlled at each production step, from half cells to the complete cavity. Inspections are carried out by means of a 3D coordinates measuring machine (CMM) and RF measurements as shown in figure 2 and 3.

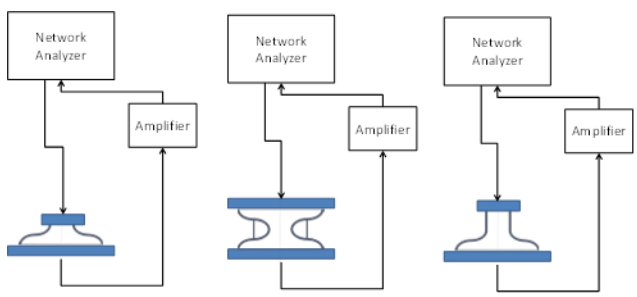

Figure 2: RF measurements set up scheme.

#enrico.cenni@cea.fr

ISBN 978-3-95450-178-6

MHI'S PRODUCTION ACTIVITIES OF SUPERCONDUCTING CAVITY

Akihiro Miyamoto, Hiroshi Hara, Kohei Kanaoka, Kazunori Okihira, Katsuya Sennyu, Takeshi Yanagisawa, Mitsubishi Heavy Industries, Ltd, Mihara, Japan

Abstract

Mitsubishi Heavy Industries, LTD. (MHI) has been developing manufacturing process of superconducting cavities. 4 topics of our recent activities, QWR, facilities of surface preparation, Superconducting RF electron gun and EBW of 4 cavities in a batch, are introduced in this report.

QWR AND CRYOMODULE

MHI has supplied superconducting RF cavities and cryostats for electron accelerators for various project such as STF and ERL project by KEK[1].

And now MHI is developing superconducting QWR cavity of heavy ion accelerator for the RIBF Upgrade plan [2] in collaboration with RIKEN and KEK.

RF frequency of prototype cavity is 75.5MHz. Cavity height is 1055mm, and diameter is 300mm. An exploded view of Superconducting QWR cavity is shown in Figure1.

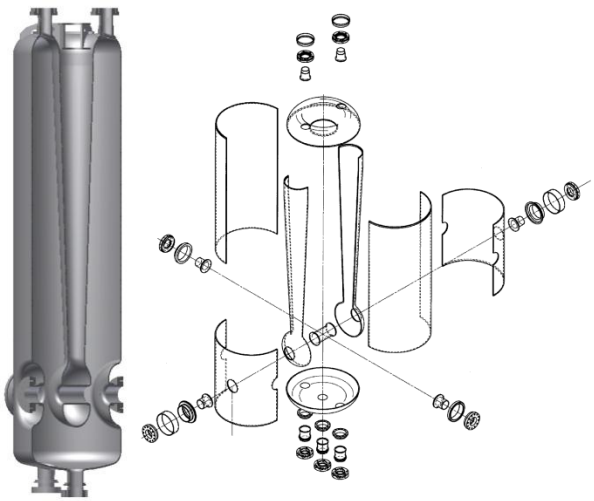

Figure 1: An exploded view of Superconducting QWR cavity.

Pure niobium is processed by machining or pressing. And each component is assembled by EB welding. In order to reduce the number of welding point, we have tested to press drift tube and stem in a one piece.

In order to avoid crack and wrinkle, adequate forming load and shape of a press mould are analysed using LS-DYNA code (See Figure 2 and Figure 3) .

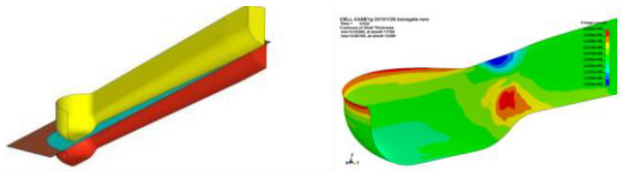

a) Model b) Contour plot of thickness

Figure 2: Forming analysis model and result.

As the result of press test, drift tube and stem are pressed successfully as a one piece. The precision of shape is below 0.5mm, and variation of thickness is below 15%.

a) Aluminum b) Niobium

Figure 3: Test piece of forming.

A plan of prototype cryostat is shown in Figure 4. In this cryostat, 2 superconducting RF cavities are installed. The operating temperature is 4.2K. Cryostat equips thermal shield for Helium 40K, and Helium 40K is cooled by small refrigerator.

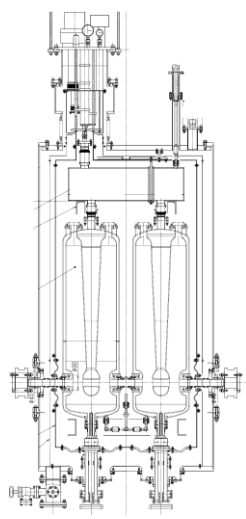

Figure 4: prototype of cryostat.

ISBN 978-3-95450-178-6

FABRICATION AND EVALUATION OF LOW RRR LARGE GRAIN 1-CELL CAVITY

Hirotaka Shimizu#, Hitoshi Inoue, Eiji Kako, Takayuki Saeki, Kensei Umemori, Yuichi Watanabe, Masashi Yamanaka,
KEK, Tsukuba, Japan

Abstract

Successive R&D studies of SRF cavities are ongoing at KEK by using existing facilities of Cavity Fabrication Facility (CFF) and other equipment of Superconducting Test facility (STF). Recently, there are studies on the low RRR of niobium material with high and uniform concentration of tantalum which could be used for the fabrication of high performance SRF cavity, and hence it could reduce the fabrication cost of cavities [1]. In order to confirm the advantage of the material, a large-grain single-cell cavity was fabricated at CFF/KEK with sheets sliced from a low RRR niobium ingot with high and uniform concentration of tantalum. The resistivity measurement of sample from sliced sheet showed the RRR value of 100, whereas it is about 400 for the nominal qualification of fine-grain sheets at KEK. The low RRR large-grain single-cell cavity was already fabricated at CFF/KEK. The quality control of the fabrication processes are well under control. Then several vertical tests of the cavity were done at STF/KEK. In this presentation, the results of the vertical tests are shown. The potential of the low RRR niobium material for SRF cavity are discussed.

INTRODUCTION

To accelerate charged particles with superconducting RF (SRF) system is a widely used scheme. Especially, for International Linear Collider (ILC), more than 17000 SRF cavities are required. According to a technical design report of the ILC, those cavities would be fabricated from high RRR (>300) niobium material by using of press forming and electron beam welding processes [2]. Improving fabrication methods and researching other types of material for the SRF cavity could reduce construction costs of the accelerator. Focusing on this point, successive R&D studies of SRF cavities are ongoing by using cavity fabrication facilities of Mechanical Engineering Center and other equipment of Superconducting Test facility in KEK [3].

Usually, SRF cavity fabrication starts from fine grain (50~150um) niobium materials. Those materials pass through electron beam melting process several times to guarantee own high purity. Instead of using the pureness, RRR of the niobium material is used as an index of quality. Niobium grain fineness of the material originates in a production process. Ordinary procedures include forging and rolling steps. During those processes, metal crystal was crushed into rather fine structures. From a workability viewpoint, this transformation sustains suitable properties of metals. So, using fine grain high RRR niobium is the world standard recipe to fabricate the SRF cavity, nowadays. But iterative electron beam melting and following forging/rolling processes push up the fabrication costs. One idea to escape from this problem is using large grain niobium material. A main difference between the large grain and the fine grain niobium material is attributed from skipping the final forging/rolling processes. During the electron beam melting, melted niobium gradually becomes colder in a melting pot, and recrystallization occurs. An aligned crystal structure in a grain boundary becomes visible size. If there's no cursing procedures like forging are followed, those aligned structures are kept and become large grain niobium materials. Usual grain size is about several centimetres. To compare with the fine grain case, skipping several processes could lead to cost reduction. A striking drawback is difficulties of fabrication originate in the large grain size. Beside the peculiar difficulties, the large grain niobium materials are studied as an alternative material of the fine grain for SRF cavity fabrications [1].

Whichever grain size is used for the cavity fabrication, the RRR value still remains as a free parameter. And naively thinking, it is thought that niobium materials with higher RRR value (>300) is preferable for the SRF cavity use. A well-known explanation about this is shown as a relationship between thermal conductivity of the cavity and the RRR value around 4.2K [4]. With this relation, the thermal conductivity of the cavity proportionally increases when the RRR of the used material increases. As a result, heat exhausting property of the cavity depends directly on the residual resistance ratio of the material. To achieve high RRR value, the electron beam melting must applied several times for one batch. In other words, cost-determining step is the electron beam melting process. From the cost reduction view point, then, the key issue is to reconsider how high the necessary RRR level is. On the other hand, there are proposals to use commercial basis niobium materials for SRF cavity use [5]. Niobium is belonging to the same family with tantalum in the periodic table. Thus, those two show quite similar physical and chemical properties. And both materials are mined the same lode. Tantalum is a typical valuable rare-metal. And during refining procedures, niobium as an impurity of tantalum would be concentrated. After all, niobium which includes high and

hirotaka@post.kek.jp

OPERATION EXPERIENCE WITH HALF CELL MEASUREMENT MACHINE AND CAVITY TUNING MACHINE IN 3 YEARS OF EUROPEAN XFEL CAVITY SERIES PRODUCTION

J.-H. Thie, A. Goessel, J. Iversen, D. Klinke, C. Mueller, A. Sulimov, D. Tischhauser
DESY, Hamburg

ABSTRACT

For the European XFEL superconducting cavity series production DESY supplied the two cavity vendors with two machines each, for production key functions: Half Cell Measurement Machine (HAZEMEMA) and Cavity Tuning Machine (CTM).

During three years of cavity series production a lot of experience was gathered about the influence of company specific surroundings and production quality on cycle times, machine drop outs, general stability time of machines and parts subject to wear.

Significant factors on cycle time for tuning operation like temperature stability and drift during tuning and measurements, precision of cell trimming before welding and tuning and geometrical factors are shown.

RF-aspects of tuning and production quality control such as additional measurements for TM011-mode to estimate quality of its damping are presented.

The performed full cavity RF measurement exceeds XFEL specifications and allows additional quality control on welding shrinkage stability and its homogeneous distribution.

INTRODUCTION

The correct mechanical trimming of cavity half cells, dumb bells and end groups is the precondition to reach the correct frequency and length of the welded and surface treated cavity.

For these key functions in total four machines, two HAZEMEMAs (Fig.1) and two CTMs (Fig.2) were supplied to the companies fabricating cavities. The general functionality of the machines was presented in previous papers [1, 2, and 3]. That is why no detailed information related to machinery functions will be given in this paper.

HAZEMEMA

For the previous prototype productions it was sufficient to perform all necessary half-cell and sub component RF measurements manually.

For the mass production all RF measurement and calculation functions were implemented into a highly automated machine. The HAZEMEMA design including control electronics, software and all interfaces with XFEL and companies databases was done by DESY for the European XFEL.

Figure 1: HAZEMEMA in use at the company.

For quality control and fulfilment of cavity RF requirements given by European XFEL specifications it is necessary to measure the RF properties of single half cells, completed dumb bells, pre turned end half-cell units, and complete cavity end groups before and after mechanical trimming.

Single cells are controlled by lots with a lot size of about 20%. All other named parts are measured 100%.

Based on 840 European XFEL cavities fabricated within 3 years, more than 2800 normal half cells, 5000 end groups and end group sub-components and around 14,000 dumb bell measurements have been performed with two HAZEMEMAs, i.e. 22,000 measurements in total.

HAZEMEMA SERVICE AND REPAIR CONCEPT

To ensure the required production quality, it is absolutely necessary to regularly control machine precision and RF calibrations. Therefor a regular service was scheduled every 6 months.

The performed checking of both machines did not reveal any relevant deviations from RF calibration.

Due to the tight European XFEL time schedules no production delays could be accepted. Both companies should have enough sub components on stock so that

ISBN 978-3-95450-178-6

RELEASE PROCESSES AND DOCUMENTATION METHODS DURING SERIES TREATMENT OF SRF CAVITIES FOR THE EUROPEAN XFEL BY USING AN ENGINEERING DATA MANAGEMENT SYSTEM

J. Iversen, J. Dammann, A. Matheisen, N. Steinhau-Kuehl
DESY, 22607 Hamburg, Germany

Abstract

For the European XFEL more than 800 superconducting cavities need to be treated. At least 65 quality documents per cavity have to be emitted and transferred to DESY by the vendor; two acceptance levels must be passed successfully to release a cavity for transportation to DESY. All quality documents, non-conformity reports and acceptance levels are automatically processed by using DESY's Engineering Data Management System (EDMS).

We summarize documentation methods, document transfer procedures, review and release processes; we describe the exchange of process information between customer and vendor; and report about experiences.

INTRODUCTION

Two companies, RI Research Instruments GmbH (RI) and Ettore Zanon S.p.A. (EZ) were contracted to fabricate and treat 800 1.3GHz superconducting cavities which are needed for the European XFEL Linac. Company EZ decided to apply the so-called "BCP Flash Scheme" for the 400 cavities contracted, while the company RI has chosen the "Final EP Scheme" to treat 400 cavities in accordance to DESY's Technical Specification for series surface and acceptance test preparation [1].

Due to the fact that such a huge amount of cavities never have been treated by the industry before in the history of SRF, DESY experts decided to implement an intensive Quality Management (QM) concept to ensure that all cavities will fulfil their requirements as specified.

REQUIREMENTS ON DOCUMENTATION

According to European Pressure Equipment Directive (PED) [2] the cavities for XFEL are pressure equipment and therefore specific formalities regarding documentation must be fulfilled. Main requirement is to ensure traceability of the delivered products, the cavity full equipped, through its complete fabrication and treatment history, back to the raw material and its inspection certificates.

It was decided that DESY wants to perform an external QC procedure in addition to the QA processes that must be performed as contracted by EZ and RI internally. That requires:

- structured and well organized repository of documents.
- a fast flow of QM documents to DESY.
- an acceptance procedure for checking the quality and releasing the cavities for AL1 [3], AL2 and AL3.

The EDMS was set up to fulfil all named requirements and was approved by TUEV Nord Systems GmbH as notified body according to PED.

QUALITY MANAGEMENT DOCUMENTS DURING SERIES TREATMENT

A dedicated selection of QC criteria for both process schemes was defined for each treatment sequences "BCP Flash" and "Final EP".

Technically all QM documents to be transferred to DESY's EDMS can be separated in two different kinds.

- Templates created by DESY using MS Excel and provided to the cavity supplier.
  Inspection sheets created based on these templates include data of test results on dimensional checks, RF-tests, etc. They are transferred by this type of documents into EDMS and forwarded to the European XFEL database for QC and statistical analysis.
- Company internal templates like leak tightness test reports, visual test reports, conformity certificates, etc.
  Documents created from these templates are accepted with its original file format or scanned to PDF and transferred into DESY's EDMS.

Depending on the treatment process scheme 63 or 65 QM documents for each single cavity had to be created and transferred into EDMS. At the end of the production the total number of QM documents will be higher than 51,000.

AUTOMATED DOCUMENT TRANSFER FROM CAVITY SUPPLIER TO DESY

Due to the high number of reports that have to be handed over to DESY during series treatment of cavities, an automated and complete paperless transfer of these QM documents was developed and implemented.

Both cavity suppliers are directly connected with their own Enterprise-Resource-Planning (ERP) system to the EDMS by using web services created by DESY (Fig. 1). That guarantees a fast and continuous flow of documents and data that follow "just in time" the treatment progress. On that way the base requirement to perform the external QC is fulfilled successfully.

A precise naming convention was created for all files which had to be transferred to DESY and for all QM documents which were created in the EDMS by the incoming files. The naming convention is the result of an

FREQUENCY MEASUREMENT AND TUNING OF A 9-CELL SUPERCONDUCTING CAVITY DEVELOPED WITH UK INDUSTRY

L Cowie, P. Goudket, A.R. Goulden, P.A. McIntosh, A.E. Wheelhouse, ASTeC, STFC, Daresbury Laboratory, Warrington, UK
B. Lamb, S. Postlethwaite, N. Templeton, Technology Department, STFC, Daresbury Laboratory, Warrington, UK
J. Everard, N. Shakespeare, Shakespeare Engineering Ltd, South Woodham Ferrers, Essex, UK

Abstract

As part of an STFC Innovations Partnership Scheme (IPS) grant, in support of enabling UK industry to address the large potential market for superconducting RF structures, Daresbury Laboratory and Shakespeare Engineering Ltd are collaborating to produce a 1.3 GHz 9-cell niobium cavity. This paper describes the procedures to ensure the cavity reaches the required frequency and field flatness. The frequency of each half-cell was measured using a custom measurement apparatus. Combined mechanical and RF simulations were used to compensate for cavity deformation during measurement. Results of Coordinate Measurement Machine measurements of one half-cell are presented. The same procedure will be used to trim the cells at the dumbbell stage, and the full 9-cell cavity will be tuned once welded.

INTRODUCTION

Daresbury Laboratory has been working with Shakespeare Engineering Ltd [1] for several years to enable the full fabrication of superconducting RF cavities in the UK. Previously the collaboration, along with Jefferson Laboratory [2], produced three single-cell niobium cavities, the last of these reaching a gradient of 40 MV/m after electro-polishing and centrifugal barrel polishing [3]. The current project is part of an STFC Innovations Partnership Scheme (IPS) grant to produce a 9-cell cavity, and has already accomplished the production of a copper 2-cell prototype cavity. A 9-cell Tesla style cavity has been designed, incorporating both spun beam pipes to remove the need for a seam weld, and steps on the equator and iris surfaces to facilitate alignment [4]. The non-welded parts for the 9-cell cavity have been delivered, and quality testing of the half-cells has been performed at Daresbury Laboratory.

HALF-CELL MEASUREMENT

Frequency Measurement

18 niobium half-cells have been received from Shakespeare Engineering. These consist of 8 female half-cells (CF1-8), 8 male half-cells (CM1-8), 1 male (EM1) and 1 female (EF1) end-cell, where the sex of the cell is defined by the alignment steps at the equator, which will be added to the cell at the dumbbell trimming stage. Currently each cell has extra length at the equator which will be trimmed to correct the frequency.

In order to measure the resonant frequency of each half-cell they were clamped between two copper plates with RF fingers flexed upward by a recessed O-ring as seen in Iversen et al [5]. RF antennas were then inserted at the top and bottom and an S21 measurement performed. Figure 1 shows the experimental setup, and Figure 2 shows the RF contact area in more detail.

Figure 1: Photograph showing the experimental arrangement used to measure the S21 of a half-cell.

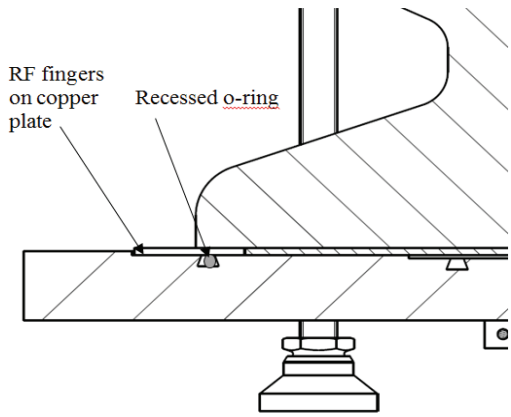

Figure 2: Detail of the RF contact area for S21 measurement.

Good RF contact, defined in this context as a bandwidth of 2 MHz or less, was achieved by the application of weight to the top of the test stand. The minimum weight possible, 3kg, was used in order to decrease deformation of the half-cell. The parallelism of

ISBN 978-3-95450-178-6

FABRICATION OF THE 3.9 GHZ SRF STRUCTURES FOR THE EUROPEAN XFEL

P. Pierini (INFN/LASA, Italy & DESY, Hamburg),
C. G. Maiano, E. Vogel (DESY, Hamburg),
M. Bertucci, A. Bosotti, J. Chen, P. Michelato, L. Monaco,
M. Moretti, R. Paparella, D. Sertore (INFN/LASA, Italy),
C. Pagani (Università degli Studi di Milano & INFN/LASA, Italy)
A. Gresele, M. Rizzi (Ettore Zanon, Italy)

Abstract

One batch of 10 cavities has been completed and eight structures have been installed in the 3.9 GHz cryomodule for the European XFEL (E- XFEL) Injector operation. A second batch of 10 RF structures for a spare injector module is under fabrication. The fabrication has been performed according to the European Pressure Vessel regulations, as needed for the E-XFEL operation. This paper describes the fabrication, quality control/assurance procedures and frequency preparation steps in order to achieve cavities at the correct frequency and length within the specifications.

INTRODUCTION

The E-XFEL injector includes a third harmonic section after the RF photocathode gun and the first 1.3 GHz accelerating module [1-2], in order for the linac to deliver beams with sufficiently low emittances for the production of 1 Å FEL light to the experimental users. The high quality beam is generated in the injector complex, where the 3.9 GHz section removes the non-linear distortions in the phase space after the first acceleration stage. The third harmonic system at 3.9 GHz of the European XFEL (E-XFEL) injector section is a joint INFN and DESY contribution to the project.

The 3rd harmonic section consists of a single module with 8 SRF cavities at 3.9 GHz and a quadrupole magnet package, currently being installed in the injector building [3]. A second module is in fabrication stage to provide the facility with a complete spare component in case of necessity.

This paper reports a short summary of the experience achieved with the production of pre-series [4] and two batches of the series cavities [5] for the 2 modules, and all the fabrication and preparation procedures followed to meet the specifications. The mechanical fabrication was planned according to the European Pressure Equipment Directive (PED) 97/23/EC [6], under the supervision of the TÜV-Nord acting as Notifying Body [7], according to the E-XFEL project specifications.

PED AND CAVITY PRODUCTION

All superconducting components of the E-XFEL linac need to comply with the European PED norms [8], under the pressure conditions set by the Project of a Maximum Allowable Working Pressure (MAWP) of 4 bar in the 2 K circuits. The most restricting procedure for Category IV vessels has been conservatively chosen, following the Module G certification path for the 3.9 GHz structures. As the cavity construction materials are not listed in the harmonised standards for the fabrication of pressure vessels, a Particular Material Appraisal (PMA) for the fabrication of the resonator has been issued by the Notifying Body, together with the design examination and the approval of fabrication drawings. Furthermore all standard provision for the fabrication of pressure vessels was followed, as the traceability of all subcomponents and components at all stages, starting from the raw material to the final cavities. All welds on pressure-bearing parts followed a weld qualification process (with the preparation of several weld specimens) with the Notifying Body and cavity fabrication was performed under its supervision, including a final pressure test of the helium tank space (up to 1.43 times the MAWP, according to the norm).

Even if a similar certification path has been followed for the 1.3 GHz cavities of the main linac [8], all formal certification steps (e.g. PMA, assessments, …) had to be officially released before the critical fabrication steps, leading in strong delays in the final cavity production.

DEVELOPMENT OF THE CAVITY FREQUENCY PREPARATION STRATEGY

High frequency superconducting RF structures have a strong sensitivity to geometry variations and preparation processes. Furthermore, the small size of the 3.9 GHz resonators require several adaptations to the processing infrastructure used for cavities of much larger volumes, to optimize and stabilize process parameters (e.g. BCP, HPR, …). As many of the sensitivity parameters depend on the actual fabrication and processing infrastructure, not all the FNAL 3.9 GHz experience for ACC39 could be applied without verification, in order to reach the desire frequency/length and performance goals.

A pre-series of 3 cavities have been launched early in the development phase in order to develop a fabrication strategy for the series, by cooperation with the industrial qualified vendor.

The series cavity for the 3.9 GHz section were fabricated, processed and tested according to the experience of the pre-series, integrating the slight

ISBN 978-3-95450-178-6

XFEL DATABASE STRUCTURE & LOADING SYSTEM

P.D. Gall, V. Gubarev, S. Yasar
DESY, Notkestrasse 85, 22607 Hamburg, Germany

Abstract

The XFEL database was designed to store cavity production, preparation, and test data for the whole LINAC on a very detailed level: from half cells up to module tests. To load this amount of data (more than 140 file types per cavity) in automatic regime a special Data Loading System was developed.

DATABASE STRUCTURE

The XFEL database for cavities and modules was developed at DESY using the ORACLE Relational Database Management System (RDBMS) [1].

According to the ORACLE RDMS strategy the structure is based on a set of tables. These tables are linked via 1to1 and 1toN relations.

The database is created to store data for more than 840 cavities from the serial production. These 9-cell cavities are produced by different European companies for the XFEL project.

In addition the database has to store data about 100 modules assembled at CEA and tested at DESY.

The content of the database is logically divided into 2 parts: cavity and module. The first one contains information about cavity production, measurements, and test results. In the module part the information about module structure, assembling information, and module test results are collected.

The XFEL database table structure repeats the structure of the real cavity production, preparation, testing, module assembling and module testing chain. Therefore the database is very flexible, and there is no problem to add new kinds of process steps.

With the help of the database the history of all steps of production are stored and can be traced very easily.

DATA SOURCES

The XFEL project is a European project, and therefore the database has to collect data from different sources in different countries:

- data about cavity production and preparation steps done at different european firms are transfered via the Engineering Data Management System (EDMS) used at DESY side;
- data about cavity measurements and tests in vertical cryostat done at the Accelerator Module Test Facility (AMTF) at DESY are collected by local database on AMTF side;
- data about module assembling process done at CEA SACLAY are transfered via EDMS and files;
- data about cavity retreatments and additional investigations done on DESY side are transfered via EDMS and files;
- data about module test results done at AMTF DESY are collected by a local database on AMTF side.

The access to EDMS is realized via JAVA API. All files of the format types XLS, XLSX, PDF, JPEG and ASCII are accepted.

The connection to AMTF is realized over a DB – DB connection via a set of views (virtual tables) to access different types of data and to trace the update status.

DATA LOADING SYSTEM

For the serial production and the big amount of data the data loading system must fulfil the following requirements:

- full automatic functionality
- checking data on consistency
- cataloging the data loading process
- include manual accessibility
- dynamically extendibility for new data types

The XFEL Data loading system fulfils all the requirements listed above. It works in this way:

- checking for new data every 30 minutes

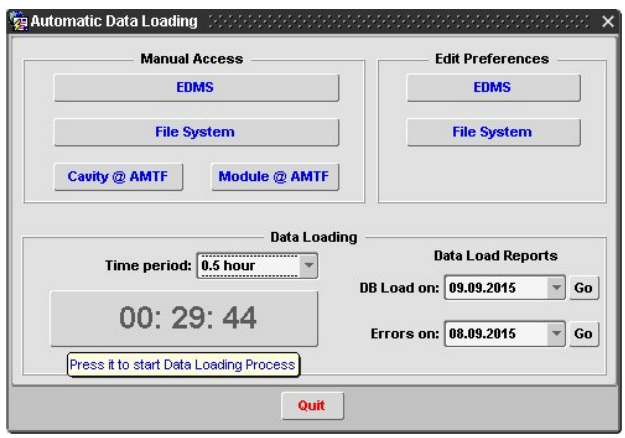

Figure 1: Data loading user interface

- daily catalogue for data loading and error reports

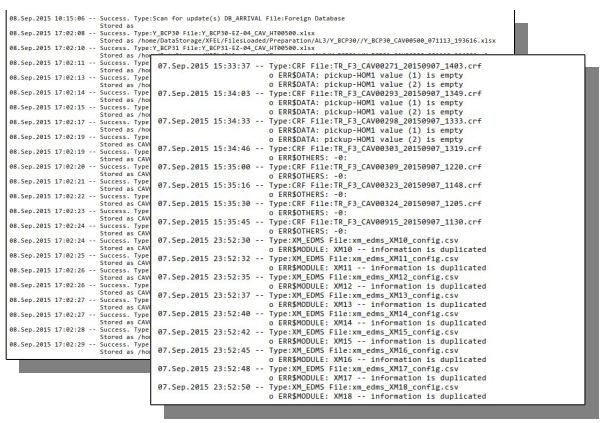

Figure 2: Data loading reports

XFEL DATABASE USER INTERFACE

P.D. Gall, V. Gubarev, D. Reschke, A. Sulimov, J.H. Thie, S. Yasar
DESY, Notkestrasse 85, 22607 Hamburg, Germany

Abstract

The XFEL database plays an important role for an effective part of the quality control system for the whole cavity production and preparation process for the European XFEL on a very detailed level. Database has the Graphical User Interface based on the web-technologies, and it can be accessed via low level Oracle SQL.

INTRODUCTION

Beginning from TTF a relational database for cavities was developed at DESY using the ORACLE Relational Database Management System (RDBMS) [1].

The database is dynamically accessible from everywhere via a graphical WEB interface based on ORACLE. At the moment we use the version Oracle Developer 10g Forms and Reports. The graphical tools are developed in Java.

The database is created to store data for more than 840 cavities coming from the serial production and about 100 modules. Therefore the main aim of the database is to store data about cavity production, cavity preparation, cavity measurement steps, assembling cavities in module, and module test results.

We have developed tools to analyse the data stored in the database for different groups of experts, which have access via WEB. Through the link http://xfel.desy.de/cavity_database you can enter the start page for the XFEL database Graphical User Interface (GUI, Fig. 1):

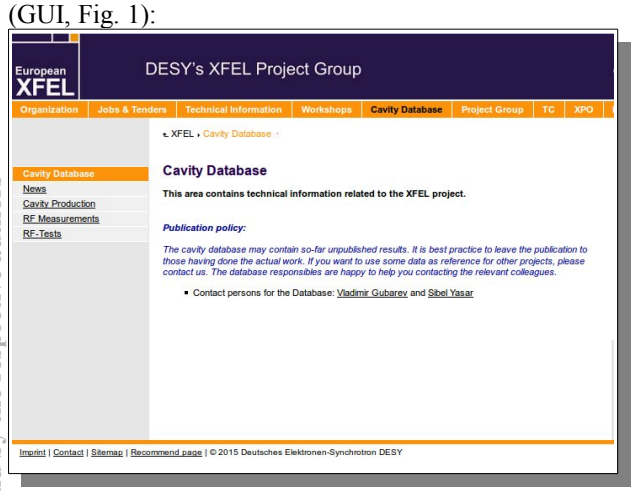

Figure 1: The XFEL database start page.

DATA PROTECTION

According to demands of production firms the grant system for the data access was designed. It is based on the group access for the different kind of information. People from the one group can have individual permissions.

Using this protection system we have divided all customers into different groups:

- RI group has permission to view production results from RI only and open information
- ZANON group has permission to view production results from ZANON only and open information
- DESY group has permission to view all results from all companies
- Not authorised people have access to the open information only

To get authorised access to the database one have to contact the responsible persons listed in the XFEL database GUI pages.

GRAPHICAL USER INTERFACE

The XFEL database GUI was developed to meet the requirements of experts involved. According to the people needs the GUI applications can logically be divided into groups:

- Cavity production control
- Cavity transportation control
- Geometry calculations for string assembly
- RF Test results in vertical cryostat
- Module Test results

Cavity Production Control

In general there exist 3 levels of the cavity production:

- Acceptance Level 1 (AL1):
  - Half cells mechanical properties
  - Half cells frequency properties
  - Dumb-bells mechanical properties
  - Dumb-bells frequency properties
  - End groups mechanical properties
  - End groups frequency properties
  - 3D-Shape measurement
  - Cavity structure
  - Cavity mechanical properties
  - Cavity frequency properties
- Acceptance Level 2 (AL2):
  - Cavity transfer measurements
  - Cavity eccentricity measurements
  - Cavity preparation steps (like BCP, EP, HPR...)
  - Cavity mechanical properties in tank
  - Cavity frequency properties in tank
- Acceptance Level 3 (AL3):
  - Further preparation steps
  - Cavity frequency check before transportation to DESY

ISBN 978-3-95450-178-6

HYDROFORMING OF LARGE GRAIN NIOBIUM TUBE*

A. Mapar, T.R. Bieler#, F. Pourboghrat, Michigan State University, East Lansing, MI 48824, USA
C.C. Compton, Facility for Rare Isotope Beams, East Lansing, MI 48824, USA,
J.E. Murphy, University of Nevada, Reno, NV, 89557, USA

Abstract

Currently most of Niobium (Nb) cavities are manufactured from fine grain Nb sheets. As-cast ingots go through a series of steps including forging, milling, rolling, and intermediate annealing, before they are deep-drawn into a half-cell shape and subsequently electron beam welded to make a full cavity. Tube hydroforming, a manufacturing technique where a tube is deformed using a pressurized fluid, is an alternative to the current costly manufacturing process. A whole cavity can be made from a tube using tube hydroforming [1,2].

This study focuses on deformation of large grain Nb tubes during hydroforming. The crystal orientation of the grains is recorded. The tube is marked with a square-circle-grid which is used to measure the strain after deformation. The deformation of the tube is going to be modeled with crystal plasticity finite element [3–5] and compared with experiments. This paper only covers the characterization of the tube and the hydroforming process.

INTRODUCTION

Large grain cavities often show better quality factor (Q) than their polycrystalline counterparts. This is due to having fewer defects per unit volume or area in the form of grain boundaries.

Seamless Nb cavities are more favorable than the welded ones, as hot spots are commonly correlated with the heat affected zone. Also, the absence of a weld potentially decreases the cost of manufacturing in the long run. Also the performance of a cavity potentially increases because the weld line is a possible source of contamination and other rare defects.

Tube hydroforming can be used to make cavity from a tube. Singer et al. [1,2] made seamless polycrystalline Nb tubes by spinning and flow forming of a disk. The tubes were then hydroformed into single-cell, or up to three-cell units. The initial values for hydroforming parameters were found from FEM simulation and were further tuned in experiments. The processing and properties of the seamless tube is critical to the success of the hydroforming process. Variations in properties of the tube such as the yield strength, thickness and grain size can result in failure of the tube or irregular final shapes [2].

*Work supported by the U.S. Department of Energy, Office of High Energy Physics, through Grant No. DE-FG02-09ER41638.
#bieler@egr.msu.edu

Large grain Nb is even more anisotropic than polycrystalline material. Therefore, a number of issues have to be addressed before the hydroforming of large grain Nb could be industrialized. Large grain seamless Nb tubes are not readily available in the market. Therefore, the first half of this paper focuses on developing a method to make large grain seamless Nb tubes and fully characterizing them. This prototype tube also provides essential data for comparing the experiment with numerical simulations using crystal plasticity models. The Second half of this paper investigates forming behavior of the tube under the hydroforming conditions.

The results of this study will be to be used as input to the crystal plasticity models developed in [4,5] that was published in SRF 2013 and this proceeding respectively. This series of studies will provide the foundation for designing a seamless large grain tube hydroformed cavity.

MAKING A LARGE GRAIN NIOBIUM TUBE

A polycrystalline Nb sheet 2 mm thick was used to make a Nb tube. The sheet was bent into a 38 mm (1.5 in) outer diameter tube and welded using full penetration electron beam welding. The tube then went through a special vacuum heat treatment to grow the grains. The heat treatment involved using a very high temperature vacuum furnace and moving a hot zone along the tube to encourage the growth of the grains in the axial direction. Figure 1 shows this tube, which is not perfectly straight. Also, the surface of the tube shows ledges and grooves that appeared to be grain boundaries. The black lines on the tube in Figure 1 trace these larger ledges and grooves. The surface of the tube also had smaller grain boundary ledge features shown in an enlargement of a portion of this tube.

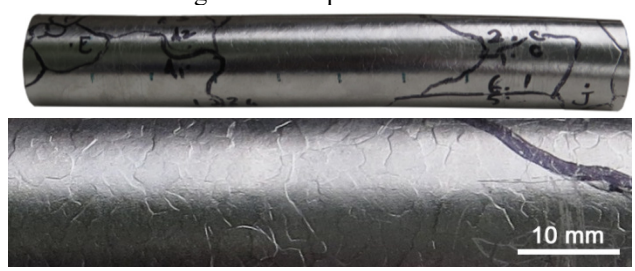

Figure 1: The large grain Nb tube. In addition to deeply grooved grain boundaries marked with black ink, the lower enlargement shows evidence for smaller grains with a few mm dimension at some point prior to growing the large grains.

ISBN 978-3-95450-178-6

HYDROFORMING SRF CAVITIES FROM SEAMLESS NIOBIUM TUBES

M. Yamanaka#, H. Inoue, H. Shimizu, K. Umemori, KEK, Tsukuba, Japan
J. A. Hocker, FNAL, Batavia, IL, USA
T. Tajima, LANL, Los Alamos, NM, USA

Abstract

The authors are developing the manufacturing method for superconducting radio frequency (SRF) cavities by using a hydroforming instead of using conventional electron beam welding (EBW). We expect higher reliability and reduced cost with hydroforming. For successful hydroforming, high-purity seamless niobium tubes with good formability as well as advancing the hydroforming technique are necessary. Using a seamless niobium tube from ATI Wah Chang, we were able to successfully hydroform a 1.3 GHz single cell cavity and obtained an E_{acc} of 36 MV/m confirming that the hydroforming technique developed at KEK is applicable for the SRF cavity.

INTRODUCTION

The major manufacture method for SRF cavities which have elliptical cell shape are the press forming of rolled niobium sheet to the cell shape and the assemble of them by a EBW. Although the inner surface of cavity should be smooth, the penetration welding is provided from outside of cavity because the electron gun of EBW is big, and a smooth rear-welding bead with small bump is required. This is very difficult welding work, which needs skills. Moreover, a chemical polishing of a groove before welding, a prevention of contamination during welding, and sometime a remove of defect occurred by welding as a post process, are required. The initial cost of an EBW machine is high and the EBW is the main factor of cost rise for cavity manufacture.

Although the welding is provided at the equator (maximum diameter) and the iris (minimum diameter) of cells where the magnetic and electric fields are largest respectively, there should be no bump like a welding bead ideally. To keep a high reliability of cavity production, very careful process control in the EBW is required. A hydroforming is one of a plastic working and applied to cavity fabrication instead of the EBW. This manufacture method is well known for a long time, and widely used for manufacture of automobile and hydraulic parts. The hydroforming involves expanding a tube with internal hydraulic pressure while simultaneously swaging it axially. The die is placed around the tube, which is formed along it. Singer has provided the study of applying the hydroforming to the cavity fabrication energetically at DESY. 1.3 GHz TESLA cavities were fabricated using a 150 mm inner diameter (ID) and 2.7 mm thickness seamless niobium tube, and the 9-cell cavities were manufactured by joining three 3-cell cavities by the EBW. The maximum accelerating gradient attained to 30 to 35 MV/m [1]. The series of research in DESY and activities at other laboratories are introduced in detail in Ref. [1], and please refer to it. KEK started the research of hydroforming since 1994. Fujino, et al. developed the seamless tube using a clad material, which joined thin niobium and fat copper sheets for the cost reduction, and manufactured 1-cell cavity by the hydroforming. The maximum accelerating gradient attained to 40 MV/m [2-4]. Afterwards, Ueno, et al. developed the necking and the hydroforming machines [5-6], and KEK can provide series of process from the seamless tube to finish the cavity in the laboratory.

It is necessary to manufacture more than 17000 1.3 GHz 9-cell cavities in the International Linear Collider (ILC) project. The cost reduction of cavity fabrication is indispensable subject. Its method by the press forming and the EBW using a high-purity (residual resistance ratio: RRR > 300) niobium is shown in the technical design report (TDR) completed in 2013 as the baseline design [7]. The authors are examining whether the cavity fabrication by the hydroforming can replace the baseline design method from the viewpoint of the cost reduction. The material is fixed as the high-purity niobium shown in the TDR. The above-mentioned method, which three 3-cell cavities are manufactured by the hydroforming and joining them by the EBW, is not sufficient for the cost reduction. The hydroforming 9-cell cavity from one long tube is significant. At present, this is not realized. The purpose of this study is the hydroforming 1.3 GHz 9-cell cavity and showing the performance of hydroformed cavity is equivalent to the cavity manufactured by the conventional method, then take a measure that the hydroforming is effective in the cost reduction. In this report, the result of manufacture of 1-cell cavity and the evaluation of performance for the first time.

SEAMLESS NIOBIUM TUBE

For successful hydroforming, high-purity seamless niobium tubes with good formability as well as advancing the hydroforming techniques are necessary. Although KEK could not obtain a good niobium tube until now, has got it manufactured by ATI Wah Chang in U.S. by cooperation of FNAL this time.

The equator ID of 1.3 GHz TESLA-like cavity is approximately 205 mm. Since the iris part is 70 mm. If we only use hydroforming from 70 mm ID tube, required elongation is 200%. Since the maximum elongation with niobium tube is 50 to 60% with suitable heat treatment and grain size. Therefore, we use a combination of necking (iris) and hydroforming (equator) from 123 mm ID tube [5]. A 2.6 mm thickness niobium sheet is used in ordinary press forming for cells; however, that of

#masashi.yamanaka@kek.jp

ADVANCE ADDITIVE MANUFACTURING METHOD FOR SRF CAVITIES OF VARIOUS GEOMETRIES*

P. Frigola#, R. Agustsson, L. Faillace, A. Murokh, RadiaBeam Technologies, Santa Monica, CA 90404, USA
G. Ciovati, W. Clemens, P. Dhakal, F. Marhauser, R. Rimmer, J. Spradlin, S. Williams, JLab, Newport News, VA 23606, USA
J. Mireles, P. A., Morton , R. B., Wicker, UTEP, El Paso, TX 79968, USA

Abstract

An alternative fabrication method for superconducting radio frequency (SRF) cavities is presented. The novel fabrication method, based on 3D printing (or additive manufacturing, AM) technology, capable of producing net-shape functional metallic parts of virtually any geometry, promises to greatly expand possibilities for advanced cavity and end-group component designs. A description of the AM method and conceptual cavity designs is presented along with material analysis and RF measurement results of additively manufactured niobium samples.

INTRODUCTION

SRF accelerating cavities are commonly used in a variety of particle accelerators for research applications, as well as emerging industrial applications. These applications place enormous demands on the development of more reliable and economic methods for fabrication of SRF accelerating cavities and end-group components such as fundamental power couplers (FPCs) and high order mode (HOM) dampers.

RadiaBeam Technologies LLC (RadiaBeam), in collaboration with Thomas Jefferson National Accelerator Facility (JLab), the University of Texas at El Paso (UTEP), and North Carolina State University (NCSU), has been developing the use of Electron Beam Melting (EBM) AM for the production of normal conducting radio frequency (NCRF) and SRF accelerating cavities and end-group components [1, 2, 3]. A review of the fabrication of copper (NCRF) components using EBM is available in reference [4]. A detailed account of the EBM fabrication and characterization of niobium can be found in reference [5].

FABRICATION PROCESS

AM (a.k.a. rapid prototyping or 3D printing) encompasses a group of technologies used to fabricate a part layer-by-layer using 3D computer aided design (CAD) data. AM is increasingly being use throughout industry, providing a quick and accurate way for designers and engineers to visualize, optimize, and fabricate functional parts directly from CAD models in a variety of materials including metals.

EBM is a so-called powder-bed fusion AM technology, originally patented and commercialized by Arcam AB, Sweden. EBM AM is unique in its use of an electron beam to fully melt powdered metals in a layer-by-layer fashion, and has several advantages compared to other AM techniques, such as reduced residual stresses, fast build rates, and better material homogeneity from the vacuum process when compared to laser based powder bed fusion technology (i.e. selective laser melting, SLM).

EBM Fabrication Process

Figure 1 shows a schematic depicting the main components of the Arcam EBM system.

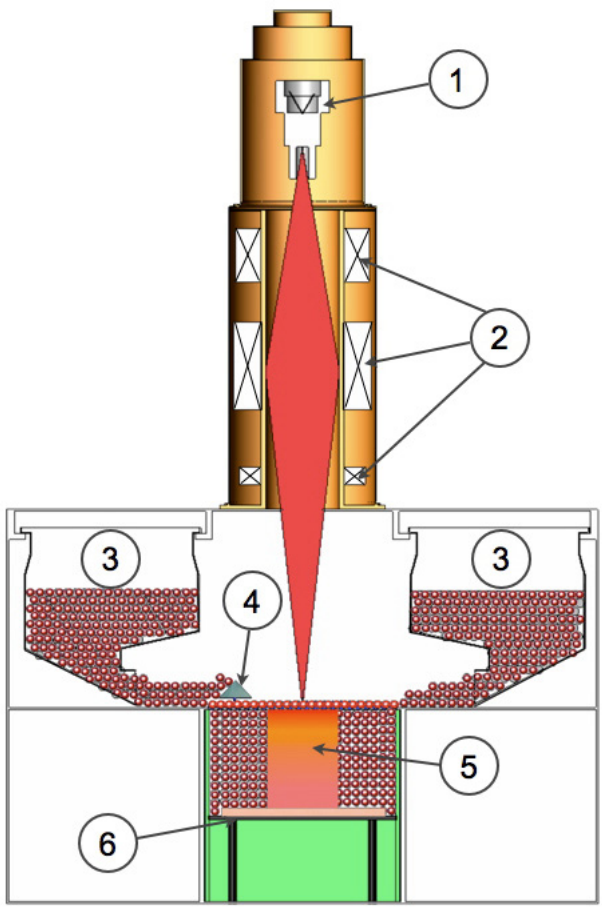

Figure 1: Arcam EBM system schematic.

*Work supported by US DOE SBIR Grant DE-SC0007666
frigola@radiabeam.com

ISBN 978-3-95450-178-6

ALTERNATIVE FABRICATION METHODS FOR THE ARIEL e-LINAC SRF SEPARATOR CAVITY

Douglas W. Storey[1,2*], Robert Edward Laxdal[2], Norman Muller[2]
[1]University of Victoria, Victoria, B.C, Canada, [2]TRIUMF, Vancouver, B.C, Canada

Abstract

The ARIEL e-Linac RF deflecting cavity is a 650 MHz superconducting deflecting mode cavity that will allow simultaneous beam delivery to both the Rare Isotope Beam program and an Energy Recovery Linac. The cavity will be operated at 4 K and with deflecting voltages of up 0.6 MV, resulting in a dissipated RF power of less than 1 W. Due to the modest performance requirements, alternative methods are being employed for the fabrication of this cavity. These include fabricating the entire cavity from reactor grade Niobium and welding the cavity using tungsten inert gas (TIG) welding in a high purity Argon environment. A post purification heat treatment will be performed in an RF induction oven to increase the cavity performance.

INTRODUCTION

An SRF deflecting cavity is being designed and constructed for use as a beam separator at the end of the ARIEL e-Linac [1]. The 650 MHz cavity will provide a nominal 0.3 MV deflecting voltage, while up to 0.6 MV is being considered to allow for flexibility of the final design.

This is a modest deflection voltage and results in low dissipated RF power on the cavity surface and low peak surface fields. For the nominal voltage of 0.3 MV and operation at 4 K, the dissipated power is only 0.2 W and is < 1 W for up to 0.6 MV. The peak electric and magnetic fields are also low, reaching 9.5 MV/m and 12 mT at 0.3 MV. Given the previous high performing results of cavities fabricated from reactor grade Niobium, [2–4], we believe this lower grade Niobium will still exceed performance requirements for this application. Material costs are an important consideration since the inner ridges will be machined from a roughly 30 kg Niobium ingot.

Additionally, we will be fabricating the cavity using high purity TIG welding. Previous weld studies on Niobium samples at MSU in collaboration with FNAL have achieved very minimal degradation of Residual Resistance Ratio (RRR) though the use of TIG welding in a high purity Argon environment with Argon torch purging [5]. Finally, high temperature heat treatments in an RF induction oven will be performed to increase cavity performance.

THERMAL STUDIES

An integrated RF-thermal study was performed using ANSYS APDL to ensure the sufficient cooling of the RF surfaces. Of particular concern was the solid inner ridge which results in a large separation of the ridge's inner surfaces and the LHe cooling bath, particularly since reactor grade Niobium will have a lower thermal conductivity than typical cavity Niobium.

Since the heat load depends on the surface temperature through the surface resistance, an iterative technique was used to determine the cavities operating temperature distribution. The outside walls of the cavity were held at 4 K and a heat load was applied to the cavity surface by calculating the local dissipated RF power on the cavity walls from the magnetic field and temperature dependent surface resistance, $R_s(T)$. The RRR of the cavity walls was assumed to be 50 for a thermal conductivity at 4 K of roughly 13 W/m K. The results of several cavity fabrication options are shown in Table 1.

Table 1: Maximum Cavity Temperature due to RF Heating

Cavity	$V_\perp = 0.3$ MV	$V_\perp = 0.6$ MV
4 mm cavity walls on both body and ridge.	4.01 K	4.03 K
3 mm walls with solid ridge.	4.08 K	4.32 K
3 mm walls, solid ridge with cooling channel.	4.07 K	4.30 K

With a solid ridge, the peak temperature that the cavity reaches under nominal operation is 4.08 K, as shown in Figure 1. The addition of a cooling channel to the ridge to move the LHe closer to the RF surfaces causes an insignificant reduction in ridge temperature and was deemed unnecessary.

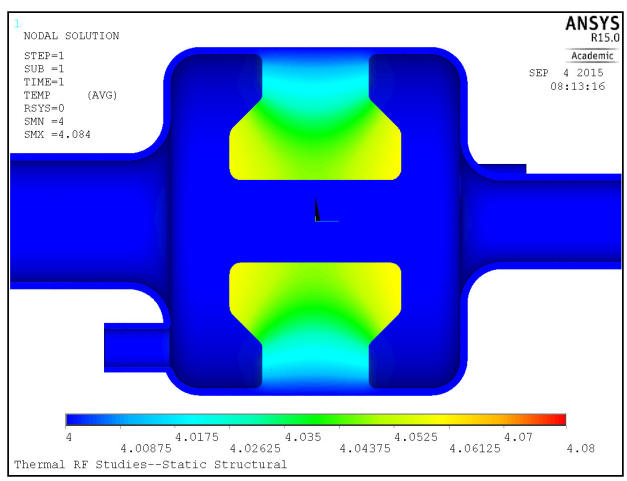

Figure 1: The cavity temperature distribution with a deflecting voltage of 0.3 MV and solid reactor grade ridges.

* dstorey@uvic.ca

ISBN 978-3-95450-178-6

A SUPERCONDUCTING RF DEFLECTING CAVITY FOR THE ARIEL e-LINAC SEPARATOR

Douglas W. Storey[1,2*], Robert Edward Laxdal[2], Lia Merminga[2], Bhalwinder Waraich[2], Zhongyuan Yao[2], Vladimir Zvyagintsev[2]
[1]University of Victoria, Victoria, B.C, Canada, [2]TRIUMF, Vancouver, B.C, Canada

Abstract

A 650 MHz SRF deflecting mode cavity has been designed for the ARIEL e-Linac to separate interleaved beams heading towards either Rare Ion Beam production or a recirculation loop for energy recovery, allowing the e-Linac to provide beam delivery to multiple users simultaneously. The cavity geometry has been optimized for the ARIEL specifications, resulting in a very compact cavity with high shunt impedance and low dissipated power. Analyses have been performed on the susceptibility to multipacting, input coupling considering beam loading and microphonics, and extensive studies into the damping of transverse and longitudinal higher order modes. The pressure sensitivity, frequency tuning, and thermal behaviour have also been studied using ANSYS. The cavity design resulting from these considerations will be discussed here.

INTRODUCTION

The ARIEL e-Linac is a MW class CW electron linear accelerator being constructed at TRIUMF to produce a 50 MeV, 10 mA electron beam for the production of rare isotopes to expand TRIUMF's Rare Isotope Beam (RIB) experimental program. The electrons are accelerated in five 9-cell, 1.3 GHz superconducting accelerating cavities housed in three cryomodules. A single cavity in the injector cryomodule (EINJ) will boost the electrons from 300 keV to ~ 10 MeV, followed by the two accelerator cryomodules (EACA/B) for a final beam energy of up to 66 MeV.

A future extension of the e-Linac will be the construction of a recirculation loop that would return electrons to make a second pass through the two accelerating cryomodules. This layout could be operated as a Recirculating Linac (RLA) to double the energy of the electron beam, or as an Energy Recovery Linac (ERL). In this mode the electrons would return for a second pass through the accelerating cavities in the decelerating RF phase, resulting in the deceleration of second pass electrons and the return of their energy back to the accelerating cavities. This beam could be used to drive an infrared or THz Free Electron Laser (FEL) or x-rays through inverse Compton scattering in the back leg of the recirculation loop.

Bunches bound for either RIB production or the ERL would be interleaved, occupying adjacent RF buckets in the 1.3 GHz accelerating RF. This requires separating the bunches bound for either the ERL or RIB at the end of the linac at a frequency of 650 MHz. Due to the high frequency of separation required, an RF separator is required to impart opposing deflections to adjacent bunches. The concept of the RF separation scheme has been laid out in [1] which describes the layout and deflections required by each element in the separation complex: an RF deflecting cavity, steering dipole, defocusing quadrupole, and septum magnet, as shown in Figure 1. The recirculated and decelerated beam would make a second pass through the deflecting cavity in the zero crossing phase to be separated from the high energy beams by the dipole magnet.

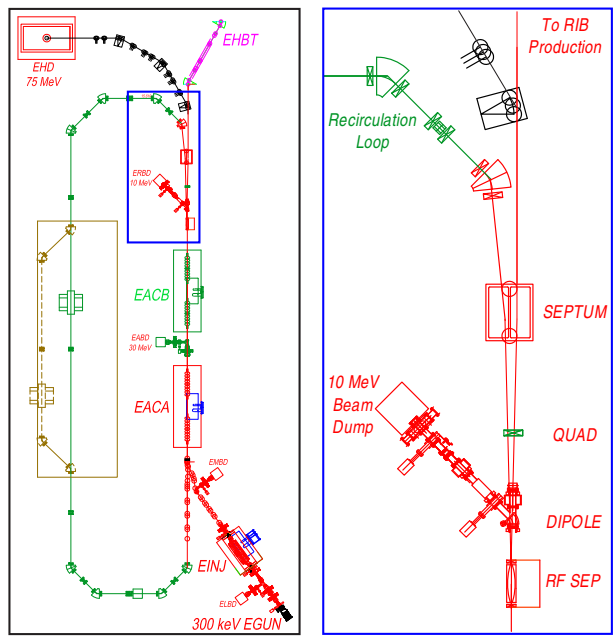

Figure 1: The ARIEL e-Linac and recirculation loop on the left and on the right, a magnified view of the separation complex.

CAVITY DESIGN

The geometry of the deflecting cavity was based on the RF Dipole [2] and Double Quarter Wave (DQW) [3] crab cavities being developed at ODU/JLab and BNL respectively. The deflection in this cavity is due to the electric field between two parallel ridge faces, with the magnetic field acting to decrease the net deflection. The cavity was optimized for increased transverse shunt impedance by reducing the magnetic field contribution to the deflection. This resulted in a "Post-and-Ridge" type design, Figure 2, where an undercut was added to the ridge to decrease the magnetic field density along the axis of the cavity. The overall length of the cav-

* dstorey@uvic.ca

ISBN 978-3-95450-178-6

PROGRESS IN IFMIF HALF WAVE RESONATORS MANUFACTURING AND TEST PREPARATION

G. Devanz, N. Bazin, G. Disset, H. Dzitko, P. Hardy, H. Jenhani, J. Neyret, O. Piquet, J. Plouin, N. Selami, CEA-Saclay, France

Abstract

The IFMIF accelerator aims to provide an accelerator-based D-Li neutron source to produce high intensity high energy neutron flux to test samples as possible candidate materials to a full lifetime of fusion energy reactors. The first phase of the project aims at validating the technical options for the construction of an accelerator prototype, called LIPAc (Linear IFMIF Prototype Accelerator). A cryomodule hosting 8 Half Wave Resonators (HWR) at 175 MHz will provide the acceleration from 5 to 9 MeV. We report on the progress of the HWR manufacturing. A pre-series cavity will be used to assess and optimize the tuning procedure of the HWR, as well as the processing steps and related tooling. A new horizontal test cryostat (Sathori) is also being set up at Saclay in the existing SRF test area. The Sathori is dedicated to the IFMIF HWR performance check, fully equipped with its power coupler (FPC) and cold tuning system. A 30 kW-RF power will be available for these tests.

LICENCING ASPECTS

Since the LIPAc cryomodule [1] will be installed in Rokkasho, Japan, its design and fabrication have to comply with HPGSL law. The nominal temperature is 4.45 K, this corresponds to a nominal pressure of 1.2 bar. Cryogenic circuits and safety equipment of the cryomodules have been designed in order to have a maximum working pressure of 0.15 MPa in the 18 L HWR helium vessel. In practice, the mechanical cavity design already presented [2] was analyzed by the manufacturer for him to propose a detailed manufacturing sequence and weld procedures following the ASME methodology. The geometries of electron beam welds (EBW) between Nb ports and NbTi flanges were modified in order to increase the joint efficiency, using ASME as a reference. For most Nb-NbTi welds, the consequence was to make them equivalent to full penetration welds. The direct effect is to reduce the amount of required inspection testing involving radiography through the complete Nb resonator and thick flanges, which in our case would have been un-conclusive. Eventually, only visual inspection and third party inspection of the welding process will be required for the Nb to NbTi welds. The requirement of 100% radiographic inspection of Nb-Nb EBW joints will be limited to those classified as longitudinal welds and to beam tube welds. The longitudinal GTAW welds of the Ti vessel will be subjected to 100% radiographic testing as well. A final pressure test will be performed with a proof pressure in the He vessel at 0.875 MPa above atmospheric pressure.

The first milestone of HWR licensing has recently been passed with the submission of the application form to the Japanese authority which processes pressure vessel applications, KHK. This document includes all manufacturing drawings, procedure, weld classification, qualification and test plan, FEM analysis of the corresponding mechanical model of the HWR with detailed description of weld areas.

MANUFACTURING

A total of 9 HWR will be manufactured. The first one, a pre-series HWR is prepared up-front to check the whole manufacturing, RF frequency tuning and final treatments procedures. The pre-series cavity will be used in Saclay test area only and can be manufactured before the weld qualification process required for the cavity licensing is complete. Several weld test samples have already been produced by the manufacturer. In particular, they cover Nb-Nb full penetration electron beam welds (EBW), and thicker EBW welds joining the NbTi flange to the FPC Nb port, with a required final thickness of 6 mm.

HWR Parts Manufacturing

The beam ports (Figure 1) have been machined from high purity bulk Nb (RRR>250).

Figure 1: beam port of the HWR.

It is also the case for the central part of the inner conductor (IC) and the toroidal end caps, shown on Figure 2 along with one conical half of the IC.

After completion of the bare resonator manufacturing, it will be delivered for chemical etching and vertical testing at Saclay. The HWR will then be heat treated in a vacuum furnace for de-hydrogenation. The final fabrication step will be the welding of the Helium vessel.

ISBN 978-3-95450-178-6

DESIGN AND DEVELOPMENT OF SUPERCONDUCTING SPOKE CAVITY FOR COMPACT PHOTON SOURCE

M. Sawamura#, R. Hajima, JAEA, Tokai, Ibaraki, Japan
T. Kubo, T. Saeki, KEK, Tsukuba, Ibaraki, Japan
Y. Iwashita, H. Tongu, H. Hokonohara, Kyoto University, Uji, Kyoto, Japan
E. Cenni, CEA/IRFU, Saclay, France

Abstract

The spoke cavity is expected to have advantages for compact ERL accelerator for X/γ-ray source based on laser Compton scattering. We have been developing the spoke cavity under a research program of MEXT, Japan to establish the fabrication process. Since our designed shape of the spoke cavity is complicated due to optimization of the RF properties, we have been designing the mold including the process of press forming and the support parts for vacuum tolerance with the mechanical simulation. In this paper we present status of the spoke cavity fabrication.

INTRODUCTION

We are developing laser Compton scattering (LCS) X-ray and gamma-ray sources combined with an energy-recovery linac (ERL) and a laser. The LCS X/γ-ray source is expected for application of non-destructive assay system of nuclear materials with nuclear resonance fluorescence [1], analysis of nano-structure, drug development, medical diagnostics and so on. We have launched a 5-year research program since 2013 to develop the superconducting spoke cavity for LCS photon sources [2]. Spoke cavities have many advantages such as shortening the distance between cavities, small frequency detune due to micro-phonics and easy adjustment of field distribution for strong cell coupling. We have almost finished cavity shape optimization [3] and been making a study of mold design and mechanical design to fabricate the niobium one-spoke cavity.

PRESS FORMING OF SPOKE CAVITY

The spoke cavity is going to be fabricated with three kinds of parts divided as shown in Figure 1.

(i) Spoke part
(ii) End-plate part
(iii) Tank part

The spoke is also divided into two half-spokes and a beam pipe. The half-spoke and the end-plate are made by press forming. The spoke base is bended into the same shape of the tank curve considering the connection to the tank.

Since the shape of the spoke is complicated, one-step press forming with one set of molds will cause so large strain to break the sheet. The strain distribution of half-spoke formed in one-step is shown in Figure 2 (top). This was calculated with 3D structural analysis software Abaqus. There were some areas of large strain near the spoke center and spoke base. In order to reduce the strain, forming process is divided into three steps as shown in Figure 3.

(i) The center die is set above the level of the die and the inner punch is forced downward to bend the sheet crossways with the die center.
(ii) Holding the sheet between the center die and the inner punch, the center die and the inner punch are forced downward at the same time to bend the sheet longways with the die.
(iii) The outer punch is forced downward to form the half-spoke base.

The simulation result of the strain distribution of half-spoke through above process is shown in Figure 2 (bottom). Though there still remains large strain area, the most of strain was reduced to less than 0.3 and this result is estimated to avoid breaking the sheet during the press forming process.

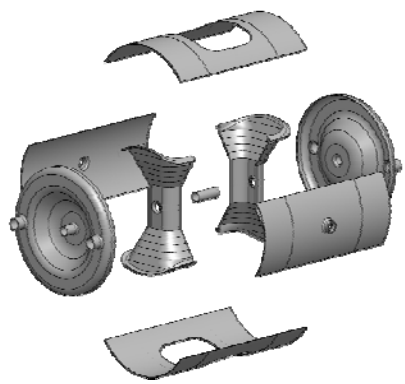

Figure 1: Exploded schematic of one-spoke cavity.

SPOKE CAVITY SUPPORTS

Mechanical analysis has been performed to control the mechanical deformations caused by the external load such as vacuum load and/or liquid/gas helium pressure. If the stress exceeds the elastic deformation to cause plastic deformation, the deformation will be accumulated to result in the frequency shift every time the external force is loaded. Figure 4 (top) shows the stress distribution when the cavity is externally loaded to 1 bar. The gray areas indicate the large stress to cause plastic deformation. The large stress occurs at the spoke base and the end-plate.

#sawamura.masaru@jaea.go.jp

ISBN 978-3-95450-178-6

ANALYSIS OF A 750 MHZ SRF DIPOLE CAVITY *

A. Castilla[1,2,3†], J. R. Delayen[1,2].
[1]Center for Accelerator Science, Old Dominion University, Norfolk, VA 23529, USA.
[2]Thomas Jefferson National Accelerator Facility, Newport News, VA 23606, USA.
[3]Universidad de Guanajuato (DCI-UG), Departamento de Fisica, Leon, Gto. 37150, Mex.

Abstract

There is a growing interest in using rf transverse deflecting structures for a plethora of applications in the current and future high performance colliders. In this paper, we present the results of a proof of principle (PoP) superconducting rf dipole, designed as a prototype for a 750 MHz crabbing corrector for the Medium Energy Electron-Ion Collider (MEIC), which has been successfully tested at 4.2 K and 2 K at the Jefferson Lab's Vertical Testing Area (VTA). The analysis of its rf performance during cryogenic testing, along with Helium pressure sensitivity, Lorentz detuning, surface resistance, and multipacting processing analysis are presented in this work. Detailed calculations of losses at the port flanges are included for completeness of the cavity's cryogenic performance studies.

INTRODUCTION

Transverse deflectors have been studied for several applications in the past, but when it comes to high performance applications that require compact superconducting designs, a few approaches have been taken. TEM parallel rod cavities showed promising performance for high $\left[\frac{R}{Q}\right]_T$ and after a long evolution and optimization of parameters such as balanced peak surface fields and low multipacting, a TE-like resonant structure was developed by S. U. De Silva *et al* [1,2], known as the rf dipole. The optimization of an rf dipole structure will depend greatly on its applications and machine-specific constraints, from the impedance budget and field flatness to its physical dimensions.

The present work has been prepared as a summary of the efforts devoted to the design and study of a superconducting 750 MHz rf dipole, developed as a PoP crab cavity for the MEIC [3]. A list of its principal parameters and rf properties can be seen in Table 1, while Fig. 1 represents a visualization of the longitudinal (a) and transverse (b) cross sections of the structure.

BEAD PULL

The cavity was deep drawn using high grade, large grain, 3mm thick Nb sheets, and e-beam welded. A bulk BCP etching after welding was perfomed by the vendor previous to several preliminary 4.2 K cryogenic tests. Once received at ODU, a series of bead pull measurements were performed to determine the symmetry of the fields (see Figs. 1(a) to (c)). Finding the frequency shift due to the perturbation on the fields by a small dielectric (teflon) bead pulled along the cavity's longitudinal axis, the transverse electric field can be determined using Eqn. 1.

$$\left[\frac{\Delta f}{f}\right]_D = -\frac{\pi a^3}{U}\left[\left(\frac{\epsilon_r - 1}{\epsilon_r + 2}\right)\epsilon_0 |E|^2\right]. \quad (1)$$

While for a perfect conductor bead, the frequency shift is given by Eqn. 2

$$\left[\frac{\Delta f}{f}\right]_C = -\frac{\pi a^3}{U}\left[\epsilon_0 |E|^2 - \frac{\mu_0}{2}|H|^2\right]. \quad (2)$$

Table 1: RF Dipole Design Parameters

Parameter	750 MHz	Units
$\lambda/2$ of π mode	200.0	mm
Cavity length	341.2	mm
Cavity radius	93.7	mm
Bars width	63.0	mm
Bars length	200.0	mm
Bars angle	45	deg
Aperture diameter -d	60.0	mm
Deflecting voltage -V_T^*	0.20	MV
Peak electric field -E_P^*	4.45	MV/m
Peak magnetic field -B_P^*	9.31	mT
B_P^*/E_P^*	2.09	$\frac{\text{mT}}{\text{MV/m}}$
Energy content -U^*	0.068	J
Geometrical factor	131.4	Ω
$[R/Q]_T$	124.2	Ω
$R_T R_S$	1.65	$\times 10^4 \Omega^2$

At E_T^*= 1 MV/m

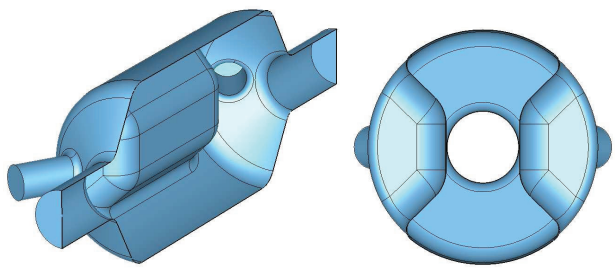

(a) Longitudinal cross section (b) Transverse cross section

Figure 1: Geometry of the optimized PoP 750 MHz rf dipole.

* Authored by Jefferson Science Associates, LLC under U.S. DOE Contract No. DE-AC05-06OR23177. This research used resources of the National Energy Research Scientific Center, supported by the Office of Science under U.S. DOE contract No. DE-AC02-05CH11231.
† acastill@jlab.org

DESIGN OF A COMPACT SUPERCONDUCTING CRAB-CAVITY FOR LHC USING Nb-ON-Cu-COATING TECHNIQUE

A. Grudiev[1,*], S. Atieh[1], R. Calaga[1], S. Calatroni[1], O. Capatina[1], F. Carra[1,2], G. Favre[1], L.M.A. Ferreira[1], J.-F. Poncet[1], T. Richard[1], A. Sublet[1], C. Zanoni[1],
[1]CERN, Geneva, Switzerland; [2]Politecnico di Torino, Turin, Italy

Abstract

The design of a compact superconducting crab-cavity for LHC using Nb-on-Cu-coating technique is presented. The cavity shape is based on the ridged waveguide resonator with wide open apertures to provide access to the inner surface of the cavity for coating. It also provides natural damping for HOMs and rather low longitudinal and transverse impedances. The results of the cavity shape optimization taking into account RF performance, coating, and thermo-mechanical considerations, as well as the design and fabrication plans of the first prototype for coating and cold tests are presented.

INTRODUCTION

The upgrade of the LHC to a higher luminosity (HL-LHC) [1], among the other things, includes using so-called crab cavities which are RF deflecting cavities operating at zero crossing and tilting the LHC bunches before and after collision point in order to provide head-on collisions. For LHC, due to requirements for RF frequency to be 400 MHz and due to given distance between the two beam pipes at the foreseen cavity locations of about 194 mm, the crab cavity transverse dimension must be significantly smaller than half of the wavelength. This requires compact cavity shapes to be used that are rather different form standard elliptical pill-box cavity type. A number of compact SRF crab cavities have been design for LHC based on the solid Nb manufacturing technology in the framework of HL-LHC program [2].

Nevertheless, there is an alternative SRF technology based on the Nb-on-Cu-coating technique developed to large extent at CERN for the largest ever-built SRF system of LEP2 at CERN. Although typically solid Nb SRF cavities show lower surface RF power loss and require less cryogenic power for cooling than Nb-on-Cu cavities, the latter ones do not have so-called quenching, a physical phenomenon related to thermal runaway process in the bulk Nb due to its relatively low thermal conductivity. On the contrary, Cu with its high thermal conductivity provides very good cooling of the superconducting Nb thin film on the cavity surface. In addition, Cu offers a possibility to create much more complex and much more accurate cavity shapes by using modern CNC 5-axis milling machines than solid Nb sheet technology. This advantage is rather important in the compact crab cavity design, whereas higher cryogenic loss can probably be accepted as it is already the case for the LHC main RF system. Last but not least, much thicker Cu cavity walls significantly reduce cavity frequency sensitivity both to the external liquid He bath pressure variations and to the Lorentz force detuning.

In this paper, we describe the design of a prototype which addresses the feasibility issues of fabrication and coating of the cavity itself with the final goal of measuring the RF power loss at 4.5 K as a function of the cavity voltage in a general purpose cryostat. No fundamental mode coupler nor HOM couplers are addressed in the prototype and are left for the future work as well as the design of a dedicated cryostat for possible beam tests.

*Alexej.Grudiev@cern.ch

RF DESIGN

The shape of the internal surface of the cavity is directly related both to its RF performance and to the Nb-coating process. One can be adapted to the needs of the other one and vice-a-versa. The existing designs of the LHC crab cavity make it very difficult if not impossible to make a Nb-coating of the inside surface. In the design of the cavity presented in this paper, the shape has been adapted to the Nb-coating process by providing access to the inner part of the cavity through the input and output beam pipes of a cross-section smaller than the cross-section of the central part which forms a resonator based on a piece of a double-ridged waveguide.

Transverse Cross-section of the Cavity

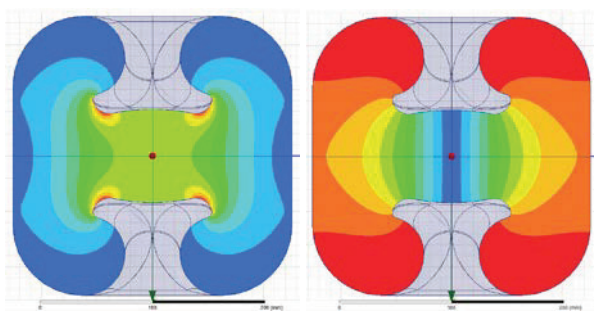

Figure 1: Transverse distributions of electric (left) and magnetic (right) fields in the middle of the cavity are presented in linear scale for deflecting voltage value of 3 MV. Maximum electric and magnetic field values on the plots (red) are 30 MV/m and 25 kA/m, respectively.

The transverse cross-section of the central part of the cavity is shown in Fig. 1 together with the electric and magnetic field distributions calculated using HFSS [3] on the left and on the right hand sides, respectively. In order to reduce the transverse dimensions of the double-ridged waveguide for given cut-off frequency close to 400 MHz,

ISBN 978-3-95450-178-6

PERFORMANCE EVALUATION OF HL-LHC CRAB CAVITY PROTOTYPES IN A CERN VERTICAL TEST CRYOSTAT

K. G. Hernández-Chahín*, DCI-UG, Guanajuato, México,
A. Macpherson, C. Jarrige, M. Navarro-Tapia, R.Torres-Sánchez, CERN, Geneva, Switzerland,
G. Burt, A. Tutte, Cockcroft Institute, Cheshire, UK, S. Verdú-Andrés, BNL, Long Island, NY, US,
S. U. De Silva, ODU, VA, USA

Abstract

Three proof-of-principle compact crab cavity designs have been fabricated in bulk niobium and cold tested at their home labs, as a first validation step towards the High Luminosity LHC project. As a cross check, all three bare cavities have been retested at CERN, in order to cross check their performance, and cross-calibrate the CERN SRF cold test facilities. While achievable transverse deflecting voltage is the key performance indicator, secondary performance aspects derived from multiple cavity monitoring systems are also discussed. Temperature mapping profiles, quench detection, material properties, and trapped magnetic flux effects have been assessed, and the influence on performance discussed. The significant effort invested in developing expertise in preparation and testing of these crab cavities has already been fruitful for all partners, and more is to come within this ongoing program.

INTRODUCTION

As part of the high luminosity upgrade of the Large Hadron Collider (LHC) [1], superconducting compact crab cavities are foreseen for beam crabbing at two of the LHC interaction points. Strong design constraints, in terms both of physical dimension and transverse crabbing voltage have resulted in three innovative designs being taken through to the proof-of-principle stage. These prototypes have been tested in their home labs, and all reached the required specification crabbing voltage of 3.4 MV. In order to gain further experience with these cavity prototypes, and to cross-calibrate the CERN SRF test facility [2] against the home labs of each of the prototypes, a set of vertical cold tests has been carried out, and the results are reported here.

The three crab cavity proof-of-principle designs [3] that have been fabricated and tested are the 4-rod cavity(UK4R) from Lancaster University, the RF Dipole (RFD) from Old Dominion University and the Double Quarter Wave (DQW) cavity from Brookhaven. Figure 1 shows the three prototypes prior to retesting at CERN.

CAVITY PREPARATION

As part of the cold test preparations, two of the cavities (UK4R and DQW) were high pressure rinsed, baked at 120 °C, and then assembled in the SRF ISO4 cleanroom, while the RFD had a similar preparation in it's home lab

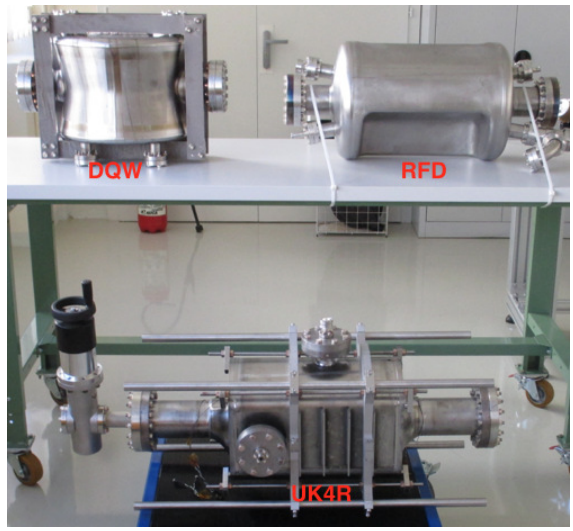

Figure 1: Picture of the crab cavities at CERN.

then shipped under vacuum to CERN. All three cavities were tested in at 2 K in the same 4 m deep cryostat in the CERN SRF facility. Preparation of the RF surface, assembly and installation of the cavity into the cryostat followed the same general steps for all cavities, and are listed below. Prior to the tests reported here, all three cavities previously had a full preparation of the RF surface in their respective home labs.

- BCP, with an average thickness removal of 20 µm
- High Pressure Rinsing, in a 100 bar rinsing cabinet. The rinse is composed of 6 cycles with a di-jet nozzle with vertical nozzle speed of 0.5 mm/s and an angular speed of 3 RPM
- Drying in an ISO4 cleanroom environment with a laminar air flow in the direction along the cavity axis
- Assembly in an ISO4 cleanroom environment
- Mounting on the cryostat insert and leak testing
- Bakeout at 120 °C up to 48 hrs
- Mounting of monitoring and diagnostic equipment, and then installation in the cryostat
- Cool down to 2 K, with the ambient magnetic field suppression.

* karim.gibran.hernandez.chahin@cern.ch

ISBN 978-3-95450-178-6

LORENTZ DETUNING FOR A DOUBLE-QUARTER WAVE CAVITY*

S. Verdú-Andrés#, Q. Wu, B. P. Xiao, BNL, Upton, NY 11973, USA
S. Belomestnykh, BNL, Upton, NY 11973, USA; SBU, Stony Brook, NY 11794, USA
J. Wang, CST of America, Inc., Framingham, MA 01701, USA

Abstract

The frequency change due to the radiation pressure on the walls of an RF cavity is known as Lorentz detuning. We present benchmarking studies of Lorentz detuning calculations for a Double-Quarter Wave Crab Cavity (DQWCC) using the codes ACE3P and CST. The results are compared with the Lorentz detuning measurements performed during the cold tests of the Proof-of-Principle (PoP) DQWCC at BNL.

LORENTZ DETUNING

Lorentz detuning is the change of frequency associated with the deformation of an RF cavity due to the pressure exerted by the electromagnetic field (known as radiation pressure) on the cavity walls.

The radiation pressure P_{rad} exerted by an electromagnetic wave on the walls of a cavity is given by:

$$P_{rad} = \frac{1}{4}\left(\mu_0 {H_{pk}}^2 - \varepsilon_0 {E_{pk}}^2\right), \quad (1)$$

where E_{pk} and H_{pk} are the peak values of the electric and magnetic field, respectively [1]. These are the field values automatically provided by simulation codes such CST and ACE3P. The expression of P_{rad} presented here is therefore the time-average radiation pressure, not the instant value.

According to Eq. (1), there will be inwards pressure in the region with dominant electric energy (negative sign – as the attractive force between two capacitive plates) and outwards pressure in the region with dominant magnetic energy (positive sign).

The Slater's perturbation theorem gives the frequency change experienced by a cavity which suffers a small change in its volume $V \to V + dV$:

$$\Delta f \propto \left(\varepsilon_0 E^2 - \mu_0 H^2\right) dV \quad (2)$$

Some conclusions can be extracted from the combination of Eqs. (1) and (2): a) the detuning is proportional to the amplitude of the electromagnetic field, thus the Lorentz detuning is especially important at high field operation; b) frequency always decreases, and c) it is impossible to design a cavity with net frequency change equal to zero.

*Work supported by US DOE via BSA LLC contract No. DE-AC02-98CH10886 and US LARP program. Used NERSC resources by US DOE contract No. DE-AC02-05CH1123.
#sverdu@bnl.gov

LORENTZ DETUNING CALCULATION

The Lorentz detuning coefficient can be calculated after a sequence of coupled simulations using electromagnetic and structural solvers. The general calculation workflow consists of three main stages:

1) Run eigenmode solver to obtain resonant frequency of the cavity and electromagnetic field distribution in the RF volume (vacuum volume).

2) Run structural solver to calculate the displacement of cavity walls (shell volume) due to the radiation pressure.

3) Run eigenmode solver to solve resonant frequency for deformed cavity.

Several simulation codes can be used to calculate the Lorentz detuning coefficient. This paper focuses on the calculation performances of two simulation codes, ACE3P [2] and CST [3].

Lorentz Detuning Calculation with ACE3P

The parallel finite-element code suite ACE3P was developed by SLAC. Omega3P is the eigenmode solver of ACE3P and TEM3P is its structural solver. Simulated volumes must be meshed in Cubit and later processed by acdtool, so that Omega3P and TEM3P can work with them. Simulation results are postprocessed with acdtool and visualized with Paraview.

Omega3P provides the resonant frequency and electromagnetic field distribution for RF volume. TEM3P takes the electromagnetic field distribution as an input. Then it calculates the corresponding radiation pressure on the inner surface of the shell model for a given accelerating gradient set by the user. From the radiation pressure and for the given boundary conditions on the shell model, TEM3P computes the corresponding displacement of the cavity walls. As a result, it generates a file with the deformed vacuum volume. This deformed vacuum volume is like the original vacuum volume, but the node coordinates have been updated according to the displacement due to pressure radiation. The deformed vacuum volume file can be used as input for Omega3P to calculate the shifted resonant frequency, and thus obtain the Lorentz detuning.

Lorentz Detuning Calculation with CST

A similar routine is used with the code package CST Suite. The eigenmode solver from the CST MWS package provides the resonant frequency and electromagnetic field distribution for the RF volume. It is equipped with a postprocessing tool that calculates the Lorentz force generated by the electromagnetic field on the cavity walls.

ISBN 978-3-95450-178-6

THERMAL LOSSES IN COUPLERS AND PORTS OF A SPS DOUBLE-QUARTER WAVE CRAB CAVITY*

S. Verdú-Andrés#, Q. Wu, B. P. Xiao, BNL, Upton, NY 11973, USA
S. Belomestnykh, BNL, Upton, NY 11973, USA; SBU, Stony Brook, NY 11794, USA
G. Burt, U. Lancaster, Lancaster, UK; STFC, Daresbury, UK
T. Jones, STFC, Daresbury, UK
R. Calaga, O. Capatina, C. Zanoni, CERN, Geneva, Switzerland
Z. Li, SLAC, Menlo Park, CA 94025, USA
F. Carra, CERN, Geneva, Switzerland; Politecnico di Torino, Turin, Italy

Abstract

The Double-Quarter Wave (DQW) crab cavity for beam tests at SPS will be equipped with a Fundamental Power Coupler (FPC), three HOM filters and one pickup. FPC and HOM couplers are located in the cavity high magnetic field region and have a hook shape. The FPC will be made in copper while HOM and pickup are in niobium. This paper explains the material choice for the FPC, HOM and pickup couplers given the calculated power dissipation for the fundamental mode. It also describes the envisaged cooling system and corresponding thermal distribution for each coupler.

INTRODUCTION

The HL-LHC Crab Cavity project aims at testing two DQW cavities with beam in SPS. The heat load budget for these tests is limited and efforts have been made during the design process of couplers and cavity interfaces among others to reduce the heat loads [1].

The SPS DQW cavity is equipped with one FPC, three HOM filters and one pickup. The SPS DQW cavity body with all its couplers is shown in Fig. 1.

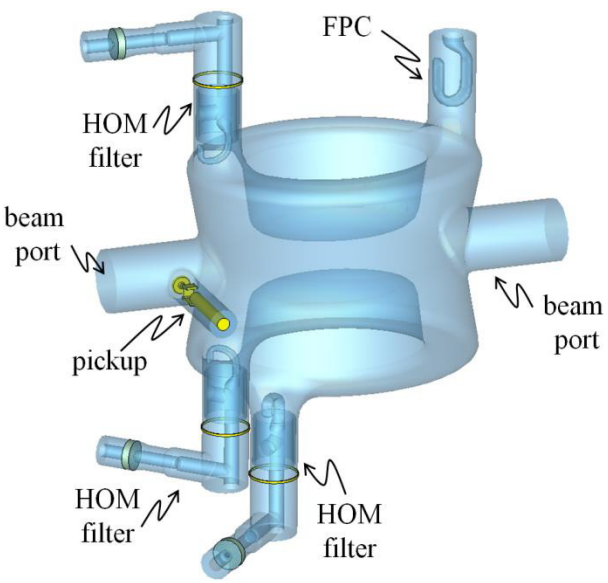

Figure 1: RF volume of SPS DQW cavity with all couplers.

FUNDAMENTAL POWER COUPLER

The FPC port is opened in the inductive region of the SPS DQW cavity. Both FPC hook and antenna will be made of bulk OFE copper. The FPC has a hook shape for better coupling to the fundamental mode of the DQW cavity.

The hook shape and penetration were chosen to provide a large enough coupling while limiting the power dissipation. The final geometry of the FPC was provided in Ref. [2]. CST simulations [3] were used to determine the RF coupling and power dissipation for the fundamental mode, respectively, 5.3×10^{5} and about 100 W for a nominal deflecting voltage of 3.34 MV. The maximum peak surface magnetic field of 8 mT is located at the hook bending for cavity operation at the nominal deflecting voltage. Posterior Omega3P [4] simulations validated these numbers.

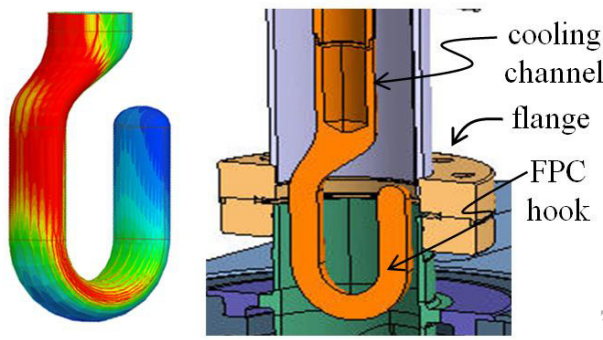

Figure 2: [Left] Surface current distribution on FPC hook provided by CST. The highest surface currents are close to the cooling channel; therefore, improving the extraction of power. [Right] CAD model of FPC hook with cooling channel.

Coupled HFSS/ANSYS simulations [5] were later used to evaluate the temperature distribution on the hook surface and calculate the corresponding radiation losses. The FPC antenna is equipped with a cooling channel for circulating water, as shown in Fig. 2. The cooling channel stops at the beginning of the hook bending. The hook has

*Work supported by US DOE via BSA LLC contract No. DE-AC02-98CH10886 and US LARP program and HiLumi LHC grant No. 284404. Used NERSC resources by US DOE contract No. DE-AC02-05CH1123.
#sverdu@bnl.gov

ISBN 978-3-95450-178-6

ELECTROMAGNETIC DESIGN OF 400 MHz RF-DIPOLE CRABBING CAVITY FOR LHC HIGH LUMINOSITY UPGRADE*

S. U. De Silva#, H. Park, J. R. Delayen, Old Dominion University, Norfolk, VA, USA
Z. Li, SLAC National Accelerator Laboratory, Menlo Park, CA USA

Abstract

The beam crabbing proposed for the LHC High Luminosity Upgrade requires two crabbing systems operating in both horizontal and vertical planes. In addition, the crabbing cavity design needs to meet strict dimensional constraints and functional specifications of the cavities. This paper presents the detailed electromagnetic design including rf properties, multipole analysis, multipacting levels of the 400 MHz rf-dipole crabbing cavity.

INTRODUCTION

The LHC High Luminosity Upgrade is proposed to use crabbing cavities for its 14 TeV beam operation. The crabbing cavities are expected to increase the luminosity at the interaction point (IP) provide luminosity levelling to reduce pile up at IP. The parallel beam pipes in the LHC sets strict dimensional constraints on the crabbing cavity system, hence requires compact crabbing cavities [1]. The rf-dipole cavity is one of the two 400 MHz crabbing cavities and will be used for horizontal crabbing of the proton beams at LHC. Prior to installation at LHC the proposed cavities will be tested at Point-6 in SPS at CERN.

RF-DIPOLE CRABBING CAVITY

A cylindrical shaped proof-of-principle (P-o-P) cavity has been designed, fabricated and successfully tested [2, 3]. The P-o-P cavity achieved at transverse voltage of 7.0 MV with an intrinsic quality factor of 1.25×10^{10} [2, 3].

The 400 MHz crabbing cavity for LHC high luminosity upgrade is adapted into a square shaped design to meet the dimensional constraints. The compact crabbing cavity is optimized to meet the current requirements for LHC [4].

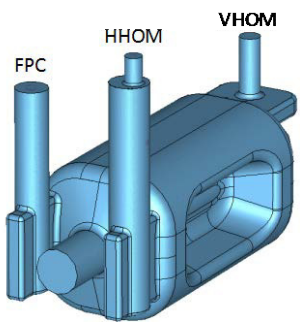

Figure 1: 400 MHz rf-dipole prototype cavity for LHC high-luminosity upgrade.

*Work supported by DOE via US LARP Program and by the High Luminosity LHC Project. Work was also supported by DOE Contract No. DE-AC02-76SF00515.
#sdesilva@jlab.org

The 400 MHz rf-dipole cavity shown in Fig. 1 operates in a TE_{11} like mode where the contribution to the transverse voltage is primarily due to the transverse electric field. The cavity is designed with transverse dimensions less than 285 mm, in order to accommodate the parallel beam line in the LHC. Hence the prototype cavity is designed with a square shaped outer conductor where all the ancillary components of the cavity are designed on the end plate of the cavity as shown in Fig. 1. Table 1 shows the cavity parameters and rf properties of the prototype cavity.

Table 1: RF Properties of Prototype RF-dipole Cavity

Parameter	Value	Units
Cavity length	775	mm
Cavity diameter	281	mm
Aperture diameter	84	mm
Deflecting voltage (V_T*)	0.375	MV
Peak electric field (E_P*)	3.6	MV/m
Peak magnetic field (B_P*)	6.2	mT
B_P* / E_P*	1.71	mT/(MV/m)
Energy content (U*)	0.13	J
Geometrical factor	107	Ω
$[R/Q]_T$	430	Ω
$R_T R_S$	4.6×10^4	Ω^2

At E_T* = 1 MV/m

Table 2 shows the operational parameters expected to be achieved at 3.4 MV and with the projected parameters of operation at 5.0 MV for the rf-dipole cavity. The cavities will be operated at 2.0 K and the power dissipation is determined assuming a surface resistance of R_s = 11.3 nΩ with a residual surface resistance of R_{res} = 10 nΩ.

Table 2: Operating Parameters at 3.4 MV and 5.0 MV

Parameter	(A)	(B)	Units
Deflecting voltage (V_T)	3.4	5.0	MV
Intrinsic quality factor (Q_0)	9.5		$\times10^9$
Peak electric field (E_P)	34	50	MV/m
Peak magnetic field (B_P)	57	84	mT
Power dissipation (P_{diss})	2.8	6.2	W

The ancillary component of the rf-dipole crabbing cavity is designed to meet the current specifications for the SPS beam test at CERN [1]. The fundamental power coupler is designed to achieve a coupling of 5.5×10^5 [5]. The optimized coupler hook has a reduced power

RF PERFORMANCE RESULTS OF THE 2nd ELBE SRF GUN

A. Arnold#, M. Freitag, P. Murcek, J. Teichert, H. Vennekate, R. Xiang, HZDR, Dresden, Germany
P. Kneisel, G. Ciovati, L. Turlington, JLAB, Newport News, USA

Abstract

An improved SRF gun (ELBE SRF Gun II) has been installed and commissioned at HZDR. This new gun replaced the first SRF gun of the ELBE accelerator which had been in operation since 2007. The new gun has an improved 3.5-cell niobium cavity those SRF performances have been studied first with a copper cathode. After the replacement by our standard Cs_2Te-cathode we observed a tremendous degradation of the cavity gradient paired with an increase of field emission.

In this contribution we will report on our in-situ investigations to find the origin and the reason for the particle contamination that happened during the first cathode transfer.

INTRODUCTION

At the superconducting (SC) electron linear accelerator of the ELBE radiation facility [1] a new superconducting electron photo injector has been installed in May 2014. This SRF gun II is replacing the previous one which had been in successful operation from 2007 until April 2014. Although SRF gun I could not reach the design specifications, it was successfully operated for R&D purposes and also some dedicated user experiments at the ELBE accelerator had been done [2].

For SRF gun II a new niobium cavity has been built, treated and tested at JLab [3]. At the same time a new cryomodule has been designed and built at HZDR [4]. In November 2013, the cavity was shipped to HZDR and assembled into the cryomodule. About half a year later, the gun was installed into the ELBE accelerator hall and since June 2014 it is under commissioning for beam tests.

The main goal of SRF gun II is to achieve medium average current (1 mA) and low emittance (1 mm mrad) at a moderate bunch charge (77 pC) as well as to test new semiconductor cathodes.

COLD MASS DESIGN

The design of the cold mass is shown in Figure 1. Most of the components are identical to the previous SRF gun I [5]. The 1.3 GHz Nb cavity, for example, consists of three TESLA like cells and a specially designed half-cell. The latter got improved stiffening and a slightly stronger electric field distribution (80% of the on-axis field in the three TESLA like cells). Another superconducting cell, called choke filter, is surrounding the cathode and prevents RF leakage into the cathode support system.

The photocathode itself is isolated from the cavity by a vacuum gap and cooled down with liquid nitrogen. Both allow the application of a normal conducting (NC) photocathodes with high quantum efficiency (QE) such as Cs_2Te or GaAs.

New is the integration of a SC solenoid in the cryomodule. Compared to the NC solenoid of SRF gun I, which was placed downstream the gun, the new design is much more compact and the distance to the cathode is smaller. The SC solenoid is placed on a remote-controlled x-y table to align its center to the electron beam axis. Additional µ-metal shields hold the solenoid remanence field as well as the field of the stepper motors on a 1 µT level near the cavity. Details of the SC solenoid design and testing are published in [6].

Q_0 vs. E_{ACC}

In order to evaluate the performance of the cavity it is most common to measure the intrinsic quality as a function of the accelerating gradient. For a strongly over coupled cavity, both quantities can be determined by the dissipated and transmitted power (P_{diss} and P_t) as well as by the external quality factor of the fundamental pickup Q_t and the normalized impedance r_s = 165 Ohm (see eq.(1)). The cavity length is L = 0.5 m.

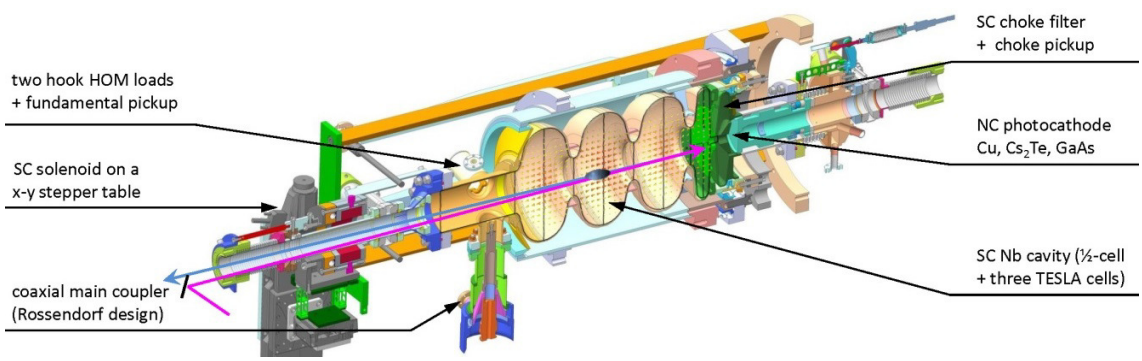

Figure 1: 3D drawing of the ELBE SRF gun II cold mass.

#a.arnold@hzdr.de

ISBN 978-3-95450-178-6

SRF GUN CAVITY R&D AT DESY

D. Kostin, C. Albrecht, A. Brinkmann, T. Büttner, J. Eschke, T. Feldmann, A. Gössel, B. van der Horst, D. Klinke, A. Matheisen, W.-D. Möller, D. Reschke, M. Schmökel, J. Sekutowicz, X. Singer, W. Singer, N. Steinhau-Kuehl, J. Ziegler, DESY, Hamburg, Germany

M. Barlach, J. Lorkiewicz, R. Nietubyc, National Centre for Nuclear Research, NCBJ, Otwock-Świerk, Poland

Abstract

SRF Gun Cavity is an ongoing accelerator R&D project at DESY, being developed since several years. Currently several SRF gun cavity prototypes were simulated, built and tested in our Lab and elsewhere [1] – [11]. Lately the 1.6 cells niobium cavity with Pb thin film cathode was tested in a vertical cryostat with a different cathode plug configurations. Cathode plug design was improved, as well as SRF gun cavity cleaning procedures. Results of the last cavity performance tests are presented.

INTRODUCTION

Goal of this R&D is to prove feasibility of all-superconducting electron source, delivering low emittance beams for FLASH / XFEL like facilities [12] – [15]. We began this R&D several years ago aiming for 1 mA current with 1 nC bunches at 1 MHz repetition rate, but:

- LCLS showed in 2009 that SASE process can take place with charge, as low as 20 pC.
- Experiments listed in the Scientific Case, which inspires the CW operating LCLS II project at SLAC, will nominally use photons generated by 100 pC bunches at 100 kHz repetition rate.

Both, led us to a revision and less demanding SRF-injector parameters in our project. We assume currently that generated electron current will be ≤ 10 μA.

SRF GUN CAVITY

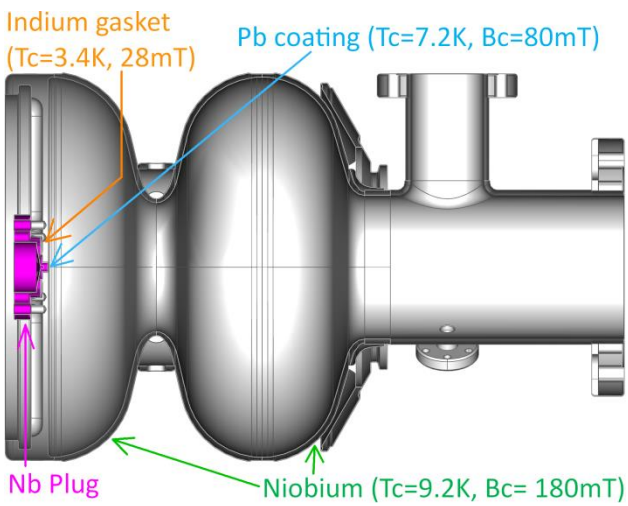

Figure 1: SRF gun cavity with a cathode plug.

In Figure 1 the 1.6 cells SRF gun cavity is presented. Figure 2 shows the cavity in a vertical test cryostat insert at DESY, Hamburg. The cavity was tested with two indium sealed niobium cathode plug (see Fig. 3) configurations: pure niobium plug and a plug coated with lead. The SRF gun cavity was electropoished at DESY before cathode plug insertion. Then the cavity was baked at 90ºC and installed in a vertical cryostat test insert with a movable input antenna (see Fig. 2), enabling variable coupling.

Figure 2: SRF gun cavity in a vertical test cryostat insert at DESY, Hamburg.

ISBN 978-3-95450-178-6

ELBE SRF GUN II – EMITTANCE COMPENSATION SCHEMES

H. Vennekate*[1,2], A. Arnold[1], D. Jansen[1], P. Kneisel[3], P. Lu[1,2], P. Murcek[1], J. Teichert[1], and R. Xiang[1]

[1]Helmholtz-Zentrum Dresden-Rossendorf
[2]Technical University Dresden
[3]Thomas Jefferson National Accelerator Facility

Abstract

In May 2014 the first SRF photo injector at HZDR has been replaced by a new gun, featuring a new resonator and cryostat. The intention for this upgrade has been to reach for higher beam energies, bunch charges and therefore an increased average beam current, which is to be injected into the superconducting, CW ELBE accelerator, where it can be used for multiple purposes, such as THz generation or Compton back-scattering. Because of the increased bunch charge of this injector compared to its predecessor, it demands upgrades of the existing and/or novel approaches to alleviate the transverse emittance growth. One of these methods is the integration of a superconducting solenoid into the cryostat. Another method, the so called RF focusing, is realized by displacing the photo cathode's tip and retracting it from the last cell of the resonator. In this case, part of the accelerating field is sacrificed for a better focus of the electron bunch right at the start of its generation. Besides particle tracking simulations, a recent study, investigating on the exact position of the cathode tip with respect to the cell's back plane after tuning and cool down, has been performed.

THE ELBE SRF GUN II

The ELBE SRF Gun, which is located at the ELBE accelerator center, Dresden, is a RF photoinjector with a 3-1/2-cell TESLA-shaped, pure niobium resonator at its heart. It is operated with a Nd-Yb UV light laser at about 260 nm, while the cavity is cooled down with superfluid helium at 2 K, hence, making it a superconducting photoinjector. In early 2014 the ELBE SRF Gun I has been replaced by its second, upgraded version. Besides a newly improved resonator, the cryostat itself has been extended in order to house an additional superconducting solenoid for emittance compensation for the generated electron bunches. [1]

Although, the gun itself is superconducting, the photocathodes are operated at liquid nitrogen temperature, i.e. 77K. During the installation of the SRF Gun II (see Fig. 1) a bulk copper cathode has been installed inside the cryostat. Since spring 2015 a transfer system has been added to the injector, making it possible to exchange the cathodes without warming up any part of the cryostat. (An updated version of this transfer system, limiting the part being exchanged each time to the very tip of the cathode, has been developed in cooperation with HZB, Berlin, and is currently in the construction phase of the first test setup, see [2].) Besides

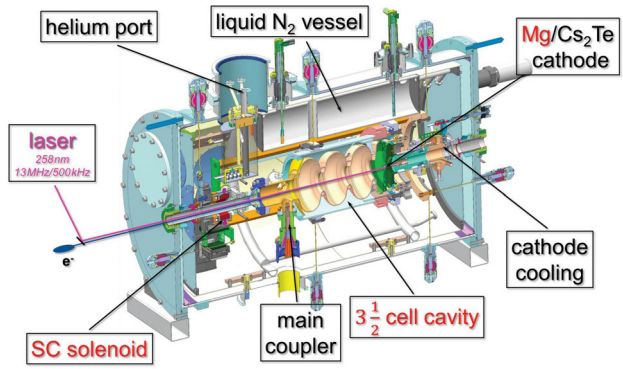

Figure 1: Overview of the design of the ELBE SRF Gun II.

the initial copper cathode, the SRF Gun II is planned to be operated with bulk Mg-tip cathodes — QE $\approx 1-2\cdot10^{-3}$ [3] — and eventually Cs_2Te coated cathodes, aiming for a QE of several percent. [4]

RF FOCUSING

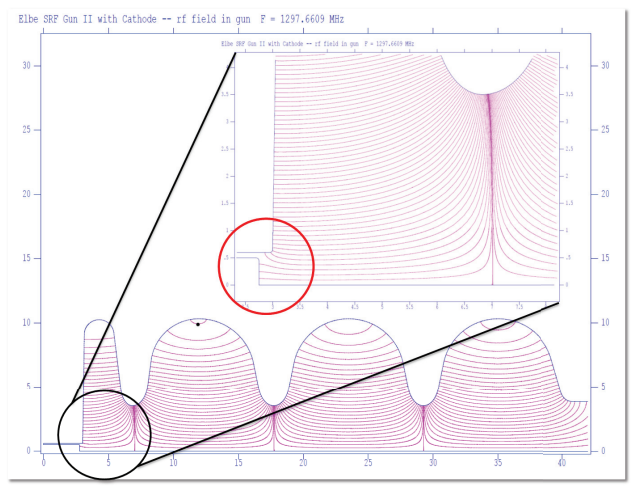

Figure 2: Example of the transverse electrical field lines affecting the cathode tip. In the indicated area the effect of RF focusing becomes visible, as the field representations indicate the additional focus towards the central gun axis for a retracted cathode.

The idea of RF focusing is born out of the geometry of the gun cavity. Since being thermally isolated from the niobium resonator, the cathode has to be inserted into the first half cell through a narrow tube. If synchronized correctly

* h.vennekate@hzdr.de

ISBN 978-3-95450-178-6

COMMISSIONING OF THE 112 MHZ SRF GUN*

S. Belomestnykh[#,1,2], I. Ben-Zvi[1,2], J. C. Brutus[1], T. Hayes[1], V. Litvinenko[1,2], K. Mernick[1], G. Narayan[1], P. Orfin[1], I. Pinayev[1], T. Rao[1], F. Severino[1],J. Skaritka[1], K. Smith[1], R. Than[1], J. Tuozzolo[1], E. Wang[1], Q. Wu[1], B. Xiao[1], T. Xin[2], A. Zaltsman[1]

[1)] Brookhaven National Laboratory, Upton, NY 11973-5000, U.S.A.
[2)] Stony Brook University, Stony Brook, NY 11794, U.S.A.

Abstract

A 112 MHz superconducting RF photoemission gun was designed, fabricated and installed in RHIC for the Coherent electron Cooling Proof-of-Principle (CeC PoP) experiment at BNL. The gun was commissioned first without beam. This was followed by generating the first photoemission beam from a multi-alkali cathode. The paper presents the commissioning results.

INTRODUCTION

A 112 MHz superconducting RF photoemission gun [1-3] is designed to provide an electron beam for the Coherent electron Cooling [4] Proof-of-Principle (CeC PoP) experiment under preparation at BNL [5]. The experiment aims to demonstrate the novel concept of cooling ions in the Relativistic Heavy Ion Collider (RHIC). The quarter-wave resonator was developed by BNL in collaboration with Niowave, Inc. The gun will be able to generate electron bunches with a charge up to 5 nC and repetition rate of 78 kHz, matching the RHIC revolution frequency. Parameters of the CeC SRF gun are listed in Table 1. A multi-alkali photocathode layer is deposited on small molybdenum pucks, several of which are stored in a "garage" under ultra-high vacuum. The garage is attached to the gun via a load lock. This allows quick exchange of the pucks inside a half-wavelength long hollow cathode stalk, which serves as an RF choke and is maintained at room temperature. Electrons are emitted when the cathode is illuminated with green (532 nm) light from a laser. Figure 1 depicts layout of the 112 MHz SRF gun components. More details of the gun design can be found in the cited references. In this paper we describe the gun installation and commissioning results, including generating the first electron beam [6]. A comprehensive analysis of the gun performance is under preparation [7].

INSTALLATION AND COMMISSIONING WITHOUT BEAM

Installation and commissioning of the CeC PoP experiment is accomplished in several phases. The gun cryomodule, together with associated sub-systems (cryogenics, RF, cooling water, vacuum, fundamental power coupler/tuner motion, cathodes insertion), was installed in RHIC during summer of 2014 as Phase I of the CeC PoP. The Phase I linac layout is shown in Figure 2. Its commissioning began in the fall of 2014 [8].

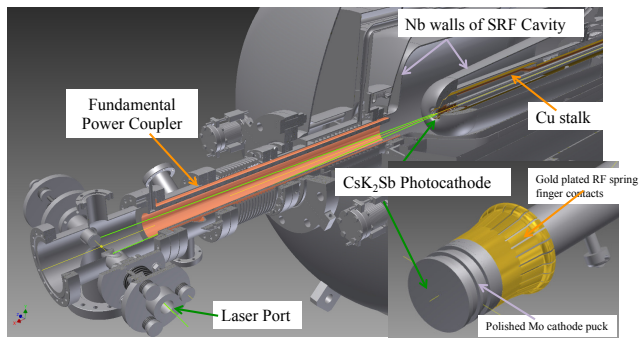

Figure 1: 112 MHz QW SRF gun with FPC, laser port and cathode stalk. Polished molybdenum cathode puck (inset) is housed inside the hollow copper stalk.

Table 1: Parameters of the 112 MHz QWR SRF Gun

RF frequency	112 MHz
Maximum energy gain	2.0 MeV
Electric field at the cathode	27.2 MV/m
Bunch charge	1 to 5 nC
Bunch repetition frequency	78 kHz
R/Q	127.3 Ohm
Geometry factor	38.5 Ohm
Cavity Q_0 at 4.5 K	1.8×10^9
Cavity RF losses at 2.0 MV	17 W
RF losses in the cathode stalk at 2.0 MV	38 W
Frequency tuning range	78 kHz
Frequency tuning with FPC	3 kHz
Q_{ext} of FPC, min.	1.25×10^7
Available RF power	2 kW
Photocathode material	CsK_2Sb
Laser wavelength	532 nm

* Work is supported by Brookhaven Science Associates, LLC under contract No. DE-AC02-98CH10886 with the US DOE
#sbelomestnykh@bnl.goc

DESIGN, FABRICATION AND PERFORMACE OF SRF-GUN CAVITY

T. Konomi#, K. Umemori, E. Kako, Y. Kobayashi, S. Yamaguchi, KEK, Tsukuba, Ibaraki, Japan
R. Matsuda, T. Yanagisawa, Mitsubishi Heavy Industries, Ltd. Japan

Abstract

KEK starts SRF gun development for studying the ERL light source from 2013. The target beam parameters is that beam current is 100 mA, repletion rate is 1.3 GHz CW and normalized emittance is less than 1 π.mm.mrad, pulse length is 3 ps. The shape of acceleration cells is elliptical and the electron emitter is photocathode. Acceleration cell and cathode head was shorted by a choke cell. A beam emittance deeply depends on the laser profile. The excitation laser is injected from backside of the photocathode to shape the laser profile easily by short focal distance. The photocathode has three layers. A substrate is $MgAl_2O_4$. A middle layer is $LiTi_2O_4$ which has two features of transparency and superconductivity. A surface layer is K2CsSb bi-alkali photocathode. The superconductivity protects the substrate from brake down. The cavity shape was designed by the SUPERFISH and GPT. The iris radius is ϕ 60 mm. The beam parameters satisfy target values. Prototype #1 cavity was fabricated without choke, cathode plug and photocathode. 1st vertical test was done. The surface peak electric field reached Esp=66 MV/m, Qo=4.19×10^9. This meets the target value Esp=42 MV/m Qo=4.5×10^9 sufficiently.

CONCEPTUAL DESIGN

Electron gun is a key component of the linac. Normalized emittance is dependent on thermal emittance of photocathode and space charge effect at low energy region. It is necessary to generate narrow energy distribution electrons and to accelerate high gradient on cathode to achieve the lower emittance beam. Thermal emittance can decrease at low temperature. Space charge effect can be suppressed by shaping profile of excitation laser. Transparent photocathode can be controlled the laser shape easily because of short focal length. Combination of SRF gun and transparent photocathode is suitable for high repletion and low emittance gun. The transparent photocathode needs the high durability under high electric RF field. A transparent superconductor $LiTi_2O_4$ which is epitaxially grown on the transparent substrate $MgAl_2O_4$ reflects the RF and transmits excitation laser [1]. Photoelectric surface is K2CsSb. It is well known as high quantum efficiency material.

Target beam and cavity parameters are listed in Table 1. These parameters based on KEK 3 GeV ERL project. Beam energy is determined from the input coupler [2]. Surface peak electric field is designed less than 50 MV/m. The cavity shape was designed based on the HZDR and HZB SRF gun [3],[4].

Table 1: Target Parameters of the SRF Gun

Parameter	Value
Beam energy	2 MeV
RF frequency	1.3 GHz
Beam current	100 mA
Pulse length (1σ)	3 ps
Projected emittance	< 1 π mm mrad
Projected energy spread	< 0.1%
Number of cells	1.5

CAVITY DESIGN

The cavity design was started from analysing relation between cavity shape and beam parameters [4]. Beam performance is affected by initial slope of the electric field and cell length. Diameter of the end iris lightly affects to the beam performance. When beam energy set to 2 MeV, it is possible to suppress the surface peak electric field in less than 50 MV/m. Half cells shape besides the cathode side half-cell were designed by same shape to supress die fabrication cost. Electric field distribution on beam axis is shown in Fig.1.

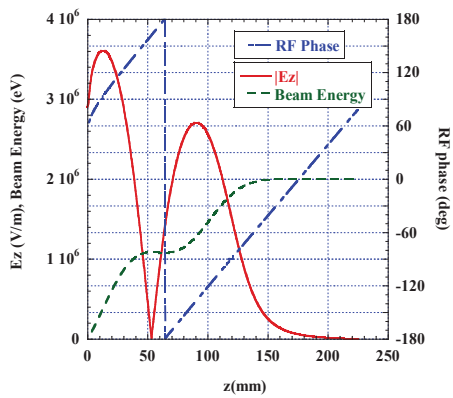

Figure 1: RF electric field and beam energy on beam axis.

Initial configuration of GPT is that beam distribution is uniform, beam radius is ϕ2 mm, beam length is 10 mm, number of macro particle is 1000, and energy distribution is 0.4 eV. Space charge effect is simulated by using "spacecharge3D". RF filed was imported from SUPERFISH. Best initial RF phase and accelerating gradient was determined from an intersection point of 2 MeV bam energy curve and minimum projected energy spread curve (Fig. 2). Best parameters are calculated by

konomi@post.kek.jp

ISBN 978-3-95450-178-6

DEVELOPMENT OF SRF CAVITY TUNERS FOR CERN*

K. Artoos, R. Calaga, O. Capatina, T. Capelli, F. Carra, L. Dassa, N. Kuder, R. Leuxe, P. Minginette, W. Venturini Delsolaro, G. Villiger, C. Zanoni, P. Zhang CERN, Geneva, Switzerland
S. Verdu-Andrés, B. Xiao, BNL, Long Island, New York, USA
G. Burt, Cockcroft Institute, Lancaster, UK
J. Delayen, H. Park, ODU, Norfolk, Virginia, USA
T. Jones, N. Templeton, STFC, Daresbury, UK

Abstract

Superconducting RF cavity developments are currently on-going for new accelerator projects at CERN such as HIE ISOLDE and HL-LHC. Mechanical RF tuning systems are required to compensate cavity frequency shifts of the cavities due to temperature, mechanical, pressure and RF effects on the cavity geometry. A rich history and experience is available for such mechanical tuners developed for existing RF cavities. Design constraints in the context of HIE ISOLDE and HL-LHC such as required resolution, space limitation, reliability and maintainability have led to new concepts in the tuning mechanisms. This paper will discuss such new approaches, their performances and planned developments.

INTRODUCTION

A new linear accelerator for the HIE ISOLDE project is currently under construction with the first cryomodule installed and being commissioned. Each cryomodule is composed of five superconducting quarter wave resonators (QWR), accelerating radio frequency (RF) cavities. Only the high-β cavities are described in this paper. The QWR are niobium sputtered, bulk copper substrate cavities, operated at 4.5 K. The operating frequency is 101.28 MHz for a 6 MV/m accelerating gradient with a power dissipation of 10 W on each cavity [1,2].

The HL-LHC upgrade requires crab cavities providing the deflecting field of 12-13 MV on the particle bunches at a frequency of 400.79 MHz. The bulk niobium cavities are operated at 2 K with a heat load of about 30 W. Two compact cavity designs with unconventional geometry are currently being developed: double quarter wave (DQW) and RF Dipole (RFD) [3,4].

The resonant RF frequency of a SRF cavity shall fit precisely to the operating frequency in order to limit the RF power required to drive it. The obtained resonant frequency will depend mainly on the dimensions and shape of the cavity and their changes during cool down. Material properties such as the RRR will have a much smaller influence on the frequency [5].

Geometrical variations due to the forming, welding and surface treatments made during the fabrication will result in a first frequency uncertainty. Stringent but realistic tolerances can be defined on the fabrication of the cavity to reduce the uncertainties. A well mastered chemical polishing combined with metrology and RF frequency measurements can improve the obtained tolerances. The precision of such measurements is however limited at room temperature due to temperature and air humidity variations.

The cool-down to the operating temperature will shift the frequency due to the thermal contraction of the components. Other environmental conditions [6] such as the vacuum conditions, helium pressure, constraints created by the support system in the cryostat and presence of mechanical vibrations can also introduce uncertainty on the resonant RF frequency.

Finally, during RF operation, Lorentz forces detune the cavity (Lorentz Force Detuning, LFD).

Facing realistic fabrication tolerances and added uncertainties, especially at the start of the production, a mechanical tuning system is required for both projects with a tuning range as large as possible. For the HL-LHC cavities, the tuner might also be required to tune the cavity away from the operating frequency when the cavities are not used during presence of beam. The cavities in both projects are operated in CW mode and require no fast pulsed tuning.

The technical solutions, status and performance of the mechanical tuners will be discussed in the next two sections for both projects.

HIE ISOLDE TUNER

During operation, the RF frequency of the QWR cavities of the HIE ISOLDE project should be within 0.5 Hz from the 101.28 MHz operation frequency. The frequency shifts from the copper substrate to the chemically polished and Nb-deposited cavity, cooled down to 4.5 K were well managed. From analytical predictions and experience during the start of the production it was possible to set a target frequency at room temperature, obtained by trimming the cavity length, changing the tip gap between inner conductor and the bottom plate, well described in [5]. To cover for the uncertainties on the production and cool-down, a tuning range of 36 kHz was aimed for by deformation of the bottom (tuning) plate. An optimisation was made on the nominal tip gap to have the best combination of tuning range, sensitivity and cost of the tuning plate design [7]. The tuning plate is machined from a 15 mm thick cold rolled Cu OFE UNS C10100 plate machined down to 0.3 mm thickness. The flat Nb-deposited plate is deformed up to 5 mm by pulling it down centrally. With an additional 0.6 mm pushing range this

*The research leading to these results has received funding from the European Commission under the FP7 project HiLumi LHC, GA no. 284404, co-funded by the DoE, USA and KEK, Japan

ISBN 978-3-95450-178-6

PERFORMANCE OF THE TUNER MECHANISM FOR SSR1 RESONATORS DURING FULLY INTEGRETED TESTS AT FERMILAB*

D. Passarelli†, J.P. Holzbauer, L. Ristori, FNAL, Batavia, IL 60510, USA

Abstract

In the framework of the Proton Improvement Plan-II (PIP-II) at Fermilab, a cavity tuner was developed to control the frequency of 325 MHz spoke resonators (SSR1). The behavior of the tuner mechanism and compliance with technical specifications were investigated through a campaign of experimental tests in operating conditions in the spoke test cryostat (STC) and at room temperature. Figures of merit for the tuner such as tuning range, stiffness, components hysteresis and overall performance were measured and are reported in this paper.

INTRODUCTION

With the goal of maintaining the cavity at the proper operational frequency: 325 MHz [1], the tuner was designed to compensate uncertainties in the frequency shift due to the cooldown from 293 K to 2 K and to minimize detuning caused by helium pressure fluctuations and microphonics perturbations. Cooldown uncertainties are estimated to be less than 135 kHz, while the amplitude of perturbations is estimated to be less than 1 kHz. These two values define respectively the requirements for coarse tuning and fine tuning. In order for the cavity to have a low pressure sensitivity (df/dp), studies showed that the stiffness of the tuner as seen by the cavity (passive stiffness) must be greater than 30 kN mm^{-1}.

Figure 1 shows the tuner prototype that was developed.

The large scale tuning (135 kHz) is accomplished via a stepper motor actuating a threaded rod and traveling nut, translating rotational motion into axial motion of a double-lever mechanism, compressing and relaxing the cavity at one of the two beam-pipes. Fine tuning (1 kHz) is achieved with piezoelectric actuators (or piezos) which act as a fine tuning mechanism for the active compensation of perturbation sources like helium bath pressure fluctuations and mechanical vibrations. Other technical specifications for the tuner are described elsewhere [1, 2].

Figure 5 shows the operating principle of the double lever mechanism that allows coarse and fine tuning of the cavity. The two main arms hinged at one end and connected to the actuation system at the other end have a probe that tunes the cavity physically pushing on the beam pipe. The actuation system consists of a stepper motor held by a bracket and connected to a second arm. This arm is hinged at the other end and keeps the piezos in series with the motor.

* Work supported by Fermi Research Alliance, LLC under Contract No. DEAC02- 07CH11359 with the United States Department of Energy

† donato@fnal.gov

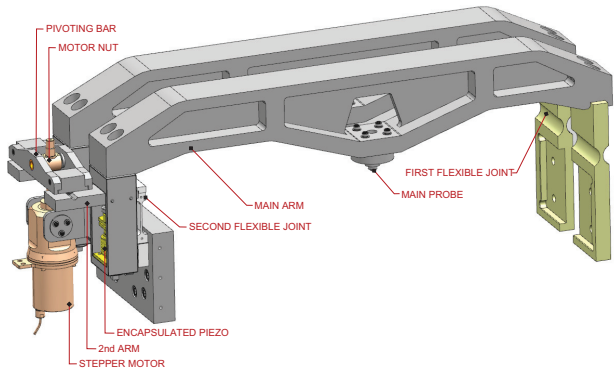

Figure 1: 3D model of the prototype model of SSR1 tuner.

TESTS AT ROOM TEMPERATURE

Several checks and preliminary measurements were done at room temperature prior to installation onto a cavity for cold testing. All structural components were checked to ensure their compliance with fabrication drawings.

Testing Encapsulated Piezos

The wire connections of the two encapsulated piezos were checked by measuring their resistance and impedance. Subsequently, both piezos were tested to monitor their elongation by applying different voltages from 0 V to 200 V (maximum applicable voltage), see Figure 2. The required stroke of 68 µm at room temperature was achieved for both piezos. The piezos are controlled in voltage by 10 V stages during the scan and both present a hysteresis loop.

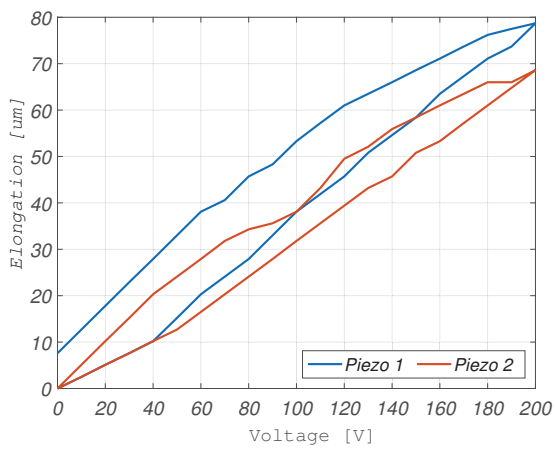

Figure 2: Elongation of Noliac piezos as a function of the voltage with an initial preload of 2000 N.

ACCELERATED LIFE TESTING OF LCLS-II CAVITY TUNER MOTOR

N. Huque, E. F. Daly, M. Abdelwhab, JLab, Newport News, VA 23606, USA
Y. Pischalnikov, FNAL, Batavia, IL 60510, USA

Abstract

An Accelerated Life Test (ALT) of the Phytron stepper motor used in the LCLS-II cavity tuner is being carried out at JLab. Since the motor will reside inside the cryomodule, any failure would lead to a very costly and arduous repair. As such, the motor will be tested for the equivalent of five lifetimes before being approved for use in the production cryomodules. The 9-cell LCLS-II cavity will be simulated by disc springs with an equivalent spring constant. Hysteresis plots of the motor position vs. tuner position – measured via an installed linear variable differential transformer (LVDT) – will be used to determine any drift from the required performance. The titanium spindle will also be inspected for loss of lubrication. This paper outlines the ALT plan and latest results.

INTRODUCTION

The LCLS-II Cavity Tuner is a lever-style tuner, consisting of the frame, two piezo actuators and a Phytron stepper motor, the LVA 52-LCLS II-UHVC-X1 (Fig. 1). In the current testing setup, the piezo actuators are not present, and replaced by solid cylinders. Table 1 describes the working parameters of the tuner and motor.

The motor itself consists of four main components: the stepper motor, gear box, titanium spindle and traveling nut. A copper collar is located at the edge of the motor section to attach to a thermal strap. The planetary gear box has a ratio of 1:50. The spindle is a titanium M12x1 thread, which attaches to a similarly sized stainless steel traveling nut. The traveling nut has a TECASIN insert which mates to the M12x1 thread [1].

TESTING SETUP

The cavity is simulated via two sets of disc springs, designed to imitate the cavity's stiffness of 3kN/mm. The tuner frame and springs are attached to an Aluminium base plate (Fig. 2), which is positioned inside the Tuner Test Can.

The can is evacuated and lowered into a vertical test area (VTA) dewar for cold testing at ~4K. Unlike the cryomodule, there is no active pumping on the test can.

An LVDT is positioned between the main lever arm of the tuner and the Aluminium base plate. The LVDT is the primary means of recording and measuring the tuner arm's movement, and the motor's operation. The feedback voltage of the LVDT is used to define the tuner arm displacement. In the provided graphs, the zero-position of the LVDT is at a readback value of 0.016V.

The motor is fitted with a thermocouple for recording the running temperature. However, its readings were found to be too noisy due to the close proximity of other wiring. Instead, a resistance temperature diode (RTD) is attached to the side of the motor portion of the assembly.

A set of limit switches are attached adjacent to the spindle to act as a safety mechanism. The limits are set just inside the maximum mechanical travel of the traveling nut. The motor is stopped once either of the switches is tripped.

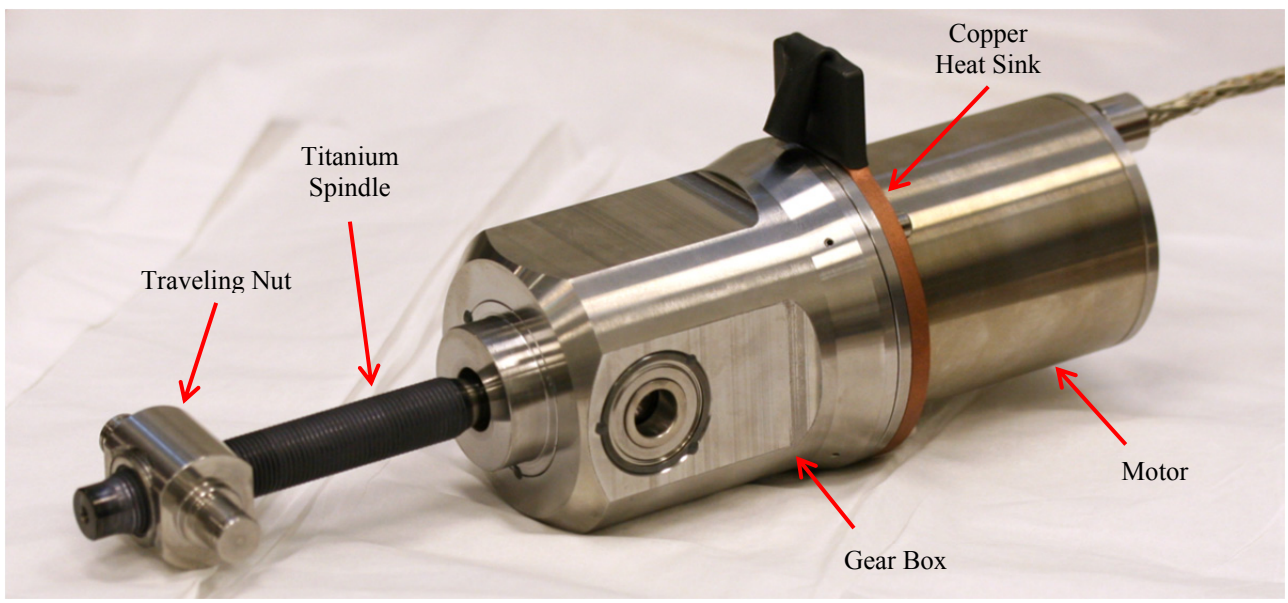

Figure 1: Phytron motor assembly, showing the main components.

ISBN 978-3-95450-178-6

BNL 56 MHz HOM DAMPER FABRICATION AT JLAB

N. Huque, E. F. Daly, W. Clemens, JLab, Newport News, VA 23606, USA
G. McIntyre, Q. Wu, S. Seberg, S. Bellavia, BNL, Upton, NY 11973, USA

Abstract

The Higher-Order Mode (HOM) Dampers for the Relativistic Heavy-Ion Collider's (RHIC) 56 MHz cavity at Brookhaven National Laboratory (BNL) are currently being fabricated at JLab. The coaxial damper is primarily constructed with high RRR niobium, with a combination of niobium and sapphire rings as the filter assembly. Several design changes have been made with respect to the performance of a prototype damper – also fabricated at JLab – which was found to quench at low power. The production dampers are being tuned and tested in the JLab vertical test area (VTA) prior to delivery. Two HOM dampers will be delivered to BNL; they are to be used in the RHIC in November, 2015. This paper outlines the challenges faced in the fabrication and tuning process.

INTRODUCTION

Work on five HOM dampers was started at Niowave Inc. in early 2014. The majority of the parts were fabricated at Niowave, as was part of the assembly. The project was transferred to JLab in July 2014. The number of dampers to be delivered was revised to two out of the original five, to allow for installation during RHIC's 2015 shutdown period (July – November). The two dampers would fit at the 225 degree and 270 degree positions on the RHIC cavity; they are named BNL01 and BNL03 respectively. The following tasks were to be carried out at JLab:

- Determine an assembly and fabrication sequence and plan, utilizing parts and assemblies received from Niowave
- Fabricate other required components
- Integrate design changes from BNL
- Conduct required welding, chemistry and inspection
- Tune fabricated dampers, including tests at 4K in the JLab vertical test area (VTA)
- Perform pressure and leak checks as required

The two dampers are scheduled to be delivered to BNL in late September, 2015.

DESIGN FEATURES

A cut-away view of the HOM damper is shown in Fig. 1. The Loop resides inside the cavity and acts as the coupling mechanism. The damper is attached to the cavity via the NbTi flange.

Cooling

The Main Inductor connects to the Loop at the cavity end of the damper, and supports the Filter Assembly at the other end. The Inductor acts as the primary cooling mechanism for the damper. Essentially, it is a Niobium tube, through which a copper rod runs. The rod is connected via an interference fit at the Loop (the area of highest heat generation) and is immersed in flowing liquid helium at the Cooling Turret [1]. Channels in the

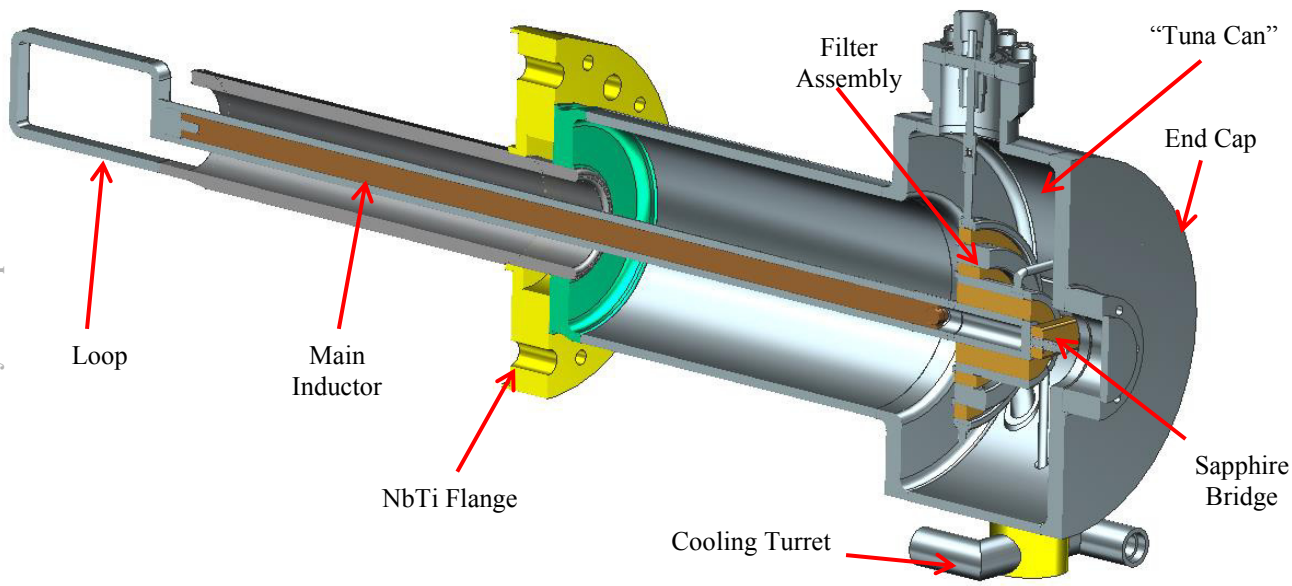

Figure 1: Cut-away view of the prototype damper, showing main components.

RELIABILITY OF THE LCLS II SRF CAVITY TUNER

Y. Pischalnikov#, B. Hartman, J. Holzbauer, W. Schappert, S. Smith, J.C. Yun
FNAL, Batavia, IL 60510, USA

Abstract

The SRF cavity tuner for LCLS II must work reliably for more than 20 years in a cryomodule environment. Tuner's active components- electromechanical actuator and piezo-actuators must work reliably in an insulating vacuum environment at low temperature for the lifetime of the machine. Summary of the accelerated lifetime tests (ALT) of the electromechanical and piezo actuators inside cold/ insulated vacuum environment and irradiation hardness test (dose level up to $5*10^8$ Rad) of tuner components are presented. Methodology to design and build reliable SRF cavity tuner, based on "lessons learned" approach, are discussed.

INTRODUCTION

Description of the design and measured parameters of the SRF cavity tuner for LCLS II project were presented at the IPAC2015 conference [1] (Figure 1).

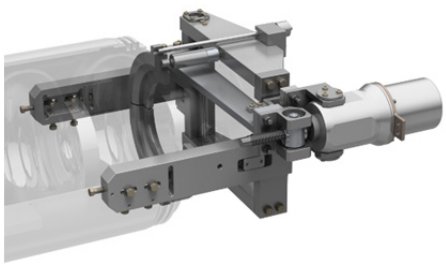

Figure 1: 3-D model of the LCLS II Tuner.

Tuner must work reliably for 20 years. Tuner will be assembled on the cavity inside the cryomodule (CM) and will work inside of the insulated vacuum vessel at cryogenic temperature. In Table 1, longevity (lifetime) requirements specifications for tuner components are presented.

Table 1: Tuner Active Components - LCLS II Lifetime Requirements (Operation for 20 Years and 40 Thermal Cycles)

Coarse Tuner/ Electromechanical Actuator	1,000 spindle rotations
Fast Tuner / Piezo-electrical Actuator	$2*10^{10}$ pulses (V_{pp}=2V, f=40Hz) & $6*10^6$ pulses (V_{pp}=50V, f=0.01Hz)

The tuner was designed such a way that the electromechanical actuator and piezo-stack are accessible and replaceable through special ports in the cryomodule vacuum vessel. As the last remedy, active components of the tuner can be replaced through designated port in the CM vacuum vessel without removing the CM from the SLAC tunnel.

RELIABILITY OF THE ELECTROMECHANICAL ACTUATOR

The electromechanical actuator is the active element of the slow/coarse tuner. The electromechanical actuator translates rotation of the stepper motor to linear motion of the tuner arms. The tuner is equipped with a Phytron actuator (LVA 52-LCLS II-UHVC-X1) [2] designed for the FNAL linear SRF project (Table 2).

Table 2: Four Main Components of the Electromechanical Actuator LVA 52-LCLS II-UHVC-X1

Stepper Motor	LVA-52, 200step/revolution, Imax=2,5A
Gear Box	type:planetary; stainless steel; dry lubrication
Spindle	Titanium; M12X1; dry lubrication
Traveling Nut	stainless steel with TECASIN-1041 insert to mates 12X1 thread

ALT of the LVA 52-LCLS II-UHVC-X1 Actuator at the FNAL HTS

As a part of the R&D efforts actuator ALT conducted during several weeks of continuous operation of the blade tuner installed on the 9-cell elliptical cavity at the FNAL HTS [3,4]. Several parameters were monitored during long test: SRF cavity frequency, temperature of the stepper motor, etc.

The motor was operated with current I=0.7A (I_{nom}=1.2 A). During the test of the actuator, the tuner pushed & pulled the cavity, the load on the actuator changed from -1200N to +1200N. Total steps accumulated by the motor during ALT test was 5000 spindle rotations or 5 LCLS II lifetime requirements (Table 1). There was no observed degradation of actuator performance. Visual inspection after ALT shows no damage or loss of lubrication to the spindle and traveling nut.

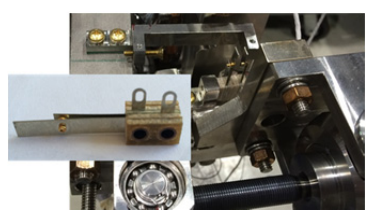

Figure 2: Limit switches mounted on the tuner.

*This manuscript has been authorized by Fermi Research Alliance, LLC under Contract N. DE-AC02-07CH11359 with U.S. Department of Energy.
#pischaln@fnal.gov

ISBN 978-3-95450-178-6

RF ANALYSIS OF EQUATOR WELDING STABILITY FOR THE EUROPEAN XFEL CAVITIES

A. Sulimov, DESY, Hamburg, Germany

Abstract

In order to guaranty a sufficient High Order Modes (HOM) damping in the European XFEL cavities, a detailed analysis of the mechanical cavity production was performed. The mechanical measurements are precise enough to control the shape of cavity parts, but cannot be used for a welded cavity. To estimate the shape deformation during equator welding, the eigenfrequencies of cavity cells are compared with frequencies of cavity parts. This simple RF analysis can indicate irregularity of 9 equator welds and was used in addition to control of mean values for longitudinal and transverse deformations.

INTRODUCTION

The mechanical and RF characteristics of all cavity parts (Fig. 1) and their positions are very important for field distribution and suppression of HOM [1, 2 and 3].

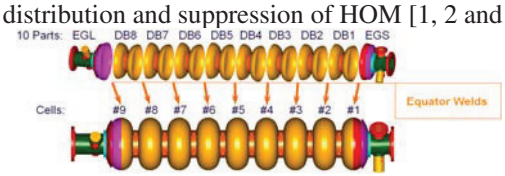

Figure 1: The European XFEL cavity and its parts: dumbbels (DB) and end-groups (short side EGS, long – EGL).

Different types of deformations during equator welding can be classified as:

- regular (the same for all welds) and irregular (specific for some cells);
- longitudinal and transverse relative cavity axis.

For the European XFEL cavities manufacturing it was planned to analyze only regular deformations (mean values of nine welds) to take them into account for cavities' sub-components preparation (trimming) [4, 5]. Organizing of new mechanical measurements is time consuming and expensive. Thus rapid RF analysis is used to find welding irregularities.

Three factors of frequency changes during equator welding (Fig. 2) have to be taken into account:

1. joint type (material overlapping due to recess);
2. longitudinal deformations due to material melting (shrinkage);
3. transverse local deformation due to outer forces (including gravity) and material softening.

ALGORITHM OF ANALYSIS

The two methods will be described in this part:

- calculation of mean values, which allow us separation of longitudinal and transverse deformations;
- analysis of welds regularity.

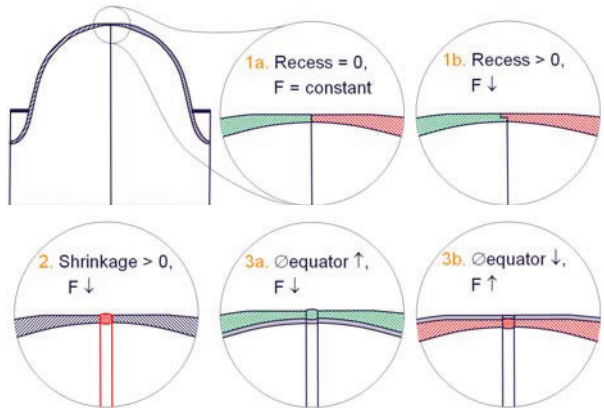

Figure 2: Influence of parts recess (1), shrinkage (2) and transverse deformation (3) on cells / cavity frequency.

Calculation of Mean Values

Based on mechanical measurements, one can calculate longitudinal deformations due to material melting:

$$\mathrm{Sh} = \frac{(\sum_{j=1}^{10} Lj - La)}{18} - R, \qquad (1.1)$$

where: Sh – mean shrinkage per each piece of a weld;
Lj – length of a cavity part (j =1 – L_{EGS}, j =2…9 – $L_{\mathrm{DB\#}(j-1)}$, j =10 – L_{EGL});
La – length of a cavity after welding;
R – planned recess per each piece of a weld.

Let us assume that we always have a constant recess parameter and any longitudinal deviations of joint between two parts will be counted in shrinkage value.

Calculation of transverse deformation is based on RF measurements:

$$\mathrm{Def} = Fa - \frac{\sum_{j=1}^{10} Fj}{18} - Fl, \qquad (1.2)$$

where: Def – frequency changes per each piece of a weld;
Fj – frequency of a cavity part (j =1 – F_{EGS}, j =2…9 – $2\,F_{\mathrm{DB\#}(j-1)}$, j =10 – F_{EGL});
Fa – pi-mode frequency of a cavity after welding;
Fl – correction due to longitudinal deformation, estimated in (1.1).

Analysis of Welds Regularity

Frequency changes in cell #(i), i = 1…9 can be described as:

$$\Delta F(i) = \frac{Fp(i)+Fp(i+1)}{2} - Fc(i), \qquad (2.1)$$

where: $Fc(i)$– eigenfrequency of a cell, which can be found, based on RF measurements (spectra and field amplitudes) after cavity welding [6];

ISBN 978-3-95450-178-6

HOM COUPLER NOTCH FILTER TUNING FOR THE EUROPEAN XFEL CAVITIES

A. Sulimov, DESY, Hamburg, Germany

Abstract

The notch filter (NF) tuning prevents the extraction of fundamental mode (1.3 GHz) RF power through Higher Order Modes (HOM) couplers. The procedure of NF tuning was optimized at the beginning of serial European XFEL cavities production. It allows keeping the filter more stable against temperature and pressure changes during cavity cool down. Some statistics of NF condition during cavities and modules cold tests is presented.

INTRODUCTION

One of the most important procedures of cavity preparation for cryo tests is tuning of HOM couplers filter [1]. The goal is reaching the minimum RF transmission on the operating mode (π-mode) at 1.3 GHz under cryo-conditions. Notch filter tuning is done by changing the gap between HOM coupler antenna end and cap (capacitance tuning) by applying a force (push or pull) on the HOM coupler cap (see Fig. 1) using a special tool.

The European XFEL cavity has 2 HOM couplers; fundamental mode NF must be tuned for both of them.

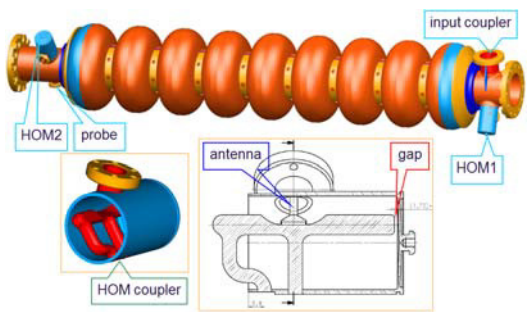

Figure 1: HOM couplers of the European XFEL cavities.

Primarily this operation is done directly before the first vertical cavity test, then constantly checked and in case of necessity adjusted before new tests or integration in the XFEL module.

Procedures of NF tuning and measurements depend on cavity conditions (see below).

CONTROL MEASUREMENTS

The two kinds of measurements will be described here:

- warm (at room temperature), done always before and after cavity tuning or adjustment;
- cold (at 2 K), control the output power of fundamental mode through HOM couplers.

Warm measurements of transmission magnitude S21 values in full TM011 bandwidth (1285 ± 15) MHz (between HOM coupler and antenna on opposite side) allow identification of the resonance frequencies (fundamental mode spectrum) and their amplitudes (9 points in Fig. 2).

Analysing the curve, built by these points, one can see:

1. Curve smoothness shows the direction of detuning:
   - local extremum (minimum) between points #5 and #9 (Fig. 2, green) – $F_{filter} < (F_{(\#8)}+F_{(\#9)})/2$;
   - smooth curve (Fig. 2, red) – $F_{filter} > (F_{(\#8)}+F_{(\#9)})/2$.
2. Amplitudes deviations between definite points (S21(#5) – S21(#8) and S21(#8) – S21(#9)) indicate the quality of the NF tuning (see criteria in "Algorithm of Tuning").

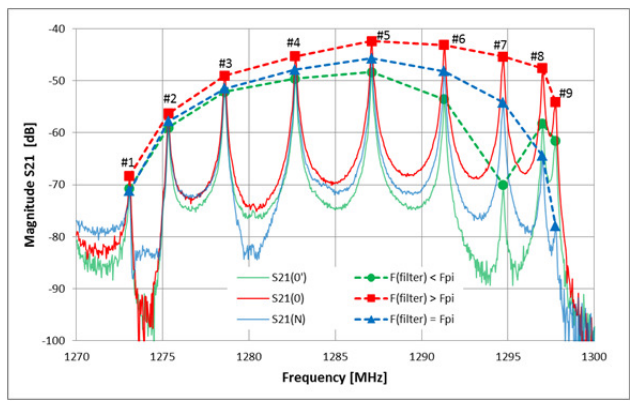

Figure 2: Fundamental mode spectrum with amplitudes (Fpi = $F_{(\#9)}$= 1297.75 MHz).

The 9 points (resonance amplitudes) are enough to analyse the NF tuning quality and direction (sometimes quantity) of detuning, therefore they are being saved and collected in the XFEL cavity database (DB) [2].

Additional criterion is used for NF of HOM2 – output power through HOM2 coupler at pi-mode should be at least two times less than through probe antenna. It means that transmission between input coupler and HOM2 should be at least 3 dB lower than between input coupler and probe (Fig. 3, Pickup – HOM2(9)).

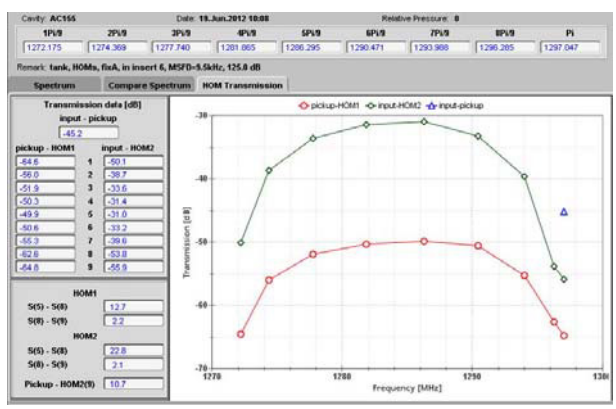

Figure 3: Control measurements at room temperature.

ISBN 978-3-95450-178-6

PRACTICAL ASPECTS OF HOM SUPPRESSION IMPROVEMENT FOR TM011

A. Sulimov, A. Ermakov, J.-H. Thie, DESY, Hamburg, Germany
A. Gresele, E. ZANON SpA, Schio, Italy

Abstract

Some Higher Order Modes (HOM) pass bands were controlled during cryo-tests at DESY for the European XFEL cavities. The second monopole mode (TM011) showed most instabilities and suppression degradation.

The authors will explain this phenomenon on the example of cavity CAV00553 and present the practical method of TM011 damping improvement.

INTRODUCTION

Suppression of the TM011 (zero mode) in the cavities was a challenging task for the European XFEL mass production. Our investigation [1] determined that damping efficiency degradation is caused by critical changes in the field distribution.

RF simulations showed that these changes are possible for geometry deviations of about ± 0.2 mm in the equator radius within specific cells.

Almost all cavities, that were produced by company E.ZANON for the European XFEL, correspond to the criteria (see Fig.1), which was achieved during pre-series production (Q load values below the "TESLA limit" of 100 000).

It was found that one sub-component of cavity CAV00533 was not trimmed to the correct length at the equator before welding and cell #1 becomes about 2 mm longer after field flatness tuning of fundamental mode. A similar situation was simulated in [1] and the measurement of HOM suppression at 2 K (see below) indicates the necessity of TM011 damping improvement.

HOM SUPPRESSION IMPROVEMENT

The detailed analysis of HOM suppression for CAV00553 shows that the most critical dipole modes (see Fig. 2 a) are damped well (points filled with red and green colours). But the second monopole mode (filled with blue) coupled not strong enough with both HOM couplers: Qload = 222 000.

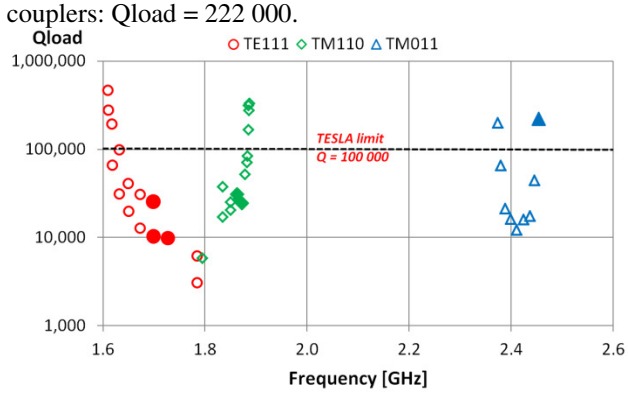

a)

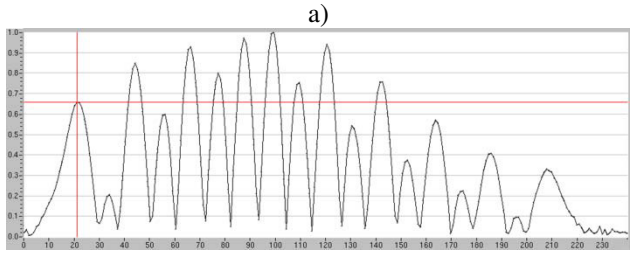

z – position on cavity axis

b)

Figure 2: HOM suppression (a) and normalized field distribution of TM011 $|E|_{r=0}$ (b) for CAV00553 after welding.

The necessary field asymmetry is lost (Fig.2 b) and the amplitude in the first cell is 35 % less than in cell #4. It also correlates with simulations in [1] for length deviation (first cell elongation) about 2 mm relative nominal value.

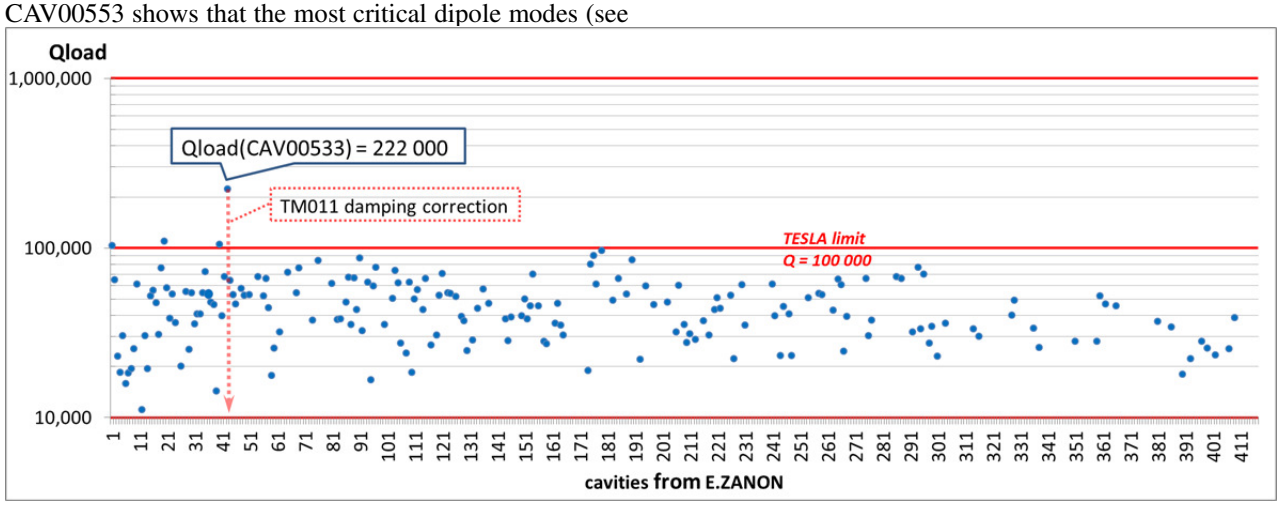

Figure 1: Measurements results of TM011 at 2K for the XFEL cavities, produced by E.ZANON.

ISBN 978-3-95450-178-6

ENGINEERING DESIGN AND PROTOTYPE FABRICATION OF HOM COUPLERS FOR HL-LHC CRAB CAVITIES *

C. Zanoni†[1], S. Atieh[1], I. Aviles Santillana[1,2], S. Belomestnykh[3,4], G. Burt[5], R. Calaga[1], O. Capatina[1], T. Capelli[1], F. Carra[1], S.U. De Silva[6], J. Delayen[6], P. Freijedo Menendez[1], M. Garlaschè[1], J.-M. Geisser[1], T. Jones[7], R. Leuxe[1], Z. Li[8], L. Marques Antunes Ferreira[1], A. May[7], T. Nicol[9], R. Olave[6], H. Park[6], S. Pattalwar[7], A. Ratti[10], E. Rigutto[1], N. Templeton[7], S. Verdu-Andres[3], Q. Wu[3], and B. Xiao[3]

[1]CERN, Geneva, Switzerland
[2]University Carlos III, 28911 Madrid, Spain
[3]BNL, Upton, NY 11973, USA
[4]Stony Brook University, Stony Brook, NY 11794, USA
[5]Cockcroft Institute, Lancaster University, UK
[6]Old Dominion University, Norfolk, VA, 23529, USA
[7]STFC Daresbury Laboratory, UK
[8]SLAC, Menlo Park, CA 94025, USA
[9]Fermilab, Batavia, IL 60510, USA
[10]LBNL, Berkeley, CA 94707, USA

Abstract

The HL-LHC upgrade relies on a set of RF crab cavities for reaching its goals. Two parallel concepts, the Double Quarter Wave (DQW) and the RF Dipole (RFD), are going through a comprehensive design process along with preparation of fabrication in view of extensive tests with beam in SPS. High Order Modes (HOM) couplers are critical in providing damping in RF cavities during operation in accelerators. HOM prototyping and fabrication have recently started at CERN.

In this paper, an overview of the final geometry is provided along with an insight in the mechanical and thermal analyses performed to validate the design of this critical component. Emphasis is also given to material selection, prototyping, initial fabrication and test campaigns that are aimed at fulfilling the highly demanding tolerances of the couplers.

INTRODUCTION

The statistical gain obtained by running LHC after 2020 with the current performance is marginal [1]. Thus, in order to keep LHC at the forefront of physics, a significant luminosity increase is foreseen through the HL-LHC (High Luminosity LHC) upgrade. The crab cavities are among the critical systems required for obtaining the desired new performance. They compensate the bunch crossing angle, and thus maximize the integrated luminosity and provide instant luminosity leveling.

Two parallel concepts for such cavities are under development: the Double Quarter Wave (DQW) and the RF Dipole (RFD). In the scope of these cavities, so called High Order Modes (HOM) couplers are also under design [2, 3], prototyping and fabrication.

The coupler is needed for damping detrimental modes with frequencies higher than the fundamental one. Such modes, induced by the passage of the charged beam in the cavity, have profound consequences in terms of power dissipation and stability of the beam [4]. Each DQW cavity needs 3 HOM couplers. The RFD have 2 HOM couplers each in 2 variants.

The geometry of the DQW and RFD HOM couplers are depicted in Figure 1. This paper overviews the thermo-mechanical assessment and early fabrication of these systems. Other aspects of the cavity design and engineering are treated elsewhere in this conference [5–7].

ASSESSMENT OF THE MECHANICAL PERFORMANCE

The DQW HOM coupler is made of a niobium shell that continues the cavity envelope and supports a hook. The hook performs the extraction of the high frequency electromagnetic modes. The external shell is in AISI 316LN (stainless steel) that contains the superfluid cryogenic helium during operation. The 316LN jacket also includes bellows that limit the effect of deformations due to welding.

The heat deposition in the hook due to the RF electromagnetic field is in the order of 17 mW. The coupler is actively cooled in order to cope with tolerances (0.1 mm shape error can determine up to 0.1 W extra load) and minimize temper-

* The research leading to these results has received funding from the European Commission under the FP7 project HiLumi LHC, GA no. 284404, co-funded by the DoE, USA and KEK, Japan
† carlo.zanoni@cern.ch

ISBN 978-3-95450-178-6

DESIGN OF DRESSED CRAB CAVITIES FOR THE HL-LHC UPGRADE*

C. Zanoni†[1], K. Artoos[1], S. Atieh[1], I. Aviles Santillana[1,2], S. Belomestnykh[3,4], I. Ben-Zvi[3,4], J.-P. Brachet[1], G. Burt[5], R. Calaga[1], O. Capatina[1], T. Capelli[1], F. Carra[1], L. Dassa[1], S.U. De Silva[6], J. Delayen[6], G. Favre[1], P. Freijedo Menendez[1], M. Garlaschè[1], M. Guinchard[1], T. Jones[7], N. Kuder[1], S. Langeslag[1], R. Leuxe[1], Z. Li[8], A. May[6], K. Marinov[6], T. Nicol[9], R. Olave[6], H. Park[6], S. Pattalwar[7], L. Prever-Loiri[1], A. Ratti[10], N. Templeton[6], G. Vandoni[1], S. Verdú-Andres[3], Q. Wu[3], and B. Xiao[3]

[1]CERN, Geneva, Switzerland
[2]University Carlos III, 28911 Madrid, Spain
[3]BNL, Upton, NY 11973, USA
[4]Stony Brook University, Stony Brook, NY 11794, USA
[5]Cockcroft Institute, Lancaster University, UK
[6]Old Dominion University, Norfolk, VA, 23529, USA
[7]STFC Daresbury Laboratory, UK
[8]SLAC, Menlo Park, CA 94025, USA
[9]Fermilab, Batavia, IL 60510, USA
[10]LBNL, Berkeley, CA 94707, USA

Abstract

RF crab cavities are one of the key systems for the HL-LHC (High Luminosity LHC) upgrade. In view of extensive tests with beam in the SPS, two cavity concepts for the design of such systems are being developed: the Double Quarter Wave (DQW) and the RF Dipole (RFD).

Cavities built out of thin niobium plates require external stiffeners in order to sustain the loads applied through their lifetime. Adequate cooling and efficient magnetic shielding are necessary to reach the required kick gradients and maintain the performance. To minimize the deformation of the cavity during assembly and operation, a design of the helium tank with bolts, for structural strength, and superficial welds, to guarantee vacuum integrity, is proposed. This approach, which is a non standard practice for helium tanks, will be reviewed in this paper.

INTRODUCTION

The statistical gain obtained by running LHC after 2020 with the current performance is marginal [1]. Thus, in order to keep LHC at the forefront of physics, a significant luminosity increase is foreseen through the HL-LHC upgrade. The crab cavities are among the critical systems required for obtaining the desired new performance.

Similar devices have already been employed at KEK [2]. However, the use of elliptical shape cavities poses major space and integration issues. This determines the need for a wholly new design. Two concepts are under development through CERN and the USLARP consortium: the Double Quarter Wave (DQW) and the RF Dipole (RFD), [3–5]. The RF design is finalized while the detailed engineering phase is underway.

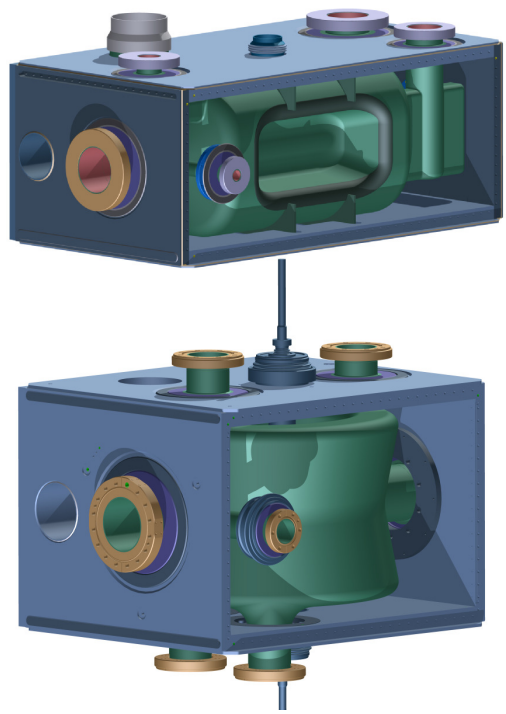

Figure 1: 3D views of the RFD (top) and DQW (bottom) dressed cavities.

The cavities are build out of niobium plates. In order to minimize the change in frequency due to fluctuations in external pressure[1] and allow some margin on the temperature

* The research leading to these results has received funding from the European Commission under the FP7 project HiLumi LHC, GA no. 284404, co-funded by the DoE, USA and KEK, Japan
† carlo.zanoni@cern.ch

[1] superfluid helium at 2 K operates at 20 mbara ± 1 mbara, while helium at 4 K at 1.3 ± 0.1 bara

DEVELOPMENTS OF SiC DAMPER FOR SuperKEKB SUPERCONDUCTING CAVITY*

M. Nishiwaki[#,1,2)] , K. Akai[1,2)] , T. Furuya[1,2)] , A. Kabe[1)] , S. Mitsunobu[1)] and Y. Morita[1,2)]
[1)] Accelerator Laboratory, KEK, Tsukuba, Japan
[2)] Department of Accelerator Science, The Graduate University for Advanced Studies (SOKENDAI), Tsukuba, Japan

Abstract

Upgrade works for SuperKEKB is in the final stage and the commissioning operation will start in this JFY. Eight superconducting accelerating cavities were operated for more than ten years at KEKB electron ring and are to be used at SuperKEKB. The cavity operation at those high current accelerators requires sufficient absorption of the beam-induced HOM power. In KEKB, the absorbed HOM power of 16 kW in two ferrite dampers attached to each cavity was achieved at the beam current of 1.4 A. On the other hand, the expected HOM power at SuperKEKB is calculated to be 37 kW in the beam current of 2.6 A. To cope with the HOM power issue, we developed additional HOM dampers made of SiC to be installed to the downstream of the cavity module. From precise calculations, it was found that the additional dampers reduce the HOM power loads of the ferrite dampers more effectively than the large beam pipe model of cavity module, which is another option to reduce the HOM loads. New SiC dampers were fabricated and high power-tested. Those SiC dampers successfully absorbed the expected HOM power. In this report, we will describe the results of calculations and high-power RF tests of new SiC dampers.

INTRODUCTION

SuperKEKB is an upgrade machine from KEKB accelerator that is an asymmetric energy electron-positron double-ring collider. The construction processes of SuperKEKB have reached the final stage and the commissioning operation will start in early 2016. The design luminosity is 8×10^{35} /cm^2/s, which is 40 times higher than that of KEKB [1]. In order to achieve this luminosity, stored beam currents have to be increased twice higher than those of KEKB, that is, 2.6 A for an electron ring (high energy ring, HER) and 3.6 A for a positron ring (low energy ring, LER), respectively.

A hybrid RF system of superconducting accelerating cavity (SCC) [2,3] and normal conducting (ARES) cavities was adopted as the RF of HER in KEKB [4]. This SCC system of eight SCC modules is to be re-used again in HER of SuperKEKB. The SCC-related parameters are listed in Table 1. The main issues are the higher beam current, the shorter bunch length and the large beam power for SCC in both KEKB and SuperKEKB. The SCC shares the beam power with ARES cavities as in the case of KEKB. Therefore, the beam power delivered by SCC can keep the same level giving the phase offset between SCC and ARES system.

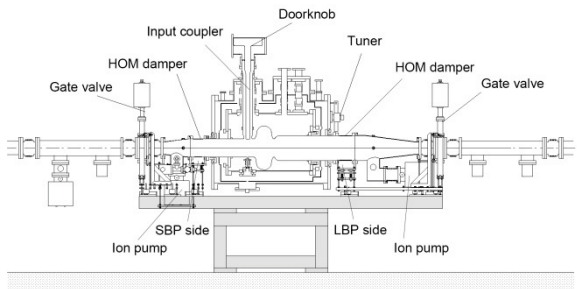

Figure 1: Cross-section drawing of the superconducting cavity module of KEKB.

Table 1: SCC-related Parameters in HER

Parameters	KEKB (operation)	SuperKEKB (design)
Energy [GeV]	8.0	7.0
Beam current [A]	1.4	2.6
Number of bunches	1585	2500
Bunch length [mm]	6	5
Number of cavities	8	8
Total beam power [MW]	~5	8.0
Beam power [kW/cavity]	400	400
Total RF voltage [MV]	15.0	15.8
RF voltage [MV/cavity]	1.5	1.5
HOM power [kW/cavity]	16	37

On the other hand, the higher-order-mode (HOM) power becomes large due to the higher beam current and shorter bunch length. To absorb HOM power, ferrite dampers are attached at the both sides of the cavity beam pipes, called small beam pipe (SBP) and large beam pipe (LBP) as shown in Fig. 1. The ferrite was sintered on copper base pipe by the hot isostatic press (HIP) method. The thickness of the ferrite is 4 mm to achieve sufficiently low Q values of higher order modes and thermal conductivity of ferrite material [5]. In KEKB, the HOM power of 16 kW at the beam current of 1.4 A was successfully absorbed with by a pair of ferrite dampers

#michiru.nishiwaki@kek.jp

ISBN 978-3-95450-178-6

HIGHER ORDER MODE DAMPING IN A HIGHER HARMONIC CAVITY FOR THE ADVANCED PHOTON SOURCE UPGRADE *

S.H. Kim#, M.P. Kelly, P.N. Ostroumov, Z.A. Conway, B. Mustapha, G. Waldschmidt,
J. Carwardine, G. Decker
ANL, Argonne, IL 60439, USA

Abstract

A superconducting higher-harmonic cavity (HHC) is under development for the Advanced Photon Source Upgrade based on a Multi-Bend Achromat lattice. This cavity will be used to improve the Touschek lifetime and the single bunch current limit by lengthening the beam. A single-cell 1.4 GHz (the 4th harmonic of the main RF) cavity is designed based on the TESLA shape. Two adjustable fundamental mode power couplers are included. The harmonic cavity voltage of 0.84 MV will be driven by the 200 mA beam. The RMS bunch length with the harmonic cavity will be >50 ps. Higher-order modes (HOM) must be extracted and damped. This will be done with two silicon carbide beamline HOM absorbers to minimize heating of RF structures such as the superconducting cavity and/or couplers and suppress possible beam instabilities. The HHC system is designed such that 1) most monopole and dipole HOMs are extracted along the beam pipes and damped in the 'beamline' silicon carbide absorbers and 2) a few HOMs, resulting from introduction of the couplers, are extracted through the coupler and dissipated in a room temperature water-cooled load. We will present time and frequency domain simulation results and discuss damping of HOMs.

INTRODUCTION

We are developing a 4th harmonic cavity for Advanced Photon Source Upgrade (APS-U) at Argonne National Laboratory. It will lengthen the beam bunch so that the Touschek lifetime and single bunch current limit will be improved [1,2]. The cavity is a single-cell 1.4 GHz superconducting cavity scaled from the TESLA shape [3]. Two moveable fundamental mode couplers are employed to separately adjust harmonic voltage and phase in combination with the slow frequency tuner [1,3].

Higher order modes (HOM) excited by relatively high current beams, 200 mA, must be damped. Otherwise, they will cause excessive cryogenic loads and beam instabilities, such as multi-bunch instabilities if resonant with the beam [4]. The damping method here is motivated by the previous work done by Cornell [5,6]. We use an enlarged beam pipe, 104 mm diameter, on the left side of the cavity as shown in Fig. 1 to extract monopole and dipole HOMs; the right side beam pipe is 70 mm, the same as the beam aperture in the cavity. Cavity HOMs propagate along the larger beam pipe and are damped in the 'beamline' silicon carbide HOM absorber which uses Coorstek SC-35 ceramic [6]. The smaller beam pipe on the right side also needs a HOM absorber to damp beam pipe modes and a portion of HOMs excited due to couplers, 'coupler modes'. Several coupler modes must be extracted out through the coupler because they cannot propagate along either beam pipe. However, we found a trapped mode if we use a traditional symmetric antenna for the coaxial coupler, therefore we developed a new coaxial antenna to resolve this issue. Details of this new antenna will be discussed in the next section.

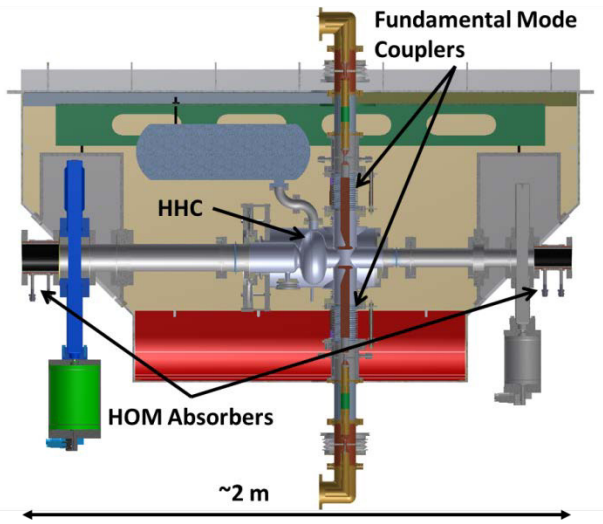

Figure 1: Conceptual model of the HHC cryomodule Details of the beamline HOM absorbers will be presented in [7] and the fundamental mode couplers in [8].

In the later of this paper, we will present monopole dipole impedances simulated using CST Wakefield Solver and cross-checked using CST Eigenmode Solver. HOM induced power losses calculated from the simulated longitudinal impedance will be also discussed. The beam current is 200 mA and currently considering operational modes are uniformly distributed 48 or 324 bunches with no gap in the bunch fill pattern as shown in Table 1.

COUPLER ANTENNA

A trapped mode was found in the initially considered design of the coupler antenna as shown in Fig. 2 (a). The larger profile antenna tip was used in this design for stronger coupling and also for minimizing the geometrical perturbation seen by the beam so that beam impedance is reduced. However, the first TE11-like mode in the coaxial coupler is trapped near the coupler tip, as shown in Fig. 2

*Results in this report are derived from work performed at Argonne National Laboratory. Argonne is operated by UChicago Argonne, LLC, for the U.S. Department of Energy under contract DE-AC02-06CH11357.
#shkim121@anl.gov

ISBN 978-3-95450-178-6

HIGH CURRENT ERHIC CAVITY DESIGN AND HOM DAMPING SCHEME *

Wencan Xu[#,1], S. Belomestnykh[1,2], I. Ben-Zvi[1,2], H. Hahn[1]
[1)] Collider-Accelerator Department, Brookhaven National Lab, Upton, NY 11973, USA
[2)] Physics & Astronomy Department, Stony Brook University, Stony Brook, NY 11794, USA

Abstract

A 5-cell 422 MHz SRF cavity, BNL4 cavity, was designed for the FFAG lattice based eRHIC, which is a high current (up to 50 mA), multi-pass (up to 16 passes) ERL. Compared with a 704 MHz SRF linac for conventional lattice eRHIC design, the 422 MHz SRF linac is chosen not only for better beam dynamics performance but also for lower linac cost. As FFAG based high luminosity eRHIC is a high current multi-pass ERL machine, it requires extremely good HOM damping to increase BBU threshold current and minimize the HOM power caused cryogenic load. So, HOM damping capability was the main concern for this cavity design. A HOM damping scheme with six coaxial-line HOM couplers and three waveguide couplers was proposed to damp the high-power, full-spectrum (up to 30 GHz) HOMs in the linac. The operation requirement for BNL4 cavity is Q_0 = 5×10^{10} at a gradient of 18.5 MV/m. As there is no experience in making such a big/heavy cavity and there is no available facility to handle a 5-cell 422 MHz cavity, a 3-cell prototype cavity is ordered to study the cavity's fabrication, processing and testing. This paper will present the design of the 5-cell 422 MHz cavity, progress on the 3-cell BNL4 prototype cavity and the progress of its HOM damping studies.

INTRODUCTION

The Collider-Accelerator Department at BNL proposed a FFAG lattice based electron-ion collider, eRHIC [1], which will use 42 5-cell 422 MHz SRF cavities as the main linac. Compared with the previous conventional lattice eRHIC design using a 704 MHz SRF linac, the 422 MHz SRF linac allows higher Beam-Break-Up (BBU) threshold current, longer bunches, lower energy loss and energy spread, higher beam polarization, easier path length control, lower transient effect, higher cavity quality factor, higher RF power efficiency and lower HOM power [2]. The 5-cell 422 MHz BNL4 cavity is an evolution design of the 5-cell 704 MHz BNL3 cavity [3,4,5]. BNL4 was designed to reduce both loss factor of monopole HOMs (HOM power) and impedance of the dipole HOMs, while maintaining similar performance of the fundamental mode. The operation requirement of BNL4 cavity is 18.5 MV/m with Q_0 @ 5×10^{10}. A 3-cell prototype cavity is undergoing fabrication to demonstrate and study this performance. This paper addresses the design of BNL4 cavity, with comparison of BNL3 cavity.

To reach full luminosity of eRHIC at intermediate energies, about 7 kW HOM power per BNL4 cavity should be damped, with 72 % of the HOM power below 5 GHz and the rest 28 % HOM power is between 5 GHz to 30 GHz. It is a big challenge to develop such a high power, full spectrum HOM damping scheme. A concept design of such HOM damping scheme is addressed in the paper.

422 MHZ 5-CELL BNL4 CAVITY DESIGN

Fundamental Mode

The same as 704 MHz BNL3 cavity, the 5-cell 422 MHz BNL4 cavity, employs a concept of using a large beam tube to propagate all HOMs but its end cells have irises that improve the confinement of the fundamental mode inside the structure. To reduce the cross-talk between neighboring cavities, tapered sections to a reduced diameter beam pipe are added on both sides of the cavity. Figure 1 (top) shows Superfish model of the BNL4 cavity. The field profile of the fundamental mode by Superfish is shown in Figure 1 (bottom). The fundamental mode's performance of the BNL3 and BNL4 cavities is listed in Table 1.

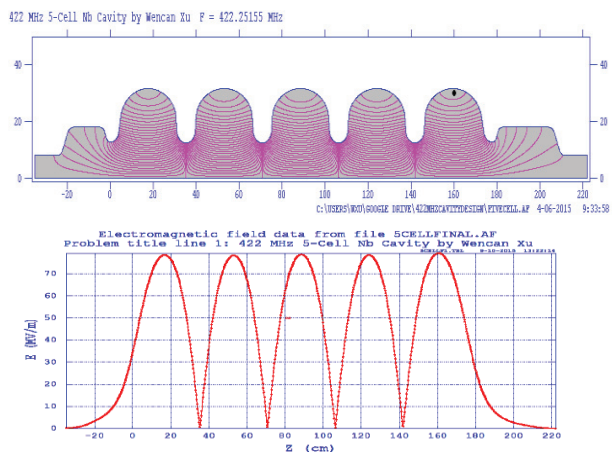

Figure 1: BNL4 cavity configuration (top) and fundamental mode field profile (bottom).

* This work is supported by LDRD program of Brookhaven Science Associates, LLC under Contract No. DE-AC02-98CH10886 with the U.S. DOE.
#wxu@bnl.gov

ISBN 978-3-95450-178-6

QUALITY CONTROL OF WELDING, BRAZING JOINTS AND CU DEPOSITION ON EU-XFEL COUPLER PARTS

A. Ermakov, W. -D. Möller, D. Kostin
DESY, Notkestrasse 85, 22607 Hamburg, Germany

Abstract

In frames of EU-XFEL Project the quality control of fundamental 1.3GHz power couplers is very important task. The power coupler consists of a several of parts including itself the different types of welding and brazing joints between ceramic, copper and stainless steel components. The quality of these joints is subject to be investigated and controlled according to EU-XFEL coupler specification taking into account the different coupler manufacturers involved. The quality of Cu deposition on some EU-XFEL coupler parts is also the issue to be qualified according to specs. The number of microscope images of different types of joints and Cu deposition on some EU-XFEL 1.3GHz coupler parts are presented.

INTRODUCTION

The superconducting architecture of EU-XFEL linear accelerator imply the producing the beam of electrons with energy of between 10 and 20 GeV. The EU-XFEL linear accelerator includes itself the number of cryogenic accelerator modules equipped with 8 superconducting cavities. As the fundamental power coupler is the object providing the vacuum and thermal interface between the cavity and wave guide components at room temperature transferring the RF wave from electromagnetic sources (klystrons) to the superconducting cavities for achieving the high accelerating gradients of electron beam, the task of producing and conditioning of high quality RF couplers becomes to be important [1-5]. Due to its complex design and rather critical operation conditions the quality control of different parts including the number of welding and brazing seams as well as the copper deposition quality have to be controlled according to EU-XFEL power coupler specification. The number of microscopic images of different coupler parts welding and brazing joints as well as copper deposition is presented.

DESCRIPTION OF COUPLERS TECHNICAL ASPECTS

Generally the EU-XFEL power couplers have a complex structure including the 2 main assemblies: warm and cold one (Fig.1a, b). Every part has a number of different welding and brazing joints between ceramic (Al_2O_3), copper (Cu-c2 or Cu-OFHC) and stainless steel (AISI 316L). Some stainless steel parts of coupler including some bellows have a copper deposition.

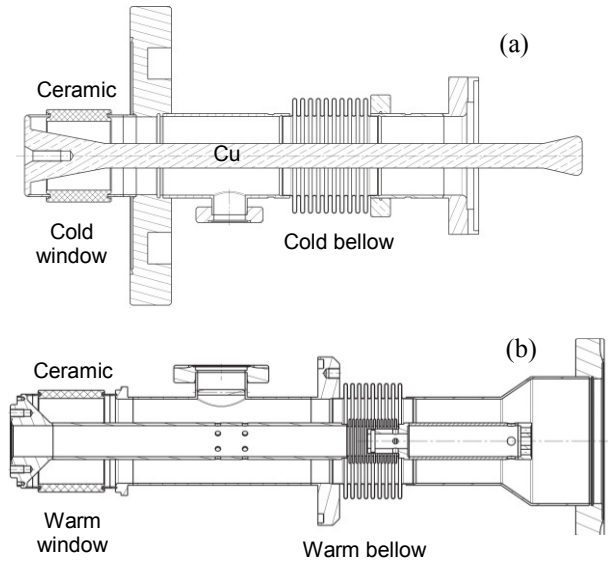

Figure 1: Main power coupler assemblies: Cold part (a), Warm part (b).

The samples for quality control and further analysis of welding and brazing seams were sectioned from the parts to be considered for investigation using linear precision saw. Taking into account the fragility of ceramic-copper brazing joints the parts before sectioning were fixed using epoxy resin. The samples for copper deposition control were cut out with special cutting blades preventing overheating the material. Each sectioned part was embedded with epoxy resin, grinded and polished thoroughly accordingly till the high quality final surface appears. In some cases the welding and brazing joints were etched in corresponding acids and its mixes (nitric acid, hydrochloric acid, hydrogen peroxide).

The measurements of thickness and quality control of copper surface deposition was done on Digital Microscope Keyence VHX-500F. The analysis of quality of welding and brazing seams was performed on inspection microscope Olympus MX-40. Hardness of copper of cold window part was done on Micro Hardness Tester Shimadzu HMV-2000. The surface roughness measurements are done using Mitutoyo ® SJ-301 surface roughness tester.

QUALITY CONTROL

Cold part as well as warm one of EU-XFEL coupler reveals itself the number of important welding, brazing parts and surfaces with copper depositions important from RF point of view. According to specification these critical

ISBN 978-3-95450-178-6

MODIFIED TTF-3 COUPLERS FOR LCLS-II*

Chris Adolphsen#, Karen Fant, Zenghai Li, Christopher Nantista, Gennady Stupakov, Jeff Tice, Faya Wang and Liling Xiao, SLAC, Menlo Park, CA 94025, USA
Ivan Gonin, Ken Premo and Nikolay Solyak, Fermilab, Batavia, IL 60510, USA

Abstract

The LCLS-II 4 GeV SCRF electron linac will use 280 TESLA-style cavities with TTF-3 power couplers that are modified for CW operation with input powers up to about 7 kW. The coupler modifications include shortening the antenna to achieve higher Q_{ext} and thickening the copper plating on the warm section inner conductor to lower the peak temperature. Another change is the use of a waveguide transition box that is machined out of a solid piece of aluminium, significantly reducing its cost and improving its fit to the warm coupler window section. This paper describes the changes, plating and surface issues, simulations and measurements of the coupler operation (heat loads and temperatures) and RF processing considerations.

INTRODUCTION

The LCLS-II project has adopted the TTF-3 coupler design (see Fig. 1) to power the 1.3 GHz TESLA-style cavities in its 4 GeV SCRF linac [1]. These couplers were designed for pulsed operation with several hundred kilowatts of input power at a ~ 1% duty factor, so the peak fields for 7 kW operation at LCLS-II will be much smaller. The low duty required the static heat load to be kept small, which was done by using only a thin (10-30 μm) layer of copper plating on the inner stainless steel surfaces. For LCLS-II CW operation, however, the inner conductor in the 'warm' section (between the windows) would overheat. Also the Q_{ext} range of the coupler is too low for the small LCLS-II beam currents (< 300 μA). Thus modifications were made as described below.

MODIFICATIONS

Thicker Copper Plating

Simulations show that with 7 kW fully reflected input power (worst case), the peak temperature of the warm inner conductor decreases from about 700 K to 400 K if its plating thickness is increased from 30 μm to 150 μm. This reduces the temperature below the 450 K level at which the couplers are baked so the vacuum levels should be manageable. LCLS-II adopted this thickness, which increases the 45 K total (static + dynamic) cryogenic load by 14 %. As a test, several ILC coupler warm sections were modified by removing their 30 μm plating and re-plating to 150 μm. The photo in Fig. 1 shows the achieved plating uniformity in the bellows region, which meets requirements. So far these couplers have worked well and vendors are producing new ones with this plating thickness.

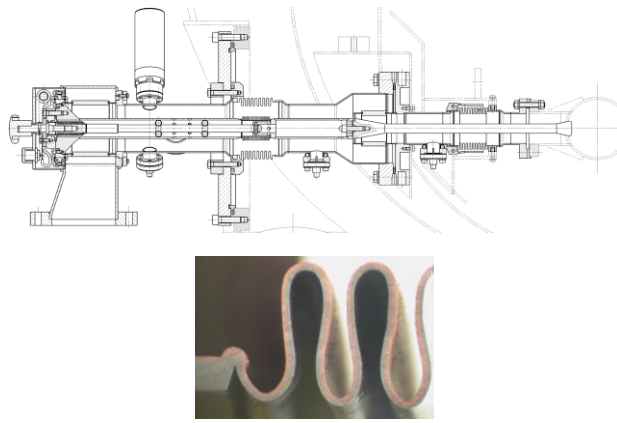

Figure 1: (top) TTF-3 coupler, (bottom) sectioned inner bellows after plating to 150 μm thickness.

Shorter Antenna

The TTF-3 couplers can move over a 15 mm range, which changes Q_{ext} by about 19 % per mm. LCLS-II will run with $Q_{ext} = 4.1\times10^7$ (about 10 times higher than XFEL), which is above the nominal TTF-3 Q_{ext} range. To shift up the range, the flared antenna tip will be shortened by 8.5 mm, keeping the same flare angle and 3 mm radius edges. For the first two cryomodules, ILC cold sections have been modified by milling down the existing antenna tips using a fixture that prevents the couplers from being damaged.

Aluminium WG Box and Flex Rings

To lower cost and improve performance, the copper waveguide box that attaches to the warm window will be replaced by one machined from a single block of aluminium, without RF matching posts (see Fig. 2). Also the capacitor ring that allows HV holdoff will be replaced by a copper flex ring to provide a better RF seal between the waveguide and the coupler body.

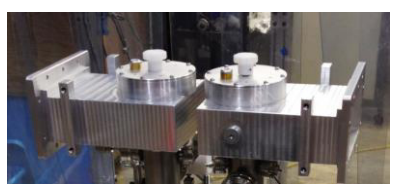

Figure 2: Pair of aluminium waveguide boxes being used for coupler RF processing.

*Work supported by the Department of Energy, Office of Science, Office of Basic Energy Science, under Contract No. DE-AC02-76SF00515
#star@slac.stanford.edu

STATUS OF THE POWER COUPLERS FOR THE ESS ELLIPTICAL CAVITY PROTOTYPES

C. Arcambal, P. Bosland, M. Desmons, G. Devanz, G. Ferrand, A. Hamdi, P. Hardy, H. Jenhani, F. Leseigneur, C. Marchand, F. Peauger, O. Piquet, D. Roudier, C. Servouin,
Irfu, CEA-Saclay, Gif-sur-Yvette, France
C. Darve, ESS-AB, Lund, Sweden

Abstract

In the framework of the European Spallation Source (ESS) project[1], the CEA Saclay is responsible for the design, the fabrication, the preparation and the conditioning of the couplers used for the Elliptical Cavities Cryomodule Technological Demonstrators (ECCTD).[2] This work is performed in collaboration with ESS and the IPNO. This paper describes the coupler architecture, its different components, the main characteristics and the specific features of its elements (RF performance, dissipated power, cooling, coupler box test for the conditioning). The status of the fabrication of each coupler part is also presented.

INTRODUCTION

The linear accelerator of the ESS is composed of a superconducting section comprising two kinds of cavities called “medium beta cavity” (beta=0.67) and “high beta cavity” (beta=0.86) [3]. All these cavities will be equipped with couplers (see Fig.1) and in the end 120 couplers will be mounted on the accelerator. In a first step, we are developing 6 couplers to equip a prototype medium beta cavity (+2 spares). That shall allow validating the RF thermo-mechanical design of the coupler, its integration in the cryomodule and its manufacturing processes.

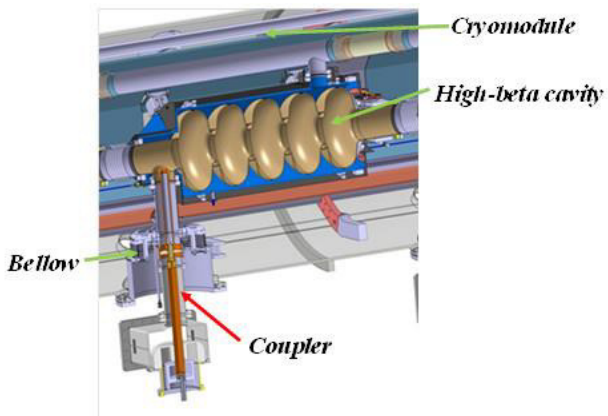

Figure 1: Coupler mounted on a high beta cavity.

COUPLER ARCHITECTURE AND CHARACTERISTICS

The ESS prototype power coupler is composed of three main parts:

*a window with its antenna to allow RF power coupling to the cavity and isolate the cavity vacuum from atmosphere thanks to an alumina disk,

*a cooled double-wall tube to keep a coaxial configuration between window and cavity and allow thermal transition between ambient and cold cavity temperatures,

*a doorknob transition to allow RF matching between the coupler and the RF power source.

The couplers mounted on the medium beta cavities are the same as the couplers of the high beta cavities; it means that the window and the doorknob are identical. Only the length of the double-wall tube changes; that allows obtaining a different antenna penetration inside the cavity and assures the correct external quality factor.

The ESS coupler is based on the coupler developed in the framework of the program HIPPI [4]. Thus, its architecture is very similar to the HIPPI one. Some elements have been modified e.g. the bellow has been removed from the double wall tube to allow an easier cleaning, the bellow is now on the ESS cryomodule. Other elements have been added such as the high voltage DC bias for the antenna and a photomultiplier port at the air window side. (see Fig. 2).

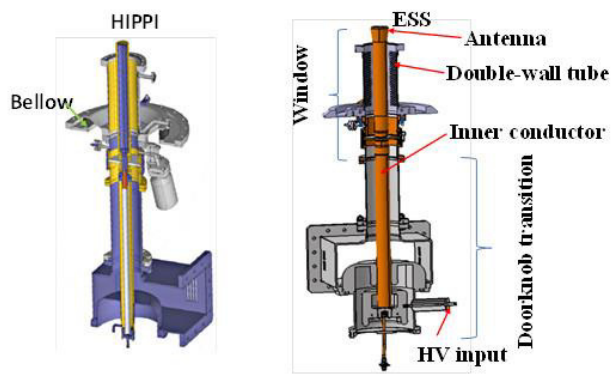

Figure 2: HIPPI coupler and ESS coupler.

In 2009 [5], the HIPPI coupler was tested until 1.2 MW for 17 minutes and at 1.1 MW for several hours, duty cycle 10%. (see Fig. 3) This last value of power is the one retained in the ESS requirements.

ISBN 978-3-95450-178-6

IMPROVED CAPACITIVE COUPLING TYPE RF POWER COUPLERS FOR A CRYOMODULE WITH TWO 9-CELL CAVITIES

Dehao Zhuang, Fang Wang, Zhanglong Wang, Peiliang Fan, Lin Lin, Liwen Feng, Shengwen Quan, Kexin Liu, Institute of Heavy Ion Physics, Peking University, China

Abstract

A capacitive coupling [1] RF power coupler has been used for the DC-SRF [2] photoinjector at Peking University. Recently, improved capacitive coupling type power couplers, which will be used for a new cryomodule with two 9-cell cavities have been designed and fabricated. The main modifications include enlarging the supporting rods of inner conductors in order to increase heat conduction, moving the bellows from the quarter-wave transformer to the 50 Ohm coaxial line to avoid the mismatch during Q_{ext} adjusting. RF conditioning of two modified power couplers has been carried out and 10kW RF power passed the couplers with a duty factor 30%. In this paper, detailed design based on multi-physics analysis and the conditioning of this improved capacitive coupling type RF Power coupler are presented.

INTRODUCTION

A cryomodule with two 1.3GHz 9-cell cavities [2] is under construction at Peking University. The capacitive coupling type RF power coupler, which has been used for the DC-SRF photo injector, will still be used for this cryomodule will still use the kind of capacitive coupling type RF power coupler.

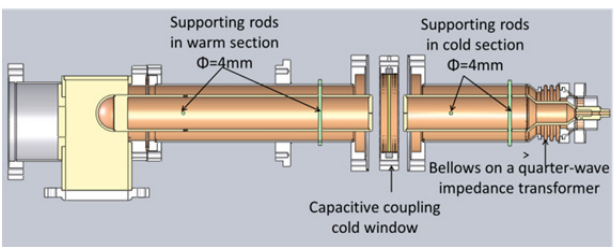

Figure 1: Structure of capacitive coupling type power coupler for the DC-SRF photoinjector at Peking University.

The capacitive coupling structure as shown in Figure 1 has the following advantages [3]: 1) the ceramic window is a whole disc, which makes it easy for fabrication and process. 2) As the inner conductor is divided into two parts, it is convenient to install the coupler into the cryomodule. 3) There is no axial stress due to the separation of inner conductor and window. However, problems of this kind of coupler have been found during the beam loading experiment of the DC-SRF photoinjector. An obvious temperature increase around supporting rods was observed when the power was over 8 kW. With the original design, the bellows is within the quarter-wave transformer. During Q_{ext} adjusting, the variation of the bellows' length will cause RF mismatching. Therefore, modified couplers have been designed and fabricated. In this paper, the design, fabrication and conditioning of this improved capacitive coupling type RF Power coupler are presented.

ENLARGING SUPPORTING RODS FOR INNER CONDUCTOR

For solving the problem of temperature increase, we try to enlarge the supporting rods for inner conductor and the thermal analysis has been carried out.

We compared the temperature distribution of couplers with original design and modified design by using ANSYS code. Figure 2 shows the temperature distribution of the original PKU coupler with the input RF power of 10kW and the supporting rod diameter of 4mm. The highest temperature is 452.5K and it occurs at the end of the inner conductor.

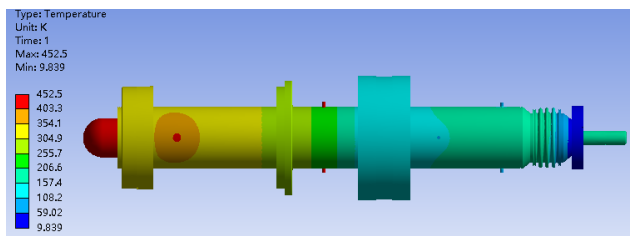

Figure 2: Temperature distribution of original power coupler at 10kW, CW.

Figure 3 shows the temperature distribution of the modified coupler with the input RF power of 10 kW and the supporting rod diameter of 24.1mm in warm section and of 18 mm in cold section. The highest temperature is 388.1K and it occurs at the end of inner conductors of the warm section.

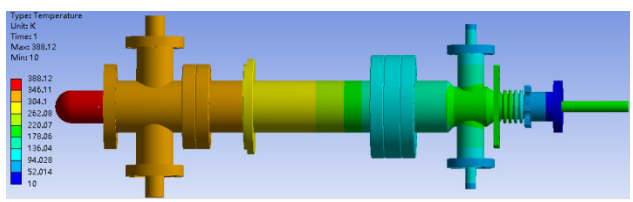

Figure 3: Temperature distribution of modified power coupler at 10kW, CW.

*Work supported by Major State Basic Research Development Program of China (Grant No. 2011CB808303 and 2011CB808304)
Email: kxliu@pku.edu.cn

ISBN 978-3-95450-178-6

NEXT GENERATION CAVITY AND COUPLER INTERLOCK FOR THE EUROPEAN XFEL

D. Tischhauser, A. Goessel, M. Mommertz,
DESY, 22603 Hamburg, Germany

Abstract

The safe operation of cavities and couplers in the European XFEL [1] accelerator environment is secured by a new technical interlock (TIL) design, which is based on the XFEL crate standard (MTCA™.4 [2]). The new interlock is located inside the accelerator tunnel. Several remote test capabilities ensure the correct operation of sensors for light, temperature and free electrons. Due to the space costs and the very high number of channels, the electronic concept was moved from a conservative, mostly analog electronic approach, with real comparators and thresholds, to a concept, where the digitizing of the signals is done at a very early stage. Filters, thresholds and comparators are moved into the digital part. The usage of an Field Programmable Gate Array (FPGA) and an additional watchdog (WD) increase the flexibility dramatically, with respect to be as reliable as possible. An overview of the system is shown.

Figure 1: RTM TIL in the field.

MOTIVATION

The primary purpose of a TIL is to protect important components, like main radio frequency (RF) coupler and superconducting cavities, which should be operated in a non self destructive way. Therefore it measures several key parameters, like temperature and illumination and compares them with known save operable values. If such a threshold is reached, it has to turn off the RF power. An additional requirement for the new TIL system arised from the fact that it is located inside the accelerator tunnel and will be physically not accessible most of the time. In order to cope with this situation, the system should be as much as possible remote operable. This includes extensive on board diagnostic and the functional test capability, including the sensors. Nevertheless the available rack space is very limited, which forces us to build a very compact system (Fig. 1). It is based on the new crate standard MTCA.4 for the XFEL. The TIL system is operated through the distributed object oriented control system (DOOCS [3]), like all the surrounding components, such as the crate and board management (through the Intelligent Plattform Management Interface (IPMI)) and the timing [4] system.

RF STATION

The default RF Station contains one klystron and a low level RF (LLRF [5]) system, 4 accelerator modules each with 8 cavities and couplers, and one TIL system (Table 1). The TIL system is split in two parts (master and slave), each for 16 cavities and couplers. Compared to the slave, the master contains additionally the cryo and vacuum channels and is generating the overall alarm sum for the RF station. Three RF stations build one cryo and cavity vacuum section.

Table 1: Interlock Signals for one RF Station

Count	Signal	Remark
96	e- sensor	current meas. with bias voltage
32	Spark	main coupler air side (waveguide)
64	PT1000	ceramic RF win. (T70K, T300K)
12	analog	IGP vacuum and high voltage
2	analog	cryo signals (He level, pressure)
1	contact	vacuum system status
1	RS422	cryo system status

MODULAR CONCEPT

The hardware is structured in simple blocks, which exists only in a low number of variants (Fig. 2). Starting at the main RF coupler there is a Coupler-Interface (CPL-IF), which does some signal conditioning and combines all interlock sensor signals from a standard XFEL coupler into one pairwise twisted (TP) cable. In the side panel of the electronic racks the Rack-Interface (Rack-IF) is mounted, which adapts the robust connectors from the outside to the high density connectors of the rear transition module (RTM) TIL boards inside. This Rack-IF combines the signals from 4 couplers to one RTM TIL board or distribute analog input channels (voltage and current) to the vacuum and cryogenic

ISBN 978-3-95450-178-6

FPC AND HOM COUPLER TEST BOXES FOR HL-LHC CRAB CAVITIES

A.Tutte, G. Burt, Lancaster University, UK

B. Xiao, BNL, US

R. Calaga, A. Macpherson, E.Montesinos, CERN, Switzerland

S. De Silva, JLab, US

Z. Li, SLAC, US

Abstract

The LHC luminosity upgrade will involve the installation of thirty-two 400 MHz SRF crab cavities. The cavities have two variants known as the RF dipole [1] and double quarter-wave [2][3] crab cavities. Each cavity has a fundamental power coupler (FPC) at 400 MHz and two or three HOM couplers. Before integration onto the cavities it is necessary to condition the FPC, and to measure the transmission on the HOM couplers at low power to ensure they operate as designed, each requiring a special test box. The FPC test box should provide a high transmission between two couplers without creating high surface fields. The low power HOM test boxes should be terminated to a load such that the natural stop and pass-bands of the couplers are preserved allowing the reflection to be measured and compared to simulations. In addition, due to the possibility of high HOM power in the LHC crab cavities, the concept of creating a broadband high power HOM coupler test box in order to condition and test the couplers at high power has been investigated. The RF design of all test boxes is presented and discussed.

INTRODUCTION

Prior to installation on the LHC, the HL-LHC crab cavities are to be tested in CERN's cryogenic test facility SM18, and on the SPS (Super Proton Synchrotron) in 2017-2018. These tests will be used to verify both the double quarter wave (DQW) and the RF dipole (RFD) cavity (shown in Fig. 1) in operation on a beam, and as such require a fully assembled cryomodule. The manufacture of the cavities for these tests has begun and is expected to be completed in 2016.

Along with the cavities themselves, the fundamental power couplers (FPCs) and the higher order mode (HOM) couplers for the crab cavities are also required. The FPC has many components already procured and is expected to be assembled and conditioned using a test box in early 2016. The HOM coupler manufacture has recently started. Once complete the HOM couplers will require testing to ensure the couplers have the stop and pass-bands at the correct frequencies, prior to their use in the cavity tests. To test the FPC and HOM couplers, various test boxes will be required.

The main focus of this testing is to ensure the components have the correct frequency response, and to condition the interior surfaces prior to operation.

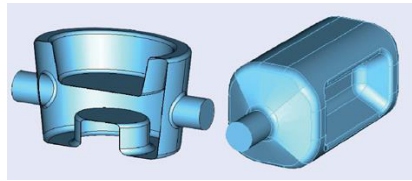

Figure 1: The DQW (left) and RF dipole (right) crab cavities for HL-LHC.

FPC TEST BOXES

For the FPCs, the primary concern is conditioning, as they need to support high power during operation. In order to condition the FPCs effectively a test box is required to ensure matching and the design frequency and which can support 0.5MW/m input power without exhibiting high peak fields.

Double Quarter Wave

The first test box to be investigated was the DQW FPC test box. The DQW FPC hook is shown in Fig. 2.

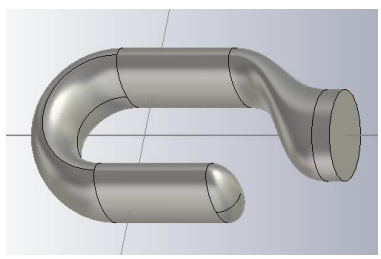

Figure 2: The DQW FPC hook.

Multiple designs were considered for the test box, with the final design being a quarter wave resonator, as shown in Fig. 3. In this design a standing wave is set up on the inner rod, with a magnetic field peak at the supported end, and an electric field peak at the open end. The hooks are positioned towards the end of the cavity as shown, this ensures that the hooks are primarily magnetically coupled.

The most important parameter in the quarter wave resonator are the length of the inner rod, which determines the resonant frequency; and the distance between the couplers and the inner rod, which determines the coupling of the hooks to the cavity, and in most cases determines the value of the peak fields in the cavity.

ISBN 978-3-95450-178-6

DESIGN OF QWR POWER COUPLER FOR THE RARE ISOTOPE SCIENCE PROJECT IN KOREA *

Ilkyoung Shin†, Myung Ook Hyun, Institute for Basic Science, Daejeon, Korea
Chang-Kyu Sung, Korea University, Sejong, Korea
Eiji Kako, KEK, Tsukuba, Japan

Abstract

A power coupler has been designed for the Rare Isotope Science Project (RISP) in Korea. The power couplers will provide 4 kW RF power to 81.25 MHz superconducting quarter wave resonators with $\beta = 0.047$. The coupler is a coaxial capacitive type with an impedance of 50 Ω using a disc type ceramic window. Design studies of the coupler are presented.

INTRODUCTION

A heavy ion accelerator, named RAON, is under construction for the Rare Isotope Science Project (RISP) at the Institute of Basic Science (IBS) in Korea [1]. A driver linac utilizes Quarter Wave Resonators (QWRs) and Half Wave Resonators (HWRs) to accelerate ions to 18.5 MeV/u. A power coupler for QWR has been designed to deliver 4 kW RF power at 81.25 MHz in CW mode. The coupler is designed to handle a full reflected power at the maximum incident power. Table 1 shows coupler design parameters.

Table 1: Coupler Design Parameters

Parameter	Value
Frequency	81.25 MHz
Operational power	4 kW
S_{11} at 81.25 MHz	< 30 dB
Impedance	50 Ω
Q_{ext}	2×10^6
Coupling type	fixed

COUPLER STRUCTURE

Figure 1 shows the coupler structure. The coaxial structure is based on 50 Ω coaxial line. The coupler has a disc type ceramic window. The structure around the ceramic window is optimized to minimize a reflected RF power and to accommodate three ports for diagnostics. Three diagnostic devices are a vacuum gauge, an e-pickup, and an arc detector. One thermal intercept is located at 40 K. A bellow structure compensates for thermal contraction and gives a flexibility in assembly with a cryomodule. The outer conductor is made of a stainless steel with 20 μm copper plating on the inside surface. The hollow inner conductor is mode of OHFC copper.

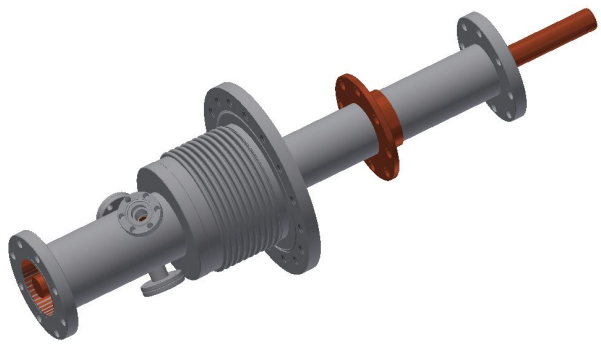

Figure 1: QWR RF power coupler. Coaxial capacitive structure with 50 Ω using a disc type ceramic window.

SIMUATIONS

Electromagnetic, thermal, and mechanical simulations were performed using the CST and ANSYS simulation packages.

Electromagnetic Simulation

CST Microwave Studio and HFSS were used to analyze and optimize RF properties of the coupler. The EM simulation results were sent to CST MPhysics and ANSYS Thermal solver for thermal analysis. Figure 2 shows an EM simulation model for CST Microwave Studio.

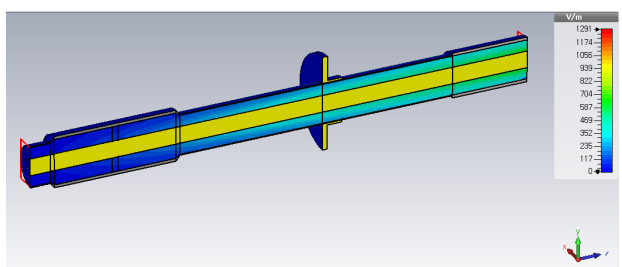

Figure 2: EM simulation model. Electric field distribution.

The location of the power and pickup couplers were simulated using CST Microwave Studio eigen mode solver. The antenna tip of the power coupler is located at 15 mm into the cavity for $Q_{ext} = 2 \times 10^6$. The Q_{ext} of the pickup coupler is 1×10^{11}, and the tip is placed at 35 mm out of cavity. Figure 3 shows the locations of the power and pickup couplers.

* This work was supported by the Rare Isotope Science Project of Institute for Basic Science funded by the Ministry of Science, ICT and Future Planning (MSIP) and the National Research Foundation (NRF) of the Republic of Korea under Contract 2013M7A1A1075764.
† ishin@ibs.re.kr

ENERGETIC COPPER COATING ON STAINLESS STEEL POWER COUPLERS FOR SRF APPLICATION*

I. Irfan#, S. F. Chapman, M. Krishnan, K. M. Velas, Alameda Applied Sciences Corporation (AASC), San Leandro, CA 94577, USA
W. Kaabi, Laboratoire de l'Accelerateur Lineaire (LAL), Orsay, France

Abstract

Delivering RF power from the outside (at room temperature) to the inside of SRF cavities (at ~4 K temperature), requires a power coupler to be thermally isolating, while still electrically conducting on the inside. Stainless steel parts that are coated on the insides with a few skin depths of copper can meet these conflicting requirements. The challenge has been the adhesion strength of copper coating on stainless steel coupler parts when using electroplating methods. These methods also require a nickel flash layer that is magnetic and can therefore pose problems. Alameda Applied Sciences Corporation (AASC) uses Coaxial Energetic Deposition (CED) from a cathodic arc plasma to grow copper films directly on stainless steel coupler parts with no Ni layer and no electrochemistry. The vacuum arc plasma consists of ~100 eV Cu ions that penetrate a few monolayers into the stainless steel substrate to promote growth of highly adhesive films with crystalline structure. Adhesion strength and coating quality of copper coatings on complex stainless steel tubes, bellows, mock coupler parts and an actual Tesla Test Facility (TTF) type coupler part, are discussed.

INTRODUCTION

In the present work our objective is to demonstrate the potential of the CED process to coat copper films on SRF power coupler parts. The details of CED process are published elsewhere [1]. We begin by demonstrating crucial requirements, such as RRR and adhesion strength that need to be fulfilled before the CED process can be considered a serious alternative to electroplating. Next, we demonstrate the capability of CED to coat complex parts. Finally, we address other issues such as thickness uniformity and average surface smoothness and establish that the CED process is ready to coat coupler parts for RF tests.

RRR OF CED COPPER FILMS

The ratio of the resistance of a film at room temperature to the resistance near 4 K temperature is called Residual Resistance Ratio (RRR) [2]. RRR is one of the crucial parameters to indirectly gauge the quality of any coated film in the SRF community [1-3]. Standards at the European X-Ray Free Electron Laser (E-XFEL) for an acceptable copper coating require RRR in the range of 30 to 80 [4]. In this section we describe the method used to measure the RRR of the CED coated copper films on stainless steel (SS) substrates.

Measuring the resistance of a metal film (Cu in this case) deposited on another metal substrate (SS in this case) is not straightforward, but we can use the formula [5] described in eqn. (1), to calculate the resistance of a copper film (R_{Cu}) at a given temperature:

$$R_{Cu} = \frac{R_{st}.R}{(R_{st} - R)} . \quad (1)$$

Where, R is the resistance of the copper coated substrate (coating plus substrate) and R_{st} is the resistance of the stainless steel substrate.

To measure the RRR, we used four stainless steel strips of dimension 3 mm x 75 mm. Two strips were 25 µm thick and the other two were 100 µm thick. The strips were cleaned in a sonicator with trichloroethylene (TCE), acetone, and isoporpylalcohol (IPA) for about 15 minutes in each chemical. One strip of each thickness was mounted in a CED chamber for the coating. We deposited a 28 µm Cu film at ~300 ºC on both strips. After the coating, the coated and the uncoated strips were sent to Fermi National Accelerator Laboratory (FNAL) for the RRR measurement. The resistance values of all four strips (two coated and two uncoated) measured at 298 K and 4.26 K are presented in the Table 1. With these resistance values we can calculate the R_{Cu} values using eqn. 1. By taking the ratio of R_{Cu} at 298 K to that at 4.26 K, we have deduced the RRR values of CED copper films.

Table 1: RRR Values of 28 µm Cu Films on 25 µm (Sub1) and 100 µm (Sub2) Stainless Steel Substrates

#	T(K)	R (Ω)	R_{Cu} (Ω)	RRR
Sub1	298	0.308796		
Sub2	298	0.073348		
Cu/Sub1	298	0.009492	0.009793	**50.9**
Cu/Sub2	298	0.008752	0.009938	**50.9**
Sub1	4.26	0.216840		
Sub2	4.26	0.050480		
Cu/Sub1	4.26	0.000192	0.000192	
Cu/Sub2	4.26	0.000195	0.000195	

*Work supported by DOE SBIR grant SC0009581
irfan@aasc.net

DESIGN OF INPUT COUPLER FOR RIKEN SUPERCONDUCTING QUARTER-WAVELENGTH RESONATOR

K. Ozeki#, O. Kamigaito, H. Okuno, N. Sakamoto, K. Suda, Y. Watanabe, K. Yamada,
RIKEN Nishina Center, Saitama, Japan
E. Kako, H. Nakai, K. Umemori,
High Energy Accelerator Research Organization (KEK), Ibaraki, Japan
K. Okihira, K. Sennyu, T. Yanagisawa,
Mitsubishi Heavy Industries Ltd. (MHI), Hiroshima, Japan

Abstract

An accelerator system based on the superconducting quarter-wavelength resonator is being constructed at the RIKEN Nishina Center. As part of the conceptual design of the input coupler, the optimal positions of the cold window and the thermal anchor were discussed according to the residual resistivity ratio of copper plating. We report on the details of that discussion.

INTRODUCTION

At the RIKEN Nishina Center, construction of an accelerator system based on the superconducting quarter-wavelength resonator (QWR) is underway with the goal of developing basic technologies for the superconducting linear accelerator for ions. A cryomodule that can mount two QWRs is now being constructed as a prototype [1]. In this system, cryocoolers for a helium recondenser and a thermal shield were considered in order to achieve a system that does not require large refrigerators. Cooling power for the recondenser is assumed to be 6 W per resonator, which can be realized by three GM/JT cryocoolers (CG310SLCR). A single thermal shield is installed and cooled to 40 K using a single-stage cryocooler. Many kinds of cryocoolers are available for cooling the thermal shield. The assumed cooling power for the thermal shield is about 90 W.

Characteristics of the input coupler are as follows: The resonance frequency of the cavity is 75.5 MHz and assumed beam loading is about 1 kW. The assumed maximum RF power is 10 kW. Disk-type double vacuum windows are adopted. The cold window is set at the vicinity of the thermal anchor. To reduce thermal conduction from the external portion, the inner and outer conductors are fabricated from 1-mm-thick copper-plated stainless steel.

Reference [2] reports significant reduction in the residual resistivity ratio (RRR) of copper plating on stainless steel due to heat treatment. At higher RRR, dynamic loss decreases and thermal conduction increases, while at lower RRR dynamic loss increases and thermal conduction decreases. As part of the conceptual design of the input coupler, the optimal positions of the thermal anchor and the cold window were discussed, based on estimations of thermal conduction and dynamic losses, in which constant thickness and various RRRs of the copper plating were assumed. Because the skin depth of the room-temperature copper is about 15 μm, the thickness of the copper plating was assumed to be 20 μm.

#k_ozeki@riken.jp

THERMAL AND ELECTRICAL CONDUCTIVITIES

The thermal conductivities of copper for various RRRs were obtained from Refs. [3] and [4]. The top panel of Fig. 1 shows the thermal conductivities of the copper for RRR = 5, 10, 30, and 100. An imaginary thermal conductivity for RRR = 1 is also shown. These thermal conductivities were converted to electrical conductivities (bottom graph in Fig. 1) using the Wiedemann–Franz law:

$$\sigma = \frac{K}{LT},$$

where K and σ are the thermal and electrical conductivities, T is temperature, and L is the Lorenz

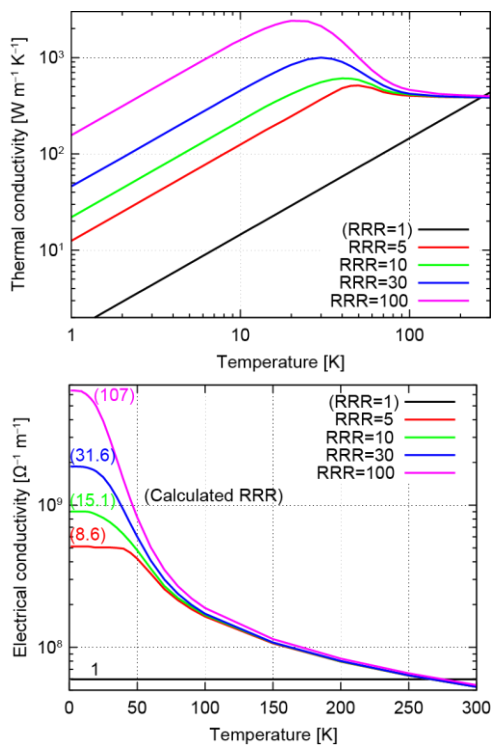

Figure 1: (top) Thermal conductivities of copper for various RRRs. (bottom) Electrical conductivities of copper derived from the thermal conductivities. Calculated RRRs are shown for each curve.

ISBN 978-3-95450-178-6

LCLS-II FUNDAMENTAL POWER COUPLER MECHANICAL INTEGRATION

Ken Premo, Tug Tacku Arkan, Yuriy M Orlov, Nikolay Solyak, Fermilab, Batavia IL, USA

Abstract

LCLS-II is a planned upgrade project for the linear coherent light source (LCLS) at Standard Linear Accelerator Centre (SLAC). The LCLS-II linac will consist of thirty-five 1.3 GHz and two 3.9 GHz superconducting RF continuous wave (CW) cryomodules that Fermilab and Jefferson Lab will assemble in collaboration with SLAC. The LCLS-II 1.3 GHz cryomodule design is based on the European XFEL pulsed-mode cryomodule design with modifications needed for CW operation. The 1.3GHz cryomodules for LCLS-II will utilize a modified TTF3 style fundamental power coupler design. Due to CW operation heat removal from the power coupler is critical. This paper presents the details of the mechanical integration of the power coupler into the cryomodule. Details of thermal straps, connections, and other interfaces are discussed.

INTRODUCTION

SLAC is responsible for the power coupler order (280 total). The Engineering Specification document (ESD), the Interface Control Document (ICD), and the Production Readiness Review (PRR) have been completed. The award for coupler production has been given to two vendors. Each vendor to produce 8 prototypes for evaluation. Prototypes are to be delivered by Sept-Oct 2015. The balance of the order will be distributed equally (132 couplers each). Expected production rate will be 16 couplers/month for each vendor. Serial production is expected to start in summer 2016, and the completion of order January 2017. Couplers will be delivered (ready to use) to the partner labs FNAL and JLAB.

COUPLER DESIGN

The coupler design basis (for production cryomodules) is as follows. A TTF3 type coupler with some modifications was originally proposed to the vendors and the vendors submitted value engineering proposals. Figure 1 presents components of the TTF3 coupler.

The following changes were made to the TTF3 ILC design: On the cold end the antenna length was shortened by 8.5mm. The CF100 55K interface mounting surface was improved by increasing the diameter from 64mm to 78mm almost doubling the mounting area. Mounting bolt size was increased from M4 to M6 to improve clamping force (> 2x). Holes for temperature sensors were added to CF100 flange. The warm end was improved by increasing the Cu plating thickness on the inner conductor from 30 micron to 150 micron in order to reduce the bellows temperature. An additional threaded hole was added to facilitate mounting a transportation support.

For the prototype production two slightly different variants will be produced by the two vendors. Both variants will be functionally equivalent. The goal is for both manufacturers will produce the same design coupler for the production CMs. There are currently licensing issues that are being worked out, but these details are beyond the scope of this paper.

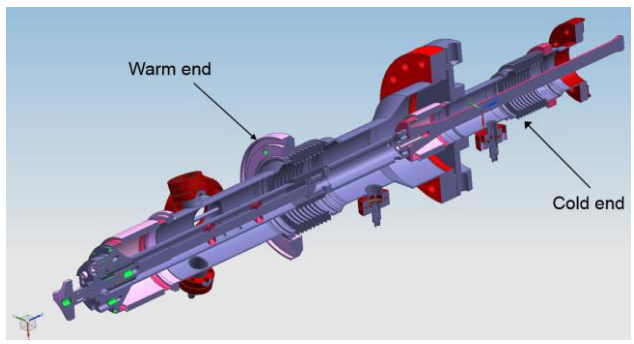

Figure 1: TTF3 Components.

COUPLER CONFIGURATIONS

For the coupler cold ends, there will be a total of 3 different configurations. Due to time constraints, for the 2 prototype cryomodules (pCMs) 16 ILC type cold ends were modified by the original manufacturer for use. It is planned that for the serial cryomodule (CM) production there will be two cold end variants, 8 of one variant from original prototype production and the remaining 272 to be the same. There will be two variants for the warm ends, with one pCM containing 8 from one vendor and the remaining cryomodules having 272 of the same warm end variation. All couplers will be functionally equivalent. Due to the variations in coupler combinations, there will be 4 different configurations of CMs. Performance of the cryomodules is expected to be the same because the couplers are functionally equivalent. Couplers will be integrated into the CM in the same way with only minor detail differences related to the different variations.

COUPLER INTEGRATION INTO CM

Integration of the coupler into the cryomodule is similar to ILC and XFEL integration. The coupler overall geometry is the same as ILC and XFEL. The lengths of cold and warm sections are also the same. The flanged connections are the same and the installation procedure is very similar to that of ILC type and XFEL. The couplers are functionally interchangeable. Coupler warm end vacuum is provided by common pumping line. Figure 2 depicts geometry similarities of the integration.

ISBN 978-3-95450-178-6

DESIGN AND SIMULATION OF HIGH POWER INPUT COUPLER FOR C-ADS LINAC 5-CELL ELLIPTICAL CAVITIES

K.X.Gu[1,2], W.M.Pan[1], T.M.Huang[1], Q.Ma[1], X.Chen[1]
[1]Key Laboratory of Particle Acceleration Physics and Technology，Institute of High Energy Physics, Chinese Academy of Sciences, Beijing 100049, China
[2]University of Chinese Academy of Sciences, Beijing 100049, China

Abstract

Two 650 MHz elliptical cavity sections (elliptical 063, elliptical 082) are chosen to accelerate medium energy protons for China Accelerator Driven sub-critical System (C-ADS) linac. For each 5-cell cavity, RF power up to 150 kW in CW mode is required to be fed by a fundamental power coupler (FPC). A coaxial type coupler is designed to meet the power and RF coupling requirements. This paper presents the RF design, thermal analysis and multipacting simulations of the coupler for C-ADS 5-cell elliptical cavities.

INTRODUCTION

In the Chinese ADS project, the main linac makes use of 650 MHz β=0.63 and β=0.82 superconducting cavities to accelerate a beam current of 10 mA covering the energy range from about 180 MeV to 1.5 GeV [1]. The superconducting cavities are designed to work at gradient of 12 MV/m, and powered by a single FPC for each. In order to meet the requirements, a FPC with the capability to deliver 150 kW continuous wave RF power is designed. Table 1 shows several parameters of the 5-cell cavities and FPC.

Table 1: Main Requirements of the Cavity and FPC

Parameter	Value
Frequency	650 MHz
Beam current	10 mA
R/Q (elliptical 082)	514.6 Ω
Peak RF power	150 kW, CW
Coupling type	Antenna
Coaxial line Impedance	50 Ω

The basic design of the 650 MHz coupler is derived from the coupler of KEKB SC cavities, in consider of its simplicity in structure and reliability in operation with high RF power [2]. Some components and mechanical dimension are redesigned because of the difference in frequency and other considerations. However, the window must be assembled with the cavity in class-10 clean room to protect the cavity from contamination. The RF structure is carefully simulated by HFSS code. Then sufficient thermal, thermal-mechanical simulations are carried on with ANSYS code. In addition, we made multipacting simulations and the results is discussed.

RF STRUCTURE DESIGN

The design of 650 MHz FPC is based on a 50 Ω coaxial line, including a doorknob transition, a planar RF windowe and an antenna. Figure 1 shows the half structure of 3-D model for RF structure analysis.

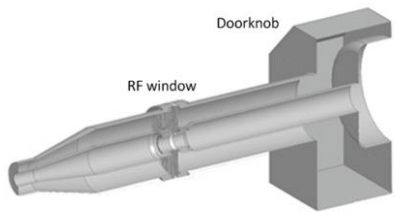

Figure 1: The half 3-D model of the 650 MHz coupler used in HFSS for RF structure design.

RF window is a critical component of the coupler. The window is made of 97.6% alumina ceramic, which works as a vacuum barrier for the cavity but let the RF power go through. The choke is an impedance-matching structure, meanwhile provides shielding for the window braze joints to reduce the electrical field. As shown in Figure 2, the electrical field near braze joints is obviously lower because of the choke structure and the window match the impedance well.

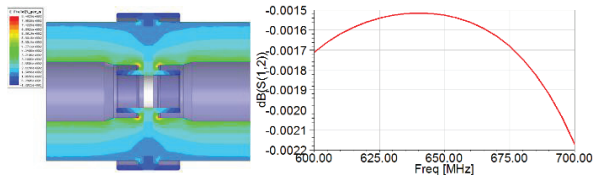

Figure 2: The E field of the window structure with 1 W RF power (left) and the S21 parameter of the RF window (right).

The transition between the coaxial line of the coupler to the WR1150 waveguide from the klystron is achieved by a doorknob configuration. The RF performance of the doorknob is sensitive to the mechanical dimensions. We have optimized dimensions of the doorknob (mainly the doorknob height, diameter and the distance from the shot circuit) aimed at a good impedance matching. Further simulations of the integrate coupler have been carried on. Figure 3 shows the calculated S11 curve of the whole

ISBN 978-3-95450-178-6

20 KW CW POWER COUPLERS FOR THE APS-U HARMONIC CAVITY*

M.P. Kelly[1,#], S.H. Kim[1], A. Barcikowski[1], Z.A. Conway[1], D. Horan[1], M. Kedzie[1], S.V. Kutsaev[3], P.N. Ostroumov[1], J.Rathke[2]
[1)]Argonne National Laboratory, Argonne, IL 60439, U.S.A.
[2)]Advanced Energy Systems, Inc., Medford, NY 111763, U.S.A.
[3)] RadiaBeam, Santa Monica, CA, 90404, U.S.A.

Abstract

A pair of 20 kW CW adjustable RF power couplers optimized for 1.4 GHz has been designed and is being built as part of the APS-U bunch lengthening system. The system uses a single superconducting RF cavity to be installed into the APS Upgrade electron storage ring and will provide a tremendous practical benefit to the majority of users by increasing the beam lifetime by 2-3 times. The 80 mm diameter, 50 Ω coaxial couplers include 4 cm (~20 dB) of adjustability. This allows optimization of bunch lengthening for a range of storage ring beam currents and fill patterns while, simultaneously, maintaining the required 0.84 MV harmonic cavity voltage. To provide bunch lengthening, the cavity/coupler system must extract RF power (up to 32 kW) from the beam. Each coupler will transmit roughly half of the total extracted power to external water-cooled loads. The design extends upon on a well-tested ANL dual RF window concept, using a pair of simple rugged 80 mm diameter alumina disks. A new feature is the 'hourglass-shaped' inner conductor designed to maximize transmission at 1.4 GHz. Results of thermal simulations, as well as, prototyping and initial RF testing are presented.

INTRODUCTION

The APS-U storage ring [1] will have a relatively short beam lifetime due to Touschek scattering [2] and a bunch lengthening cavity is required to mitigate the effect. Harmonic cavities provide lengthening by modifying the longitudinal potential, reducing the slope near the bunch center [3]. Normal and superconducting RF (SRF) cavities are in use elsewhere for this purpose [4,5].

SRF cavities have advantages over normal conducting cavities in many high-current, high-power CW applications, including for the 6 GeV, 200 mA electron storage ring in the APS-U:

- One beam-driven single-cell harmonic cavity easily provides the required 0.84 MV potential
- Large-bore SRF cavities have no trapped monopole or dipole modes; HOM damping is, therefore, relatively less complex
- The high intrinsic quality factor, $Q_0>10^8$, combined with a variable coupler, permit adjustment of the loaded quality factor, Q_L, for near-optimal lengthening for various beam currents

The coupler/cavity design for the 4th harmonic system is shown in Figure 1. Some basic features are similar to the Cornell ERL injector couplers [6]. Two couplers reduces the time average power density and the symmetry reduces the transverse impedance presented to the beam.

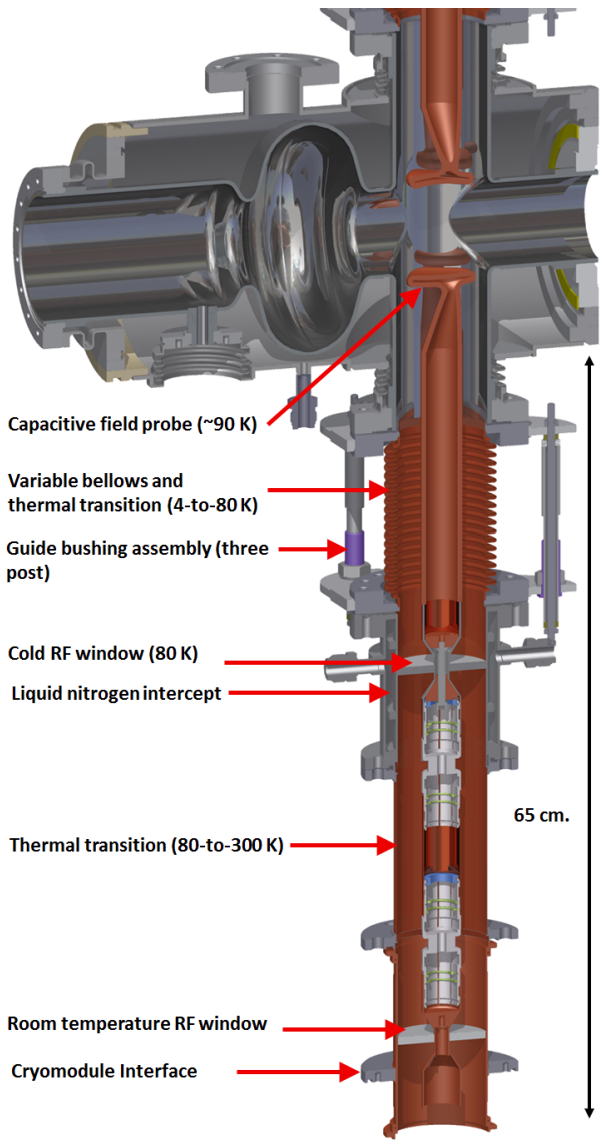

Figure 1: A pair of 80 mm diameter dual-window RF power couplers mounted to a 4th harmonic cavity

* This work was supported by the U.S. Department of Energy, Office of Nuclear Physics, under Contract No. DE-AC02-06CH11357. This research used resources of ANL's ATLAS facility, which is a DOE Office of Science User Facility.
#mkelly@anl.gov

HOM COUPLER PERFORMANCE IN CW REGIME IN HORIZONTAL AND VERTICAL TESTS

N. Solyak#, M. Awida, A. Grassellino, C. Grimm, A. Hocker, J. Holzbauer, T. Khabibobulline, O. Melnychuk, A. Rowe, D. Sergatskov, FNAL, Batavia, IL, 60510, USA
J. Sekutowicz, DESY, Hamburg, Germany

Abstract

Power dissipation in HOM coupler antenna can limit cavity gradient in cw operation. XFEL design of HOM coupler, feedthrough and thermal connection to 2K pipe was accepted for LCLS-II cavity based on simulation results. Recently a series of vertical and horizontal tests was done to prove design for cw operation. In vertical test was found no effect of HOM coupler heating on high-Q cavity performance. In horizontal cryostat HOM coupler was tested up-to 23MV/m in continuous wave mode. Result proves that XFEL HOM coupler meets LCLS-II specifications.

INTRODUCTION

Higher order modes (HOM) are excited in the particle accelerator's superconducting cavities by the particle beam causing instabilities and affecting the particle accelerator performance. In this perspective it is essential to couple them away from the cavity through specially designed HOM antennas [1]. However, the RF losses accumulated on the HOM antenna surface will induce heating and might cause the antenna surface to heat up and eventually quench if the temperature exceeds 9.2 K, the critical temperature for niobium. The problem is rather more critical for continuous wave (CW) machines compared to pulsed machines [2-3].

LCLS-II, a proposed coherent light source to be built at SLAC, is a continuous wave linear accelerator that would utilize state of the art superconducting cavities. Heating of HOM couplers is one of the technical challenges. Our simulation shows that antenna overheating for the ILC style of HOM couplers and feedthroughs will limit cavity gradient to ~10 MV/m in CW operation.

Given that we would like to utilize several existing ILC cavities in the LCLS II project, we investigate in this paper the possible shape modifications of the current ILC HOM antenna that could lower the RF losses (the goal is to reduce the losses by a factor of 4), while relatively preserving the current coupling (LCLS-II requirements for HOM damping is $Q_{ext} < 1.e6$ for the most dangerous modes, so our goal is to avoid reducing the coupling more than 10 times [4-5]). Another option is to use a better design for the feedthrough with improved thermal conductance to remove power dissipated in the antenna. In both options we assume that the design of the HOM coupler itself (f-part and can, see Figure 1) remains untouched from the original one used in XFEL and ILC cavities. A recent proposal [2] aimed at reducing heating of the HOM antenna requires a modification of the f-parts. We don't consider this option here, since it is not a viable solution for existing ILC cavities; moreover, it would require prototyping.

HOM COUPLER

The LCLS-II project is based on ILC/XFEL technology. However some modifications are required to accommodate a much higher heat load in CW operations (gradient 16 MV/m; beam: 300pC, 1MHz; σ_z=25μm at the end of the linac).One of the constraints on the LCLS-II project is that the first two cryo-modules will use existing ILC cavities provided by Fermilab with "short-short beam pipe" configuration, as shown in Figure 1(a). Therefore no modification of the HOM coupler design (except the feedthrough) is possible.

Figure 1(a) shows the geometry of the conventional ILC 9-cell elliptical cavity. The cavity has a power coupler and a HOM antenna (HOMc) on one side and a pick-up and a HOM antenna (HOMpu) on the other side. Figure 1 also shows the front projection of the cavity showing the details of both HOM antennas, and the f-parts. Possible modifications to the current ILC design of the HOM antenna are either changing the gap size or changing the tip size.

More than a hundred TESLA HOM couplers have operated for many years in TTF and around the world in short pulse regimes (few % duty factor) with a beam current up to 9 mA. In acceptance tests of these couplers and in multi-year operation in facilities, it was found that this design is robust (no overheating, no multipactoring), and cavities can operate up to 35 MV/m gradient if the couplers are properly cleaned. However, at long pulse regimes in some cavities with attached HOM feedthroughs, DESY [2] and JLAB [3] observed heating of the HOM couplers, which might be a serious limitation for CW operation. To improve heat removal performance new designs of the feedthrough were developed by JLAB and DESY to reduce heating. For XFEL applications the configuration of antenna was modified (tip diameter was reduced from 11mm to 7.8mm). For 3.9 GHz cavities, FNAL modified the JLAB feedthrough design to prevent internal resonances up to 10 GHz .

All feedthrough designs have these common features:

- Sapphire window instead of Alumina (x3 higher thermal conductivity at 2K)
- Molybdenum internal pin connector instead of SS (x200 higher thermal conductivity at 2K)
- Use copper socket for better cooling

*Work supported by US DOE Contract DE-AC02-766SF00515
solyak@fnal.gov

ISBN 978-3-95450-178-6

MECHANICAL DESIGN OF A HIGH POWER COUPLER FOR THE PIP-II 325 MHz SSR1 RF CAVITY*

O. Pronitchev#, S. Kazakov
FNAL, Batavia, IL 60510, USA

Abstract

The Project X Injector Experiment (PXIE) at Fermilab will include one cryomodule with eight 325 MHz single spoke superconductive cavities (SSR1). Each cavity requires approximately 2 kW CW RF power for 1 mA beam current operation. A future upgrade will require up to 8 kW RF power per cavity. Fermilab has designed and procured ten production couplers for the SSR1 type cavities. Status of the 325 MHz main coupler development for PXIE SSR1 cryomodule is reported.

INTRODUCTION

A multi-MW proton accelerator facility based on an H- linear accelerator using superconducting RF technology, Proton Improvement Plan-II (PIP II), is being developed at Fermilab to support the intensity frontier research in elementary particle physics. The PIP-II baseline design includes two types of 325 MHz superconducting cavities, single spoke resonators, SSR1, with a β=0.22 and single spoke resonators, SSR2, having β of 0.47. The first cryomodule consists of eight SSR1 cavities and will be installed in PXIE at Fermilab. Both types of cavities have a similar design and are equipped with the same size power coupler flanges. This will allow the use of the same design for power couplers that feed the RF power to both types of cavities. Power consumption of the cavities for both projects varies from 2 kW to 8 kW, thus the 325 MHz power couplers should operate up to 10 kW in the CW regime. The PIP-II upgrade plan intends to use the Linac in a continuous wave (CW) mode [1]. This means that the main coupler must reliably operate at a power level > 20 kW under conditions of full reflection. Prototype 325 MHz couplers were designed and tested at power levels ~ 8 kW in both CW modes: travelling wave (TW) and standing wave (SW) [2].This paper presents the mechanical design and production status of 325 MHz main coupler for PXIE SSR1 cryomodule.

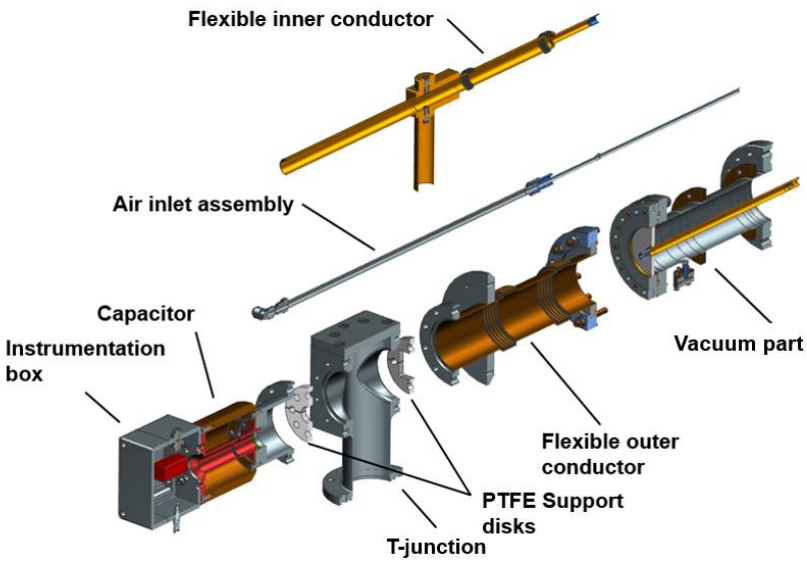

Figure 1: Exploded view of 325 MHz main coupler.

* Work supported by DOE.
# olegp@fnal.gov

MECHANICAL DESIGN OF A HIGH POWER COUPLER FOR THE PIP-II 162.5 MHz RF QUADRUPOLE*

O. Pronitchev#, S. Kazakov
FNAL, Batavia, IL 60510, USA

Abstract

PXIE is a prototype front end system [1] for the proposed PIP-II accelerator upgrade at Fermilab. An integral component of the front end is a 162.5 MHz, normal conducting, continuous wave (CW), radiofrequency quadrupole (RFQ) cavity. Two identical couplers will deliver approximately 100 kW total CW RF power to the RFQ. Fermilab has designed and procured main couplers for the CW RFQ accelerating cavity. The mechanical design of the coupler, along with production status, is presented below.

INTRODUCTION

A multi-MW proton facility, PIP-II, has been proposed and is currently under development at Fermilab. A prototype of the PIP-II front end, PXIE, is planned to validate the conceptual design. PXIE will supply a 25 MeV 50 kW beam, and will include an H- ion source, a CW RFQ, and a two superconducting RF cryomodule providing up to 25 MeV energy gain at an average beam current of 1 mA (upgradable to 2 mA) [1]. The ion source will deliver up to 10 mA of H- at 30 keV to the RFQ. The 162.5 MHz RFQ (Fig. 1) accepts and accelerates this beam to 2.1 MeV. The RFQ is designed to dissipate ~80 kW of RF power under nominal operating conditions. To reduce coupler power demands, two couplers will be integrated with the RFQ [2].

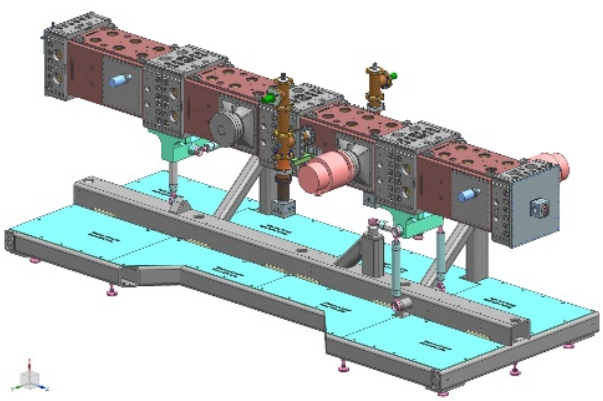

Figure 1: 3D CAD model of RFQ.

Table 1: RFQ Parameters

Parameter	Value
Ion type	H-
Beam current	1-10 mA
Beam energy	0.03-2.1 MeV
Frequency	162.5 MHz
Duty factor (CW)	100%
Total RF power	≤ 130 kW
Number of couplers	2

RFQ COUPLER

Requirements

Parameters of the RFQ (Table 1) define the requirements for the two couplers. Coupler parameters are listed in Table 2.

Table 2: Coupler Requirements

Parameter	Value
Frequency	162.5 MHz
Operating power	75 kW
Coupling type	Loop
Output port diameter	~3"
Input impedance	50 Ohm

Coupler Structure

The PXIE RFQ power coupler includes all components necessary to transport up to 75kW (each) of RF power from a 50 Ohm source into the RFQ vacuum while maintaining the RFQ vacuum integrity.

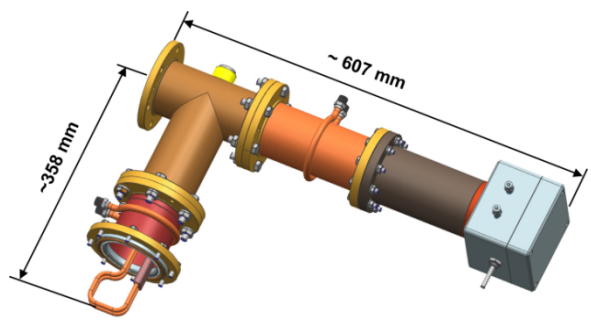

Figure 2: Overall dimensions of RFQ coupler.

*Work supported by DOE.
#olegp@fnal.gov

ISBN 978-3-95450-178-6

A 1.3 GHZ WAVEGUIDE TO COAX COUPLER FOR SUPERCONDUCTING CAVITIES WITH A MINIMUM KICK

R. Eichhorn#, J. Robins, C. Egerer, and V. Veshcherevich
Cornell Laboratory for Accelerator-Based Sciences and Education, Cornell University,
Ithaca, NY 14853-5001, USA

Abstract

Transversal forces as a result of asymmetric field generated by the fundamental power couplers have become a concern for low emittance beam in future accelerators. In pushing for smallest emittances, Cornell has finished a physics design for a symmetric coupler for superconducting accelerating cavities. This coupler consists of a rectangular waveguide that transforms into a coaxial line inside the beam pipe, eventually feeding the cavity. We will report on the RF design yielding to the extremely low transversal kick. In addition, heating, heat transfer and thermal stability of this coupler has been evaluated.

BACKGROUND

Many new accelerator designs, especially for light source applications, reply on high quality, low emittance electron beams. This not only results in highly optimized photo guns (DC, RF, or SRF), but also requires a careful control of the emittance growth in the injector linac. This is usually achieved by a highly sophisticated beam dynamics optimization, as in described in [1-3]. It has been realized that transversal kicks introduced by the fundamental power coupler and the higher order mode coupler give a significantly contribution to the emittance growth.

Due to axial asymmetry that usually exist in these couplers, the electromagnetic fields, have transverse components and produce a transverse kick to the electron beam. A way to compensate the dipole kick is using two identical couplers placed symmetrically to feed the RF into the cavity, like done in the Cornell ERL injector [4]. This complicates the cryo-module design significantly while higher than dipole moment kicks still remain.

To explore opportunities to further minimize transversal kicks to the beam of any order we designing a waveguide-to-coaxial type coupler as shown in Fig. 1, resulting in super-symmetric fields. That coupler has a tube inside the beam pipe which forms a coaxial line with the beam pipe while shielding the beam from the asymmetric fields. Couplers of that type were designed, built and used for the 3 GHz superconducting cavities at the S-DALINAC in the early 90s and are operational since then [5,6]. Later similar couplers were considered at DESY [7] and FNAL [8].

In this paper, we shortly review the RF optimizations of this coupler design while focusing on the mechanical and cryogenic properties.

#r.eichhorn@cornell.edu

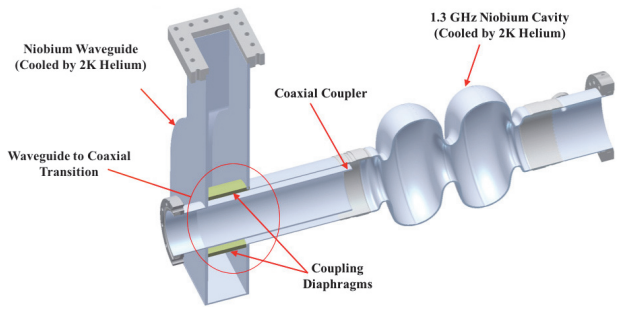

Figure 1: Cornell design of a super-symmetric fundamental power coupler, based on a waveguide-to-coax transition.

RF DESIGN

For practical sizes of the beam pipe, two modes can propagate in the beam pipe coaxial line: a fully axially symmetric TEM mode and a dipole TE11 mode. The TE11 mode is excited in the coaxial line due to asymmetric coupling to the transmission line. This dipole mode produces a transverse kick to the beam and therefore needs to be minimized.

Our design started from a scaled version of the Darmstadt coupler. For the Cornell injector cavities with a beam pipe diameter of 106 mm, the diameter of the coaxial coupling tube was chosen to be 78 mm. The external quality factor of the coupler can be adjusted by choosing an appropriate length of the tube. Figure 2 describes this behaviour while Fig. 3 reports the transverse associated with this.

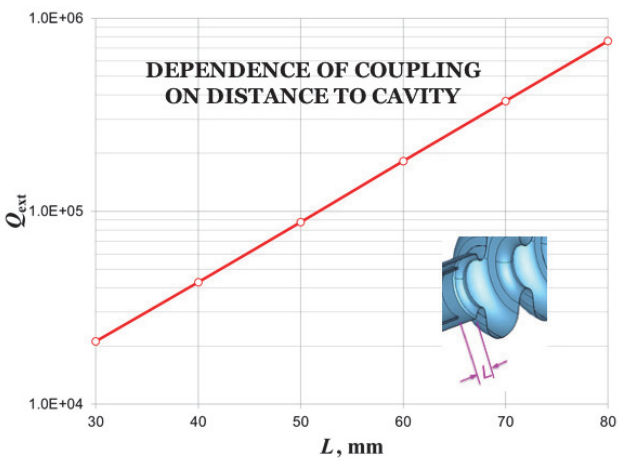

Figure 2: External Q of the coupler as a function of the distance from the coaxial tube to the first iris of the cavity, indicating an ideal cut-off behaviour of the fields.

STATUS OF THE FUNDAMENTAL POWER COUPLER PRODUCTION FOR THE EUROPEAN XFEL ACCELERATOR

C. Lievin, S.Sierra#, THALES, Vélizy, France
G.Garcin, G.Vignette, THALES, Thonon les Bains, France
M.Knaak, M.Pekeler, L.Zweibaeumer, RI Research Instruments, Bergisch Gladbach, Germany
A.Gallas,W.Kaabi, LAL, Orsay, France

Abstract

For the XFEL accelerator, Thales, RI Research Instrument and LAL are working on the manufacturing, assembly and conditioning of fundamental power couplers. 670 couplers have to be manufactured according to strict specifications. This paper describes the full production activity from the program starting to the current phase with main measurements for the coupler characteristic: copper and TiN coating characteristics. The status of the production is given with an output rate of 8 couplers per week. The status for more than 500 couplers manufactured and conditioned is presented.

INTRODUCTION

Fundamental coupler main parameters are[1]:

- RF frequency: 1.3 GHz
- Peak Power: 150 kW
- Pulse length: 1.3 ms
- Repetition rate 10 Hz
- Tuning : ± 10 mm
- Coupling (Qext) $2x10^{6} \rightarrow 2x10^{7}$
- Two ceramics windows

The main metallic sub-assemblies of a coupler are the Warm External Conductor (WEC), Warm Internal Conductor (WIC), The Cold External conductor(CEC) and the antenna, illustrated in Fig.1.

The two other critical components are the two cylindrical ceramics.

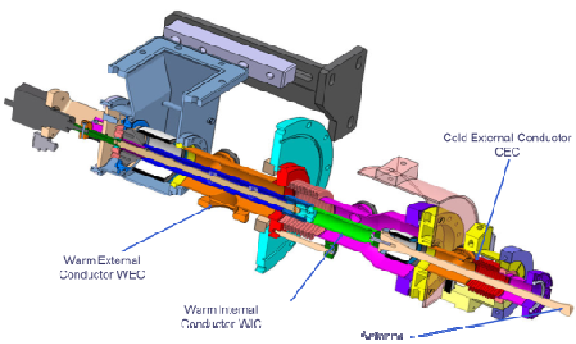

Figure 1: Coupler general layout.

COUPLER FABRICATION

Main steps in the coupler fabrication are: parts assemblies, copper coating of RF surfaces, TiN coating of ceramics windows. When all these parts are ready, parts are EB Welded in order to achieve Warm part and Cold part of individual couplers. Then the coupler parts are clean in an ISO 4 clean room and after drying, they are integrated by pair on a transition waveguide. After a leak check and a RGA is operated couplers are send to LAL in special design shipping box. In LAL couplers are then RF conditioned up to 1 MW peak before being sent to IRFU for complete integration on cryomodules.

Thales Production Process

The XFEL couplers sub-assemblies are based on a brazing technology. This technology allows having a better reproducibility than a welded one, which is more operator dependant and also could be performed by batches, which is useful for a mass production.

Brazing material Cu-Au (50-50) is mainly used. At the beginning of the program, all interfaces particularly brazing grooves, and mechanical tolerances have been defined and qualified in order to avoid centricity problem between tubular parts and avoid gaps, edge or excessive brazing material on RF surfaces.

During the preparation of manufacturing tests have been done also on bellows in order to study the effect of brazing temperature. It has been observed that the stiffness of bellows increases by a few percent remaining in the range of the actuator capabilities for tuning the coupler.

Once the sub-assemblies are brazed and prepared, the three main one (WEC, WIC and CEC) are copper coated, as illustrated in Fig.2 and Fig.3.

The copper plating process is the trickiest step for the coupler manufacturing. This is due to the combination of very demanding specifications on thickness tolerances on complicated geometries (bellows, conical parts, big flanges), quality on the copper visual aspect and RRR specifications.

Thickness and tolerances on WEC and CEC are of 10 µm ±20 % on tubular parts and ± 30% on bellows, For WIC thickness is of 30 µm ±20 % on tubular parts and ± 30% on bellows.

RRR value initial specification was from 30 to 80.

ISBN 978-3-95450-178-6

AUTOMATIC RF CONDITIONING TEST BENCH OF FUNDAMENTAL POWER COUPLERS FOR THE EUOPEAN XFEL ACCELERATOR

C. Lievin, P. Rouillon, S. Sierra, THALES, Vélizy, France
H. Guler, W. Kaabi,A.Verguet LAL, Orsay, France

Abstract

In order to perform the RF conditioning of the fundamental power coupler for the XFEL accelerator, Thales and LAL developed together a test bench being able to make the automatic RF conditioning. The capability of this test bench is of 4 pairs of coupler at the same time with automatic sequences of increasing the RF power.

The test bench is composed of the overall RF station providing up to 5 MW peak power at 1.3 GHz. The waveguide distribution allows 4 individual RF lines for conditioning, and the automatic sequence applied to the couplers in respect with all signals monitored and controlled during the RF process.

.

INTRODUCTION

LAL contribution to the XFEL project is the delivery of 670 fundamental power couplers to equip 80 Cryomodules.

The fundamental coupler is composed of the following parts[1] as illustrated in Fig.1.

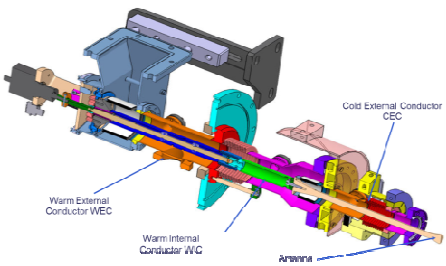

Figure 1: Schematic of XFEL fundamental power coupler.

The preparation and RF conditioning of XFEL couplers are done at LAL ORSAY in a dedicated ISO5 clean room (70m2).

The Automatic conditioning test bench provided by Thales and developed jointly with LAL is part of the industrial capabilities developed for mass production of XFEL RF couplers. The test presented and all auxiliaries are compatible with a production rate from 8 to 10 couplers/week.

GENERAL DESCRIPTION OF THE TEST BENCH

The RF test bench system consists of a fully integrated power station including for the RF power station:

- High voltage modulator
- A 5 MW klystron TH2104C
- Interlocks controls and data acquisition system.

An automatic control system manages the conditioning procedure with diagnostics, monitoring and analysis of signals.

The 1.3 GHz power station could provide a maximum output power of 5 MW. The RF signal is divided in 4 channels which allow a conditioning of 4 coupler pairs in parallel, Fig.2.

Figure 2: General layout of four channels for coupler conditioning.

The general layout of test bench is presented in the figure n°3.

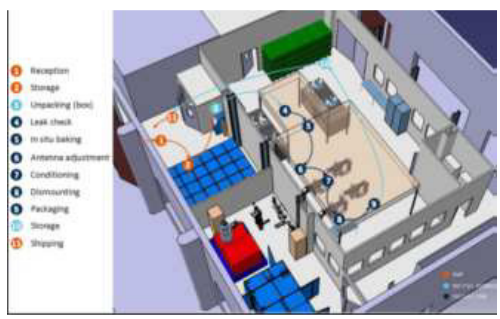

Figure 3: General layout of test bench.

ISBN 978-3-95450-178-6

LESSON LEARNED ON THE MANUFACTURING OF FUNDAMENTAL POWER COUPLERS FOR THE EUROPEAN XFEL ACCELERATOR

C. Lievin, S.Sierra#, THALES, Vélizy, France
G.Garcin, G.Vignette, THALES,Thonon les Bains, France
M.Knaak, M.Pekeler, RI Research Instruments GmbH, Bergisch Gladbach, Germany

Abstract

In this paper, we described lessons learned during the production of Fundamental Power Coupler(FPC) for the European XFEL accelerator and different steps necessaries to obtain a rate of 8 couplers a week, from the manufacturing of individual components up to the RF conditioning. This document also proposes some possible ways to be optimized for a future mass production of such components. With comparison of processes and adaptation which could benefit to an increase rate or a more secure program. Some of them, which could be studies from the coupler definition to the manufacturing process in order to obtain a stable and possible increase rate or lower cost of production by decreasing risks on programs. This analysis is based on a current production of more than 500 couplers, see Fig. 1.

INTRODUCTION

For the European XFEL accelerator, 670 fundamental power couplers are under manufacturing by Thales and RI Research Instruments[1].

These couplers are RF conditioned by LAL in Orsay before being sent to Saclay for Cryomodule integration[2].

The main metallic sub-assemblies of a coupler are the Warm External Conductor (WEC), Warm Internal Conductor (WIC), The Cold External Conductor(CEC) and the antenna, as illustrated on Fig. 2.
The two other critical components are the two cylindrical ceramics.

For the fundamental power coupler production a weekly rate of 10 couplers a week has been demonstrated over few months.

A current production of more than 500 couplers delivered to LAL (Laboratoire de l'Accélérateur Linéaire) has been achieved.

Ramp up for such a rate is a fundamental parameter to be considered by experience on the XFEL FPC program.

This ramp up period is needed in order to solve the following issues:

- Common understanding and sharing on visual acceptance criteria for each individual production phase.
- Stability of manufacturing process.

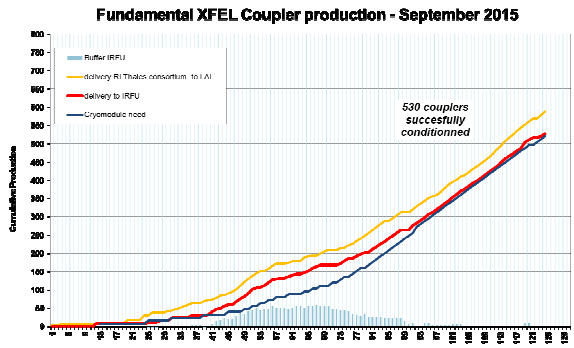

Figure 1: FPC production status.

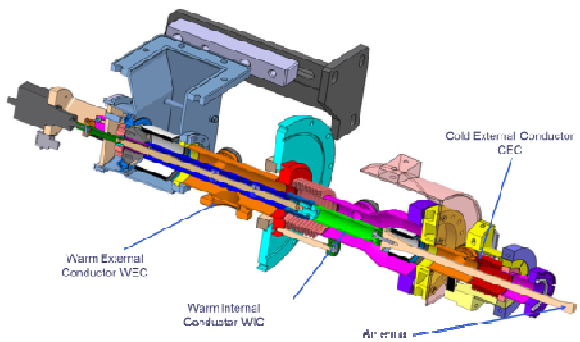

Figure 2: Coupler general layout.

VISUAL INSPECTION CRITERIA

Visual inspection criteria process shared with all participants of such a program is one of the major lessons learned during the XFEL FPC production.

Objective and measurable criteria are to be shared between all parties involved in the production program.

Often some of the visual acceptation criteria given in specifications are difficult to be understood commonly. As example of such criteria if copper coating quality is defined as "special attention to the aspect", this criterion is not measurable and could be interpreted differently by operators.

This is the reason why it is of the most importance to define commonly such criteria. For the XFEL FPC

ISBN 978-3-95450-178-6

NEW POSSIBLE CONFIGURATION OF 3.9 GHz COUPLER*

S. Kazakov#
FNAL, Batavia, IL 60510, USA

Abstract

The LCLS-II superconducting accelerator supposedly will use 3.9 GHz (3-d harmonic) superconductive cavities. A new possible configuration of 3.9 GHz main coupler is presented in the paper. This configuration contains two coaxial ceramic windows, a cold and a warm one. Inner conductors of windows are connected through the capacitive gap and have no mechanical no thermal contacts. It allows to avoid using bellows and thus avoid the problem of heating and cooling. The windows have shields protecting shields against the electron, and this prevents the window ceramics from charging. Results of computer simulation of the new coupler are posted.

INTRODUCTION

The main coupler is the key element of a superconducting accelerator. The purpose of the coupler is to transmit RF power from a room temperature RF source to a cold superconducting cavity. The coupler must have a small ohmic losses in order to prevent a cold cavity from heating. At the same time, the coupler should have small thermal conductivity in order to minimize the heat flow from a room temperature environment to a superconductive cavity. Common elements of a coupler are bellows. There are two major purposes of bellows usage. The first one is to compensate thermal shrinking-expansion and movements of accelerator parts. The second one is to reduce the thermal conductivity of the coupler's conductors. However, utilizing the bellows has several drawbacks. In a high power coupler, the bellows themselves may reach high temperatures due to their low thermal conductivity and the ohmic losses. This is especially true for the inner conductor of the coaxial coupler. The inner conductor has a smaller size, hence its losses density is higher. In addition, bellows make the coupler more expensive. Moreover, if the coupler includes two windows, it is necessary to provide a reliable and demountable electrical contact between the two parts of inner conductor. We suggest a new approach which eliminates the drawbacks described above.

We propose using a capacitive gap instead of bellows. The gap has no thermal conductivity (except thermal radiation, which is small). There are no ohmic losses, no electrical or mechanical contacts, no high temperatures, and there is no need to cool it. The gap tolerates displacements that can compensate for the thermal shrinking-expansion. We used this approach to design the 3.9 GHz coupler. The structure of the coupler is presented on Figure 1. This coupler still has bellows, but all of them are placed in the air, room temperature side. It reduces requirements to bellows and simplifies the cooling. The design includes the shields in front of windows to protect the ceramics from charged particles coming from the cavity. The shields also match the windows.

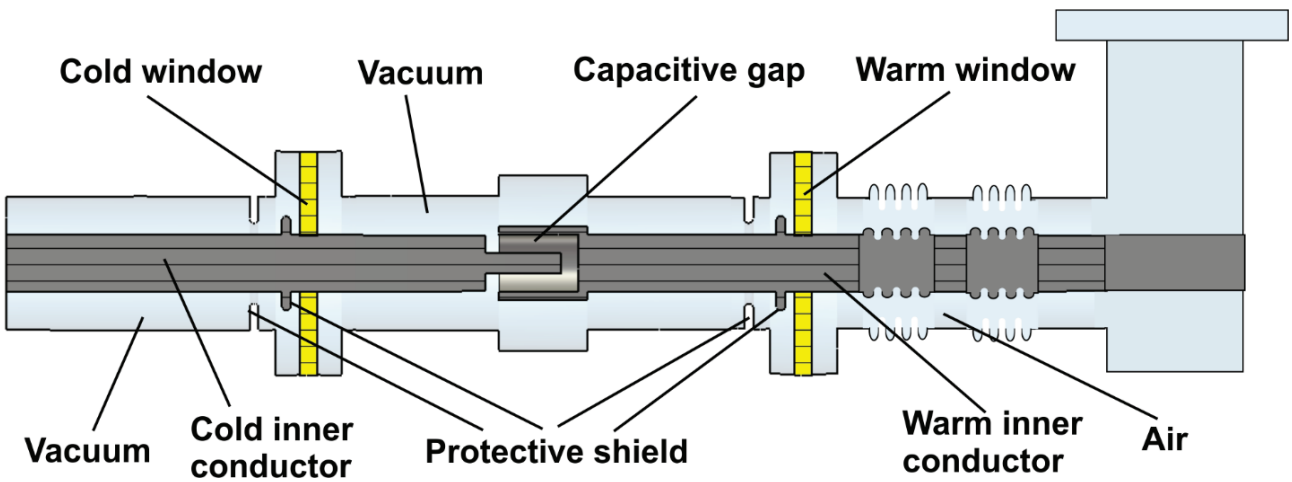

Figure 1: Structure of the coupler. The coupler contains two coaxial ceramic windows, a cold and a warm one. The inner conductors of windows are connected through the capacitive gap, i.e. have no mechanical contact.

*Work supported by DOE.
#skazakov@fnal.gov

ISBN 978-3-95450-178-6

TESTING OF 325 MHz COUPLERS AT TEST STAND IN RESONANCE MODE

S. Kazakov#, B. Hanna, O. Pronitchev, FNAL, Batavia, IL 60510, USA

Abstract

The linear accelerator for the PIP-II program utilizes two types of 325 MHz Single Spoke resonator cavities: SSR-I and SSR-II. Operating power of SSR-II is about 17 kW and requires input couplers which can reliably work at power levels > 20 kW with full reflection at any reflected phase. Currently only one 10 kW RF amp is available for coupler testing. To increase testing power, a special resonance configuration was used. This configuration allows us to raise RF power approximately 3 times. The testing scheme and results are discussed in the paper.

INTRODUCTION

The proton accelerator facility based on an H- linear accelerator which utilizes superconducting RF technology, PIP-II, is now being developed at Fermilab to support the intensity frontier research in elementary particle physics. The PIP-II design includes two types of 325 MHz superconducting cavities, single spoke resonators SSR-I, with β=0.22 and single spoke resonators, SSR-II, with β=0.47. The total number of spoke cavities is 51. Both types of cavities have similar design and utilize the same design of the main coupler. Maximum RF power per cavity is 17 kW. The PIP-II upgrade plan intends to use the Linac in a continuous wave (CW) mode [1]. This means that the main coupler must reliably operate at a power level > 20 kW under conditions of full reflection. Prototype 325 MHz couplers were designed and tested at power levels ~ 8 kW in both CW modes: travelling wave (TW) and standing wave (SW) [2]. Power was limited by the maximum power of RF amplifier. In order to further increase RF power, a resonance scheme with a movable reflector was designed and built. A set of shorted coaxial waveguides with different lengths was used to change reflection phases. RF power that circulated between the movable reflector and RF short was more than 3 times higher than input power from amplifier.

325 MHz COUPLER AND DC-BLOCK

The structure of the 325 MHz coupler is presented in Fig. 1. A more detailed description of the coupler's configuration is presented in [2]. Three couplers were produced. Two of them were tested on the coupler test stand [3] at room temperature. The third coupler was tested with a cold superconducting spoke cavity in the test cryomodule.

*Work supported by DOE.
#skazakov@fnal.gov

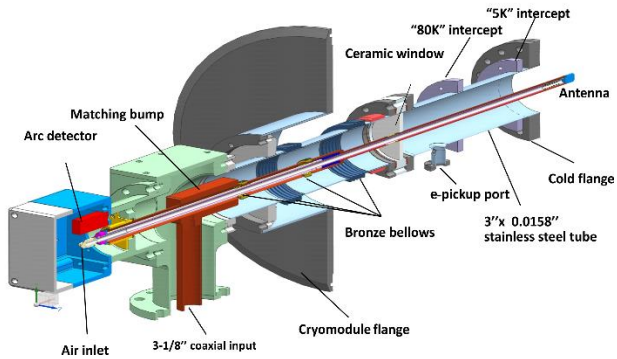

Figure 1: Structure of 325 MHz coupler.

To supress multipactor in the coupler, high voltage (HV) bias is used. To isolate the coupler input and protect the RF amplifier from HV bias, a DC-block is utilized. The structure of the DC-block is shown in Fig. 2 [2]. Power requirements for the DC-block are similar to coupler power requirements: reliable operation at power level > 20 kW, CW. Two DC-blocks were installed on the test stand and tested simultaneously with two couplers. A HV bias of up to 5 kV was applied during the test.

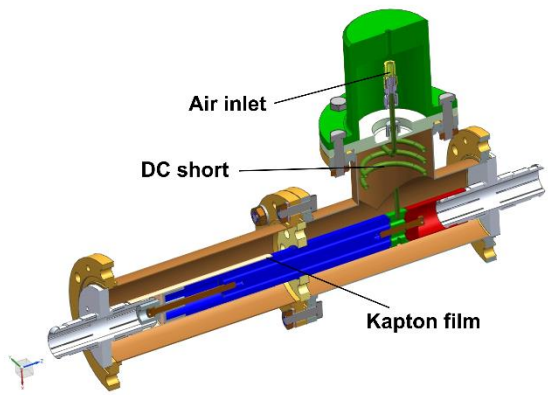

Figure 2: Structure of 325 MHz DC-block.

Configuration of the test stand is presented in Fig. 3 [3]. Two couplers are connected to a 6'' stainless steel cavity. Two DC-blocks are attached to the couplers inputs. The movable reflector (not presented at the drawing) is connected to the input of the first DC-block. Several directional couplers are used for power measurement and shape monitoring. RF power is measured twice: before and after the reflector. The ratio of these values is the power amplification of this resonance setup.

Nb COATINGS ON BELLOWS USED IN SRF ACCELERATORS

S.F. Chapman, I. Irfan, M. Krishnan, K.M. Velas, AASC, San Leandro, CA 94577, USA

Abstract

Alameda Applied Sciences Corporation (AASC) is developing bellows with the strength and flexibility of stainless steel and the low surface impedance of a superconductor. Such unique bellows would enable alignment of SRF cavity sections with greatly reduced RF losses. To that end, we grow Nb thin films via Coaxial Energetic Deposition (CED) from a cathodic arc plasma. Films of Nb were grown on stainless steel bellows, with and without an intermediate layer of Cu deposited via the same technique, to produce a working bellows with a well adhered superconducting inner layer. The Nb coated bellows have undergone tests conducted by our collaborators to evaluate their RF performance.

MOTIVATION

Any radio-frequency superconducting (SRF) accelerator including multiple cells of cavities must allow for fine adjustment of the joints between beam components, to correct for misalignment and to allow for thermal expansion. Flexible metal bellows are a common choice.

The bellows must be strong and flexible enough to hold vacuum and maintain integrity during tens of thousands of compressions and thermal cycling. Thus, stainless steel is the usual choice. Thin-walled stainless steel bellows also provide the advantage of some measure of thermal isolation between the components it joins.

However, a bellows made of non-superconducting material will increase beam impedance and lead to RF power losses [1]. In some cases, these power losses can eventually damage the bellows and lead to instabilities. Unfortunately, there are no currently known superconductors able to compete with the mechanical advantages of stainless steel.

One possible solution, aside from planning and budgeting for RF power losses to stainless steel bellows, is to add a superconducting shield to the inner surface of the bellows, such as layers of fine mesh or overlapping finger stock, thereby blocking the beam's view of any non-superconducting material. Unfortunately, such a shield necessarily reduces the flexibility of the coupling, while increasing its complexity and reducing available space. Additionally, as such shields are less robust than stainless steel, repeated flexing may result in particulates that can also be harmful to beam performance.

The bellows can also be coated with some other material, such as copper, that, while not a superconductor, has a significantly lower impedance than stainless steel.

AASC is working to develop and benchmark another solution. By coating the inner surface of a stainless steel bellows with multiple skin-depths worth of niobium, we can create a bellows with the mechanical advantages of stainless steel while adding minimal beam impedance and no additional obstacles to proper operation of the accelerator.

COATING TECHNIQUE

To coat the bellows, we grow a thin (microns to tens of microns) film of Nb on their inner surface via energetic condensation. Specifically, we use a proprietary variation on high vacuum (~10^{-7} Torr) cathodic arc plasma that we call CED.

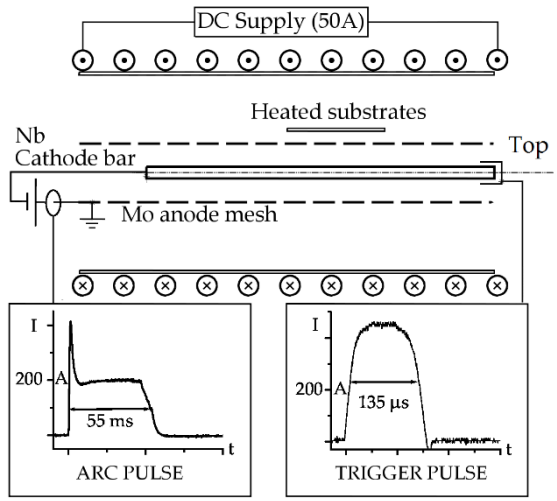

Figure 1: CED process schematic drawing.

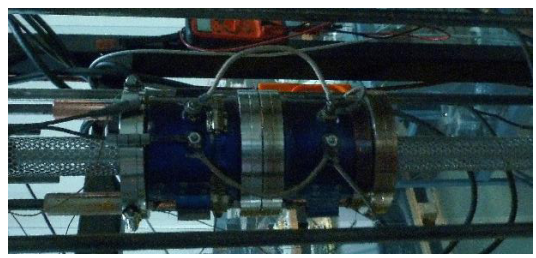

Figure 2: Bellows mounted in CED apparatus.

Figure 1 shows a schematic drawing of the CED process, while Fig. 2 shows two bellows mounted in the CED apparatus before insertion into the vacuum chamber. On the central axis of the apparatus we locate a rod (0.5" O.D.) of the desired coating material, which will act as a cathode. Surrounding the cathode is a coaxial cylindrical mesh anode (1.25" I.D.) made of a refractory metal such as molybdenum or stainless steel. Surrounding the anode, we place the substrate or substrates to be coated. The assembly is then placed inside a vacuum chamber located inside a coaxial DC (~50 Gauss) solenoidal magnet.

By triggering and maintaining a vacuum arc (30-100V, 100-200A) between the cathode and anode we produce an energetic (60-120 eV, in the case of Nb) highly ionized plasma consisting solely of cathode material [2, 3]. By manipulating the average instantaneous location of the

ISBN 978-3-95450-178-6

HIGH POWER INPUT COUPLERS FOR C-ADS

T.M. Huang#, Q. Ma, X. Chen, F.B. Meng, H.Y. Lin, W.M. Pan, G.W. Wang, K.X. Gu, X.Y. Zhang,
Key Laboratory of Particle Acceleration Physics and Technology,
Institute of High Energy Physics (IHEP), Chinese Academy of Science, Beijing 100049, China

Abstract

High power input couplers are key components of the of the high power input couplers for C-ADS.

INTRODUCTION

Accelerator Driven sub-critical System (ADS) is a proton accelerator-based facility to produce energy and to destroy nuclear waste efficiently. China ADS (C-ADS) project is aiming at constructing a 15 MW continuous wave (CW) proton linac of 1.5 GeV and 10 mA from 2011 to 2030s. For Phase-I, the goal is to build a CW proton linac of 25 MeV and 10 mA by around 2016 [1]. The phase-I linac consists of two injectors and one main linac section, as shown in Fig. 1. Four types of superconducting cavities (SCCs) of two frequencies are adopted.

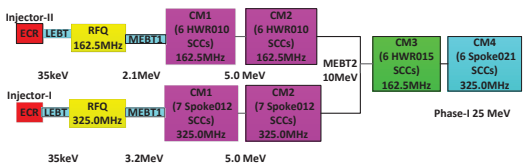

Figure 1: The schematic of C-ADS (Phase-I).

All input couplers for the SCCs are developed in IHEP. Up to now, all injector couplers have been assembled with both the Test Cryomodules (TCM) and the first formal cryomodules (CM1); joined the cavity RF processing and beam commissioning. In the meanwhile, the design of the input couplers for the main linac has been completed and to be fabricated soon.

In this paper, we will describe the design, manufacture, high power test on the test stand and the RF processing in the cryomodule of the couplers.

DESIGN OF THE COUPLERS

Both injectors and the main linac consist of two cryomodules; each cryomodule houses six or seven cavities; and each cavity is equipped with one input coupler. The main parameters of each coupler are listed in Table 1. Since the requirements of the input couplers for the same type of cavities for injectors and main linac are similar, only the design of the injector couplers will be illustrated here. Thoroughly and carefully simulations were done to determine the RF dimensions, mechanical structures, cooling methods and so on, which have been described in detail [2], [3].

Table 1: Main Parameters of the High Power Input Couplers for C-ADS SCC (Phase-I)

Parameters	Spoke -012	HWR -010	Spoke -021	HWR -015
Frequency (MHz)	325	162.5	325	162.5
RF power (kW)	10	20	25	25
Qext	7.0E5	7.0E5	8.0E5	6.7E5
Dynamic losses to 2K (W)	0.24	/	/	/
Dynamic losses to 4K (W)	2.20	0.18	3.10	1.85

The general layouts of couplers for two injectors are shown in Fig. 2. As can be seen, both couplers can be divided into three main parts.

An open-ended 50 Ω coaxial line provides coupling to the cavity. The inner conductor is made of OFHC and cooled by water. The outer conductor is a stainless steel tube, with the inner surface copper-plated with 3 times of skin-depths of copper to reduce RF losses. The cooling of the outer conductor decides by the cavity operation temperature and the heat losses. The outer conductor of the coupler for Spoke-012 cavity is cooled by a thermal anchor at 4 K by helium and at 80 K by nitrogen; and the outer conductor of the coupler for HWR-010 cavity is cooled with 4 K helium gas through a double-wall tube.

A RF window affords RF-transparent vacuum barrier. The window is similar to that of the coupler for BEPCII SCC which proved excellent performance [4]. A coaxial planar ceramic made of 97.6% alumina is applied. The RF design of the window focuses on impedance matching, the resonant mods far from working frequency and no multipacting on the operation power level; the mechanical design of the window biased towards on a safe thermal stress, the easier ceramic-copper brazing and fully protection of the window. The window is equipped with three monitor ports to detect electron current, vacuum pressure and discharging light. The inner conductor of the window is also cooled by water.

A T-box provides the matching to the coaxial line. Due to the very low working frequency, the traditional transition structures of “doorknob” [4] and coaxial line with quarter wave short-circuit are too large. The T-box, which consists of one outer box, one inner box and one moveable short-circuit plate, is an ingenious design to solve the problem. The size of outer and inner boxes, the radius of chamfers, and the position of the short-circuit plate were carefully optimized aiming at good impedance matching and low peak electric field. The T-box is made of aluminum for weight reduction. Based on the RF-thermal analysis using ANSYS, no cooling of the

Email: huangtm@ihep.ac.cn

ISBN 978-3-95450-178-6

XFEL COUPLERS RF CONDITIONING AT LAL

H. Guler*, W. Kaabi, A. Gallas, C. Magueur, M. Oublaid, D. Le Pinvidic, A. Thiebault, A. Verguet
Laboratoire de l'Accélérateur Linéaire (LAL), IN2P3/CNRS, Orsay, France

Abstract

In the framework of the French contribution to XFEL project, The LAL has in charge the development, the production and the RF conditioning of 800 power couplers to equip 100 cryo-modules. Thus, LAL's tasks consist on the industrial monitoring and coupler quality control at two different production sites, in addition to the RF conditioning at LAL.

The conditioning process and all the preceding preparation steps are performed in a 70m^2 ISO5 clean room. This infrastructure, its equipment and the RF station are designed to allow the treatment of 8 couplers in the same time, after a ramp-up phase.

Clean room process and first conditioning results are presented and discussed.

INTRODUCTION

The large experience acquired by LAL in power coupler treatment within the last ten years made it one of the key players in this field. Several studies were carried in various domains (mechanical design, RF simulation, vacuum studies, cleaning–assembling procedure and RF conditioning [1]), to better understand the RF behaviour, to improve coupler treatment procedure and to make the RF conditioning shorter and more efficient.

Historically, LAL's activities in power coupler started years ago with TTF3 couplers, base model of XFEL ones, that were prepared and conditioned at LAL to be installed later at FLASH machine. Therefore, Thanks to the experience accumulated, LAL is involved in the industrialisation and the preparation of the 800 XFEL couplers. LAL's tasks consist on the industrial monitoring at two production sites: Thales Electron Devices-Thonon les bains-France (TED) and Research Instruments-Cologne-Germany (RI), in addition to the RF conditioning at LAL. The first task goes from the specifications setting to the final coupler quality control. The second is held in a 70 m^2 ISO5 clean room especially constructed for this purpose. In the following, we will present details on the coupler preparation process in LAL's clean room and the first conditioning results.

COUPLER CONDITIONING AT LAL

Both processes: Coupler preparation and RF conditioning occurred in a 70 m^2 ISO5 clean room especially constructed for XFEL coupler treatment.

The clean room and the equipment installed are optimised to treat 8 couplers per week after a rump up phase.

Coupler Preparation Process

Several steps are carried out prior to RF conditioning. Upon reception at LAL, the coupler pairs are introduced in clean room and after a quick visually checked, pumping groups composed of getter pump, vacuum valve and gauge (Fig. 1) are mounted in each warm part and in the set of the two cold parts and the transition waveguide box. Then, a leak test is performed (Fig. 2). Once the tightness is verified, an in-situ under vacuum baking cycle is carried out (with a landing at 150 °C during 75 h) to remove the residual water vapour. The clean room is equipped with 3 ovens allowing the treatment of 12 couplers in the same time (Fig. 3). At the exit of the oven, the next step is the getter pump starting and the RGA mounting. A residual gas spectrum is then recorded and compared to a coupler pair "standard spectrum" (Fig. 4). The final step, before installing the coupler pair in RF test bench, is the couplers antenna tuning in order to guaranty a good RF matching and avoid power reflection (Fig. 5). Once all these steps are successfully performed, the coupler pair is than installed in RF test bench ready for conditioning (Fig. 6).

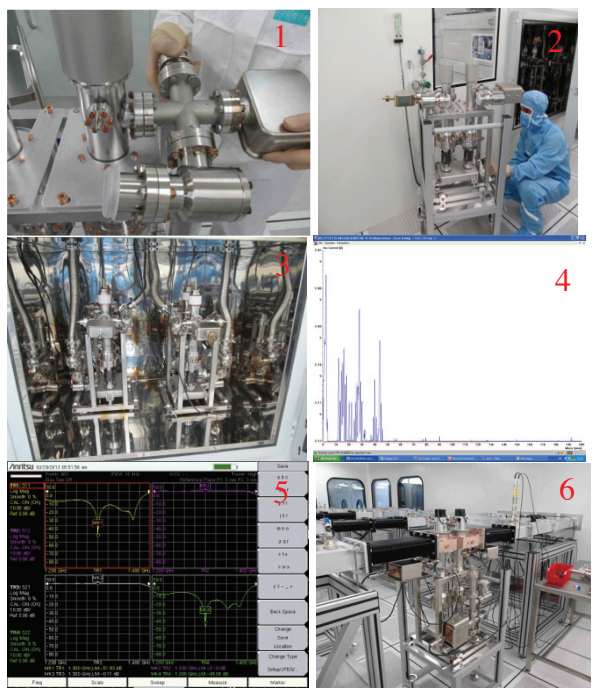

Figure 1-6: (1) Pumping group mounting, (2) Leak check, (3) In-situ baking, (4) RGA spectrum record, (5) Antenna tuning, (6) installation in RF test bench.

ISBN 978-3-95450-178-6

HIGH POWER COUPLER TEST FOR ARIEL SC CAVITIES

Y.Y. Ma#, V. Zvyagintsev, R.E. Laxdal, B.S. Waraich, D. Lang, P. Harmer
TRIUMF, 4004 Wesbrook Mall, Vancouver, BC, Canada, V6T 2A3

Abstract

TRIUMF ARIEL [1] (The Advanced Rare Isotope Laboratory) project employs five 1.3 GHz 9-cell superconducting elliptical cavities [2] for acceleration of 10 mA electron beam up to energy of 50 MeV. 100 kW CW (continuing wave) RF power will be delivered into each cavity by means of pair of Power Couplers: 50 kW per each coupler. Before installing the power couplers with the cavities, they have to be assembled on Power Coupler Test Stand (PCTS) and conditioned with a 30 kW IOT. Six couplers have been conditioned at room temperature and four of them have been installed to the cavities and tested during beam commissioning. Test results of the power couplers will be described and discussed in this paper.

INTRODUCTION

E-Linac for ARIEL project [1] consists of three cryomodules with 5 superconducting 1.3 GHz 9-cell elliptical cavities [3]. 100 kW CW RF power will be delivered into each cavity by means of pair of Power Couplers: 50 kW per each coupler (Fig. 1).

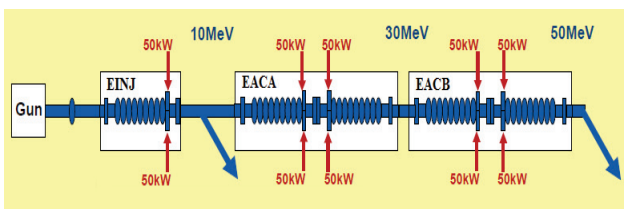

Figure 1: Schematic of the E-Linac.

We employ CPI [4] Power Coupler VWP 3032 [5] capable to deliver up to 75 kW CW RF power at 1.3 GHz to superconducting cavity operating at 2K temperature of liquid He. The coupler design is presented on Fig. 2, it consists of 2 assembly units: 'cold' assembly which has to be mounted to the superconducting cavity RF port and 'warm' assembly which to be connected to waveguide and operates like a warm-cold transition.

'Cold' assembly is a coaxial line loaded with antenna and terminated on other end by 'cold' window, which separates 'cold' cavity and 'warm' assembly vacuum volumes. 'Warm' assembly consists of a coaxial line between 'cold' and 'warm' windows and a coaxial-waveguide transformer at the 'warm' window side. Outer conductor of the 'cold' assembly, 'warm' assembly inner conductor and 'warm' assembly outer conductor have bellows to provide coupling antenna adjustment and reduce thermal flow to the cavity.

#mayanyun@triumf.ca

PCTS was developed at TRIUMF [6] for power couplers conditioning before installation to the cavity. The PCTS is designed for conditioning of two RF power couplers at the time which are installed in series with an RF waveguide box. The coupler which is connected to IOT through waveguide is an 'input coupler' and the coupler which is connected with RF dummy load or variable movable short plate is an 'output coupler'. We are doing RF conditioning in travelling wave mode with water cooled RF dummy load and in standing wave mode with variable movable short plate with air cooling.

There are three valves for vacuum insulation. The turbo pump, three ion pumps and three ion gauges are installed to provide and monitor the vacuum in the PCTS. The warm assemblies of 'input coupler' and 'out coupler' have separated vacuum spaces. The 'cold' sections and waveguide box have a common vacuum.

One Hamamatsu H10722-01 PMT attached to each power coupler, it is sensitive to photons generated by multipacting in the region between the warm and cold RF windows. Ten thermocouples are attached in various points to the exterior of the couplers and the waveguide box. Two PT100 temperature sensors are built (by CPI) inside the inner conductor of the couplers near the inner conductor bellows. Two Raytek MI series IR sensors measure the temperature of the 'cold' window ceramics through view ports in the waveguide box.

The forward and reverse power measurement is provided with power meter connected to directional couplers. In order to protect couplers during RF conditioning, the PMT signals, ion gauge signal are using to fast trip of RF drive with Mini-Circuits ZASWA-2-50DR+GaAs RF switch.

As PCTS works under room temperature we use water loops which installed in the middle of bellows and external fans which set beside the bellows for cooling as shown in Fig.3. In cryomodule, the 'cold' bellows are equipped with 4 K Siphon loop at antenna side, an 80K heat link in the middle of cold bellows and an 80K Nitrogen cryogenic cooling loop at the cold window side. In cryomodule, the 'warm' bellows are equipped with a thermal link connected to the 80K thermal shield.

During 2013-2014 six RF power couplers have been conditioned at TRIUMF with PCTS. Four conditioned couplers have been installed to EINJ and EACA; EACA presently equipped with one single 9-cell cavity and a 'dummy' cavity. During the 1st stage of ARIEL E-Linac commissioning EINJ and EACA cryomodules in the present configuration produced a final energy of 23MeV [7]. Another two pre-conditioned power couplers will be installed to VECC Injector cryomodule [8].

HIGHER ORDER MODES SIMULATION AND MEASUREMENTS FOR 2400 MHz CAVITY*

Ya.V. Shashkov, N.P. Sobenin, M.V. Lalayan, D.S. Bazyl, R.V. Donetskiy,
National Research Nuclear University MEPHI, Moscow, Russia
A. Zavadtsev, LLC, Nano Invest, Moscow, Russia
M.M. Zobov, LNF-INFN, Frascati, Italy
R. Calaga, European Organization for Nuclear Research (CERN), Geneva, Switzerland

Abstract

In the frameworks of the High Luminosity LHC upgrade program an application of additional harmonic cavities operating at multiples of the main RF system frequency of 400 MHz is currently under discussion. The 800 MHz superconducting cavities with grooved beam pipes were suggested as one of the design options. A scaled aluminum prototype with a frequency of the operational mode of 2400 MHz was manufactured for testing the results of simulations. The load reflection coefficient measurements were performed as well as the Q_{load} measurements for cavities with the load. Here we discuss the prototype design and report the obtained measurement results.

INTRODUCTION

At present the project aimed at Large Hadron Collider luminosity upgrade (HL-LHC) is being developed at CERN [1]. The implementation of 800 MHz harmonic cavities in LHC should provide a possibility to vary the length of colliding bunches in LHC which can lead in number of positive effects [2]. In order to supply the required harmonic voltage several single cell superconducting cavities are to be used.

One of the main goals of the cavity design is to fulfill strict Higher Order Modes (HOM) damping requirements. Several techniques for HOM damping such as beam pipe grooves, fluted beam pipes, ridged beam pipes etc. were investigated and compared [3]. In our opinion the solution with grooves (see Fig. 1), similar to that used in KEKB [4], is preferable due to the structure cylindrical symmetry, design simplicity and absence of dangerous HOMs. That is why in order to check the simulation results and to investigate eventual HOM properties the scaled version of this cavity was manufactured.

SIMULATIONS

Based on the results obtained during the calculations carried out with the MWS [5] and ABCI [6] codes the dimensions of the grooved beam pipe were chosen in such a way that the external quality factor of the most dangerous dipole HOMs was below 100 and below 1000 for HOMs in the higher frequency range. As it is seen in Fig. 2 the wake potential decays almost to zero when the distance between bunches is 15 m and on the graph of longitudinal impedance there are no sharp peaks corresponding to the HOM with high Q values. This has been achieved due to the fact that the cut-off frequency of the drift tube is lower than the frequency of HOMs.

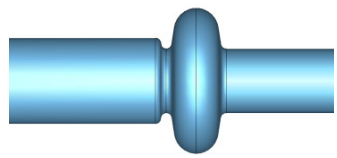

Figure 1: Cavity with grooved beam pipes.

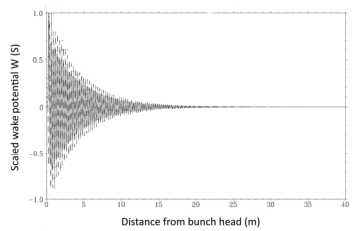

Figure 2a: Transverse wakefield potential in the cavity with the grooved beam pipe.

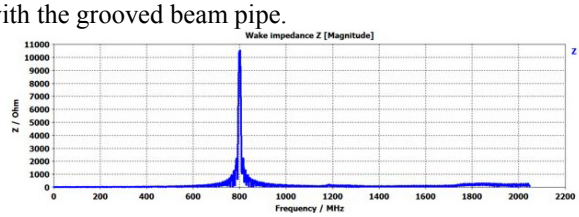

Figure 2b: Longitudinal impedance in the cavity with the grooved beam pipe.

In order to verify the results obtained by numerical simulations a scaled aluminium cavity prototype with the frequency of the fundamental mode of 2400 MHz was built. The prototype was designed in a modular form (Fig. 3, 4) so that it is possible to carry out measurements for different lengths and shapes of the drift tubes and to further carry out measurements for a chain consisting of two such cavities. The prototype assembly consists of the beam pipe with a larger radius, the cavity body, the beam tube with a smaller radius having a feedthrough for power input and two shorting plates.

*Work supported by Ministry of Education and Science grant 3.245.2014/r and the EU FP7 HiLumi LHC – Grant Agreement 284404

DEMONSTRATION OF COAXIAL COUPLING SCHEME AT 26 MV/M FOR 1.3 GHZ TESLA-TYPE SRF CAVITIES *

Yi Xie†, A. Kanareykin (Euclid TechLabs, Solon, Ohio)
T. Khabiboulline, A. Lunin, V. Poloubotko, A. Rowe,
N. Solyak, V. Yakovlev (Fermilab, Batavia, Illinois), J. Rathke (AES, Medford, New York)

Abstract

Superconducting ILC-type cavities have an rf input coupler that is welded on. A detachable input coupler will reduce conditioning time (can be conditioned separately), reduce cost and improve reliability. The problem with placing an extra flange in the superconducting cavity is about creating a possible quench spot at the seal place. Euclid Techlabs LLC has developed a coaxial coupler which has an on the surface with zero magnetic field (hence zero surface current). By placing a flange in that area we are able to avoid disturbing surface currents that typically lead to a quench. The coupler is optimized to preserve the axial symmetry of the cavity and rf field. The surface treatments and rf test of the prototype coupler with a 1.3 GHz ILC-type single-cell cavity at Fermilab will be reported and discussed.

INTRODUCTION

The standard 1.3 GHz TESLA type SRF cavity has a fundamental power coupler and two asymmetric HOM couplers both upstream and downstream. The couplers break the cavity axial symmetry that in turn causes a rf field distortion and transverse wake field which may cause beam emittance dilution [1]. In order to preserve the axial symmetry of the acceleration channel, different schemes of coaxial coupler were proposed and developed [2], [3].

We suggested another design for the coupling unit, as shown in Fig. 1. This coupler has the following features:

- The coupler unit preserves the axial symmetry of the acceleration channel. There are no RF kicks or wakes that lead to emittance dilution;
- It is a quarter-wave resonant coupler for the operating mode;
- The coupler is detachable, because in the operating mode the currents are small in the coupler corners, and non-welded superconducting joints may be used. Thus, the coupler unit can be a separate device that can be treated independently of the structure;
- It may be manufactured of low RRR niobium (reduced cost) compared with the main cavity;
- It is compact.

The magnetic field distribution for the operating mode is shown in Fig. 2. One can see that the field in the corners is much smaller than in the main cavity. For the maximal acceleration gradient of 35 MeV/m the surface magnetic field is 147 mT. In this case in the corner it is about 0.15 mT, lower enough to definitely permit superconducting joints.

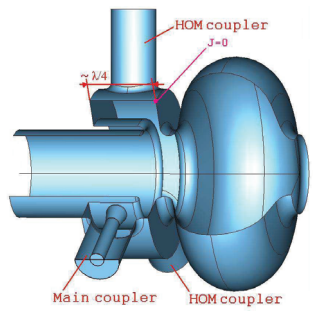

Figure 1: Schematic of Euclid proposed quarter-wave coaxial coupler.

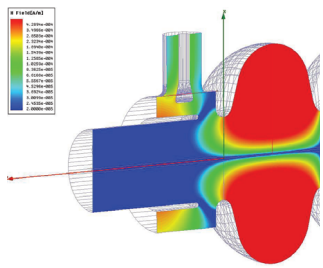

Figure 2: The magnetic field pattern in the coupler for the operating mode.

ELECTROMAGNETIC DESIGN

The first step in the coaxial coupler development was an adjustment of the shape to get the zero of the magnetic field at an accessible point for split flanges. The coaxial coupler which behaves like the coaxial resonator has an rf magnetic field and surface current minimum at the point $\lambda_{rf}/4$ from the corner (λ_{rf} is the wavelength in vacuum). This position can't be changed by appropriate choice of radii of the coaxial unit. Figure 3 shows the position of the magnetic field zero in the final design of the coaxial coupler. It satisfies the detachable design requirements.

The coupling to the fundamental mode has been modeled by the HFSS eigenmode solver for the shape depicted above. For the adjustment of the feed coupler the external Q-factor of the nearest semicell was calculated. The computed Q_{ext} for the fundamental power coupler vs its pene-

* This Work is supported by the US DOE SBIR Program DE-SC0002479.
† yixie@fnal.gov, now at Fermilab.

ISBN 978-3-95450-178-6

ESS SPOKE CRYOMODULE AND TEST VALVE BOX

Denis Reynet, Sylvain Brault, Patxi Duthil, Matthieu Pierens, Patricia Duchesne, Guillaume Olry, Nicolas Gandolfo, Emmanuel Rampnoux, Sébastien Bousson, IPNO, UMR 8608 CNRS/IN2P3 - Université de Paris Sud 15, rue G. Clémenceau, BP1, 91406 ORSAY cedex, France
Christine Darve, ESS Lund, Sweden

Abstract

The future European Spallation Source is based on a superconducting linac which includes a Spoke section. For prototyping purpose, a Spoke cryomodule and a valve box are being built and will be assembled by the end of 2015 and tested at full power. Design, fabrication and procurement of those components provide an insight of the series phases. The valve box will also be used for the test of the 13 series cryomodules.

INTRODUCTION

17 European countries are involved in the development of the European Spallation Source (ESS), a project for building the world's most powerful neutron source feeding multidisciplinary researches. This machine includes a linear accelerator based on superconducting radiofrequency (SRF) technologies [1]. Among 146 SRF resonators housed in 43 cryomodules, 26 paired β = 0.5 352.2 MHz SRF niobium double Spoke cavities will be used for the first time in an operating linac. They will function at a temperature of about 2 K in a saturated superfluid helium bath within 13 cryomodules.

A prototype cryomodule containing two cavities, fully equipped, was designed [2] at IPNO and will be tested by the end of 2015 by use of a dedicated prototype valve box. All components of this cryomodule, among which the SRF cavities and the RF power couplers, were procured during the last two years. They were received at IPNO and tested. Among others, those test phases included assembly tasks, alignment using dedicated tooling, cryogenic tests in vertical cryostat, RF tests, etc. Beyond the consecutive validation or eventual modification of the pieces design, experience was gained concerning the procurement phase and the relating technical specifications and will be useful for the series.

The prototype valve box is now being constructed to achieve two main objectives. On the one hand it is thought as a prototype valve box: it must validate the cryogenic operation of the prototype cryomodule as it would be on the linac; it might prove the legitimacy of the mechanical and thermal designs and, consecutively, the assembly procedure. This will be preliminary done at IPNO test stand. On the other hand, this valve box will be used for the tests of all the series cryomodules at the FREIA test stand in Uppsala University. Those environments differ one from each other and are far from the linac cryogenic installations. The valve box hence requires a very versatile configuration.

THE SPOKE CRYOMODULE PROTOTYPE

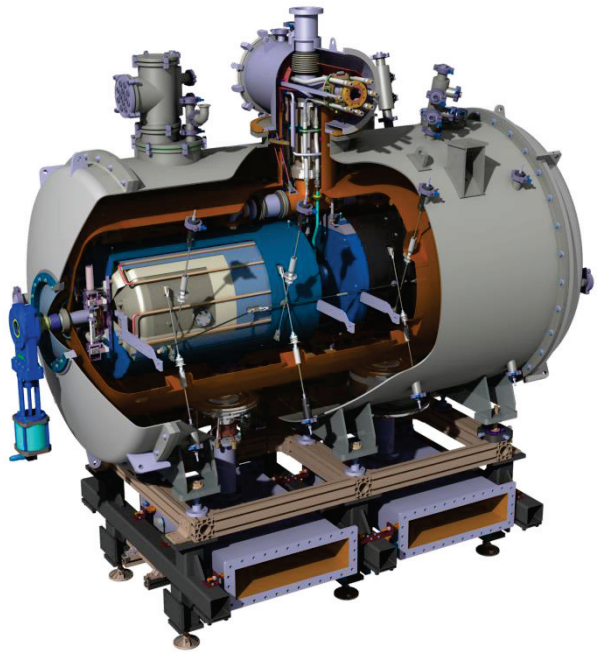

Figure 1: The Spoke cryomodule prototype.

The Spoke cryomodule (cf. Figure 1) holds two SRF double Spoke cavities equipped with two RF power couplers, positioned vertically with the antennas standing up and two cold tuning systems. This cold mass is covered by MLI blankets manufactured by Jehier and made of 10 layers of reflective aluminised PET films (Mylar) separated by polyesters. The direct contact between the cold mass and the MLI blankets might be useful in case of loss of insulation vacuum by preventing the air condensation directly on the metallic surfaces of the cavities liquid helium tanks, smoothing the consecutive pressure increase within the cryogenic distribution. Each cavity is entirely enclosed in a double shield consisting in an inner and an outer shell made of Cryophy® and manufactured by Mecamagnetic. A copper serpentine allows for the cooling down of the magnetic shield expecting therefore to reach a large magnetic permeability before the Meissner transition of the cavity. To complete the tests of the Spoke cavities [3], they were equipped with their MLI blankets and their cold magnetic shield on a specific handling tool (cf. Figure 2).

ISBN 978-3-95450-178-6

PROCUREMENTS FOR LCLS-II CRYOMODULES AT JLAB*

E. F. Daly#, G. Cheng, G.K. Davis, T. Hiatt, N.A. Huque, F. Marhauser, H. Park, J.P. Preble, K.M. Wilson
Thomas Jefferson National Accelerator Facility, Newport News, VA 23606, U.S.A.

Abstract

The Thomas Jefferson National Accelerator Facility (Jlab) is currently engaged, along with several other DOE national laboratories, in the Linac Coherent Light Source II project (LCLS II). The SRF Institute at Jefferson Lab will be building one prototype and seventeen production cryomodules (CMs) based on the TESLA / ILC / XFEL design. Each CM will contain eight nine cell cavities with coaxial power couplers operating at 1.3 GHz. Procurement of components for cryomodule construction has been divided amongst partner laboratories in a collaborative manner. JLab has primary responsibility for six procurements including the dressed cavities, cold gate valves, higher-order-mode (HOM) and field probe (FP) feedthroughs, beamline bellows cartridges, cavity tuner assemblies and HOM absorbers. For procurements led by partner laboratories, JLab collaborates and provides technical input on specifications, requirements and assembly considerations. This paper will give a detailed description of plans and status for JLab procurements.

INTRODUCTION

The Linac Coherent Light Source (LCLS)-II project at the SLAC National Accelerator Laboratory (SLAC) requires a 4 GeV continuous-wave (CW) superconducting radio frequency (SRF) linear accelerator in the first kilometer of the SLAC tunnel as part of a high repetition rate X-ray free-electron laser. The collaborative project brings together six US institutions, which in alphabetical order are Argonne National Laboratory (ANL), Cornell University, Fermi National Accelerator Laboratory (FNAL aka Fermilab), Thomas Jefferson National Accelerator Facility, Lawrence Berkeley National Laboratory (LBNL), and SLAC [1].

As part of shared responsibilities Fermilab and JLab will build the 1.3 GHz accelerating cavity cryomodules (CMs) concurrently in two assembly lines in order to meet the overall project schedule. In preparation for CM assembly, Fermilab has been leading the CM design efforts based on extensive experience with TESLA-style CM design and assembly. The starting point for the design is existing models and drawings of similar ILC CMs (e.g. Type III+) with modifications to enable continuous-wave (CW) operation [2]. JLab and Cornell are partners in R&D and design contributing to development activities, design reviews, integration, cost estimation and production. Both Cornell and JLab have valuable CW CM design experience. JLab has directly applicable recent 12 GeV Upgrade production experiences which will be applied to both procurement and production efforts for LCLS-II.

Currently, activities and preparations are underway for assembling two prototype CMs, one at each laboratory. Following the prototyping efforts, thirty-three production CMs are planned - sixteen at Fermilab [3], seventeen at JLab – for a total of thirty-five CMs in order to provide reliable 4 GeV energy gain.

LEVERAGING XFEL/ILC CM EXPERIENCE

A very important part of the CM procurement plan is to leverage XFEL's existing CM experience ("know-how") gained during procurement activities [4]. DESY has entered into licensing agreements to share their successes, current issues and supply-chain challenges for key areas of cavity, main coupler and cryomodule component procurement. This allows LCLS-II to learn from DESY's experiences and to adjust both procurement and production plans accordingly.

In addition, CEA Saclay colleagues responsible for the production of ~100 XFEL CMs [5] have hosted workshops for the SRF community and several focused meetings with LCLS-II staff to share their experiences with production in order to understand the staffing, technical and logistics issues related to such a large scale production effort. This experience includes integration issues related to procured components and can be directly applied to LCLS-II procurement efforts.

Finally, LCLS-II can leverage Fermilab's ILC-style CM production development activities and experience during integration activities for components utilized to build two pre-production CMs – CM1 and CM2 – from kits of subassemblies and components provided by DESY.

PROCUREMENT STRATEGY

The procurement of CM components is distributed between Fermilab and JLab, with the exception of SLAC who will procure the main RF power couplers [6]. The goals for CM assembly are that the two prototype CMs will be identical and the thirty-three production CMs will be identical, and that all CMs will meet or exceed the

* Authored by Jefferson Science Associates, LLC under U.S. DOE Contract No. DE-AC05-06OR23177 with supplemental funding from the LCLS-II Project U.S. DOE Contract No. DE-AC02-76SF00515. The U.S. Government retains a non-exclusive, paid-up, irrevocable, world-wide license to publish or reproduce this manuscript for U.S. Government purposes.
# edaly@jlab.org

ISBN 978-3-95450-178-6

TRIUMF'S INJECTOR AND ACCELERATOR CRYOMODULES

N. Muller, R.E. Laxdal, P. Harmer, J. Kier, D. Kishi, P. Kolb, A. Koveshnikov, C. LaForge, D. Lang, Y. Ma, A.K. Mitra, R. Nagimov, R. Smith, B. Waraich, L. Yang, Z. Yao, V. Zvyagintsev
TRIUMF, Vancouver, Canada

Abstract

TRIUMF's ARIEL project includes a 50 MeV-10mA electron linear accelerator (e-Linac) using 1.3 GHz superconducting technology. The accelerator consists of three cryomodules; an injector cryomodule with one cavity and two accelerating cryomodules, each having two cavities. One injector cryomodule and one accelerator cryomodule have been assembled and commissioned at TRIUMF, and a second injector cryomodule for VECC is being assembled in Kolkata. Both injector and accelerator cryomodules utilize a top-loaded cold mass design contained in a box-type cryomodule. The design and early test results of both cryomodules are presented.

INTRODUCTION

TRIUMF's new high intensity superconducting electron linear accelerator (e-Linac) is configured as a 50 MeV 10mA device consisting of five 1.3 GHz nine-cell niobium cavities. Each cavity is designed to supply 10MV of acceleration with two 50kW power couplers that supply the required beam loaded RF power of 100kW. The cavities are housed in three cryomodules, one injector cryomodule and two identical accelerator cryomodules, ICM, ACM1 and ACM2 respectively. TRIUMF has recently commissioned the ICM and ACM and is now building a second ICM for the VECC laboratory in Kolkata. The second ICM cryomodule will be completed this year and will be tested using TRIUMF's e-Linac facilities prior to shipment to India.

CRYOMODULE DESIGN

The cryomodule design has been reported elsewhere [1-3]. In brief the module is a top-loading box-like structure with a stainless steel vacuum chamber. The ICM is show in Fig. 1 and the ACM is shown in Fig. 2. The cold mass is suspended from the lid and includes a stainless steel strongback, a 2K phase separator pipe, cavity support posts and the cavity hermetic unit. The hermetic unit consists of the niobium cavities, the end assemblies, an inter-cavity transition (ICT) with a stainless steel HOM damper, the power couplers (FPC) and an rf pick-up.

The niobium cavity (Fig. 3) is a nine cell 1.3GHz cavity based on a TESLA design with modified end sections to accommodate two 50kW power couplers and mitigate higher order modes [4].

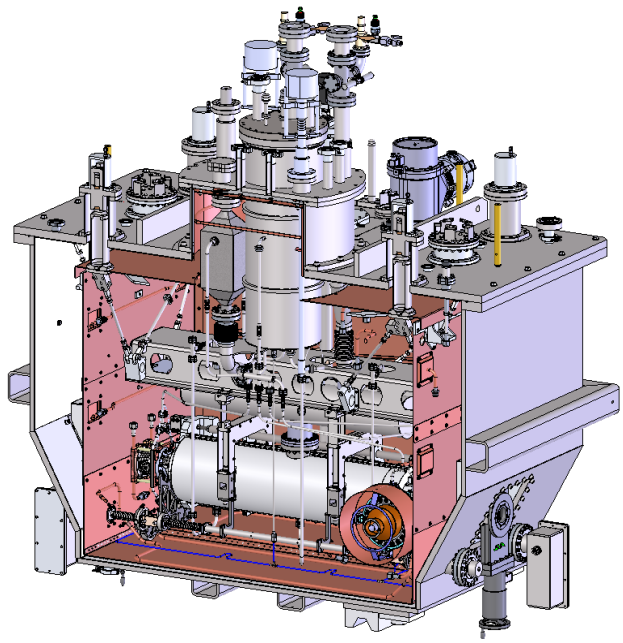

Figure 1: Injector Cryomodule (ICM).

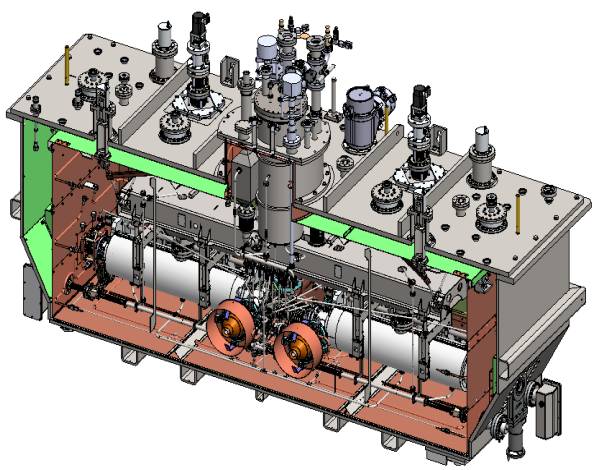

Figure 2: Accelerating Cryomodule (ACM).

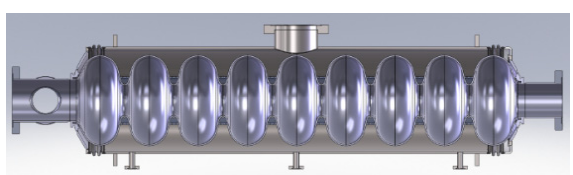

Figure 3: The e-Linac nine cell cavity with jacket.

ISBN 978-3-95450-178-6

MODIFIED ELBE TYPE CRYOMODULES FOR THE MAINZ ENERGY-RECOVERING SUPERCONDUCTING ACCELERATOR MESA*

T. Stengler†, K. Aulenbacher, R. Heine, F. Schlander, D. Simon, KPH Mainz, Germany
M. Pekeler, D. Trompetter, RI Research Instruments GmbH, Bergisch Gladbach, Germany

Abstract

At the Institut für Kernphysik of Johannes Gutenberg-Universität Mainz, the new multi-turn energy recovery linac MESA is under construction. Two modified ELBE-type cryomodules with two 9-cell TESLA/XFEL cavities each will provide an energy gain of 50 MeV per turn. Those are currently in the production process at RI Research Instruments GmbH, Bergisch Gladbach, Germany. Modifications for the tuner and the HOM damper are under development. In addition, a 4K/2K Joule Thomson expansion stage will also be integrated into the cryomodule. The current status of the development of the cryomodules and their modifications will be discussed.

INTRODUCTION

At the Mainz Energy-Recovering Superconducting Accelerator MESA, superconducting radio frequency (SRF) accelerator modules are of particular importance. The cryomodules, based on the ELBE-type cryomodule [1], have been ordered at RI Research Instruments GmbH, Bergisch Gladbach, Germany.

The ELBE-type cryomodule has to be modified to comply with the special requirements of MESA, e.g. the c.w. beam. Each cryomodule will contain two 9-cell TESLA/XFEL-type cavities that will provide 12.5 MeV energy gain each. Besides smaller adaptations, three major modifications are made: the tuner, the feedthrough of the higher order mode antenna, and the helium supply.

MAINZ ENERGY-RECOVERING SUPERCONDUCTING ACCELERATOR MESA

The Mainz Energy-Recovering Superconducting Accelerator MESA will be a new recirculating electron accelerator and shall operate in two different modes: an energy recovering (ER) mode and an external beam (EB) mode. It will provide a continuous wave beam with a duty cycle of 100 %. A possible design can be seen in Fig. 1.

At the ER mode there will be high beam currents from 1 mA up to 10 mA and an energy of 105 MeV, while at the EB mode the electrons will be polarized with a current of 150 µA and 155 MeV [2].

A photoemissive source will produce the electrons [3], which will be pre-accelerated by a normal conducting linac up to 5 MeV before they are guided into the main accelerator

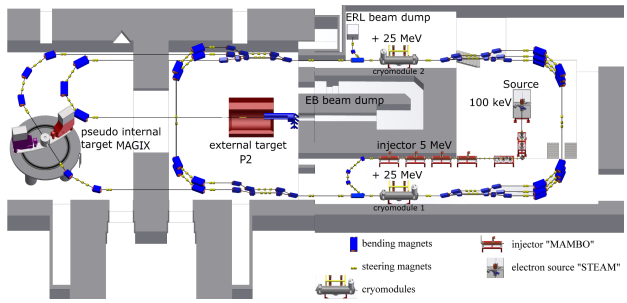

Figure 1: Possible configuration of the MESA design. The beam pipe is allocated around an existing beam dump which will be used in external beam (EB) mode.

[4]. Two cryomodules accelerate and decelerate the electrons depending on the mode of operation. The beamline will be stacked at two arcs similar to CEBAF [5].

In EB mode there will be three passes through the cryomodules. In ERL mode four passes are made (two ramp up, two ramp down). A pseudo internal target experiment will be done in ERL mode with a high resolution spectrometer facility named MAGIX [6]. The external beam mode will be used for an fixed target experiment P2 which aims at a precise measurement of the Weinberg angle [7].

MESA CRYOMODULE

The MESA cryomodules are based on ELBE-type cryomodules, which are in use at the Helmholtz-Zentrum Dresden-Rossendorf (HZDR), Germany. Each module contains two 9-cell TESLA/XFEL cavities and operates at 2 K. Each cryomodule will provide an energy gain of $\Delta E \geq 25$ MeV. The dimensions of the cryomodule are given in Fig. 2.

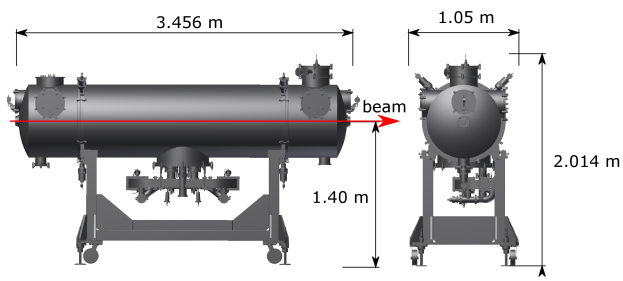

Figure 2: Dimensions of the cryomodule. The beam pipe is at a height of 1.40 m.

To suit the purposes and considering the beam parameters of MESA, there will be some modifications of the ELBE-type cryomodules. Because of multi turn ERL operation, it

* Work supported by the German Research Foundation (DFG) under the Cluster of Excellence "PRISMA"
† stengler@kph.uni-mainz.de

ISBN 978-3-95450-178-6

LCLS-II 1.3 GHz CRYOMODULE DESIGN – MODIFIED TESLA-STYLE CRYOMODULE FOR CW OPERATION*

T. Peterson#, T. Arkan, C.M. Ginsburg, Y. He, J. Kaluzny, M. McGee, Y. Orlov
Fermi National Accelerator Laboratory, Batavia, IL 60510, USA

Abstract

We will present the design of the 1.3 GHz cryomodule for the Linear Coherent Light Source upgrade (LCLS-II) at SLAC. Fermilab is responsible for the design of this cryomodule, a modified TESLA-style cryomodule to accommodate continuous wave (CW) mode operation and LCLS-II beam parameters, consisting of eight 1.3 GHz superconducting RF cavities, a quadrupole-corrector magnet package, and instrumentation. Thirty-five of these cryomodules, approximately half built at Fermilab and half at Jefferson Lab, will become the main accelerating elements of the 4 GeV linac. The modifications and special features of the cryomodule include: thermal and cryogenic design to handle high heat loads in CW operation, magnetic shielding and cool-down configurations to enable high quality factor (Q0) performance of the cavities, liquid helium management to address the different liquid levels in the 2-phase pipe with a 0.5% SLAC tunnel longitudinal slope, a support structure design to meet California seismic design requirements, and with the overall design consistent with space constraints in the existing SLAC tunnel. The prototype cryomodule assembly will begin in September 2015 and is to be completed in March 2016.

INTRODUCTION

The LCLS-II main linac cryomodule is based on the XFEL design, including TESLA-style superconducting accelerating cavities, with modifications to accommodate CW operation and LCLS-II beam parameters [1]. Thirty-five 1.3 GHz cryomodules and two 3.9 GHz cryomodules will be connected to form four linac segments (L0, L1, L2, and L3) which are separated by three warm beamline sections, shown in Fig. 1.

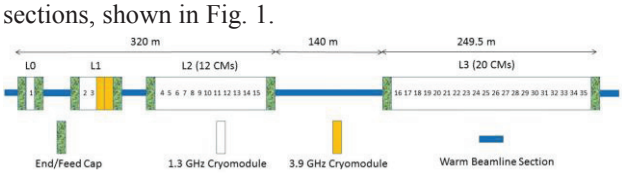

Figure 1: LCLS-II Linac with cryomodules in sections.

The cryomodule houses eight superconducting cavities which are operated at 2 K, and it provides mechanical support and thermal insulation to the RF cavities. These 9-cell, 1.3 GHz cavities with an envisaged Q0 of 2.7×10^{10} will provide an energy gain of 16 MV/m. The cryomodule installed "slot length" is 12.222 m.

The general layout of the module is shown in Fig. 2.

* Work supported, in part, by Fermi Research Alliance, LLC under Contract No. DE-AC02-07CH11359 with the United States Department of Energy and the LCLS-II Project
# tommy@fnal.gov

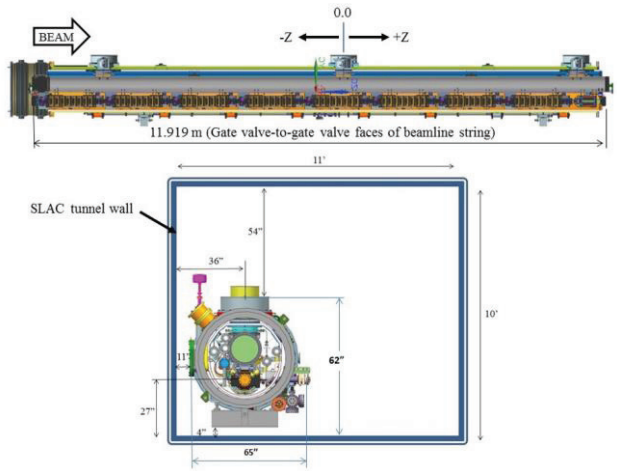

Figure 2: LCLS-II 1.3 GHz cryomodule.

The high Q0 requirement and CW operation drive some modifications for the LCLS-II module with regard to the TESLA-style module. The major features of the LCLS-II cryomodules are listed in Table 1.

Table 1: Major Features of the LCLS-II Cryomodules

Key Requirement	Major Features
Series configuration	Continuous insulating vacuum; no external parallel transfer line; cold beam pipe through the interconnect
0.5% longitudinal tunnel slope	One 2 K supply valve in each module for individual steady-state management of helium liquid level
Retention of high Q0 cavity performance	Active external magnetic field cancellation coils provide magnetic shielding and residual field of ≤5 mG at the cavities; a cool-down/warm-up cryogenic valve in the closed-ended cool-down circuit in each module provide high thermal gradient during cool-down through 9.2 K transition temperature to minimize flux trapping; using non-magnetic materials in the module
Seismic safety	Comply with SLAC seismic loading requirements under various accelerations and oscillatory modes
Removal of high heat loads in CW operation	Increased size and closed-ended 2-phase pipe allows sufficient conduction of the heat from the cavities through the superfluid helium; copper plating on beamline components; improved thermal intercepts at 5 K and 45 K

ISBN 978-3-95450-178-6

STATUS OF LCLS-II QA SYSTEMS COLLABORATION FOR CYROMODULE CONSTRUCTION AT TJNAF AND FNAL

E.A. McEwen#, J. Leung, V. Bookwalter, Jefferson Lab, Newport News, VA, USA
J. Blowers, J. Szal, Fermilab, Batavia, Illinois, USA

Abstract

At the Thomas Jefferson National Accelerator Facility (Jefferson Lab), we are supporting the LCLS-II Project at SLAC. The plan is to build thirty-five 1.3 GHz continuous wave cryomodules, production to be split between JLab and FNAL (Fermilab). This has required a close collaboration between the partner labs, including enhancing our existing quality systems to include this collaboration. This overview describes the current status of the Quality System development as of August 2015, when the partner labs start the assembly of the prototype cryomodules.

INTRODUCTION

Responding to a call to build a revolutionary new X-ray laser, SLAC is developing an upgrade of its Linac Coherent Light Source (LCLS) that will be at the forefront of X-ray science

The upgrade project, LCLS-II includes the design and construction of an accelerator, where Fermilab is responsible for the cryomodule design, in collaboration with JLab and SLAC.

Procurement, fabrication, assembly and test are shared by Fermilab and JLab. JLab will build 18 cryomodules and Fermilab 17. This has required a close collaboration between the labs, including enhancing our existing quality systems to support this joint construction effort.

Cryomodules (Figure 1) at both labs are being built to the same design using identical components. The end result will be cryomodules that are all mechanically identical in meeting the functional requirements.

The partner labs recognize that staff, tooling, and processes will not be identical, therefore are working on a set of common parameters that both labs will include in their production processes for reporting and comparison. Electronic travelers will be used in both labs, and as they are being developed we are sharing and comparing.

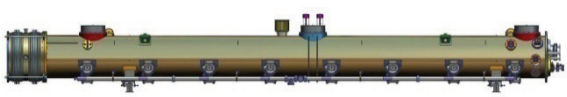

Figure 1: LCLS-II cryomodule [1].

QA staff from SLAC, JLab, and Fermilab have been working closely to coordinate quality efforts related to LCLS-II cryomodule work. All three have formal QA programs, and LCLS-II-specific QA Plans have been put in place. JLab and Fermilab QA have frequent coordination meetings (teleconference every three weeks or so with SLAC participating as necessary.) The SLAC LCLS-II QA Manager has assessed the QA programs at JLab and Fermilab (so-called "crosswalk"), and gave them both passing marks (Nov/Dec 2014). Both JLab and Fermilab are including SLAC-specific QA requirements into their plans (e.g. Acceptance Criteria Strategies), following the Graded Approach policies of both labs.

PROCUREMENT STRATEGY

Distributing procurements between the two labs minimizes administrative costs. For any given procurement, a "Lead Lab" has been identified. As the name implies, the "Lead Lab" leads and makes the procurement (i.e. procuring parts for all 35 cryomodules) while the other lab acts in a support role. The procurement strategy is described in full in the SLAC Procurement Procedure. Procurement Responsibility Matrix LCLSII-4.1-PM-0229-R0 (June2014)

As an example, Fermilab has the lead for niobium procurement; JLab has the lead for cavity & helium vessel procurement

Suppliers will ship approximately half of each order to each lab, and so each lab will perform receiving inspections on the materials they will use. This allows for each lab to work in their preferred way (to a common set of requirements), and eliminates the natural tendency to reproduce/redo work.

Each lab has named a technical person to work on each procurement (for both leading and supporting); called the Sub-contracting Officer's Technical Representative (SOTR).

The SOTR holds an important and responsible position, and is the "glue" between design, prototyping, procurement and assembly phases, while lending technical expertise for sub-system components through all phases of the project.

Design Phase

- SOTR develops technical specifications from higher level requirements.
- Prepares drawings and supporting technical documents.

Prototyping Phase

- Works with Acquisition/Procurement to procure prototypes from industry/partner labs.
- Participates in prototype development and testing.
- Feeds experience into production process.

* Co-authored by Jefferson Science Associates, LLC under U.S. DOE Contract No. DE-AC05-06OR23177, and by Fermilab Research Alliance LLC under Contract No. DE-AC02-07CH11359 with support from the LCLS-II Project.
# mcewen@jlab.org

OVERVIEW OF RECENT TUNER DEVELOPMENT ON ELLIPTICAL AND LOW-BETA CAVITIES

R. Paparella, INFN Milano - LASA, Segrate (MI), Italy

Abstract

This paper aims to provide an overview on the latest advances of tuner development for SRF applications. Issues and present approaches on how to resolve them will be emphasized for both TM and TEM cavities and examples from various labs and projects (XFEL, LCLS-II, ESS, SPL, ARIEL, SPIRAL2, FRIB, ANL, IFMIF) will be given in order to better explain issues and solutions.

TUNERS FOR SRF STRUCTURES

Tuning SRF structures poses peculiar challenges to designers, mainly due to the subject overlapping different disciplines as mechanics, radiofrequency, cryogenics, controls and electronics.

Operating a cavity steadily at its set point within usually strict, project-driven, field amplitude and phase stability limities involves, as of the current state-of-art techniques, an interleaved combination of Low Level RF control on forward power, quasi-static (slow) tuning mechanism and a fast tuning action in the μ-meter range. Beforehand, the most effective way to avoid tune disturbances comes from cavity and cryomodule design by either decoupling or damping the contribution of largest resonant modes in the system.

In view of a global overview of various tuning systems for different accelerating machines, some general considerations about the tuner design are here recalled:

- **Deformation vs. Insertion**: a bulk and heavy structure is required to deform an SRF structure but this tuning scheme can preserve cavity RF shape (within its elastic limits). On the other end, light and simple plunger-like solutions directly induce local perturbations in the RF field regions, therefore surface properties become crucial.
- **Continuous Wave (CW) vs. Pulsed RF**: while stochastic background noise or microphonics (MP) will be the main disturbance in the former scenario, synchronized Lorenz Force detuning (LFD) issue will likely be dominating in the latter. A much simpler, feed-forward control scheme is enough to provide a satisfactory compensation in case of LFD.
- **Large loaded Q (Ql) vs. Large bandwidth**: where a large Ql is set by the project, the resonator bandwidth can be easily pushed to tenths of Hz level, a value critically comparable to usual MP operational levels. Lower Ql requirements allow for a spontaneous rejection to background noise.
- **Accessibility vs. Heat load**: the choice of having directly accessible actuators placed outside the vacuum vessel ("warm" actuators) is usually paid in terms of additional heat loads transferred by the actuating shaft. On the other end, a fully "cold" scenario (XFEL-like) is demanding in terms of component reliability. Nonetheless, a trade-off is still viable, as illustrated later on for LCLS-II case.
- **Active MP compensation, Yes vs. No**: stability of a complex closed control loop involving several resonant RF and mechanical modes is likely the price to pay for an active MP suppression, while extra RF power cost should be budgeted if LLRF controls is asked to drive a noisy cavity. Fortunately, a high stiffness of the cavity constraints helps in both cases: dominant structural modes are pushed up dropping their contribution to phase error and piezo-stroke transfer efficiency is simultaneously maximized.
- **At beam tube vs. Around**: severe spatial constraints usually exist in the inter-cavity area (also related to phasing and beam dynamics) but moving the tuner far from beam ports makes tuner stroke and force transfer crucial.

This review will discuss tuner concepts and recent results by aggregating the different accelerating structures on which they are used.

QW AND HW CAVITIES

ATLAS at ANL

In the framework of the ATLAS Efficiency and Intensity Upgrade program, a cryomodule with 7 SC quarter-wave resonators at 72 MHz β=0.077 has been recently commissioned [1].

A dual strategy has been developed at ANL, separating the slow tuner mechanism from the fast tuning action for a better individual optimization.

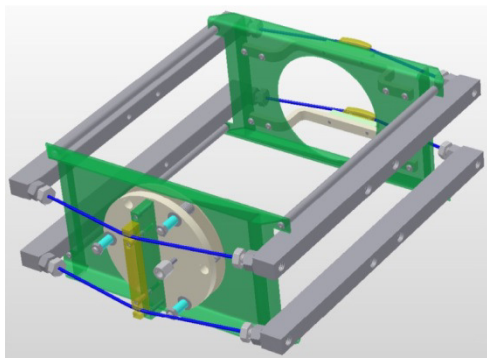

Figure 1: ANL Intensity Upgrade QWR pneumatic tuner.

Slow tuning action is provided by a well-known pneumatic type tuner (Fig. 1): a cold, Hegas-filled bellows expands and pushes outward on the wire ropes

ISBN 978-3-95450-178-6

HIGH GRADIENT PERFORMANCE IN FERMILAB ILC CRYOMODULE*

E. Harms#, C. Baffes, K. Carlson, B. Chase, D. Crawford, E. Cullerton, D. Edstrom, A. Hocker, A. Klebaner, M. Kucera, J. Leibfritz, J. Makara, D. McDowell, O. Nezhevenko, D. Nicklaus, Y. Pischalnikov, K. Premo, P. Prieto, J. Reid, W. Schappert, W. Soyars, P. Varghese, A. Warner
Fermilab, Batavia, IL 60510, USA

Abstract

Fermilab has assembled an ILC like cryomodule using U.S. processed high gradient cavities and achieved an average gradient of 31.5 MV/m for the entire cryomodule. Test results and challenges along the way will be discussed.

INTRODUCTION

An intermediate S1 goal of the International Linear Collider is to, "achieve 31.5 MV/m average operational accelerating gradient in a single cryomodule as a proof-of-existence. In case of cavities performing below the average, this could be achieved by tweaking the RF distribution accordingly [1]." With this in mind Fermilab has assembled and brought into operation an ILC-type cryomodule, the 2nd of this type at Fermilab. In Fermilab parlance this device is known as RFCA002 or simply CM-2. CM-2 is composed of eight nine-cell cavities resonating at 1.3 GHz. All eight cavities were fabricated in industry and tested extensively prior to assembly into a single cryomodule. Fabrication and testing results to date have been documented previously [2,3].

CM-2 was first installed in the test cave in March 2012, however leak checking of the 2-phase helium circuit revealed a leak which was in an inaccessible location for further localization, thus necessitating its removal. A faulty bellows was replaced and installation for a second time occurred in April 2013. Warm coupler conditioning was carried out on each cavity individually in parallel with ongoing interconnect and leak checking activities.

INDIVIDUAL CAVITY CHARACTERIZATION

Once the entire cryomodule could be cooled down, a program to individually characterize each cavity was carried out. The suite of tests is typical for testing such cavities at Fermilab and other SRF facilities:

- Tune cavity to resonance
- Map out and set Q_L
- System calibrations, calculate gradient, k
- On-resonance conditioning
- Determine peak performance
- Final (high power) LLRF calibration
- Lorentz Force Detuning Compensation set-up
- Document dark current, x-rays vs. gradient
- Dynamic Heat Load measurements (Q_0).

Typical operating parameters were set to match ILC design ones as much as possible: fill time = 596 microseconds, flattop length = 969 microseconds, Q_{Ext} = 3.5 x 10^7, and pulse repetition = 5 Hz. In this phase the output of the 5MW klystron was directed to one cavity at a time, to a peak of order 1 MW.

The duration of this characterization step was 57 days for the first cavity, but was reduced to as short as six days as experience was gained.

Peak Gradient

An administrative limit of 31.5 MV/m was the maximum allowed peak gradient each cavity was run up to until this first stage of testing as a unit was completed. All cavities but #6 were able to reach this limit. Figure 1 compares the achieved peak gradients for all cavities in bare cavity vertical tests at Jefferson lab, horizontal tests as dressed cavities at Fermilab, and as contained within the cryomodule.

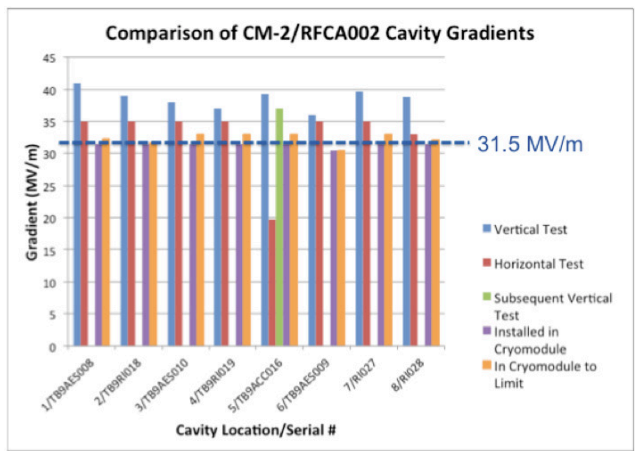

Figure 1: Comparison of CM-2/RFCA002 cavity gradients: vertical test (blue), horizontal (red), in CM-2 (purple) during initial tests, and to absolute gradient in cryomodule (orange). An administrative limit of 31.5 MV/m was set for initial CM-2 testing.

Q_0

The Q_0 of each cavity was also determined by measuring the dynamic heat load at discrete points just below the peak gradient. Figure 2 summarizes these results. At their peak gradient the Q_0 values ranged from a low of 5.7 x 10^9 on cavity #7 to as high as 1.4 x 10^{10} on cavity #2. There is a large uncertainty on these values owing the nature of the measurement.

* Operated by Fermi Research Alliance, LLC under Contract No. DE-AC02-07CH11359 with the United States Department of Energy
# harms@fnal.gov

PERFORMANCE OF THE CORNELL ERL MAIN LINAC PROTOTYPE CRYOMODULE

F. Furuta#, B. Clasby, R. Eichhorn, B. Elmore, M. Ge, D. Gonnella, D. Hall, G. Hoffstaetter, R. Kaplan, J. Kaufman, M. Liepe, T. O'Connell, S. Posen, P. Quigley, D. Sabol, J. Sears, E. Smith, V. Veshcherevich, Cornell University, Ithaca, NY 14850, USA

Abstract

Cornell has designed, fabricated, and completed initial cool down test of a high current (100 mA) CW SRF main linac prototype cryomodule for the Cornell ERL. This paper will report on the design and performance of this very high Q0 CW cryomodule including design issues and mitigation strategies.

INTRODUCTION

Cornell University has proposed to build Energy Recovery Linac (ERL) as drivers for hard x-ray sources because of their ability to produce electron bunches with small, flexible cross sections and short lengths at high repetition rates. The proposed Cornell ERL is designed to operate in CW at 1.3GHz, 2ps bunch length, 100mA average current in each of the accelerating and decelerating beams, normalized emittance of 0.3mm-mrad, and energy ranging from 5GeV down to 10MeV, at which point the spent beam is directed to a beam stop [1, 2]. The design of main linac prototype cryomodule (MLC) for Cornell ERL had been completed in 2012. The fabrication and testing of MLC components (cavity, high power input coupler, HOM dampers, tuners, etc.,) and assembly of MLC cold mass had been completed in 2014. MLC installation and cooldown preparations began in this summer. We will describe about MLC and initial cool down results in this proceeding.

MLC GENERAL LAYOUT

The general layout of an ERL main linac cryomodule (MLC) is shown in Fig. 1. It is 9.8 m long and houses six 1.3 GHz 7-cell superconducting cavities with Individual HOM absorbers and one magnet/BPM section. Each cavity has a single coaxial RF input coupler which transfers power from an RF power source to the beam loaded cavity. The specification values of 7-cell cavities are Qo of 2.0e10 at 16.2MV/m, 1.8K. Due to the high beam current combined with the short bunch operation, a careful control and efficient damping of higher order modes (HOMs) is essential. So HOMs are installed next to each cavity. To minimize ambient magnetic field of high-Q 7-cell cavities, MLC has three layers of magnetic shielding; 1) Vacuum Vessel (carbon steel), 2) 80/40 K magnetic shield enclosing the cold mass, and 3) 2 K magnetic shield enclosing individual cavities. All components within the cryomodule are suspended from the Helium Gas Return Pipe (HGRP). This large diameter (280mm) titanium pipe will return the gaseous helium boiled off the cavity vessel to the liquefier and act as a central support girder. The HGRP will be supported by 3 support post. The middle one is fixed; the other side posts are not and will slide by 7-9mm respectively during the cooldown from room temperature to cold.

7-CELL CAVITIES FOR MLC

Vertical Test Results

All 7-cell cavities for MLC were fabricated in house. Three of six cavities were stiffened cavity and the other three were un-stiffened cavity. Cavity surface preparation recipe consists of bulk Buffered Chemical Polishing (BCP, 140um), degassing (650degC*4days), frequency and field flatness tuning, light BCP (10um), low temperature baking (120degC*48hrs), and HF rinse [3]. Figure 2 shows best Q(E)curve of MLC 7-cell cavities during vertical test (VT) at 1.8K. All 7-cell cavities had surpassed the specification values of Qo=2.0e10 at 16.2MV/m, 1.8K. In fact, average Qo=(3.0±0.3)*1e10 had been achieved during VT at 16.2MV/m, 1.8K. All VT was limited by administrative limit, no radiation or no quench were detected during VT.

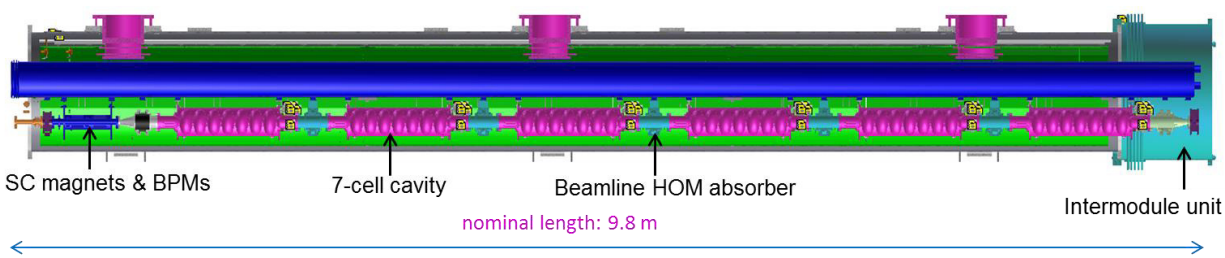

Figure 1: Cornell ERL Main Linac Prototype Cryomodule

* Work is supported by NSF Grants NSF DMR-0807731 and NSF PHY-1002467
#ff97@cornell.edu

ISBN 978-3-95450-178-6

A 1.3 GHZ CRYOMUDULE WITH 2X9-CELL CAVITY FOR SETF AT PEKING UNIVERSITY*

F.Zhu, S.W.Quan, L.Lin, F. Wang, L.W. Feng, J.K. Hao, S.L. Huang, D.H. Zhuang, Y.F. Gao, X D.Wen, K.X. Liu#, J.E. Chen,
Institute of Heavy Ion Physics & State Key Laboratory of Nuclear Physics and Technology, Peking University, Beijing, 100871, China

Abstract

The straight beam line of SETF at Peking University is under construction, which consists of a DC-SRF photoinjector and a superconducting linac with two 9-cell cavities. Stable operation of the DC-SRF photoinjector has been realized and the design, manufacture and assembly of the cryomodule with two 9-cell cavities have been completed. Improved capacitive coupling RF power coupler and fast tuner with piezo are adopted.

INTRODUCTION

Since we reported the project of Superconducting ERL Test Facility (SETF) at Peking University (PKU) in SRF 2009 [1] and SRF2011 [2], the progress has been made step by step. After the DC-SRF was put into stable operation in 2014 [3], the efforts have been made to establish the straight beam line which is shown in Figure 1. The most important component in this straight beam line is a 1.3GHz superconducting linac containing two 9-cell cavities, which will accelerate the electrons from DC-SRF photoinjector up to 25MeV. The electron beam with MHz high repetition rate will used to generate infrared free electron laser and THz radiation. In this paper, we mainly report the design, manufacture and assembling of the cryomudule with 2×9-cell cavity.

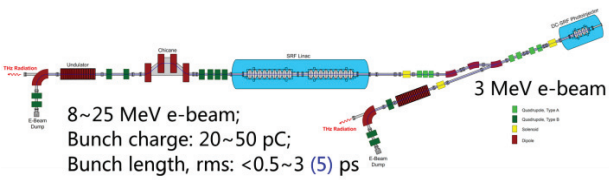

Figure 1: Schematic drawing of the layout of PKU FEL facility.

STABLE OPERATION OF THE DC-SRF PHOTOINJECTOR

The DC-SRF photocathode gun [4, 5] combines a DC pierce structure and a 3.5-cell superconducting cavity. It can provide electron beam with energy higher than 3 MeV and average current of about 1mA. The accelerating gradient of the cavity reached 23.5 MV/m and the intrinsic quality factor Q_0 is higher than 1.2×10^{10} in vertical test [6].

The wavelength of the seed drive laser is 1064 nm. The repetition rate of laser pulses is 81.25 MHz, which is 1/16 of the resonate frequency of the 3.5-cell SRF cavity. The harmonic generators convert the infrared pulses to UV pulses with a wavelength of 266 nm. The drive laser system can provide 1 W power in a train of 6 ps UV pulses with 5% power instability. The quantum efficiency of Cs_2Te photocathode was about 4% for the injector operation.

Figure 2: Beam experiment layout of the DC-SRF photoinjector.

For machine safety, the beam experiments were carried out at an Eacc of 8.5 MV/m. The duty factor of RF power was 7% with a repetition rate of 10 Hz. Average beam current in macro pulses at 1mA for about 10 minutes was obtained and stable operation for more than 6 hours at 0.55mA were tested. Figure 2 shows the beam experiment layout of the DC-SRF injector. The detailed experiment results were published this year [3].

By adding an undulator after the DC-SRF injector and the 3.5-cell cavity works as both the acceleration and RF bunch compression roles, we got successfully THz radiation (700~1200 μm) in early 2015.

2×9-CELL CAVITY CRYOMODULE

The main accelerator contains two 9-cell TESLA cavities, input power couplers, frequency tuners, helium vessel, liquid nitrogen shield, magnetic shield and its associated auxiliary systems. The sectional view of the cryomodule is shown in Figure 3.

*Work supported by National Basic Research Project (No. 2011CB808304 and 2011CB808302）and NDRC project
#kxliu@pku.edu.cn

ISBN 978-3-95450-178-6

CONSTRUCTION AND PERFORMANCE OF FRIB QUARTER WAVE PROTOTYPE CRYOMODULE*

S. Miller#[1], B. Bird[1], G. Bryant[1], B. Bullock[1], N. Bultman[1], F. Casagrande[1], C. Compton[1], A. Facco[1, 2], P. Gibson[1], J. Hulbert[1], D. Morris[1], J. Popielarski[1], L. Popielarski[1], M. Reaume[1], R. Rose[1], K. Saito[1], M. Shuptar[1], J. Simon[1], B. Tousignant[1], J. Wei[1], K. Witgen[1], T. Xu[1]

[1] Facility for Rare Isotope Beams, Michigan State University, East Lansing, MI 48824 USA
[2] INFN - Laboratori Nazionali di Legnaro, Legnaro (Padova), Italy

Abstract

The driver linac for the Facility for Rare Isotope Beams (FRIB) will require the production of 48 cryomodules. FRIB has completed the fabrication and testing of a β=0.085 quarter-wave cryomodule as a pre-production prototype. This cryomodule qualified the performance of the resonators, fundamental power couplers, tuners, and cryogenic systems of the β=0.085 quarter-wave design. In addition to the successful systems qualification; the ReA6 cryomodule build also verified the FRIB bottom up assembly and alignment method. The lessons learned from the ReA6 cryomodule build, as well as valuable fabrication, sourcing, and assembly experience are applied to the design and fabrication of FRIB production cryomodules. This paper will report the results of the β=0.085 quarter-wave cryomodule testing, fabrication, and assembly; production implications to future cryomodules will also be presented.

INTRODUCTION

FRIB is a high-power heavy ion accelerator facility now under construction at Michigan State University under a cooperative agreement with the US DOE [1]. Its driver linac operates in continuous wave mode and accelerates stable ions to energies above 200 MeV/u with the beam power on target up to 400 kW. The linac has a folded layout as shown in Figure 1, which consists of a front-end, three linac segments connected with two folding segments, and a beam delivery system to deliver the accelerated beam to target [2].

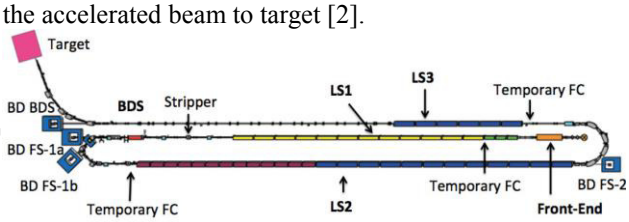

Figure 1: Schematic layout for FRIB driver linac.

Due to the heavy mass and correspondingly low velocity of the accelerated ions, the FRIB driver linac utilizes four different low-beta SRF resonator designs in cryomodules as described in Table 1. For high-beta applications superconducting RF has become an established technology with a history of industrial optimization efforts; however, for low-beta structures, FRIB will be the first facility utilizing industrially produced resonators on a larger scale [3].

Table 1: Required cryomodule configurations for FRIB. Resonator and solenoid quantities per cryomodule are shown in parenthesis. The β=0.041 will cryomodule utilize a L_{eff} =0.25 m solenoid and all other cryomodules will utilize a L_{eff} =0.50 m solenoid.

Type	Cryomodule Qty.	Resonator Qty.	Solenoid Qty.
β=0.041	3	12 (4)	6 (2)
β=0.085	11	88 (8)	33 (3)
β=0.29	12	72 (6)	12 (1)
β=0.53	18	144 (8)	18 (1)
Matching Modules	3 (β=0.085) 1 (β=0.53)	12 (4) 4 (4)	N/A
Total	**48**	**332**	**69**

Each cryomodule will be equipped with niobium resonators operating at 2 K with focusing solenoids, which include x-y steering, operating at 4.5 K. Due to the large number of cryomodules the FRIB project lends itself to a manufacturing mind-set that incorporates large scale production into the design of individual module types. As a part of this manufacturing mind-set FRIB has manufactured a prototype cryomodule that utilizes two superconducting quarter-wave resonators (QWR) and one superconducting solenoid, and is referred to as the ReA6 cryomodule as seen in Figure 2. The completion of the ReA6 cryomodule not only tested the general cryomodule design, but also the manufacturing methods and assembly [4].

CRYOMODULE DESIGN

The FRIB cryomodules are based on a modular bottom-supported design which is optimized for mass-production and efficient precision-assembly. Figure 3 displays the subsystem break down of the cryomodule. Four types of superconducting resonators (β=0.041, β=0.085, β=0.29, β=0.53) and two solenoid lengths (L_{eff} = 0.25 m and 0.50

* This material is based upon work supported by the U.S. Department of Energy Office of Science under Cooperative Agreement DE-SC0000661. Michigan State University designs and establishes FRIB as a DOE Office of Science National User Facility in support of the mission of the Office of Nuclear Physics.
# millers@frib.msu.edu

TECHNICAL AND LOGISTICAL CHALLENGES FOR IFMIF-LIPAC CRYOMODULE CONSTRUCTION

H. Dzitko, G. Devanz, N. Bazin, S. Chel, N. Berton, A. Bruniquel, P. Charon, P. Contrepois, G. Disset, P. Gastinel, P. Hardy, V. Hennion, H. Jenhani, J. Neyret, O. Piquet, J. Relland, B. Renard, N. Sellami, R. Vallcorba-Carbonell, IRFU CEA/Saclay, France
D. Regidor, F. Toral, CIEMAT, Madrid, Spain
D. Gex, G. Phillips, F4E, Garching, Germany
J. Knaster, IFMIF EVEDA Projet Team, Rokkasho, Japan
A. Kasugai, H. Nakajima, K. Yoshida, JAEA, Naka, Japan

Abstract

This paper provides an overview of the final design and fabrication status of the IFMIF cryomodule, including the design issues, and deals with the strategies implemented in order to mitigate the main technical and logistical risks identified. The seismic constraints as well as licensing requirements, transportation issue and assembly process are also addressed. The IFMIF cryomodule presented here will be part of the Linear IFMIF Prototype Accelerator (LIPAc) whose construction is ongoing [1, 2]. It is a full scale prototype of one of the IFMIF accelerators, from the injector to the first cryomodule, aiming at validating the technical options for the future accelerator-based D-Li neutron source to produce high intensity high energy neutron flux for testing of candidate materials for use in fusion energy reactors. The cryomodule contains all the equipment to transport and accelerate a 125 mA deuteron beam from an input energy of 5 MeV up to 9 MeV. It consists of a horizontal cryostat of about 6 m long, 3 m high and 2 m wide, which includes 8 superconducting HWRs for beam acceleration working at 175 MHz and at 4.5 K, 8 power couplers to provide RF power to cavities, and 8 Solenoid Packages as focusing elements.

OVERVIEW OF THE IFMIF LIPAC PROJECT

The International Fusion Materials Irradiation Facility (IFMIF) aims at producing intense neutron fluxes so as to characterize materials envisioned for future fusion reactors. To this end, two identical Linacs, each accelerating a continuous-wave 125-mA deuteron beam at the final energy of 40 MeV, would be necessary to produce by break-up interactions of the D^+ beam with the Li target the required 10^{17} neutrons per seconds with the appropriate energy [3]. Because the accelerators have to reach unprecedented performances, the feasibility is being tested through the design, manufacturing, installation, commissioning and testing activities of a 1:1-scale prototype accelerator from the injector to the first cryomodule referred to as the Linear IFMIF Prototype Accelerator (LIPAc) shown in Figure 1. The IFMIF project is carried out under the framework of the Broader Approach Agreement between Europe and Japan. It is presently in its Engineering Validation and Engineering Design Activities (EVEDA), and the accomplishment in summer 2013, on schedule, of its Engineering Design Activities (EDA) allowed the successful development of the IFMIF Intermediate Engineering Design Report (IIEDR) [4]. The EU contributions to the LIPAc accelerator (CEA-Saclay, CIEMAT, INFN Legnaro and SCK-CEN Mol) are coordinated by the Fusion for Energy organization. The D^+ injector and LEBT have been installed and are nowadays being tested on the Rokkasho site (JAEA) in Japan.

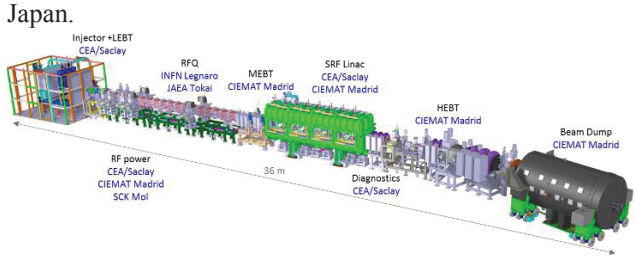

Figure 1: IFMIF LIPAc accelerator.

CRYOMODULE DESIGN

The IFMIF SRF LINAC for the LIPAc phase mostly consists of a cryomodule designed to be as short as possible along the beam axis so as to meet the beam dynamics requirements [5]. Figure 2 shows the 12.5-ton cryomodule made up with a rectangular section vacuum vessel, room temperature magnetic shield, MLI, thermal shield cooled down by GHe from the phase separator return line, and cold-mass wrapped in MLI.

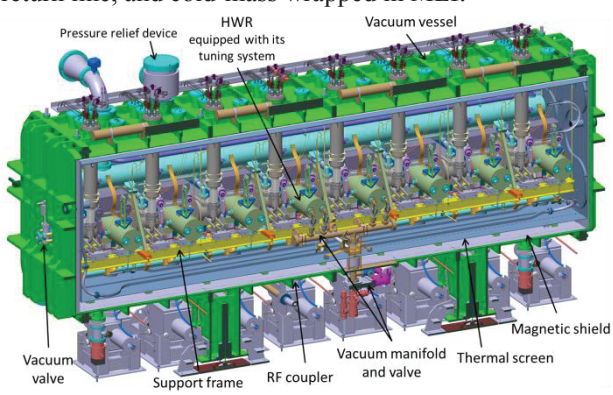

Figure 2: IFMIF LIPAc cryomodule cut view.

The cold mass is made up of the cylindrical phase separator, cryogenic circuit, titanium cavity support frame, hanging from the top of the vacuum vessel thanks to ten TA6V rods plus 4 TA6V rods ensuring lateral and horizontal positioning; 8 HWRs equipped with their

ISBN 978-3-95450-178-6

CRAB CAVITY AND CRYOMODULE DEVELOPMENT FOR HL-LHC*

F. Carra#[1], A. Amorim Carvalho[1], K. Artoos[1], S. Atieh[1], I. Aviles Santillana[1,2], S. Belomestnykh[3,4], A. Boucherie[1], J.P. Brachet[1], K. Brodzinski[1], G. Burt[5], R. Calaga[1], O. Capatina[1], T. Capelli[1], L. Dassa[1], S. U. De Silva[6], J. Delayen[6], T. Dijoud[1], H. M. Durand[1], G. Favre[1], P. Freijedo Menendez[1], M. Garlaschè[1], M. Guinchard[1], T. Jones[5,7], N.Kuder[1], S. Langeslag[1], R. Leuxe[1], Z. Li[8], A. Macpherson[1], K. Marinov[7], L. Marques Antunes Ferreira[1], P. Minginette[1], E. Montesinos[1], F. Motschmann[1], T. Nicol[9], R. Olave[6], C. Parente[1], H. Park[6], S. Pattalwar[7], L. Prever-Loiri[1], D. Pugnat[1], A. Ratti[10], E. Rigutto[1], V. Rude[1], M. Sosin[1], N. Templeton[7], G. Vandoni[1], S.Verdú-Andrés[3], G. Villiger[1], Q. Wu[3], B. P. Xiao[3], C. Zanoni[1]

[1]CERN, Geneva, Switzerland
[2]University Carlos III, 28911 Madrid, Spain
[3]BNL, Upton, NY 11973, USA
[4]Stony Brook University, Stony Brook, NY 11794, USA
[5]Cockroft Institute, Lancaster University, UK
[6]Old Dominion University, Norfolk, VA, 23529, USA
[7]STFC / Daresbury Laboratory, Daresbury, UK
[8]SLAC, Menlo Park, CA 94025, USA
[9]Fermilab, Batavia, IL 60510, USA
[10]LBNL, Berkeley, CA 94707, USA

Abstract

The HL-LHC project aims at increasing the LHC luminosity by a factor of 10 beyond the design value. The installation of a set of RF crab cavities is one of the key upgrades in the frame of this program: two concepts (Double Quarter Wave – DQW – and RF Dipole – RFD) have been proposed and are being designed in parallel in view of tests in the SPS before aiming at the final design for LHC.

This paper overviews the main design choices for the cryomodule and its different components, which have the goal of optimizing the structural, thermal and electro-magnetic behaviour of the system, while respecting the existing constraints in terms of integration in the accelerator environment. Prototyping and testing of the most critical components, fabrication, preparation and installation strategies are also described.

INTRODUCTION

The LHC uses a 60 m common focusing channel on each side of the interaction region (IR), where the two counter-rotating beams have to be separated transversely to avoid parasitic collisions. The separation is performed by introducing a crossing angle at the interaction point (IP), which increases with the inverse proportionality of the transverse beam size at the collision point. The non-zero crossing angle implies an inefficient overlap of the colliding bunches, thus reducing the luminosity. To recover the loss, one of the key element of the HL-LHC upgrade will be the adoption of a crab-crossing scheme, provided by a set of compact SRF crab cavities [1]. Prior to installation in the LHC, a prototype two-cavity cryomodule will be built and tested in the SPS in 2017. An overview of the project planning until installation in the LHC is provided in Table 1 [2].

Table 1: Overview of Crab Cavity Planning

2013-2014	Cavity Testing & Cryomodule Design
2015-2016	SPS Cryomodule Fabrication
2017-2018	SPS Tests & LHC Pre-Series Module
2019-2024	LHC Cryomodule Construction & Testing
2024-2025	LHC Installation

The design and development of the cryomodule components is at an advanced stage [3]; the main sub-assemblies are summarized in Fig. 1 and described in the following paragraphs.

*The research leading to these results has received funding from the European Commission under the FP7 project HiLumi LHC, GA no. 284404, co-funded by the DoE, USA and KEK, Japan
#federico.carra@cern.ch

SRF, COMPACT ACCELERATORS FOR INDUSTRY & SOCIETY

R. Kephart, B. Chase, I. Gonin, A. Grassellino, S. Kazakov, T. Khabiboulline, S. Nagaitsev,
R. Pasquinelli, S. Posen, O. Pronitchev, A. Romanenko, V. Yakovlev
Fermi National Accelerator Laboratory, Batavia, Illinois 60510, USA
S. Biedron, S. Milton, N. Sipahi
Colorado State University, Fort Collins, Colorado 80523, USA
S. Chattopadhyay and P. Piot
Northern Illinois University, DeKalb Illinois 60115, USA

Abstract

Accelerators developed for science now are used broadly for industrial, medical, and security applications. Over 30,000 accelerators [1] touch over $500B/yr in products producing a major impact on our economy, health, and well being. Industrial accelerators must be cost-effective, simple, versatile, efficient, and robust. Many industrial applications require high average beam power. Exploiting recent advances in Superconducting Radio Frequency (SRF) cavities and RF power sources as well as innovative solutions for the SRF gun and cathode system we have developed a design for a compact SRF high-average power electron linac. Capable of 5-50 kW average power and continuous wave operation this accelerator will produce electron beam energies up to 10 MeV. Small and light enough to mount on mobile platforms, such accelerators will enable new in-situ environmental remediation, in-situ crosslinking of materials, and security applications. More importantly, we believe this accelerator will be the first of a new class of simple, turn-key SRF accelerators that will find broad application in industry, medicine, security, and science.

OVERVIEW

Use of Superconducting Radio-Frequency (SRF) cavities allow linear accelerators (linacs) less than 1.5 M in length to create electron beams beyond 10 MeV with average beam powers measured in 10's of kW. Such compact SRF accelerators can have high wall plug power efficiencies and will require smaller radiation enclosures reducing overall installation costs. Recent technological breakthroughs are expected to reduce capital costs such that such accelerators can be cost effective for many existing and proposed industrial applications. Examples include radiation crosslinking of plastics and rubbers; creation of pure materials with surface properties radically altered from the bulk; modification of bulk or surface optical properties of materials; radiation driven chemistry; food preservation; sterilization of medical instruments; sterilization of animal solid or liquid waste, and destruction of organic compounds in industrial waste water effluents. Small and light enough to be located on a mobile platform, such accelerators will enable new in-situ remediation methods for chemical and biological spills and may create entire new industries by enabling in-situ crosslinking of materials.

A team from Fermilab, Colorado State University, Northern Illinois University, Euclid Techlabs, and PAVAC has started an effort to design, construct, and validate a compact, 10 kW average power linac capable of operating continuous wave (CW); delivering beam energies up to 10 MeV; weighing less than 3,000 pounds; and that can be palletized and made portable for a variety of industrial applications. This will be done by exploiting recent, robust, technological advancements in Superconducting Radio Frequency (SRF) and RF power source technologies as well as innovative solutions for the SRF gun and cathode system.

A major design choice for high-average power, compact SRF accelerators is the choice of RF frequency. As the frequency goes up, the size and weight of an SRF accelerator decreases. However, as the frequency goes up, the SRF cryogenic cooling requirements grow with the square of the frequency leading to the need for large cryogenic systems that without additional technological advances outpace the gains in going to higher frequencies. Until recently the mitigation approach was to adopt low frequencies (~350 MHz) that in turn lead to large physical size and weight for the cavities [2], cryomodule, and the required radiation shielding. Fortunately, due to several recent breakthroughs, low cryogenic loss elliptical cavities operating at 650 MHz or 1.3 GHz are now a viable and excellent choices that can be used to create more compact and efficient solutions.

BREAKTHROUGH TECHNOLOGY

There are six transformational, technological advances in SRF and peripheral equipment that pave the way for our ability to create a viable, compact, robust, high-power, high-energy, electron-beam or x-ray source. When these advances are integrated into a single design they enable an entire new class of compact, mobile, high-power electron accelerators.
These technologies are:

1) A new niobium surface processing technique "N-doping" [3] has been developed and demonstrated at Fermilab which dramatically reduces the cryogenic

ISBN 978-3-95450-178-6

SRF FOR FUTURE CIRCULAR COLLIDERS

A. Butterworth, O. Brunner, R. Calaga †, E. Jensen
CERN, Geneva, Switzerland

Abstract

The future circular colliders (FCC) will require superconducting RF (SCRF) systems for the proton-proton, electron-positron and lepton-hadron modes of the collider operation. The SCRF systems will accelerate the protons beams to 50 TeV and the lepton beams from 45.5 to 175 GeV in a staged approach with a possible 60 GeV energy recovery linac for the lepton-hadron to option as an intermediate step. The expected stored beam currents in some modes exceed 1 A with very short bunch lengths. A first conceptual design of the FCC RF system is proposed along with highlights of specific R&D topics to reach the design performance. Challenges related to RF structure design, intensity limitations due to beam loading, RF powering and higher order modes are addressed. Synergies between the different collider modes and the present LHC are identified.

INTRODUCTION

The scope of the FCC design study phase can be highlighted into three main categories [1]:

- FCC-hh: A 50 TeV proton-proton collider as a long term goal
- FCC-ee: A 45-175 GeV e^+e^- collider as an intermediate step
- FCC-he: Integration study to include an electron ring between 60-200 GeV electrons to collide with the 50 TeV protons.

A schematic of the foreseen 80-100 km FCC ring is shown in Fig. 1. A first conceptual design of the RF system for the different collider modes is proposed with highlights on specific SCRF challenges and related R&D to reach the design performance. Synergies between the different options are identified.

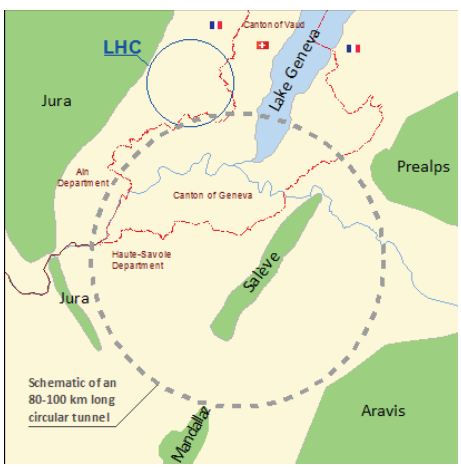

Figure 1: Schematic of the 80-100 km future circular collider tunnel at CERN (courtesy FCC study group).

SUPERCONDUCTING RF FOR FCC-HH

The FCC-hh collider will become the new energy frontier with a potential for direct discovery of new particles and explore physics well beyond the LHC. The primary function of the RF system for the FCC-hh would be to efficiently capture of up to 0.5 A (10600 bunches) at proposed energy of 3.3 TeV [2], accelerate to 50 TeV in approximately 30 minutes and store the colliding beams at 50 TeV for several hours. The high beam current and the uneven filling scheme, including the long abort gap, will result in transient beam loading that will strongly modulate the voltage vector. The situation is almost identical to that of the present LHC which employs 8 SCRF cavities at 400 MHz with high power RF to compensate for the strong reactive beam loading. Superconducting RF cavities with the large apertures and high stored energy are ideally suited to minimize the transient beam loading and thereby the required RF power for the proposed design voltage. To limit the sharp changes in the demanded power from the RF amplifier and keep the voltage vector constant, a 1/2-detuning scheme [3] similar to the LHC is appropriate.

Table 1: Relevant parameters for the FCC-hh option. The detailed parameter list can be found in Ref. [2].

	Unit	LHC	HL-LHC	FCC-hh
Energy	TeV	7.0	7.0	50.0
p/bunch	10^{11}	1.15	2.2	1.0 (0.2)
Beam current	A	0.55	1.1	0.51
Bun. Spacing	ns	50-25	25	25 (5)
St. Energy	MJ	392	694	8400
SR loss/turn	MeV	7×10^{-3}		3.9
RF Frequency	MHz	400		
Harmonic #		35640		133689
Total voltage	MV	16		32
RF power	kW	300	450	340
Peak Lumi	10^{34}	1.0	8.4	5-29

In this scheme, the cavity detuning is set to value where the RF power required is equal in the segments with and without beam. Only the sign of the generator phase is flipped for the two cases. This ensures that the required instantaneous peak power is kept almost constant. Fig. 2 shows the power requirements as a function of Q_L for injection and top energy parameters assuming the present $\frac{1}{2}$-detuning scheme. The detuning values and the optimum Q_L are listed in Table 2. The detuning at injection is beyond the the revolution frequency and and at top energy is quite close.

† Rama.Calaga@cern.ch